Laterally Loaded Piles

Models and Measurements

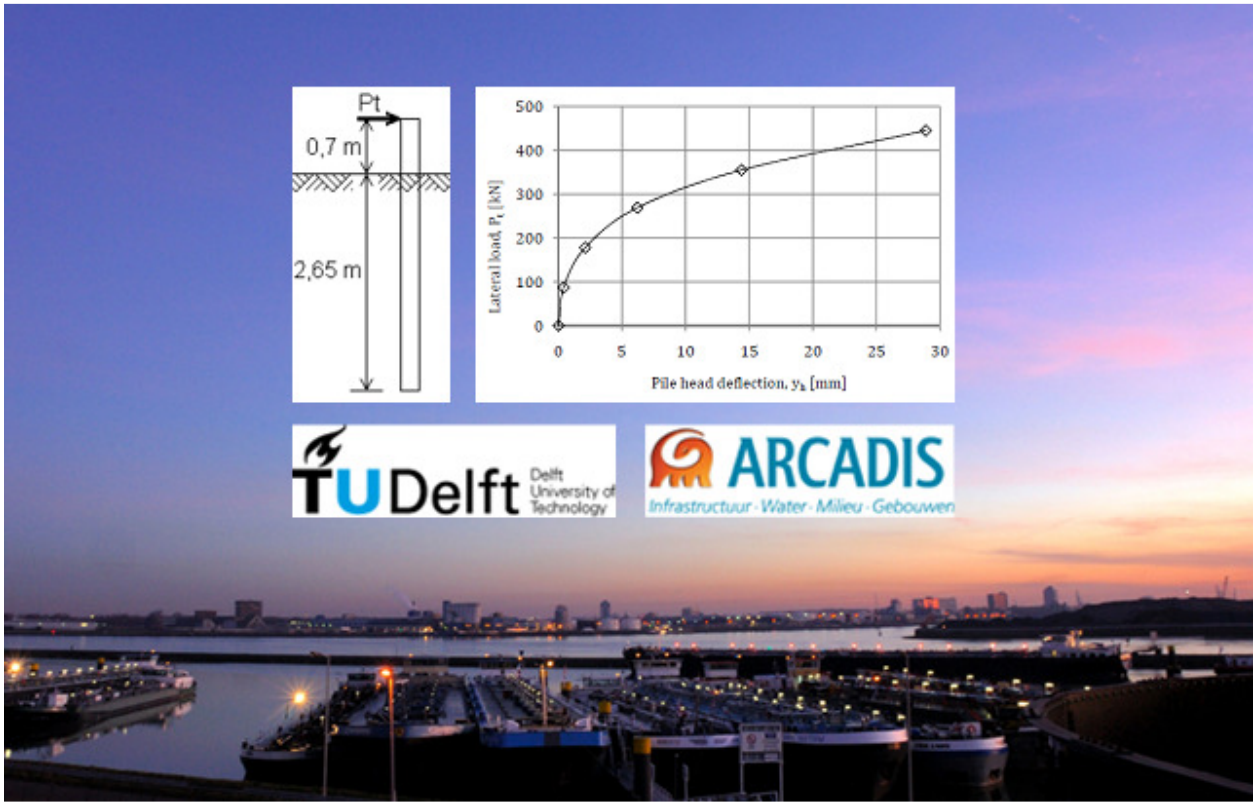

J.A.T. Ruigrok

A thesis presented on the comparison between different geotechnical models for single piles, which are loaded laterally at the top, on the basis of field measurements. The considered models are Blum, Brinch Hansen, Broms, the Characteristic Load Method, the Nondimensional Method, the Single Pile Module of MSheet, p-y Analysis by MPile and Finite Element Analysis by Plaxis.

Laterally Loaded Piles

Models and Measurements

J.A.T. Ruigrok
Delft, 2010

TU Delft
Faculty of Civil Engineering and Geosciences
Section of Geo-engineering

ARCADIS
Department of Hydraulic Engineering

Supervisory committee:

Chairman	Prof. Ir. A.F. van Tol	TU Delft, Deltares
Daily Supervisor TU Delft	Ing. H.J. Everts	TU Delft, ABT
Daily Supervisor ARCADIS	Ir. S. Azzouzi	ARCADIS Nederland bv
Supervisor TU Delft	Dr. Ir. R.B.J. Brinkgreve	TU Delft, PLAXIS bv
Supervisor TU Delft	Dr. Ir. J.G. de Gijt	TU Delft

PREFACE

In this master thesis a study to the available models for the design of laterally loaded piles is made. The research was initiated by a partnership between Arcadis and the TU Delft. The research was executed at the TU Delft, faculty of Civil Engineering and Geosciences at the department of Geo-engineering, and at Arcadis Rotterdam within the consulting group of Hydraulic Engineering.

I would like to thank my supervisory committee for their support and helpful input. Special thanks to my girlfriend Roos for her support and my parents for their support and advice throughout the many many years of education I enjoyed. Others I would like to thank are my friends, family, roommates and colleagues at Arcadis. Gratitude, I also owe to Saïd Azzouzi, for proposing the research question at the university, arranging for me a place at the office of Arcadis in Rotterdam and for the numerous discussions on the subject of laterally loaded piles.

PRINTING THIS REPORT

The report exists of four parts, the main report and three appendixes. All parts have their own table of contents and can be seen as separate reports. The first appendix, appendix A, contains detailed descriptions on the theoretical background of the used models. Appendix B contains descriptions on a number of field measurements. And appendix C contains all executed calculations. In the main report the findings of the appendices are summarized elaborated and conclusions are drawn. If you wish to print the report please check which of the parts are relevant to you. Especially consider appendix C. This appendix is 173 pages thick and merely contains all in and output of all calculations, which have a very repetitive character. Appendix C is therefore best to be used as reference.
This report can be printed in black and white, without losing its readability.

SUMMARY

This thesis is a comparison between different geotechnical models which can be used to design single laterally loaded piles. The comparison is useful, because in the daily practice of geotechnical engineering many discussions arise on which model is most suitable in which situation. This is also mainly due to the differences in results between different models. Sharp designs can reduce cost massively.
Of course, in literature several researches were already conducted in comparing different models. However, these comparisons were either theoretical comparisons, or comparisons between a single model and measurements. With today's most used models, comparisons between the models and measurements have not yet been made.
The objective of this thesis is therefore to compare the accuracy of the different models and find recommendations on which model can be used best in which situation.

The problem of a single laterally loaded pile is complex due to the presence of multiple nonlinearities. Firstly, the soil stiffness is nonlinear. For small deformations, the soil reacts stiffer than for larger deformations. The maximum soil resistance and stiffness increase nonlinearly with depth and depend nonlinearly on the pile diameter. Then, also the mobilization of the soil resistance along the pile develops nonlinearly. The pile deformation at the top is largest, if the load increases on the pile, deeper soil layers become more active.

Eight different models were chosen and compared. These are:

- Blum
- Brinch Hansen
- Broms
- Characteristic Load Method (CLM)
- Nondimensional Method (NDM)
- MSheet
- p-y Curves
- Plaxis 3DFoundation

Blum is an easy analytical design method. Its output is the length of a pile, if the maximum load and diameter of the pile and the friction angle and volumetric weight of the soil are given. Blum is therefore an ultimate strength model.
Brinch Hansen is, like Blum, an analytical ultimate strength model. The differences are that cohesion and layered soils can be taken into account. To do this, the ultimate soil resistance is determined differently and different assumptions are made in the calculation.
Broms method is in essence also an ultimate strength model. However the assumption is made that the deformations at a load of 0,3 and 0,5 times the ultimate load increase linearly and between these loads the deformations can be calculated. This, and the design of piles are done with the help of a number of design graphs.
The *Characteristic Load Method* (CLM) is a method based on a large amount of p-y analysis. The developers desired a quick design method which does not require the use of a computer but does take the multiple nonlinearities of the problem into account. The result was a number of design graphs with which a pile could be designed and deformations and moments along the pile could be calculated.

The *Nondimensional Method* (NDM) is, like the CLM, a method which is based on p-y analysis. The multiple nonlinearities are taken into account. Although the method does not require the use of a computer, the results are not obtained quickly. This, because the procedure is iterative and multiple values from nondimensional graphs have to be determined. The advantage of the model is that different p-y curves can easily be implemented and compared. In the comparative calculations, the p-y curves as recommended by Reese *et al.* were used. The model can be used both for design and prediction of the deformations of the pile.
MSheet, is an often used spring model. The method can be used to design piles and to predict deformations. The ultimate soil resistance at each depth is, in the standard settings, determined according to Brinch Hansen and the linear modulus of subgrade reaction according to Ménard. Equilibrium is then iteratively found between the soil springs and the load.
p-y Curves, is like MSheet a spring model. However, the spring stiffnesses are nonlinear as can be expected from soil. The p-y analyses have been executed with the cap model of the program MPile. The possibilities of this model are also larger than MSheet. Pile groups, for instance, can also be designed with this program. In the comparative calculations, the p-y curves as recommended by the API were used.
Plaxis 3DFoundation, is a 3D finite element method. The theoretical background and calculation method is closest to the reality with this model, since fundamental soil behavior is implemented. The program iterates until equilibrium is reached between the load and the soil reaction.

The comparison between the different models on accuracy and theoretical background resulted in a multi-criteria analysis (MCA). Of the models, Broms and the CLM are least usable. The methods are unpractical and inaccurate. The NDM is very accurate, however *very* unpractical. Blum and Brinch Hansen, the ultimate strength models, cannot be compared on the basis of measurements, since the prediction of the deformations of the pile under working loads is not the way these models are originally supposed to be used. The three models which require the use of a computer, MSheet, p-y analyses with MPile and Plaxis, all score high in the MCA. The methods are approximately equally accurate, are easy to use and offer lots of possibilities. These are the models which are recommended to be used in the case of single pile design.
For a more substantiated choice between these three models, consider the complexity of the situation, the design phase and the amount of time available. In very early design phases, or to find dimensions of a pile which can be used as starting point for a design in for instance MPile, Blum can be used. However, great care is needed if Blum is used since several variations of this model circulate. The recommended version of the method of Blum is described in the German codes and in the Spundwand-Handbuch by the German sheet-pile producer Hoesch.

From the research it became clear that on some subjects further research is desirable. Additional tests would increase the reliability on the statements made on accuracy. If these tests would reach failure, the accuracy of Blum and Brinch Hansen could also be examined. In Plaxis accuracy could increase if the stiffnesses are more precisely determined. Development of better correlations between strength and stiffness could also increase the accuracy of Plaxis. Considering the good results of the NDM, the accuracy of the use of p-y curves in MPile can be examined. Also p-y curves can be developed specially for Dutch soils, e.g. peat and sandy clays.

Finally, it can be concluded that single pile design is a tedious procedure and all models should only be used while considering their limitations, possibilities and theoretical backgrounds.

SAMENVATTING

Dit afstudeerwerk omvat een vergelijking tussen verschillende geotechnische modellen die gebruikt worden om alleenstaande horizontaal belaste funderingspalen te ontwerpen. De vergelijking is nodig, omdat in de praktijk vele discussies ontstaan over welk model het best toepasbaar is in welke situatie. Dit komt, omdat ervaring leert welke modellen conservatief rekenen en welke progressief. Scherpe ontwerpen kunnen de kosten enorm beperken.
In het verleden zijn al enkele onderzoeken naar dit onderwerp gedaan. Echter, deze vergelijkingen waren of een vergelijking gebaseerd op theorie, of een vergelijking van een enkel model met een meting. Niet eerder zijn de huidige vaak gebruikte modellen met elkaar op basis van metingen vergeleken.
Het doel van dit afstudeerwerk is het maken van deze vergelijking en concluderen welk model het preciest het paalgedrag voorspeld en welk model het best gebruikt kan worden in welke situatie.

Het probleem van de horizontaal belaste paal is complex door de vele niet-lineaire verbanden. Zo is de stijfheid van de grond niet-lineair afhankelijk van de rek. Ook nemen de maximale weerstand en de stijfheid van de grond niet lineair toe met de diepte en ook niet met de diameter van de paal. Ook de mobilisatie van de weerstand van de grond verloopt op een complexe manier. De weerstand van de grond is afhankelijk van de vervorming van de paal die nergens over de diepte gelijk is.

Acht verschillende modellen die dit probleem aanpakken zijn vergeleken. Deze zijn:

- Blum
- Brinch Hansen
- Broms
- Characteristic Load Method (CLM)
- Nondimensional Method (NDM)
- MSheet
- p-y Curves
- Plaxis 3DFoundation

Blum is een simpel analytisch ontwerpmodel. Het berekent de benodigde lengte van een paal als de diameter, maximum belasting en grondeigenschappen gegeven zijn. Blum ontwerpt daarom op de bezwijkgrens toestand.
Brinch Hansen is een gelijksoortig model als Blum. Het verschil is dat cohesie en een gelaagde bodemopbouw in rekening gebracht kunnen worden. Ook wordt de grondweerstand anders bepaald en de berekening op een andere manier uitgevoerd.
Broms rekent ook op de bezwijkgrens toestand. Maar stijfheidberekeningen zijn ook mogelijk, omdat wordt aangenomen dat de verplaatsingen lineair toenemen bij toenemende belasting onder normale belastingscondities. De berekening wordt uitgevoerd met ontwerpgrafieken.
De *Characteristic Load Method* (CLM) is gebaseerd op een groot aantal p-y analyses. De ontwikkelaars wilden een snelle ontwerpmethode ontwerpen die de verschillende niet lineaire verbanden in rekening zou brengen. Dit leidde tot enkele ontwerpgrafieken waarmee de verplaatsingen en momenten langs de paal berekend kunnen worden.

De *Nondimensional Method* (NDM) is net als de CLM gebaseerd op p-y berekeningen. De verschillende niet lineaire verbanden worden in rekening gebracht. Hoewel de methode geen computer vereist is het geen snelle ontwerpmethode. Dit, omdat er verschillede iteraties moeten plaatsvinden en uit verschillende grafieken waarden moeten worden afgelezen. Het voordeel van de methode is dat verschillende p-y curven eenvoudig kunnen worden ingevoerd en vergeleken. In de vergelijking van de modellen zijn de p-y curven van Reese *e.a.* gebruikt.
MSheet, is een veel gebruikt verenmodel. De uiterste grondweerstand wordt in de standaard instellingen bepaald met Brinch Hansen en de lineaire bedingconstante met Ménard. Het model zoekt evenwicht tussen de belasting en de grondveren.
p-y Curves, is net als MSheet een verenmodel. Echter, de veerstijfheden zijn niet lineair zoals van grond kan worden verwacht. De p-y analyses zijn gedaan met het cap model van MPile. De mogelijkheden van dit pakket zijn groter dan die van MSheet, zo kunnen bijvoorbeeld paalgroepen in rekening worden gebracht. In de berekeningen zijn de aanbevolen p-y curves van de API gebruikt.
Plaxis 3DFoundation, is een 3D eindige elementen methode. De theoretische achtergrond en berekeningsmethode van dit model benaderen de werkelijkheid het dichtst van alle modellen. Plaxis itereert totdat er evenwicht is tussen de belasting en de grondreactie.

De vergelijking tussen de verschillende modellen op precisie en theoretische onderbouwing resulteerde in een multi-criteria analyse (MCA). Van alle modellen zijn Broms en de CLM het minst bruikbaar. De methodes zijn niet praktisch en niet precies. De NDM is heel precies, maar *heel* onpraktisch. Blum en Brinch Hansen, die in de bezwijktoestand rekenen, kunnen niet worden vergeleken op basis van de metingen, dit, omdat de modellen niet bedoeld zijn voor het berekenen van verplaatsingen onder normale belastingen. De drie modellen die werken met hulp van een computer, MSheet, p-y Curves en Plaxis, scoren hoog in de MCA. De methodes zijn ongeveer even precies, zijn eenvoudig in gebruik en zijn theoretisch goed onderbouwd. Dit zijn de aanbevolen methodieken voor het ontwerp van palen.
Om een onderbouwde keuze tussen deze modellen te maken, beschouw dan de complexiteit van de situatie, de ontwerpfase en de beschikbare hoeveelheid tijd. In een zeer vroeg ontwerpstadium, of om paaldimensies te bepalen die als uitgangspunt kunnen dienen voor, bijvoorbeeld, een MPile berekening, kan de methode Blum gebruikt worden. Deze methode dient voorzichtig gebruikt te worden, omdat verschillende varianten in omloop zijn. De aanbevolen variant is beschreven de Duitse normen en het Spundwand-Handbuch van de Duitse damwandenleverancier Hoesch.

Uit het onderzoek werd duidelijk dat op sommige onderwerpen aanvullend onderzoek wenselijk is. Extra metingen zouden de vergelijking op precisie waardevoller kunnen maken. Als bij deze metingen palen belast zouden worden tot bezwijken, dan zouden ook Blum en Brinch Hansen op precisie vergeleken kunnen worden. De precisie van Plaxis zou kunnen toenemen als de stijfheden nauwkeuriger bepaald worden. Ontwikkeling van betere correlaties tussen sterkte- en stijfheidparameters zouden de precisie van Plaxis verbeteren. Gezien de goede resultaten van de NDM zou ook de precisie van MPile met de curven ontwikkeld door Reese *e.a.* onderzocht kunnen worden. Er zijn geen uitgesproken aanbevelingen voor curven voor veengronden, zanderige klei enz. Ontwikkeling van deze zou de toepasbaarheid van het model in Nederland kunnen vergroten en vereenvoudigen.
Tot slot kan worden geconcludeerd dat het ontwerpen van alleenstaande horizontaal belaste palen ingewikkeld is. De modellen zouden alleen gebruikt mogen worden als rekening wordt gehouden met hun beperkingen, mogelijkheden en theoretische onderbouwing.

TABLE OF CONTENTS

1 INTRODUCTION

1.1 PROBLEM DESCRIPTION

In geotechnical engineering a large number of models are available which engineers can use to design at the top laterally loaded piles. Unfortunately, in practice it often appears that there is conflict between different partners if a decision has to be made on which model to use. This is due to the fact that there are no clear guidelines which prescribe which model to use in which situation. Clear guidelines on this issue are necessary to avoid conflicts, to save time in the decision making process and to make sharp designs which fulfill the safety and usability requirements.
In the past, some comparisons were made between different models. However, this way no comments on accuracy of the models could be made and no solution to the above problem could be given.

Note: This research does not include models for piles loaded by laterally moving soils.

1.2 TYPES OF MODELS

In this thesis eight models are described and compared. These models range from simple methods which do not require the use of a computer to very advanced finite element software packages. The considered models can be divided in roughly two groups. To the first group belong the so called ultimate state models. With this group it is only possible to design a pile on strength, since only the load at failure is considered. The models which belong to this group are models Blum* and Brinch Hansen*. The second group concerns all other models which are capable of designing a pile of both strength and stiffness. These models are called: the method Broms*, the Characteristic Load Method (CLM), the Nondimensional Method (NDM), the single pile module by MSheet, the *p-y* analyses by MPile and the finite element analyses by Plaxis. Of this last group of models the first three use a graphical-analytical approach. The last three are models which require the use of a computer.
From this overview of models it can be seen that a wide variety of models is used. This is due to the fact that there were no selection criteria on the theoretical background of the models. The only criterion on which the selection was based was that a model has or had to be part of the daily practice in geotechnical engineering.

**Note: The models are sometimes named after their developer's. If an author is named without the year of publication, the model is meant and not a reference work.*

1.3 OBJECTIVES OF THESIS

The main objective of the thesis is to find recommendations on which model to use in which situation for the design of laterally loaded piles. This is to be done by comparing the results of the different models with full scale field tests. This allows a comparison on accuracy between models on a variety of soil profiles. With accuracy the preciseness with which a model can predict the deformations of and moments in a pile under lateral loading is meant. The models also have to be compared on model characteristics and usability to fulfill the main objective.
The secondary objective is to find recommendations on how Blum can best be used. This because Blum is one of the most frequently used models in dolphin design and during the process it appeared that different versions of Blum circulate. Also the model Blum could not be compared on accuracy with the other models since this is an ultimate strength model.

1.4 RANGE OF THESIS

Because of the limited number of field tests which were used in the comparison, the conclusions and recommendations of the thesis are valid within a certain range. This range is elaborated in paragraph 3.2.2 and 3.2 of the main report. There are several ranges. The tests were executed with piles with deferent diameters and made of different materials. There were also different soil types and different loading conditions. The summary of the range is given in table 1-1.

Pile		**Soil**		**Loads**	
Diameter:	0,3m<D<1,5m	*Types:*	Cohesive (c_u), cohesionless (φ) and layered	*Direction:*	Only Lateral
Materials:	Steel tube & bored piles			*Duration:*	Tens of seconds/ minutes

Table 1-1 Range of field tests used in thesis

1.5 OUTLINE OF THESIS

The thesis started with an extensive literature research. The results of the literature research are summarized in chapter 2 and 3. In chapter 2 each of the considered models is described on its most important features and the limitations of the model. In chapter 3 the field tests are summarized. Not all the field tests available in literature have been used for this thesis. A selection of the tests is made in this chapter.
With the measurement, the models can be compared on accuracy. This is done by considering the results of the measurements as unknown and predicting the outcome of the measurements with the model. This way the predictions can be considered as Class A predictions. The results of these calculations are shown and discussed in chapter 4.
With the results of chapters 2 and 4, it is now possible to compare the models on accuracy and theory. To do this adequately a Multi Criteria Analysis is used. This MCA is described in chapter 5. From Chapter 2 and 5 it appeared that it is not possible to compare Blum and Brinch Hansen with measurements. Blum, the most frequently used model of the two is elaborated in detail

in chapter 6. Also recommendations are given on how this method should be used, since multiple variants of the method circulate. Chapter 7 gives the conclusions and recommendations of the thesis. The structure of the thesis is given in table 1-2.
Finally, there are three appendices. Appendix A gives a detailed description of the models. Here, the theoretical background is elaborated in detail, the existing validation of the model and the method of application of the model are given and, after this, the limitations of the models are summarized.
Appendix B gives detailed descriptions of all the field tests extracted from literature. The data is divided in four parts: the soil information, pile information, load information, test results and, if available, the used instrumentation on the pile.
Appendix C gives the full elaboration of all the executed calculations. Each calculation can be considered as a Class A prediction of the accompanying results of a field test.

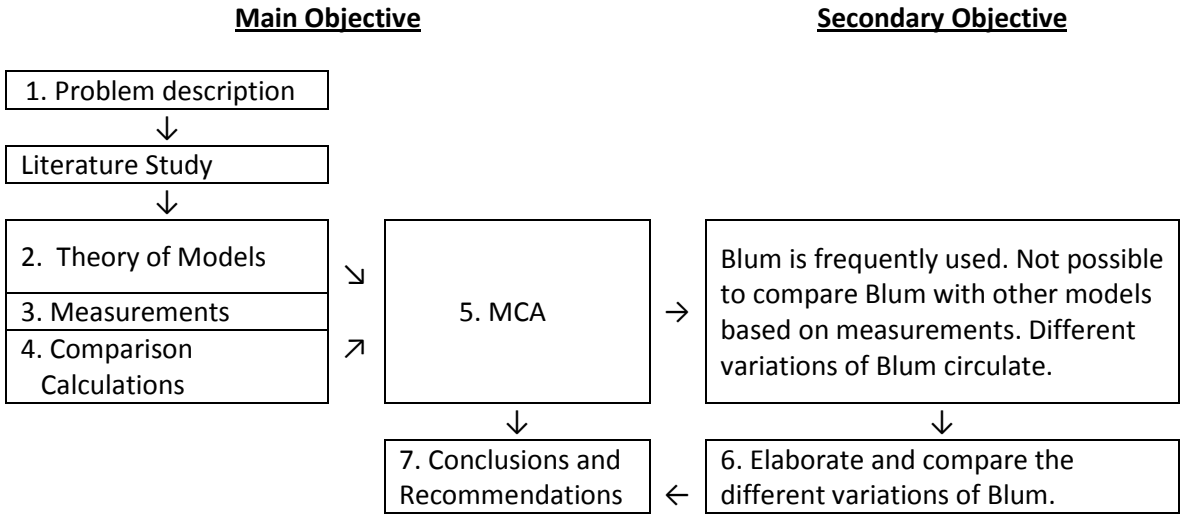

Table 1-2 Structure of Thesis. The numbers represent the chapter numbers.

2 MODELS

In this chapter a description of each of the considered models is given. The descriptions are relatively brief, since their purpose is only to give the basis of the theoretical background, the possibilities and the limitations of the models. Each model is first briefly introduced followed by the main reference(s). For more detailed references and descriptions of the models, see *appendix A*. The models in this chapter are increasing in complexity and modernity.

2.1 BLUM – 1932

The method developed by H. Blum is one of the most widely used methods. It is still used today even though the model is nearly 80 years old. Its simplicity and fast results make it an attractive alternative to the more expensive and complex computer calculations. (Blum, 1932) For a more detailed description, see Appendix A, chapter 1.

2.1.1 Background

Since the method of Blum was established in a period when no calculations could easily be executed by computers, Blum made some crude assumptions. The pile is considered to be fixed against deflections at theoretical penetration depth, t_0. The moment at this depth is assumed to be zero, a lateral force is allowed at this point. This is allowed, if the real length of the pile is taken to be $1{,}2t_0$. (Figure 2-1 B)

Above the fixed point, there are two forces on the pile. The first force is the lateral load which is applied at the top of the pile. The second force is caused by the soil resistance. It is assumed that the soil mobilizes the full passive resistance. The passive resistance is found by assuming a soil wedge, figure 2-1 A, which is pushed upwards by a lateral deflection of the entire pile. This soil resistance is supposed to be independent of the deformation of the pile.

To calculate displacements Blum assumes the moment and rotation to be zero at the theoretical penetration depth. Then with mere rules of mechanics Blum calculates the displacements in the ultimate state.

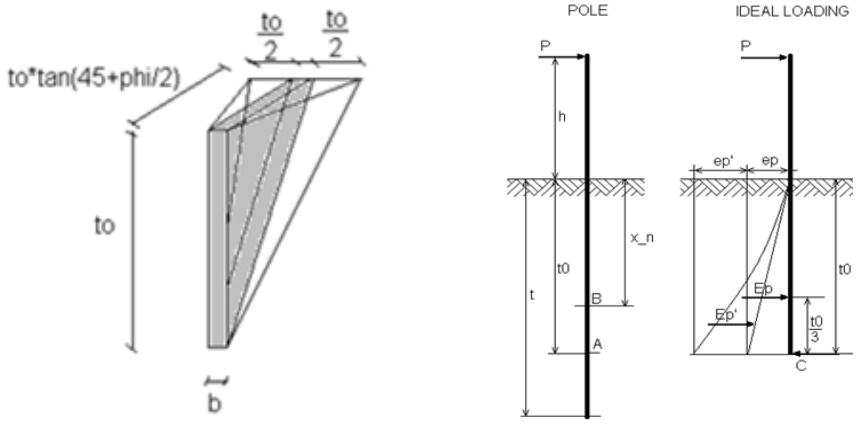

Figure 2-1 A: The soil wedge which causes the passive resistance. B: The pile schematization with the actual pile and the pile in the ideal loading situation. The soil resistance is depicted on the wrong side. The soil resistance "ep" is caused by the grey part of the wedge and "ep'" by the other two parts.

2.1.2 Possibilities and Limitations of method Blum

The method Blum is suitable to use for short and rigid piles in a sandy soil. For this situation, it can well be used to obtain a quick indication of the pile length. The method does not give the behavior of longer and more slender piles. Also the term of cohesion does not play a role in the model. Because the method Blum is also an ultimate strength model, its purpose is not to design a pile in the serviceability limit state. This can be done, for example, by assuming the soil resistance to increase linearly with depth. These assumptions will not be used in this thesis, since the model was not designed to be used in this way.

It should be noted that the model of Blum does not represent in any way the actual pile-soil interaction behavior. The method of Blum is therefore usable only to give a quick estimate of the final pile design.

It has been noted that in the daily practice of engineering adapted versions of Blum are used in the form of calculation sheets. These versions include layered soils, sleeve friction and sloping groundlines. In the case of layered soils, the engineer should ask himself if the value of $1{,}2t_0$ is still valid. The implementation of sleeve friction and sloping surfaces is examined further in chapter 6.

2.2 BRINCH HANSEN

Brinch Hansen published his method in 1961. The method is not as widely used as Blum, but the lateral earth pressure coefficients are used to determine the ultimate resistance of the soil in combination with a modulus of subgrade reaction in the program MSheet which is discussed later in this paper. (Brinch Hansen, 1961) For a detailed description, see Appendix A, chapter 3.

2.2.1 Background

Brinch Hansen is, like Blum, an ultimate limit state model. There are some differences. Brinch Hansen separates the soil resistance at different depths. And Brinch Hansen allows the term of cohesion in the calculation. The model is also suitable for layered systems with different types of soil. On the pile behavior there is another difference. Brinch Hansen does not fix the pile at a fixed depth, but keeps this point variable. If the load and the pile width are known, the pile length and the location of the rotation point can be found by means of an iterative procedure.

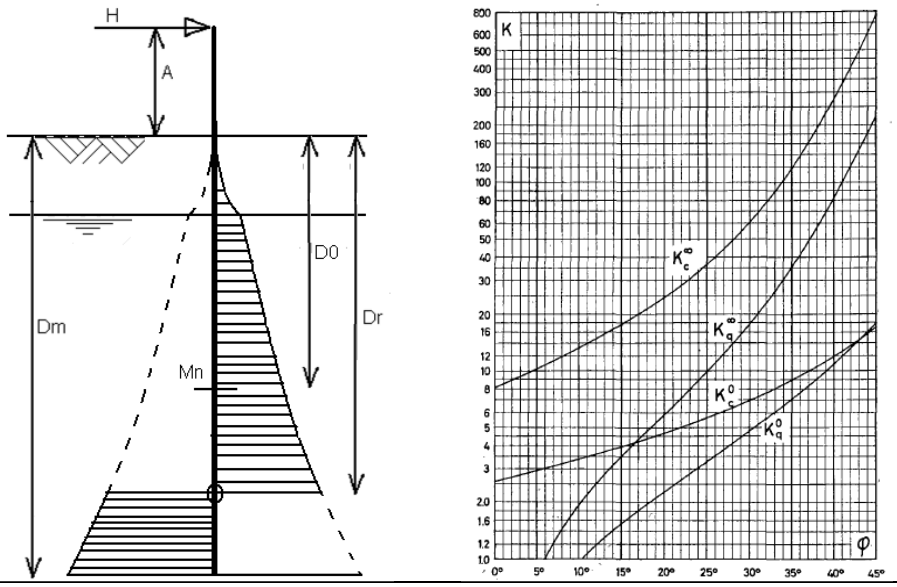

Figure 2-2 Schematization Brinch Hansen and lateral earth pressure coefficients

On the soil pressures, Brinch Hansen takes into account both the active and passive earth pressures. The earth pressures can then be visualized in a graph. This graph is shown in figure 2-2 on the right. With the earth pressure coefficients known the lateral earth pressures, shown in figure 2-2 on the left can be calculated with the following formula:

$$e^D = qK_q^D + cK_c^D \qquad eq.\ 2.1$$

The model of Brinch Hansen was validated by performing load tests on small wooden piles. Now the ultimate lateral earth pressure is used in the much used spring model MSheet.

2.2.2 Possibilities and Limitations of method Brinch Hansen

The method of Brinch Hansen is suitable for all types of soil and for layered systems. It is therefore a more complete model than Blum. The downsides are: the fact that the model is not capable of calculating deflections at the ultimate load and the calculation takes a lot of time because of the iterative character.

Fortunately, most of these issues can be solved with the aid of a computer. Deflections can be calculated if one more boundary condition is assumed. Now, the only boundary condition is that the pile does not deflect laterally at the rotation point.

2.3 BROMS

The method developed by Broms is used regularly outside of the Netherlands, especially for cohesive soils. Initially the method was developed for short, rigid and unfixed, piles in cohesive soils, but was expanded to long piles with fixed heads and cohesionless soils. (Broms, Lateral resistance of piles in cohesionless soils, 1964) (Broms, Lateral resistance of piles in cohesive soils, 1964) (Broms, 1965) For a more detailed description, see Appendix A, chapter 5.

2.3.1 Background

Broms introduced methods to calculate the ultimate lateral resistance. The assumption for short piles is that the ultimate lateral resistance is governed by the passive earth pressure of the surrounding soil. The ultimate lateral resistance for piles with large penetration depths is governed by the ultimate or yield resistance of the pile. This is shown in figure 2-3.
Broms also separates clayey soils from sandy soils. A remarkable feature of the soil resistance in clay, is that Broms sets the soil resistance for the first 1,5 pile diameters at zero.
Broms produced a series of nondimensional graphs with this method to quickly find the penetration depth of the pile, if the load, diameter and soil strength are known.
It is also possible, to predict the deflections of the pile under working loads. To do this, the pile deformations are assumed to be linear elastic where the load is approximately between 0,3 and 0,5 times the ultimate load.
The model has been validated by a large number of field tests. The conclusion was that the calculated deflections had a large variation compared to the measured deflections. On strength, the method is conservative if the soil is cohesionless and reasonably accurate if the soil is cohesive.

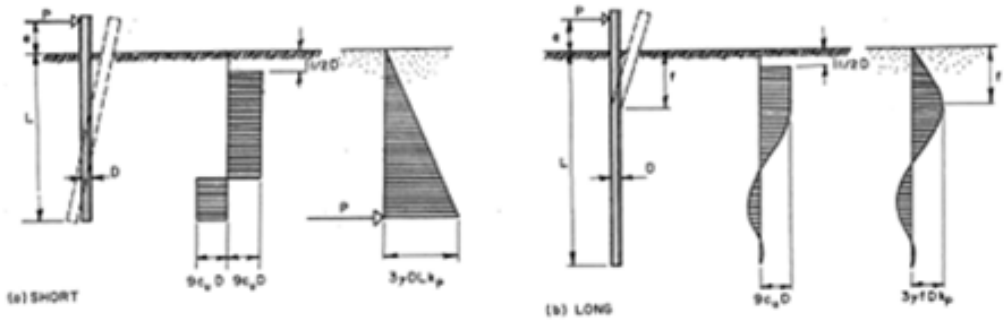

Figure 2-3 Soil reaction and failure mechanisms for short and long piles, according to Broms

2.3.2 Possibilities and Limitations of method Broms

Broms is very usable to quickly design a pile. However the model is not very reliable. It is best to use it for homogeneous cohesive soils. Also calculation of the serviceability limit state is possible, but not very accurate, since the pile-soil reaction is assumed to be linearly elastic and the validation showed large differences between calculation and measurement.

2.4 NONDIMENSIONAL METHOD (NDM)

This model, developed by Matlock and Reese, 1956, is based on *p-y* curves and numerical solutions that were obtained by hand-operated calculators. This model offered at the time a desirable solution to fully design piles in both the ultimate limit state and serviceability limit state while including nonlinear soil behavior. (Reese & Van Impe, 2001) For a more detailed description, see Appendix A, chapter 4.

2.4.1 Background

The main assumption, which forms the basis of this calculation, is that the stiffness of soil increases linearly with the depth and is zero at the ground line. Then if the p-y curves are established, paragraph 2-7, it is possible to iteratively calculate moments and deflections along the pile. This procedure is time consuming. The p-y curves have to be manually created, and then at least two iterations follow. For each iteration, multiple values have to be determined from the graphs.

Now that computers can numerically perform real p-y analyses, the nondimensional method is not used a lot. However, the results can be used to check p-y analyses and the method gives good insight in the nonlinearity of the problem.

2.4.2 Possibilities and Limitations of the NDM

With the NDM it is possible to check on real p-y analyses and good insight into the problem can be obtained. Another major possibility is that the decision on which p-y curve to use is completely open.

The disadvantages of the model are that the soil has to be homogeneous. The pile has to have a constant bending stiffness over the length of the pile. And most important, the calculation procedure is time consuming.

Note, in this research full p-y analyses have been executed with the program MPile. This program uses p-y curves recommended by the American Petrol Institute, (API). Therefore, the analyses with the NDM use other p-y curves. Namely those developed by Reese and Matlock. The p-y curves are described later in paragraph 2.7.

2.5 CHARACTERISTIC LOAD METHOD

The characteristic load method, CLM, was developed to quickly obtain results, which incorporate nonlinear behavior. Like the nondimensional method, the CLM is based on nondimensional graphs that were deduced from numerous *p-y* analyses. (Duncan, Evans, & Ooi, 1994) For a more detailed description, see Appendix A, chapter 6.

2.5.1 Background

The characteristic load method was developed by performing nonlinear *p-y* analysis for a wide range of free- and fixed head piles and drilled shafts in clay and sand. The results were presented in the form of relationships, graphs, among dimensionless variables. The method can be used to determine ground line deflections, maximum moments and the location of the maximum moment. The dimensionless variables are the lateral load divided by a characteristic load and the applied moment divided by the characteristic moment. The deflections are divided by the pile width. There are separate design graphs for cohesive soils and cohesionless soils.

2.5.2 Possibilities and limitations of the CLM

The CLM has some limitations. The soil has to be modeled as a homogeneous layer. The pile must have a constant bending stiffness over the height of the pile. The largest limitation lies in the validation. The model overestimated the deformations in some situations.

2.6 MSHEET, SINGLE PILE MODULE

MSheet is a software application; build to design earth retaining structures like building pits. The first version of this program was released in 1990. In 2004 the single pile module was added to the application. (GeoDelft, 2004) For a more detailed description, see Appendix A, chapter 7.

2.6.1 Background

In this module the soil is modeled as a bilinear springs. The method of Brinch Hansen is commonly used to find the maximum possible horizontal resistance of soil against lateral movements of the foundation. The maximum horizontal resistance can also be calculated and introduced into the program manually by choosing the correct active, passive and neutral horizontal earth pressures. To find the modulus of subgrade reaction of the soil, the user can choose to use the theory of Ménard, or he can manually give the values of this modulus for each layer. These two parameters describe the soil as a bilinear spring.

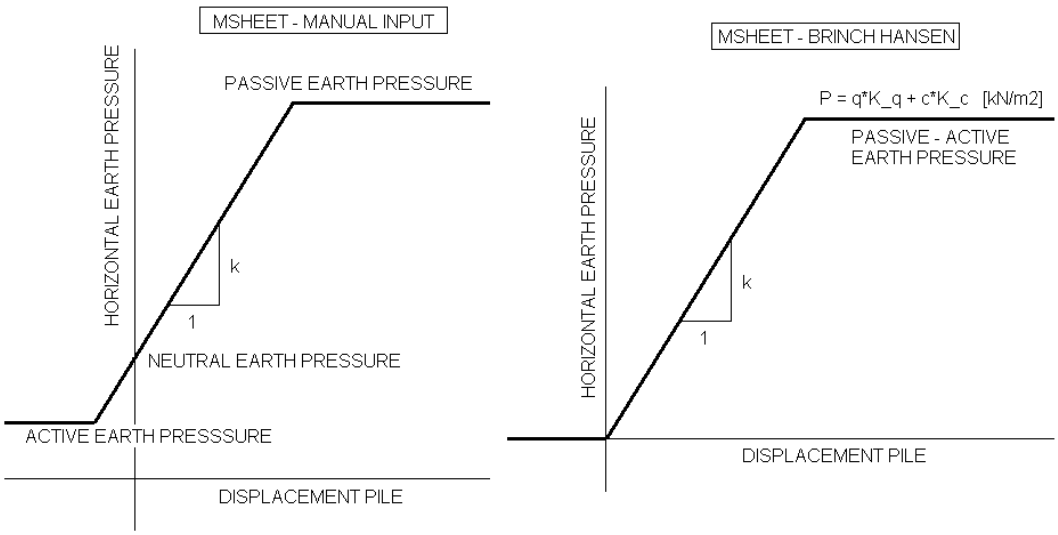

Figure 2-4 Bilinear springs in MSheet – Single Pile Module

2.6.2 Possibilities and limitations of MSheet

MSheet has a lot of possibilities. The model can be used on layered soils. The bending stiffness can vary over the length of the pile. Both ultimate state en serviceability limit state calculations are possible.

The main disadvantage is that the soil is modeled as a bilinear spring. This is unrealistic for soils. The stiffness is also independent of stress and strain. The independency of stress can be taken away by generating a lot of layers in the soil model with increasing elasticity with increasing depth. The ultimate horizontal earth pressure is usually only reached at the top of the pile, where the deflection is largest. This strength parameter, determined by Brinch Hansen or manually, is in contradiction to the stiffness, depending on the surrounding stress.

2.7 P-Y CURVES

The first ideas of this model, based on p-y curves, first arose halfway the previous century. Now it has fully been adopted in computer software like MPile. (MPile, version 4.1, 3D modelling of single piles and pile groups) (Reese & Van Impe, Single piles and pile groups under lateral loading, 2001) For a more detailed description, see Appendix A, chapter 2.

2.7.1 Background

Like MSheet the method of the p-y curves is based on a mass-spring model. Except that the springs are nonlinear and for large parts based on curves found by performing field tests.

The shapes of the curves depend on the strength parameters of the soil and the surrounding stress level. This makes the model easy to apply, because little soil data is required.

The program MPile uses p-y curves as they are recommended by the API in the standard settings. MPile does offer a possibility to manually apply p-y curves, but this was too time-consuming for this thesis. The recommendations by the API say that the soil stiffness is modeled as a parabolic curve until an ultimate strength is reached. A typical p-y curve is given in figure 2-5.

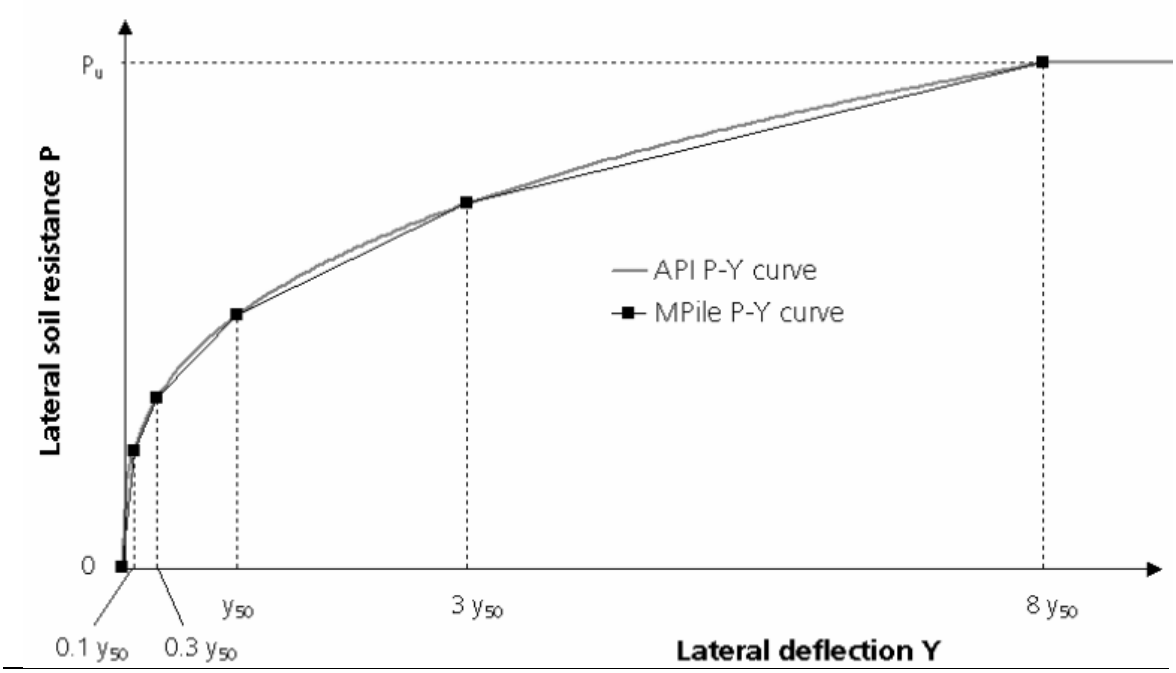

Figure 2-5 Typical p-y curve by the API. MPile models the parabolic part of the curve as five linear parts. Source: (MPile, version 4.1, 3D modelling of single piles and pile groups)

2.7.2 Possibilities and limitations of MPile

There are a lot of possibilities with the method of the p-y curves implemented in a computer program. It is now possible to model the soil nonlinearly. The pile can consist of sections with different bending stiffnesses. Axial loads can be applied. And calculations can be executed in both the ultimate limit state and the serviceability limit state.

In the case of the single pile problem, with only a lateral load at the top of the pile, the p-y method has no limitations. Everything can be modeled, even sloping surfaces. This last thing is not a standard option, but this and many other conditions can be implemented in the program by manually generating the p-y curves. Many guidelines and recommendations on how to generate the p-y curves exist apart from those of the API.

2.8 PLAXIS – 3D FOUNDATION

Plaxis – 3DFoundation is a three dimensional finite element program, specifically developed to predict soil-foundation interaction. The program was released in 2004 and the second, current version appeared in 2007. (PLAXIS 3D Foundation, Material models manual, Version 2) For a more detailed description, see Appendix A, chapter 8.

2.8.1 Background

Various models can be selected in Plaxis to simulate the soil behavior. The simplest model available is a linear elastic perfectly plastic model, known as the Mohr-Coulomb (MC-) model. Here, it is assumed that the soil resistance increases linearly with displacement, until the failure criterion is reached. The failure criterion is determined by Mohr-Coulomb. Also more advanced models are available. These are the hardening soil model, HS model, and the hardening soil model which includes small strain stiffness, HSSmall model. The last model includes the stress and strain dependency of the soil. Whereas, the HS-model only includes stress dependency and the MC-model includes neither of the two. Because the pile has a large

penetration depth and the deformations of the soil are small, except near the top of the pile, the HSS-model is the preferred model in this situation.
The calculation method used by Plaxis is a so called finite element calculation. The calculation method solves the problems numerically. It continues with the iteration procedure until equilibrium is reached between load and soil reaction.

2.8.2 Possibilities and limitations of Plaxis

The limitations of Plaxis are very few. The program is capable of performing complex calculation with all different types of loads. There are however several disadvantages. The use of the model is difficult compared to the other models. Lots of input parameters have to be determined. The time necessary to setup the model takes some time. And finally the calculation time necessary can go up to more than a day.

2.9 EVALUATION OF MODELS

In table 2-1 the results of the literature study are summarized. By means of the table it is possible to see which model is applicable in which situation. There are some characteristics mentioned of the model which do not apply to the single pile problem as used in this thesis. These characteristics does however, give a good idea of the possibilities of a model in a broader context.
The models can roughly be divided in two types. The first type is the ultimate strength model. Its purpose is not to design a pile in the serviceability limit state. This is important, because this type of model can therefore not be compared on the basis of field tests which do not reach failure. The tests did not reach failure as will be seen in the following chapter. The second type is obviously the type which can predict deformations at service loads.
To the first type belong the models Blum and Brinch Hansen. To the second type the models CLM, NDM, p-y analyses, MSheet and Plaxis belong. It's not clear to which of the two types the model of Broms belongs. Broms is in essence an ultimate strength model, but some tricks are used to predict deformations of the pile as long as the load is between certain margins below the ultimate limit load.

MODEL	Blum	Brinch Hansen	Broms	CLM	NDM	p-y Analyses	MSheet Single - Pile	PLAXIS 3D Foundation
GENERAL								
Year	1932	1961	1965	1994	1962	1940-now	2004[4]	2004
Validation	Yes[8]	yes	Yes	Yes	No	Yes	No	Yes
Common practice	Yes	No	Yes[5]	No	No	Yes	Yes	Yes[9]
MODEL TYPE								
Ultimate load	Yes	Yes	Yes	Yes	Yes	Yes	Yes	Yes
Working load	No	No	Yes[6]	Yes	Yes	Yes	Yes	Yes
Based on tests	No[8]	No	No	No	No	Yes	No	Yes
Based on analytics	Yes[8]	Yes	Yes	No	No	Yes	Yes	Yes
Based on p-y Analyses	No	No	No	Yes	Yes	Yes	No	No
SOIL								
Clay	No	Yes	Yes	Yes	Yes	Yes	Yes	Yes
Sand	Yes	Yes	Yes	Yes	Yes	Yes	Yes	Yes
Layered	No	Yes	No	Yes	No	Yes	Yes	Yes
Nonlinear soil	No	No	No	Yes	Yes	Yes	Bilinear	Yes
Time dep.	No	No	No	No	No	Yes	No	Yes
Sloping surface	No	No	No	No	No	Yes	No	Yes
LOAD AT MUDLINE								
Horizontal	Yes	Yes	Yes	Yes	Yes	Yes	Yes	Yes
Moment	Yes	Yes	Yes	Yes	Yes	Yes	Yes	Yes
Axial	No	No	No	No	No	Yes	No	Yes
Cyclic[1]	No	No	No	No	No	Yes	No	Yes
PILE								
Nonlinear pile[2]	No	No	No	Yes	Yes	Yes	No	Yes
Not constant EI[3]	No	No	No	No	No	Yes	No	Yes
Shell factor dependent on diameter	No	Yes	No	No	No	No	Yes[7]	Yes

Table 2-1 Summary of models. Notes: 1, Cyclic loading is not part of this thesis. 2, Nonlinear pile means that the EI of the pile is dependent on moment. 3, Not constant EI means that it is* possible to divide the pile in different sections with different EI's. *4, MSheet was introduced in 1990, the single pile module in 2004. 5, Broms is common practice internationally. 6, Only if the working load is between ,3 and ,5 times the ultimate load. 7, The modulus of subgrade reaction is dependent on the pile diameter if Ménard* and/or Brinch Hansen *is used. 8, Not all articles which formed the foundation of the method by Blum could be retrieved, therefore these statements are assumptions based on Blum's Theory (Blum, 1932). 9, Plaxis is very commonly used, however not for the considered problem.

3 MEASUREMENTS

In this chapter the field tests are presented on which the models of chapter two are to be compared. Since the tests are obtained from literature, some minimum criteria for the field tests had to be established to make selection of the tests possible. These criteria are described in paragraph 3.1. This resulted in a large number of tests, which are summarized in paragraph 3.2. For the full description of the tests and references, see appendix B. The amount of tests was too large to include all tests in the comparison because of the limited available time for this thesis. Thus a selection had to be made. The selection and the way this selection was made are described in paragraph 3.3. Finally, this chapter is summarized in paragraph 3.4.

3.1 CRITERIA FOR FIELD TEST SELECTION FROM LITERATURE

From the field tests found in literature it is to be preferred that all available data found during the test is published. However, this is rarely the case. Due to practical reasons and restrains in allowed number of pages, the soil and pile data etc. are merely summarized in most articles. Thus, minimum criteria had to be established. Field tests have to fulfill these criteria before they can be implemented in the comparison. These criteria are divided in four groups.

The first group concerns pile data: the pile the penetration depth, the bending stiffness, the material, the shape (diameter!) and strength should be known. Of these parameters, the material and the strength of the pile are least important. The material is not really important as long as the bending stiffness, or M-κ curve, is known. The strength is not really important as long as the pile did not fail during the test. Another condition is that the pile is not allowed to be restrained at the top.

The second group is about the soil data. The characteristics of the soil determine for a great part the deflection of the pile under a certain load. From the soil, the material (sand, clay), the position of the water table, the strength properties and the unit weight should be known. The modulus of subgrade reaction is not necessary (although preferred) to be known, since this parameter is determined by the theoretical background of most of the models or can be deduced from correlations with the strength parameters.

Pile	**Soil**	**Loading**	**Instrumentation**
Length and penetration depth	Classification of soil	Point of application above soil surface	Arrangement for applying load
Bending stiffness	Position water table	Loading type (force and/or moment)	Methods of measuring moments, deformation
Material	Strength	Magnitude	
Shape, width	Unit weight	Static, dynamic or long lasting load	
Strength			
Free headed			
Installation method			

Table 3-1 Overview of criteria for field test selection from literature

The third group is on the loads which were applied during the test. Of this load the point of application above the soil surface, the type of loading, moment/lateral load, and magnitude should be known. The duration of the load is important, because it is important to be able to determine if the soil reacted drained or undrained. The preferred loading type is static which means that the pile is loaded within, tens of, minutes. This is a loading situation which is frequently encountered in mooring situation in harbours.
The fourth group is about instrumentation. It is not really important to know which instrumentation exactly was used, but it can help to understand why the results of the tests show a certain behavior. Of the instrumentation it is most interesting to know how the loads were applied. Were the loads applied with a pulse, or were the loads applied gradually? The soil behavior depends on this difference. Furthermore, it is interesting to know how the deformations and moments were measured during the test. An overview of the four groups of requirements is given in table 3-1.
Another requirement which was not given as a separate group is that the results of the test are clearly documented. The minimum requirement is a load-displacement curve.

3.2 FIELD TESTS

In paragraph 3.2.1, an overview of the field tests is given. Then in paragraph 3.2.2 the limitations of these field tests are presented. This last paragraph will then automatically present the range (in pile lengths, pile diameters, soil types and so on) for which this research and thus the final recommendations are valid.

3.2.1 Overview of field tests

In this study 17 field experiments were executed on a total of 20 piles. In table 3-2, the field tests are summarized on some of the important characteristics. These characteristics are chosen, because they provide the information to determine which models can be applied.

Case	Soil type	Single soil type	Ultimate state reached	Pile type	Not constant E_pI_p over length pile	Axial load
I-cu	Cohesive, unsaturated	Yes	No	Steel	No	No
II-cu	Cohesive, unsaturated	Yes	No	Bored	No	No
III-cu	Cohesive, unsaturated	Yes	No	Steel	No	No
IV-cu	Cohesive, unsaturated	Yes	No	Steel	No	No
V-cs	Cohesive, saturated	Yes	No	Steel	No	No
VI-cs	Cohesive, saturated	Yes	No	Steel	No	No
VII-cs	Cohesive, saturated	Yes	No	Steel	Yes	No
VIII-cl	Cohesionless	Yes	No	Steel	No	No
IX-cl	Cohesionless	Yes	No	Bored	No	No
X-cl	Cohesionless	Yes	No	Steel	No	No
XI-l	Layered	No	Yes	Steel	No	Yes
XII-l	Layered	No	No	Bored	No	No
XIII-l	Layered	No	No	Steel	Yes	No
XIV-l	Layered	No	No	Steel	Yes	No
XV-cφ	*c-φ* soil	No	No	Bored	No	No
XVI-cφ	*c-φ* soil	No	No	Bored	No	No
XVII-cφ	*c-φ* soil	No	No	Steel	No	No

Table 3-2 Summary Field Tests

The cases are sorted on soil type. The additions to the field test number (cu, cs, cl, l and c*φ*) stand for the soil type in which the test was executed. Here, *"cu"* stands for Cohesive Unsaturated soil, *"cs"* for Cohesive Saturated soil, *"cl"* for Cohesionless soil, *"l"* for layered soil and *"cφ"* for *c-φ* soil. For full descriptions of the soil tests, please see appendix B.
It can immediately be seen that case XI is different from the others. It is the only case where failure immersed and also the only case where an axial load was applied. Other cases that differed, apart from the soil type, were cases II, IX, XII, XV and XVI, since here bored piles were used and cases VII, XIII and XIV, since the bending stiffness of these piles was not constant over the length of the pile.

3.2.2 Limitations of field tests

Results of some of the field tests have been used as empirical input for creating the *p-y* curves. This is a limitation, because the models which use *p-y* curves cannot be validated on those field tests. The following cases have been used to create the recommendations for the *p-y* curves: Case II-cu, Case V-cs, Case VII-cs and Case VIII-cl.
Furthermore, the soil data is very limited. In most of the cases this is limited to the undrained shear strength and/or the angle of internal friction and a volumetric weight for each soil layer. In all cases, except for the case in Delft the soil test results are not available. This means that the available soil data is assumed to be correct and correctly interpreted by means of thorough soil investigations.
The number of tests is not high enough to be able to judge the models in all possible situations. The range of the diameters of the different piles is between 0,3m and 1,5m. Thus no large diameter piles are included in this research.
No tests on wooden piles are included and the number of concrete piles is small.
In all the field tests the piles were subjected to loads of a short duration. This means that the load should not be considered as an impulse. It also means that the soil will react partially drained, especially if sand is considered, and partially undrained, in the cases of a clayey soil. This also limits the range in which this research is valid to loads of a short duration. These types of loads can be expected in mooring situations, if a boat collides with a dolphin. Those collisions usually last for (tens of) seconds. But the loads in the field tests lasted from tens of seconds to tens of minutes.
The range of the field tests are summarized in table 3-3.

Pile		**Soil**		**Loads**	
Diameter:	0,3m<D<1,5m	*Types:*	Cohesive (c_u), cohesionless (*φ*), layered and c-*φ* soils	*Direction:*	Only Lateral
Materials:	Steel tube & bored piles			*Duration:*	Tens of seconds/ minutes

Table 3-3Range of all field tests

3.3 SELECTION OF FIELD TESTS WHICH ARE TO BE USED IN THE COMPARISON

Not all measurements can be used in this research. This is due to the limited amount of time available to perform all the calculations with all models for all measurements. The selection of the measurements was based first on type of soil. It was decided to make for the two most occurring soils, clayey soil and sandy soil, a comparison between the models on three cases. This excluded the field tests in layered soils and c-*φ* soils. Of the remaining cases, case II, V, VII and VIII are excluded since these tests were executed and used by the developers of the method of p-y curves. The remaining tests have been used for calculation. Unfortunately, only

two cases in sandy soil remained. Therefore case XIII-l has also been used. The soil layer in this case is layered, but the thick top layer consisted of cohesionless soil. For the calculations in clayey soils four cases remained. Here, case IV-cu was left out since it was executed with the goal to examine the pile behavior in earthquake conditions. In summary, the used tests are for cohesive soil: Case I-cu (from) Bagnolet, III-cu Brent Cross and VI-cs Sabine. And for cohesionless soil: Case IX-cl Garston, X-cl Arkansas River and XIII-l Florida.
This selection of field tests also has a more narrow range than all the field tests together. The narrowing affected the range of soil type most. The other ranges stayed similar, but it must be taken into account that, if fewer cases are considered within the ranges, the accuracy of the comparison and the conclusions become less accurate.
The final range is given in table 3-4.

Pile		**Soil**		**Loads**	
Diameter:	0,3m<D<1,5m	*Types:*	Cohesive (c_u), cohesionless (φ) and layered	*Direction:*	Only Lateral
Materials:	Steel tube & bored piles			*Duration:*	Tens of seconds/ minutes

Table 3-4 Range of field tests used in research

3.4 SUMMARY OF CHAPTER 3

In this chapter and in appendix B, 17 field tests with test results on 20 piles are described. Because of the time constraint, a selection of the field tests had to be made. These field tests would be used for comparing the geotechnical models described in chapter 2. The selection resulted in three cases in cohesive soil and three cases in cohesionless soil. These cases are: for cohesive soil: Case I-cu (from) Bagnolet, III-cu Brent Cross and VI-cs Sabine. And for cohesionless soil: Case IX-cl Garston, X-cl Arkansas River and XIII-l Florida.
Logically and unfortunately these six cases do not cover the full spectrum of laterally loaded piles that can be thought of. Therefore, this research is only valid within a certain range. This range is given in table 3-4.

4 COMPARISON CALCULATIONS

This chapter gives the results of all calculations performed with the models on the six cases. Realize that the ultimate state models are not used in this comparison. The results of these calculations give insight into the accuracy of the models. First in paragraph 4.1, the structure of the calculations is given. In paragraph 4.2, the results of the calculations are presented and discussed. Finally, the results are evaluated in paragraph 4.3. The actual elaborations of all single calculations are not presented here. They are given in appendix C.

4.1 STRUCTURE OF CALCULATIONS

In appendix C, the calculations have been sorted per model. However, to compare the models and not the measurements, the results in the following paragraph have been ordered on measurement. All calculations are shown in table 4-1. From the table it can be seen that not all the calculations could be, or were executed.

It was already known that comparison on ultimate state models Blum and Brinch Hansen was not possible on the basis of measurements. This, because Blum can only calculate the deflections at the ultimate load and Brinch Hansen cannot calculate deflections at all. But also the CLM could not perform all calculations. This is due to two conditions of the field tests that have to fulfill the CLM-requirements. The piles in cases Bagnolet I and Florida had a too small length-diameter ratio. In the cases of Sabine and Garston the deformations were measured above the ground line. Furthermore, with the CLM it is only possible to calculate the deformations at the ground line. In the case of Florida, the calculation could not be performed with the NDM, because in Florida the soil was layered and the pile had an inconstant bending stiffness, two things which cannot be handled by the NDM. Calculations, which could not be performed, are marked with an "X" in the table.

Also with the method Broms not all calculations were done. After calculating the cases Arkansas River and Brent Cross, Broms proved to be very inaccurate and not capable of recalculating the deflections in all loading steps. It was decided not to continue with this model. See appendix C, chapter 4. The calculations which were not done with this model are marked with "ND". The remaining calculations which were performed are marked with a "*V*"

Model / *Case*	**Blum**	**Brinch Hansen**	**Broms**	**CLM**	**NDM**	**MSheet**	**MPile**	**Plaxis 3DF**
I-cu Bagnolet I	X	X	ND	X	*V*	*V*	*V*	*V*
I-cu Bagnolet II	X	X	ND	*V*	*V*	*V*	*V*	*V*
I-cu Bagnolet III	X	X	ND	*V*	*V*	*V*	*V*	*V*
III-cu Brent Cross	X	X	*V*	*V*	*V*	*V*	*V*	*V*
VI-cs Sabine	X	X	ND	X	*V*	*V*	*V*	*V*
IX-cl Garston	X	X	*ND*	*X*	*V*	*V*	*V*	*V*
X-cl Arkansas River	X	X	*V*	*V*	*V*	*V*	*V*	*V*
XIII-l Florida	X	X	ND	X	X	*V*	*V*	*V*

Table 4-1 Overview of calculations. "X" = Calculation not possible. "ND" = Calculation Not Done. "V" = Calculation performed.

4.2 RESULTS OF CALCULATIONS

As stated in the chapter 3 the six cases that have been evaluated, are chosen such that three of the cases have been executed in a cohesive soil and three of the cases in a cohesionless soil. The results are summarized per case. First, the three field tests in cohesive soil are evaluated. For each case, the calculated displacements are plotted versus the measured displacements. The closer a measured value is to the line x=y, the more precise the calculated value is. Then the different models can be compared. This is first visually done. If the models are compared visually, not only the closeness of the calculated displacement to the measured displacement can be taken into account, but also the shape of the curve and the relative accuracy for low and high loads. Low loads give small deflections and a miscalculation of say: 5mm can be considered as a larger error than a miscalculation of 5mm if a higher load is applied. In paragraph 4.3 the results are compared analytically.

4.2.1 Results cohesive soil

Here the three cases in cohesive soil are summarized. The first two cases, Bagnolet and Brent Cross, have been executed in unsaturated conditions. The third case, Sabine, has been executed in submerged conditions.

4.2.1.1 Case I-cu, Bagnolet

Graphs 4-1 to 4-3 on the following page show that in all three tests MPile predicted the measured displacement most accurate.

For test I, after MPile, the best result was generated by MSheet. It can be argued that the result generated by the NDM is more precise. However, MSheet generated the better results at higher loads. The CLM was not able at all to produce results in this situation since the pile was too short compared to its diameter.

For test II, MSheet, NDM and MPile approximated the deformations closely, MPile almost exactly. However, Plaxis and the CLM predicted deflections which were almost twice as large as the measured deflections.

For the third test, again MPile makes the closest approximation of the deflections, but is followed closely by Plaxis, NDM and MSheet. The NDM underestimated the deflections and the CLM overestimated the deflection. MPile predicts the deformations almost exactly.

The results are summarized in table 4-2.

Model	Bagnolet Test I	Bagnolet Test II	Bagnolet Test III	Bagnolet Total
CLM	NA	-	-	-
NDM	+	+	+	+
MSheet	+	+	+	+
MPile	+	+	+	+
Plaxis	-	-	+	-

Table 4-2 Comparison models Bagnolet total, on displacements

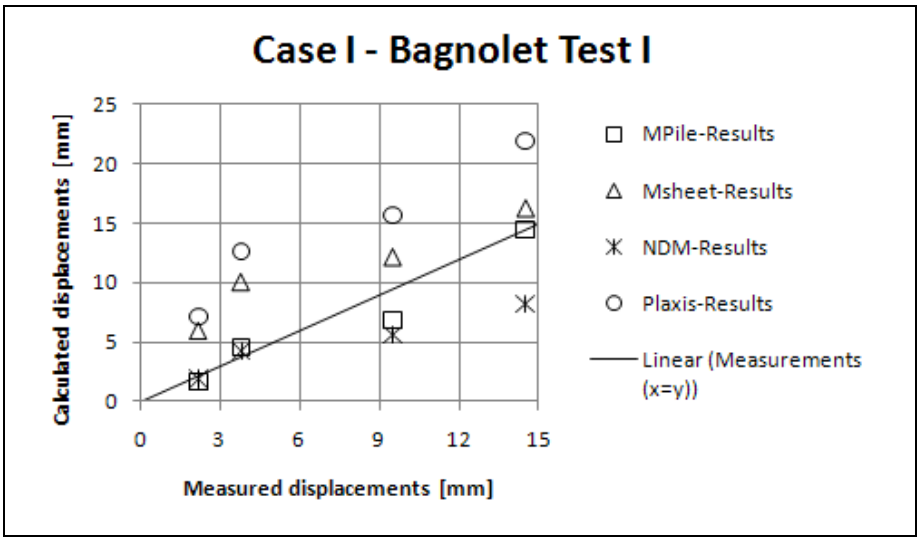

Graph 4-1 Comparison models Bagnolet, test I – Displacements

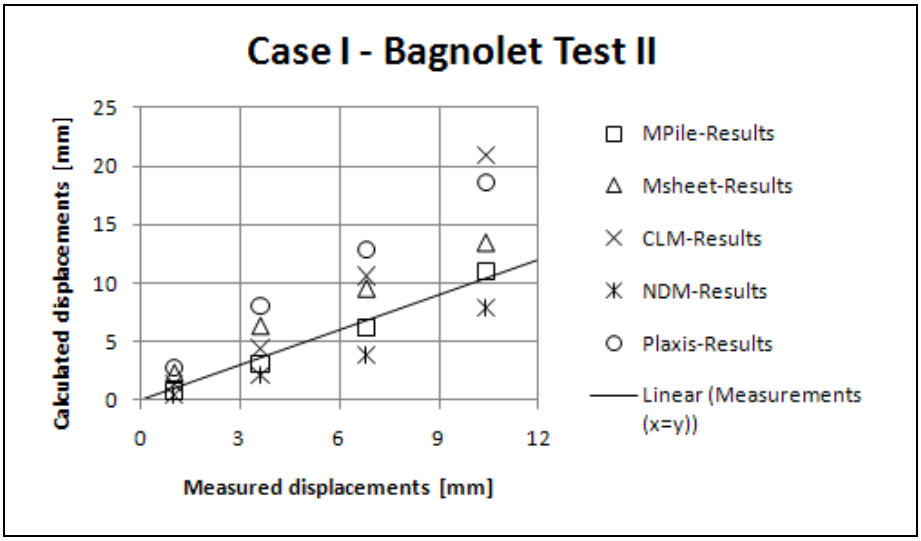

Graph 4-2 Comparison models Bagnolet, test II - Displacements

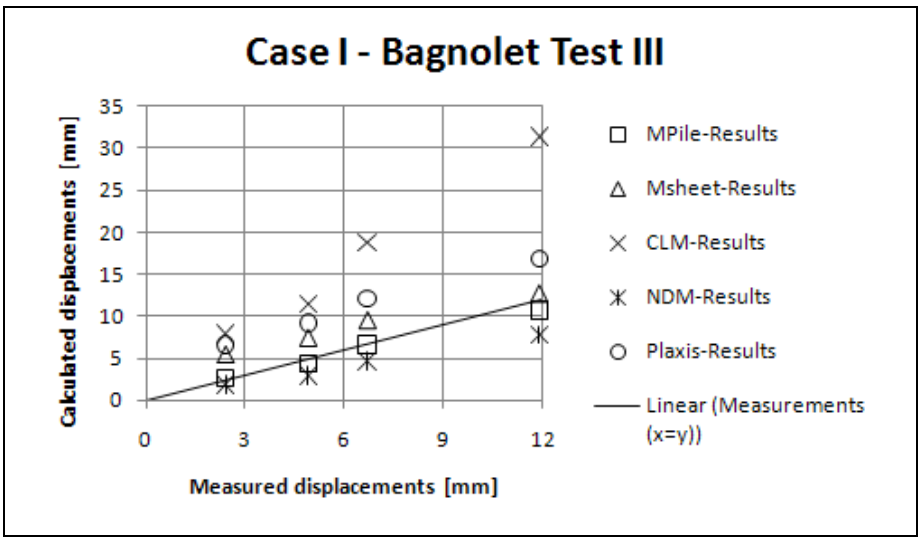

Graph 4-3 Comparison models Bagnolet, test III - Displacements

During the field test, also the maximum moments were measured. These moments have been calculated by the different models. The results are given in the graphs 4-4 to 4-6.
From the graphs it appears that all of the models predict the maximum occurring moment reasonably accurate. The exception is the CLM. For test I, the CLM was not able to calculate the maximum moment and for test three the moments were significantly more inaccurate than the other models. The results of the comparisons are given below. Plaxis was not used for calculation of the maximum moment. This decision is explained in paragraph 4.3.2.

Model	Bagnolet Test I	Bagnolet Test II	Bagnolet Test III	Bagnolet
CLM	NA	+	-	-
NDM	+	+	+	+
MSheet	+	+	+	+
MPile	+	+	+	+
Plaxis	NA	NA	NA	NA

Table 4-3 Comparison models Bagnolet, on maximum moments

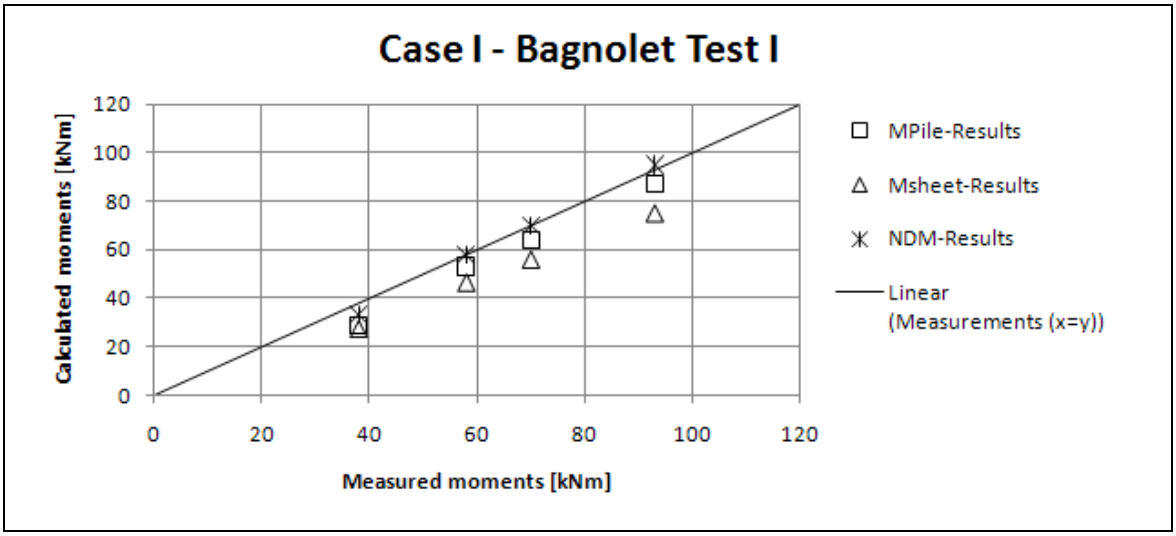

Graph 4-4 Comparison models Bagnolet, test I – Maximum moments

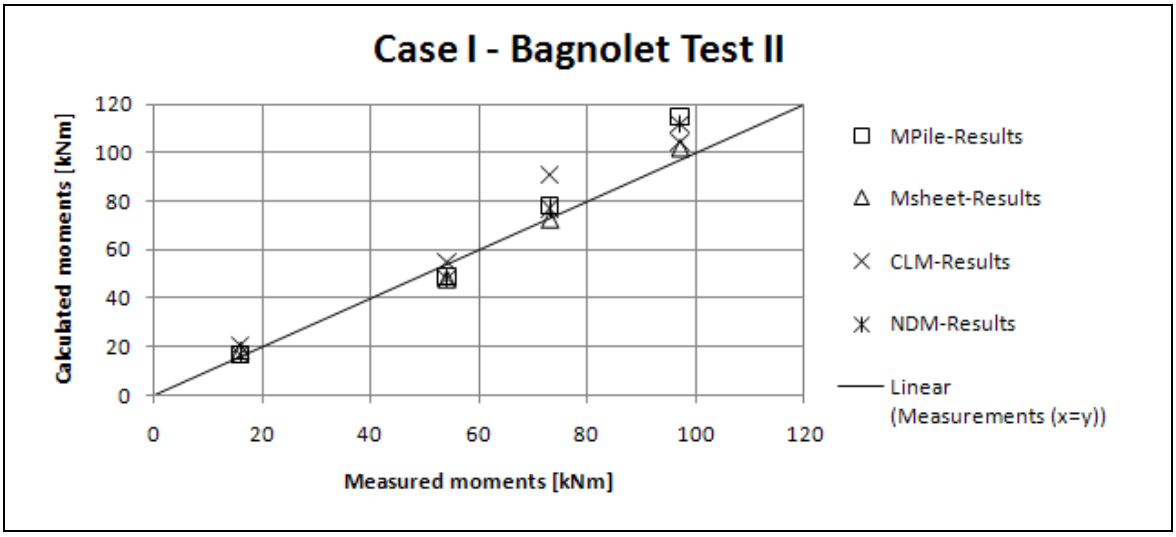

Graph 4-5 Comparison models Bagnolet, test II – Maximum moments

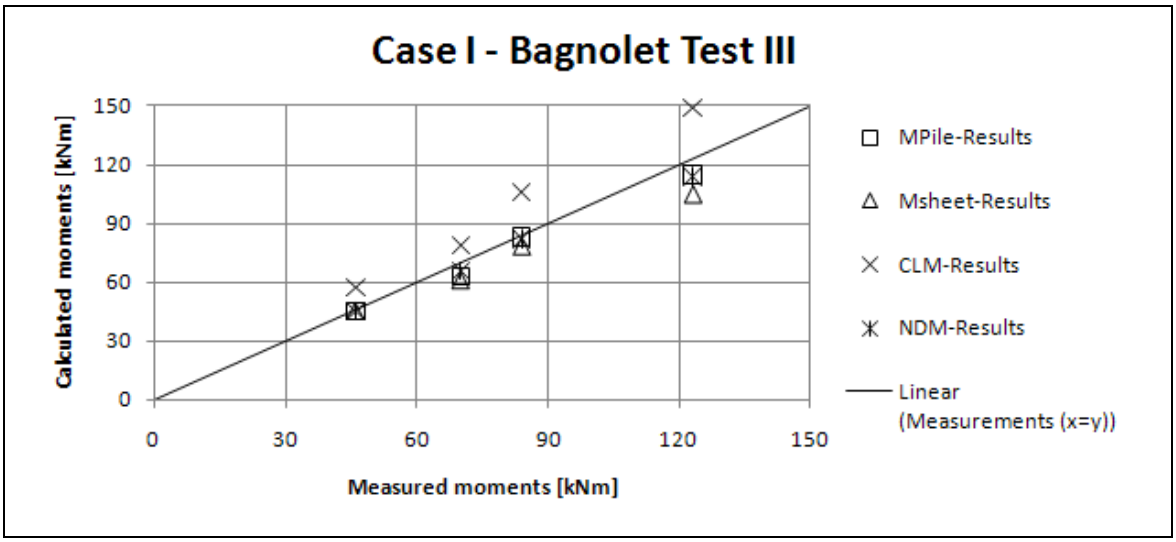

Graph 4-6 Comparison models Bagnolet, test III – Maximum moments

4.2.1.2 *Case III-cu, Brent Cross*

Graph 4-7 shows that the NDM calculation has the best fit with the measurements. This is based on the shape of the curve and the accuracy. The NDM is followed by the MSheet and MPile programs. The results of the Plaxis calculation overestimated the deflections, but it seems that the curve will not deviate further from the measurements for higher loads. The CLM was not applicable, since the pile-head deformations were measured.

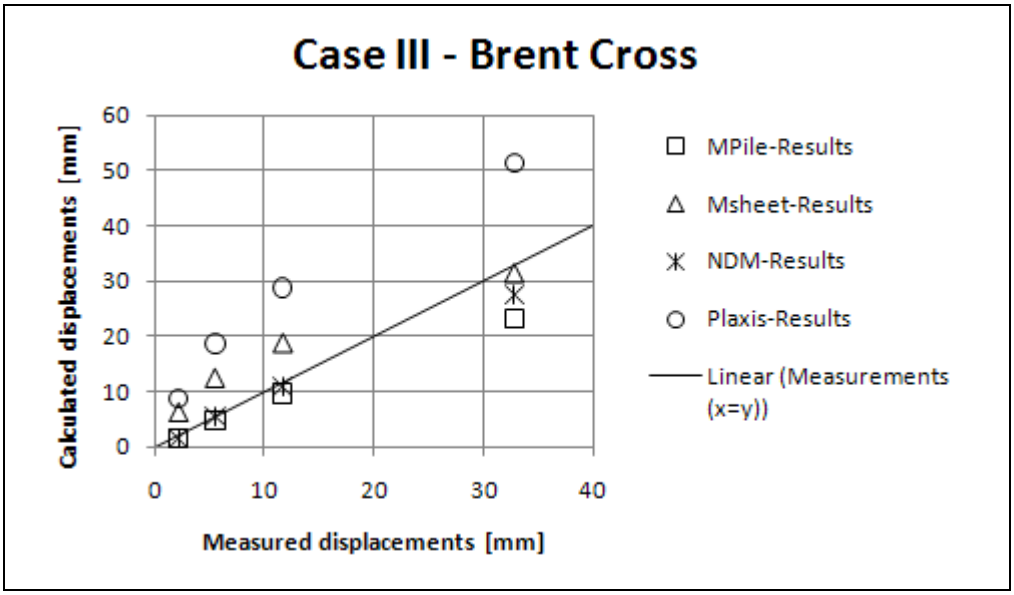

Graph 4-7 Comparison models Brent Cross – Displacements

4.2.1.3 *Case VI-cs, Sabine*

The models produced inconsistent results. This might be because only very little soil data was available. (Only one strength and one volumetric weight parameter.)

It is clear from graph 4-8 that the Plaxis calculation produced the most accurate results followed closely by MSheet. The NDM and MPile overestimated the displacements with almost a factor two. The CLM could not produce results for the two highest loads. The deflections became too large to be able to read them from the design graphs.

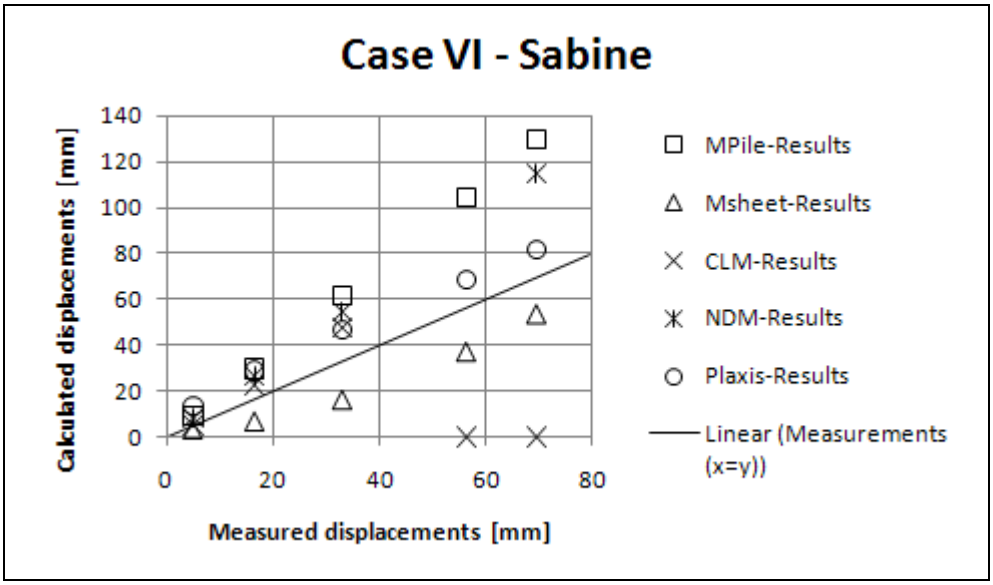

Graph 4-8 Comparison models Sabine – Displacements

When the maximum moments are considered, it can be concluded that the calculated moments do not deviate much from the measured moments. The CLM is the exception, since the maximum moment could not be calculated for the highest two loads.

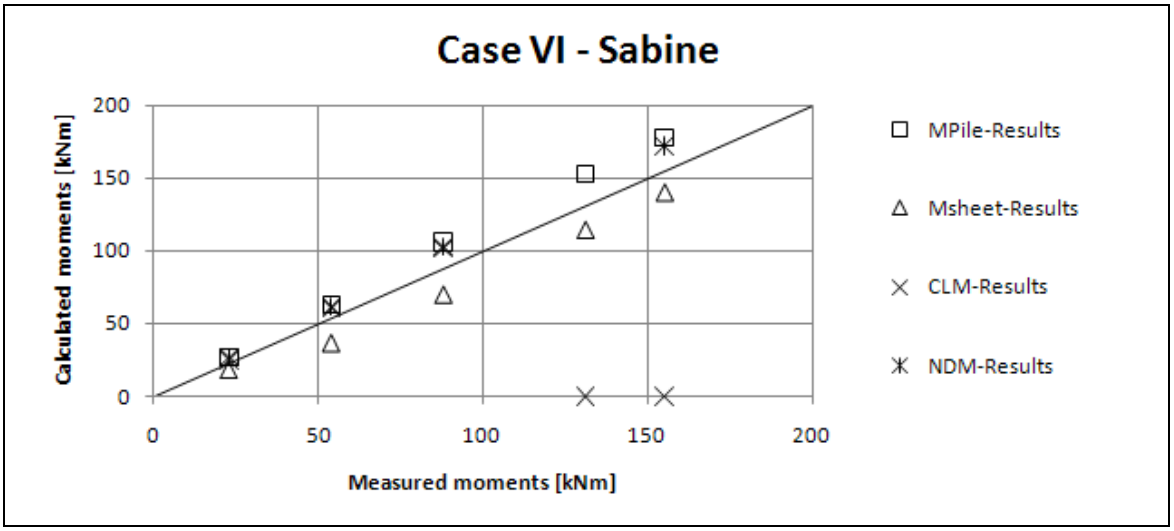

Graph 4-9 Comparison models Sabine – Maximum moments

4.2.2 Results cohesionless soil

Here the results of the three cases in cohesionless soil are summarized.

4.2.2.1 Case IX-cl, Garston

All calculation that could be executed returned fairly good results. The CLM was not applicable, since the pile-head deformations were measured. MSheet generated an almost perfect fit with the measurements. Plaxis overestimated the deflections, but did show a similar shape of the curve. MPile underestimated the deflections. The NDM results did not deviate a lot from the measurements; however the shape of the curve was totally different.

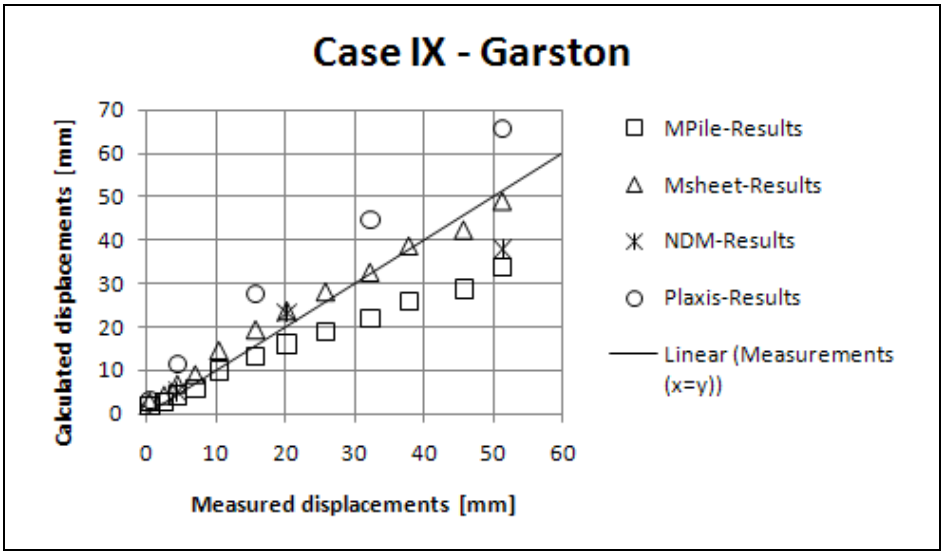

Graph 4-10 Comparison models Garston – Displacements

At Garston the maximum moments were also measured. These measurements are given in graph 4-11. Unfortunately, the maximum moment was only given for two loads. All the models returned similar results. The MSheet calculation was closest to the measurements. All of the calculations gave an underestimation of the maximum moment for the higher load.

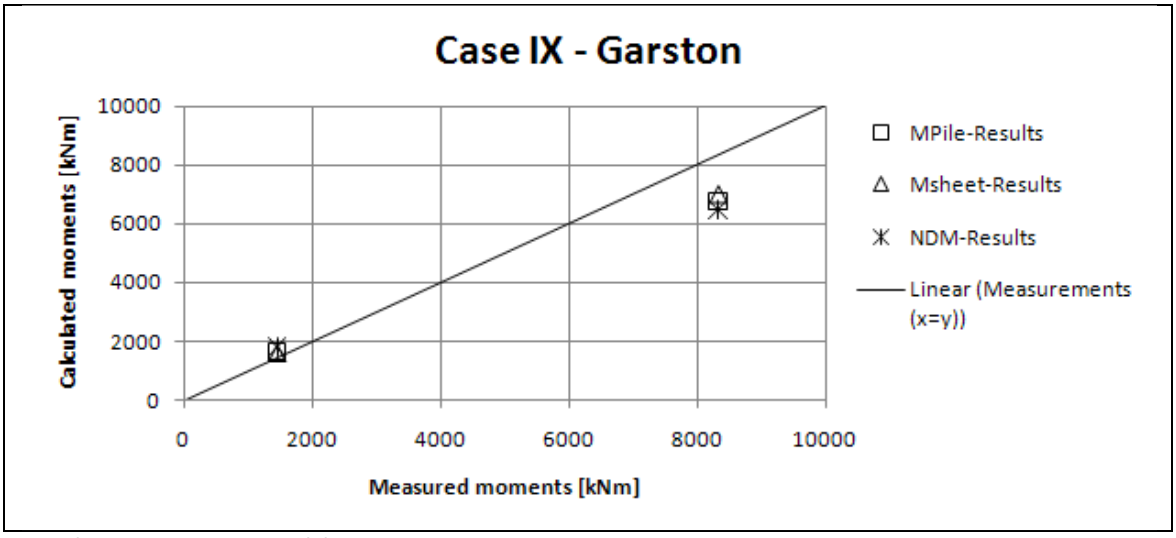

Graph 4-11 Comparison models Garston – Maximum moments

4.2.2.2 *Case X-cl, Arkansas River*

From graph 4-12, it can be seen that the NDM, Plaxis and MPile calculation predicted the deformations almost perfectly. The CLM and MSheet calculation overestimated the deformations by almost a factor two for the highest load.

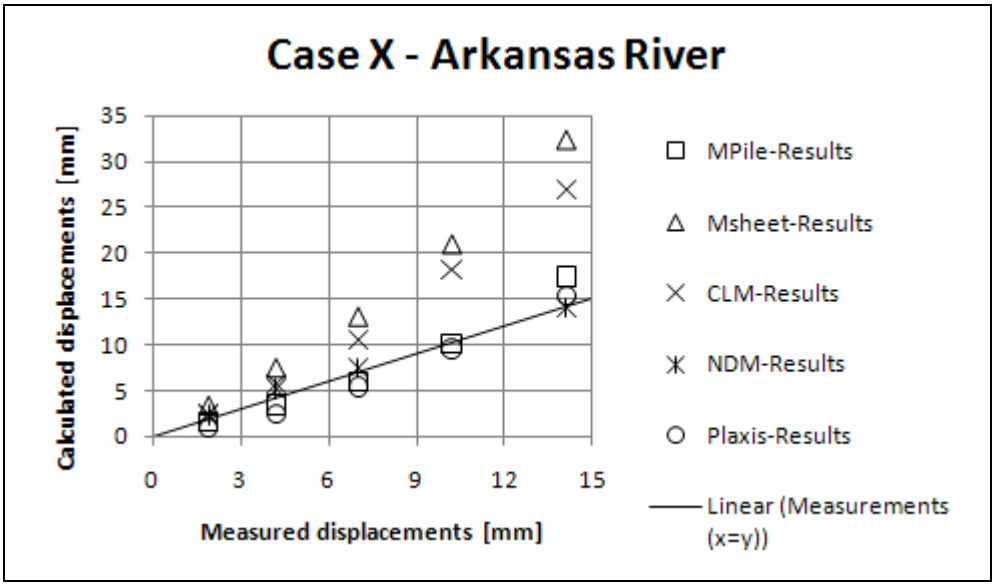

Graph 4-12 Comparison models Arkansas River – Displacements

4.2.2.3 *Case XIII-l, Florida*

In this case it was not possible to use the CLM and the NDM because of the layering of the soil and the changing stiffness over the length of the pile. From graph 4-13 it can be seen that the models which were allowed to be used returned results which were not close to the measurements. The reason for this is unclear. Because the calculation results of all previous cases are not as far off of the measurements as in this situation, it is likely that there is an error in the soil data or measurements.

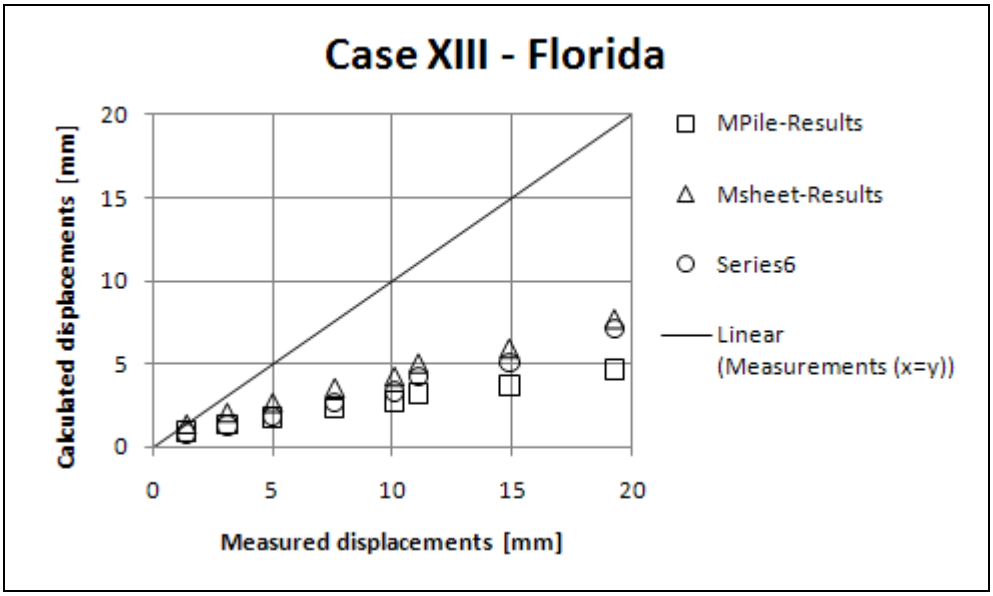

Graph 4-13 Comparison models Florida – Displacements

4.3 REMARKS ON PLAXIS

The attentive reader might have noticed that Plaxis was not used to its full capabilities. For cohesive soils the Mohr-Coulomb model was used instead of one of the advanced models. The maximum moments were not determined with Plaxis. This paragraph explains why these decisions were made

4.3.1 Why Mohr-Coulomb for cohesive soils?

In these special cases it was decided not to use the HS or HSSmall model in Plaxis. This was due to the fact that all cohesive layers were modeled with just an undrained shear strength and these layers therefore had to have an angle of internal friction of zero. The loads were of short duration, thus modeling of undrained behavior for clayey soils is recommendable.

If the angle of internal friction is chosen to be zero in the HS or HSSmall model, the soil stiffnesses will exclude their stress-dependency. This is assumed to be the reason why this resulted in excessive deformations at the ground line, which on their turn resulted in instability of the iteration process. The reason for the excluding of the stress-dependency can be explained if the following formulas are considered. In these formulas: cot(φ)=cos(φ)/sin(φ), if then φ=0, cot(φ) becomes infinite. Thus, if φ=0 is entered in the formulas below, then: $E_{50} = E_{50}^{ref}$ and $E_{ur} = E_{ur}^{ref}$.

$$E_{50} = E_{50}^{ref} \left(\frac{\sigma_3 + c \cot \varphi_p}{\sigma^{ref} + c \cot \varphi_p} \right)^m \qquad \textit{eq. 6.1}$$

$$E_{ur} = E_{ur}^{ref} \left(\frac{\sigma_3 + c \cot \varphi_p}{\sigma^{ref} + c \cot \varphi_p} \right)^m \qquad \textit{eq. 6.1}$$

This problem could have been solved by modeling the soil as c-φ-soil. Correlations exist which could have been used to model the clay with effective strength parameters based on the undrained shear strength of the soil.

However, a more practical solution was chosen. The Mohr-Coulomb model does not have the above described problems. The stress dependency can be approximated with the $E_{increment}$ option in the advanced soil parameter menu. This is no real stress-dependency, but a depth-dependency.

4.3.2 Why were the maximum moments not determined with Plaxis?

The maximum moments were not determined with Plaxis because this is a very tedious procedure. The recommended way to find the moments in the pile is by integrating the axial stresses. This is a time consuming procedure. The fact that the pile is not round but angular in Plaxis makes this procedure even more complicated. The determination of the maximum moments was because of the limited amount of time available not done.

Other ways of determining the moments are by differentiating the deformations of the pile over its length. This procedure was also not followed, because it is time consuming. Deformations have to be retrieved for each node around the pile for each load step. This is the time consuming part. Differentiation with help of, for instance, an excel calculation sheet is then an easy task.

4.4 REMARKS ON P-Y CURVES

Also some remarks on the methods which use p-y curves should be made. It is to be expected that all three methods, CLM, NDM and p-y analysis with MPile, generate similar accurate results. This is clearly not the case, see paragraph 4.4.1 for explanation. It should also be remarked that p-y analysis with the curves recommended by the API generate different results than p-y analysis with the method of Reese *et al.* The results of both curves are examined in the paragraph 4.4.2. Finally, in paragraph 4.4.3, some remarks are made on the soil types used in this comparison and other soil types which are less commonly encountered.

4.4.1 Why are the results of the three methods, which use p-y curves, significantly different?

The results of the CLM method differentiated most from the other methods and from the measurements. This was also noted by the developers of the method (Duncan, Evans, & Ooi, 1994). The differences occurred due to the crude assumptions, appendix A chapter 6, which had to be made. The assumptions did eliminate the use of a computer, but lots of possibilities were lost. Losing the layering of the soil is an important example of this.

The differences between the NDM-results and the p-y analysis with MPile differ less. However, there are differences. This is probably due to the different type of p-y curves which were used. This is examined further in the next paragraph.

4.4.2 How do the results generated with API-p-y analysis differ from Reese *et al.*-p-y analysis?

As this can only be examined if the two types of curves are used in the same model, some additional calculations have to be executed. For this the NDM was chosen since implementation of different curves is fairly simple with this method. The comparison has been executed on a case in cohesionless soil, Case X-cl Arkansas River, and in cohesive soil, Case III-cs, Brent Cross. The results of these calculations are respectively presented in chapter 6.5.3 and chapter 6.2.4 of Appendix C. It can be concluded that the curves of the API are more optimistic than the curves by Reese in the case of sand. In cohesive soils, the results are approximately equal.

This can be explained if the two types of p-y curves are plotted in the same graph, see figure 4-1. In both cases, the soil reaction by the API is stiffer. However, the curves in cohesionless soils differ a lot, whereas the curves in cohesive soils are approximately equal. The shapes of the curves thereby clearly explain the results found in the above described NDM calculations. This result was also found by L. Bekken (Bekken, 2009) who discovered that p-y curves by the API were stiffer than the p-y curves from the more realistic soil model Plaxis.

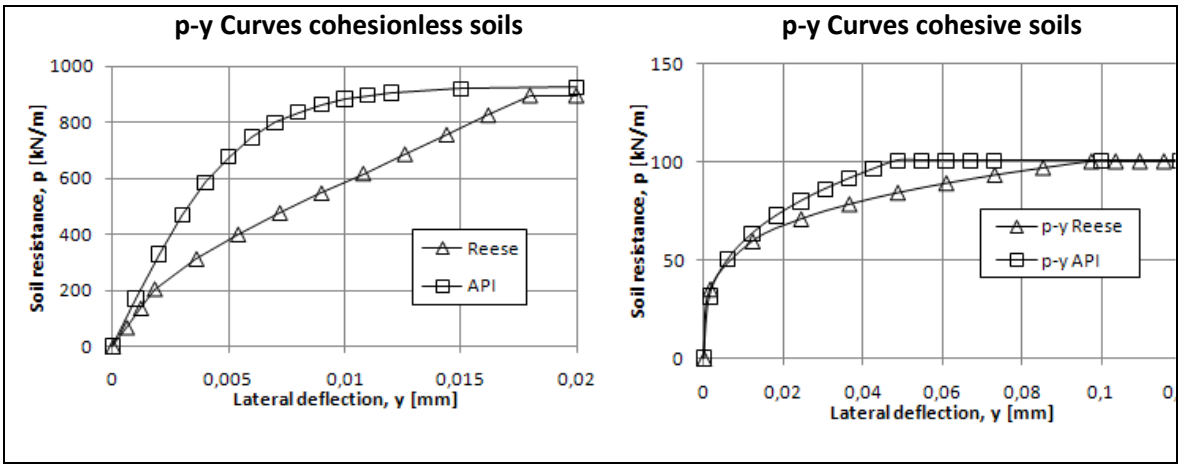

Figure 4-1 p-y Curves. The left graph represents the p-y curves in the cohesionless sand of Arkansas River on a depth of 3,36m. The graph on the right represents the p-y curves of Brent Cross at a depth of 0,86m.

4.4.3 Remarks on the use of p-y curves in Dutch soils in the context of this comparison

It is important to note that the comparative calculation which have been executed were good for the p-y curves which already exists. The soils in the cases either consisted of sand which could well be described with an angle of internal friction, or of clay which could well be modeled with an undrained shear strength. In practice however, it is not unlikely that soil types are found which cannot be classified that easily. These soils are preferred to be modeled as c-φ soils. Reese developed recommendations for these soils but assumed these soils to be cemented sands etc and not, for instance, sandy clay (Reese & Van Impe, 2001). Also it was found that no p-y curves for peaty soils are developed. Especially in undrained loading conditions, peat can contribute to the soil resistance. This research shall not continue on this subject since it is out of the scope, however, further research on this and development of new curves may be of great additional value to the practicability of p-y models like MPile.

4.5 EVALUATION OF RESULTS

With the results of all cases, the models can now be compared on accuracy. To do this all calculated deflections of a single model are plotted versus the measured values. This is done in one graph for all the cases. If then the smallest square method is applied to find the best linear fit through the origin of the graph, the slope of this best fit can be used as a measure on accuracy of the model. In the graph however, all the cases must be equally represented. This is accomplished by setting the maximum measured displacement of each separate case at the value of 1,0. The calculated displacements and other measured displacements are then recalculated to be proportional to this value of 1,0. This method produces graph 4-14.

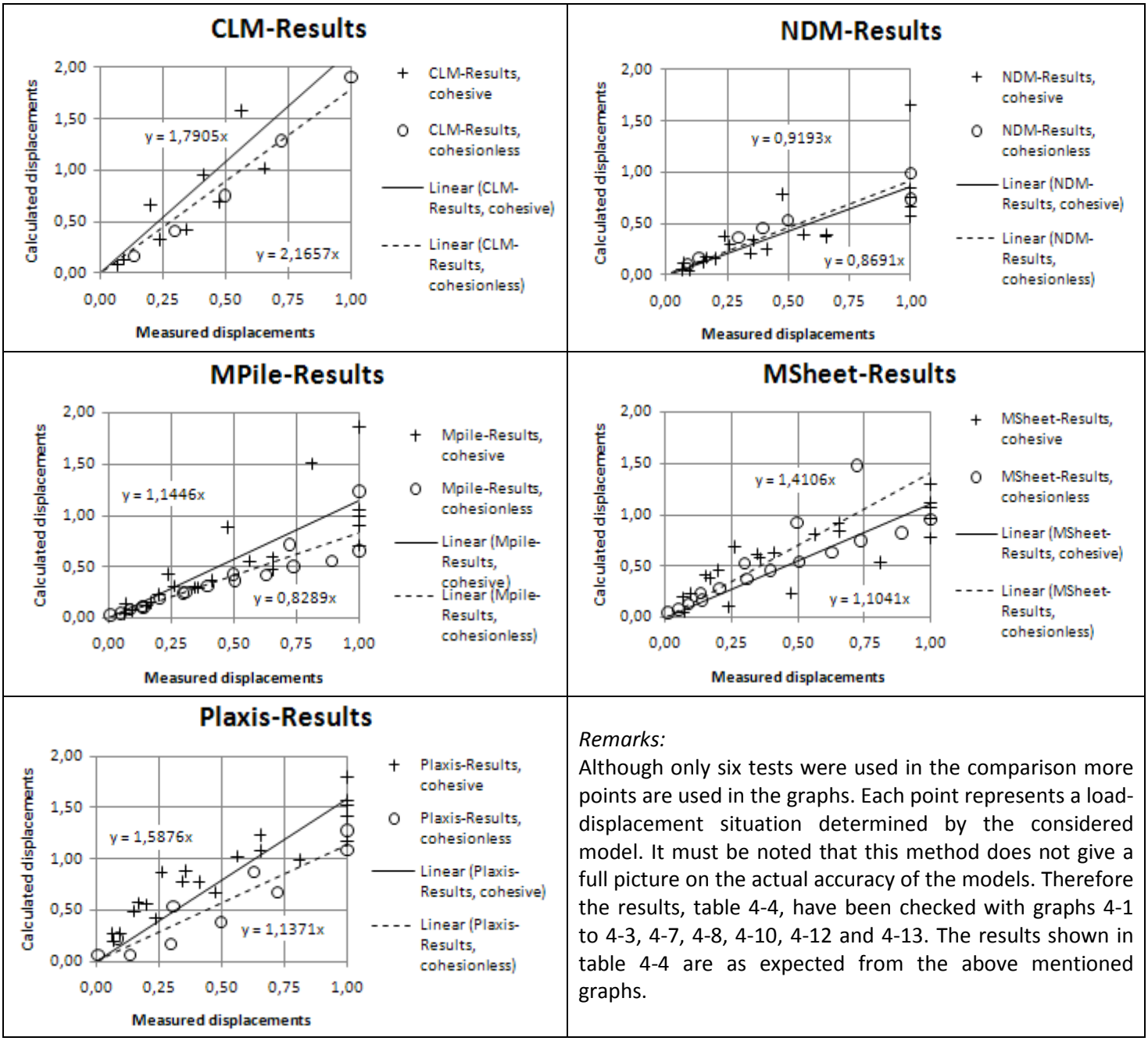

Remarks:
Although only six tests were used in the comparison more points are used in the graphs. Each point represents a load-displacement situation determined by the considered model. It must be noted that this method does not give a full picture on the actual accuracy of the models. Therefore the results, table 4-4, have been checked with graphs 4-1 to 4-3, 4-7, 4-8, 4-10, 4-12 and 4-13. The results shown in table 4-4 are as expected from the above mentioned graphs.

Graph 4-14 Accuracy of models

	CLM	NDM	MPile	MSheet	Plaxis
Cohesive	2,17	0,87	1,14	1,10	1,59
Cohesionless	1,79	0,92	0,83	1,41	1,14

Table 4-4 Summary of slopes of accuracy graphs

The results found in the graphs are summarized in table 4-4. The closer the slope of the best fit is to the value of 1,0, the more accurate the results of a model are. This way it can be seen that for cohesive soils the NDM, MPile and MSheet are the most accurate models. For cohesionless soils the NDM, MPile and Plaxis are most accurate. The CLM is the most inaccurate model for all soil types. The results found in table 4-4 are in line with the results which were obtained visually in paragraph 4.2.
Note, that in the graphs the results of the calculations of the case in Florida are not taken into account. It is shown in paragraph 4.2.2.3 that it is most likely that there is an error in the soil data or measurement in this case.
Also the model of Broms has not been compared to the other models. This is due to the fact that the results of the two calculations by Broms were very inaccurate and it was decided not to continue with this model. In chapter 4 of appendix C, the results of the calculations with Broms are given.

When the maximum moments are now considered; graphs 4-4, 4-5, 4-6, 4-9 and 4-11, it can be concluded that all the models predict the maximum moments quite accurately. Apparently, the calculated maximum moment is not very sensitive related to of the type of model.

With the accuracy of the models known, the models can be compared in a Multi Criteria Analysis. The Multi Criteria Analysis is presented in chapter 5.

5 MULTI CRITERIA ANALYSIS

A Multi Criteria Analysis, MCA, is a simple way to compare different alternatives on different grounds. The advantages of a MCA over informal judgment are that it is open and explicit, which means that the results and procedure can be checked and discussed. The approach of the MCA will be used here to compare the different models. Different criteria will be established on which the models can earn points (0 to 1). These criteria are described in paragraph 5.1. Then, in paragraph 5.1.4, the criteria will be given a different weight/multiplying factor to differentiate between important and less important criteria. In paragraph 5.2 the MCA is presented. In 5.3 the score accreditation of the models in the MCA are explained. Finally in 5.4 the results are evaluated.
(Department_for_communities_and_local_government, 2009)

5.1 CONSIDERED CRITERIA AND WEIGHT ACCREDITATION

Different alternatives, or in this thesis; different models, are compared on different criteria. It is important that all relevant criteria are established in such a way that the characteristics of the models can be taken into account. These characteristics can roughly be divided in three groups. These are: the *general characteristics*; practicability and common practice, the *theoretical characteristics*; what are the possibilities and limitations of a certain model and the *accuracy* of the model; how precise can a model predict the pile-soil behavior.
In the MCA, some criteria have been adopted even though there is not a strong relation with the problem of laterally loaded piles. This is done to let the MCA also be a practical guideline for engineers, if they want to select a model for their specific situation.

5.1.1 General Criteria

The general criteria are very important. These comprise the practicability and whether or not the model is commonly used in today's engineering practice. With practicability, the ease of use is meant. Is there a lot of geotechnical knowledge and experience required to use the model or is it a straightforward, "easy" model? The more "easy" a model is, the higher the score in the MCA will be, since these models are on this criterion more valuable than "harder" types of model. The other general criterion, common practice, has been taken in the MCA, since a model which is already used a lot has a huge advantage over a model with which nobody has real experience with.

5.1.2 Theoretical Criteria

There are a large number of theoretical criteria. Which situations can the model deal with? Different criteria have been established on model type, soil behavior/type, load types and pile types/behavior.
In *model type,* the design possibilities of the model are taken as criteria. Can the model design a pile in the serviceability limit state or in the ultimate limit state? Or, both?
The *soil* criteria, take into account the types of soil, which can be used in the model. These are cohesionless soil, cohesive soil and layered systems with both types of soil. But there are more soil criteria. These are on soil behavior. Can the model take the nonlinearity of the modulus of subgrade reaction into account? This criterion is called "nonlinear soil" in the MCA. And can

the model deal with time dependency, i.e. creep, or can it separate between drained and undrained behavior, or neither. The final criterion on soil is whether or not the model takes sloping surfaces into account.
There are also different types *loads* on which the model can score. A model must be able to deal with a lateral force at the top of the pile. But can it also handle a moment, an axial load, or cyclic loads. The more loading types a model can deal with, the higher the score.
Finally there are four *pile* criteria. Can the model deal with nonlinear behavior of the pile, i.e. is the model able to deal with a bending stiffness which is dependent on the rotation of the pile? This criterion is called nonlinear "M-κ". The second criterion is whether or not the pile may consist of different sections with a different bending stiffness. The third criterion is more a soil criterion than a pile criterion. However, the criterion depends on the pile diameter and is therefore mentioned among the pile criteria. The criterion is whether or not the shell factor of the model depends on the pile diameter. The last pile criterion is whether or not the model can be used to design pile-groups, because sometimes lateral loads have to be carried by multiple piles.

5.1.3 Accuracy Criteria

The accuracy criterion is obviously the preciseness with which the models can predict the deformations of the pile under lateral loads. The criterion is divided in accuracy in cohesive soils and cohesionless soils. This is done since in chapter 4 this deviation is also made, and to be able to better judge the different model compared to each other.

5.1.4 Weight Accreditation

Different weights have to be accredited to the different criteria. This, because some criteria are considered to be more important than other criteria. There are 17 theoretical criteria, two general criteria and two accuracy criteria.
All theoretical criteria are weighted with a factor of one. The more of these criteria the model fulfills the higher the score in the MCA. There are two exceptions. These are the theoretical criteria whether or not the model can deal with axial loads and cyclic loads. These two types of loads are not enclosed in the research objective. However, they are important to get insight in the possibilities of the models. The weights, these criteria are accredited with, are zero.
A model can now score a total of 15 points in the MCA on theoretical criteria. The weight which now has to be accredited to the general and accuracy criteria must be in balance with theoretical criteria. The weights of the general criteria add up to a total of eight points. The same is valid for the accuracy criteria. The theoretical criteria now possess approximately half and the general and accuracy approximately 1/4 of the total number of points.
The theoretical criteria are given twice as much weight as the other two groups of criteria, because the theoretical background of a model determines its possibilities and limitations. This is considered more important than accuracy, since it was also shown in chapter 4 that the differences between the models on this criterion are small. And more important than the general criteria which only show the possibilities the models have of being used in practice.
In summary the weight accreditation is given in table 5-1.

Criteria Groups	**Points Possible**	**Percentage**
General	8	26%
Theoretical	15	48%
Accuracy	8	26%
Total	31	100%

Table 5-1 Weights accredited to different criteria groups

5.2 MCA

	Blum	BH	Broms	CLM	NDM	MPile	MSheet	Plaxis	Factor	Blum	BH	Broms	CLM	NDM	MPile	MSheet	Plaxis
GENERAL																	
Common practice	1	0	1	0	0	1	1	1/2	4	4	0	4	0	0	4	4	2
Practicability	1	1	1/2	1/2	0	1	1	3/4	4	4	4	2	2	0	4	4	3
MODEL TYPE																	
Design pile on strength	1	1	1	1	1	1	1	1	1	1	1	1	1	1	1	1	1
Design pile on stiffness	0	0	1	1	1	1	1	1	1	0	0	1	1	1	1	1	1
SOIL																	
Clay	0	1	1	1	1	1	1	1	1	0	1	1	1	1	1	1	1
Sand	1	1	1	1	1	1	1	1	1	1	1	1	1	1	1	1	1
Layered	0	1	0	1	0	1	1	1	1	0	1	0	1	0	1	1	1
Nonlinear soil	0	0	0	1	1	1	1/2	1	1	0	0	0	1	1	1	1/2	1
Time dep.	0	0	0	0	0	0	0	1	1	0	0	0	0	0	0	0	1
Separates drained/undrained	0	0	0	0	1	1	1/2	1	1	0	0	0	0	1	1	1/2	1
Sloping surface	0	0	0	0	1	1	1/2	1	1	0	0	0	0	1	1	1/2	1
LOADS																	
Horizontal	1	1	1	1	1	1	1	1	1	1	1	1	1	1	1	1	1
Moment	1	1	1	1	1	1	1	1	1	1	1	1	1	1	1	1	1
Axial	0	0	0	0	0	1	0	1	0	0	0	0	0	0	0	0	0
Cyclic	0	0	0	0	1	1	1/2	1	0	0	0	0	0	0	0	0	0
PILE																	
Nonlinear M-κ	0	0	0	0	0	0	0	1	1	0	0	0	0	0	0	0	1
Not constant EI	0	1	0	0	0	1	1	1	1	0	1	0	0	0	1	1	1
Shell factor dependent pile diameter	0	1	0	0	0	0	1	1	1	0	1	0	0	0	0	1	1
Pile Groups	0	0	0	0	0	1	0	1	1	0	0	0	0	0	1	0	1
ACCURACY																	
Cohesionless soil	NA	NA	0	1/4	1	3/4	1/2	1	4	NA	NA	0	1	4	3	2	4
Cohesive soil	NA	NA	0	0	3/4	1	1	1/2	4	NA	NA	0	0	3	4	4	2
									SUM	12	12	12	11	16	27	24,5	26

5.3 MCA, INPUT EXPLAINED

In this paragraph the input of the MCA in paragraph 5.2 is explained. This is done to explain the method of reasoning which was used to get to the values as they are presented in the table. The explanations are sorted in the three main criteria groups: General criteria, Theoretical criteria and Accuracy criteria.

5.3.1 General criteria

Common Practice: The models Brinch Hansen, CLM and NDM are nowadays not used in daily practice. Therefore they get here 0,0 points on a 0,0 to 1,0 scale. On the other hand the models Blum, Broms (internationally), MSheet and MPile are used a lot. Of these models Blum and MSheet are commonly used in the Netherlands. These models score 1 on this criteria. Plaxis is also used a lot in practice, however not for single laterally loaded piles. Therefore the model scores 1/2.

Practicability: Models which can easily be used with a computer received a score of 1. To these models belong Blum (Excel), Brinch Hansen (Excel), MPile and MSheet. The models score 1/2, if graphs have manually to be read; Broms and CLM. The NDM received zero points, because first p-y curves have to be established, then multiple graphs have to be read and an iterative procedure has to be followed. Plaxis is an exception. This model is basically a computer model and thus requires no manual calculation of the user. However the calculation time is considerably longer that with the other models and lots of soil parameters are required. These have to be examined with laboratory tests or estimated with correlations. Therefore Plaxis scores 3/4.

5.3.2 Theoretical criteria

Design on pile strength: It is possible to perform a ultimate limit state calculation with all of the models.

Design on pile stiffness: It is not possible to execute a serviceability limit state calculation with the models Blum and Brinch Hansen. This is possible with all other models.

Clay: Blum was originally not designed to use the influence of cohesion in the calculation. The other models can deal with cohesive soils.

Sand: All the models can perform pile designs in cohesionless soils.

Layered: Models which are developed only for homogeneous soils are Blum, Broms and the NDM. These models score 0. The other models which do allow layered soils score 1.

Nonlinear soil: When deflections are considered, Blum and Brinch Hansen score 0, because these are ultimate state models. Broms also scores 0, because it assumes a linear relation between load and deflection between 0,3 and 0,5 times the ultimate load. MSheet scores 1/2, because the relation is bilinear and therefore can be considered neither linear nor nonlinear. The other models do contain nonlinear soil behavior.

Time dependency: The only model which can include time dependency, or creep, is Plaxis. Plaxis therefore scores 1 and the other models 0.

Separates Drained/Undrained: Models which can make this difference are models which use p-y curves, except the CLM. The ultimate load methods and Broms cannot make this difference. The modulus of subgrade reaction and shear strength in MSheet can be altered to obtain the undrained behavior. This is therefore no real model characteristic. MSheet scores 1/2. Plaxis can also differentiate between drained and undrained behavior.

Sloping surface: A sloping surface can be taken into account by models where p-y curves are used, except the CLM. The ultimate load methods and Broms cannot model this situation. The modulus of subgrade reaction in MSheet can be altered to obtain the behavior with a sloping

surface. This is therefore no real model characteristic. MSheet scores 1/2. Plaxis 3D can handle this situation and scores 1.
Horizontal load: A model which cannot deal with a lateral load is not usable in this research. All models score 1.
Moment: All models can deal with moments at the mud line. A moment is a logical consequence if a lateral load is applied at some distance above the surface. All models score 1.
Axial load: Not all models can deal with both lateral and axial loads. Models which can deal with this situation are MPile and Plaxis and score 1. All other models score 0.
Cyclic load: Cyclic loading behavior can be implemented in methods which use the p-y curves, except the CLM and score 1. Furthermore it is possible in MSheet to manually alternate the stiffnesses. This is therefore no real model characteristic. MSheet scores 1/2. Plaxis can handle this type of loading and scores 1.
Nonlinear M-κ: This extra complexity can only be implemented in Plaxis. Plaxis scores 1, the other models 0.
Not constant EI: Pile that consists of different sections with different bending stiffnesses can only be designed with MPile, MSheet, Plaxis and Brinch Hansen. These models score 1. The other models 0.
Shell factor dependent on diameter: In most models the shell factor is constant regardless of the pile diameter. The exception is Plaxis, because of the finite element character. Plaxis scores 1, the other 0. The other exceptions are Ménard and Brinch Hansen. Here the ultimate soil resistance and respectively the modulus of subgrade reaction are diameter dependent.
Pile Groups: MPile and Plaxis are the only two models which can model pile-soil-pile behavior. These models therefore score 1, the other models score 0.

5.3.3 Accuracy criteria

The accuracy criteria are determined on a different way than the above criteria. Here the results of chapter 4 are used. The more a calculation result differs from the measurements the lower the score will be. The criteria for the score accreditation are as shown in table 5-2.
The results in table 4-4 can be seen as the percentage the results differ from the actual measurement. The criteria are chosen in such a way that the model scores 0 if the model predicts a deflection which is approximately twice (>180%), or half (<60%) the measured deflection. This automatically leads to the scores described in table 5-2. The determination of the scores can than easily been seen in table 5-3 to 5-5. First the slopes, determined by the smallest square method, are recalculated to percentages. Then the on the basis of these percentages, the scores are accredited. The scores of table 5-5 are then implanted in the MCA.

Score, if:	Criteria
0	60%>S>180%
1/4	60%<S<180%
1/2	70%<S<160%
3/4	80%<S<140%
1	90%<S<120%

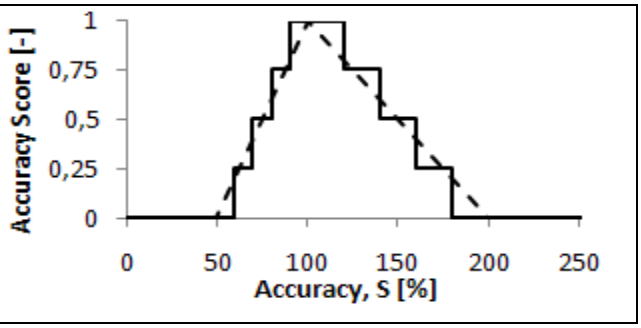

Table 5-2 Scores on accuracy both in tabular as in graphical form. "S" is the value of accuracy as determined in table 5-4

	MPile	MSheet	CLM	NDM	Plaxis
cohesive	1,14	1,10	2,17	0,87	1,59
cohesionless	0,83	1,41	1,79	0,92	1,14

Table 5-3 Accuracy of models. A value of 1,00 means a perfect fit for the average of all recalculated cases.

	MPile	MSheet	CLM	NDM	Plaxis
cohesive	114	110	217	87	159
cohesionless	83	141	179	92	114

Table 5-4 Accuracy recalculated as percentage

	MPile	MSheet	CLM	NDM	Plaxis
cohesive	1,0	1,0	0,0	3/4	1/2
cohesionless	3/4	1/2	1/4	1,0	1,0

Table 5-5 Scores of models determined by combining tables 5-2 and 5-4

5.4 EVALUATION OF MCA

If the results of the MCA are considered merely on scores, it can be seen that MPile is the best model, graph 5-1. However, ***the final scores of the MCA should not be considered without the MCA itself***. The MCA places the results in a context. Therefore, MPile, the highest scoring model, is not necessarily the best model. Below, the results are discussed.

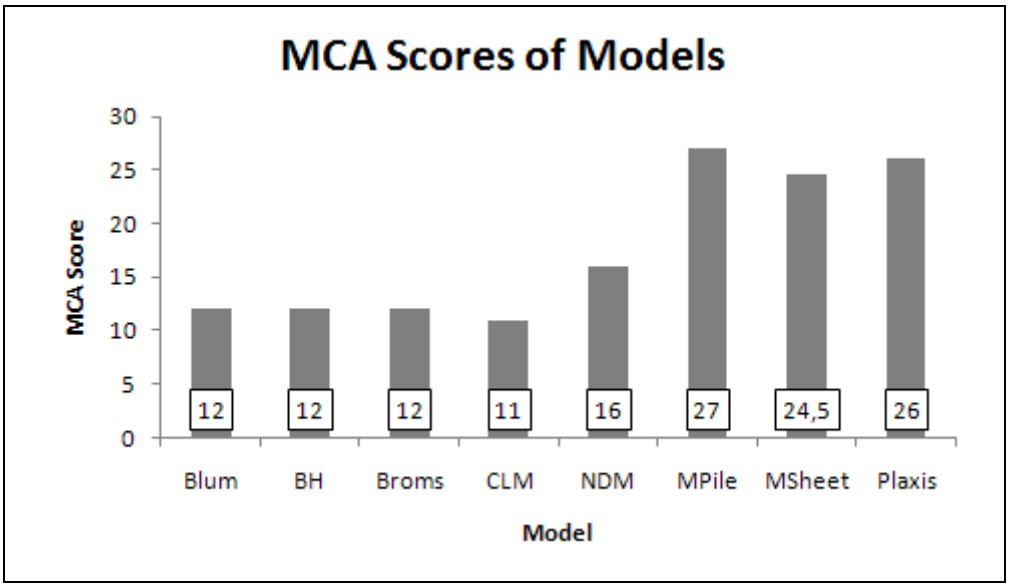

Graph 5-1 Graphical presentation of MCA results

To evaluate the MCA the ultimate state models Blum and Brinch Hansen have to be considered first. These models have been unfairly judged since they could not score points on accuracy. Thus the scores of these two models should be considered lightly. However, it can be seen that the model of Brinch Hansen has a considerable more complete theoretical background than Blum, but is not used in practice. These two even out, resulting in approximately equal scores for both models.

Now the graphical-analytical models Broms and the CLM are considered. They both have low scores in the MCA. This is due to the limited possibilities of both models and they were both

inaccurate in predicting the deformations. Since the CLM is based on p-y analyses it does have a more sound theoretical background than Broms. However, the model is not frequently used in practice. Broms has fewer possibilities, but is used in practice internationally.

The NDM is like the CLM and Broms a graphical-analytical method, but must be mentioned separately when the MCA is considered. The results of the method were very accurate. Of course, the basis of this method is the p-y curve and gives the NDM a good theoretical background. The assumptions on the model however, do limit the possibilities a lot compared to real p-y analysis. It must be remarked that the NDM in this research used p-y curves recommended by Reese and Matlock, where the curves recommended by the API are used by MPile. The NDM scores no points on the general criteria, since the model is time consuming and complicated. Because of the high score on accuracy and slightly more possibilities, the NDM scores higher than the CLM, Broms, Brinch Hansen and Blum. It must be noted that most of the considered cases were almost “tailor made” for the NDM, since the soil profiles could easily be modeled as homogeneous.

Finally, the three computer models are considered. The MCA scores of these three models are much higher than the scores of the other models. The models have high scores on common practice, practicability and accuracy. Furthermore, the theoretical background of these models and their possibilities exceed the others. Between the three models, MPile, MSheet and Plaxis there are some differences resulting from the MCA which have to be considered.
Plaxis scores fewer points on the general criteria than MPile and MSheet. This is due to higher complexity of the model and the longer calculation time. However, if the theory and possibilities of the models are elaborated, it is Plaxis which has the higher scores. With Plaxis it is possible to contemplate complex three dimensional situations, time dependency and all different types of loads and load combinations. The spring models MPile and MSheet basically have the same possibilities, except that MPile is capable of analyzing the pile-soil-pile behavior and axial loading. The main difference of MPile and MSheet is the spring. MPile uses nonlinear springs and MSheet bilinear springs.
Looking at accuracy, MPile and MSheet are both accurate for cohesive soils. Plaxis is less accurate for cohesive soils but most accurate for cohesionless soils. MPile is also very accurate for cohesionless soils, but less accurate than Plaxis. MSheet is least accurate for cohesionless soils. Note that, although one model is more precise that the other, all three models are quite accurate and that hard statements on the most accurate model cannot be made, because of the little amount of field tests which have been used.

6 ELABORATIONS ON BLUM

The use of Blum is very simple and so is modifying the model. Therefore, it is not strange that four different variations of the model were found in literature and engineering practice. The results of these models differ from each other. The differences and similarities are of these variations are therefore important to be examined.

6.1 VERSIONS OF BLUM

In this paragraph the four versions of Blum are described on the basis of several important model characteristics, compared to the original version of Blum.

6.1.1 Original Blum

Original Blum is the method developed by Blum in 1932 without modifications. (Blum, 1932)
The basic structure and assumptions behind this method are stated in chapter 1 of appendix A. The main assumptions of this method are that the soil is homogeneous and that the soil can be described with only the total volumetric weight and angle of internal friction. The other assumption is that the pile is fixed against lateral deflection at a certain point , t_0, below the soil surface. The bending moment at this point is assumed to be zero. A lateral (point-)load is imposed here to require balance between the horizontal load and soil resistance. Since a point load on a soil surface cannot exists, because the stresses are infinite, Blum states that an additional length of 20% of the penetration depth of the pile is enough to sustain the point load.

6.1.2 Blum according to the former version of the Spundwand-Handbuch Berechnung

The former Spundwand-Handbuch from 1977, states that the method of Blum was found to be on the conservative side. Therefore the method was adapted. (Lupnitz, 1977)
The adoptions were small, but did change the results. The effective volumetric weight is used instead of the total volumetric weight. And finally, the additional length of 20% was considered to be unnecessary as long as wall friction was not taken into account. Thus, the theoretical penetration depth is now equal to the real penetration depth.

6.1.3 Blum according to the current version of the Spundwand-Handbuch Berechnung

New insights and rapid development of computers, a new variation of Blum was developed. (Lupnitz & al., 2007)
It was desired to implement layered systems, wall friction and cohesive layers into the model. The soil pressures by Blum remained unaltered, however passive earth pressure coefficients are retrieved from the DIN 4085 (2002). Also the implementation of cohesive soils and the effective volumetric weight of the soil are now used. Introducing wall friction of (2/3)φ and layered soils, the additional length of 20% is no longer valid. Situations are thinkable that the soil resistance at the theoretical penetration depth is very low compared to the layers above this point. Thus, an entirely new calculation method was developed. The soil resistance at the theoretical penetration depth has to be determined in kN per meter of pile length. Then, to fulfill the requirement of horizontal balance, the soil resistance has to work over a certain pile length. The method stated that half of this resistance works above the theoretical penetration

depth and half of it below. This method is therefore based on analytics and horizontal balance. Finally, it is important to realize that the influence of the diameter of the pile is taken into account.

6.1.4 Blum used in practice

All this recommendations leaded to several spreadsheets to ease the work of engineers. These sheets are still widely used in practice because of the quick results/designs. One frequently used sheet has a somewhat different approach on Blum.
The sheet is used as follows. The earth pressure coefficient is determined according to the CUR166 and wall friction can be taken into account. The effective unit weight of the soil is used. Layered systems are also possible, however cohesive soils have to be modeled with a friction angle in both drained and undrained situations. Since the sheet was found to be on the optimistic side, wall friction has to be taken into account for 50%, or (1/3)φ. After the sheet determined the theoretical penetration depth, the real penetration depth is found by adding an additional length of 20% to the theoretical penetration depth.

6.1.5 Summary of methods Blum

In table 6-1 the four methods of Blum are compared on their most important characteristics. Since the current version of the SWHB and the version used in practice use totally different passive earth pressure coefficients, it is difficult to say if it is justified to refer to this methods as Blum.

Model / Properties	Original Blum	Blum SWHB 1977	Blum SWHB 2007	BLUM Practice
Volumetric weight soil	Total	Effective	Effective	Effective
Passive earth pressure coefficient	$\tan^2(45+\varphi/2)$	$\tan^2(45+\varphi/2)$	According to DIN4085 (2002)	According to CUR166
Penetration depth, t	$t=1,2t_0$	$t=t_0$	t Is found by means of analytics and horizontal balance	$t=1,2t_0$
Wall friction	No	No	Yes	Yes

Table 6-1 Summary of different variations of Blum on important characteristics of which they differ, SWHB stands for Spundwand-Handbuch

6.2 CALCULATIONS

To compare Blum, a fictive subsurface is made up. In this soil a pile is placed with a fictive diameter. The length of the pile is then calculated with all four versions of Blum for increasing friction angle of the soil. This way, statements can be made on how conservative or progressive each variation of Blum is compared to the others.

6.2.1 Situation

The soil consists of one homogeneous layer of cohesionless sand. The friction angle lies between 25^o and 35^o. The volumetric weight is $20kN/m^3$ and the wall friction is 2/3 of the friction angle with a limit of 20^o. The water table is located above the ground line and the point of application of the lateral load of 3000kN is ten meters above the ground line. The pile has a diameter of 1,5m.

6.2.2 Calculations

To design the pile with Blum the passive earth pressure has to be determined. Blum originally proposed for this the formula $\lambda_p = \tan^2(45+\varphi/2)$. This gives a value of $\lambda_p = 3{,}0$, if $\varphi=30^o$. The version of Blum which incorporates wall friction uses formula 6.1.

$$K_p = \frac{cos^2(\varphi)}{\left[1+\sqrt{\frac{\sin(\varphi-\delta)\sin(\varphi+\beta)}{\cos(-\delta)\cos(\beta)}}\right]^2} \qquad \textit{eq. 6.1}$$

This formula gives a value of $K_p = 5{,}737$, if: $\delta=20^o$ and $K_p = 3{,}0$, if: $\delta=0^o$. Logically it can be expected that a higher value K_p will lead to shorter pile lengths. β In this formula represents the slope of the surface. In the considered situation sloping surfaces are not considered.

The calculations are performed according to the different sources where the different variations of Blum were found. The references are stated in paragraphs 6.1.1 to 6.1.4.

6.2.3 Results

The results of the calculations by Blum are presented in graph 6-1. The results are remarkable. The former version of the Spundwand-Handbuch stated that Blum was too conservative. However, the variation on Blum suggested by that version of the Spundwand-Handbuch is even more conservative. The origin of this contradiction may be explained by the use of the volumetric weight. The original Blum uses the total volumetric weight in its calculations. The SWHB uses the effective volumetric weight. The difference in soil resistance f_w then becomes almost a factor two. The influence of this is huge. This can clearly be seen from the soil resistance in graph 6-2. The total soil resistance calculated according to the former version of the SWHB is half the soil resistance of the soil resistance according to Blum.
Furthermore, it can be seen in graph 6-1 that the current version of the SWHB is the most conservative method. This is due to the calculation method of the additional penetration depth. It can be seen that for higher friction angles, the method becomes less conservative.
From graph 6-1 it can be seen that for sandy soils ($\varphi \geq 30^o$) all models generate results within a margin of 10%.

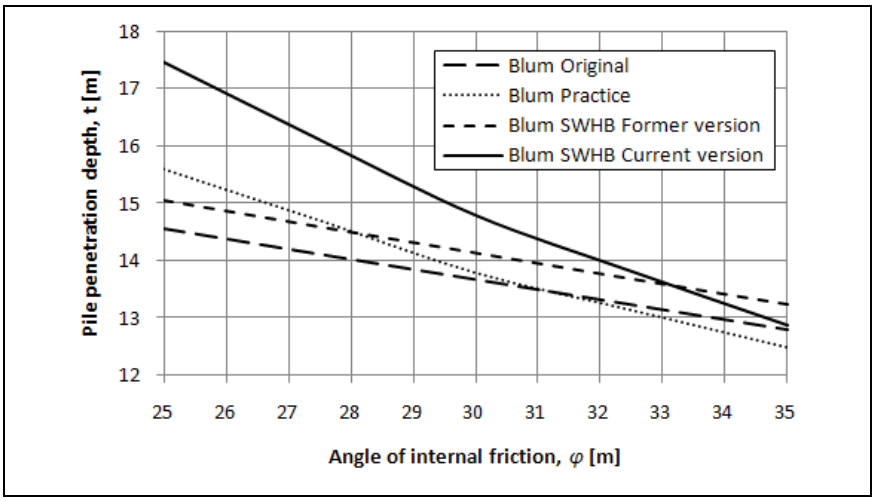

Graph 6-1 Results of Blum calculations for different angles of internal friction

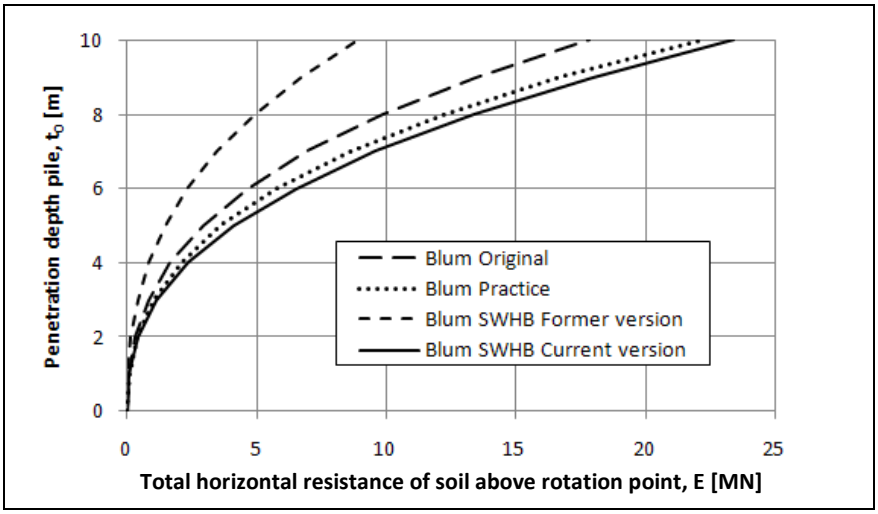

Graph 6-2 Horizontal resistance of piles depending on the theoretical penetration depth, t0, of a pile with diameter = 1,5m, in a soil with φ = 35°, δ=2φ/3, γ=20kN/m³ and γ'=10kN/m³. The load is the resultant load of the soil resistance, which works over the pile length above the rotation point.

6.3 EVALUATION ON BLUM

Many versions of Blum exist. Of these versions the method proposed by the current version of the Spundwand-Handbuch Berechnung is most complete and theoretical just. If an engineer wishes to use Blum, this is the method to use. The method is already used in practice, however note that the additional length should not be determined by multiplying the theoretical penetration depth with 1,2, but should be found by horizontal balance as suggested by the current version of the SWHB. If another version of Blum is chosen, note that the soil must be cohesionless and homogeneous.

Remarkable is that the former version of the SWHB proposed an alternative method of Blum, because Blum was found to be too conservative. The alternative version turned out to be even more conservative. From this it can be concluded that the use of the right volumetric weight is very important. Original Blum uses the total volumetric weight, whereas the former version of the SWHB uses the effective volumetric weight. Since the old version of the SWHB has already been replaced, it is unlikely that this version will frequently be used.

7 CONCLUSIONS AND RECOMMENDATIONS

This chapter will consist of three parts. The first part, paragraph 7.1, will give the conclusions of the calculations and the MCA. Paragraph 7.2 will represent the main objective of this research, namely the recommendations on which model to use in which situation for the design of laterally loaded piles. Paragraph 7.3 will present recommendation for further research on this subject.

7.1 MAIN CONCLUSIONS

Geotechnical software packages, mass-spring models and finite element analyses, are more complete and more accurate models than manual methods or graphical-analytical methods.
This can clearly be seen in the MCA. MPile, MSheet and Plaxis score much higher points on these criteria. However, only on practicability the software packages are equaled by the manual methods. This, because these methods have been, or can be, implemented in excel sheets. It must be remarked that the accuracy of the three software packages lies very close to each other. Therefore, on this number of considered cases, it is not possible to make statements on which of the three models is most accurate.

Ultimate state models cannot be compared with other models on the basis of field tests.
This is impossible, because the ultimate state models, Blum and Brinch Hansen, cannot calculate deformations under working loads and during the field tests the piles were not loaded up to failure of the pile or soil. It is noted, that assumptions can be made to make it possible to calculate deflections with both of the models. But, since this procedure is an adaption of the model, this is not done for this comparison.

Broms and the Characteristic Load Method are not appropriate models to design laterally loaded piles.
The methods are unpractical and inaccurate. This clearly follows from the MCA.

The nondimensional method is a good model, yet too unpractical.
The results of the NDM are accurate. However, the model is very tedious and time consuming and therefore too unpractical. Furthermore, it must be remarked that the considered cases were perfect for the NDM since all soil profiles could easily be modeled as single homogeneous layers. In practice, homogeneous soils are rarely found.

Parameter selection for the Plaxis HSSmall input with correlations is allowed for cohesionless soils.
On the basis of two field cases, it can be concluded that the used correlations (*reference*) were acceptable. The deflections for both cases were slightly overestimated, thus the correlations are on the safe side.

Blum is a quick and easy method. Because the model is simple to modify, many variations on the model exist and great care is necessary if this model is used.
Four variations on Blum were retrieved from literature and practice. The results they produced are similar for cohesionless and homogeneous soils. However, only the variation proposed by the German codes includes layering of the soils and cohesive soils and is therefore the recommended version.

7.2 RECOMMENDATIONS ON MODEL CHOICE FOR THE DESIGN OF LATERALLY LOADED PILES

On pile design the preferred models are MPile, Plaxis and MSheet, because of the better theory, higher amount of possibilities and the higher accuracy (Conclusion 1). The decision between the models however must be properly considered.

Guidelines for model choice:
MSheet can be chosen, if the considered problem has a soil structure with horizontal layers. The influence of surrounding structures and other influences may not be too high. Second order effects of axial loads may be applied by adding an extra moment at the top of the pile. This procedure is iterative. MSheet is convenient to make a quick design if limited soil data is available.

MPile can be chosen, if the engineer wishes to optimize the results. The springs in the model are depending on the surrounding stresses and the stiffness of the soil is nonlinear. Thus, the stiffnesses are higher for low deformations and vice versa. Also the effects of external influences and pile groups may be examined with this program.

Plaxis is a three dimensional program and therefore multiple external effects can be taken into account. Plaxis may be used, if the situation is very complicated and enough soil data is present. However, the results of Plaxis are equally good as those of MPile and MSheet and therefore in most designs the use of Plaxis is not required.

The NDM, Broms and the CLM model are not to be used for pile designs. The first model is too unpractical and the others are too inaccurate compared to the above mentioned models.

If an engineer wishes to design a pile quickly in a very early stage in the design process, he can use the recommendations by the German codes which are described in the current version of the Spundwand-Handbuch. The original version of Blum can only be used in homogeneous and cohesionless sand.

7.3 RECOMMENDATION FOR FURTHER RESEARCH

The comparison calculations can be expanded with more cases. This will give better insight into the accuracy of the models.

The models Blum and Brinch Hansen cannot be compared with the other models on accuracy. This can be solved by checking the pile designs of Blum and Brinch Hansen with an accurate model like MPile, or by pile tests in which the piles are loaded until failure is reached.

In Plaxis the Mohr-Coulomb model is used. Better correlations to find the stiffnesses than Table 1 can be established to improve the results of Plaxis. This can be done by calibrating

Plaxis on a number of field tests and find relations between the stiffness and strength parameters. This way less or no laboratory tests are needed to determine the soil stiffness.

Examine accuracy of MPile with p-y curves recommended by Reese et al.
In MPile the p-y curves recommended by the API were used. From the calculations with the NDM it appeared that p-y curves recommended by Reese *et al.* produced good results. It is recommendable to examine the combination of these curves and MPile. The curves can be implemented in the manual curve input of MPile. Or, LPile can be used, a mass-spring software package like MPile, which has these curves implemented as a basic setting.

From the literature study it appeared that p-y curves are only established for characteristic soils, i.e. clay and sand. However in Dutch soils pure sand or pure clay are rarely found. It can be recommended to examine if separate recommendations for *p-y* curves for Dutch soils (peat, sandy clays etc.) have to be developed since they are not available.

8 DISCUSSION

The number of field tests is limited to six. To compare the different models on accuracy, larger amounts of field tests are required to increase the preciseness of the comparison. These tests are available and presented in the second appendix of this report. The time constraint on this thesis was the limiting factor for not fulfilling all calculations.
I do not consider this to be a huge loss for the results. In the MCA, mainly the relative accuracy is compared, since no hard line can be drawn on when a measurement is accurate and when a measurement is inaccurate. If the amount of available data of the measurements is considered, all of the models produce very accurate results. However, the differences in results are large enough to support the main conclusion firmly. The main conclusion states that the computer models, MPile, MSheet and Plaxis, are the most accurate and user friendly models. It is not unexpected that the models did not predict the pile deformations as accurate as other models can predict, for instance, the deflection of a horizontal steel beam. Accuracy of this order can be expected never to be reached. Therefore, I reckon that the results of all of the computer models reached a very acceptable degree of preciseness with which safe designs can be made as long as the safety requirements are being fulfilled.
Comparisons of the models with more measurements would be put to better use, if recommendations are found to improve the models. The model which has the best potential for this is Plaxis, because this model requires a lot of parameters to be determined. The other models, MSheet and MPile, have fewer possibilities for modifications in the standard settings. But recommendations can be found for the manual input and/or for improving or adapting the standard settings of the models.

Tests in Dutch soils are not used in the comparison. These tests should be used to make the comparison better applicable for Dutch situations. Dutch soils are often layered with different types of soft soils, e.g. clay, peat, sand and combinations of the three. The CLM, Blum, Broms and the NDM would not be advisable, because they are developed for homogeneous soils. MPile is difficult to use, if the strength of the soil consists of both a friction angle and cohesion. No soil model is present in MPile for these types of soil. A model for peaty soils is also missing. MSheet and Plaxis can easily be used for all types and combinations of soils which are frequently encountered in the Netherlands. The conclusions of the thesis might therefore be different if the comparison calculations were made on the basis of Dutch soil tests.

Finally, Plaxis has not been fairly used in comparison, compared to the other models. The other models were used to their full capabilities. Plaxis, however, was not. Very advanced soil models are present in the program. These were not used in the calculations, if the soil was clayey. This is due to the available soil data, which was very limited. Results of soil testing were not available at all.

APPENDIX A

Models

CONTENTS APPENDIX A

INTRODUCTION

In this chapter the most conventional models are evaluated on their theoretical background, the way they are validated and their limitations. In most cases some remarks are made on the calculation of the models and an example calculation is presented.
The selection of a model depended on the following characteristics. The model has to be able to design a single pile. And the soil behavior or reaction has to be taken into account. Thus, no mere rules of thumb are considered to be valid models. Another important characteristic should be that the model is or was frequently used in practice. This resulted in a wide variety of models ranging from quick design methods that have already been used for many decades to very modern and advanced finite element models.
Important note: Unless given otherwise all the information, graphs, figures and formulas in a chapter are derived from the reference given in the introduction of each chapter.

1 BLUM – 1932

The method developed by H. Blum (Blum, 1932) is one of the most widely known methods. It is still used today even though the model is nearly 80 years old. Its simplicity and fast results make it an attractive alternative to the more expensive and complex computer calculations.
Note: The figures in this chapter are drawn by J. Ruigrok.

1.1 BACKGROUND

Just like the calculation of sheet pile walls, the assumption is made for an ideal loading situation. This is shown in *figure 1-1*. The first picture, "pole", in the figure shows a side view from the situation, together with some important points over the height of the pile. "Loading", shows the load *P* on the pile and the shear forces generated over the length of the pile. "Ideal loading", shows the loading situation with which Blum performs his calculations. Here the theoretical penetration depth is considered. The soil reaction consist of two parts, E_p and $E_{p'}$, these will be explained later. At point *C,* the moment is assumed to be zero, but a horizontal force is imposed to get horizontal balance. Note that in this picture the soil reaction forces on the pile are drawn on the wrong side of the pile in regard to the direction of *P*. "Moment", shows the moments along the pile. The moments increase until point *B* where the moment reaches its maximum. In the ideal loading situation, the moments are zero at the theoretical penetration depth. "Deflection", shows the deflection of the pile at the ground line, *d'*, and at the top of the pile, *d*. Keep in mind that the calculated deflections are only to be calculated at the ultimate load. The used symbols are listed on the next page.

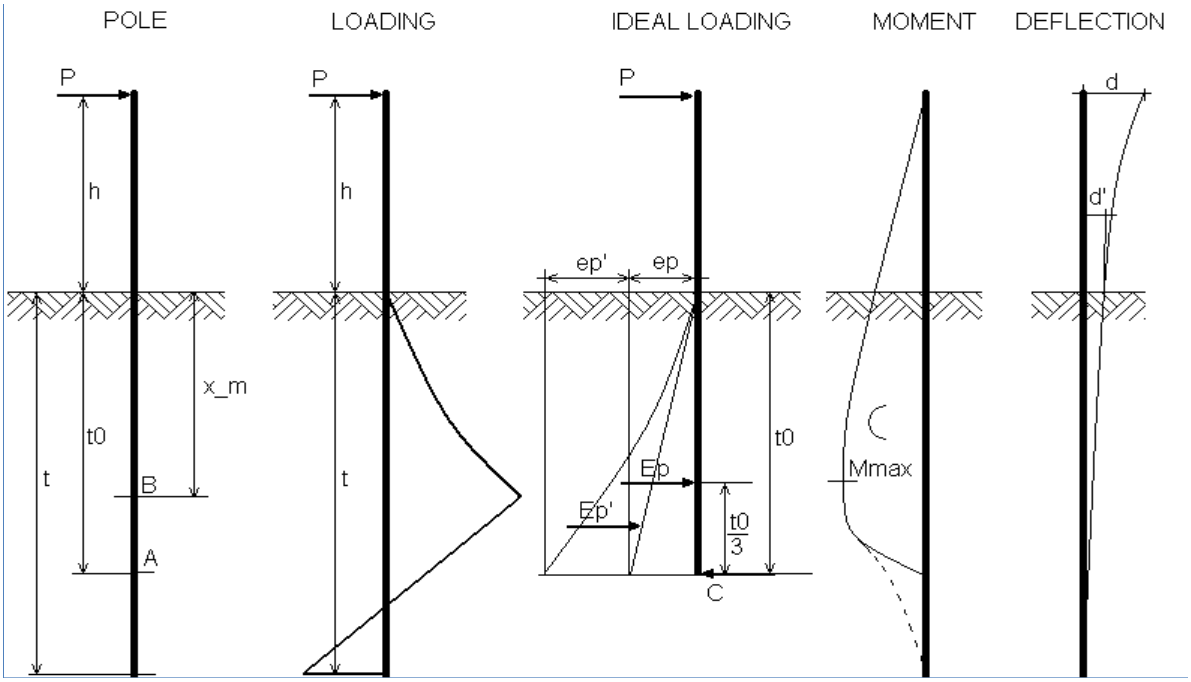

Figure 1-1 Drawings of Pile, loads, schematized loads, moment and deflection *– Picture by J. Ruigrok*

The list of symbols by Blum:

P = Horizontal force at static loading [kN]
d = Deflection at top of pile [m]
d' = Deflection at ground level [m]
f_w = Soil resistance = $\gamma\lambda_p$ [kN/m^3]
γ = Volumetric weight of soil above water table [kN/m^3]
γ_0 = Volumetric weight of soil below water table [kN/m^3]
h = height where load P is applied [m]
b = width of the pole perpendicular to the direction of the force [m]
x_m = Location M_{max} below surface [m]
t_0 = Theoretical penetration depth, here in the ideal loading situation, the moments are zero [m]
t = Real penetration depth = $1{,}2t_0$ [m]
I = Modulus of inertia in the direction of P [m^4]
W = Section modulus in the direction of P [m^3]
E = Modulus of elasticity [kN/m^2]
M_{max} = Maximum moment in ideal loading situation [kNm]

Below, the solutions to find either the maximum moment and load, or the minimum dimensions. The derivation of the solution is stated at the bottom of this abstract. The strength design formulas are:

$$\frac{24P}{f_w} = 4x_m^2(x_m + 3b) \qquad \textit{eq. 1.1}$$

And:

$$\frac{24P}{f_w} = t_0^3\frac{t_0 + 4b}{h + t_0} \qquad \textit{eq. 1.2}$$

With *eq. 1.2* it is possible to determine either the maximum load, if the dimensions of the pile are known, or the minimum dimensions of the pile, if the load is known. With *eq. 1.1* it is possible to determine the location of the maximum moment. Then, with *eq. 1.3*, M_{max} can be calculated.

$$M_{max} = \frac{f_w}{24}x_m^2\{3x_m^2 + x_m(4h + 8b) + 12bh\} \qquad \textit{eq. 1.3}$$

To calculate displacements at the critical load Blum found *eq. 1.4* and *eq. 1.5*:

$$d = \frac{P(h + t_0)^3}{3EI} - \frac{f_w t_0^4}{360EI}\{2.5t_0^2 + t_0(3h + 12b) + 15bh\} \qquad \textit{eq. 1.4}$$

$$d' = \frac{Pht_0^2}{2EI} + \frac{Pt_0^3}{3EI} - \frac{f_w}{EI}\left(\frac{t_0^6}{144} + \frac{bt_0^5}{30}\right) \qquad \textit{eq. 1.5}$$

Derivation of the strength design formulas

Because the system is in balance there will be moment equilibrium. At point A, at the bottom of the theoretical penetration depth: $\Sigma M_A = 0$. This equilibrium gives the following equation:

$$P(h + t_0) - \frac{t_0}{3} f_w \frac{b t_0^2}{2} - \frac{t_0}{4} f_w \frac{t_0^3}{6} = 0 \qquad \textit{eq. 1.6}$$

Before continuing, first the above formula will be elaborated. The second and third term are calculated with the equilibrium of the passive earth pressure and the load caused by the weight of the soil on the pile. The volume pressing horizontally on the pile has a wedge shape, *figure 1-2*.

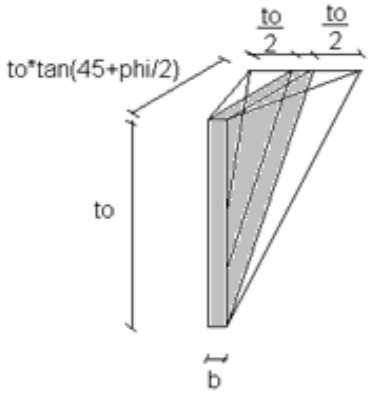

Figure 1-2 Volume of soil pressing on pile

The second term is found by first calculating the middle, grey, part of the soil wedge. This volume weights:

$$\gamma \frac{(b t_0 t_0 \tan\left(45 + \frac{\varphi}{2}\right))}{2} = G_1\ [kN] \qquad \textit{eq. 1.7}$$

The third term is found by the rest of the weight of the soil volume. This is:

$$\gamma \frac{(t_0 t_0 \tan\left(45 + \frac{\varphi}{2}\right) 2\frac{t_0}{2})}{6} = G_2\ [kN] \qquad \textit{eq. 1.8}$$

If the situation is viewed from the side the equilibrium between load and soil resistance can be visualized, figure 1-3.

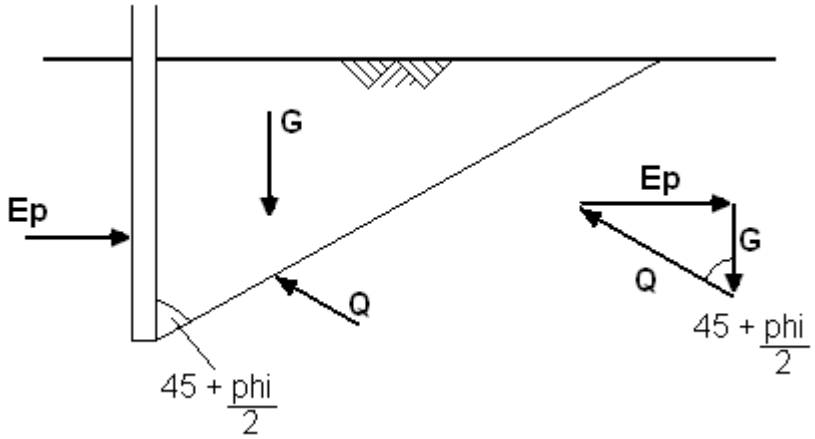

Figure 1-3 Soil wedge pressing on pile and force equilibrium

With the force equilibrium, shown in figure 1-3, E_p can be calculated for both G_1 and G_2.

$$E_p = G_1 \tan\left(45 + \frac{\varphi}{2}\right) = \gamma \quad \frac{bt_0^2 tan^2(45 + \frac{\varphi}{2})}{2} = \frac{bt_0^2}{2}\gamma\lambda_p = \frac{bt_0^2}{2} f_w \qquad \textit{eq. 1.9}$$

$$E_{p'} = G_2 \tan\left(45 + \frac{\varphi}{2}\right) = \gamma \quad \frac{t_0^3 tan^2(45 + \frac{\varphi}{2})}{6} = \frac{t_0^3}{6}\gamma\lambda_p = \frac{t_0^3}{6} f_w \qquad \textit{eq. 1.10}$$

To find the balance in moment at point *A*, the level, at which E_p and $E_{p'}$ are active, needs to be determined. The stresses of e_{p1} increase linearly with depth, this results that E_p is active at a level of $t_0/3$ above point *A*. The stresses of e_{p2} increase quadratic with depth this results that $E_{p'}$ is active at a level of $t_0/4$ above point *A*. The sum of all moments can now be calculated around point *A*.

$$\Sigma M_A = P(h + t_0) - \frac{t_0}{3}E_{p1} - \frac{t_0}{4}E_{p2} = P(h + t_0) - \frac{t_0}{3} f_w \frac{bt_0^2}{2} - \frac{t_0}{4} f_w \frac{t_0^3}{6} = 0 \qquad \textit{eq. 1.11}$$

This can be simplified to obtain *eq. 1.6*:

$$\Sigma M_A = P(h + t_0) - f_w(\frac{bt_0^3}{6} + \frac{t_0^4}{24}) = 0 \qquad \textit{eq. 1.6}$$

Eq. 1.6 can be rewritten, to find the moment at every depth in the ideal load schematization:

$$M_x = P(h + x) - f_w(\frac{bx^3}{6} + \frac{x^4}{24}) \qquad \textit{eq. 1.12}$$

The place of the maximum moment can be found at the location where: $dM_x/d_x = 0$:

$$\frac{dM_x}{dx} = 0 = P - f_w(\frac{3bx^2}{6} + \frac{4x^3}{24}) \qquad \textit{eq. 1.13}$$

From which the value of *P* can be derived: (Keep in mind that M_{max} is found at $x=x_m$)

$$P = f_w(\frac{bx_m^2}{2} + \frac{x_m^3}{6}) \qquad \textit{eq. 1.14}$$

If P is substituted in *eq. 1.12* then M_{max} becomes:

$$M_{max} = f_w\left\{(h + x_m)(\frac{bx_m^2}{2} + \frac{x_m^3}{6}) - (\frac{bx_m^3}{6} + \frac{x_m^4}{24})\right\} \qquad \textit{eq. 1.15}$$

Simplification gives the result of the derivation for M_{max}, i.e. *eq. 1.3*.

$$\boldsymbol{M_{max} = \frac{f_w}{24}x_m^2\{3x_m^2 + x_m(4h + 8b) + 12bh\}} \qquad \textit{eq. 1.3}$$

If the value of P is now substituted in *eq. 1.6* it is found that:

$$f_w\left(\frac{bx_m^2}{2}+\frac{x_m^3}{6}\right)(h+t_0)=f_w(\frac{bt_0^3}{6}+\frac{t_0^4}{24}) \qquad \textit{eq. 1.16}$$

After simplification *equations 1.1 and 1.2* are obtained.

$$\frac{\boldsymbol{24P}}{\boldsymbol{f_w}}=\boldsymbol{t_0^3}\frac{\boldsymbol{t_0+4b}}{\boldsymbol{h+t_0}}=\boldsymbol{4x_m^2(x_m+3b)} \qquad \textit{eq. 1.1 \& 1.2}$$

Derivation of the displacement design formulas

The detailed derivation will not be given here, because the background on the soil resistance is already given in the derivation of *equations 1.1, 1.2 and 1.3*. To calculate the displacements, Blum assumes the bottom of the pile at depth t_0 to be fixed. Thus no horizontal movement of the pile tip and a horizontal load may be present for horizontal balance. The moment at the fixation is zero, when the ultimate load is present. With the fixation, the load, the bending stiffness of the pile and the earth pressure known, it is possible to calculate the deflection of the pile at every depth. Blum only gives the solutions to calculate the displacements at ground level and at the top of the pile, *eq. 1.4 and 1.5.*

1.2 CALCULATIONS

As stated in the background, the calculation can go two ways. One can either calculate the minimum dimensions of the pile, if the load and the location of the load are known, or the maximum load, if the dimensions of the pile are known. If the dimensions of the pile are set, or the ultimate load is known the moments along the pile can be calculated. It is also possible to calculate the deflections of the pile under the maximum load.

The calculations are very easy. The difficulty lies with the determination of λ_p. λ_p Can be calculated with the theory of Rankine, (Verruijt, 1983), *eq. 1.17*. However, if the wall friction and the inclination of the surface are desired of being taken into account, great care is necessary and the user should ask himself, if all assumptions and formula's are still valid.

$$K_p=tan^2(45+\frac{\varphi}{2}) \qquad \textit{eq. 1.17}$$

1.3 LIMITATIONS

The limitations of Blum's theory are:

- In general:
  - Only capable to find the ultimate resistance of the soil
  - No calculations possible under working loads
- On soil behavior:
  - No cohesion (although it is possible by adapting the formulas)
  - No layered soils (although it is possible by adapting the formulas)
  - No time dependent behavior
  - No nonlinear soil behavior
- On loading types:
  - No cyclic loads
  - No axial load (although it is possible by adapting the formulas)
- On pile behavior:
  - No differences of the bending stiffness over the height of the pile (although it is possible by adapting the formulas)
  - Bending stiffness independent of moment

A note must be made on the first limitation. The model Blum can be adapted to find the displacements of the pile for working loads. To do this, assumptions have to be made. For instance, deflections can be assumed to increase linearly with increasing loads. These type of assumptions however are not part of the model and will therefore not be made in this thesis.

2 P-Y CURVES – 1950'S – TODAY

With the model of the p-y curves a numerical model is meant that models the soil resistance as predefined nonlinear springs. The deflections and moments are calculated by iterations until the load and soil resistance (depending on the deformation of the pile) are in equilibrium. Interest in the model was first developed in the 1940's and 1950's when energy companies build offshore structures that had to sustain heavy horizontal loads from waves. An exact publication date of the model is not available since the input of the model, the p-y curves, is still modified and improved today. The earliest recommendations on p-y behavior date from the 1950's by the work of Skempton and Terzaghi. In this paper the latest methods of describing the p-y curves are elaborated, (Reese, Isenhower, & Wang, 2006).

2.1 BACKGROUND

There are two types of nonlinearity in the problem of the laterally loaded piles. The first is the nonlinear behavior of the soil surrounding the pile. At small deflections, soil react more stiff than soil at larger deflections. The second nonlinearity is in the behavior of the pile. The bending stiffness of the pile decreases as the moment in the pile increases. A differential equation is written to take into account the effect of axial loading on the bending moment. Now the equation can also take into account the effect of buckling. Numerical methods are developed to solve the differential equation. How to solve the equation is discussed later.

Basis for useful solutions

Detailed analysis and successful design of a laterally loaded pile depends principally on the predictions of the response of soil with appropriate accuracy. A computer is necessary to solve the complex problems fast. The prediction of the p-y curves is very important and data acquisition at the site is indispensable.

Characteristics of p-y curves

A typical p-y curve is shown in figure 2-1 A. The curve simulates a short term static loading on the pile. The initial portion is a straight line through the origin and

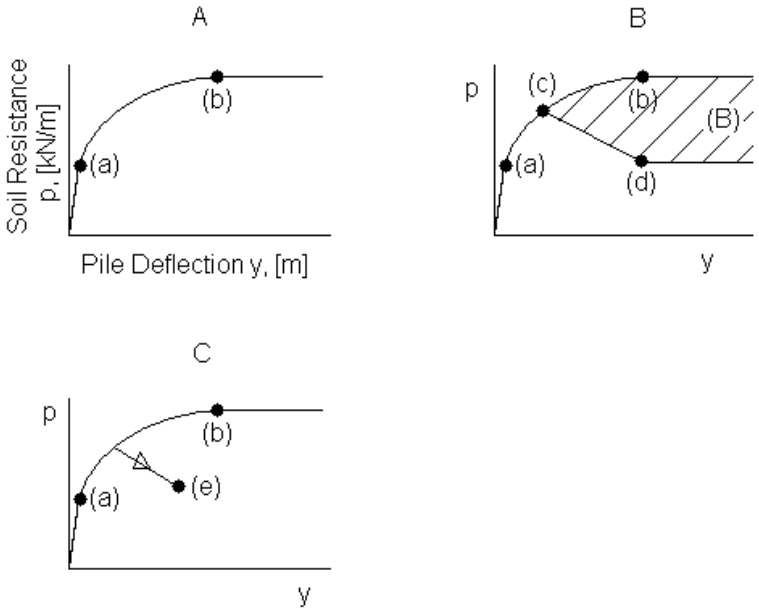

Figure 2-1 Typical shapes of p-y curves A: static load, B: cyclic load, C: sustained load – Picture by J. Ruigrok

point (a), assuming that the soil resistance, p, is linearly related to pile displacement, y, for small strains. Analytical methods are established for this relationship.
In the second portion, from point (a) to (b), it can be seen that the soil resistance is increasing at a decreasing rate with respect to the pile deflection. This simulates the nonlinear behavior of the soil. The horizontal portion of the curve is the ultimate soil resistance. The soil behaves plastically after point (b).
The shaded portion in figure 2-1 B shows the decreasing value of p, from point (c) to point (d). This decrease reflects the effect of cyclic loading. Figure A and B are identical until point (c), this implies that small cyclical loading has little or no effect on the soil behavior.
The possible effect of sustained loading is shown in figure 2-1 C. If the permeability of the soil is low the increased pore water pressures will dissipate slowly. This means that initially the stiffness of the soil is high, but reduces over time. Line (e) shows this time effect under constant loading. The reduced value of p, indicates that as the deflection increases, the resistance shifts to other elements of the pile.

Influence of diameter
In the analytical solutions to the problem it appears that the diameter of the pile appears to the first power in the expressions of the *p-y* curves. This means that shell factor of pile is constant with the diameter of the pile. Experimental data show that this is not true. The shell factor becomes smaller, if the diameter of the pile increases. In the recommendations that follow to calculate the *p-y* curves the diameter *b* appears to the first power (constant shell factor) this does not seriously contradict any available experimental data. For large diameter piles in over-consolidated clay below the water table further studies are recommended.

Recommendations to find p-y curves for clays
To find the initial portion of the curve, the stiffness, E_{smax}, for small strains has to be determined. This is not easy. Studies found values from E_{smax} ranging from 40 times to 2840 times the undrained shear strength. The current best approach is to use values for the initial slope of *p-y* curves from experiments. Next the ultimate resistance p_u of the soil has to be determined. For the top part of the pile the ultimate resistance can be modeled by simulating the soil as a wedge that is pushed and up and out the soil. The wedge is shown in figure 2-2 A. The resistance of the wedge is modeled as the friction along the three sides of the wedge and the friction along the shaft of the pile. Taking into account the frictions along the sides of the wedge and the weight of the wedge, the following expression for p_{u1} can be derived:

$$p_{u1} = c_a b[\tan \alpha_s + (1+\kappa)\cot\ \alpha_s] + \gamma' bH + 2c_a H(\tan \alpha_s \sin \alpha_s + \cos \alpha_s) \qquad \textit{eq. 2.1}$$

With:

p_{u1} = ultimate resistance near ground surface per unit of length along the pile [*kN/m*]
c_a = average undrained shear strength over the depth [kN/m^2]
α_s = angle of inclined plane with vertical [*degree*]
γ' = effective unit weight of soil [*kN/m^3*]
κ = reduction factor for shearing resistance along the face of the pile [*k*]

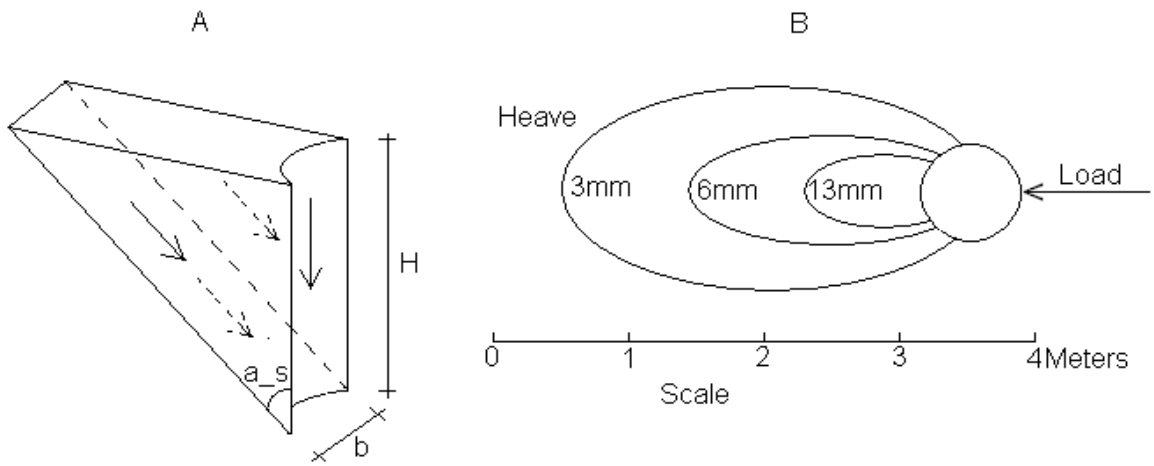

Figure 2-2 A: Soil wedge, B: Approximation of expected heave in practice – Figure by J. Ruigrok

Eq. 2.1 can be simplified by assuming κ to be equal to zero and α_c to be equal to 45°:

$$p_{u1} = 2c_a b + \gamma' bH + 2.83c_a H \qquad \textit{eq. 2.2}$$

Of course the assumption of an exact failure of the soil over a wedge like depicted in figure 2-2 A is discussable. Measurements show that the heave around a pile is not rectangular. The heave has a more or less oval shape, figure 2-2 B.
The second model is to calculate the ultimate soil resistance below the top part, where the ground only moves horizontally. The resistance of the soils is modeled in four parts. The first one is the direct resistance, *sigma_6 x b*, figure 2-3. Two parts are located on the sides of the pile. These are simulating the friction between the sides of the pile and the soil. Because the pile is round, the friction is only active over a width of half the diameter of the pile. The friction is a function of the cohesion. And one part, *sigma_1 x b*, is located behind the pile. This last part causes a negative resistance, because the soil pushes against the pile in the same direction as the movement of the pile.

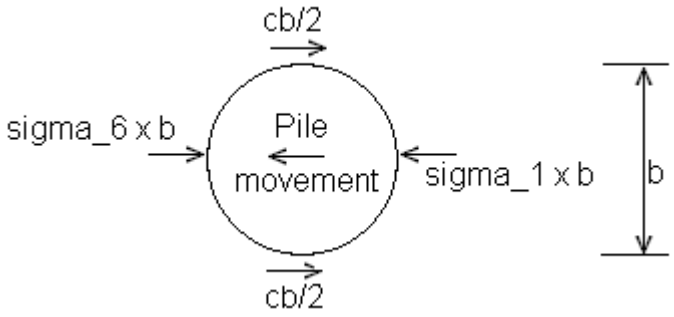

Figure 2-3 Soil resistance in case of horizontal movement of soil – Picture by J. Ruigrok

This leads to the following equation:

$$p_{u2} = (\sigma_6 - \sigma_1 + c)b = 11cb \qquad \textit{eq. 2.3}$$

The simplification to *11cb*, is derived from an equilibrium equation of all stresses around the pile. The authors found that: $\sigma_6 - \sigma_1 = 10c$.

Above, the situation was sketched for the general situation of clays. Below, some recommendations follow for constructing the p-y curves in more specific situations.

Response of soft-clays in the presence of free-water.
The following procedure is for calculating p-y curves for short-term static loading. Cyclical loading and sustained loading are skipped since these situations are not part of this thesis. The experiment that was executed by Matlock (1970) served as basis for the p-y curves. The location was Lake Austin (Reese, Isenhower, & Wang, 2006, p. 453).

1. Obtain the best possible estimate of the variation of undrained shear strength *c* and submerged unit weight with depth. Also, obtain the value of ε_{50}, the strain corresponding to one-half of the maximum principal stress difference. If no stress-strain curves are available, typical values of ε_{50} are given in table 2-1.

Undrained shear strength c_u [kN/m^2]	**ε_{50} [-]**
<12	0,02
12-24	0,02
24-48	0,01
48-96	0,006
96-192	0,005
>192	0,004

Table 2-1 Typical values for ε_{50} related to the undrained shear strength

2. Compute the ultimate soil resistance per unit length of the pile using the smaller of the values given by the following equations:

$$p_{uz} = \left[3 + \frac{\gamma'}{c_{uz}} + \frac{J}{b}z\right] c_z b \qquad \textit{eq. 2.4}$$

$$p_{uz} = 9 c_{uz} b \qquad \textit{eq. 2.5}$$

with:

p_{uz} = Ultimate soil resistance at depth *z* [*kN/m*]
γ' = Average effective unit weight from ground surface to p-y curve [*kN/m^3*]
z = Depth below ground surface to *p-y* curve [*m*]
c_{uz} = Undrained shear strength at depth *z* [*kN/m^2*]
b = Diameter (width) of the pile [*m*]
J = Experimentally determined parameter (0,5 for soft clays, 0,25 for medium clays. the value of 0,5 is frequently used for *J* [-]

3. Compute the deflection y_{50} at one-half of the ultimate soil resistance from the following equation:

$$y_{50} = 2.5\varepsilon_{50}b \qquad \textit{eq. 2.6}$$

4. Compute the p-y curve from the following relationship:

$$\frac{p}{p_u} = 0.5\left(\frac{y}{y_{50}}\right)^{\frac{1}{3}} \qquad \textit{eq. 2.7}$$

The value of p/p_u remains constant beyond $y = 8y_{50}$, the ultimate soil resistance is reached at this deflection.

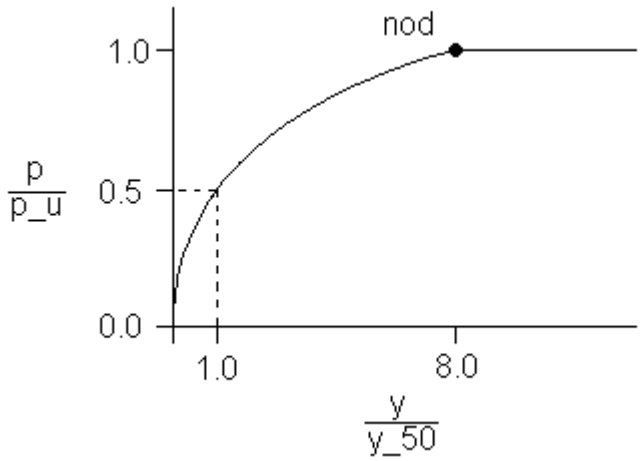

Figure 2-4 p-y Curve for soft-clays in the presence of free-water – Picture by J. Ruigrok

Response of stiff-clays in the presence of free-water.
The following procedure is for calculating p-y curves for short-term static loading. Cyclical loading and sustained loading are skipped since these situations are not part of this thesis. The test that served as basis for the development of this recommendation was performed by Reese et al. in 1975 (Reese, Isenhower, & Wang, 2006, p. 456). In figure 2-6 an example curve is given.

1. Obtain values of the undrained shear strength *c*, average soil submerged unit weight *γ'* above the location of the curve and pile diameter *b*.
2. Compute the average undrained shear strength c_a over depth *z*. To find the resistance of the wedge.
3. Compute the ultimate soil resistance per unit length of the pile using the smaller of the values given by the following equations:

$$p_{u1} = 2c_a b + \gamma' bz + 2.83c_a z \qquad \textit{eq. 2.8}$$

$$p_{u2} = 11cb \qquad \textit{eq. 2.9}$$

c_a = average undrained shear strength over the depth above depth '*z*' [kN/m^2]

4. Choose the appropriate value of A_s from the figure for shaping the p-y curves:

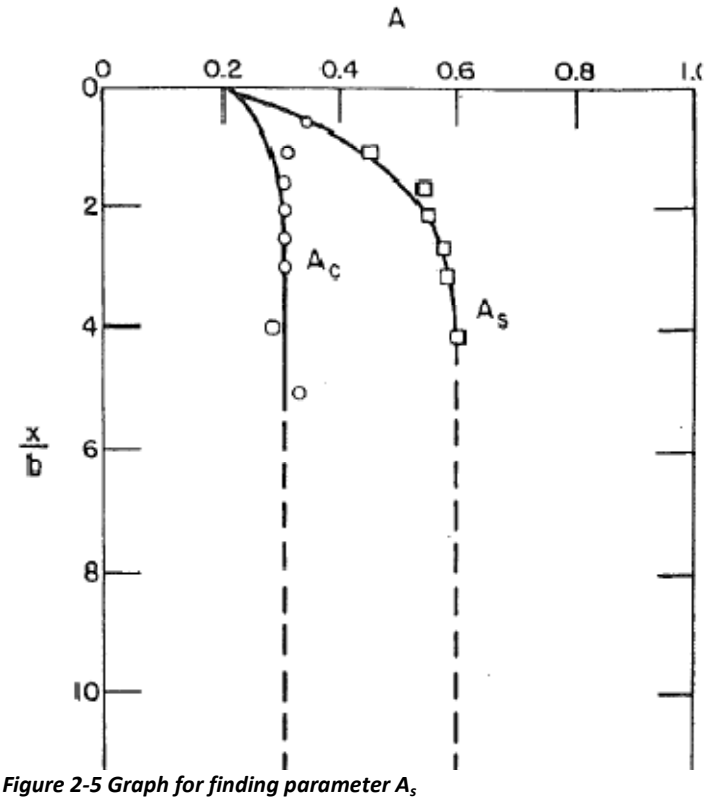

Figure 2-5 Graph for finding parameter A_s

5. establish the initial straight line portion of the p-y curve. Use the appropriate value of K_{py} from table 2-2.

$$p = (K_{py} z) y \qquad \textit{eq. 2.10}$$

	Average undrained shear strength c_a [*kPa*]		
	50-100	**200-300**	**300-400**
K_{py} **(static) [*MN/m³*]**	135	270	540
K_{py} **(cyclic) [*MN/m³*]**	55	110	540

2-2 Initial stiffness p-y Curves

6. Compute y_{50}:

$$y_{50} = \varepsilon_{50} b \qquad \textit{eq. 2.11}$$

Determine ε_{50} from laboratory tests, or use table 2-1.

7. Establish the first parabolic portion of the curve with:

$$p = 0.5 p_u \left(\frac{y}{y_{50}}\right)^{\frac{1}{2}} \qquad \textit{eq. 2.12}$$

This equation should be used to define the portion of the *p-y* curve from the point of intersection with eq. 2.10 to the point where $y = A_s y_{50}$.

8. Establish the second parabolic portion of the *p-y* curve:

$$p = 0.5 p_u \left(\frac{y}{y_{50}}\right)^{\frac{1}{2}} - 0.055 p_u \left(\frac{y - A_s y_{50}}{A_s y_{50}}\right)^{\frac{5}{4}} \qquad \textit{eq. 2.13}$$

This equation defines the portion of the p-y curve from the point where $y = A_s y_{50}$ to the point where $y = 6A_s y_{50}$.

9. Establish the next straight line portion of the p-y curve:

$$p = 0.5 p_u (6A_s)^{\frac{1}{2}} - 0.411 p_u - \frac{0.0625}{y_{50}} p_u (y - 6A_s y_{50}) \qquad \textit{eq. 2.14}$$

10. Establish the final straight line portion of the p-y curve:

$$p = p_u \left[1.225 (A_s)^{\frac{1}{2}} - 0.75 A_s - 0.411\right] \qquad \textit{eq. 2.15}$$

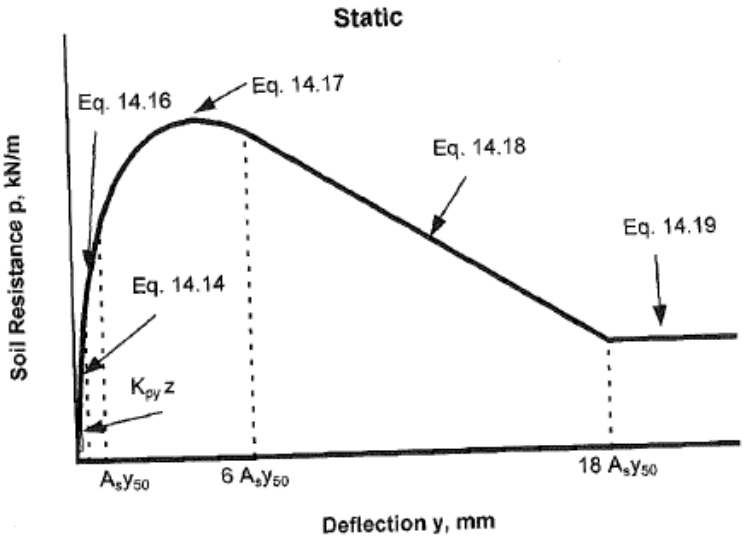

Figure 2-6 p-y Curve for clay. Note: Eq. 14.14, 14.16-14.19 matches with Eq. 2.10, 2.12-2.15 of this literature study

Note: This method suggests that there are intersections between all portions of the p-y curve. This may not be the case for the part described in step5. If this portion does not intersect with one of the other equations step 5 describes the entire p-y curve.

Response of stiff-clays with no free-water.

The way to find the response of stiff clays with no free water is exactly the same as the way to find the response of soft clay with the presence of free water. However, there are differences. Here, the relationship between p and y is as follows:

$$\frac{p}{p_u} = 0.5\left(\frac{y}{y_{50}}\right)^{\frac{1}{4}} \qquad \textit{eq. 2.16}$$

The value of p/p_u remains constant beyond $y = 16y_{50}$, the ultimate soil resistance is reached at this deflection. Notice that the effective stress equals the total stress, since there is no presence of free water.

Response of clays according to API

According to the API (MPile, version 4.1, 3D modelling of single piles and pile groups), the ultimate lateral resistance depends upon the failure mechanism of the clay which differs for shallow, p_{us}, and deep, p_{ud}, depth. They are to be determined with respectively equation 2.17 & 2.18.

$$p_{us} = 3C_u + \gamma' H + JC_u \frac{H}{D} \qquad \textit{eq. 2.17}$$

$$p_{ud} = 9C_u \qquad \textit{eq. 2.18}$$

with:

p_{us} = Ultimate lateral resistance at shallow depth [kN/m^2]
p_{us} = Ultimate lateral resistance at deep depth [kN/m^2]
C_u = Undrained shear strength [kN/m^2]
γ' = Effective unit weight of the soil [kN/m^3]
H = Depth below soil surface [m]
J = Dimensionless empirical constant. A value ranging from 0,25 to 0,5 is recommended
D = Pile diameter [m]

The p-y curve is now defined by two lines: the curve describing the nonlinear behavior and the line describing the ultimate soil resistance.

$$p = \begin{cases} 0{,}5 p_u (y/y_{50})^{(1/3)} & for\ y < 8\ y_{50} \\ p_u & for\ y \geq 8\ y_{50} \end{cases} \qquad \textit{eq. 2.19}$$

with:

p = Lateral soil resistance at depth H [kN/m^2]
p_u = Ultimate lateral resistance, the smaller value of p_{us} and p_{ud} [kN/m^2]
y = Actual lateral deflection [m]
y_{50} = $2{,}5\varepsilon_{50}D$ [m]
ε_{50} = Strain which occurs at one-half of the maximum stress on laboratory undrained compression tests of undisturbed soil samples. An estimated value can be obtained from table 2-1 [-]
D = Pile diameter [m]

Recommendations to find p-y curves for sands

The initial stiffness of sand is a function of the confining pressure. Recommendations were derived from experiments at Mustang Island by Cox et al. in 1974 (Reese, Isenhower, & Wang, 2006, p. 468). These recommendations for the initial stiffness are in the table below:

Relative density sand	Loose ($\varphi < 30^o$)	Medium ($30^o \leq \varphi < 36^o$)	Dense ($\varphi \geq 36^o$)
K_{py} below water table [MN/m^3]	5,4	16,3	34
K_{py} above water table [MN/m^3]	6,8	24,4	61

Table 2-3 Recommendations for initial stiffness for sands

There are, like for clays, two models to calculate the ultimate resistance. The first model is to calculate the ultimate resistance for the upper part of the pile. The total lateral force may be computed by subtracting the active force F_a, computed by using Rankine theory, from the passive force F_p, computed from the model where it is assumed that the Mohr-Coulomb failure condition is satisfied on planes, *ADE*, *BCF* and *AEFB*. The wedge is shown in figure 2-7:

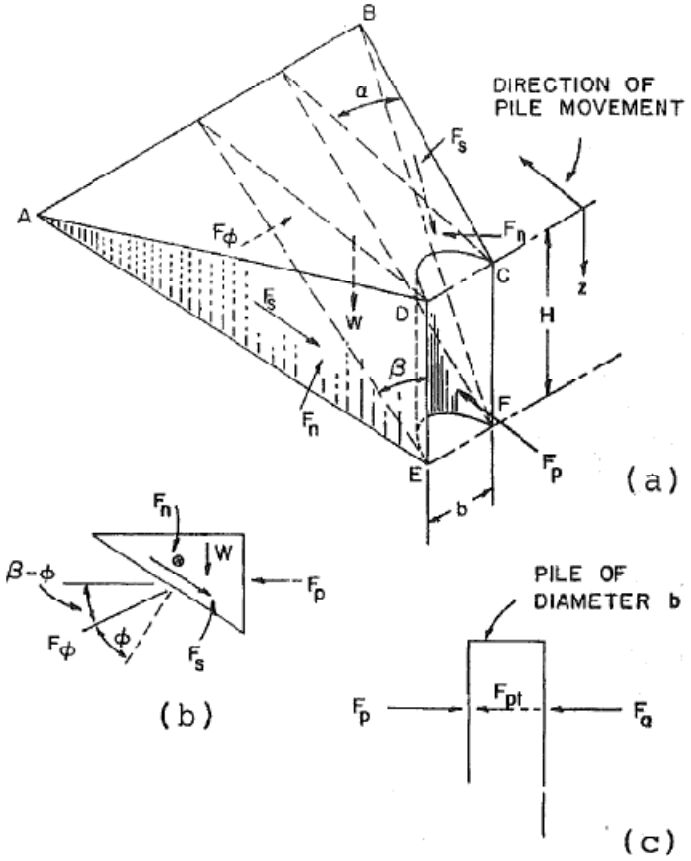

Figure 2-7 Soil resistance at the top part of the pile

The ultimate soil resistance near the ground surface per unit length of the pile is found by differentiating the elaborated equation of $F_{pt} = F_p - F_a$. This gives:

$$p_{u1} = \gamma z \left[\frac{K_0 z \, tan\, \varphi \sin\beta}{tan(\beta - \varphi)\cos\alpha_s} + \frac{\tan\beta}{tan(\beta - \varphi)}(b + z\tan\beta\tan\alpha_s) + K_0 z \tan\beta\,(\tan\varphi\sin\beta - \tan\alpha_s) - K_a b \right] \qquad \textit{eq. 2.20}$$

with:
φ = Friction angle [*degrees*]
K_0 = Coefficient of earth pressure at rest = *1- sin φ* [-]
K_a = Minimum coefficient of active earth pressure = $tan^2(45 - \varphi/2)$ [-]
β = Approximated to be *45 + φ/2* [*degrees*]
α_s = Ranging from *φ/3*, to *φ/2* (The last is also used by Blum) [*degrees*]

The second formula is used to calculate the ultimate soil resistance at some point below the ground surface. The pressure at the back of the pile must be equal to, or larger than, the minimum active pressure. If not, the soil could fail by slumping. The ultimate soil resistance at some depth below the soil surface is calculated with the same kind of equilibrium equation as used to find the ultimate resistance for clays.

$$p_{u2} = K_a b\gamma z\, tan^8(\beta - 1) + K_0 b\gamma z \tan\varphi\, tan^4\beta \qquad \textit{eq. 2.21}$$

The equations for p_{u1} and p_{u2} , *eq. 2.20 &2.21*, are approximations because of the elementary nature of the models used in the computations. However serve a useful purpose in indicating the form of the ultimate soil resistance.

Response of sand above and below the water table
The procedure is for short-term static loading and for cyclic loading.

1. Obtain values for the friction angle *φ*, the effective soil unit weight γ' and the pile diameter *b*. (note: use the buoyant unit weight for sand below the water table and total unit weight for sand above the water table)

2. Compute the ultimate soil resistance per unit length of the pile by using the smaller of the values given by the following equations.

$$p_{u1} = \gamma z \left[\frac{K_0 z \, tan\, \varphi \sin\beta}{tan(\beta - \varphi)\cos\alpha_s} + \frac{\tan\beta}{tan(\beta - \varphi)}(b + z\tan\beta\tan\alpha_s) + K_0 z \tan\beta\,(\tan\varphi\sin\beta - \tan\alpha_s) - K_a b \right] \qquad \textit{eq. 2.22}$$

$$p_{u2} = K_a b\gamma z\, tan^8(\beta - 1) + K_0 b\gamma z \tan\varphi\, tan^4\beta \qquad \textit{eq. 2.23}$$

with: $\alpha_s = \varphi/2$

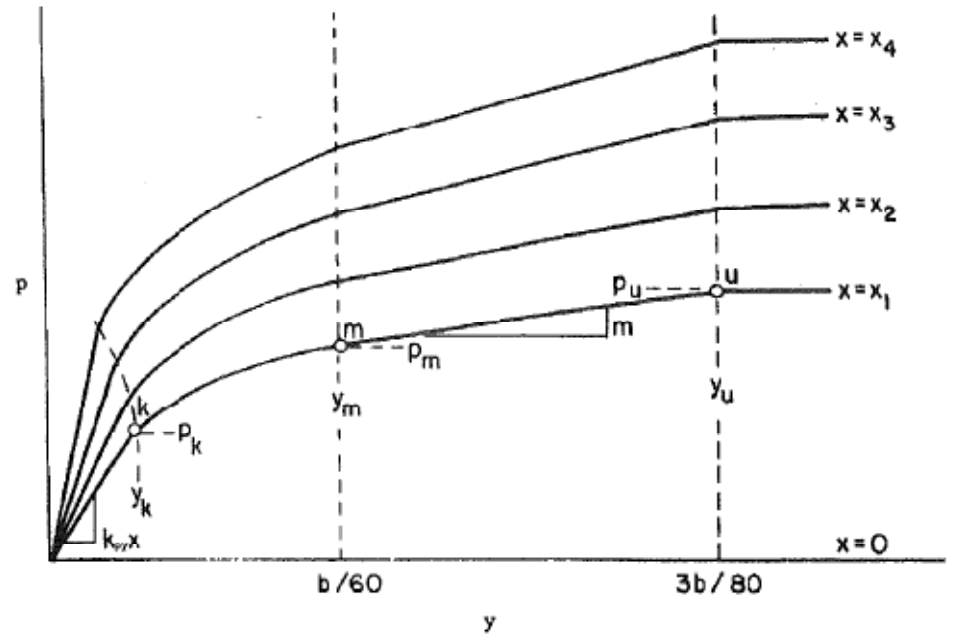

Figure 2-8 Shape of p-y curves for sands

3. The p-y curves will look as in figure 2.8 above. Take y_u = 3b/80. compute p_u by the following equation:

$$p_{us} = A_s p_u \qquad \textit{eq. 2.24}$$

Get the value of A_s from the graph, figure 2-9:

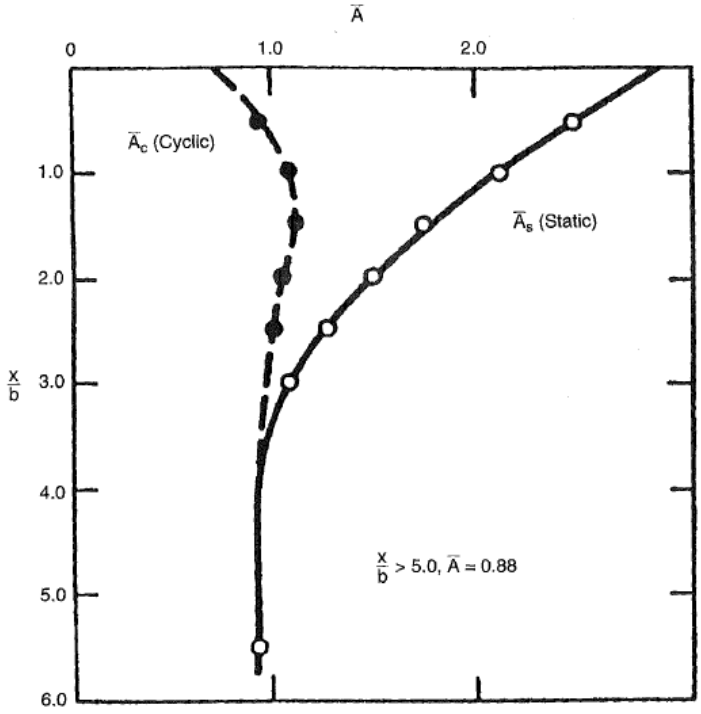

Figure 2-9 Dimensionless parameters Ac and As to find the ultimate soil resistance

4. Take y_m = b/60. Compute p_m by the following equation:

$$p_{ms} = B_s p_u \qquad \textit{eq. 2.25}$$

Get the value of B_s from the graph, figure 2-10:

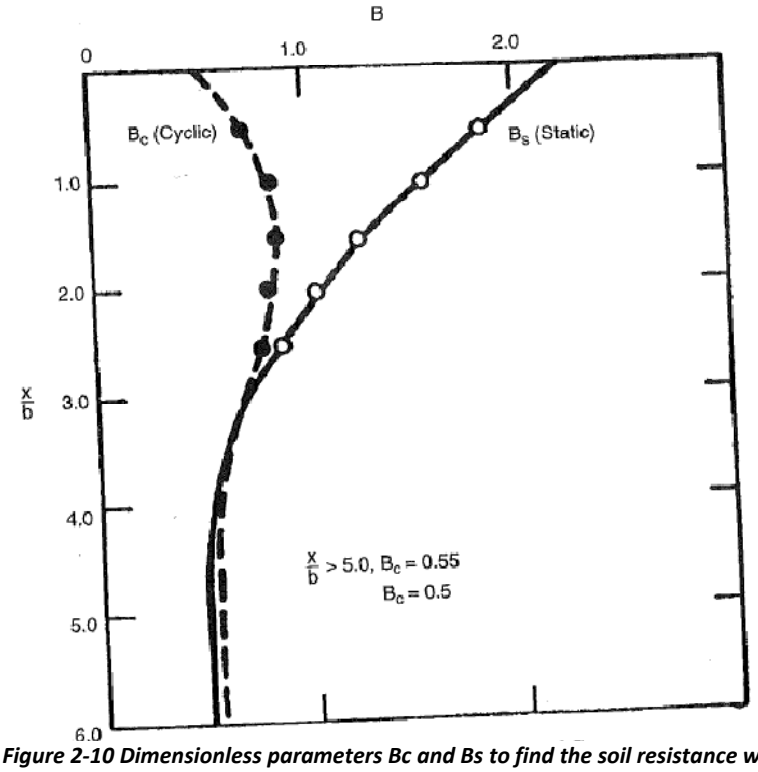

Figure 2-10 Dimensionless parameters Bc and Bs to find the soil resistance were y=b/60

5. Compute the initial straight line portion of the p-y curve:

$$p = K_{py} z y \qquad \textit{eq. 2.26}$$

Get the correct value of K_{py} from table 2-3.

6. Establish the parabolic section of the *p-y* curve between point *k* and *m*.

$$p = C y^{1/n} \quad \text{with;} \qquad \textit{eq. 2.27}$$

$$m = \frac{p_u - p_m}{y_u - y_m}, \quad n = \frac{p_m}{m y_m}, \qquad C = p_m \Big/ y_m^{1/n} \qquad \textit{eq. 2.28, 2.29, 2.30}$$

7. Determine point *k* as:

$$y_k = \frac{C}{K_{py} z} \qquad \textit{eq. 2.31}$$

Note: The procedure suggests that all portions intersect. This may not be the case at point k. If this happens, the p-y *curve is described by* eq. 2.26 *, until this intersects with another branch of the curve.*

Triaxial tests are recommended for finding the internal friction angle. The procedure above can be used for sand above the water table if appropriate adjustments are made in the unit weight and angle of internal friction of the sand.

Response of sand above and below the water table, according to the API.
Another method for constructing the *p-y* curves is described in the API RP2A (1987). The assumption made was that the method can be used both above and below the water table. However, the API recommendations were developed only for submerged sand.

1. Obtain values for the friction angle φ, the soil unit weight γ and the pile diameter *b*. (note: use the buoyant unit weight for sand below the water table and total unit weight for sand above the water table)

2. There are two equations that can be used to determine the ultimate lateral resistance, p_u. The first equation is for shallow depths, the second for deep depths. The ultimate lateral resistance is the smallest value of:

$$p_{us} = (C_1 z + C_2 b)\gamma z \qquad \textit{eq. 2.32}$$

$$p_{ud} = C_3 b \gamma z \qquad \textit{eq. 2.33}$$

Here C_1, C_2 and C_3 are coefficients that have to be determined from figure 2.11.

3. Develop *p-y* curves with:

$$p = A p_u \tanh\left(\frac{k_{py\,max}\, z}{A p_u} y\right) \qquad \textit{eq. 2.34}$$

Where A = 0,9 for cyclic loading and (3 – 0,8(z/b)) ≥ 0,9 for static loading. k_{py} Is found in figure 2.12.

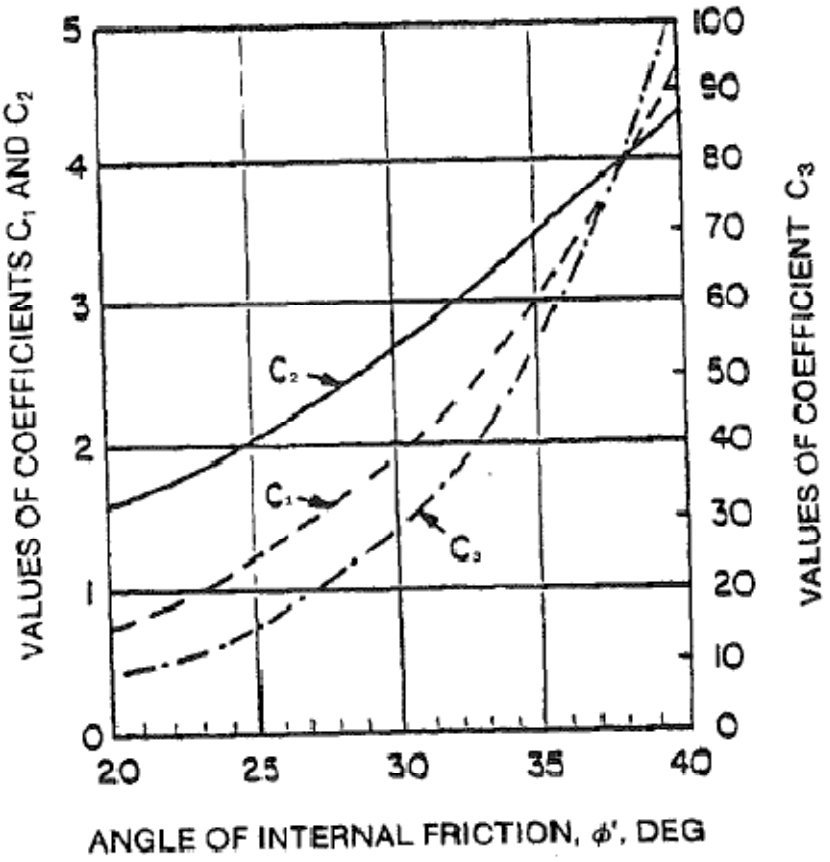

Figure 2-11 Values of coefficients of C_1, C_2 and C_3 versus the friction angle

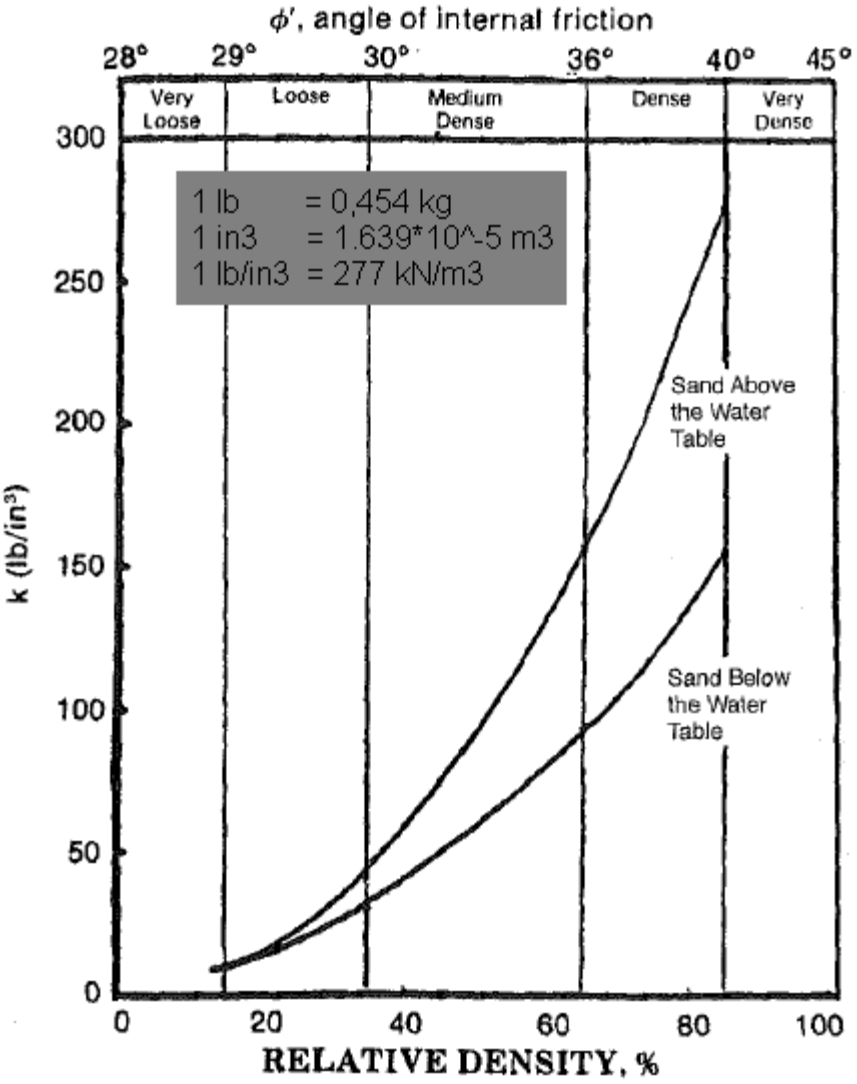

Figure 2-12 Graph to determine the initial stiffness for the p-y curve according to the API

Recommendations for p-y curves with cohesion and a friction angle

There are no available recommendations on developing *p-y* curves for soil with cohesion and a friction angle that are generally accepted. The following procedure for developing *p-y* curves is for short-term static loading and cyclic loading. The tests of Kuwait and Los Angeles, described in appendix B: Case XV and XVI allowed the development of the recommendations described below. However, it should be noted that the two field tests were not executed to examine the soil response. To do this a fully instrumented pile would have been needed.

The ultimate soil resistance is calculated as the passive earth pressure plus the sliding resistance on the sides of the pile minus the active soils pressure. The sliding resistance and the active soil pressure tend the cancel each other out. The recommended equation of the ultimate soil resistance is given in eq. 2.35.

$$p = \sigma_p D = C_p \sigma_h D \qquad \textit{eq. 2.35}$$

with:

σ_p = Passive pressure including three dimensional effect of wedge [kN/m^2]
D = Diameter / width pile [m]

and:

$$\sigma_h = \gamma z\, tan^2\left(45 + \frac{\varphi}{2}\right) + 2c \tan\left(45 + \frac{\varphi}{2}\right) \qquad \textit{eq. 2.36}$$

with:

σ_h The Rankine passive pressure for a wall with infinite length [kN/m^2]
γ Unit weight of soil [kN/m^3]
z Depth at which passive resistance is considered [m]
φ Friction angle [degrees]
c Cohesion [kN/m^2]
C_p Dimensionless modifying facto to account for the three dimensional effect of the wedge [-]

The factor C_p can be divided in two parts. $C_{p\varphi,}$ to modify the friction term of equation and C_{pc}, to modify the cohesion term. It is now possible to rewrite eq. 2.35:

$$p_{ult} = \left[C_{p\varphi}\gamma z\, tan^2\left(45 + \frac{\varphi}{2}\right) + C_{pc}c \tan\left(45 + \frac{\varphi}{2}\right)\right] D \qquad \textit{eq. 2.37}$$

Equation 2.37 will be rewritten as:

$$p_{ult} = A_s p_{ult\varphi} + p_{ultc} \qquad \textit{eq. 2.38}$$

The value of A can be obtained from figure 2-9. The friction component, $p_{ult\varphi}$, will be the smaller value of equations 2.22 and 2.23. The cohesion component, p_{ultc}, will be the smaller value of equations 2.4 and 2.5. Because the behavior of c-φ soil looks more like the behavior of cohesionless soils than the behavior of cohesive soil, the procedures described for sands by Reese *et al.* will be used to develop the *p-y* curves. An example curve is given in figure 2-13.

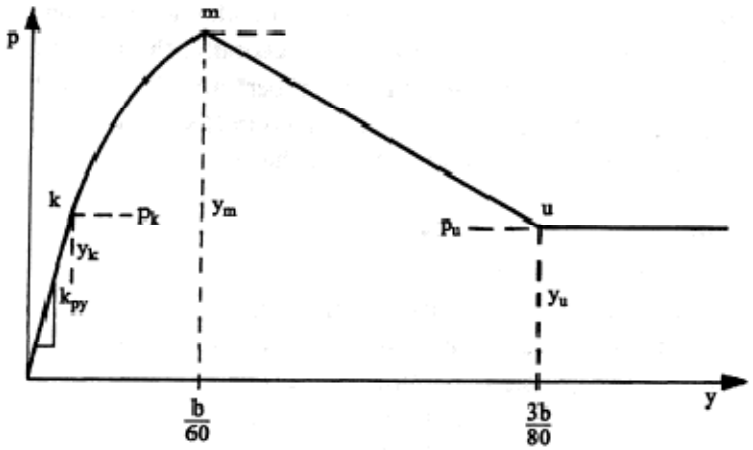

Figure 2-13 Characteristic shape of p-y curves for c-phi soil. (Reese & Van Impe, 2001, p. 92)

Procedure

1. Establish y_u as 3b/80 and compute p_{ult} with equation 2.38.

2. Compute y_m as b/60 and compute p_m with equation 2.25. Use in this case $p_{ult\varphi}$ for p_u. The two straight line portions beyond point m, figure 2-13, can now be established.
3. The initial straight line portion of the curve can be found with equations 2.39 and 2.40 and figures 2-14 and 2-15.

$$p = (k_{py}z)y \qquad \textit{eq. 2.39}$$

with:

$$k_{py} = k_c + k_\varphi \qquad \textit{eq. 2.40}$$

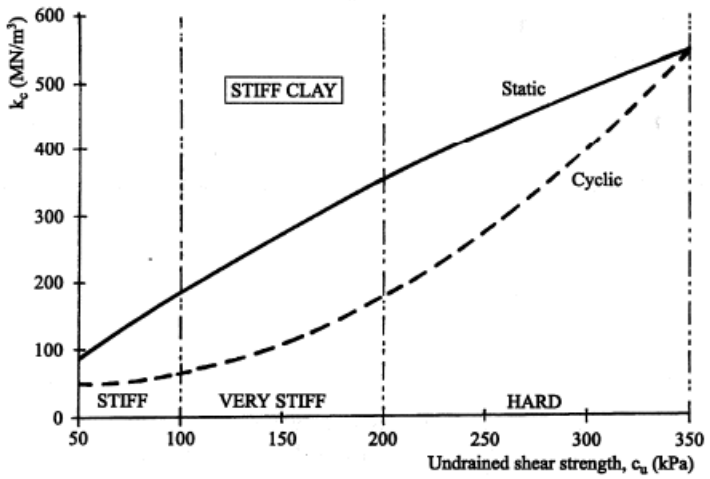

Figure 2-14 Values of k_c for cohesive soil. (Reese & Van Impe, 2001, p. 94)

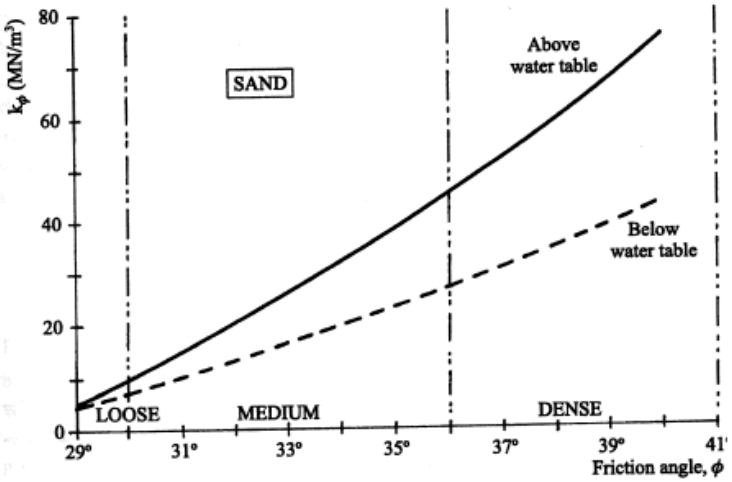

Figure 2-15 Values of k_φ for cohesionless soils. (Reese & Van Impe, 2001, p. 95)

4. The parabolic part of the p-y curve is established the same way as the parabolic part in the p-y curves for sands. Use equations 2.27 to 2.30. Determine point y_k with:

$$y_k = \left(\frac{C}{k_{py}z}\right)^{n/(n-1)} \qquad \textit{eq. 2.41}$$

2.2 CALCULATIONS

Calculations with the p-y curve method are bounded to be executed on a computer. The iterative procedure and complexity make manual calculation very hard and time-consuming. Of course calculation with the nondimensional method, chapter 4, is an option, but not for complex situations with layered soil and axial loads. Fortunately, several software packages are developed that make it possible to calculate the pile-soil behavior within seconds. Examples of such programs are LPile (LPILE Plus 5.0 for windows) and MPile (MPile, version 4.1, 3D modelling of single piles and pile groups).

The mathematical hearth of the Cap model in MPile (Bijnagte & Luger, MPile Version 4.1, 3D Analysis of single piles and pile groups, 2006) program will be used to describe the calculation procedure of the *p-y* method.

The lateral soil resistance in MPile is modeled as a number of parallel springs, which define *p-y* curves. To calculate the stiffness of the springs, the recommendations by the API are used. With the rules of the API, MPile separates *p-y* recommendations for five different cases: clay under a static lateral load, clay under a cyclic lateral load, sand under a static lateral load, sand under a cyclic lateral load and undrained sand under al lateral load. In MPile it is also possible to apply user defined *p-y* curves to manually model the soil stiffness. It should therefore also be possible to apply the curves proposed by Reese *et al.* into the program.

The calculation process is designed in such a way that, after several numerical iterations, equilibrium is reached between the mobilized soil resistance, caused by the deformation of the pile, and the load applied on the pile. To speed up the calculation MPile simplifies the *p-y* curves as they are recommended by the API. Instead of a curve, MPile generates five linear portions to approach the *p-y* curve before p_u is reached. In figure 2-13, the *p-y* curve for clays by the API is plotted together with the curve MPile uses. The values of the two curves match at a displacement of $0{,}1y_{50}$, $0{,}3y_{50}$, y_{50}, $3y_{50}$ and $8y_{50}$ m. In figure 2-14, the *p-y* curve for sands by the API is plotted together with the curve of MPile. The values of the two curves match at a displacement of $0{,}25y_{max}$, $0{,}5\ y_{max}$, y_{max}, $1.5\ y_{max}$ and $2.5\ y_{max}$ m. Here y_{max} is calculated with equation 2.42.

$$y_{max} = \frac{Ap_u}{k_{py}H} \qquad \textit{eq. 2.42}$$

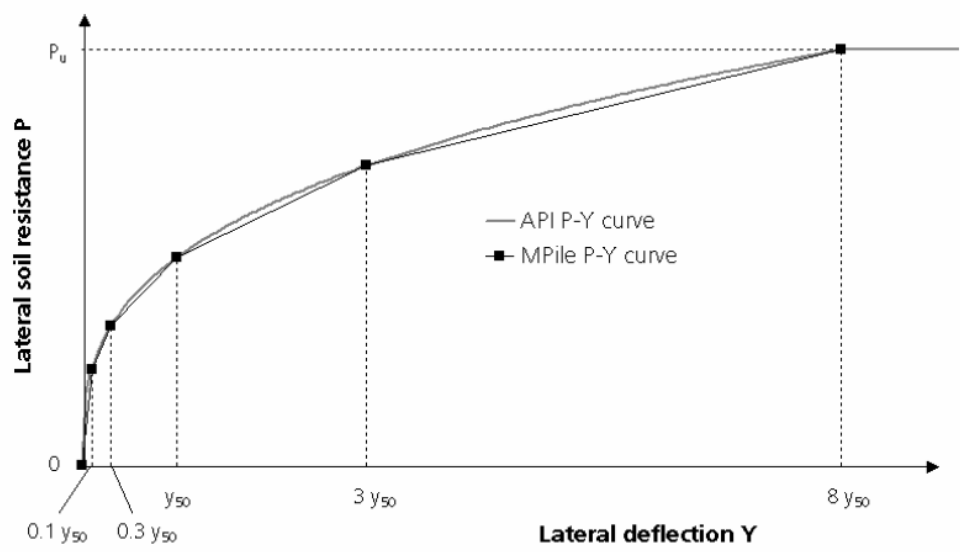

Figure 2-16 Modeling of p-y curve for clay and static loading (Bijnagte & Luger, MPile Version 4.1, 3D Analysis of single piles and pile groups, 2006)

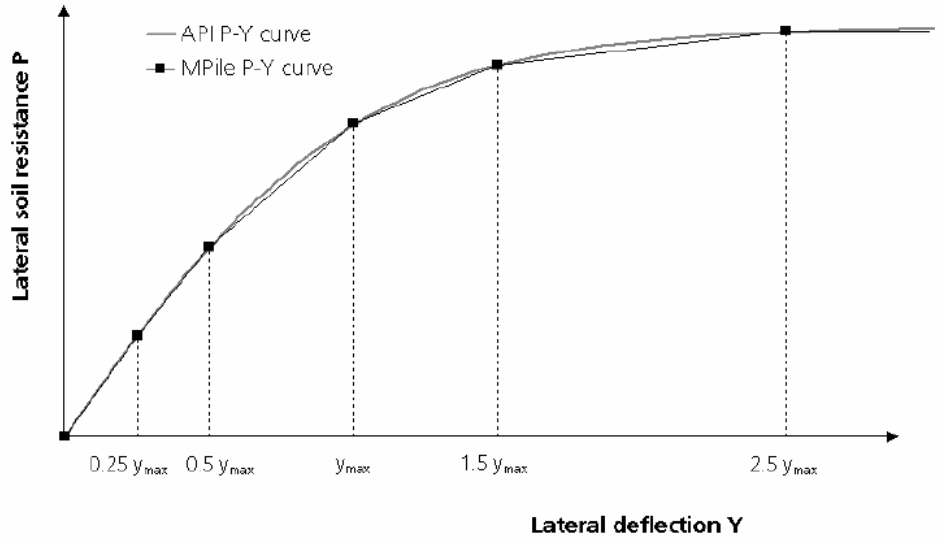

Figure 2-17 modeling of p-y curve for sand (Bijnagte & Luger, MPile Version 4.1, 3D Analysis of single piles and pile groups, 2006)

Now the spring stiffness is known the differential equation can be solved. The differential equation is formulates as stated below, eq. 2.43 (Reese, Isenhower, & Wang, 2006, pp. 382-386).

$$E_p I_p \frac{d^4y}{dx^4} + P_x \frac{d^2y}{dx^2} - p + W = 0 \qquad \textit{eq. 2.43}$$

with:

E_pI_p = Bending stiffness [kNm^2]

y = lateral deflection of the pile at a point x along the length of the pile [m]

P_x = axial load on the pile [*kN*]
p = soil reaction per unit length = $E_{py}y$ [*kN/m*]
W = Distributed load along the length of the pile [*kN/m*]

The assumption is made that a bar, figure 2-18, on an elastic foundation is subjected to horizontal loading and to a pair of compressive forces P_x acting in the center of gravity of the end cross section of the bar. If an infinitely small unloaded element bounded by two horizontals a distance *dx* apart is cut out of this bar the equilibrium of moments leads to the following equation:

$$(M + dM) - M + P_x dy - V_v dx = 0 \qquad \textit{eq. 2.44}$$

Or, if written in incremental form:

$$\frac{dM}{dx} + P_x \frac{dy}{dx} - V_v = 0 \qquad \textit{eq. 2.45}$$

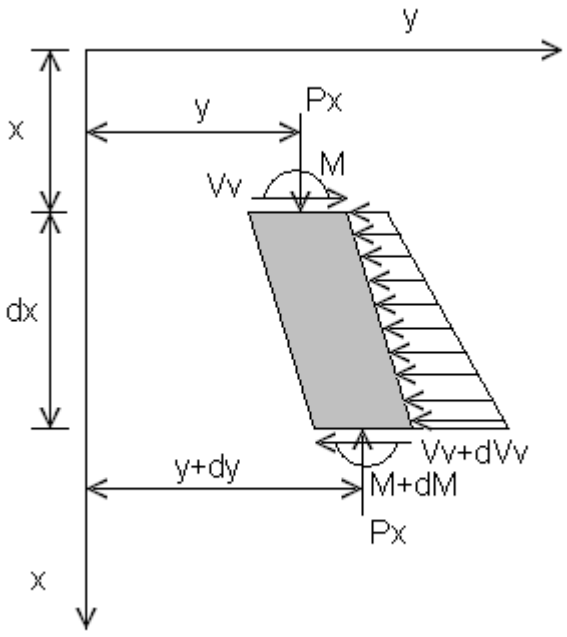

Figure 2-18 Element from a beam column

Differentiation of eq. 2.45 with respect to *x,* gives:

$$\frac{d^2M}{dx^2} + P_x \frac{d^2y}{dx^2} - \frac{dV_v}{dx} = 0 \qquad \textit{eq. 2.46}$$

The following identities are noted:

$$\frac{d^2M}{dx^2} = E_p I_p \frac{d^4y}{dx^4} \qquad \textit{eq. 2.47}$$

$$\frac{dV_v}{dx} = p \qquad \textit{eq. 2.48}$$

$$p = E_{py} y \qquad \textit{eq. 2.49}$$

Substituting these values in eq. 2.46 gives:

$$E_p I_p \frac{d^4 y}{dx^4} + P_x \frac{d^2 y}{dx^2} - E_{py} y = 0 \qquad \textit{eq. 2.50}$$

To allow a distributed force per unit length along the pile can be convenient for solving a number of practical problems. If the distributed force *W* is added to equation 2.50, the final differential equation, eq. 2.43 is obtained.

2.3 VALIDATION

The method of the *p-y* curves has been extensively validated. But remarks must be made. The curves of Reese and the API are based upon measurements of full-scale tests. All recommendations both by Reese and the API are based on single field tests. (This means that for the recommendations for *p-y* curves on, for instance, saturated clay depend fully on a single field test.) To validate the model the measurements of other tests should be compared with calculated values. To validate MPile, as a software program, it is allowed to compare the outcome of MPile with the measurements that were the basis of creating the API recommendations. The results of this comparison, performed by MPile (Bijnagte & Luger, MPile Version 4.1, 3D Analysis of single piles and pile groups, 2006), are given in figure 2-19. As expected, the calculations and measurements agree almost exactly. This validates that the MPile software is correctly programmed.

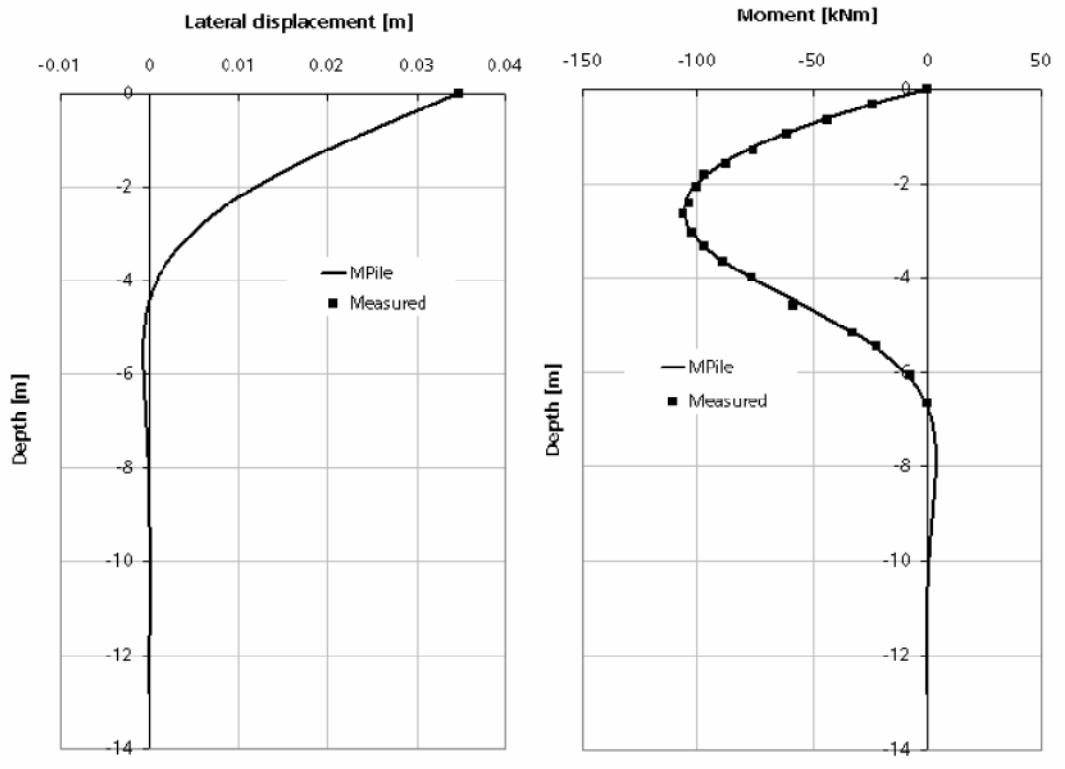

Figure 2-19 Measured and calculated values for displacement and moment at test pile Lake Austin

Apart from validating the software also the basis of the model, namely the *p-y* curve has to be checked. A lot of comparative calculations have been made (Reese & Van Impe, 2001, pp. 259-299). Here it is concluded that agreement between the computed maximum bending moment and the maximum moment from experiments is “excellent”. A review of all of the curves showing computed and experimental deflections shows that, in general, the computation yields acceptable results. However in the cyclic loading cases in soft clays, the deflections where highly underestimated. If deflections are the critical parameter, the engineer might wish to execute field tests.

2.4 LIMITATIONS

The method of the p-y curves is used in the Cap model of MPile. This software package is used in the calculations. The possibilities and limitations of the p-y model are thereby also influenced by the software. The limitations of the MPile software are according to the manual (Bijnagte & Luger, MPile Version 4.1, 3D Analysis of single piles and pile groups, 2006):

- In general
  - The unit weight of water cannot be changed, but is set to 9,81 kN/m^3.
  - A horizontal groundwater level is assumed within each soil profile.
- On soil behavior
  - The program does not support sloping ground surface. (But can be simulated by manual p-y curve input.)
  - No excess pore pressures can be applied, except by manually defining *p-y* curves.
  - K_0, the coefficient of horizontal effective stress over vertical effective stress is constant with depth within each soil layer.
- On loading types
  - Loads are static, except the dynamic load in the *Dynamic* model.
  - Loads/displacements, moments/rotations can only be applied to the top of the pile through the pile cap.
- On pile behavior
  - The pile is modeled as a linear elastic beam with compression and bending (no shearing), but may be build-up in sections with different dimensions and stiffness's.
  - Single piles have no torsion resistance.

3 BRINCH HANSEN - 1961

The method developed by Brinch Hansen (Brinch Hansen, 1961) is in essence the same type of model as the model developed by Blum. The method of calculating the ultimate soil resistance is different and more expanded. It is possible to use the model on layered and cohesive soils.

3.1 BACKGROUND

With the method proposed by Brinch Hansen the pile is assumed to be rigid and square (*B x L*). The driving depth is D_m. The horizontal force, *H*, is acting at a height, *A*, above the ground surface. The surface may be loaded with a surcharge, *P*. The soil properties consist of cohesion, *c*, friction angle, *φ*, the effective unit weight above the groundwater table, *y*, and the effective unit weight below the groundwater table, *y'*. The soil is assumed to be uniform. The effective vertical overburden pressure at depth *D* is:

$$q_D = P + yD_d + y'D_s \qquad eq.\ 3.1$$

In *eq. 3.1* D_d is the depth above the groundwater table. D_s Is the depth below the groundwater table. It is assumed that the rigid pile rotates around a point that is located at depth D_r.

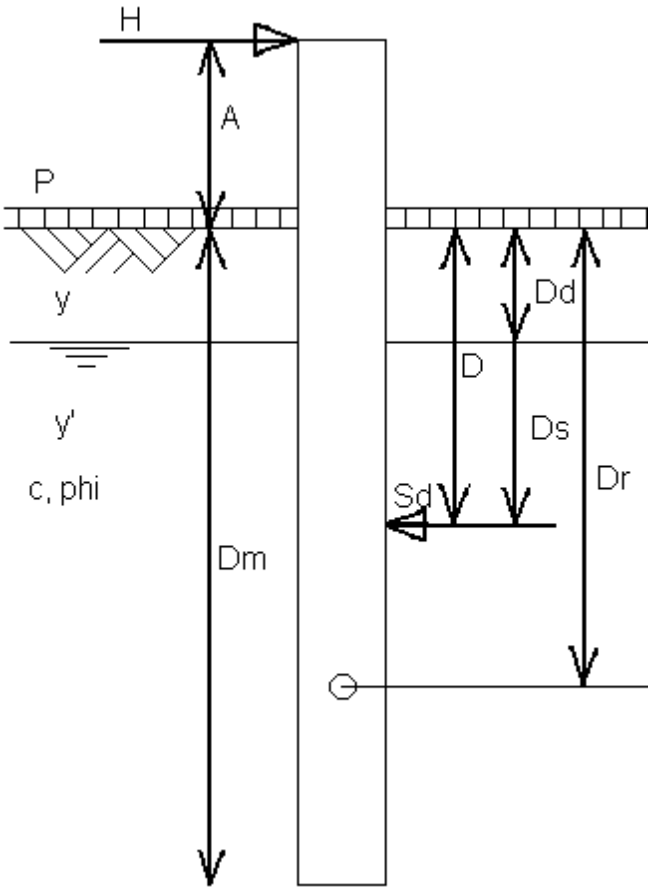

Figure 3-1 Schematization lateral loaded pile, according to Brinch Hansen – Picture by J. Ruigrok

To calculate the resultant earth pressures (passive minus active earth pressures) at depth *D*, Brinch Hansen has developed a set of formulas. He separates the resultant earth pressure in two parts. One caused by the vertical effective overburden pressure and the other by the cohesion of the material. The general formula is:

$$e^D = qK_q^D + cK_c^D \qquad eq.\ 3.2$$

e^D = Resultant horizontal pressure [kN/m^2]
q = Effective vertical overburden pressure [kN/m^2]
K^D_q = Resultant earth pressure coefficient caused by the vertical effective overburden pressure [-]
c = Cohesion [kN/m^2]
K^D_c = Resultant earth pressure coefficient caused by the cohesion [-]

Now Brinch Hansen considers K^D_q and K^D_c for three different depths. First, the earth pressure coefficients at ground level are determined. Second, for moderate depths. And third, for great depths. After this the values are elaborated and formulas that combines the three situations are established in such a way that the coefficients can easily be found at every depth.

Pressure at ground level
At ground level, the earth pressure coefficient K^0_q takes both passive and active earth pressures into account. But for the coefficient K^0_c only the passive earth pressure is taken into account. This is done to be on the safe side, because this might otherwise lead to negative earth pressures on the active side of the pile.

$$e^0 = qK_q^0 + cK_c^0 \qquad \textit{eq. 3.3}$$

$$K_q^0 = e^{\left(\frac{\pi}{2}+\varphi\right)\tan(\varphi)} \cos(\varphi) \tan\left(\frac{\pi}{4}+\frac{\varphi}{2}\right) - e^{\left(-\frac{\pi}{2}+\varphi\right)\tan(\varphi)} \cos(\varphi) \tan\left(\frac{\pi}{4}-\frac{\varphi}{2}\right) \qquad \textit{eq. 3.4}$$

$$K_c^0 = \left[e^{\left(\frac{\pi}{2}+\varphi\right)\tan(\varphi)} \cos(\varphi) \tan\left(\frac{\pi}{4}+\frac{\varphi}{2}\right) - 1\right] \cot(\varphi) \qquad \textit{eq. 3.5}$$

Pressure at moderate depth
For the resultant pressures at moderate depth Brinch Hansen uses the passive Rankine state. If the pile is pushed horizontally the soil will fail over a diagonal slip surface from depth D to the earth surface.

Pressure at great depth
At great depth slip surfaces will not go up to the ground surface, but they will go horizontally around the pile. The following formulas are found for the earth pressure coefficients:

$$K_c^\infty = N_c d_c^\infty \qquad \textit{eq. 3.6}$$

$$K_q^\infty = K_c^\infty K_0 \tan(\varphi) \qquad \textit{eq. 3.7}$$

$$N_c = \left[exp^{\pi \tan(\varphi)} tan^2\left(\frac{\pi}{4}+\frac{\varphi}{2}\right) - 1\right] \cot(\varphi) \qquad \textit{eq. 3.8}$$

$$d_c^\infty = 1.58 + 4.09 tan^4(\varphi) \qquad \textit{eq. 3.9}$$

Pressure at arbitrary depth – combining the formulas

Two formulas are needed to find K^D_q and K^D_c that must fulfill the condition for $D \rightarrow 0$, that $K^D \rightarrow K^0$ and for $D \rightarrow \infty$, that $K^D \rightarrow K^\infty$. Brinch Hansen presents the following formulas which fulfill these criteria.

$$K_q^D = \frac{K_q^0 + K_q^\infty \alpha_q \frac{D}{B}}{1 + \alpha_q \frac{D}{B}} \qquad \textit{eq. 3.10}$$

$$\alpha_q = \frac{K_q^0}{K_q^\infty - K_q^0} \frac{K_0 \sin(\varphi)}{\sin\left(\frac{\pi}{4} + \frac{\varphi}{2}\right)} \qquad \textit{eq. 3.11}$$

$$K_c^D = \frac{K_c^0 + K_c^\infty \alpha_c \frac{D}{B}}{1 + \alpha_c \frac{D}{B}} \qquad \textit{eq. 3.12}$$

$$\alpha_c = \frac{2K_c^0}{K_c^\infty - K_c^0} \sin\left(\frac{\pi}{4} + \frac{\varphi}{2}\right) \qquad \textit{eq. 3.13}$$

With the coefficients, K^D_q and K^D_c, the horizontal stresses at every depth can be calculated with the general formula.

3.2 VALIDATION

The validation of the model of Brinch Hansen was performed by N.H. Christensen (Christensen, 1961). He performed 26 pile load tests on wooden piles. He found that the model of Brinch Hansen was in most of the situations a little on the safe side. It must be noted however that the used piles were scaled. The cross-section of the pile was 5x5cm and the penetration depth varied from 25 to 50cm.

3.3 CALCULATIONS

Like the calculations of Blum the calculations of Brinch Hansen can go two ways. One can either calculate the maximum horizontal force on a pile, or it is possible to calculate the minimum penetration depth of the pile, if the horizontal force is given.

Calculation of the maximum load H

The point of application of the load above the soil surface, *A,* the width of the

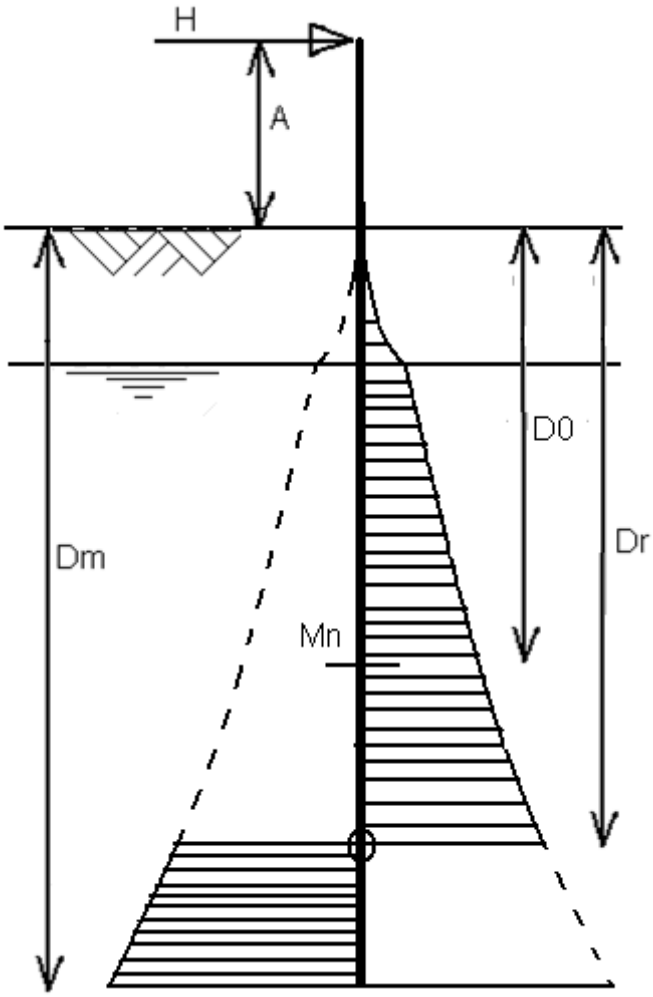

Figure 3-2 Schematization stresses on pile according to Brinch Hansen – figure by J. Ruigrok

pile and the driving depth D_m are given. The unknowns are the point of rotation and the maximum horizontal force. These are determined by two equilibrium conditions. First D_r is fixed, by trial, in such a way that the two pressure areas (above and below the rotation point) give an equal moment about the line of load *H*. Then the maximum force is found by horizontal load equilibrium. Thus, the maximum horizontal load is the difference between the two pressure areas.

Calculation of the penetration depth of the pile, Dm

The unknowns are the driving depth D_m and the rotation point D_r. *H* and *A* should be known. First, the depth D_0 of the maximum moment, i.e. the depth where the transversal force is zero, is calculated. The soil pressure above this point should be equal to the horizontal force. Then the moment M_n is calculated at this point. Finally, the driving depth and the depth of the rotation centre should be found in such a way that the two additional pressures (the area between depth D_0 and D_r and the area below depth D_r) are numerically equal and give a moment equal to M_n. This is an iterative process.

3.4 LIMITATIONS

The limitations of Brinch Hansen's theory are:

- In general
  - Only capable to find the ultimate resistance of the soil
  - No calculations possible under working loads
  - Not possible to calculate deflection. The moments along the pile can be calculated, but to get to deflection the moments should be integrated twice. This imposes two more unknowns. Brinch Hansen only has one boundary condition that is that the displacements of the rotation point are zero. Other boundary conditions are not given by Brinch Hansen.
  - The model was validated on scaled wooden piles.
- On soil behavior
  - No time dependent behavior
  - No nonlinear soil behavior
- On loading types
  - No cyclic loads
  - No axial load (although it is possible by adapting the formulas)
- On pile behavior
  - No differences of the bending stiffness over the height of the pile (although it is possible by adapting the formulas)
  - Bending stiffness independent of moment

4 ANALYSIS WITH NONDIMENSIONAL CHART - 1962

This model, developed by Matlock and Reese, (Reese, Isenhower, & Wang, 2006), is based on *p-y* curves and numerical solutions were obtained by hand-operated calculators. Examination of the analytical parameters in the numerical solutions led to the proposal of a formal analytical procedure for $E_{py} = k_{py}x$ (Reese & Matlock, 1956) and later to the use of nondimensional methods to develop a wide range of solutions for a pattern of variations of E_{py} with depth (Matlock & Reese, 1962).

4.1 BACKGROUND

Engineers understood many years ago, that the physical nature of soils led to the argument that E_{py} should be zero at the mudline and increase linearly with depth.

$$E_{py} = k_{py}x$$

The following equations can be derived by numerical analysis for the case where stiffness of the soil increases linearly with depth. A lateral load may be imposed at the pile head, and the length of the pile may be considered.

$$y = A_y \frac{P_t T^3}{E_p I_p} + B_y \frac{M_t T^2}{E_p I_p} \qquad S = A_s \frac{P_t T^2}{E_p I_p} + B_s \frac{M_t T}{E_p I_p} \qquad M = A_m P_t T + B_m M_t$$

$$V = A_v P_t + B_v \frac{M_t}{T} \qquad T = \sqrt[5]{\frac{E_p I_p}{k_{py}}} \qquad Z_{max} = \frac{L}{T}$$

Where:

y = Deflection [m]
S = Slope [*degree*]
M = Moment [kNm]
V = shear [kN]
T = Relative stiffness factor [m]
P_t = Applied lateral load at pile head [kN]
M_t = Applied moment at pile head [kNm]
A_y, B_y, A_s, B_s, A_m, B_m, A_v, B_v = nondimensional parameters for respectively: deflection by lateral load, deflection by moment, slope by lateral load, slope by moment, moment by lateral load, moment by moment, shear by lateral load and shear by moment.

Nondimensional are given in figures 4-1 to 4-8 on the following pages.

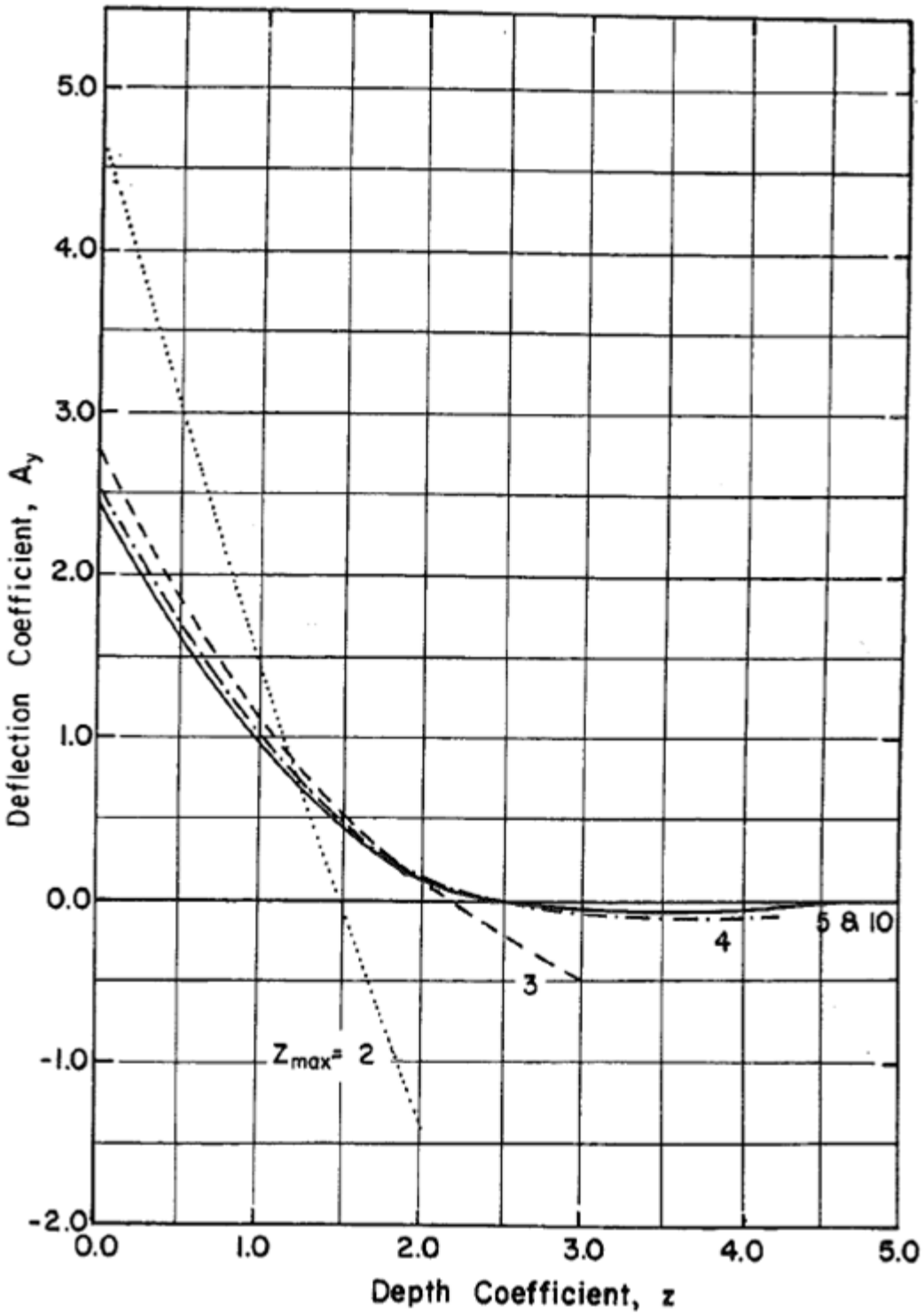

Figure 4-1 Pile deflection produced by a lateral load at the mudline

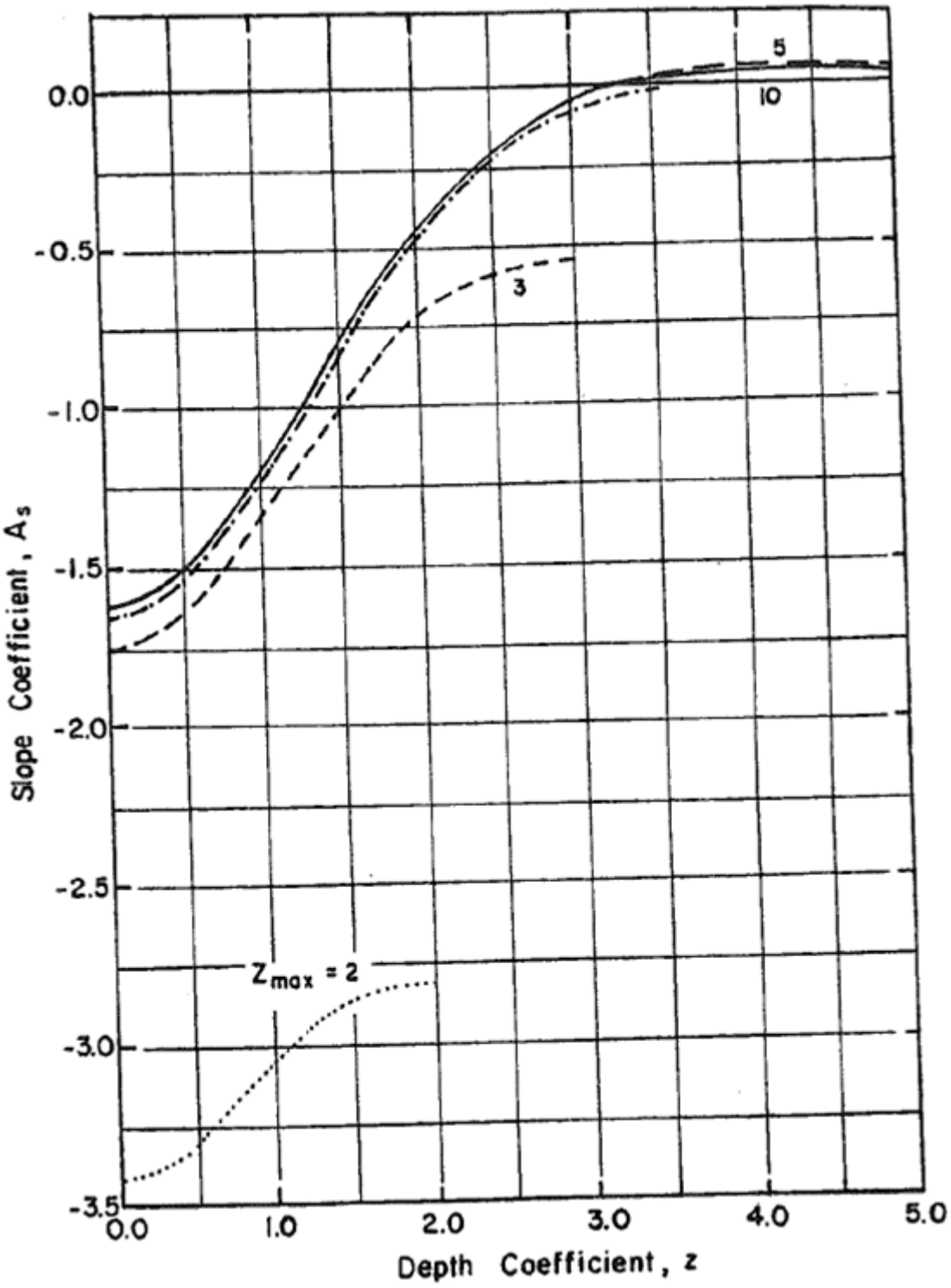

Figure 4-2 Slope of a pile caused by a load at the mudline

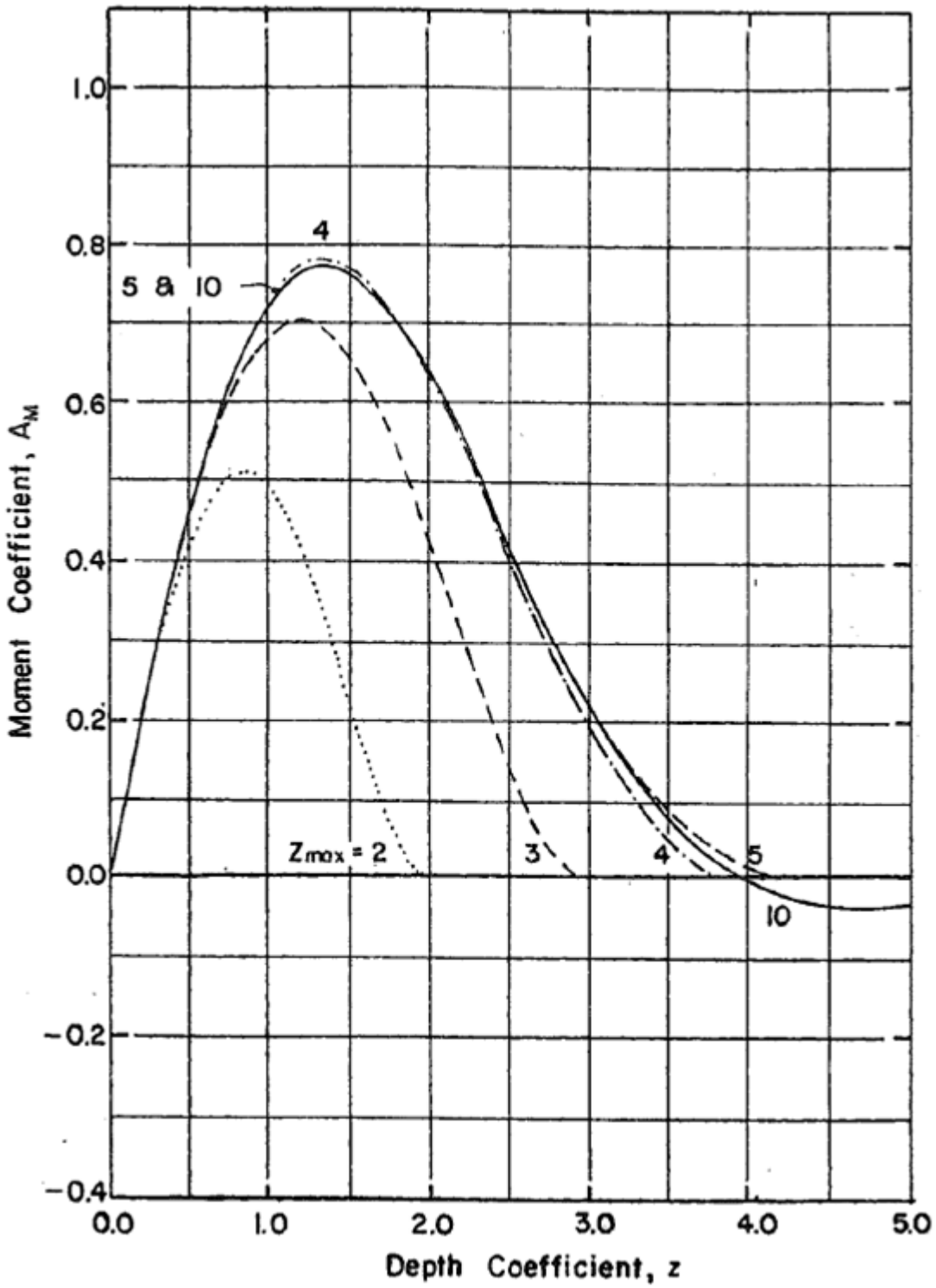

Figure 4-3 Bending moment caused by a lateral load at the mudline

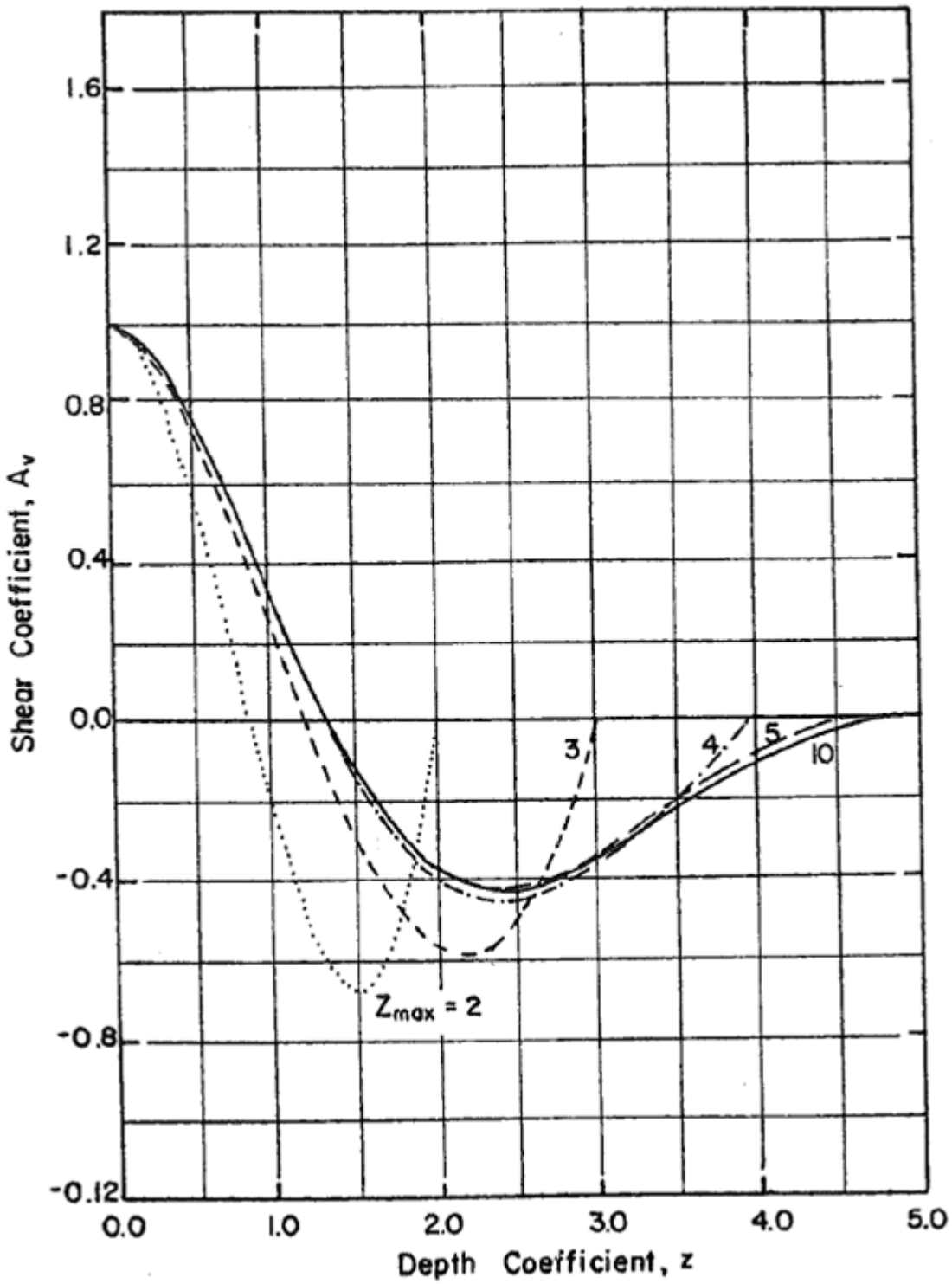

Figure 4-4 Shear produced by a lateral load at the mudline

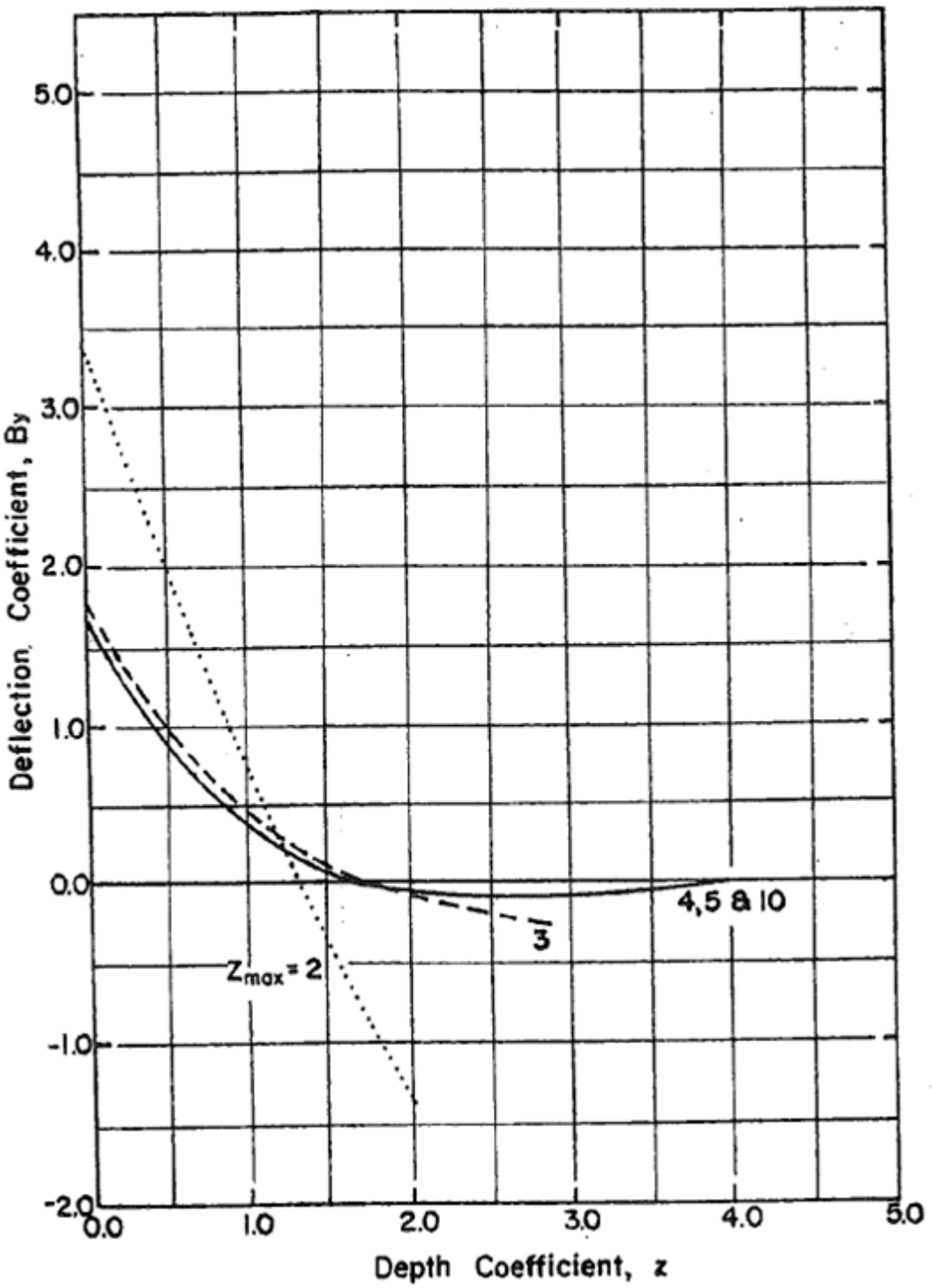

Figure 4-5 Deflections caused by a moment at the mudline

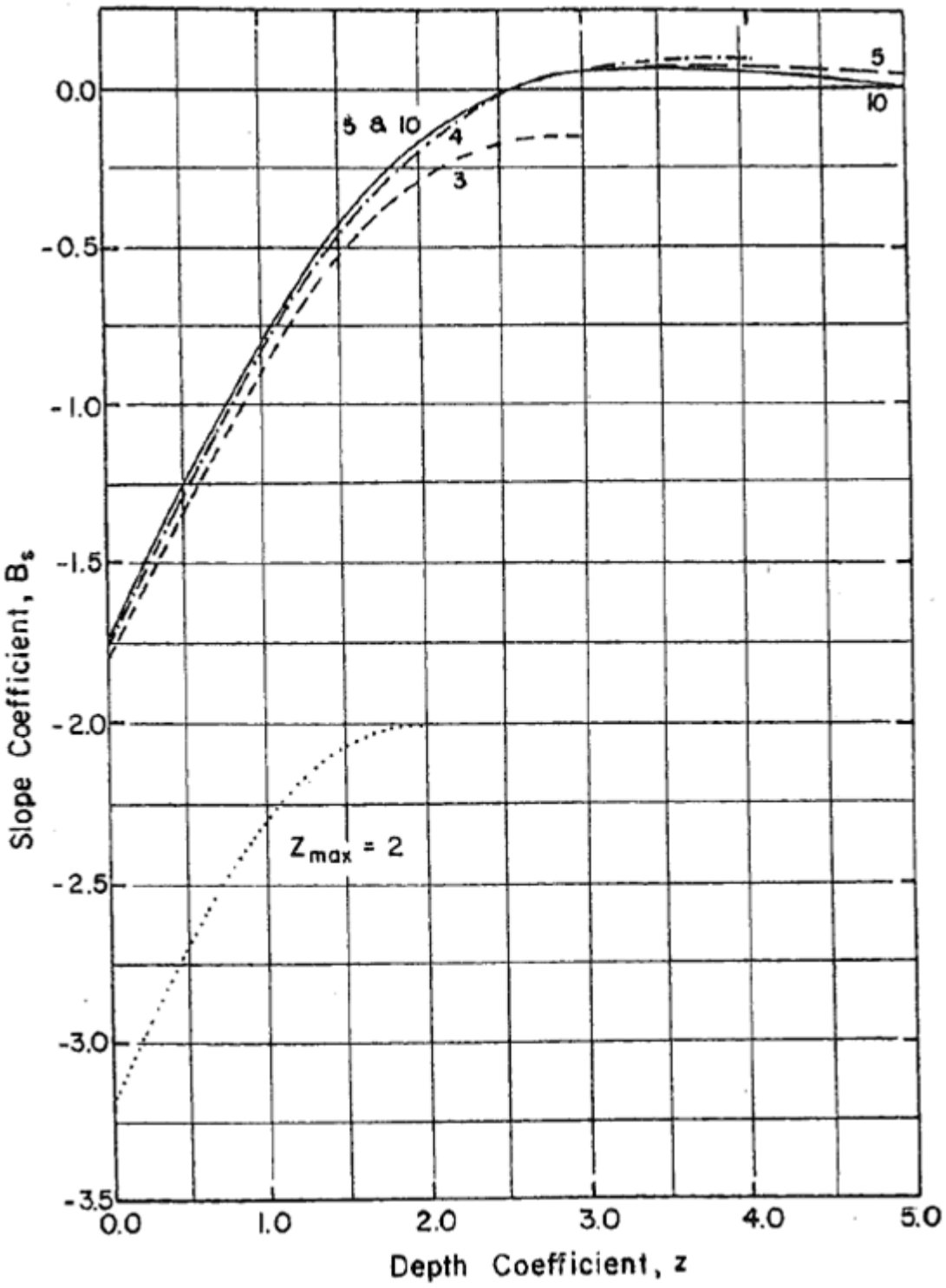

Figure 4-6 Slope of a pile caused by a moment at the mudline

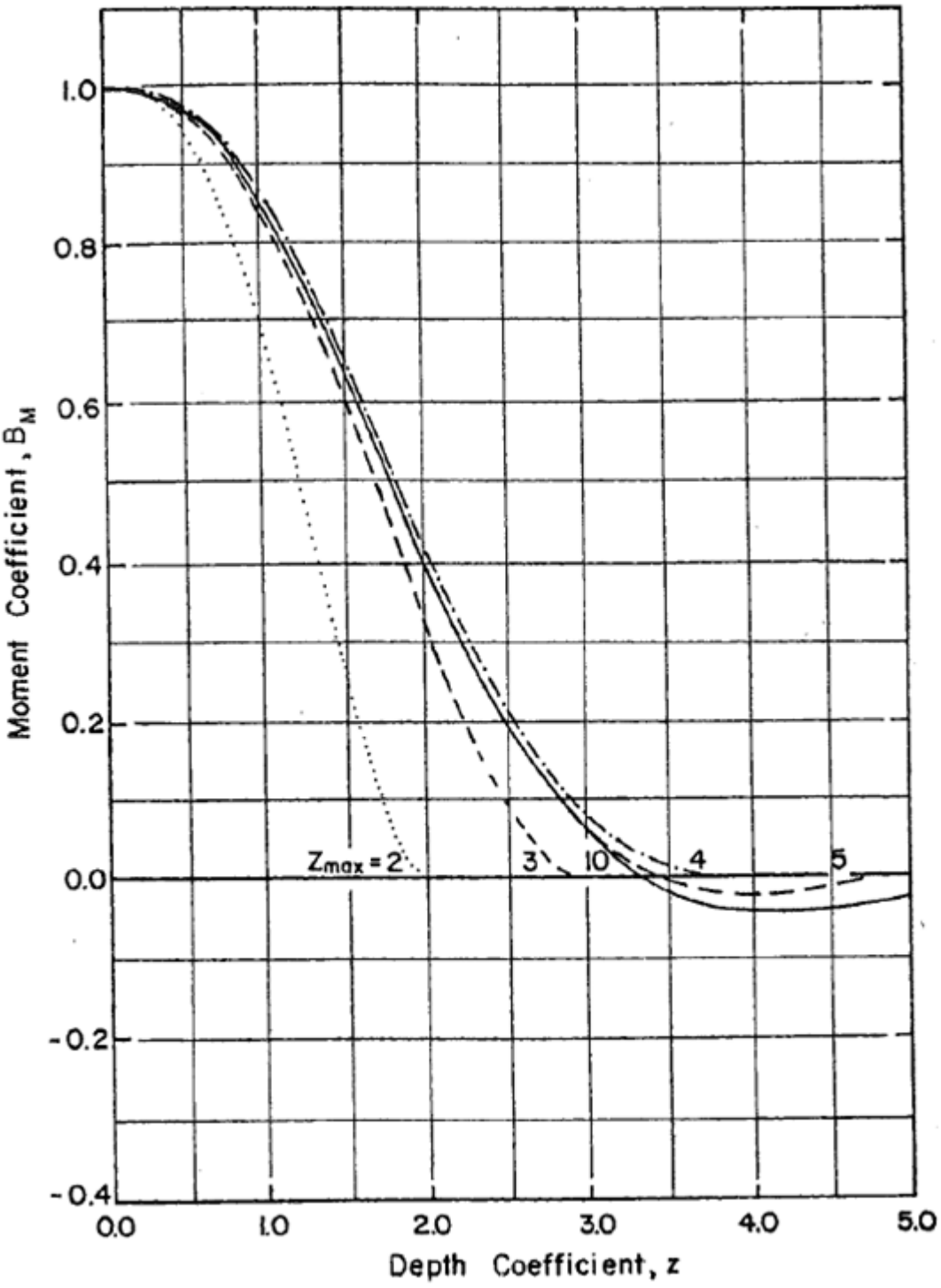

Figure 4-7 Bending moment produced by a moment at the mudline

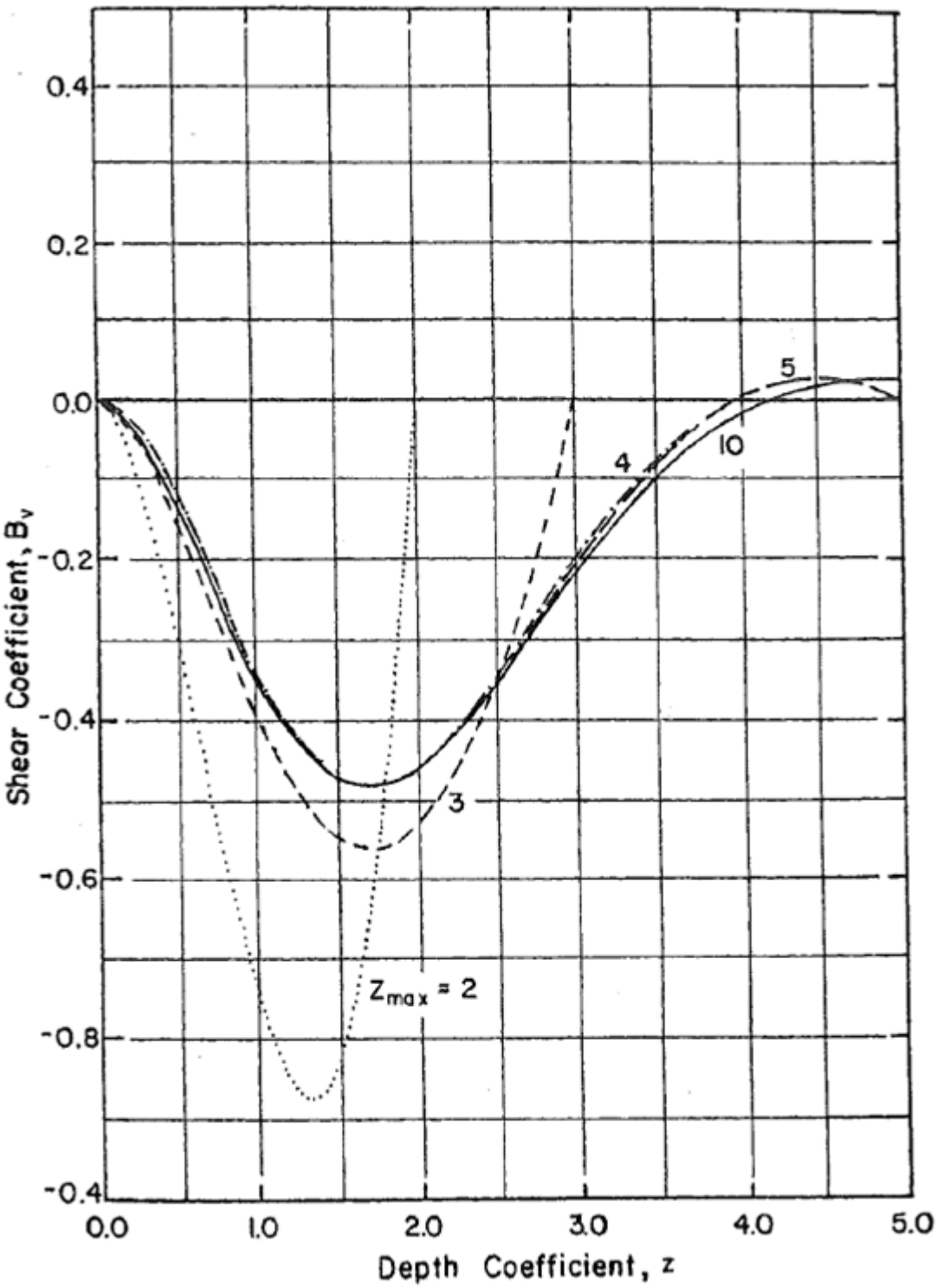

Figure 4-8 Shear produced by a moment at the mudline

4.2 VALIDATION

The nondimensional method has been created with the use of numerical solutions. The model is validated on those solutions, figure 4-9. The values of deflection for the top of the pile obtained with the nondimensional method and computer calculations that use the *p-y* method are in reasonable agreement. The values and location of the maximum moment agree almost exactly. The numerical solutions on itself are checked thoroughly. This is stated in Chapter 2 – validation.

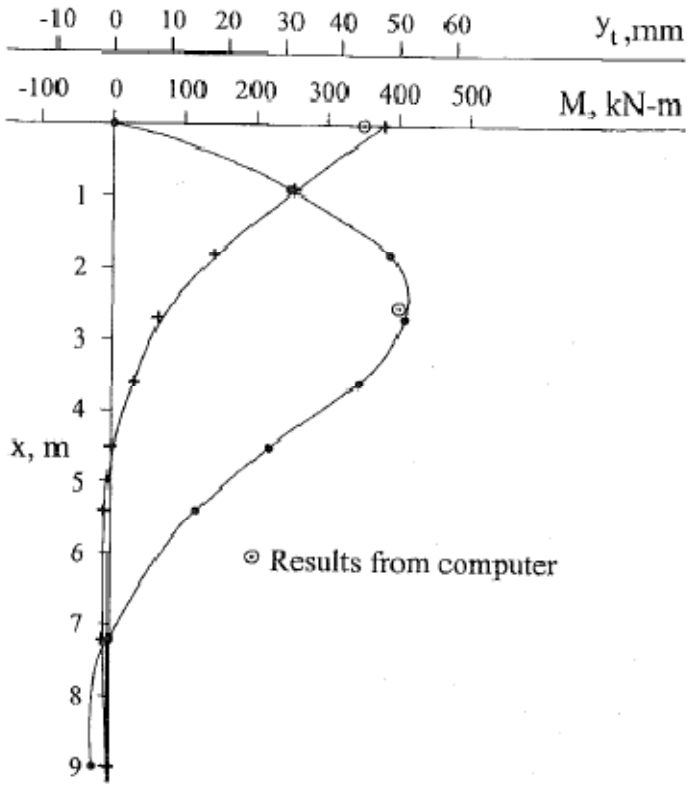

Figure 4-9 Computed values of deflection and maximum bending moment for an example problem - (Reese, Isenhower, & Wang, 2006, p410)

4.3 CALCULATIONS

Compared with the computer calculations, the nondimensional method is time consuming and tedious. This, because the values must be estimated from curves and the nonlinearity of the problem requires iteration. The method is valuable, because computer calculations can be checked and the solution gives good insight into the problem.

To start the calculation a family of *p-y* curves has to be developed. How to do this is written in chapter 2 of the literature and abstracts. Next, assume a value of T, T_{tried}. Then calculate Z_{max} to select the curve to use in the nondimensional plots. (See plots on the bottom of this summary.) Now, compute a trial deflection of the pile using equation for *y*. Now with the *p-y* curves determine the corresponding *p*. By dividing *p* with *y*, E_{py} is obtained for every depth a *p-y* curve is generated. Now all the values E_{py} are plotted versus the depth. $E_{py}=k_{py}x$, the line through the values should be linear and pass through the origin. The slope of the graph is k_{py}. With this value and the formula for *T*, a new value for *T*, $T_{obtained}$, can be calculated. If, $T_{obtained} \neq T_{tried}$, the procedure must be repeated with another value of T_{tried}. This is the iteration needed because

of the nonlinearity of the soil. The iteration procedure can be speed up by finding the intersection between the line connecting two iterations and the line, $T_{tried} = T_{obtained}$, figure 4-10.

With *T* known, the correct curves for the nondimensional parameters can be selected and *y* and *M* can be calculated.

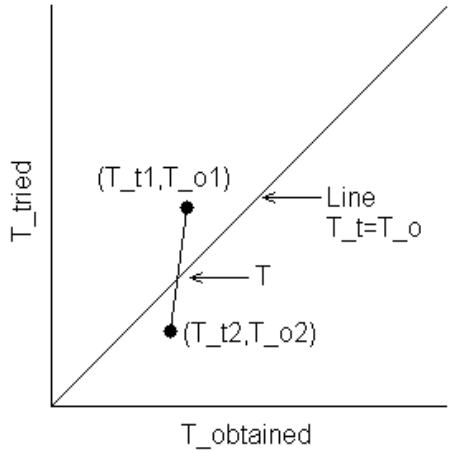

Figure 4-10 Method of iteration for the Nondimensional method – Picture by J.

4.4 LIMITATIONS

The limitations of the Nondimensional method are:

- In general
  - Tedious and iterative calculation procedure.
- On soil behavior
  - No layered soils
- On loading types
  - No axial load
- On pile behavior
  - No differences of the bending stiffness over the height of the pile
  - Bending stiffness independent of moment
  - No influence of diameter of the pile of the pile on the soil resistance

5 BROMS - 1964

The method developed by Broms (Broms, 1965) is used a lot outside of the Netherlands, especially for cohesive soils. Initially the method was developed for short, rigid and unfixed, piles in cohesive soils, but was expanded to long piles, fixed heads and cohesionless soils.

5.1 BACKGROUND

Broms introduces methods to calculate the ultimate lateral resistance. The assumption for short piles is that the ultimate lateral resistance is governed by the passive earth pressure of the surrounding soil. The ultimate lateral resistance for piles with large penetration depths is governed by the ultimate or yield resistance of the pile.

Ultimate lateral resistance cohesive soils: The lateral earth pressure acting at failure on a laterally loaded pile in a saturated cohesive soil is approximately $2C_u$ at the ground surface, in which C_u is the undrained cohesive strength as measured by undrained triaxial, direct shear or vane tests. The lateral reaction increases with depth and reach a maximum of eight to twelve times C_u at approximately three pile diameters below the ground surface. At failure, the soil located in front of the pile down to a depth of three pile diameters will move upwards and will cause the soil to heave in front of the pile. The soil located below three pile diameters will move laterally. The lateral soil reactions may be assumed zero down to a depth of 1,5 pile diameters and equal to $9C_uD$ below this depth.

Ultimate lateral resistance cohesionless soils: The ultimate lateral earth pressure at failure can be safely estimated as three times the passive Rankine earth pressure. It should be noted that available test data are limited and that additional data are required to use the proposed design method with confidence.

The ultimate lateral resistance of a laterally loaded pile is governed by the ultimate lateral resistance of the surrounding soil and by the moment resistance of the pile section. In the graphs the ultimate lateral resistance for both cohesive and cohesionless soil is shown both for free piles and restrained piles. The ultimate lateral resistance of short piles was found to be governed by the penetration depth of the pile and to be independent of the ultimate bending resistance of the pile section. The ultimate lateral resistance of long piles was found to be governed by the ultimate bending resistance of the pile section and to be independent of the penetration depth.

If it is not clear whether a pile is long or short, the pile should be checked on failure as being a short pile and as being a long pile.

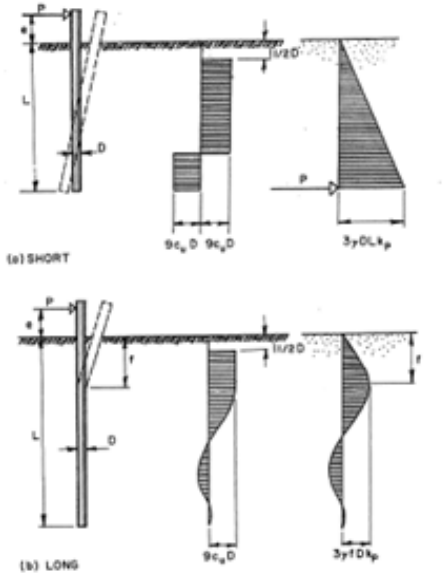

Figure 5-1 Failure modes for free piles

Calculation of the ultimate load, P_{ult}

To find the ultimate lateral load, for given dimensions of the (short) pile, use figure 5-3, for cohesive soils and figure 5-4, for cohesionless soils. Enter the proper graph on the *x-axis* by calculating the Length-Diameter, *L/D*, ratio. Then select the right graph based on the fixation at the ground line and the ratio between the eccentricity of the load and the diameter of the pile. Then the value at the *y-axis* can be determined. Multiplying this value with c_uD^2 for cohesive soils and with $K_pD^3\gamma$ for cohesionless soils gives the ultimate lateral load, P_{ult}.

To find the ultimate lateral load of the (long) pile corresponding to the yield moment, use *figure 5-5* for cohesive soils and figure 5-6 for cohesionless soils. Enter the proper graph on the *x-axis* where: M_{yield}/c_uD^3. Then select the right graph based on the fixation at the ground line and the ratio between the eccentricity of the load and the diameter of the pile. Then the value at the *y-axis* can be determined. Multiplying this value with c_uD^2 for cohesive soils and with $K_pD^3\gamma$ for cohesionless soils gives the ultimate lateral load, P_{ult}.

Because it is sometimes difficult to determine whether a pile is long or short the ultimate lateral load is found by taking the lesser outcome for P_{ult} of the two given procedures above.

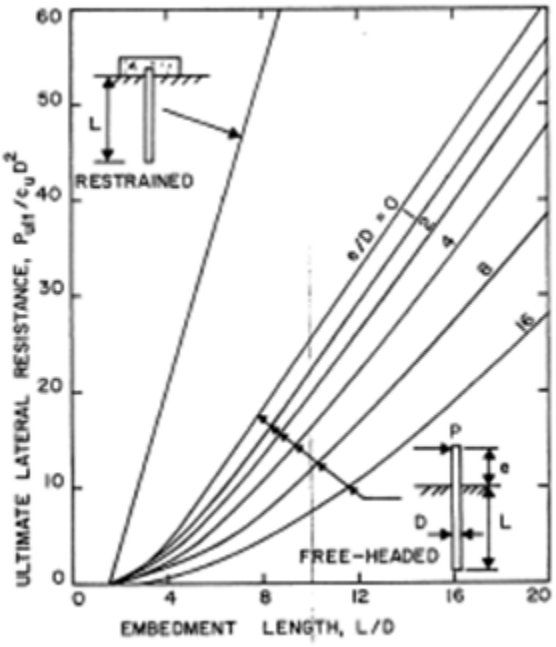

Figure 5-3 Ultimate lateral resistance for cohesive soils related to embedment length

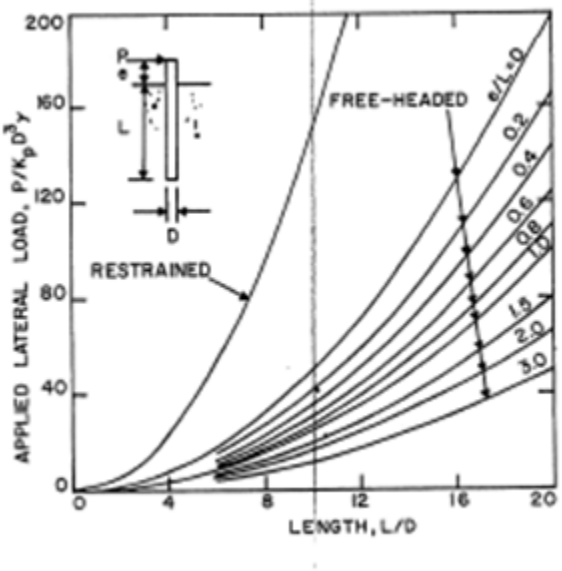

Figure 5-4 Ultimate lateral resistance for cohesionless soils related to embedment length

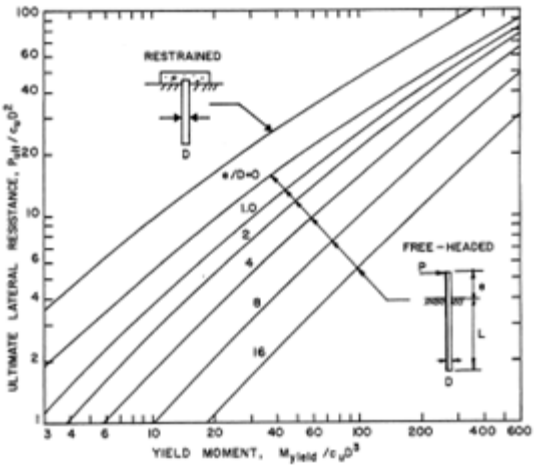

Figure 5-5 Ultimate lateral resistance for cohesive soils related to yield moment

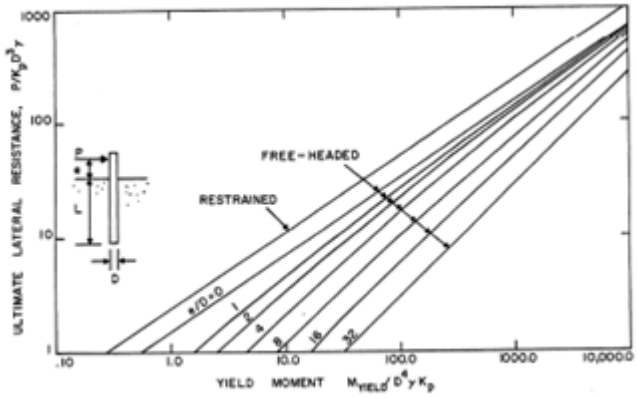

Figure 5-6 Ultimate lateral resistance for cohesionless soils related to yield moment

Lateral deflections according to Broms

At working loads (at approximately 0,5 – 0,3 times the ultimate lateral resistance) the lateral deflections can be estimated by assuming that the unit soil reaction, p, increases linearly with increasing lateral deflection.

$$p = k_h y \qquad \textit{eq. 3.1}$$

k_h = the modulus of horizontal subgrade reaction [kN/m^3]
p = unit soil reaction [kN/m^2]
y = lateral deflection [m]

Cohesive soil: At working loads the modulus of horizontal subgrade reaction can be assumed to be constant with depth. The dimensionless lateral deflections at the ground surface have been plotted in figure 9 as a function of the dimensionless length βL in which:

$$\beta = 4\sqrt{\frac{k_h D}{4EI}} \qquad \textit{eq. 3.2}$$

With βL it is possible enter the graph and calculate the deflections at ground level.

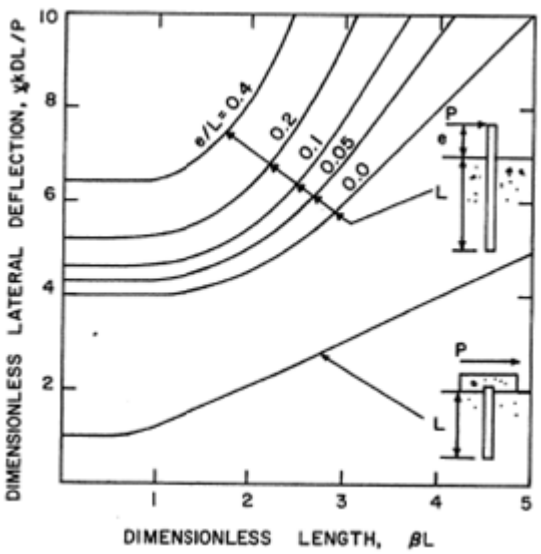

Figure 5-7 Lateral deflections at ground surface for cohesive soils

Cohesionless soil: The lateral deflections of a pile in a cohesionless soil can be calculated by assuming the modulus of subgrade reaction increases linearly with depth.

$$k_h = \frac{n_h z}{D} \qquad \textit{eq. 3.4}$$

k_h = the modulus of horizontal subgrade reaction [kN/m^3]
z= depth below ground surface [m]
n_h = coefficient that depends on the relative density of the soil [kN/m^3]
D = Diameter or side of loaded area [m]

The dimensionless lateral deflections at the ground surface have been plotted in figure 10 as a function of the dimensionless length ηL in which:

$$\eta = \sqrt[5]{\frac{n_h}{EI}} \qquad \textit{eq. 3.5}$$

With ηL it is possible enter the graph and calculate the deflections at ground level.

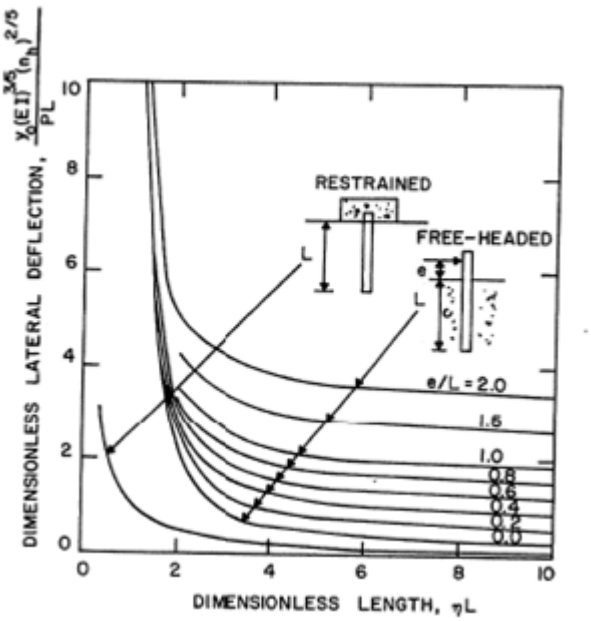

Figure 5-2 Lateral deflections at ground surface for cohesionless soils

For the calculation of β and η the values of k_h and n_h are difficult to determine. The suggested way to obtain these values is by means of full scale test on site. This is not really practical since you want to know the displacements on beforehand. Another approach, to calculate k_h, is from the vertical subgrade reaction.

$$k_h = \frac{0.4 k_0 D}{B} \qquad \textit{eq. 3.6}$$

With:
K_0 = vertical subgrade reaction [kN/m^3] for a square or circular plate with the side or diameter B [m]
D = diameter or side of loaded pile [m]

For n_h several guideline figures are given. If the groundwater table is located below the depth of $\eta L = 2$, n_h can be taken to be *7, 21* and *56 tons per cu ft* for respectively a loose, medium and dense sand. If the water is near or above the ground surface, one can take the values to be *60%* of the values given before.

5.2 VALIDATION

Broms divided the validation of his model. He validated his model separately for cohesionless and cohesive soils.

Cohesionless soils
For the lateral deflections Broms compared his calculation to actual measured deformations, (Broms, 1964 Lateral resistance of piles in cohesionless soils). He did this for 19 cases. He found that in nearly all cases that the calculated lateral deflection exceeded considerably the measured lateral deflection. The observation was made for single piles, pile groups, restrained

piles and unrestrained piles. Broms draws the conclusion that the values recommended by Terzaghi will in general over-estimate at working loads the deflections at the ground surface, and thus will yield results which are on the safe side, except for piles which have been placed by jetting.
For the ultimate resistance Broms compared his calculated values with measured values. He did this for 7 cases. The average measured ultimate lateral resistance exceeded the calculated resistances by more than 50%. The conclusion can be drawn that the ultimate lateral resistance of the piles is estimated conservatively by taking the ultimate lateral soil resistance as three times the Rankine lateral earth pressure.
Cohesive soils
Broms also compared his calculations with test results for cohesive soils, (Broms, 1964 Lateral resistance of piles in cohesive soils). For the lateral displacement he considered five separate cases. The measured lateral deflections at the ground surface varied between 0,5 to 3,0 times the calculated deflections. It should be noted that the calculated lateral deflections are for short piles inversely proportional to the assumed coefficient of subgrade reaction and thus to the measured average unconfined compressive strength of the supporting soil. Thus small variations of the measured average unconfined compressive strength will have large variations on the calculated lateral deflections. It should also be noted that the agreement between measured and calculated lateral deflections improves with decreasing shearing strength of the soil. According to Broms the test data indicate that the proposed method can be used to calculate the lateral deflections at working loads (at loads equal to 0,5 to 0,3 times the ultimate lateral capacity of the pile) when the unconfined compressive strength of the soil is less than *1,0 t/f*^{2} (*108 kN/m*^{2}). However if the unconfined compressive strength exceeds *1,0 t/f*^{2}, the actual deflections at the soil surface can be considerably larger than the calculated lateral deflections due to the erratic nature of the supporting soil.
Finally, the calculated ultimate bearing capacity for cohesive soils has been compared with measurements for three separate cases. This has been done by calculation of the maximum occurring moment in the pile. By entering the graph of *figure 3-5* on the *y-axis*, not with P_{ult}, but with the applied load P, the maximum moment along the pile can be found. The agreement between calculated and measured moment is good. The main reason for this outcome is that the bending moment is not really sensitive to small variations in the assumed distribution of lateral soil resistance or to small variations in the measured cohesive strength of the soil. The test data indicate that the proposed method of analysis can be used with confidence to predict the maximum bending moment for both restrained and unrestrained piles. However, it should be noted that the experimental verification was limited. Additional test data are desirable.

5.3 CALCULATIONS

Unlike Blum and Brinch Hansen, Broms provides a method that is fully capable of designing a pile on the two most important aspects. It can calculate the ultimate bearing capacity of the load, i.e. it can perform a calculation on strength. And it can predict the deformations under working loads, something the methods by Blum and Brinch Hansen are not capable of.
The method is used a lot internationally although the validation shows that the calculations of the deflections are not accurate.

5.4 LIMITATIONS

The limitations of Broms's theory are:

- In general
  - Calculations of deflection are merely indicative and only if the load is between 0,3 and 0,5 times P_{ult}.
- On soil behavior
  - No time dependent behavior
  - Only homogeneous soils
  - For sands a shell factor of 3 is used. Broms found that this was already too high. Keep in mind that for larger diameter piles the shell factor can be considerably lower
- On loading types
  - No cyclic loads
  - No axial load
- On pile behavior
  - No differences of the bending stiffness over the height of the pile
  - Bending stiffness independent of moment

6 CHARACTERISTIC LOAD METHOD - 1994

The characteristic load method, CLM, (Duncan, Evans, & Ooi, 1994) was developed to quickly design piles, which incorporate nonlinear behavior. Like the nondimensional method the CLM is based on nondimensional graphs which were deduced from numerous *p-y* analyses. The CLM is faster than the nondimensional method since the iterative character of the procedure is eliminated.

6.1 BACKGROUND

Deep foundations should satisfy three conditions. They must carry the imposed load. The deflection may not be larger than a maximum. The soil may not be loaded so heavily that it reaches its ultimate load carrying capacity.

Even though the ultimate carrying capacity of the soil is reached the soil response is nonlinear. Doubling of the load can result in a deflection that is four times as large and a maximum moment that is more than twice as large. This has two causes. One: The load deflection behavior of the soil around the pile is nonlinear. Two: As the strength of the upper part of the soil becomes mobilized, additional loads must be transferred to greater depth, where the strength of the soil is not yet mobilized to the same degree.

The *p-y* method appears to be the most practical and useful procedure for the design of deep foundations under lateral loading. The reaction of the soil is related to the deflection by means of *p-y* curves. The drawback of the method is the time required to develop input and perform the detailed computer analysis. There are situations where these detailed analysis are not warranted or needed, but answers are desired quickly that include the nonlinear behavior.

The characteristic load method was developed by performing nonlinear *p-y* analysis for a wide range of free- and fixed head piles and drilled shafts in clay and sand. The results were presented in the form of relationships, graphs, among dimensionless variables, figures 6.1 to 6.3. The method can be used to determine ground line deflections, maximum moments and the location of the maximum moment. The dimensionless variables are the lateral load P_t divided by a characteristic load P_c, the applied moment M_t divided by a characteristic moment M_c and deflections are divided by the pile width *D.* Below the formula's to calculate P_c and M_c. There are separate formulas for cohesive soils and cohesionless soils.

$$P_c = 7.34D^2\left(E_pR_I\right)\left(\frac{S_u}{E_pR_I}\right)^{0.68} \quad \textit{(Cohesive soils)} \qquad \textit{eq. 6.1}$$

$$P_c = 1.57D^2\left(E_pR_I\right)\left(\frac{\gamma\prime D\varphi\prime K_p}{E_pR_I}\right)^{0.57} \quad \textit{(Cohesionless soils)} \qquad \textit{eq. 6.2}$$

$$M_c = 3{,}86D^3\left(E_pR_I\right)\left(\frac{S_u}{E_pR_I}\right)^{0{,}46} \quad \textit{(Cohesive soils)} \qquad \textit{eq. 6.3}$$

$$M_c = 1{,}33D^3\left(E_pR_I\right)\left(\frac{\gamma\prime D\varphi\prime K_p}{E_pR_I}\right)^{0{,}40} \quad \textit{(Cohesionless soils)} \qquad \textit{eq. 6.4}$$

With:

P_c = Characteristic Load [*kN*]
M_c = Characteristic Moment [*kNm*]
D = Diameter Pile [*m*]
E_p = Pile or drilled shaft elasticity [kN/m^2]
R_I = Moment of inertia ratio = I_p / Icircular [m^4/m^4] $I_{circular} = \frac{\pi D^4}{64}$
S_u = Undrained shear strength of clay [kN/m^2]
y' = Effective unit weight of soil, which is total unit weight above ground water table and buoyant unit weight below ground water table [kN/m^3]
K_p = Rankine coefficient of passive earth pressure [-] $K_p = tan^2(45 + \frac{\varphi'}{2})$
φ' = Effective stress friction angle of sand [*degrees*]

Note: The soil near the top of the pile is most important with regard to response to lateral load. To calculate P_c or M_c, S_u and φ' should be averaged over a depth equal to *8D* below the ground surface.

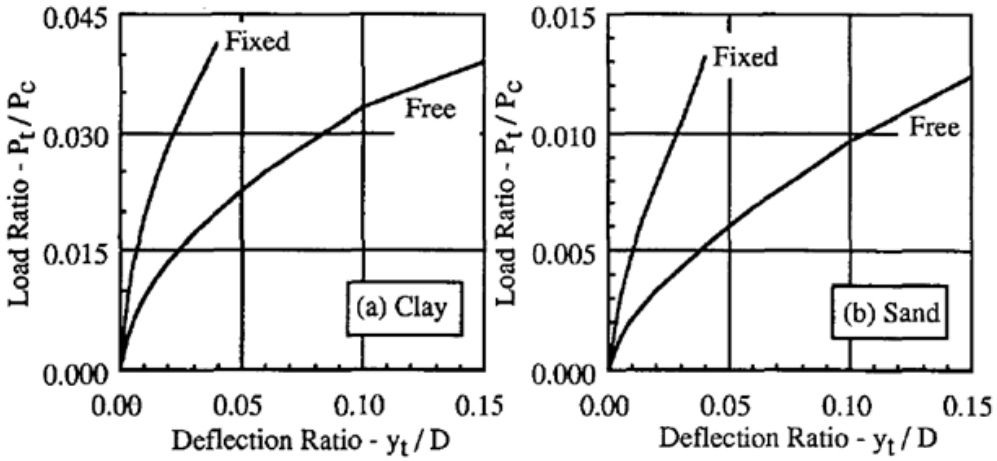

Figure 6-1 Load-deflection curves: (a) Clay; (b) Sand

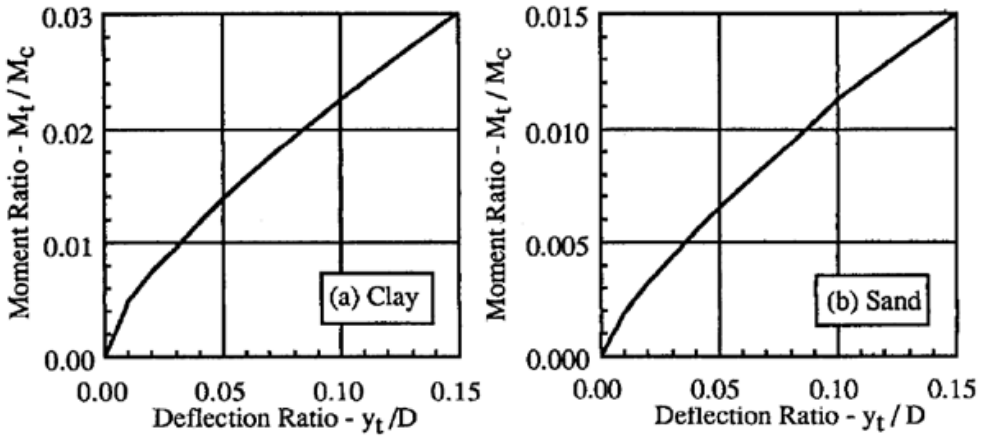

Figure 6-2 Moment-deflection curves: (a) Clay; (b) Sand

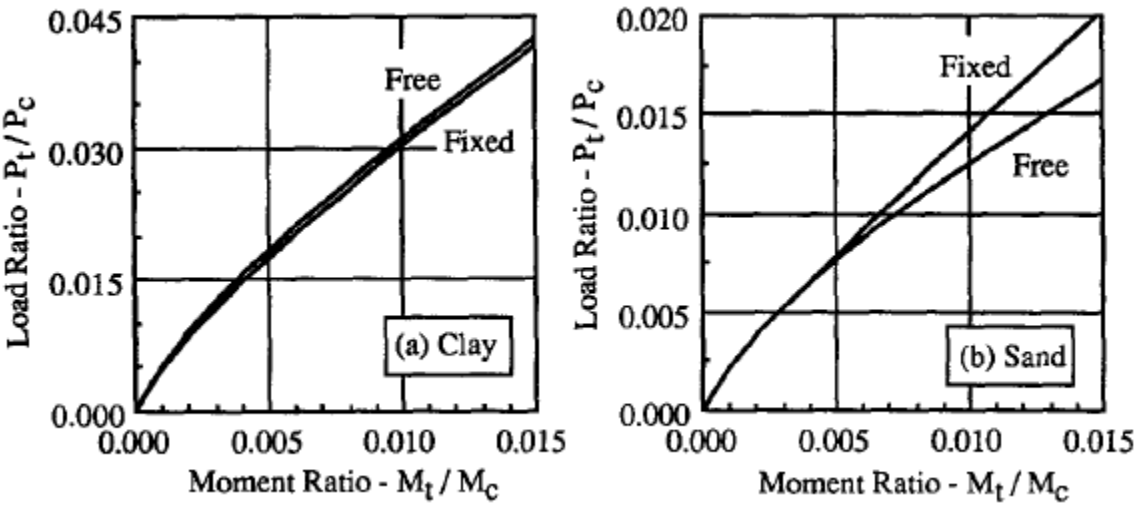

Figure 6-3 Load-moment curves: (a) Clay; (b) Sand

z/T (1)	A_m (2)	B_m (3)
0	0.00	1.00
0.5	0.46	0.98
1.0	0.73	0.85
1.3	0.77	0.73
1.5	0.76	0.64
2.0	0.63	0.40

Table 6-1 Moment coefficients A_m and B_m (after Matlock and Reese 1961)

Type of soil (1)	Criterion (2)	Minimum length (3)
Clay	$E_pR_I/S_u = 100{,}000$	6 diameters
Clay	$E_pR_I/S_u = 300{,}000$	10 diameters
Clay	$E_pR_I/S_u = 1{,}000{,}000$	14 diameters
Clay	$E_pR_I/S_u = 3{,}000{,}000$	18 diameters
Sand	$E_pR_I/(\gamma' D\phi' K_p) = 10{,}000$	8 diameters
Sand	$E_pR_I/(\gamma' D\phi' K_p) = 40{,}000$	11 diameters
Sand	$E_pR_I/(\gamma' D\phi' K_p) = 200{,}000$	14 diameters

Table 6-2 Minimum pile lengths for characteristic load method

6.2 VALIDATION

The CLM was derived from p-y analyses, therefore it can be expected that these two types of analyses would agree fairly closely when used to analyze the same conditions. However because of the simplifications in the CLM there are differences. Duncan *et al.* compared the results by both methods. The results are given in table 6-3. It can be concluded that for static loading on clay the results of the CLM approximate the p-y analysis closely, except in the case

of stiff saturated clay where the deformations were overestimated by a factor larger than two. For sands, the results calculated using the CLM are in fairly close agreement with the p-y analysis results for static and cyclic loads.

The CLM was also validated by comparing the results with a field load tests. The results of this test are given in figures 6-4 and 6-5. The first test, performed by Reese *et al.* (1975), was on a 641mm diameter pipe pile in stiff preconsolidated clay. In figure 6-4 it can be seen that the calculated values of lateral deflection are about 70% larger than those measured. The calculated values of maximum bending moment agree well with those measured. The second test, performed by Cox *et al.* conducted tests on steel pipe piles in clean fine sand to silty fine sand below water. From figure 6-5 it can be deduced that the calculated values of deflection are about 10% higher than the measured values. The calculated values of moment agree quite well with the measured values.

	P_t = 44.5 kN (10 kips)				P_t = 89.0 kN (20 kips)			
	y_t		M_{max}		y_t		M_{max}	
Method (1)	mm (2)	in. (3)	kN·m (4)	kip-in. (5)	mm (6)	in. (7)	kN·m (8)	kip-in. (9)
(*a*) Piles embedded in clay with S_u = 48 kPa (1,000 psf)								
Characteristic load	6.1	0.24	44	390	20.6	0.81	108	960
p-y, Soft clay, static	5.1	0.20	41	365	21.8	0.86	97	860
p-y, Soft clay, 10,000 cycles	5.1	0.20	41	365	21.8	0.86	97	860
p-y, Stiff clay above water, static	4.3	0.17	40	355	21.3	0.84	101	890
p-y, Stiff clay above water, 100 cycles	5.8	0.23	44	390	37.3	1.47	104	920
p-y, Stiff clay above water, 10,000 cycles	6.9	0.27	47	415	53.6	2.11	105	930
p-y, Stiff clay below water, static	3.8	0.15	39	342	8.6	0.34	84	740
p-y, Stiff clay below water, 100 cycles	Failure indicated	—	Failure indicated	—	Failure indicated	—	Failure indicated	—
(*b*) Piles embedded in sand with ϕ = 35 degrees								
Characteristic load	5.1	0.20	43	380	13.7	0.54	103	910
p-y, Static	5.1	0.20	44	390	14.0	0.55	105	930
p-y, 100 cycles	5.3	0.21	49	430	15.0	0.59	116	1,030
p-y, 10,000 cycles	5.3	0.21	49	430	15.0	0.59	116	1,030

Table 6-3 Comparison of Characteristic load method and p-y analyses

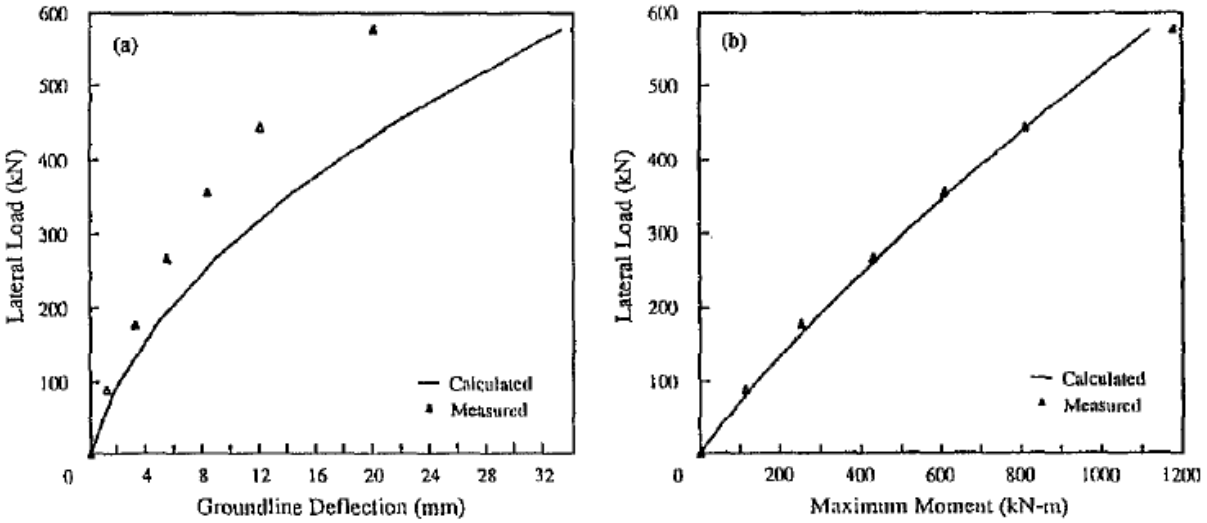

Figure 6-4 Comparison of measured and calculated deflections and moments for pipe pile in stiff clay [Measured values from Reese et al. (1975)]: (a) deflection; (b) Moment

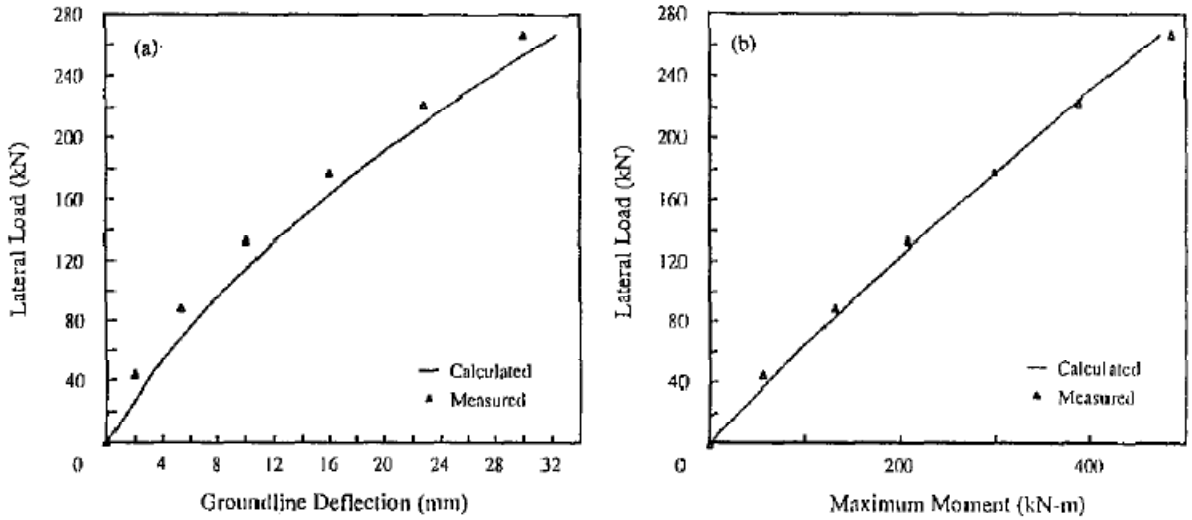

Figure 6-5 Comparison of measured and calculated deflections and moments for pipe pile in sand [Measured values from Cox et al. (1974): (a) Deflection; (b) Moment

6.3 CALCULATIONS

The CLM assumes that the dimension of the pile and the soil conditions are known. Then it is possible to calculate the deflections at the ground line and the (maximum) bending moments. How to do this for different types of loads is stated below.

Calculate deflections due to loads applied at ground line.

Step 1: Calculate P_c and P_t/P_c.

Step 2: Use the load-deflection curves to find y_t/D

Step 3: Multiply y_t/D by D to find the deflection of the pile at ground level.

(The chart can also be used to find the load corresponding to a certain deflection.)

Calculate deflections due to moments applied at ground line.
Step 1: Calculate M_c and M_t/M_c.
Step 2: Use the moment-deflection curves to find y_t/D
Step 3: Multiply y_t/D by D to find the deflection of the pile at ground level.
(The chart can also be used to find the moment corresponding to a certain deflection.)

Calculate deflections due to a load applied above the ground line.
Loads applied above the ground line induce both a load, P_0, and a moment, M_0, at the ground line. Because the behavior is nonlinear, it is not sufficient to merely add the deflections caused by the load and the moment. The nonlinear effect should be taken into account by using a nonlinear superposition procedure.
Step 1: Calculate deflections, y_p, as would occur by the load, P_0, alone.
Step 2: Calculate deflections, y_m, as would occur by the moment, M_0, alone.
Step 3: Determine the load, P_1, that would have caused the same defections as the moment, M_0, would cause alone as calculated in step 2.
Step 4: Determine the moment, M_1, that would have caused the same defections as the load, P_0, would cause alone as calculated in step 1.
Step 5: Calculate the ground line deflection, y_{pm}, which would be caused by the real load plus the equivalent load ($P_0 + P_1$).
Step 6: Calculate the ground line deflection, y_{mp}, which would be caused by the real moment plus the equivalent moment ($M_0 + M_1$).
Step 7: Calculate the ground line deflection by taking the average of y_{pm} and y_{mp}.

By taking both moment and load the nonlinear effect of load and moment is averaged.

Calculate maximum moment – Fixed head piles
In fixed head piles the maximum moment occurs at the top of the pile. The calculations are only necessary for a load at the ground line. In the case of a moment at the ground line, M_{max} equals M_t and is located at the top of the pile.
Step 1: Calculate P_c and M_c.
Step 2: Calculate P_t/P_c.
Step 3: Use the Load-Moment curve to find the value of M_t/M_c.
Step 4: Multiply this value by M_c to find the maximum moment in the pile M_{max}.

Calculate maximum moment – Free headed piles
The maximum moment of free headed piles under a certain load occur at some depth below the ground surface. The magnitude and location of the maximum moment can be estimated with the theory for soil modulus increases linearly with depth.
Step 1: Calculate the "characteristic length", *T*, of the pile. The value of *T* is found by solving formula 6.5.

$$y_{combined} = \frac{2.43P_t}{E_p I_p} T^3 + \frac{1.62M_t}{E_p I_p} T^2 \qquad \textit{eq. 6.5}$$

$y_{combined}$ = estimated ground line deflection due to both load and moment [*m*]
T = Characteristic Length of pile [*m*]

Step 2: When T is determined the bending moments in the upper part of the pile can be calculated with the following equation.

$$M_z = A_m P_t T + B_m M_t \qquad eq.\ 6.6$$

with:
M_z = Moment at depth z [kNm]
Z = Depth below ground line [m]
A_m = Dimensionless moment coefficient
B_m = Dimensionless moment coefficient

Values of A_m and B_m are given in table 6-1. The maximum moment for a load at the ground line, P_t, occurs at a depth of $z=1.3T$, where A_m is maximum. The maximum moment for a moment, M_t, occurs at the ground line, where B_m is maximum. When both a moment and a load are present at the ground line, the maximum moment occurs at depth between $z=0$ and $z=1.3T$.

The CLM is only applicable at piles that are long. This means that their behavior is not significantly influenced by their lengths. If the length of the pile is less than listed in table 6.2, the CLM method is no longer valid. Shorter piles deform more and bending moments will be smaller. CML is based on uniform soil. To calculate P_c and M_c, the soil properties S_u and φ' should be averaged over the first $8D$ of the earth below the ground line.

6.4 LIMITATIONS

The limitations of the characteristic load method are:

- In general
  - The CLM was generated by lots of *p-y* analyses therefore the limitations of the CLM are nearly the same as the limitations of the *p-y* curves. However for the CLM crude assumptions had to be made. Therefore, the results can differ from the *p-y* analyses.
- On soil behavior
  - No time dependent behavior
  - No sloping ground
- On loading types
  - Not usable for cyclic loads in stiff clays
  - No axial load
- On pile behavior
  - No differences of the bending stiffness over the height of the pile
  - No influence of pile diameter on soil reaction
  - Bending stiffness independent of moment

7 MSHEET, SINGLE PILE MODULE – 2004

MSheet is a software application; build to design earth retaining structures like building pits. The first version of this program was released in 1990. In 2004 the single pile module was added to the application. In this module the soil is modeled as a bilinear springs. (GeoDelft, 2004)

7.1 BACKGROUND

In the manual of MSheet (GeoDelft, 2004) the mathematical motor of the single pile module of MSheet is described. In this module, the method of Brinch Hansen, Appendix A, chapter 3, is commonly used to find the maximum possible horizontal resistance of soil against lateral movements of the foundation. The maximum horizontal resistance can also be calculated and introduced into the program manually by choosing the correct active, passive and neutral horizontal earth pressures. To find the modulus of subgrade reaction of the soil, the user can choose to use the theory of Ménard, or he can manually give the values of this modulus for each layer. These two parameters describe the soil as a bilinear spring.

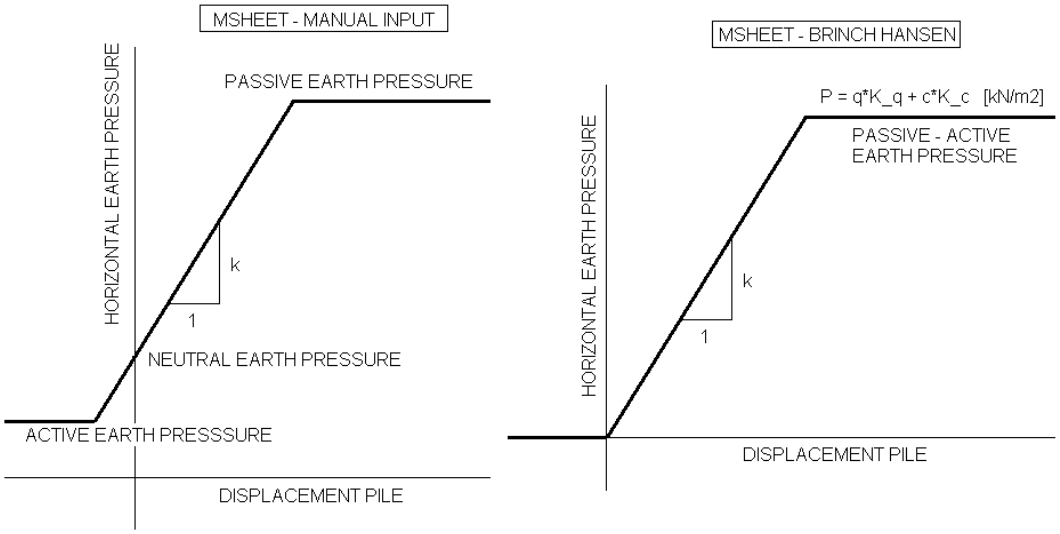

Figure 7-1 Bilinear spring curves that can be used as input in the single pile module in MSheet – Picture by J. Ruigrok

7.2 THEORY OF MÉNARD

To understand the principles of the modulus of subgrade reaction, by Ménard, a brief description of the Ménard pressure meter test and underlying theory are described (Roctest).

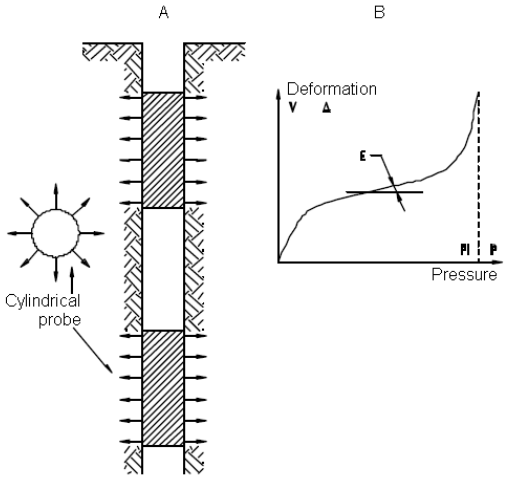

Figure 7-2 Ménard pressure meter test (Roctest) A: An impression of the cylindrical probe in the soil. B: A typical graph that is obtained with the test.

In figure 7-2 the basic principle of the Ménard pressure meter test is shown. A cylindrical probe is penetrated into the soil and by pressing gas or fluid into the probe it expands laterally. If then the volume is plotted versus the pressure in the probe the graph, figure 7-2 B is obtained. This relation between deformation and stresses can be analyzed, if several assumptions are made. The instrument exerts a radial and uniform field of stresses on a given length of the probe. The deformation of the soil or rock comprises a pseudo-elastic and a plastic phase. When the determination is done by a volumetric mean the medium is considered to be isotropic in the test zone.

Figure 7-3 shows a typical pressure meter curve. It shows the injected volumes in the probe versus the pressures. The normalized test must comprise of ten equal increments of pressure. This procedure therefore requires a previous estimation of the limit pressure. The readings of the deformation are made at each step of pressure at 10, 30 and 60 seconds after reaching each pressure level. The pressures versus volumes curve, crosses in 7-3, present three phases: The recompression phase, the pseudo-elastic phase and the plastic phase. The creep curve, dots in 7-3, is obtained by drawing the deformations between 30 and 60 seconds versus the pressures. It presents also three phases.

From the graph basically three parameters can be obtained. Namely, the limit pressure, P_L, the pressure meter modulus, E, and the creep pressure P_F. In MSheet the only required parameter is E. The pressure meter modulus is based on the Lame equation giving the radial increment of a radial cavity in function of the pressure in an elastic medium. The formula which gives the shear modulus G is $G = V_X (\partial P/\partial V)$, where V is the volume of the cavity and P the pressure in the cavity. $\partial P/\partial V$ Is the slope of the pressure meter curve in its linear pseudo-elastic part, taken for the volume V_M, located in the middle of the segment V_O - V_F. V_O is the volume corresponding to the pressure of recompression of the walls on the borehole, which is more or less the “at rest” pressure of the soil. V_F corresponds to the creep pressure. In an elastic medium the relations between the shear modulus G and the Young’s modulus E is: $E = 2G(1+v)$

where *v* is the poisons ratio. In the case of the pressure meter modulus E_M, the Poissons ratio is equal to 0,33. If V_C is the "at rest" volume of the probe, E_M can be calculated with:

$$E_M = 2{,}66(V_C + V_M)\frac{\partial P}{\partial V} \qquad \textit{eq. 6.5}$$

Because pressure meter tests are rare in the Netherlands in comparison to Cone Penetration Tests, CPT, relations were established between the point resistance of a CPT and the pressure meter modulus, table 7-1. With the pressure meter modulus known, the modulus of subgrade reaction is then calculated with the following formula (GeoDelft, 2004):

$$\frac{1}{k_h} = \frac{1}{3E_M}[1{,}3R_0(2{,}65\frac{R}{R_0})^{\alpha} + \alpha R] \;\; (for: R \geq R_0) \qquad \textit{eq. 6.5}$$

$$\frac{1}{k_h} = \frac{2R}{E_M}\frac{4(2{,}65)^{\alpha} + 3\alpha}{18} \; (for: R \geq R_0) \qquad \textit{eq. 6.5}$$

with:

E_M = pressiometric modulus [kN/m^2]
R_0 = 0,3 meter
R =half diameter of pile [m]
α = rheological coefficient [-]
k_h = modulus of horizontal subgrade reaction [kN/m^3]

Soil	Em [kPa]
Peat	(3-4)*qc
Clay	(2-3)*qc
Loam	(1-2)*qc
Sand	(0,7-1)*qc
Gravel	(0,5*0,7)*qc

Table 7-1 Relation cone resistance and pressure meter modulus for different types of soil

Soil	Peat	Clay	Loam	Sand	Gravel
Over consolidated	-	1	2/3	1/2	1/3
Normally consolidated	1	2/3	1/2	1/3	1/4
Decomposed ,weathered	-	1/2	1/2	1/3	1/4

Table 7-2 Rheological coefficients for different types of soil

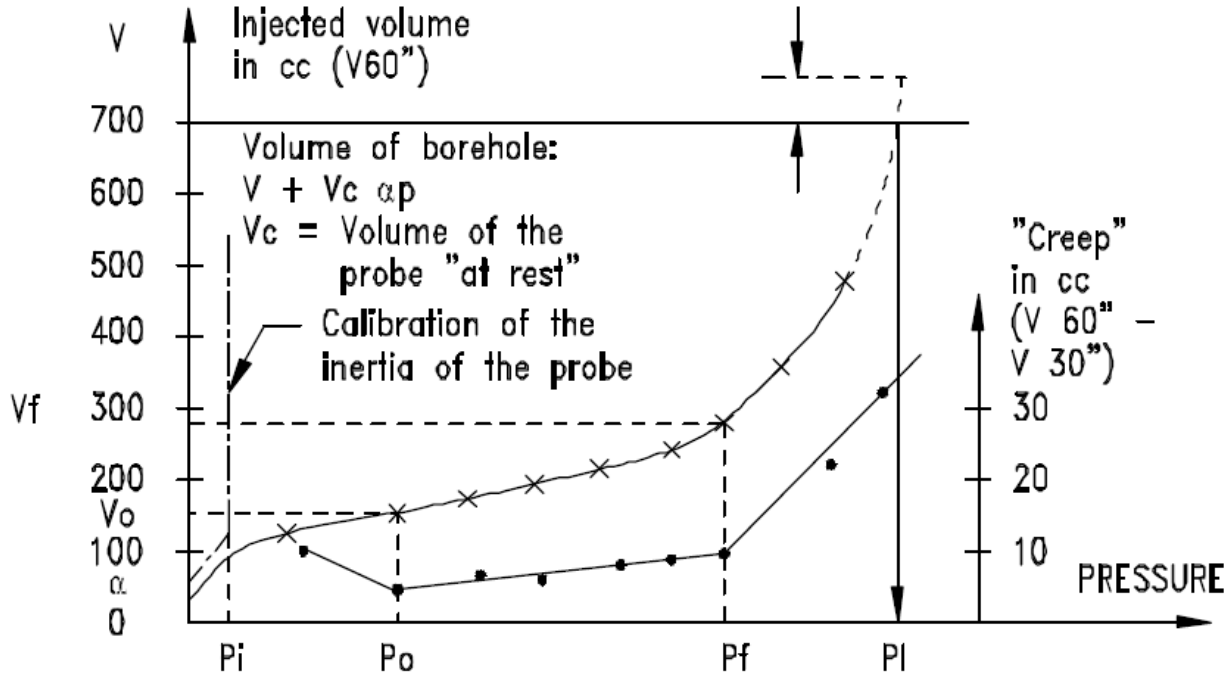

Figure 7-3 Typical result normalized Ménard pressure meter test

For more background information on Ménard, see literature: Ménard, L et al; Méthode générale de calcul d'un rideau ou d'un pieu sollicité horizontalement en fonction des resultats pressiométriques, Solssoils 22-23 VI, 1971

7.3 VALIDATION

The unique combination of Ménard and Brinch Hansen in a program is not validated with field load tests. The code of the program, however, is validated by a number of benchmarks. These benchmarks have not (yet) been published.

7.4 CALCULATION

Calculation of a single pile in the MSheet program is executed in a similar way as in the MPile program. The program tries to establish equilibrium between the loads and soil resistance. Details on the program can be found in the manual (GeoDelft, 2004). The result of the calculation is a series of graphs giving the moments, stresses and displacements at every height of the pile.

7.5 LIMITATIONS

The limitations of the MSheet single pile module are:

- In general
  - The MSheet program weakest link is the modeling of bilinear springs. The stiffness of the soil should decrease with increasing deformation. Also, the stiffness of the soil should increase with depth. In MSheet however this is not the case. Within one soil layer the stiffness is the same at every depth, if Ménard is used. To simulate depth depended soil stiffness multiple layers should be defined. There is a second reason why the stiffness should increase more depth. The deformations of the pile are large near the mud line and become smaller at deeper sections of the ground. If the user is not adapting the input of the model (soil layers and modulus of subgrade reaction) it is expected that the results will be on the conservative side.
    Note that it is possible to implement depth dependent stiffness, if the manual input is used.
- On soil behavior
  - No nonlinear soil. The soil is modeled as bilinear soils
  - No sloping ground
  - Only horizontal layers
- On loading types
  - No cyclic loads
  - No axial load
- On pile behavior
  - No differences of the bending stiffness over the height of the pile
  - Pile stiffness not dependent on moment

8 PLAXIS – 3D FOUNDATION – 2004

Plaxis – 3D Foundation is a three dimensional finite element program, specifically developed to predict soil-foundation interaction. The program was released in 2004 and the second, current version appeared in 2007. (PLAXIS 3D Foundation, Material models manual, Version 2), (Plaxis 3D Foundation, Validation manual, version 2)

8.1 BACKGROUND

Various models can be selected in Plaxis to simulate the soil behavior. The simplest model available is a linear elastic perfectly plastic model, known as the Mohr-Coulomb model. Here it is assumed that the soil resistance increases linearly with displacement, until the failure criterion is reached. The failure criterion is determined by Mohr-Coulomb. Also more advanced models are available. These are the hardening soil model, HS model, and the hardening soil model which includes small strain stiffness, HSSmall model. The models include the nonlinear behavior of the soil, which means that the stiffness of the soil depends on the strains. In Plaxis 3DFoundation also a creep module is implemented. This model is not used since the loads on the piles in this research are only occurring for very short times. For the problem of laterally loaded piles the HSSmall is preferred to be used. This model seems to be the most appropriate model, because over the length of the pile both very small deformations at greater depths and large deformations at the top occur. A more detailed description of this model is given below.

THE HS MODEL

This part is written on the basis of an article provided by Plaxis on their website. (Schanz, Vermeer, & Bonnier, 1999) The origin of the HSSmall model is the HS model. The HS model involves two types of hardening, namely shear hardening and compression hardening. Shear hardening is used to model irreversible strains due to primary deviatoric loading. Compression hardening is used to model irreversible strains due to primary compression in oedometer loading and isotropic loading.

The basic idea of the formulation of the HS model is the hyperbolic curve that is obtained from triaxial testing. Because a triaxial test is described it is assumed that, $\sigma_2' = \sigma_3'$ and σ_1' is the effective major compressive stress. The yield curve of standard triaxial test can be described by the following relation.

$$\varepsilon_1 = \frac{q_a}{2E_{50}} \frac{(\sigma_1 - \sigma_3)}{q_a - (\sigma_1 - \sigma_3)} \; for \; q < q_f \qquad \textit{eq. 8.1}$$

Here, q_a, is the deviatoric stress which describes the maximum stress that the hyperbole will approach asymptotically. This maximum will not be reached in real loading situations. Therefore there is a cut-off on the hyperbola which is described by q_f. q_f Is found by the Mohr-Coulomb failure criterion, which involves cohesion, c, and friction angle, φ_p. The relation between q_a and q_f is given by failure ratio R_f. Furthermore, the parameter E_{50} is the stiffness

modulus at a stress where 50% of the maximum shear strength, q_f, is mobilized. The formula's to determine q_f, q_a and E_{50} are given in equations 8-2 to 8-4.

$$q_f = \frac{6 \sin \varphi_p}{3 - \sin \varphi_p} (p + \cot \varphi_p) \qquad \textit{eq. 8.2}$$

$$q_a = \frac{q_f}{R_f} \qquad \textit{eq. 8.3}$$

$$E_{50} = E_{50}^{ref} \left(\frac{\sigma_3 + c \cot \varphi_p}{\sigma^{ref} + c \cot \varphi_p} \right)^m \qquad \textit{eq. 8.4}$$

E_{50}^{ref} Is a reference stiffness modulus, corresponding to the reference stress, σ^{ref}. The actual stiffness depends on the minor principal stress, σ_3', which is the confining pressure in a triaxial test. The amount of stress dependency is given by the power, m. With this stress dependent stiffness modulus the stiffness of the soil increases automatically with depth in the model.

For unloading and reloading another stress dependent stiffness is used. The relation between the two is given in the following relation.

$$E_{ur} = E_{ur}^{ref} \left(\frac{\sigma_3 + c \cot \varphi_p}{\sigma^{ref} + c \cot \varphi_p} \right)^m \qquad \textit{eq. 8.5}$$

Although the unloading and reloading stiffness is stress dependent, it is not strain dependent. The elastic strains can be described with the following formulas, where ν_{ur} is the constant Poisson's ratio for un- and reloading.

$$\varepsilon_1^e = \frac{q}{E_{ur}} \qquad \varepsilon_2^e = \varepsilon_3^e = \nu_{ur} \frac{q}{E_{ur}} \qquad \textit{eq. 8.6}$$

The soil's stress-strain behavior for triaxial loading can now be simulated. See graph 8-1.

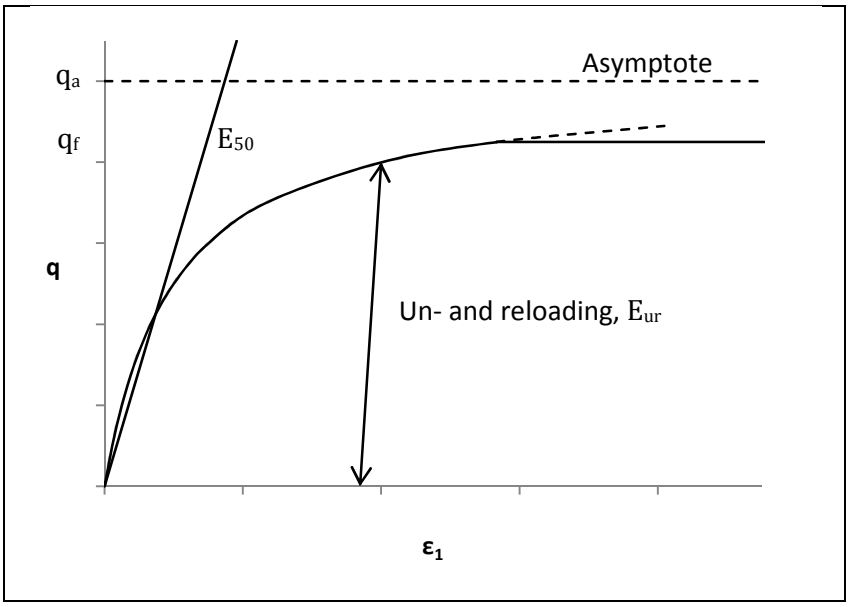

Graph 8-1 Hyperbolic stress-strain relation for a standard drained triaxial test. Figure by J. Ruigrok

On the previous pages the stress strain behavior was described. Now a further elaboration is given on the yield surface, the failure condition and the hardening law. In a triaxial test two yield surfaces can be found, f_{12} and f_{13}. They are defined by equation 8.7 and 8.8.

$$f_{12} = \frac{q_a}{E_{50}} \frac{(\sigma_1 - \sigma_2)}{q_a - (\sigma_1 - \sigma_2)} - \frac{2(\sigma_1 - \sigma_2)}{E_{ur}} - \gamma^p \qquad \textit{eq. 8.7}$$

$$f_{13} = \frac{q_a}{E_{50}} \frac{(\sigma_1 - \sigma_3)}{q_a - (\sigma_1 - \sigma_3)} - \frac{2(\sigma_1 - \sigma_3)}{E_{ur}} - \gamma^p \qquad \textit{eq. 8.8}$$

γ^p Is the measure of plastic shear strain. It is determined by equation 8.9 and is used as parameter for the frictional hardening. γ^p Can be found by using the following definition.

$$\gamma^p = \varepsilon_1^p - \varepsilon_2^p - \varepsilon_3^p = 2\varepsilon_1^p - \varepsilon_v^p \approx 2\varepsilon_1^p \qquad \textit{eq. 8.9}$$

If the combination of stresses stays below the yield criterion, the soil behaves still elastically, E_{ur}. However, as soon as the stresses reach the failure criterion the soil starts to behave also plastically, E_{50}, until it reaches the strength criterion. The yield surface moves along with the imposed stresses. If the soil is unloaded after some plastic deformations, the plastic deformations are not reversed.

Now, the plastic shear strain is known, also the plastic volumetric strain has to be determined. The relation between the two types of strains, $\dot{\varepsilon}_v^p$ and $\dot{\gamma}^p$, is linear and is called a flow rule.

$$\dot{\varepsilon}_v^p = \dot{\gamma}^p \sin\psi_{\mathrm{m}} \qquad \textit{eq. 8.10}$$

$$\sin\psi_{\mathrm{m}} = \frac{\sin\varphi_m - \sin\ \varphi_{cv}}{1 - \sin\varphi_m\ \sin\ \varphi_{cv}} \qquad \textit{eq. 8.11}$$

$$\sin\varphi_{\mathrm{m}} = \frac{\sigma_1 - \sigma_3}{\sigma_1 + \sigma_3 - 2c\cot\varphi_p} \qquad \textit{eq. 8.12}$$

In these equations ψ_m is the mobilized dilatancy angle, φ_{cv} is the critical value for the friction angle and φ_m is the mobilized friction angle.

In the HS model a second hardening rule is present. The first hardening rule, described above, showed the hardening that occurs during shear loading. It did not explain the plastic volume strain which occurs during isotropic loading. Therefore a second yield surface in principal stress space is introduced, which is governed by E_{oed}^{ref}, instead of E_{50}^{ref}. The yield surface of the cap, f_c, is determined by the following relations.

$$f_c = \frac{\tilde{q}^2}{M^2} + (p + a)^2 - (p_c + a)^2 \qquad \textit{eq. 8.13}$$

Where:

$$a = c\cot\varphi \qquad \textit{eq. 8.14}$$

$$\tilde{q} = \sigma_1 + (\alpha - 1)\sigma_2 - \alpha\sigma_3 \qquad \textit{eq. 8.15}$$

$$\alpha = \frac{3 + \sin\varphi}{3 - \sin\varphi} \qquad \textit{eq. 8.16}$$

$$p = (\sigma_1 + \sigma_2 + \sigma_3)/3 \qquad \textit{eq. 8.17}$$

The value of M is a model parameter and will be discussed later. To find the volumetric strain, if the stress path reaches the yield cap, another flow rule has to be established. The formula to determine the volumetric strain is as follows.

$$\varepsilon_v^c = \frac{H}{m+1}\left(\frac{p_c}{\sigma^{ref}}\right)^{m+1} \qquad \textit{eq. 8.18}$$

This second hardening law relates to the pre-consolidation stress p_c. m And σ^{ref} have already been discussed. H is a model constant. M and H are cap parameters, but they are not input paramaters. The values of M and H are related to K_0^{NC} and E_{oed}^{ref}. These parameters are used as input for the model and are therefore input parameters in Plaxis.

Finally the HS model has the possibility to include a dilatancy cut-off. The volume strains cannot continue forever. In order to model this behavior the initial void ratio, e_0, and maximal void ratio, e_{cv}, are entered. As soon as the maximum void ratio is reached, the dilatancy angle is immediately set to zero. The mobilized dilatancy angle can be determined by the following two relations.

$$for\ e < e_{cv} \quad \sin\psi_m = \frac{\sin\varphi_m - \sin\varphi_{cv}}{1 - \sin\varphi_m \sin\varphi_{cv}} \qquad \textit{eq. 8.19}$$

$$for\ e \geq e_{cv} \quad \psi_m = 0 \qquad \textit{eq. 8.20}$$

The void ratio is related to the volumetric strain, ε_v, by the relation.

$$\varepsilon_{v0} - \varepsilon_v = ln\left(\frac{1+e}{1+e_0}\right) \qquad \textit{eq. 8.21}$$

THE HSSMALL MODEL (PLAXIS 3D Foundation, Material models manual, Version 2)
But how is the hardening soil model with small strain stiffness different from the hardening soil model? The HS model assumes linear elastic behavior in reloading and unloading phases. This is of course not a very realistic assumption. With increasing strain amplitude (unloading-loading), the soil stiffness decays nonlinearly. Two additional parameters are necessary to describe this behavior. G_0 is the initial, or very small shear strain modulus. And, $\gamma_{0,7}$, is the strain level at which the initial shear modulus is reduced to 72,2% of its original value, $G_s = 0{,}722G_0$.
In this research to laterally loaded piles, the focus is not on cyclic loading. Therefore the use of the small strain stiffness overlay on the HS model is mainly important for the initial soil stiffness in the model. The value of $\gamma_{0,7}$, is therefore not that important since it is used to calculate the stiffness in the un- and reloading phases. The relation between the small strains and the shear stiffness is given below.

$$\frac{G_s}{G_0} = \frac{1}{1 + 0{,}385\left(\frac{\gamma}{\gamma_{0,7}}\right)} \qquad \textit{eq. 8.22}$$

In graphical form the relation looks as show in figure 8-2. The stiffness reduction curve reaches into the plastic domain. In the HSSmall model the small strain stiffness is bounded by a lower limit. This is done because the hardening rule says that stiffness degradation due to plastic straining is simulated with strain hardening.

The cut-off value can be calculated with the following formulas.

$$G_{ur} = \frac{E_{ur}}{2(1+\nu_{ur})} \qquad \textit{eq. 8.23}$$

$$\gamma_{cut-off} = \frac{1}{0{,}385}\left(\sqrt{\frac{G_0}{G_{ur}}} - 1\right)\gamma_{0,7} \qquad \textit{eq. 8.24}$$

Keep in mind that the there is a difference in stiffness degradation for virgin loading and reloading. Degradation for virgin loading happens twice as fast. Therefore, if is reloading is considered, $\gamma_{0,7}$ should be taken twice the original value: $\gamma_{0,7\,reloading} = 2\gamma_{0,7}$.

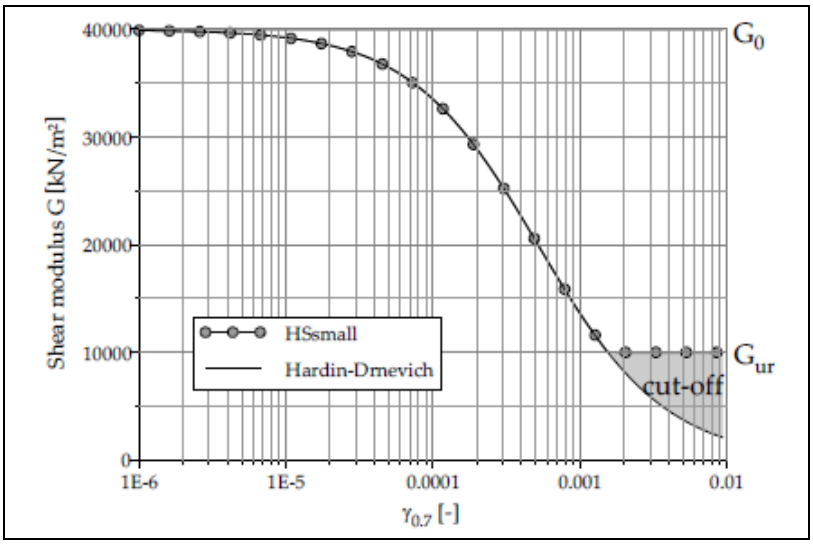

Graph 8-2 Small strain degradation curve as used in the HSSmall model (PLAXIS 3D Foundation, Material models manual, Version 2)

Finally, if a triaxial test is considered the HSSmall will simulate the result as shown in graph 8-3.

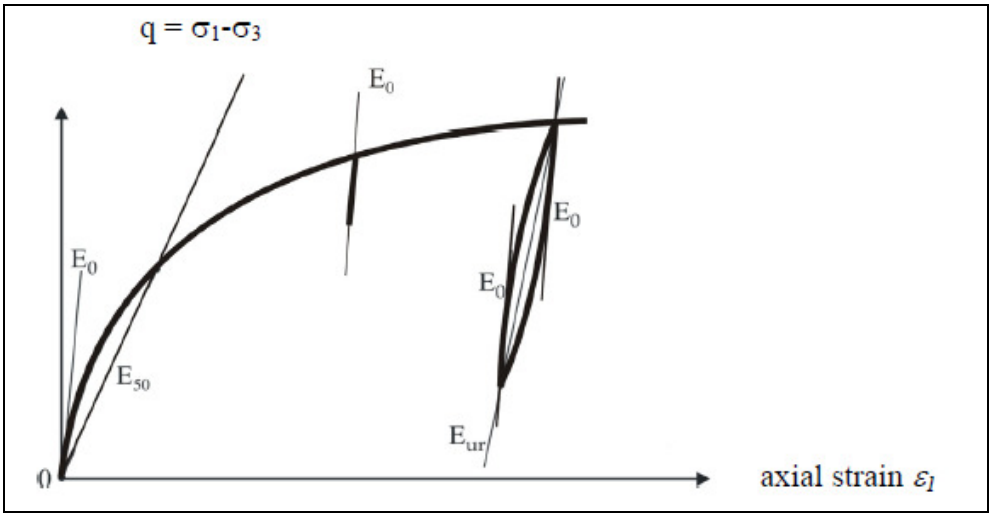

Graph 8-3 Stiffness parameters E_{50}, E_{ur} and E_0 of the HSSmall model in a triaxial test (PLAXIS 3D Foundation, Material models manual, Version 2)

8.2 VALIDATION

Plaxis has been tested by a number of benchmarks. The material models that have been used have proved their use. With the software it is also possible to simulate soil tests. This way the model can be validated if the output of the virtual soil test is approaching the input of the model.

8.3 CALCULATIONS

The calculation method used by Plaxis is a so called finite element calculation. The calculation method solves the problems numerically. It continues with the iteration procedure until equilibrium is reached between load and soil reaction. To do this 3D meshes have to be generated, and the material model has to be rewritten to incremental form.

The selection of the correct model and the values of the parameters are very important. In the case of a laterally loaded pile large and small deformations occur over the height of the pile. The model that involves this behavior is the HSSmall model. The determination of the values of the parameters is different for every case, since it depends on the soil and available soil data. Therefore this will not be discussed here.

8.4 LIMITATIONS

The limitations of Plaxis are very few. The application is capable of performing complex calculation with all different types of loads. There are however several disadvantages. The model is difficult compared to the other models. The amount of input parameters is largest for this model. The time necessary to setup the model and so on takes a lot of time. And finally the calculation time necessary can go up to more than a day.

9 SUMMARY

In the table the results of the literature study are summarized. By means of the table it is possible to see which model is applicable in which situation.
Discussion and elaboration of the table are given in chapters 2, 5, 6 and 7 of the main report.

MODEL	Blum	Brinch Hansen	Broms	CLM	NDM	p-y Analysis	MSheet Single - Pile	PLAXIS 3D Foundation
GENERAL								
Year	1932	1961	1965	1994	1962	1940-now	2004[4]	2004
Validation	Yes	yes	Yes	Yes	No	Yes	No	Yes
Common practice	Yes	No	Yes[5]	No	No	Yes	Yes	No
MODEL TYPE								
Ultimate load	Yes	Yes	Yes	Yes	Yes	Yes	Yes	Yes
Working load	No	No	Yes[6]	Yes	Yes	Yes	Yes	Yes
Based on tests	No	No	No	No	No	Yes	No	Yes
Based on analytics	Yes	Yes	Yes	No	No	Yes	Yes	Yes
Based on p-y Analyses	No	No	No	Yes	Yes	No	No	No
SOIL								
Clay	No	Yes	Yes	Yes	Yes	Yes	Yes	Yes
Sand	Yes	Yes	Yes	Yes	Yes	Yes	Yes	Yes
Layered	No	Yes	No	Yes	No	Yes	Yes	Yes
Nonlinear soil	No	No	No	Yes	Yes	Yes	Bilinear	Yes
Time dep.	No	No	No	No	No	Yes	No	Yes
Sloping surface	No	No	No	No	No	Yes	No	Yes
LOAD AT MUDLINE								
Horizontal	Yes	Yes	Yes	Yes	Yes	Yes	Yes	Yes
Moment	Yes	Yes	Yes	Yes	Yes	Yes	Yes	Yes
Axial	No	No	No	No	No	Yes	No	Yes
Cyclic[1]	No	No	No	No	No	Yes	No	Yes
PILE								
Nonlinear pile[2]	No	No	No	Yes	Yes	Yes	No	Yes
Not constant EI[3]	No	No	No	No	No	Yes	No	Yes
Shell factor depen-dent on diameter	No	No	No	No	No	No	No[7]	Yes

Table 7-9-1 Summary of models. Notes: 1, Cyclic loading is not part of this thesis. 2, Nonlinear pile means that the EI of the pile is dependent on moment. 3, Not constant EI means that it is* possible to divide the pile in different sections with different EI's*. 4, MSheet was introduced in 1990, the single pile module in 2004. 5, Broms is common practice internationally. 6, Only if the working load is between ,3 and ,5 times the ultimate load. 7, The modulus of subgrade reaction is dependent on the pile diameter if Ménard* and/or Brinch Hansen *is used. 8, Not all articles which formed the foundation of the method by Blum could be retrieved, therefore these statements are assumptions based on Blum's Theory (Blum, 1932). 9, Plaxis is very commonly used, however not for the considered problem.

SUMMARY

APPENDIX B

Measurements

CONTENTS

INTRODUCTION

This overview of field test data is meant to give insight into the reliability of the tests and their capabilities to serve as a test on which the different models can be compared. The models that will be compared are described in Appendix A.
The data of the field tests are divided in five groups: the pile properties, the soil properties, the load properties, the test and measurement instrumentation and the results. With the information of the first four groups, table I-1, it is possible to determine which of the models is applicable in the separate field tests. This depends mostly on the soil properties. Nearly all the models can deal with homogenous soil, but as soon as the soil consists of two or more layers some models can no longer be applied. This is mostly the case for the models that do not make use of a computer. Computer software can more easily deal with large amounts of data and make iterative calculations.
Each chapter in this literature study represents a separate case. Within the chapter the case is first introduced. Then data belonging to the five groups is presented as detailed as there is data available. And finally, the chapter is concluded with a list of models that can be used to reproduce the results of the measurements.

Pile	**Soil**	**Loading**	**Instrumentation**
Length and penetration depth	Classification of soil	Point of application above soil surface	Arrangement for applying load
Bending stiffness	Position water table	Loading type (force and/or moment)	Methods of measuring moments, deformation
Material	Strength	Magnitude	
Shape, width	Unit weight	Static, dynamic or long lasting load	
Strength			
Free headed			
Installation method			

Table I-0-1 Required pile, soil and loading information for laterally pile analysis. Instrumentation information is desirable, not required.

1 FIELD TESTS IN COHESIVE SOILS – NO FREE WATER

This series of cases involve only researches to laterally loaded piles in cohesive soils where the groundwater table lies below the penetration depth of the piles. Descriptions of the tests can be found in: (Reese & Van Impe, 2001, pp. 260-269).

1.1 CASE I – BAGNOLET, FRANCE (1965)

In 1965, Kerisel reported results of three short-term static laterally load tests. All the tests were performed on the same pile which was recovered and reinstalled after each test. The penetration depth and point of application varied between each test. The pile head was free to rotate in each test.

Pile

The test pile was constructed by connecting two steel sheet piles. This gave a difficulty in determining the width of the pile, since it has not been given. Reese and Van Impe determined, after an examination of the shape of the cross-section of the pile, that a width of 0,43m is appropriate. It is assumed that this width is appropriate for all calculations with the different models. However, the exact shape of the pile remains unknown. The bending stiffness, E_pI_p, was given as 25.500 kNm^2.

Soil

The tests were performed near Paris in a fairly uniform deposit of medium stiff clay. The properties of the soil are shown in table 1-1. The properties were obtained by unconfined compression tests and cone tests. The water table was below the tips of the piles. The saturation grade was 90%.

Loading

As stated before, the loading consisted of a short-term lateral static load, applied at a certain distance above the ground line.

Instrumentation

Unfortunately, very little is known about the used instrumentation. Maximum moment, Ground line deflection and the magnitude of the lateral load were measured. The method of measuring however was not.

Depth [*m -gl*]	**Water content [*%*]**	**Undrained shear strength c_u [*kPa*]**	**Total unit weight [*kN/m^3*]**
0	-	100	17,9
3,96	31,5	125	17,9
4,69	29,0	130	17,9

Table 1-1 Reported soil properties at Bagnolet

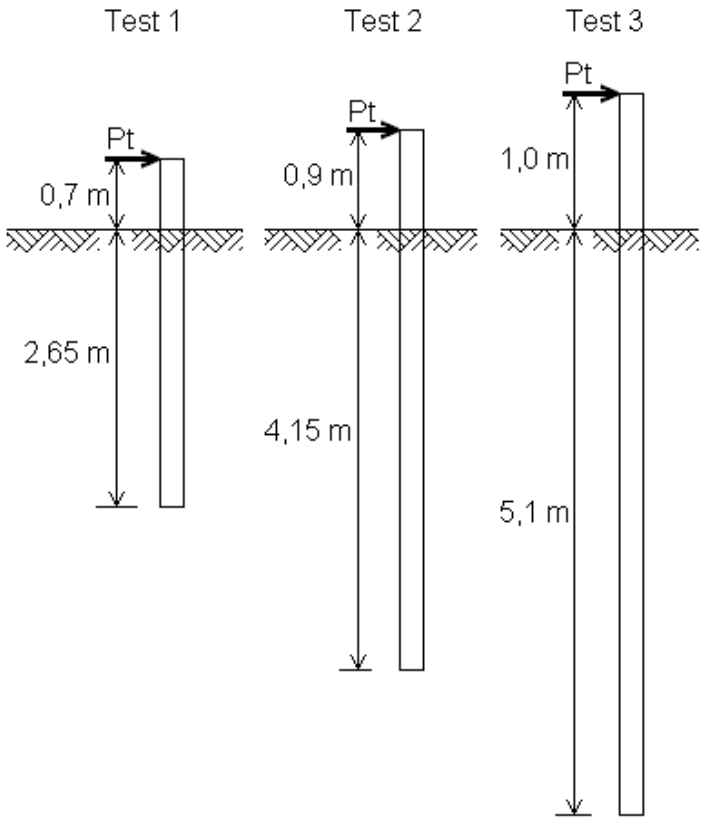

Figure 1-1 Pile penetration depth and point of application for the three cases.

Results

The results of all three tests consist of two graphs. The first graph is the lateral load, P_t, versus the ground line deflection, y_{gl}. The second graph is the load, P_t, versus the maximum bending moment, M_{max}, in the pile. The test data is presented both in tabular form, table 1-2, and graphically, graphs 1-1 to 1-6.

Test 1			**Test 2**			**Test 3**		
P_t [kN]	**y_{gl} [mm]**	**M_{max} [kNm]**	**P_t [kN]**	**y_{gl} [m]**	**M_{max} [kNm]**	**P_t [kN]**	**y_{gl} [m]**	**M_{max} [kNm]**
29	2,2	38	15	1,0	16	34	2,4	46
49	3,8	58	39	3,6	54	46	4,9	70
59	9,5	70	59	6,8	73	59	6,7	84
79	14,5	93	83	10,4	97	79	11,9	123

Table 1-2 Numerical presentation of the test results at Bagnolet

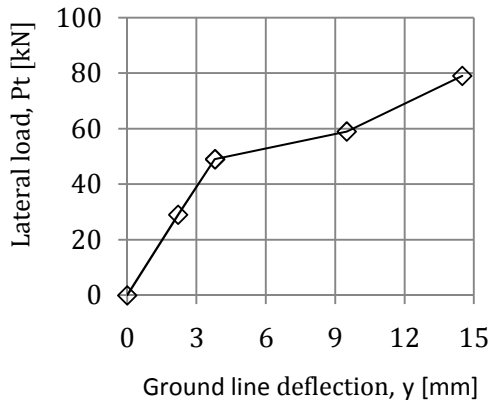

Graph 1-1 Ground line deflection vs. load test 1 Bagnolet

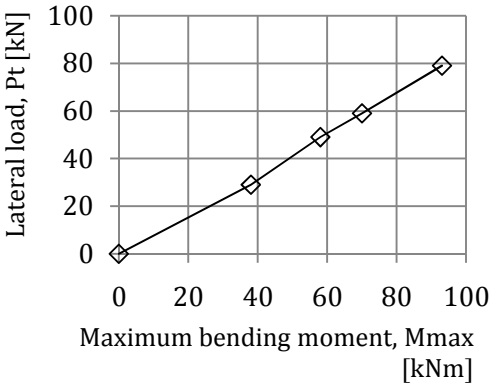

Graph 1-2 Maximum bending moment vs. load test 1 Bagnolet

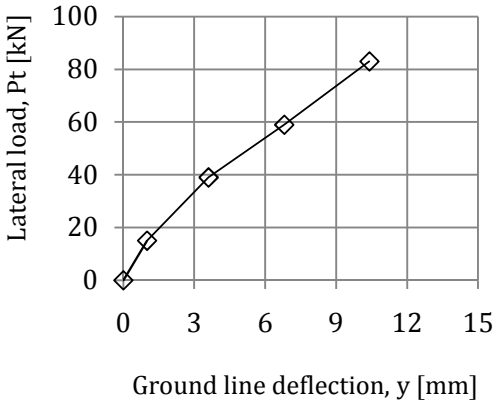

Graph 1-3 Ground line deflection vs. load test 2 Bagnolet

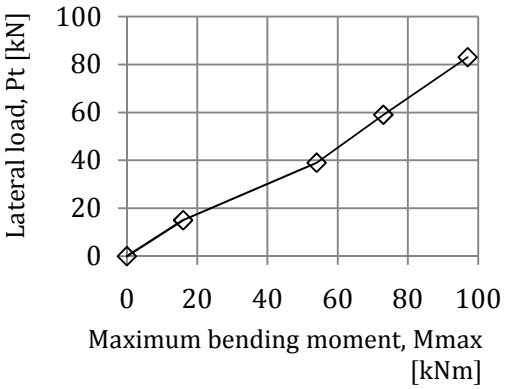

Graph 1-4 Maximum bending moment vs. load test 2 Bagnolet

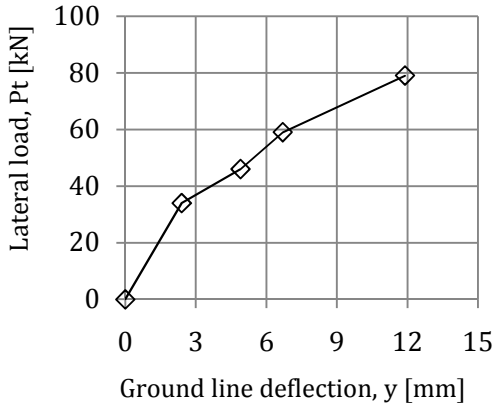

Graph 1-5 Ground line deflection vs. load test 3 Bagnolet

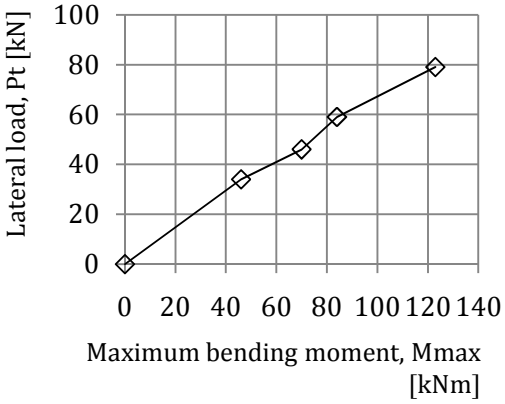

Graph 1-6 Maximum bending moment vs. load test 3 Bagnolet

1.2 CASE II – HOUSTON, TEXAS USA (1975)

This test was used to develop the recommendations of the p-y curves. Therefore it is not allowed to use this case to compare the models based on the p-y curves. These are MPile, the nondimensional method and the characteristic load method. However, the other models can be compared on this case.

Pile

In 1975 Reese and Welch reported the results from a test on a bored pile with a diameter of 0,762 m and a penetration of 12,8 m. A steel pile was placed within the middle of the pile for the measuring equipment. The diameter of this pile was 0,26 m and the wall thickness 6,35 mm. Around the instrument pile a rebar case was placed consisting of 20 bars with a diameter of 44,5 mm and placed in a circle with a diameter of 0,61 m, figure 1-2.

The bending stiffness of the pile was not calculated but measured during the test with strain gauges on the opposites of the steel instrument pipe. The researchers found an E_pI_p of $4{,}0 \times 10^5$ kNm^2. The bending moment at which a plastic hinge would occur was computed to be *2030 kNm*.

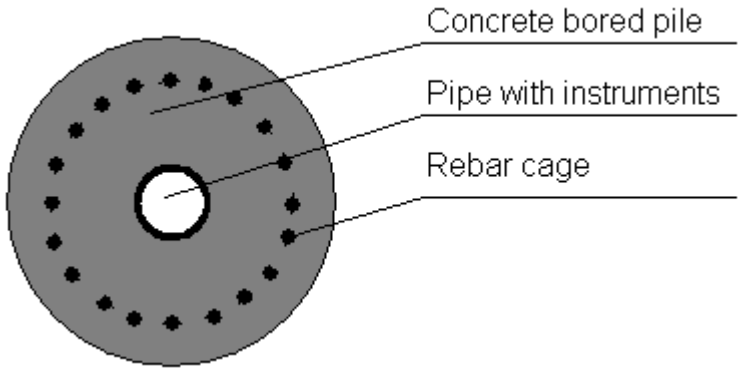

Figure 1-2 Cross-section bored pile Houston

Soil

The soil was overconsolidated clay. The water table was located at 5,5 m below the soil surface. The soil properties were determined by laboratory tests on samples. The soil properties as far as they have been determined are shown in table 1-3.

Depth [m]	Water Content [%]	Undrained shear strength [kPa]	Total unit weight [kN/m^3]
0	18	76	19,4
0,4	18	76	19,4
1,04	22	105	18,8
6,1	20	105	19,1
12,8	15	163	19,9

Table 1-3 Soil properties Houston

Loads

The lateral loads were applied at 0,076 m above the ground line.

Instrumentation

As stated before the instruments were applied in a steel tube within the bored pile. In this pile strain gauges were placed to measure the strain, differential strain on both sides of the pipe and the occurring moment.

Results

The measurements resulted in three graphs: P_t, versus the pile head deflection, y_h, P_t versus the maximum bending moment, and the bending moment, M, for every depth at a load of 445 kN, which was the maximum applied static lateral load. The results are presented in tabular form, table 1-4, and graphical form, graphs 1-7 to 1-9.

P_t [kN]	y_h [mm]	M_{max} [kNm]
87	0,4	62
178	2,1	148
269	6,2	264
355	14,4	429
445	28,9	619

Depth [m]	M [kNm]
0,5	198
1,0	379
1,5	495
2,0	569
2,5	610
3,0	619
3,5	602
4,0	569
5,0	478
6,0	326
7,0	181
8,0	78
9,0	12

Table 1-4 Numerical test date Houston graphs 1 to 3.

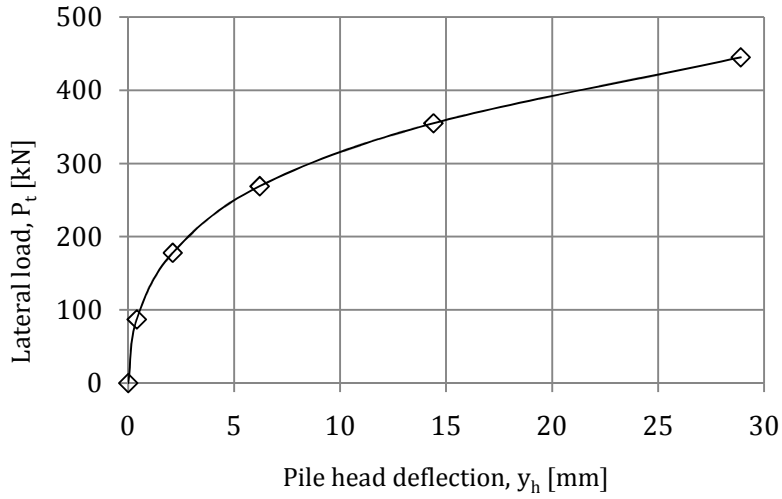

Graph 1-7 Pile head deflection vs. load, Houston

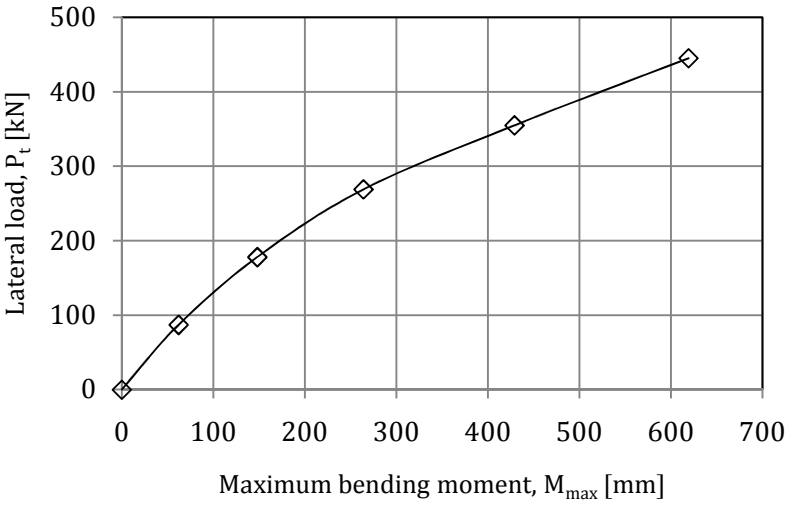

Graph 1-8 Maximum bending moment vs. load, Houston

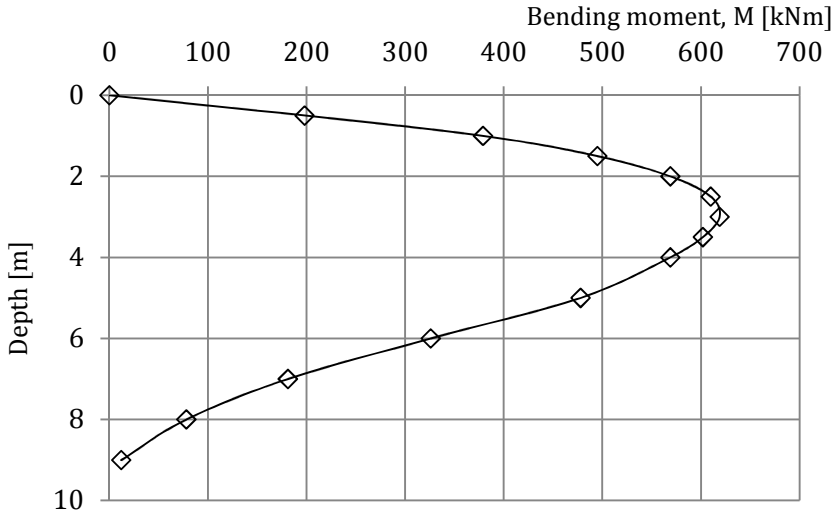

Graph 1-9 Bending moment along the pile, where P_t = 445kN, Houston

1.3 CASE III – BRENT CROSS, LONDON UK (1981)

The results of this experiment were reported by Price and Wardle. The test results were also used for further study by Gabr *et al.* in 1994.

Pile

The test pile was a steel pipe with a diameter of 0,406 m and its penetration depth was 16,5 m. The moment of inertia, I_p, was reported to be 2,448 x 10^{-4} m^4. The bending stiffness, E_pI_p, was 5,14 x 10^4 kNm^2. The bending moment at which the extreme fibers would suffer the first yield was computed to be 301 *kNm*. A plastic hinge would occur at a bending moment of 392 *kNm*.

Soil

The properties of the London clay were determined by laboratory tests and are shown in table 1-5. The location of the water table was not reported, but was presumably at some depth below the soil surface.

Depth [m]	Undrained shear strength [kPa]
0	44,1
4,6	85,2
6,2	80,6
19,0	133,3

Table 1-5 Soil properties Brent Cross

Loads

The lateral load was applied at a distance of 1,0 m above the soil surface. Before the static lateral load test commenced, a test was executed for cyclical lateral loads. The loads however were small and it can be assumed that the cyclic loading test had no influence on the static loading test.

Instrumentation

As far as Reese and Van Impe (2001) are concerned, no data is reported on the instrumentation used on this test.

Results

As in the cases above the results are presented in tabular-, table 1-6, and graphical form, graph 1-10. However, only data on the pile-head deflection, y_h, is known. Keep in mind that the pile head is located on meter above the ground line.

P_t [*kN*]	y_h [*mm*]
20	2,2
40	5,5
60	11,7
100	32,8

Table 1-6 Numerical presentation of test results Brent Cross

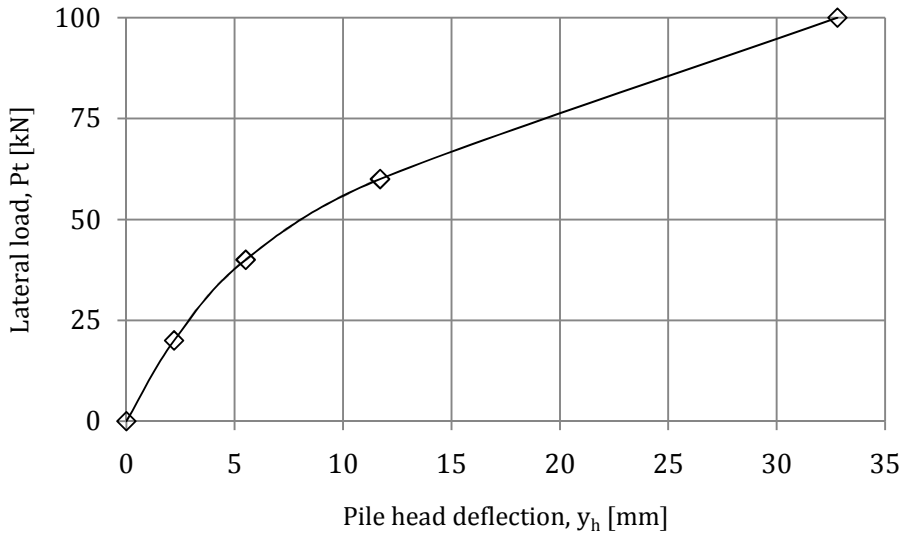

Graph 1-10 Pile head deflection vs. load, Brent Cross

1.4 CASE IV – JAPAN (1965)

In 1965 a Japanese committee was established to examine the influences of earthquakes on piles. To do this, they performed a full scale lateral load test.

Pile

The steel pipe pile had an outside diameter of 305 mm, a wall thickness of 3,18 mm and a penetration depth of 5,18 m. The moment of inertia, I_p, was 3,43x10^{-5} m^4, the bending stiffness, E_pI_p, was 6868 kNm^2. The bending moment at which yielding of the extreme fibers would occur was computed to be 55,9 kNm and the ultimate bending moment was computed to be 71,8 kNm.

Soil

The soil at the site was a soft, medium to highly plastic, silty clay. The soil parameters were obtained from laboratory tests. The results are shown in table 1-7.

Depth [m]	Undrained shear strength [kPa]	Submerged unit weight [kN/m^3]
0	27,3	4,9
5,18	43,1	4,9

Table 1-7 Reported properties of soil at Japan

Load

The static loading was applied at a height of 0,201 m above the ground line.

Instruments

There is very little known on the methods the researchers used for the experiment. Load, displacement of the pile head and the maximum bending moment were measured.

Results

Results are displayed in tabular form, table 1-8, and graphical form, graphs 1-11 and 1-12.

P_t [*kN*]	y_h [*mm*]	M_{max} [*kNm*]
3,2	0,96	4,1
8,1	2,55	5,7
14,2	4,83	17,3

Table 1-8 Results test Japan

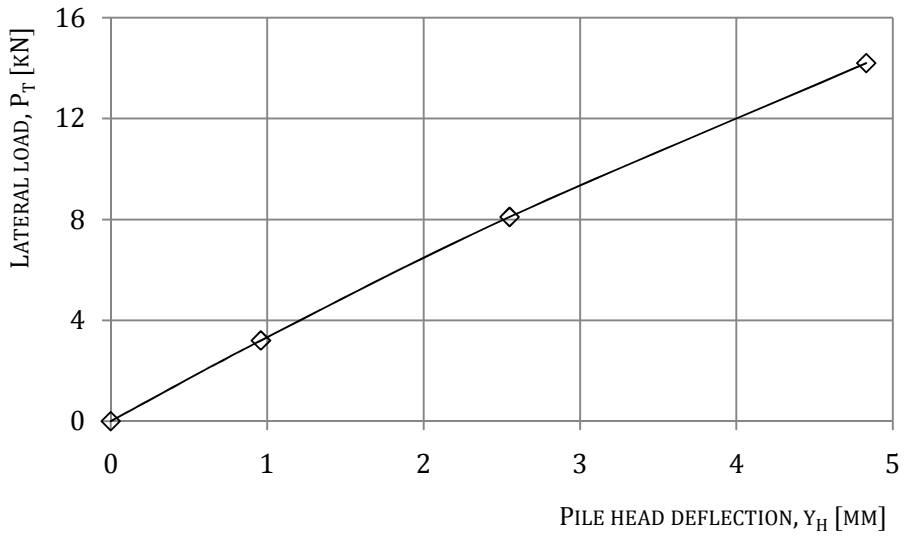

Graph 1-11 Pile head deflection vs. load, Japan

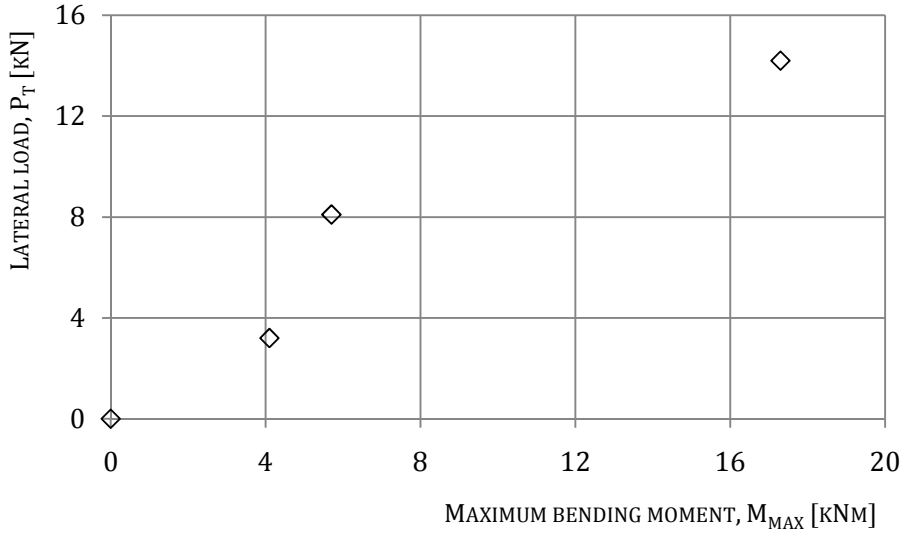

Graph 1-12 Maximum bending moment vs. load, Japan

2 FIELD TESTS IN COHESIVE SOILS, WATER TABLE ABOVE SOIL SURFACE

Since the recommendations on p-y curves separate cohesive soils below the water table from cohesive soils above the ground water table, the same separation have been made in this paper between the cases. This is done since three of the models are depending on the p-y curves and the initial number of cases is large enough to make the separation. (Reese & Van Impe, 2001, pp. 269-276)

2.1 CASE V – LAKE AUSTIN, TEXAS USA (1970)

In 1970, Matlock presented results of a test on a steel pipe pile. The test, executed around the year 1956 was visited by Terzaghi, who, before then, did not believe that it was possible to examine the soil behavior by using strain gauges. This test has been used to produce the p-y curves in the presence of free water and the results can therefore not be used to compare the method of the p-y curves with the other methods.

Pile

The steel pipe pile used at Lake Austin had a diameter of 0,319 m, a wall thickness of 12,7 mm and a penetration depth of 12,8 *m*. The E_pI_p, was 31280 kNm^2. The bending moment at which yielding of the extreme fibers would occur was computed to be 231 *kNm* and the ultimate bending moment was computed to be 304 *kNm*.

Soil

The pile was driven into slightly overconsolidated clay near Lake Austin. The undrained shear strength was measured with field vane tests and was found to be almost constant with depth. The undrained shear strength $c_{u,vane}$ averaged 38,3 kPa. The vane strengths were then modified to obtain the undrained shear strength of clay. The submerged unit weight of the clay had an average value of 10,0 kN/m^3. The results of the soil investigation are shown in table 2.1. Water was kept above the ground surface at all times during testing.

Depth [m]	Water content [%]	Undrained shear strength [kPa]
0	29,0	30,2
1,14	33,5	32,2
1,14	33,5	42,3
3,39	50,1	17,5
3,70	49,6	30,1
4,30	48,3	23,4
5,69	46,1	51,8
7,25	54,5	29,8
9,47	55,5	32,6
15,0	-	32,6

Table 2-1 Properties of soil at Lake Austin

Load
The load was static and was applied at 0,0635 m above the ground line.

Instruments
The pile was instrumented internally with electrical resistance strain gauges for the measurement of bending moment. Each load increment had to be maintained long enough to read the strain gauges. because of creep of the clay the pressure in the hydraulic ram that controlled the load had to be adjusted to maintain a constant load.

Results
The test results are shown in tabular form, table 2-2, and as graphs, graphs 2-1 to 2-3.

P_t [*kN*]	y_h [mm]	M_{max} [*kNm*]
10	2,1	12
21	6,2	27
33	11,4	44
46	16,1	58
58	21,8	73
69	27,5	88
81	34,8	106
93	43,1	123
105	56,1	150

Depth [m]	M [kNm], where P_t = 81 kN
0,3	24
0,6	43
0,9	61
1,2	75
1,5	87
1,8	96
2,2	100
2,5	103
2,7	106
3,1	102
3,4	97
3,7	88
4,0	76
4,5	58
5,1	32
5,4	21
6,1	8
6,6	0

Table 2-2 Numerical results test Lake Austin

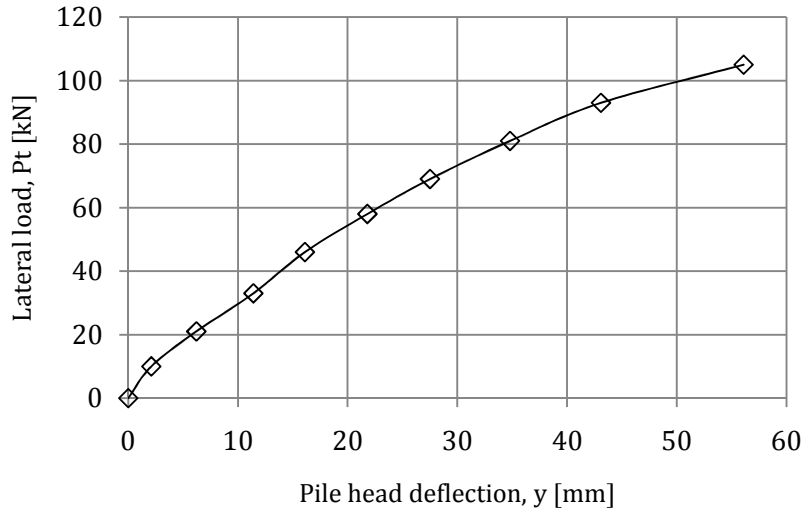

Graph 2-1 Pile head deflection vs. load, Lake Austin

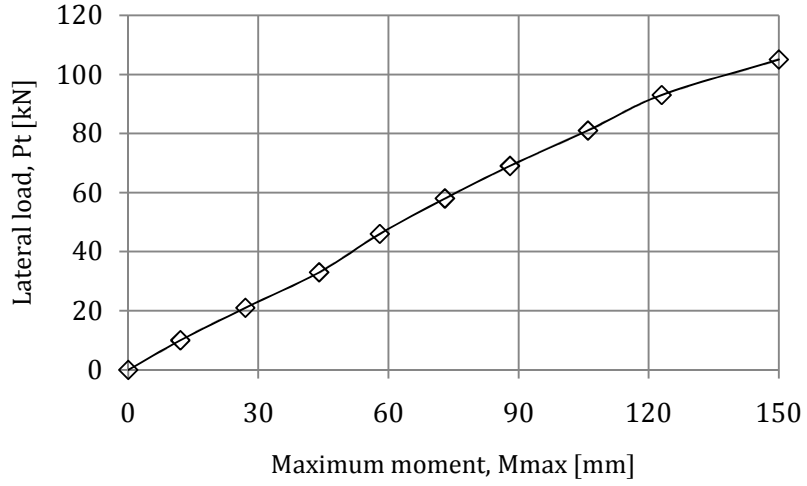

Graph 2-2 Maximum bending moment vs. load, Lake Austin

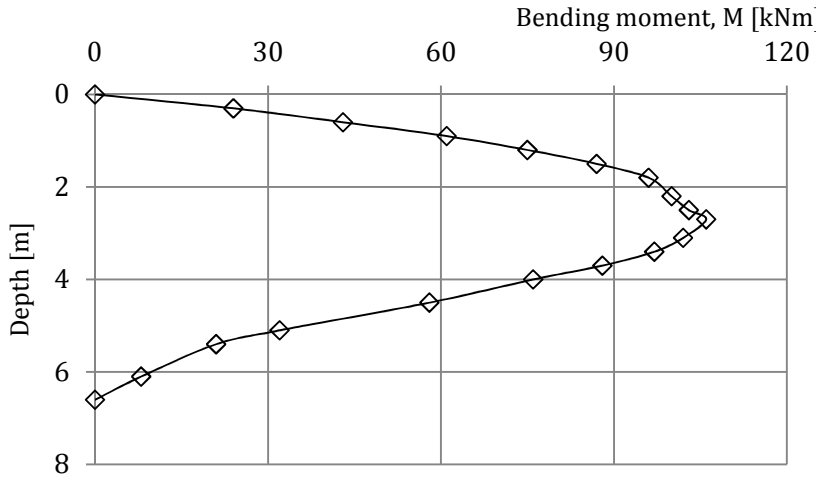

Graph 2-3 Bending moment along the pile, where P_t = 81kN, Lake Austin

2.2 CASE VI – SABINE, TEXAS USA (1979)

The pile was removed from Lake Austin and reinstalled at Sabine to perform another test on the already instrumented pile. The results were analyzed by Meyer in 1979.

Pile

The pile is similar to the pile used in Lake Austin, Case V.

Soil

The soil was considered to be soft clay. The clay was a slightly overconsolidated marine deposit and had a shear strength of 14,4 kN/m^2, and a submerged unit weight of 5,5 kN/m^3.

Load

The lateral loads were applied at a 0,305 m above the ground line. Also cyclic loads were applied, but after the static loading test had been applied.

Instrumentation

The instrumentation was similar to the instrumentation used at Lake Austin.

Results

The test results are shown as tabular form, table 2-3, and as graphs, graphs 2-4 and 2-5.

P_t [*kN*]	y_h [*mm*]	M_{max} [*kNm*]
18	5,0	23
35	16,6	54
53	33,1	88
71	56,4	131
80	69,6	155

Table 2-3 Numerical results Lake Austin

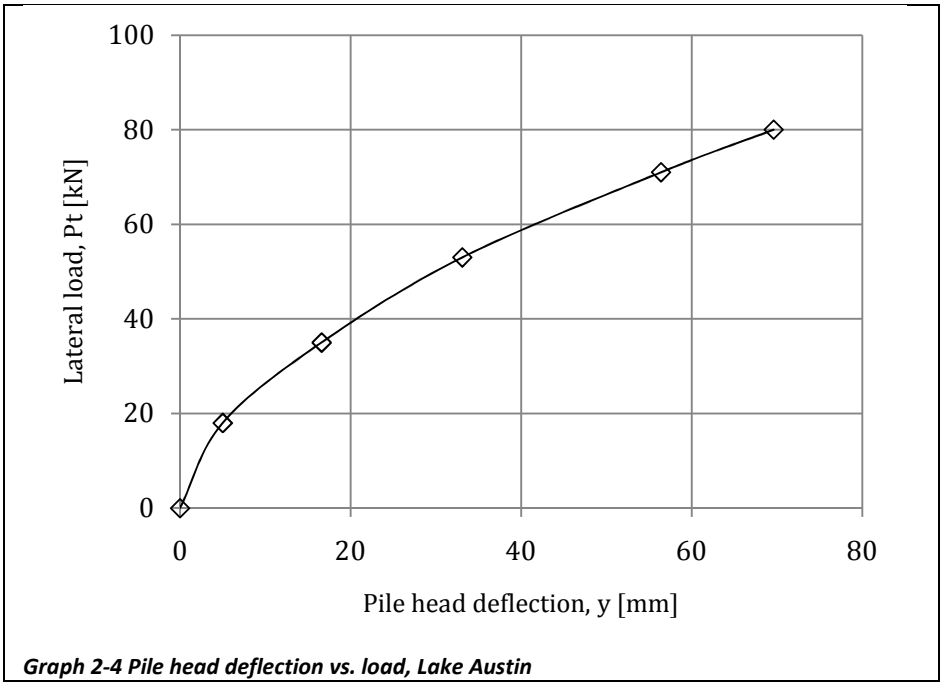

Graph 2-4 Pile head deflection vs. load, Lake Austin

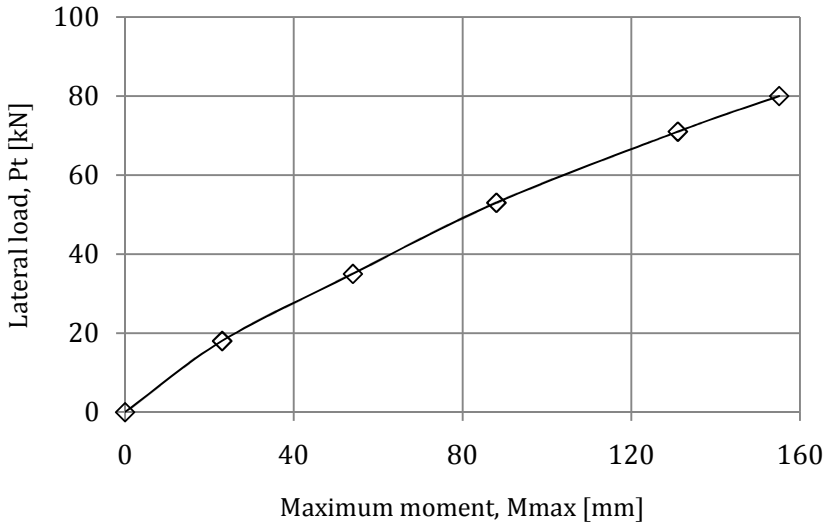

Graph 2-5 Maximum bending moment vs. load, Lake Austin

2.3 CASE VII – MANOR, TEXAS USA (1979)

In 1975 Reese *et al.* described an test at Manor. The difference from the other tests was that the bending stiffness of the pile was not constant over the length of the pile.

Pile

The steel pipe pile was composed of two sections with different bending stiffness. The mechanical properties of the pile are shown in table 2-4.

Section [m]	I_p [m^4]	E_pI_p [kNm^2]	M_{yield} [kNm]	M_{ult} [kNm]
Top 0 – 7,01	0,002335	493.700	1.757	2.322
Bottom 7,01 – 15,24	-	168.400	-	-

Table 2-4 Pile properties, Manor

Soil

The clay at the site was strongly overconsolidated. The undrained shear test was found by performing laboratory tests on soil samples. The site was excavated to a depth of one meter and water was kept above the surface of the site for several weeks prior to obtaining data on soil properties. The soil properties are displayed in table 2-5.

Depth [m]	Water content [%]	Undrained shear strength [kPa]	Total unit weight [kN/m^3]
0,00	-	25	-
0,90	37	70	18,1
1,52	27	163	19,4
4,11	22	333	20,3
6,55	22	333	20,3
9,14	19	1100	20,8
20,00	-	1100	-

Table 2-5 Soil properties Manor

Load

The static load was increased with increments. The point of application of the load was at 0,305 m above the ground line.

Instrumentation

The pile was instrumented with electrical resistance strain gauges for measurement of the bending moment.

Results

The test results are shown in tabular form, table 2-6, and in graphical form, graphs 2-6 and 2-7.

Lateral load, P_t [kN]	Deflection ground line, y [mm]	Maximum bending moment, M_{max} [kNm]
38	0,1	38
64	0,4	77
102	1,4	154
127	1,9	183
178	3,1	260
229	3,8	346
267	5,0	442
318	6,9	529
356	8,1	615
395	9,6	712
445	12,3	913
484	13,8	1058
535	17,7	1173
566	19,2	1212
598	21,5	1269

Table 2-6 Raw data test results Manor

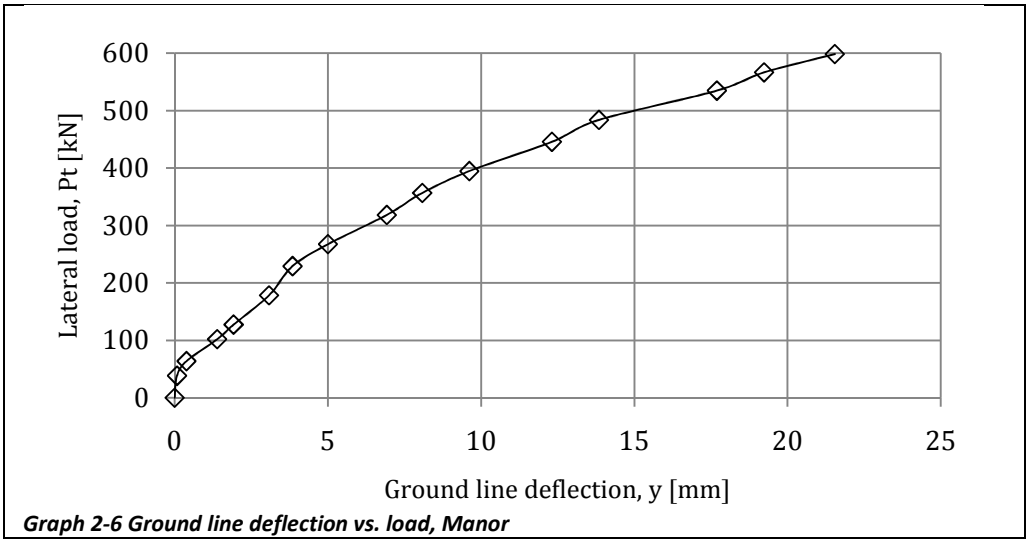

Graph 2-6 Ground line deflection vs. load, Manor

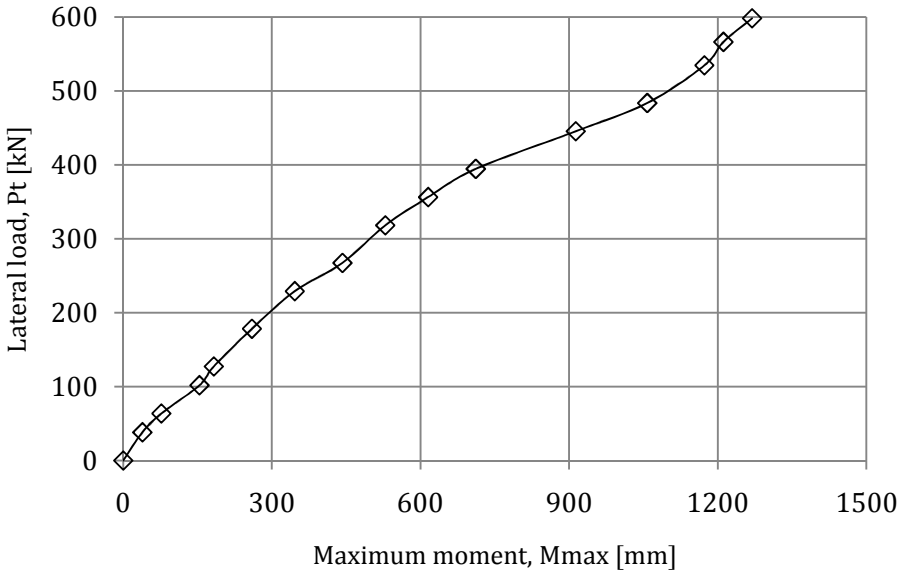

Graph 2-7 Maximum bending moment vs. load, Manor

3 FIELD TESTS IN COHESIONLESS SOILS

In contradiction to cohesive soils there are cohesionless soils. There are three cases described here. Two of them were executed in the US and the third was executed in the United Kingdom. (Reese & Van Impe, 2001, pp. 276-283)

3.1 CASE VIII – MUSTANG ISLAND, TEXAS USA (1974)

In 1974 the results of a lateral load test were described by Cox *et al.* The test was performed near Corpur Christi, Texas. The results of this test were used by Reese *et al.* to develop their recommendations on the p-y curves.

Pile

The steel pipe pile had a length of 21 m and was 610 mm wide. The other properties of the pile were: I_p = 8,0845 x 10^{-4} m^4, E_pI_p = 163.000 kNm^2, M_y = 640 kNm and M_{ult} = 828 kNm. The pile was placed open-ended. Change of the soil might have been less than if a closed-ended pile was used.

Soil

The soil was uniformly graded fine sand with a friction angle of 39 degrees. the submerged unit weight was 10,4 kN/m^3. The water surface was maintained at 150 mm above the ground line during the entire test.

Load

The pile was subjected to static loading. The load was applied at 0,305 m above the ground line.

Instruments

The pile was instrumented on the inside with strain gauges for the measurement of the bending moment.

Results

The results are presented in tabular form, table 3-1, and graphical form, graphs 3-1 to 3-3.

P_t [*kN*]	y_g [mm]	M_{max} [*kNm*]
22	0,6	22
33	0,8	39
44	1,7	56
52	2,2	72
78	3,9	111
100	6,1	150
122	8,3	189
144	11,1	233
167	14,4	278
207	21,1	361
241	26,1	428
267	30,0	478

Depth [m]	M [kNm], where P_t = 210 kN
0,6	121
1,2	230
1,9	315
2,5	362
3,0	337
3,6	290
4,3	236
4,9	184
5,5	126
6,1	74

Table 3-1 Results test Mustang Island

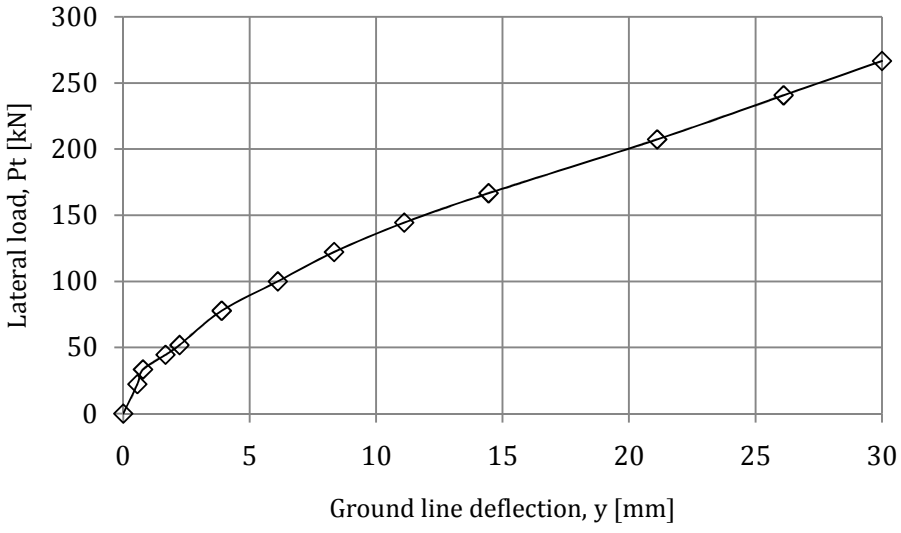

Graph 3-1 Ground line deflection vs. load, Mustang Island

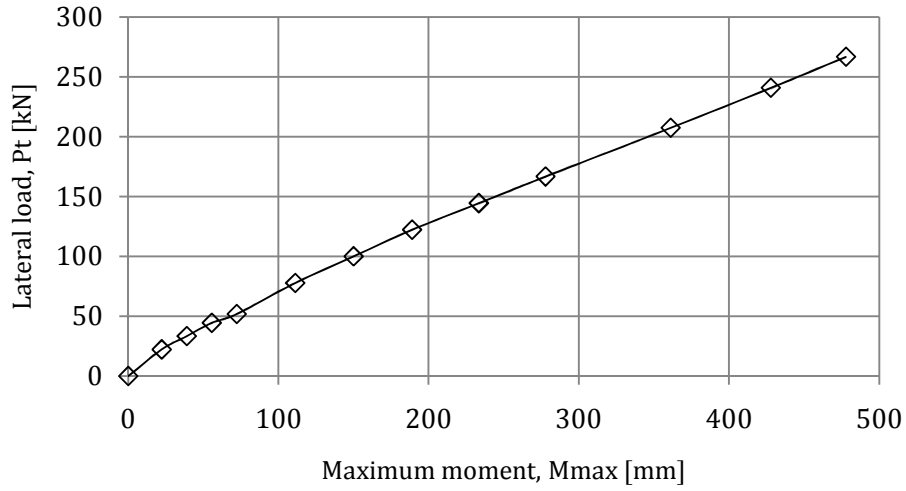

Graph 3-2Maximum bending moment vs. load, Mustang Island

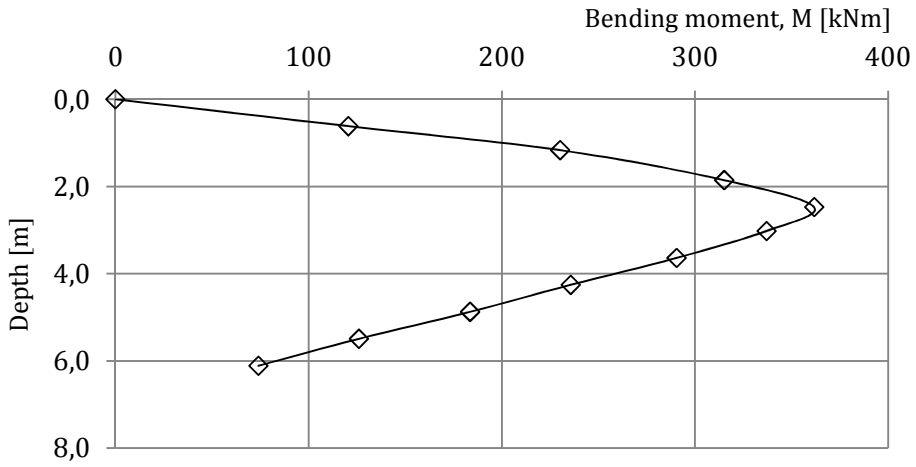

Graph 3-3 Bending moment along the pile, where P_t = 210kN, Mustang Island

3.2 CASE IX – GARSTON, LIVERPOOL UK (1987)

In 1987, Price and Wardle reported the results of a lateral-load test of a bored pile.

Pile

The bored pile had an diameter of 1,5 m and was 12,5 m long. The reinforcement consisted of 36 bars round bars with a diameter of 50 mm in a circle of 1,3 m in diameter. The yield strength of the steel was 425 N/mm^2. The cube strength of the concrete was 49,75 N/mm^2. M_{ult}, was calculated to be 15900 kNm.

Soil

The soil properties are shown in table 3-2.

Depth [m]	Description	N_{SPT}	Unit weight [kN/m^3]	Friction angle [degrees]
0 - 0,36	Fill	18	-	-
0,36 – 3,5	Dense sandy gravel	≈65	21,5	43
3,5 – 6,5	Course sand and gravel	30	9,7	37
6,5 – 9,5	Weakly cemented sandstone	≈61	11,7	43
9,5 -	Highly weathered sandstone	≈140	-	-

Table 3-2 Soil properties, Garston

Load

The lateral load was applied at 0,9 m above the ground line. Each load held until the lateral movement was less than 0,05 mm in 30 minutes

Instrumentation

Very little is reported on the instrumentation along the length of the pile. All that is known, is that highly precise measuring equipment was installed and the bending moment could be determined reasonably accurate. However, the results on bending moment were not reported by Reese and Van Impe.

Results

The results of the test at Garston are displayed in tabular form, table 3-3, and graphical form, graph 3-4 and 3-5.

P_t [kN]	y_g [mm]	M_{max} [kNm]
234	0,5	
374	2,6	
607	4,5	1463
794	7,1	
981	10,5	
1215	15,8	
1402	20,3	
1589	25,9	
1776	32,3	
2009	37,9	
2150	45,8	
2383	51,4	8325

Table 3-3 Results test data Garston

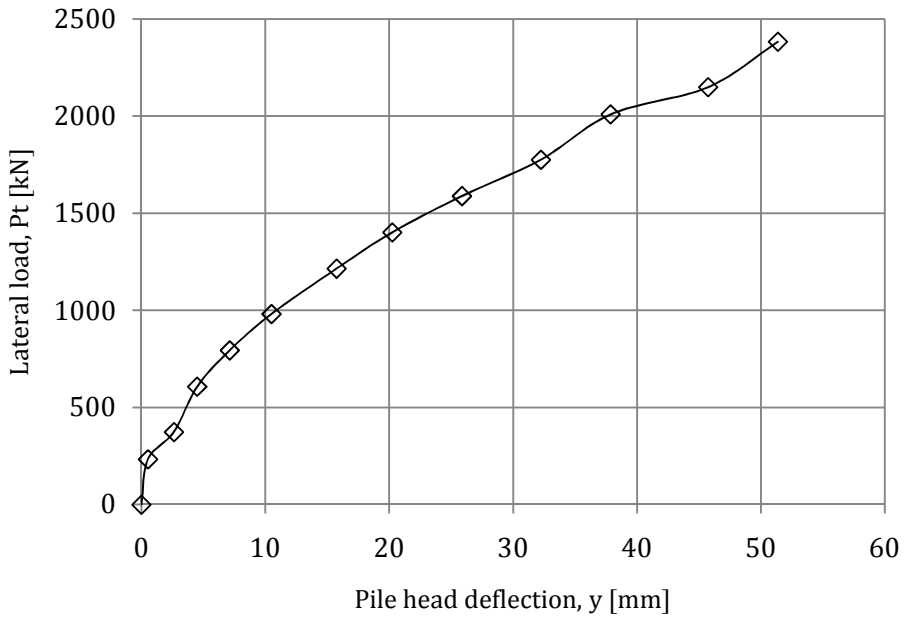

Graph 3-4 Pile head deflection vs. load, Garston

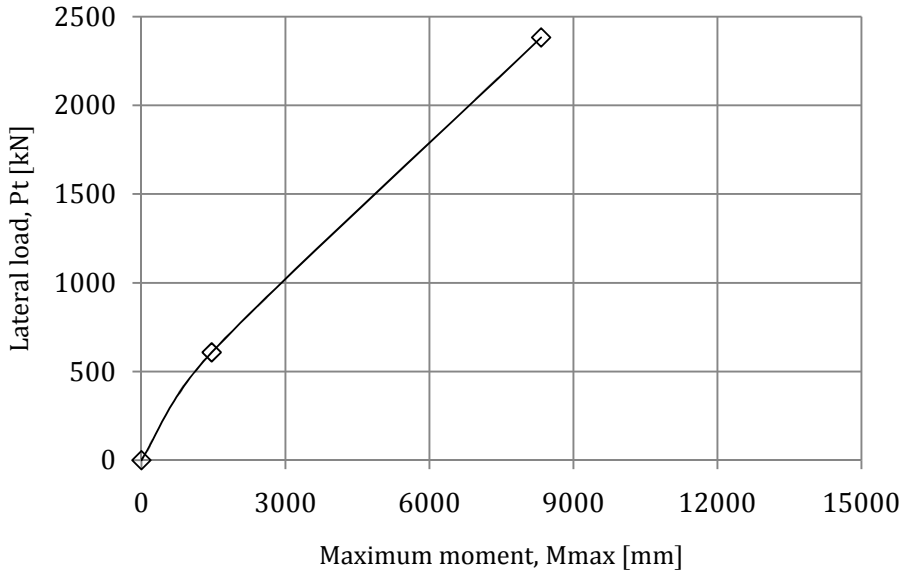

Graph 3-5 Maximum bending moment vs. load, Garston

3.3 CASE X – ARKANSAS RIVER, USA (1970)

In 1970 Mansur & Hunter and Alizadeh & Davisson reported the results of lateral load tests for a number of piles in connection with a navigation project. One of the tests is used here. The data of the other tests were not retrieved.

Pile

The steel pipe pile had a length of 15 m, diameter of 406 mm and a wall thickness of 8,153 mm. To apply the measuring equipment four steel bars were welded to the sides of the pile. This is shown in figure 3-1. The additional steel bars influenced the bending stiffness and width of the pile. The effective width of the pile was 480,3 mm, the moment of inertia, I_p, was $3{,}494 \times 10^{-4}$ m^4 and the bending stiffness was 69900 kNm^2. Estimating the yield strength of the steel to be 248×10^3 kPa, M_y becomes 361 kNm.

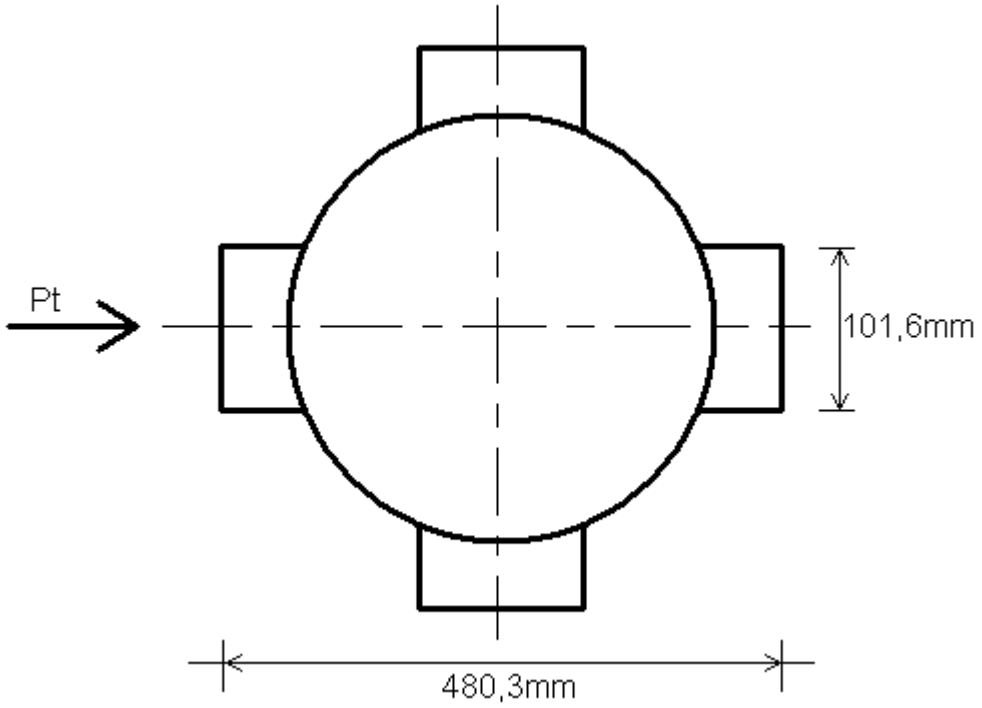

Figure 3-1 Schematization cross-section pile Arkansas River

Soil

Several borings were made to determine the soil parameters. They showed a considerable variation of soil properties around the site. The soil in the top 5,5 m was a poorly graded sand with some gravel and little to no fines. The deeper soils were fine sands with some organic silt. The water table was at a depth of 0,3 m. The total unit weight above the water table was 20 kN/m^3 and below it was 10,2 kN/m^3. Data from the site showed that the site had been preconsolidated by an overburden of 6 meters that was removed prior to testing. The reported soil data is given in table 3-2.

Depth [m]	σ_v [Mpa]	N_{SPT}	q_c [Mpa]	σ_v/q_c	φ [degree]	Es [Mpa]	n_E
0	0	12	5,0	-	-	15,0	4,0
0,6	0,012	12	5,0	417	45	15,0	4,0
2,4	0,039	14	5,5	183	42	15,0	4,0
4,0	0,056	20	10,0	179	42	22,5	3,0
4,6	0,062	17	8,0	129	41	19,5	3,0
5,0	0,071	25	13,0	183	42	27,0	3,0
7,0	0,086	28	14,0	163	42	28,5	3,0
8,5	0,102	18	12,0	118	40	19,5	3,0
10,0	0,117	27	15,0	128	41	30,0	2,5
11,6	0,133	29	15,0	113	40	30,0	2,5
20,0	0,219	29	15,0	68	36	30,0	2,5

Figure 3-2 Soil data Arkansas River. n_E is a multiplier of E_s, based on the degree of overconsolidation

Loads

The loading was static and was applied at the ground line.

Instrumentation

As stated before, the instrumentation of the pile was installed in steel bars that were connected to the pile. This indicated that the occurring moment along the pile was measured. Unfortunately, the obtained data of these measurements were not reported by Reese and Van Impe. The pile head deflection, y_h, was measured.

Results

Very little results have been published by Reese and Van Impe. However the results that were published are useful. The results are given in tabular form, table 3-4 and in graphical form, graph 3-6.

P_t [*kN*]	y_h[mm]
46	1,9
92	4,2
140	7,0
191	10,2
248	14,1

Table 3-4 Results test, Arkansas River

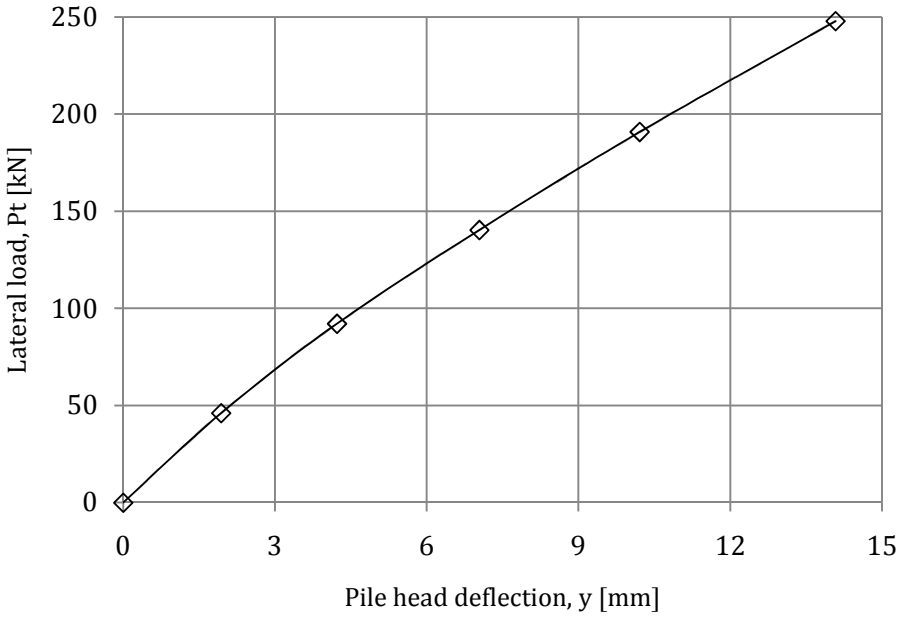

Graph 3-6 Pile head deflection vs. load, Arkansas River

4 FIELD TESTS IN LAYERED SOILS

In the cases described above, it is possible to schematize the soil as homogeneous layers. However, in practice the soil is often layered. These field tests have been added to determine the accuracy of the models in case of layered soils. (Reese & Van Impe, 2001, pp. 283-290)

4.1 CASE XI – BOGALUSA, LOUISIANA USA (1984)

In 1984, Gooding *et al.* published tests for the Louisiana Power and Light Company. Here a steel pipe pile was tested at Bogalusa to measure the behavior of the foundation for a transmission tower. An interesting part of this research was that the loading continued until failure.

Pile

The pile had an outside diameter of 0,9144 m, a wall thickness of 9,525 mm and a penetration depth of 4,27 m. The moment of Inertia, I_p, was 0,002772 m^4, the bending stiffness, E_pI_p, was 554400 kNm^2, the bending moment of first yield, M_y, was 1516 kNm and the ultimate bending moment, M_{ult}, was 1950 kNm.

Soil

The soil can be schematized as two layers. The first layer was classified as stiff sandy clay. The shear strength was found by unconfined compression tests. The second layer was classified as a dense fine sand where the uncorrected values of N from the standard penetration test averaged 71. The friction angle was determined from this value together with the overburden pressure. This resulted in a friction angle, φ, of 50^o. The soil data is summarized in table 4-1.

Depth [m]	Water content [%]	Total unit weight [kN/m^3]	Undrained shear strength [kPa]	Friction angle [degrees]
0	17,3	18,7	59,2	-
1,83	17,3	18,7	59,2	-
1,83	21,6	20,1	-	50
6,0	21,6	20,1	-	50

Table 4-1 Soil properties, Talisheek

Load

The load that was applied consisted of three parts: a lateral load, which was applied at a point 10,36 m above the soil surface, an axial load, which was applied by an weight on the pile, and a moment, which was produced by placing the load eccentrically. A schematization of the situation is shown in figure 4-1. The loads that were applied are given in table 4-2.

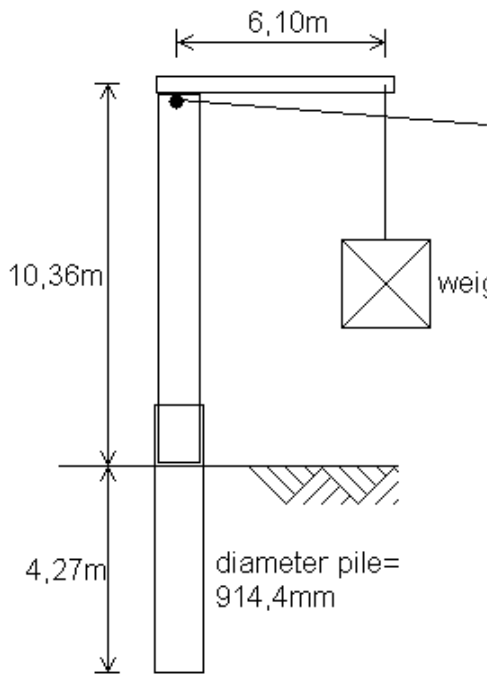

Figure 4-1 Loading of test pile at Talisheek

Load Nr.	Lateral Load P_t [kN]	Bending Moment M_t [kNm]	Axial Load P_x [kN]	Deflection y_t [mm]
1	44,1	456,8	4,5	9,1
2	66,1	685,0	8,9	16,8
3	79,4	822,3	8,9	22,9
4	88,2	913,6	13,3	27,4
5	97,0	1004,9	13,3	30,5
6	0	328,1	107,2	15,2
7	0	641,3	211,9	19,8
8	0	939,5	309,8	25,9
9	13,2	1076,4	314,3	25,9
10	26,4	1213,3	314,3	30,5
11	39,6	1350,2	318,7	35,1
12	52,8	1487,1	318,7	42,7
13	66,1	1624,1	323,1	48,8
14	79,3	1761,0	323,1	56,4
15	88,1	1852,2	323,1	-
16	92,5	1897,9	327,6	-
17	96,9	1943,5	327,6	-
18	103,5	2012,2	327,6	73,2

Table 4-2 Set of loads applied at Talisheek

Instrumentation

The only reported measurements are the deflections at the ground line, y_t.

Results

The results have been given in table 4-2. A graphical presentation of the of the results is also given, graph 4-1.

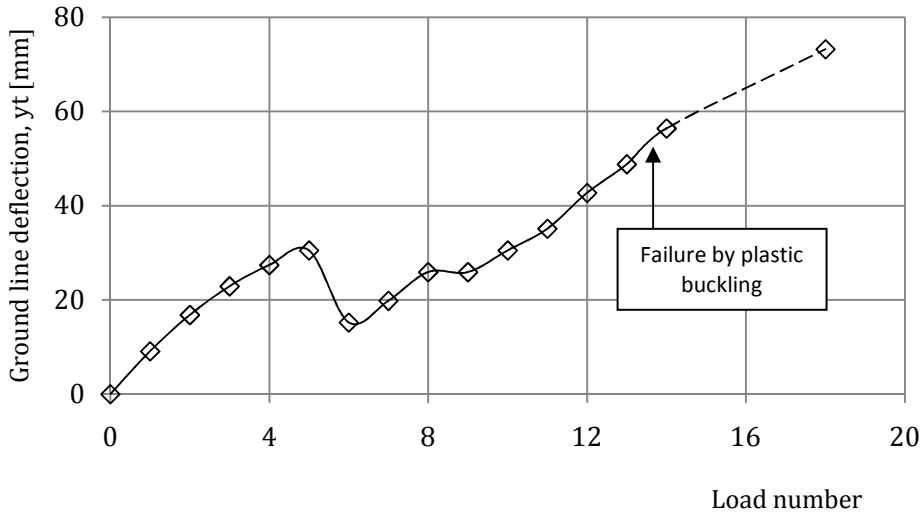

Graph 4-1Ground line deflection vs. Load number, Talisheek

4.2 CASE XII – ALCÁCER DO SOL, PORTUGAL (1993)

In 1993, Portugal and Sêco e Pinto described the testing of a bored pile at the site of a bridge at Alcácer do Sol. They did this at the second international seminar on deep foundations on bored and auger piles in Ghent, Belgium.

Pile

The pile was a 40 m long bored pile with a diameter of 1,2 m. The reinforcement consisted of 35 bars with a diameter of 25mm. The strengths of the concrete and the steel were reported to be 33,5 and 400 MPa respectively. The cover of the reinforcement was 50 mm. The bending stiffness, E_pI_p, was computed to be $3{,}29 \times 10^6$ kNm^2 and the ultimate bending moment was computed to be 3370 kNm.

Soil

The soil could be divided in four separate layers. The soil properties were found form SPT, CPT and vane tests. The found values are shown in table 4-3. The position of the water table was not reported, but it was assumed that it was located close below the ground line.

Depth [m]	Water content [%]	Total unit weight [kN/m^3]	Undrained shear strength [kN/m^2]	Friction angle [degrees]
0	62,5	16	20	-
3,50	62,5	16	20	-
3,50	28,6	19	-	30
8,50	28,6	19	-	30
8,50	62,5	16	32	-
23,0	62,5	16	32	-
23,0	28,6	19	-	35
40,0	28,6	19	-	35

Table 4-3 Soil properties, Alcácer do Sol

Load

The lateral load was applied 0,2 meters above the ground line. The load was static.

Instrumentation

The moments were measured along the length of the pile, but the applied techniques are not reported.

Results

The test results are displayed in table 4-4 and graphs 4-2 and 4-3.

Lateral Load P_t [kN]	Deflection y_h [mm]	Bending Moment M_t [kNm]
0	0	0
101	1,7	265
202	4,5	582
300	8,0	1010

Table 4-4 Results test, Alcácer do Sol

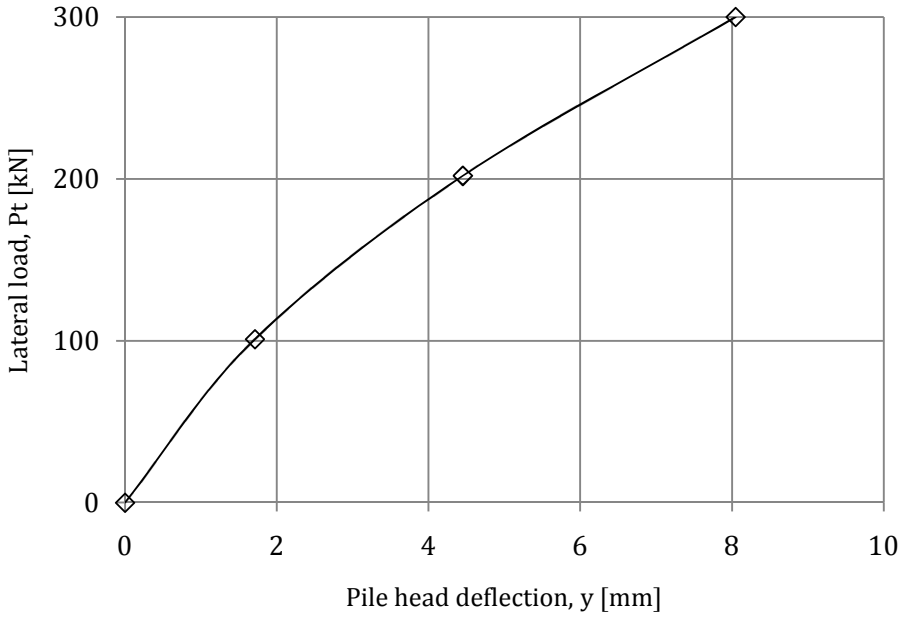

Graph 4-2 Pile head deflection vs. load, Alcácer do Sol

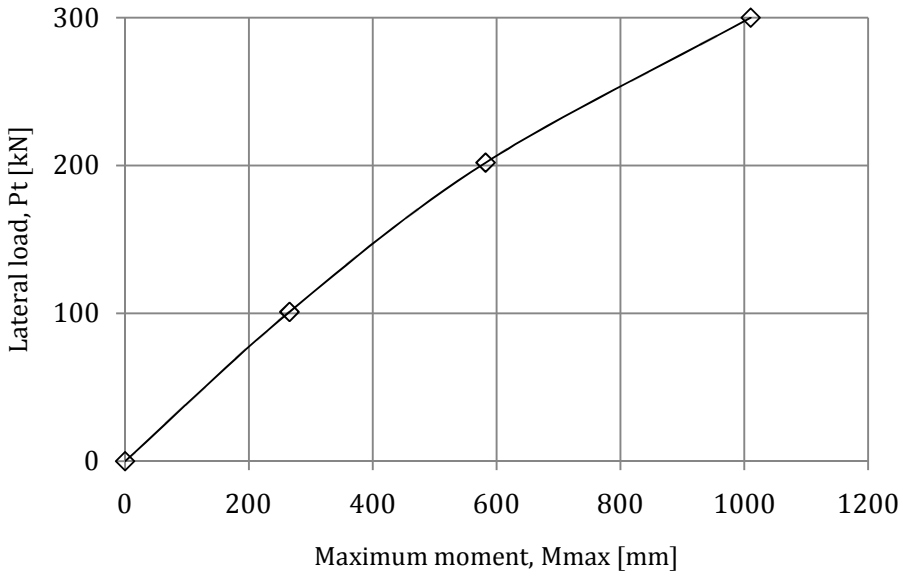

Graph 4-3 Maximum bending moment vs. load, Alcácer do Sol

4.3 CASE XIII – FLORIDA USA (1977)

In 1977 Davis described the testing of a steel pipe pile, but it was Meyer in 1979 who analyzed the results.

Pile

The pile was a steel pipe pile. The pile had a diameter of 1,42 m and a penetration depth of 7,92 m. The pile was filled with concrete until a depth of 1,22 m below the ground line. The bending stiffness and ultimate moment are therefore not constant over the height of the pile. The bending stiffness and ultimate moment for the top 1,22 m of the pile are 5.079.000 kN/m^2 and 6280 kNm respectively and 2.525.000 kN/m^2 and 4410 kNm for the bottom part.

Soil

The soil consisted of two layers. The top layer of 3,96 m consisted of sand with a volumetric weight of 19,2 kN/m^3 and a friction angle of 38 degrees. Below this layer there was a saturated clay layer with a submerged volumetric weight of 9,4 kN/m^3 and an undrained shear strength of 120 kPa. The water table was located at 0,61 m below the ground line.

Load

The load was static and was applied at 15,54 m above the soil line.

Instrumentation

Very little is known about the methods measurements were taken. The only measurements that are reported are the pile head deflections at different loads.

Results

The results are presented in tabular form, table 4-5, and graphical form, figure 4-4.

Lateral Load P_t [kN]	**Deflection y_t [mm]**
46	1,4
67	3,1
87	5,0
113	7,6
133	10,1
157	11,1
180	14,9
226	19,3

Table 4-5 Results test, Florida

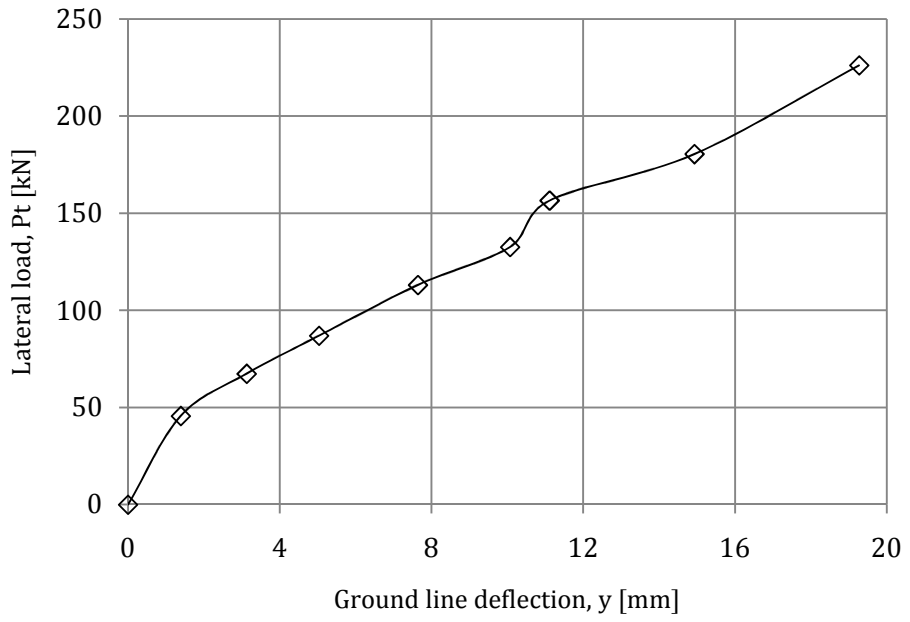

Graph 4-4 Ground line deflection vs. load, Florida

4.4 CASE XIV – APAPA, NIGERIA (1972)

In 1968 and 1972, Coleman and Coleman & Hancock describe the testing of Raymond piles near Apapa. The results were analyzed by Meyer in 1979.

Pile

Two Raymond piles were installed. A Raymond pile is a step-tapered pile. The diameter of the pile is small at the tip of the pile and large at the top. As the piles are installed the pile heads were capped with concrete blocks. The properties of the pile are given in table 4-6.

Depth [m]	Diameter [m]	E_pI_p kN/m^3
0 - 2,44	0,442	22.400
2,44 - 6,10	0,417	20.100
6,10 - 15,3	0,391	18.700

Table 4-6 Pile properties, Apapa

Soil

The soil consisted of two layers. The first layer consisted of a dense sand with a friction angle of 41 degrees and a volumetric weight of 18,9 kN/m^3. The friction angle was found by means of triaxial tests. Below this layer there was a thick layer of soft organic clay with a submerged unit weight of 4,9 kN/m^3, and the shear strength, found by means of an in situ vane test, was found to be 23,9 kPa.

Load

The static load was applied at 0,61 meters above the ground line.

Instrumentation

The pile deflection was measured at the point of application of the load. The load was applied by means of a hydraulic jack that was placed between the two piles. Therefore two tests were conducted at the same time.

Results

The results are given in tabular form, table 4-7, and graphical form, graph 4-5.

Lateral Load, P_t [kN]	Pile head deflection, Pile 1 $y_{t,1}$ [mm]	Pile head deflection, Pile 2 $y_{t,2}$ [mm]
8	1,5	1,3
18	3,1	3,1
26	4,4	5,2
35	5,7	6,8
44	7,4	8,8
53	9,6	12,9
63	11,8	18,6
71	18,2	24,7
81	22,8	-
89	27,2	-

Table 4-7Results test, Apapa

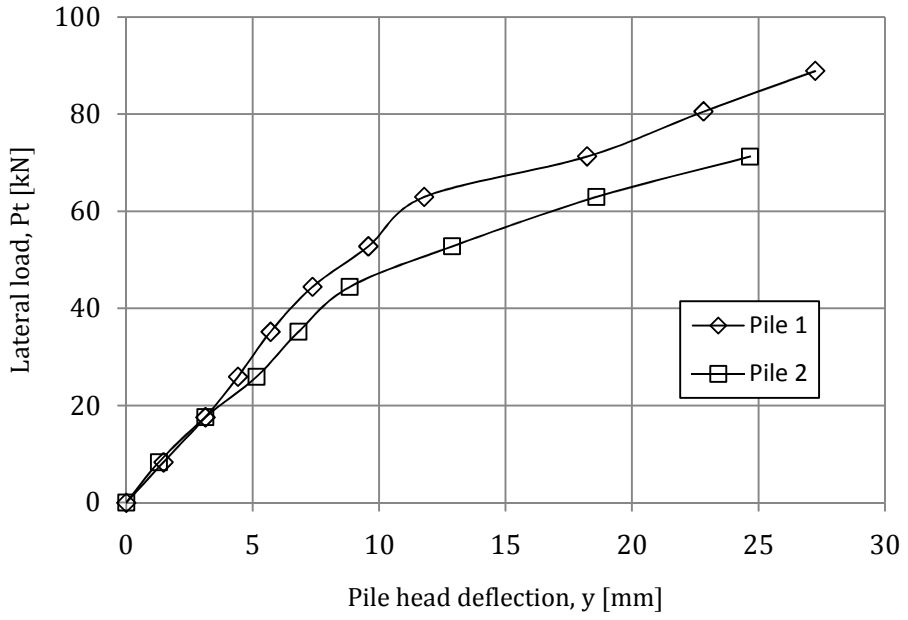

Graph 4-5Pile head deflection, Pile 1 and Pile 2, Apapa

5 FIELD TESTS IN C - Φ SOILS

In some situations, soil can have both cohesion and a friction angle. This is possible for cemented sands, sandy clays etc. In this chapter tests are performed in cemented sands

5.1 CASE XV – KUWAIT (1990)

In Kuwait, Ismael reported the results on a laterally loaded pile in 1990.

Pile

The pile was a bored pile with a diameter of 0,3 m and five meter long. The reinforcement was composed of six 22 mm bars in a 0,25 m diameter. A 36 mm diameter bar was placed in the middle of the pile. The bending stiffness was calculated from the initial slope of the moment-curvature curves to be 20,2 MNm^2. This value is significantly higher than the bending stiffness that was calculated, but it was decided that the measured bending stiffness was considered to be the valid value.

Soil

In the subsurface two layers could be separated. The first layer was a medium dense cemented silty sand, with a thickness of about 3,5 m. The cohesion and friction angle were found, by drained triaxial compression tests, to be 20 kPa and 35^o respectively. The unit weight averaged 17,9 kN/m^3. This top layer was underlain by a medium dense to very dense silty sand with cemented lumps. This layer has been found to have a cohesion of zero and is thus no $c - \varphi$ soil. The friction angle was 43^o and the unit weight was 19,1 kN/m^3.

Load

The point of application of the load was not reported in the summary of Reese and Van Impe. Therefore it is assumed that the load was applied at ground line.

Instrumentation

The test piles were instrumented with electrical-resistance strain gauges. After the test the soil around the pile was removed until a depth of 2 m. With the gauges exposed the pile was reloaded and the curvature was found from readings of strain.

Results

The results are given in tabular form, table 5-1, and graphical form, graph 5-1.

Lateral load, Pt [kN]	Pile head deflection, y_h [mm]
0	0
24	0,3
49	1,3
75	3,0
100	6,2
124	9,4
150	19,6
155	22,9

Table 5-1 Results test, Kuwait

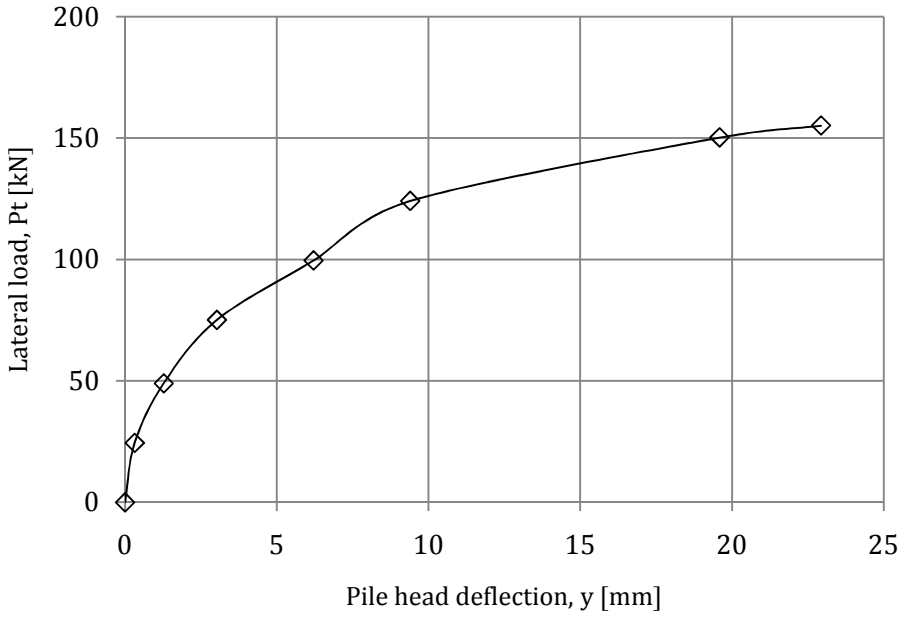

Graph 5-1 Pile head deflection vs. load, Kuwait

5.2 CASE XVI –LOS ANGELES, CALIFORNIA USA (1986)

This field test was conducted in 1986 by Caltrans, The Californian Department of Transport, in Los Angeles.

Pile

The bored pile was 1,22 m in diameter and had a penetration depth of 15,85 m. The pile was reinforced 24 bars with an total area of 0,001065 m^2. The distance between the outside of the reinforcement and the wall of the pile was 76,2 mm. The compressive strength of the concrete was 24.800 kPa and the tensile strength of the steel was 413.700 kPa.

Soil

The soil was schematized as five separate layers. For which the top and bottom layer are considered to be cohesive and the other layers to be c-φ soils. The properties of the soil layers are given in table 5-2.

Depth [m]	Soil type	Cohesion [kPa]	Friction angle [degrees]	Unit weight [kN/m^3]
0 – 1,5	Plastic clay	179	-	19,2
1,5 – 7,4	Sand and some clay	4,8	30	19,8
7,4 -10,5	Sandy clay	19,2	35	19,8
10,5 – 13,4	Sandy silt	19,2	21	18,9
13,4 - 20	Plastic clay	110	-	18,4

Table 5-2 Soil properties, Los Angeles

Load

The static load was applied at 0,61 m above the ground line. The loads were applied in increments.

Instrumentation

The pile was instrumented with strain gauges and Carlson cells for measurements on bending moment. Information on the calibration however, was not given.

Results

The results of the test at Los Angeles are given in tabular form, table 5-3, and graphical form, graphs 5-2 and 5-3.

Lateral load Pt, [kN]	Pile head deflection, y_h [mm]	Maximum bending moment, Mmax [kNm]
0	0	0
673	14,8	1420
891	26,5	2222
1089	38,9	2963
1307	52,5	3704
1703	98,1	5741

Table 5-3 Results test, Los Angeles

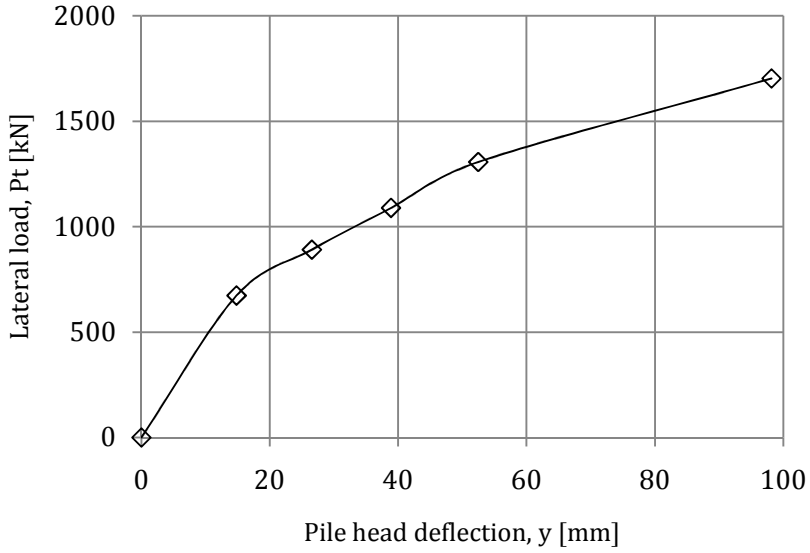

Graph 5-2 Pile head deflection vs. load, Los Angeles

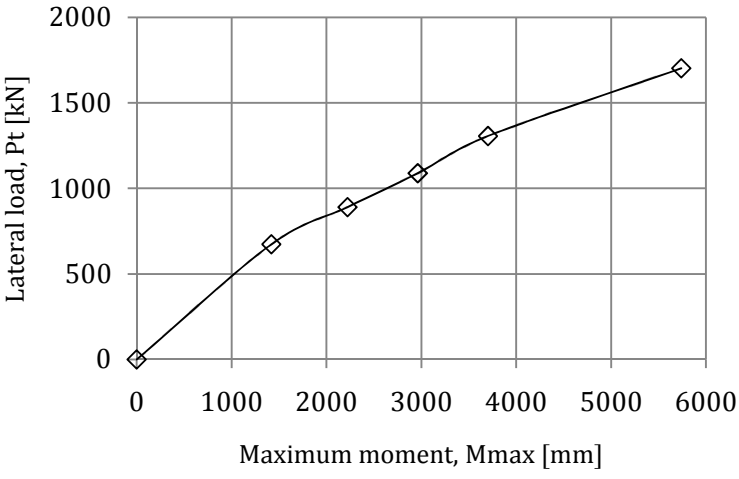

Graph 5-3 Maximum bending moment vs. load, Los Angeles

5.3 CASE XVII –DELFT, NETHERLANDS (1991)

This field test was conducted to find the accuracy of several finite element models. (Bijnagte, Van den Berg, Zorn, & Dieterman, 1991) It is the only full scale test that was found that was not already used by (Reese & Van Impe, 2001) as an example case. In figure 5-1, an overview of the test setup is given.

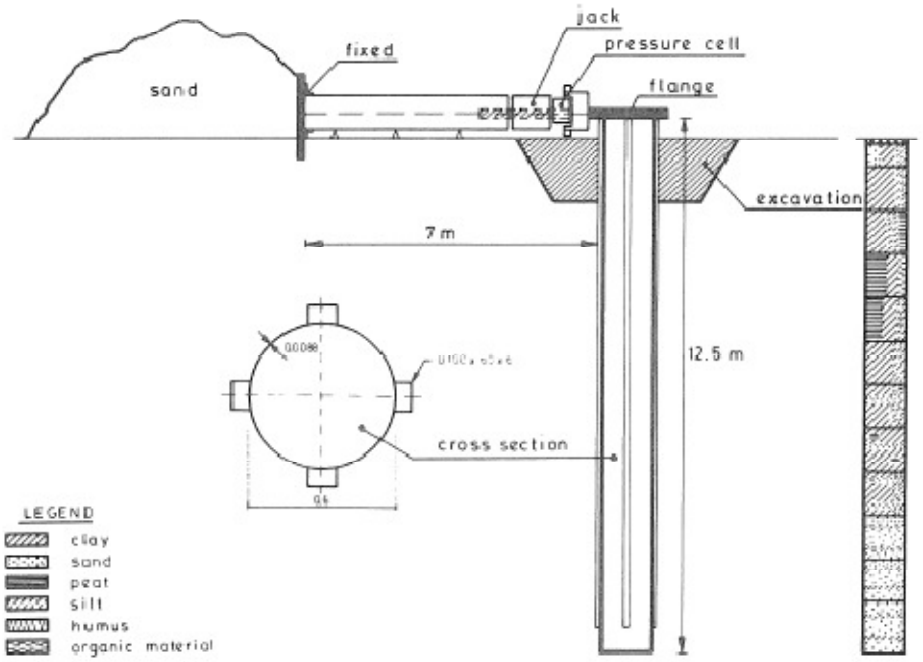

Figure 5-1 Test setup, soil layers and cross-section pile, Delft

Pile

The steel pipe pile had a diameter of 0,61 m, a wall thickness of 8,8 mm and a length of 12,5 m. To protect the measuring equipment, steel U-profiles, 100x50x6mm, were welded on four sides of the pile, figure 5-1.

Soil

The soil parameters were determined very precisely with field tests and laboratory tests. First of all a three CPT's were made which showed good correlation. The results of CPT 1A, figure 5-2, were presumed to be representative. Apart from the CPT also borings were made. This was done with the Delft continuous sampler. With the samples the soil was classified and soil properties were determined, tables 5-4, 5-5 and 5-6. The sand lump that was used to bear the horizontal load was placed at a distance of more than 10D. It is assumed that this weight had no influence on the test results. Around the pile the soil was excavated 1,5 m below the surface in a square of 2,6x2,6 m.

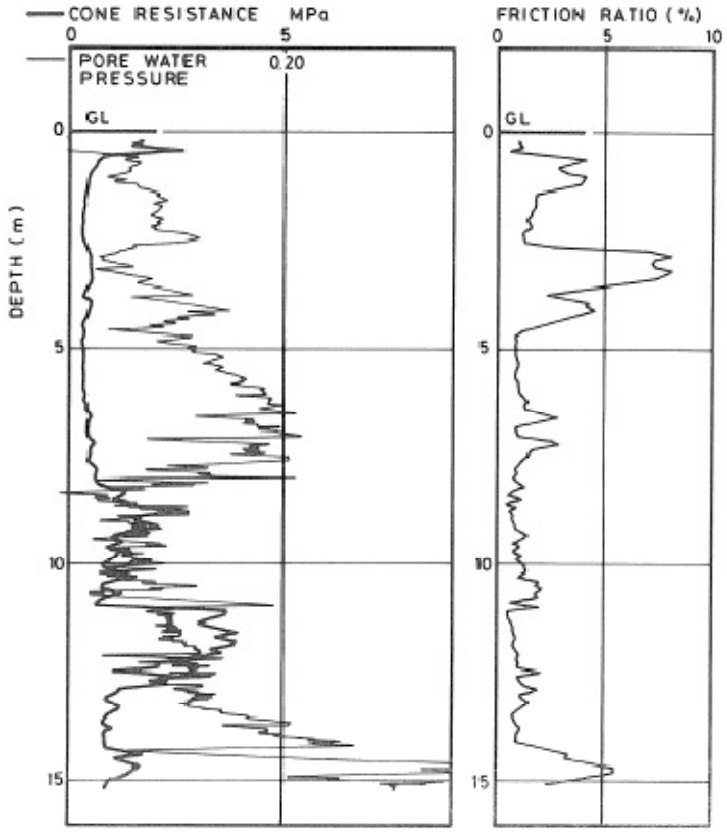

Figure 5-2 CPT 01A, representative CPT Delft

Depth [m]	Soil type	Unit weight [ton/m^3]
0 - 0,15	Pavement	-
0,15 - 0,66	Sand/clay, silty	1,88
0,66 - 2,68	Clay, silty, humus, peat	1,52
2,68 - 4,70	Peat/clay, silty	1,22
4,70 - 8,77	Clay, silty	1,54
8,77 - 13,85	Sand with silt/clay layers	1,73

Table 5-4 (Simplified) soil classification and wet densities

Sample nr.	Depth sample in m -ground line	Soil type	Liquid limit [%]	Plastic limit [%]	Plasticity index [%]
2	1,16-1,26	Clay silty	77,2	22,3	54,9
3	2,07-2,17	Clay silty with humus	71,8	23,5	48,3
4	2,98-3,08	Peat	631,0	234,4	396,6
5	4,39-4,49	Clay silty	43,0	18,1	24,9
6	5,30-5,40	Clay silty	59,2	18,7	40,5
7A	6,20-6,30	Clay silty with humus	121,1	28,0	93,1

Table 5-5 Results of Atterberg limits tests for clay and peat samples

Sample nr.	Depth sample in m - ground line	Soil type	Wet density [ton/m^3]	Water content [weight %]	Undrained shear strength c_u [kN/m^2]
2	1,16-1,20	Clay silty	1,53	72,5	36,2
3	2,07-2,11	Clay silty with humus	1,62	58,9	17,2
4	2,98-3,02	Peat	1,02	522,0	34,8
5	4,39-4,43	Clay silty	1,70	48,3	9,9
6	5,27-5,31	Clay silty	1,58	62,0	16,8
7A	6,21-6,25	Clay silty with humus	1,40	109,6	26,9
7B	6,51-6,56	Clay with peat	1,19	210,9	-
8A	7,10-7,15	Peat with clay	1,13	251,6	-
8B	7,48-7,52	Clay with humus	1,52	73,7	21,0
9	8,25-8,29	Clay- and sand layers	1,65	54,5	6,8

Table 5-6 Results of water content determinations and laboratory vane tests

Loads

The loading scheme can be divided in a quasi static and a cyclic part. First a quasi static, sine shaped load with an amplitude of 235kN was applied in 20 seconds. After that three series of alternating loads were applied. In this study, only the static part will be examined.

Instrumentation

The following data were recorded during the test with an interval of five measurements per second:

-The load at the pile top

-The horizontal displacement of the pile top

-The horizontal displacement of the pile 1 m below the pile top

-The bending moment by means of 34 strain gauges

Results

The results of the test comprise two plots that are of interest for this research. First of all there is the load displacement curve of the quasi-static loading. Secondly, there are the moment curves measured from the strain gauges while the quasi-static load was applied. The results are reported here in both tabular form, tables 5-7 and 5-8, and in graphical form, graphs 5-4 to 5-6.

Lateral load, Pt [kN]	Pile head deflection, y [mm]	Maximum bending moment, Mmax [kNm]
25	3,0	0
50	8,0	54
75	14,0	114
100	21,0	175
125	30,1	242
150	41,1	316
175	52,1	403
200	66,1	490
225	82,1	584
238	100,0	786

Table 5-7 Results test, pile head deflection and maximum bending moment, Delft

Depth [m –gl]	Bending moment over the length of the pile [kNm], where:								
	P_t = 25kN	P_t = 50kN	P_t = 75kN	P_t = 100kN	P_t = 125kN	P_t = 150kN	P_t = 175kN	P_t = 200kN	P_t = 238kN
-0,5	0	0	0	0	0	0	0	0	0
0,0	20	32	44	55	67	79	91	102	118
1,2	40	74	114	154	195	228	269	302	369
2,4	54	114	175	242	309	376	450	531	658
3,6	47	101	168	235	316	403	490	584	752
4,8	34	81	134	195	269	356	443	544	786
6,0	20	47	81	128	188	255	322	403	604
7,2	7	13	34	60	87	134	175	228	396
8,4	0	0	0	7	20	40	60	87	121
9,6	-7	-4	0	0	0	1	7	13	54
10,8	-9	-5	0	0	0	0	0	0	0
12,0	0	0	0	0	0	0	0	0	0

Table 5-8 Results test, bending moment, Delft

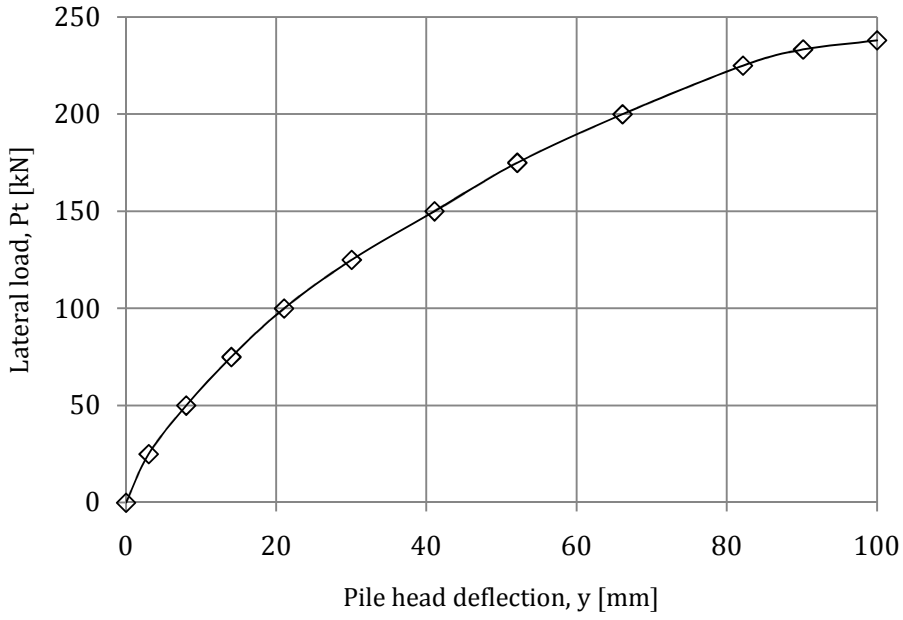

Graph 5-4 Pile head deflection vs. load, Delft

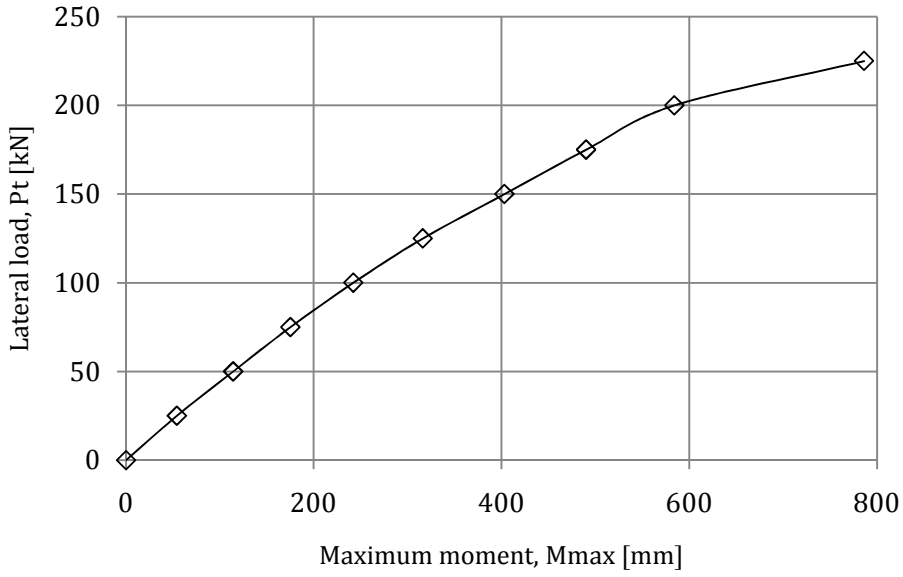

Graph 5-5Maximum bending moment vs. load, Delft

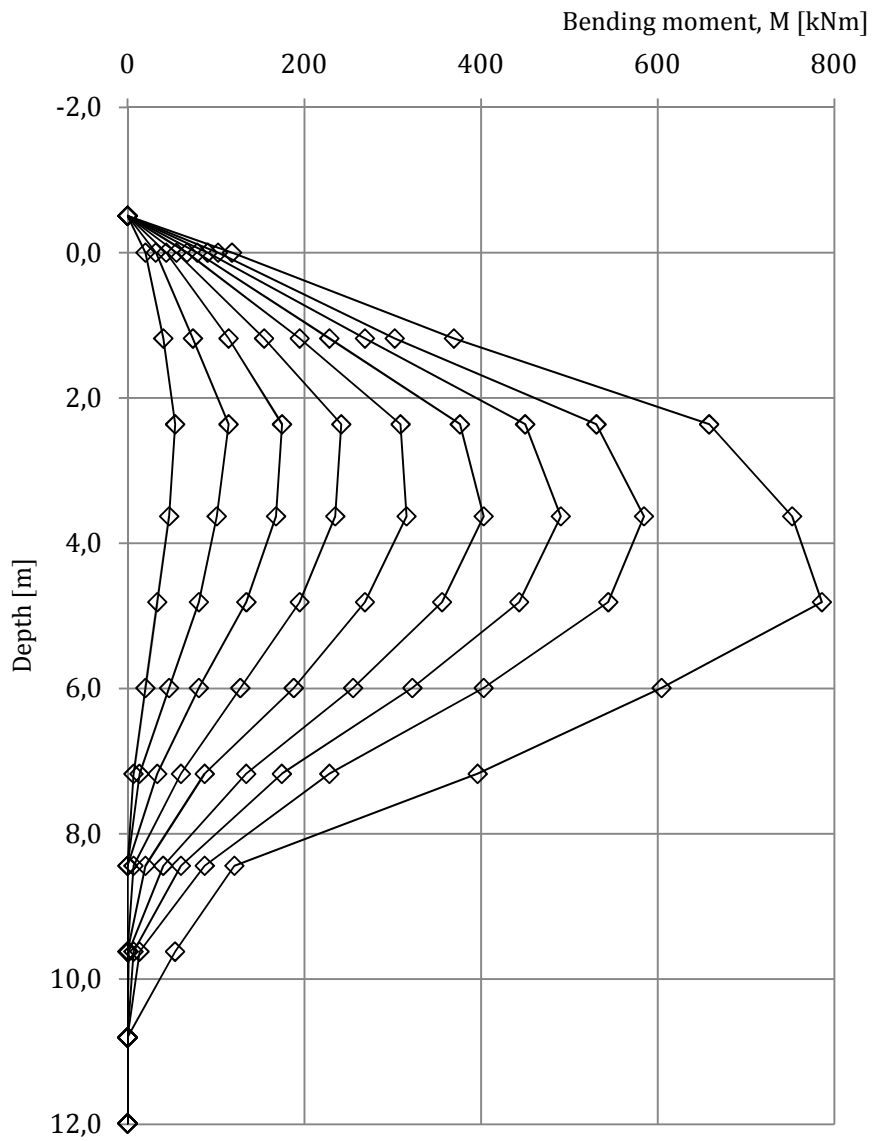

Graph 5-6 Bending moments as a function of depth for a lateral load of 25, 50, 75, 100, 125, 150, 175, 200 and 238 kN, Delft

6 EVALUATION

In this study 17 field experiments were executed on a total of 20 piles. Below, in table 6-1, the field tests are summarized on some of the important characteristics. These characteristics are chosen, because they together provide the information whether or not a certain model (Appendix A) is valid for the situation of that particular case.

Case	Soil	Homogeneous	Ultimate stat reached	Pile type	Not constant E_pI_p over length pile	Axial load
I-cu	Cohesive, unsaturated	Yes	No	Steel	No	No
II-cu	Cohesive, unsaturated	Yes	No	Bored	No	No
III-cu	Cohesive, unsaturated	Yes	No	Steel	No	No
IV-cu	Cohesive, unsaturated	Yes	No	Steel	No	No
V-cs	Cohesive, saturated	Yes	No	Steel	No	No
VI-cs	Cohesive, saturated	Yes	No	Steel	No	No
VII-cs	Cohesive, saturated	Yes	No	Steel	Yes	No
VIII-cl	Cohesionless	Yes	No	Steel	No	No
IX-cl	Cohesionless	Yes	No	Bored	No	No
X-cl	Cohesionless	Yes	No	Steel	No	No
XI-l	Layered	No	Yes	Steel	No	Yes
XII-l	Layered	No	No	Bored	No	No
XIII-l	Layered	No	No	Steel	Yes	No
XIV-l	Layered	No	No	Steel	Yes	No
XV-cφ	*c-φ* soil	No	No	Bored	No	No
XVI-cφ	*c-φ* soil	No	No	Bored	No	No
XVII-cφ	*c-φ* soil	No	No	Steel	No	No

Table 6-1 Summary Field tests

It can immediately be seen that case XI is different from the others. It is the only case where failure immersed and also the only case where an axial load was applied. Other cases that differed, apart from the soil type, were cases II, IX, XII, XV and XVI, since here bored piles were used and cases VII, XIII and XIV, since the bending stiffness of these piles was not constant over the length of the pile.

Limitations of the available field tests

Some of the field tests have been used as empirical input for creating the *p-y* curves. This is a limitation, because the models which use *p-y* curves cannot be validated on those field tests. The following cases have been used to create the recommendations for the *p-y* curves: Case II-cu, Case V-cs, Case VII-cs and Case VIII-cl.

Furthermore, the soil data is very limited. In most of the cases this is limited to the undrained shear strength and/or the angle of internal friction and a volumetric weight for each soil layer. In all cases, except for the case in Delft the soil test results are not available. This means that the available soil data is assumed to be correct and correctly determined by means of thorough soil investigations.
The number of tests is not high enough to be able to judge the models in all possible situations. The range of the diameters of the different piles is between 0,3m and 1,5m. Thus no large diameter piles are included in this research.
No tests on wooden piles are included and the number of concrete piles is small.
In all the field tests the piles were subjected to loads of a short duration. This means that the load should not be considered as an impulse. It also means that the soil will react partially drained, especially if sand is considered, and partially undrained, in the cases of a clayey soil. This also limits the range in which this research is valid to loads of a short duration. These types of loads can be expected in mooring situations, if a boat collides with a dolphin. These types of collisions usually last for (tens of) seconds.

APPENDIX C

Comparison Calculations

CONTENTS

1 INTRODUCTION

In this appendix the models are compared on accuracy. This means that the models are compared on how accurate they can predict the deflections of the pile. This is an important parameter on the decision on which model is the best in a specified situations. The models that are used here are described in detail in appendix A and the field tests in appendix B. This appendix is divided in ten chapters. Apart from the introduction, each chapter contains all the calculations which have been executed with the model stated in the chapter title. Each paragraph of the chapters is a calculation. The results are given on the end of each paragraph. In the evaluation in chapter four of the main report, the results are summarized. In those graphs, the accuracy of the different models can be compared.

Notes:
Not all the models have been used for all the cases. The models Blum and Brinch Hansen could not be used to evaluate field tests. The model of Broms produced results that were very different from the reality. In addition to that, it appeared that it is not possible to use Broms in all loading situations. Therefore, Broms is only used in two cases. The Nondimensional Method, with p-y curves according to the API is also used in only two cases. After calculating the two cases, the MPile program became available to the author, and this program also uses p-y curves according to the API. In addition to that, the Nondimensional Method returned better results for the two cases if the p-y curves where generated according to Reese *et al.* Because of these reasons and the fact that using the Nondimensional Method is very time intensive, it was decided to not continue with this method with p-y curves according to the API.

In addition to that not all measurements have been used either. This was due limited amount of time available to perform all the calculations with all models for all measurements. The selection of the measurements was based first on type of soil. It was decided to make for the two most occurring soils, clayey soil and sandy soil, a comparison between the models on three cases. This excluded the field tests in layered soils and c-φ soils. Of the remaining cases, case II, V, VII and VIII are excluded since these tests were executed en used by the developers of the method of p-y curves. The remaining tests have been used for calculation. Unfortunately, only two cases in sandy soil remained. Therefore case XIII-l has also been used. The soil layer in this case is layered, but the thick top layer consisted of cohesionless soil. For the calculation in clayey soil four cases remained. Here case IV-cu was left out since it was executed with the goal to examine the pile behavior in earthquake conditions. In summary the used tests are for cohesive soil: Case I-cu, III-cu and VI-cs. And for cohesionless soil: Case IX-cl, X-cl and XIII-l.

2 BLUM

The method to design laterally loaded piles that was developed by H. Blum is not suitable to be compared with other models. This is due to the fact that loading of the test piles did not go all the way up to failure. Although the method does allow the user to calculate the displacement of the pile, unfortunately the only displacement that can be calculated is the displacement at failure. Therefore no calculations have been performed with Blum.

3 BRINCH HANSEN

The method of Brinch Hansen has the same limitation as the method proposed by Blum. This model is also designed to calculate only the ultimate load on the pile. Since the pile is modeled with only one boundary condition, one rotation point at a certain depth below the soil surface, it is not possible at all to calculate deflections with this model. For this reasons the results of the field tests cannot be recalculated with this model.

4 BROMS

The method Broms only gives an estimate for deflections if the imposed load is between approximately 0,3 and 0,5 times the ultimate load. Thus to calculate the deflections for these loads first the ultimate load has to be found. The method has been applied on two cases, Arkansas River and Brent Cross. The first is field test in cohesionless soil, the second in a cohesive soil.

4.1 CASE X-CL, ARKANSAS RIVER

4.1.1 Input

The input necessary to enter the design graphs for long piles in cohesionless soil consists of the following parameters:

Yield moment: $M_{yield} = 361\ kNm$

Pile diameter: $D = 0{,}48\ m$

Volumetric weight:

$\gamma = 14{,}4\ kN/m^3 (see\ calculation\ Arkansas\ River\ by\ CLM, chapter\ x.x)$

Friction angle: $\varphi = 42{,}8°\ (see\ calculation\ Arkansas\ River\ by\ CLM, chapter\ x.x)$

Passive horizontal earth pressure coefficient:

$$K_p = tan^2\left(45 + \frac{42{,}8}{2}\right) = 5{,}23$$

Point of application: $e = 0\ m$

Modulus of horizontal subgrade reaction:

$$n_h = 56\ tons\ per\ cu\ ft = 1794\ kN/m^3$$

Bending stiffness pile: $EI = 69900\ kNm^2$

4.1.2 Calculation

For a long pile in cohesionless soil, figure 5-6 of chapter 5 in the literature study has to be used.

$$\frac{M_{yield}}{D^4 \gamma K_p} = \frac{361}{0{,}48^4 \times 14{,}4 \times 5{,}23} = 90$$

$$\frac{e}{D} = \frac{0}{0{,}48} = 0$$

If these parameters are used in the figure, the value “8” is found. This gives:

$$8 = \frac{P_{ult}}{K_p D^3 \gamma} \longrightarrow P_{ult} = 8 K_p D^3 \gamma = 8 \times 5{,}4 \times 0.48^3 \times 20 = 93 kN$$

Deformations can now be calculated for:

$0{,}3 \times 93 \leq P \leq 0{,}5 \times 93 \longrightarrow 28kN \leq P \leq 47kN$

Since Broms stated that the deformations can be calculated for loads between the approximate values of 0,3 and 0,5 times the ultimate load, the deformation can only be determined for the load of 46 kN. For this calculation figure 5-3 of chapter five of appendix A has to be used. The input for this graph is:

$$\eta = \sqrt[5]{\frac{n_h}{EI}} = \left(\frac{1794}{69900}\right)^{0,2} = 0{,}48\, m^{-1}$$
$$\eta L = 0{,}48 * 15 = 7{,}2$$

If these parameters are used in the figure, the value “0,33” is found. This gives the following displacements:

$$\gamma_{h,92kN} = \frac{0{,}33PL}{(EI)^{0,6} n_h^{0,4}} = \frac{0{,}33 \times 46 \times 15 \times (1000)}{69900^{0,6} \times 1794^{0,4}} = 14{,}1\, mm$$

4.1.3 Output

The maximum load prescribed by Broms is lower than the loads that have been applied during the field test. Broms predicts the ultimate load to be 93kN, however 248kN has been applied without failure of the pile. The calculated deformation deferred a lot from the measurements. Also Broms was not able to calculate the deflections at all of the imposed loads during the test. In graph 4-1 the results are given in graphical form.

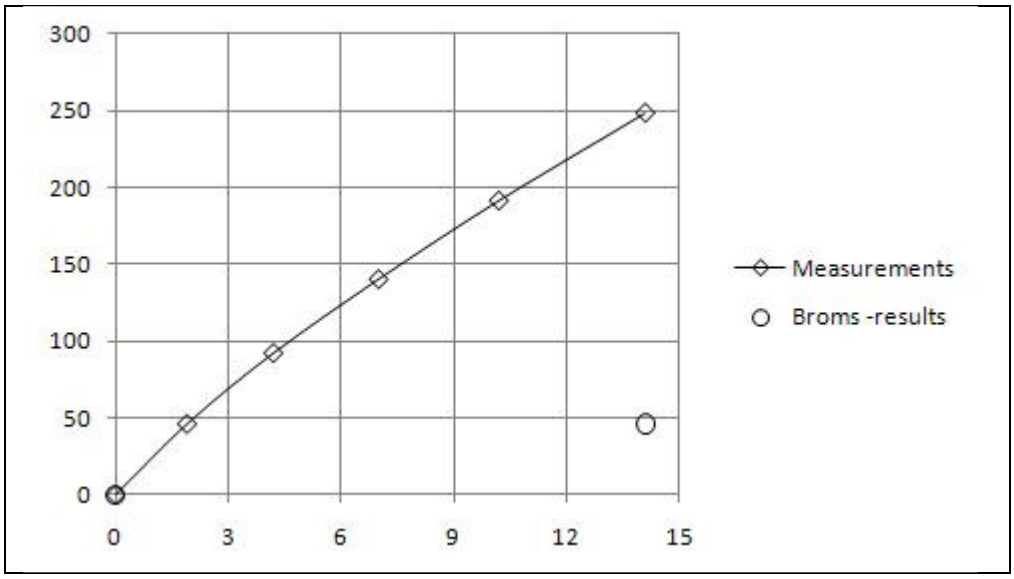

Graph 4-1 In this graph the lateral load [kN] is plotted on the y-axis versus the deformations [mm] on the x-axis. The graph visualizes the result obtained with Broms compared to the measurement in the case of Arkansas River.

4.2 CASE III-CU, BRENT CROSS

4.2.1 Input

The input necessary to enter the design graphs for long piles consists of the following parameters:

Yield moment: $M_{yield} = 392\ kNm$
Pile diameter: $D = 0{,}406\ m$
Undrained shear strength: $c_u = 44{,}1kPa$
Point of application: $e = 1\ m$
Modulus of horizontal subgrade reaction: $k_h = 8300\ kN/m^3$
Bending stiffness pile: $EI = 5{,}14 \times 10^4\ kNm^2$
Length pile: $L = 16{,}5\ m$

4.2.2 Calculation

For a long pile in cohesive soil, figure 5-6 of chapter 5 in appendix A has to be used.

$$\frac{M_{yield}}{D^3 c_u} = \frac{301}{0{,}406^3 \times 44{,}1} = 102$$
$$\frac{e}{D} = \frac{1}{0{,}406} = 2{,}46$$

If these parameters are used in the figure, the value “20” is found. This gives:

$$20 = \frac{P_{ult}}{c_u D^2} \longrightarrow P_{ult} = 20 c_u D^2 = 20 \times 44{,}1 \times 0{,}406^2 = 145kN$$

Deformations can now be calculated for:

$$0{,}3 \times 145 \leq P \leq 0{,}5 \times 145 \longrightarrow 43kN \leq P \leq 73kN$$

Since Broms stated that the deformations can be calculated for loads between the approximate values of 0,3 and 0,5 times the ultimate load, the deformations will be determined for the loads of 40kN and 60kN. For this calculation figure 5-7 of chapter five of appendix A has to be used. The input for this graph is:

$$\beta = \sqrt[4]{\frac{k_h D}{4EI}} = \left(\frac{8300 \times 0{,}406}{4 \times 5{,}14 \times 10^4}\right)^{0{,}25} = 0{,}36\ m^{-1}$$
$$\beta L = 0{,}36 * 16{,}5 = 5{,}94$$

If these parameters are used in the figure, the value “14,4” is found. This gives the following displacements:

$$\gamma_{h,40kN} = \frac{14{,}4P}{LDk_h} = \frac{14{,}4 \times 40}{16{,}5 \times 0{,}406 \times 8300} = 10{,}4\ mm$$

$$\gamma_{h,60kN} = \frac{14{,}4P}{LDk_h} = \frac{14{,}4 \times 60}{16{,}5 \times 0{,}406 \times 8300} = 15{,}5\ mm$$

4.2.3 Output

The results found by Broms differ from the measured values. The calculated deflections are higher than the measured deflections. An overview the results is given in graphical form in graph 4.2.

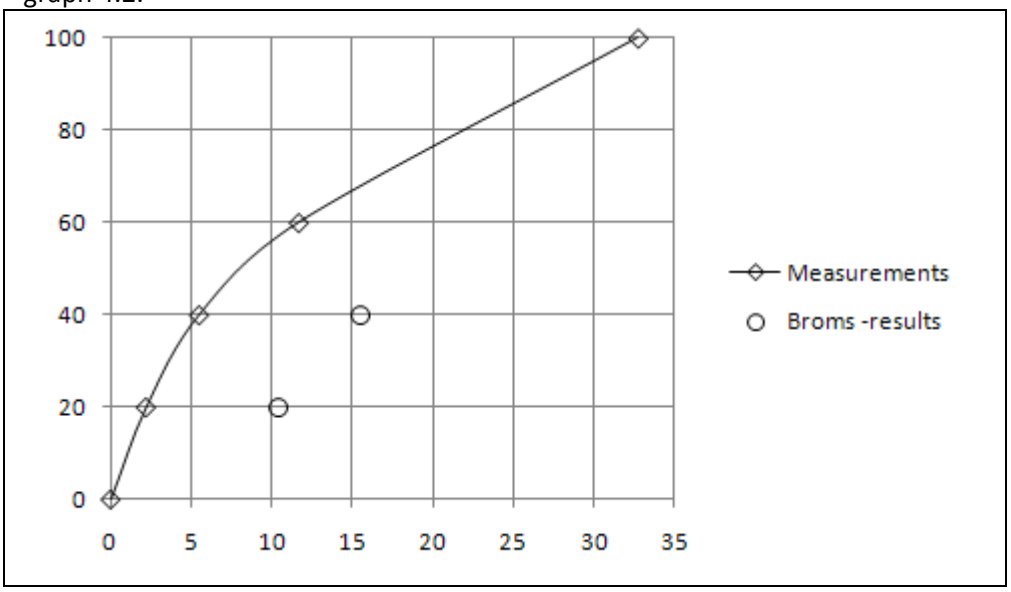

Graph 4-2 In this graph the lateral load [kN] is plotted on the y-axis versus the deformations [mm] on the x-axis. The graph visualizes the result obtained with Broms compared to the measurement in the case of Brent Cross.

5 CHARACTERISTIC LOAD METHOD

The Characteristic Load Method, CLM, is developed for homogeneous soil. The developers proposed to average the soil parameters over the first eight pile diameters of the soil, because the properties of the top layers are most important. Six field tests have been considered. Of these field test, three have been executed in cohesive soils, the others in cohesionless soil.

5.1 CASE I-CU, BAGNOLET

5.1.1 Calculation

Determine if the deflections are measured at the ground line.

Yes, the ground line deformation has been measured. Also the maximum occurring moment has been measured.

Determine the average soil parameters over the first eight diameters of the pile

The diameter of the pile is determined to be 0,43m. Because the soil data describes a top layer of 3,96m thick, the soil parameters are as follows:

$c_u = 100kPa$
$\gamma' = 17{,}9kN/m^3$

Determine if the pile is long enough to perform a CLM-calculation.

This can be determined by table 6-2 of Appendix A.

$$\frac{E_p R_I}{c_u} = \frac{2{,}1 \times 10^8 \times \left(\frac{25.500}{2{,}1 \times 10^8}\right) \Big/ \left(\frac{\pi \times 0{,}43^4}{64}\right)}{100} = 151.949$$

The minimum length is, if the values of the table are linearly interpolated, seven pile diameters.

The lengths of the three piles in the three tests performed at Bagnolet are:

$Test\ 1: L/D = 2{,}65/0{,}43 = 6{,}16 \times D$
$Test\ 2: L/D = 4{,}15/0{,}43 = 9{,}65 \times D$
$Test\ 3: L/D = 5{,}10/0{,}43 = 11{,}86 \times D$

This means that the CLM-calculation can only be performed for Test 2 and 3.

Determine the Characteristic load, P_c, and moment, M_c.

$$R_I = \left(\frac{25.500}{2{,}1 \times 10^8}\right) \Big/ \left(\frac{\pi \times 0{,}43^4}{64}\right) = 72{,}4 \times 10^{-3}$$

$$P_c = 7{,}34 \times 0{,}43^2 \times (2{,}1 \times 10^8 \times 72{,}4 \times 10^{-3}) \times \left(\frac{100}{2{,}1 \times 10^8 \times 72{,}4 \times 10^{-3}}\right)^{0{,}68} = 6.177\ kN$$

$$M_c = 3{,}86 \times 0{,}43^3 \times (2{,}1 \times 10^8 \times 72{,}4 \times 10^{-3}) \times \left(\frac{100}{2{,}1 \times 10^8 \times 72{,}4 \times 10^{-3}}\right)^{0{,}46} = 19.280\ kNm$$

Determine P_0/P_c to find y/D and subsequently ground line deformation, y_p.

The ground line deformations caused only by the lateral load for **Test 2** are:

$P_0/P_c = 15/6177 = 0{,}00243 \rightarrow y_p/D = 0{,}001 \rightarrow y_{p,15kN} = 0{,}43\ mm$
$P_0/P_c = 39/6177 = 0{,}00631 \rightarrow y_p/D = 0{,}005 \rightarrow y_{p,39kN} = 2{,}15\ mm$
$P_0/P_c = 59/6177 = 0{,}00955 \rightarrow y_p/D = 0{,}011 \rightarrow y_{p,59kN} = 4{,}73\ mm$
$P_0/P_c = 83/6177 = 0{,}01344 \rightarrow y_p/D = 0{,}019 \rightarrow y_{p,83kN} = 8{,}17\ mm$

The ground line deformations caused only by the lateral load for **Test 3** are:

$P_0/P_c = 34/6177 = 0{,}00550 \rightarrow y_p/D = 0{,}004 \rightarrow y_{p,34kN} = 1{,}72\ mm$
$P_0/P_c = 46/6177 = 0{,}00745 \rightarrow y_p/D = 0{,}008 \rightarrow y_{p,46kN} = 3{,}44\ mm$
$P_0/P_c = 59/6177 = 0{,}00955 \rightarrow y_p/D = 0{,}011 \rightarrow y_{p,59\ kN} = 4{,}76\ mm$
$P_0/P_c = 79/6177 = 0{,}01279 \rightarrow y_p/D = 0{,}018 \rightarrow y_{p,79kN} = 7{,}74\ mm$

Determine M_0/M_c to find y/D and subsequently ground line deformation, y_m.

The ground line deformations caused only by the moment at the groundline for **Test 2** are:

$M_0/M_c = 15 \times 0{,}9/19280 = 0{,}0007 \rightarrow y_m/D = 0{,}0014 \rightarrow y_{m,34kN} = 0{,}60\ mm$
$M_0/M_c = 39 \times 0{,}9/19280 = 0{,}0018 \rightarrow y_m/D = 0{,}0036 \rightarrow y_{m,39kN} = 1{,}55\ mm$
$M_0/M_c = 59 \times 0{,}9/19280 = 0{,}0028 \rightarrow y_m/D = 0{,}0056 \rightarrow y_{m,59\ kN} = 2{,}41\ mm$
$M_0/M_c = 83 \times 0{,}9/19280 = 0{,}0039 \rightarrow y_m/D = 0{,}0078 \rightarrow y_{m,83kN} = 3{,}35\ mm$

The ground line deformations caused only by the moment at the groundline for **Test 3** are:

$M_0/M_c = 34 \times 1{,}0/19280 = 0{,}0018 \rightarrow y_m/D = 0{,}0036 \rightarrow y_{m,34kN} = 1{,}55\ mm$
$M_0/M_c = 46 \times 1{,}0/19280 = 0{,}0024 \rightarrow y_m/D = 0{,}0048 \rightarrow y_{m,46kN} = 2{,}06\ mm$
$M_0/M_c = 59 \times 1{,}0/19280 = 0{,}0031 \rightarrow y_m/D = 0{,}0062 \rightarrow y_{m,59kN} = 2{,}67\ mm$
$M_0/M_c = 79 \times 1{,}0/19280 = 0{,}0041 \rightarrow y_m/D = 0{,}0082 \rightarrow y_{m,79kN} = 3{,}57\ mm$

Determine load, P_1, that would have caused the same deflections as moment, M_0.

This is determined first for **Test 2**:

$y_{m,15kN}/D = 0{,}0014 \rightarrow P_{1;15kN}/P_c = 0{,}0017 \rightarrow P_{1;15kN} = 10{,}5\ kN$
$y_{m,39kN}/D = 0{,}0036 \rightarrow P_{1;39kN}/P_c = 0{,}0042 \rightarrow P_{1;36kN} = 25{,}9\ kN$
$y_{m,59kN}/D = 0{,}0056 \rightarrow P_{1;59kN}/P_c = 0{,}0067 \rightarrow P_{1;59kN} = 41{,}4\ kN$
$y_{m,83kN}/D = 0{,}0078 \rightarrow P_{1;83kN}/P_c = 0{,}0094 \rightarrow P_{1;83kN} = 58{,}1\ kN$

And for **Test 3**:

$y_{m,34kN}/D = 0{,}0036 \rightarrow P_{1;34kN}/P_c = 0{,}0043 \rightarrow P_{1;34kN} = 26{,}6\ kN$
$y_{m,46kN}/D = 0{,}0048 \rightarrow P_{1;46kN}/P_c = 0{,}0058 \rightarrow P_{1;46kN} = 35{,}8\ kN$
$y_{m,59kN}/D = 0{,}0062 \rightarrow P_{1;59kN}/P_c = 0{,}0074 \rightarrow P_{1;59kN} = 45{,}7\ kN$
$y_{m,79kN}/D = 0{,}0082 \rightarrow P_{1;79kN}/P_c = 0{,}0098 \rightarrow P_{1;79kN} = 60{,}5\ kN$

Determine moment, M_1, that would have caused the same deflections as load, P_0.

This is determined first for **Test 2**:

$y_{p,15kN}/D = 0{,}001 \rightarrow M_{1;15kN}/M_c = 0{,}0005 \rightarrow M_{1;15kN} = 9{,}6\ kNm$
$y_{p,39kN}/D = 0{,}005 \rightarrow M_{1;39kN}/M_c = 0{,}0025 \rightarrow M_{1;36kN} = 48{,}2\ kNm$
$y_{p,59kN}/D = 0{,}011 \rightarrow M_{1;59kN}/M_c = 0{,}0055 \rightarrow M_{1;59kN} = 106{,}0\ kNm$
$y_{p,83kN}/D = 0{,}019 \rightarrow M_{1;83kN}/M_c = 0{,}0095 \rightarrow M_{1;83kN} = 183{,}2\ kNm$

And for **Test 3**:

$y_{p,34kN}/D = 0{,}004 \rightarrow M_{1;34kN}/M_c = 0{,}0020 \rightarrow M_{1;34kN} = 38{,}6\ kNm$
$y_{p,46kN}/D = 0{,}008 \rightarrow M_{1;46kN}/M_c = 0{,}0040 \rightarrow M_{1;46kN} = 77{,}1\ kNm$

$y_{p,59kN}/D = 0{,}011 \rightarrow M_{1;59kN}/M_c = 0{,}0055 \rightarrow M_{1;59kN} = 106\ kNm$
$y_{p,79kN}/D = 0{,}018 \rightarrow M_{1;79kN}/M_c = 0{,}0090 \rightarrow M_{1;79kN} = 173{,}5\ kNm$

Now calculate the displacements that are caused by the combined load of P_0 and P_1.

For **Test 2**:

$P_0 + P_{1;15kN} = 15 + 10{,}5 = 25{,}5\ kN$
$P_0 + P_{1;39kN} = 39 + 25{,}9 = 64{,}9\ kN$
$P_0 + P_{1;59kN} = 59 + 41{,}4 = 100{,}4\ kN$
$P_0 + P_{1;83kN} = 83 + 58{,}1 = 141{,}1\ kN$

$P_{0+1}/P_c = 25{,}5/6177 = 0{,}00413 \rightarrow y_{pm}/b = 0{,}004 \rightarrow y_{pm,15kN} = 1{,}72\ mm$
$P_{0+1}/P_c = 64{,}9/6177 = 0{,}01051 \rightarrow y_{pm}/b = 0{,}012 \rightarrow y_{pm,39kN} = 5{,}16\ mm$
$P_{0+1}/P_c = 100{,}4/6177 = 0{,}01625 \rightarrow y_{pm}/b = 0{,}027 \rightarrow y_{pm,59kN} = 11{,}6\ mm$
$P_{0+1}/P_c = 141{,}1/6177 = 0{,}02284 \rightarrow y_{pm}/b = 0{,}050 \rightarrow y_{pm,83kN} = 21{,}5\ mm$

For **Test 3**:

$P_0 + P_{1;34kN} = 34 + 26{,}6 = 60{,}6\ kN$
$P_0 + P_{1;46kN} = 46 + 35{,}8 = 81{,}8\ kN$
$P_0 + P_{1;59kN} = 59 + 45{,}7 = 104{,}7\ kN$
$P_0 + P_{1;79kN} = 79 + 60{,}5 = 139{,}5\ kN$

$P_{0+1}/P_c = 60{,}6/6177 = 0{,}00981 \rightarrow y_{pm}/b = 0{,}032 \rightarrow y_{pm,34kN} = 13{,}8\ mm$
$P_{0+1}/P_c = 81{,}8/6177 = 0{,}01324 \rightarrow y_{pm}/b = 0{,}043 \rightarrow y_{pm,46kN} = 18{,}5\ mm$
$P_{0+1}/P_c = 104{,}7/6177 = 0{,}01695 \rightarrow y_{pm}/b = 0{,}065 \rightarrow y_{pm,59kN} = 28{,}0\ mm$
$P_{0+1}/P_c = 139{,}5/6177 = 0{,}02258 \rightarrow y_{pm}/b = 0{,}099 \rightarrow y_{pm,79kN} = 42{,}6\ mm$

Now calculate the displacements that are caused by the combined moments M_0 and M_1.

For **Test 2**:

$M_0 + M_{1;15kN} = 15 \times 0{,}9 + 9{,}6 = 23{,}1\ kNm$
$M_0 + M_{1;39kN} = 39 \times 0{,}9 + 48{,}2 = 83{,}3\ kNm$
$M_0 + M_{1;59kN} = 59 \times 0{,}9 + 106 = 159{,}1\ kNm$
$M_0 + M_{1;83kN} = 83 \times 0{,}9 + 183{,}2 = 257{,}9\ kNm$

$M_{0+1}/M_c = 23{,}1/19280 = 0{,}00120 \rightarrow y_{pm}/b = 0{,}0024 \rightarrow y_{mp,15kN} = 1{,}03mm$
$M_{0+1}/M_c = 83{,}3/19280 = 0{,}00432 \rightarrow y_{pm}/b = 0{,}0086 \rightarrow y_{mp,39kN} = 3{,}7\ mm$
$M_{0+1}/M_c = 159{,}1/19280 = 0{,}00825 \rightarrow y_{pm}/b = 0{,}022 \rightarrow y_{mp,59kN} = 9{,}5\ mm$
$M_{0+1}/M_c = 257{,}9/19280 = 0{,}01338 \rightarrow y_{pm}/b = 0{,}047 \rightarrow y_{mp,83N} = 20{,}2\ mm$

For **Test 3**:

$M_0 + M_{1;34kN} = 34 \times 1{,}0 + 9{,}6 = 43{,}6\ kNm$
$M_0 + M_{1;46kN} = 46 \times 1{,}0 + 48{,}2 = 94{,}2kNm$
$M_0 + M_{1;59kN} = 59 \times 1{,}0 + 106 = 165\ kNm$
$M_0 + M_{1;79kN} = 79 \times 1{,}0 + 183{,}2 = 262{,}2\ kNm$

$M_{0+1}/M_c = 43{,}6/19280 = 0{,}00226 \rightarrow y_{pm}/b = 0{,}0045 \rightarrow y_{mp,34kN} = 1{,}9\ mm$
$M_{0+1}/M_c = 94{,}2/19280 = 0{,}00489 \rightarrow y_{pm}/b = 0{,}0098 \rightarrow y_{mp,46kN} = 4{,}2\ mm$
$M_{0+1}/M_c = 165/19280 = 0{,}00856 \rightarrow y_{pm}/b = 0{,}022 \rightarrow y_{mp,59kN} = 9{,}5\ mm$
$M_{0+1}/M_c = 262{,}2/19280 = 0{,}01360 \rightarrow y_{pm}/b = 0{,}047 \rightarrow y_{mp,79N} = 20{,}2\ mm$

Calculate the groundline deflections by taking the average between y_{pm} and y_{mp}.

For **Test 2**:

$\boldsymbol{y_{15kN}} = (1{,}72 + 1{,}03)/2 = \mathbf{1{,}4}\ \boldsymbol{mm}$
$\boldsymbol{y_{39kN}} = (5{,}16 + 3{,}7)/2 = \mathbf{4{,}4}\ \boldsymbol{mm}$
$\boldsymbol{y_{59kN}} = (11{,}6 + 9{,}5)/2 = \mathbf{10{,}6}\ \boldsymbol{mm}$
$\boldsymbol{y_{83kN}} = (21{,}5 + 20{,}2)/2 = \mathbf{20{,}9}\ \boldsymbol{mm}$

For **Test 3**:

$\boldsymbol{y_{34kN}} = (13{,}8 + 1{,}9)/2 = \mathbf{7{,}9}\ \boldsymbol{mm}$
$\boldsymbol{y_{46kN}} = (18{,}5 + 4{,}2)/2 = \mathbf{11{,}4}\ \boldsymbol{mm}$
$\boldsymbol{y_{59kN}} = (28{,}0 + 9{,}5)/2 = \mathbf{18{,}8}\ \boldsymbol{mm}$
$\boldsymbol{y_{79kN}} = (42{,}6 + 20{,}2)/2 = \mathbf{31{,}4}\ \boldsymbol{mm}$

Calculate the maximum moments

This calculation is best executed in excel to speed up the iterative process. In excel the calculations have been executed according to Chapter 6 in Appendix A.

For **Test 2**:

$\boldsymbol{M_{max,15kN}} = \mathbf{20{,}5}\ \boldsymbol{kNm}$
$\boldsymbol{M_{max,39kN}} = \mathbf{55{,}2}\ \boldsymbol{kNm}$
$\boldsymbol{M_{max,59kN}} = \mathbf{91{,}0}\ \boldsymbol{kNm}$
$\boldsymbol{M_{max,83kN}} = \mathbf{104{,}3}\ \boldsymbol{kNm}$

For **Test 3**:

$\boldsymbol{M_{max,34kN}} = \mathbf{57{,}6}\ \boldsymbol{kNm}$
$\boldsymbol{M_{max,46kN}} = \mathbf{78{,}9}\ \boldsymbol{kNm}$
$\boldsymbol{M_{max,59kN}} = \mathbf{106{,}3}\ \boldsymbol{kNm}$
$\boldsymbol{M_{max,79kN}} = \mathbf{148{,}8}\ \boldsymbol{kNm}$

5.1.2 Output

At Bagnolet three tests were performed. Two of them were allowed to be calculated with the CLM. In the first test the pile length was too short compared to the pile diameter. The result of the calculations on test two and three is a set of four graphs, two load-displacement graphs and two load-maximum moment graphs. These graphs are given below. It can be seen that the maximum moment were calculated reasonably accurate. Displacements however differed more. The lateral deflection of the pile was calculated to be approximately two times as large as the measured deflection for test II and three times as large as the measured deflection for test III.

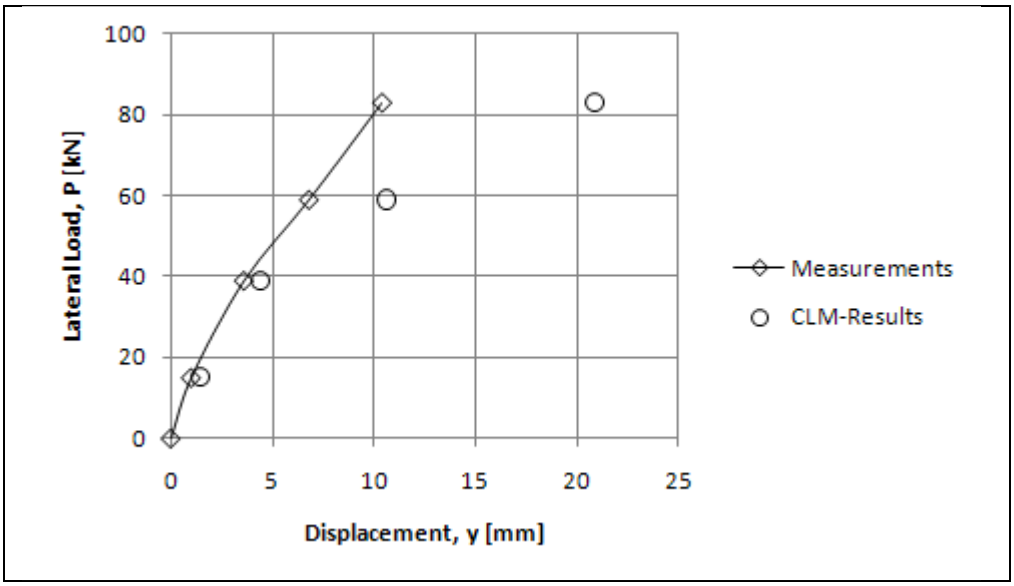

Graph 5-1 Lateral load vs. displacement Test II

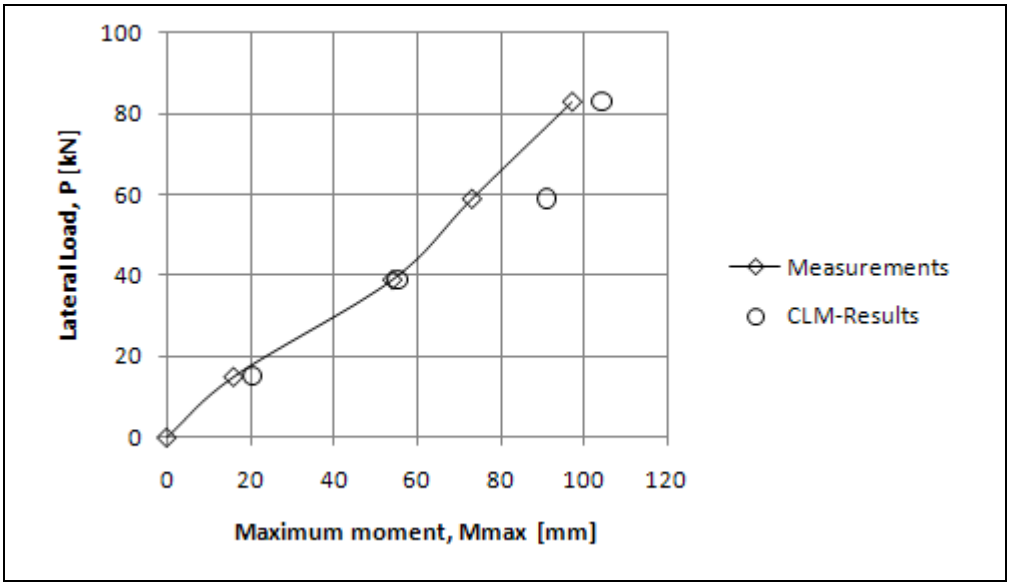

Graph 5-2 Lateral load vs. maximum moment Test II

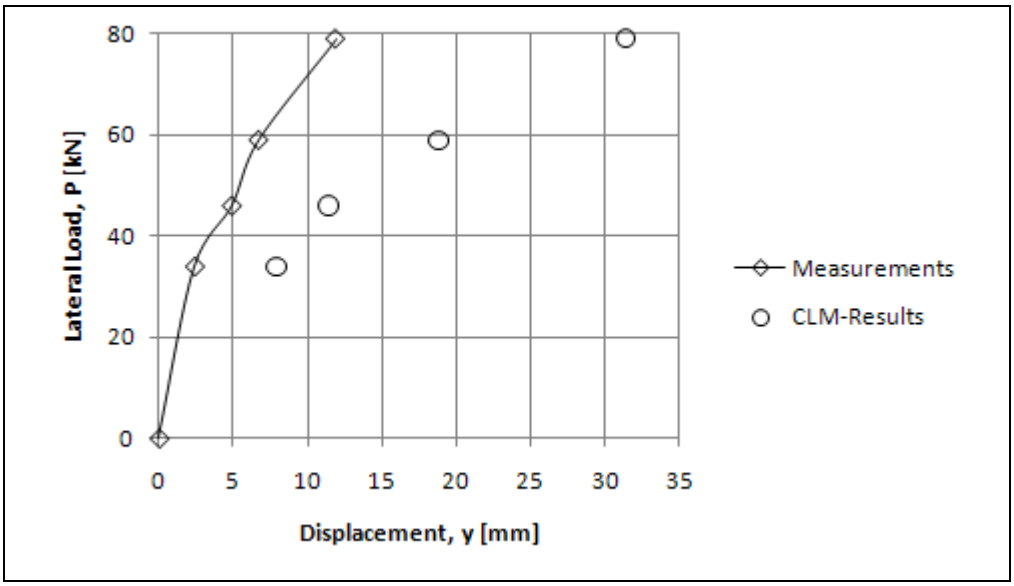

Graph 5-3 Lateral load vs. displacement Test III

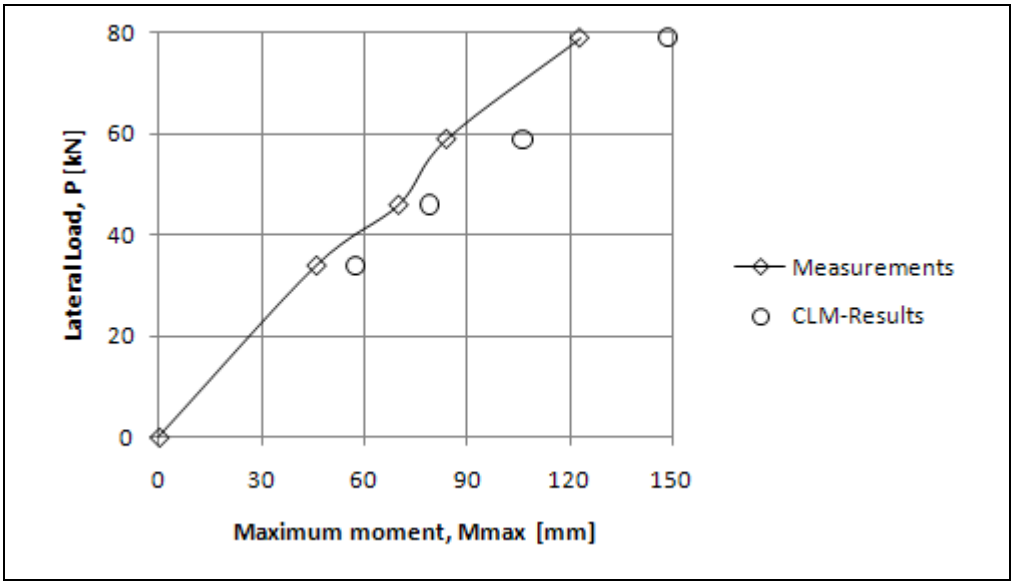

Graph 5-4 Lateral load vs. maximum moment Test III

5.2 CASE III-CU, BRENT CROSS

5.2.1 Calculation

Determine if the deflections are measured at the ground line.

No, the pile head deformation has been measured. Therefore, it is not possible to calculate these displacements with the CLM.

5.3 CASE VI-CS, SABINE

5.3.1 Calculation

Determine if the deflections are measured at the ground line.

No, the pile-head deformation has been measured. Also the maximum occurring moment has been measured. The pile head deformations can be assumed to be equal to the groundline deformations, since the pile head is located close to the ground line. A slight underestimation of the deflections can be expected.

Determine the average soil parameters over the first eight diameters of the pile

The soil data describe a homogeneous subsurface with the following soil parameters.

$c_u = 14{,}4kPa$
$\gamma' = 5{,}5kN/m^3$

Determine if the pile is long enough to perform a CLM-calculation.

The length of the pile is 12,8m. This length equals 12,8/0,319=40 pile diameters, which is longer than the maximum required minimum length.

Determine the Characteristic load, P_c, and moment, M_c.

$$R_I = \left(\frac{31.280}{2{,}1 \times 10^8}\right) \Big/ \left(\frac{\pi \times 0{,}319^4}{64}\right) = 293 \times 10^{-3}$$

$$P_c = 7{,}34 \times 0{,}319^2 \times (2{,}1 \times 10^8 \times 293 \times 10^{-3}) \times \left(\frac{14{,}4}{2{,}1 \times 10^8 \times 293 \times 10^{-3}}\right)^{0{,}68} = 1.424\ kN$$

$$M_c = 3{,}86 \times 0{,}319^3 \times (2{,}1 \times 10^8 \times 293 \times 10^{-3}) \times \left(\frac{14{,}4}{2{,}1 \times 10^8 \times 293 \times 10^{-3}}\right)^{0{,}46} = 6.870\ kNm$$

Determine P_0/P_c to find y/D and subsequently ground line deformation, y_p.

$P_0/P_c = 18/1424 = 0{,}0126 \rightarrow y_p/D = 0{,}018 \rightarrow y_{p,18kN} = 5{,}74\ mm$
$P_0/P_c = 35/1424 = 0{,}0246 \rightarrow y_p/D = 0{,}055 \rightarrow y_{p,35kN} = 17{,}55\ mm$
$P_0/P_c = 53/1424 = 0{,}0372 \rightarrow y_p/D = 0{,}131 \rightarrow y_{p,53kN} = 41{,}79\ mm$
$P_0/P_c = 71/1424 = 0{,}0499 \rightarrow y_p/D = NA \rightarrow y_{p,71kN} = NA$
$P_0/P_c = 80/1424 = 0{,}0562 \rightarrow y_p/D = NA \rightarrow y_{p,80kN} = NA$

The values of P_0/P_c, for the loads of 71 and 80kN exceed the range of the design graphs of the CLM. Therefore the calculation continues without these measurements.

Determine M_0/M_c to find y/D and subsequently ground line deformation, y_m.

$M_0/M_c = 18 \times 0{,}305/6870 = 0{,}00080 \rightarrow y_m/D = 0{,}0016 \rightarrow y_{m,18kN} = 0{,}51\ mm$
$M_0/M_c = 35 \times 0{,}305/6870 = 0{,}00155 \rightarrow y_m/D = 0{,}0031 \rightarrow y_{m,35kN} = 0{,}99\ mm$
$M_0/M_c = 53 \times 0{,}305/6870 = 0{,}00235 \rightarrow y_m/D = 0{,}0047 \rightarrow y_{m,53kN} = 1{,}50\ mm$

Determine load, P_1, that would have caused the same deflections as moment, M_0.

$y_{m,18kN}/D = 0{,}0016 \rightarrow P_{1;18kN}/P_c = 0{,}0022 \rightarrow P_{1;18kN} = 3{,}1\ kN$
$y_{m,35kN}/D = 0{,}0031 \rightarrow P_{1;35kN}/P_c = 0{,}0042 \rightarrow P_{1;35kN} = 6{,}0\ kN$
$y_{m,53kN}/D = 0{,}0047 \rightarrow P_{1;53kN}/P_c = 0{,}0064 \rightarrow P_{1;53kN} = 9{,}1\ kN$

Determine moment, M_1, that would have caused the same deflections as load, P_0.

$y_{p,18kN}/D = 0{,}018 \rightarrow M_{1;18kN}/M_c = 0{,}004 \rightarrow M_{1;18kN} = 27{,}5\ kNm$
$y_{p,35kN}/D = 0{,}055 \rightarrow M_{1;35kN}/M_c = 0{,}015 \rightarrow M_{1;35kN} = 103{,}0\ kNm$
$y_{p,53kN}/D = 0{,}131 \rightarrow M_{1;53kN}/M_c = 0{,}028 \rightarrow M_{1;53kN} = 188{,}9\ kNm$

Now calculate the displacements that are caused by the combined load of P_0 and P_1.

$P_0 + P_{1;18kN} = 18 + 3{,}1 = 21{,}1\ kN$
$P_0 + P_{1;35kN} = 35 + 6{,}0 = 41{,}0\ kN$
$P_0 + P_{1;53kN} = 53 + 9{,}1 = 62{,}1\ kN$

$P_{0+1}/P_c = 21{,}1/1424 = 0{,}015 \rightarrow y_{pm}/D = 0{,}023 \rightarrow y_{pm,18kN} = 7{,}3\ mm$
$P_{0+1}/P_c = 41{,}0/1424 = 0{,}029 \rightarrow y_{pm}/D = 0{,}080 \rightarrow y_{pm,35kN} = 25{,}5\ mm$
$P_{0+1}/P_c = 62{,}1/1424 = 0{,}044 \rightarrow y_{pm}/D = NA \rightarrow y_{pm,53kN} = NA$

Now calculate the displacements that are caused by the combined moments M_0 and M_1.

$M_0 + M_{1;18kN} = 18 \times 0{,}305 + 27{,}5 = 33{,}0\ kNm$
$M_0 + M_{1;18kN} = 18 \times 0{,}305 + 103{,}0 = 113{,}7\ kNm$
$M_0 + M_{1;18kN} = 18 \times 0{,}305 + 188{,}9 = 205{,}1\ kNm$

$M_{0+1}/M_c = 33{,}0/6870 = 0{,}0048 \rightarrow y_{pm}/D = 0{,}011 \rightarrow y_{mp,18kN} = 3{,}5\ mm$
$M_{0+1}/M_c = 113{,}7/6870 = 0{,}0165 \rightarrow y_{pm}/D = 0{,}063 \rightarrow y_{mp,18kN} = 20{,}1\ mm$
$M_{0+1}/M_c = 205{,}1/6870 = 0{,}0299 \rightarrow y_{pm}/D = 0{,}150 \rightarrow y_{mp,18kN} = 47{,}9\ mm$

Calculate the groundline deflections by taking the average between y_{pm} and y_{mp}.

$\boldsymbol{y_{18kN}} = (7{,}3 + 3{,}5)/2 = \boldsymbol{5{,}4\ mm}$
$\boldsymbol{y_{35kN}} = (25{,}5 + 20{,}1)/2 = \boldsymbol{22{,}8\ mm}$
$\boldsymbol{y_{53kN}} = (NA + 47{,}9)/2 = \boldsymbol{47{,}9\ mm}$ (Low estimate, since the deflections of P_{0+1} are higher for the loads of 18 and 35 kN than the deflections of M_{0+1}.

Calculate the maximum moments

This calculation is best executed in excel to speed up the iterative process. In excel the calculations have been executed according to Chapter 6 in Appendix A.

$\boldsymbol{M_{max,18kN}} = \boldsymbol{24{,}9\ kNm}$
$\boldsymbol{M_{max,35kN}} = \boldsymbol{60{,}8\ kNm}$
$\boldsymbol{M_{max,53kN}} = \boldsymbol{101{,}6\ kNm}$

5.3.2 Output

The CLM was not capable of calculating the deflections for all the loads. At some point the design graphs were not sufficiently expanded to read all the values. Therefore only three measurements can be compared with the calculation. The results are given below in graphical form.

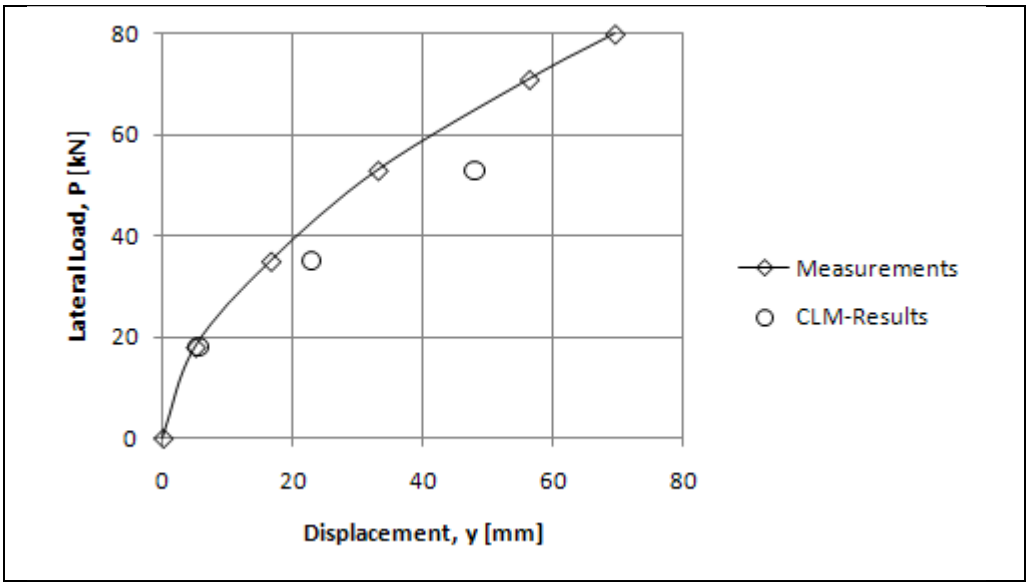

Graph 5-5 Lateral load vs. displacement, Sabine

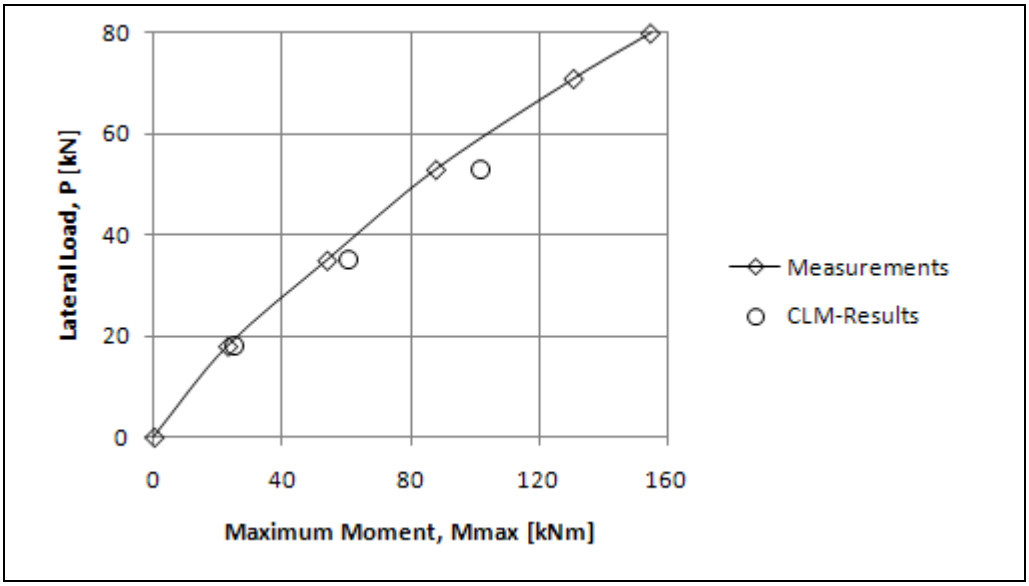

Graph 5-6 Lateral load vs. maximum moment, Sabine

5.4 CASE IX-CL, GARSTON

In contradiction to the above CLM-calculation, this, and the following field tests have been executed with a sandy soil.

5.4.1 Calculation

Determine if the deflections are measured at the ground line.

Yes, the pile head deformations have been measured at 0,9m above the groundline. This makes it impossible to correctly compare the measurements with the groundline deformation.

5.5 CASE X-CL, ARKANSAS RIVER

5.5.1 Calculation

Determine if the deflections are measured at the ground line.

Yes, the ground line deformation has been measured, therefore the calculation can legitimately be used to predict the measurements.

Determine the average soil parameters over the first eight diameters of the pile

The diameter of the pile is determined to be 0,48m. This means that the soil properties have to be averaged over the first 8x0,48=3,84m below the soil surface. It is assumed that the soil properties of the fill are equal to the soil properties of the soil layer below the fill.

$$\varphi = \frac{2{,}4 \times 45 + (3{,}84 - 2{,}4) * 42}{3{,}84} = 43{,}9°$$

$$\gamma' = \frac{1{,}5 \times 20 + (3{,}84 - 1{,}5) \times 10{,}2}{3{,}84} = 14{,}03\ kN/m^3$$

Determine if the pile is long enough to perform a CLM-calculation.

The pile is 15/0,48=31 diameters long. This length is sufficient to perform a CLM-calculation according to table 6-2 of appendix A.

Determine the Characteristic load, P_c.

$$R_I = (3{,}494 \times 10^{-4}) \Big/ \left(\frac{\pi \times 0{,}48^4}{64}\right) = 134 \times 10^{-3}$$

$$P_c = 1{,}57 \times 0{,}48^2 \times (2{,}0 \times 10^8 \times 134 \times 10^{-3}) \times \left(\frac{14{,}03 \times 0{,}48 \times 43{,}9 \times tan^2(45 + 43{,}9/2)}{2{,}0 \times 10^8 \times 134 \times 10^{-3}}\right)^{0{,}57} = 38.369\ kN$$

Determine P_0/P_c to find y/D and subsequently ground line deformation, y_p.

$P_0/P_c = 46/38369 = 0{,}00120 \rightarrow y_p/D = 0{,}005 \rightarrow y_{p,46kN} = 2{,}4\ mm$
$P_0/P_c = 92/38369 = 0{,}00240 \rightarrow y_p/D = 0{,}012 \rightarrow y_{p,92kN} = 5{,}8\ mm$
$P_0/P_c = 140/38369 = 0{,}00365 \rightarrow y_p/D = 0{,}022 \rightarrow y_{p,140kN} = 10{,}6\ mm$
$P_0/P_c = 191/38369 = 0{,}00498 \rightarrow y_p/D = 0{,}038 \rightarrow y_{p,191kN} = 18{,}2\ mm$
$P_0/P_c = 248/38369 = 0{,}00646 \rightarrow y_p/D = 0{,}056 \rightarrow y_{p,248kN} = 26{,}9\ mm$

5.5.2 Output

The CLM method is easy to use if the loads are applied at the groundline. The results of the calculation were deflections for all the applied loads. The calculated deflections were approximately twice as large as the measured deflections. This result is shown in the graph below.

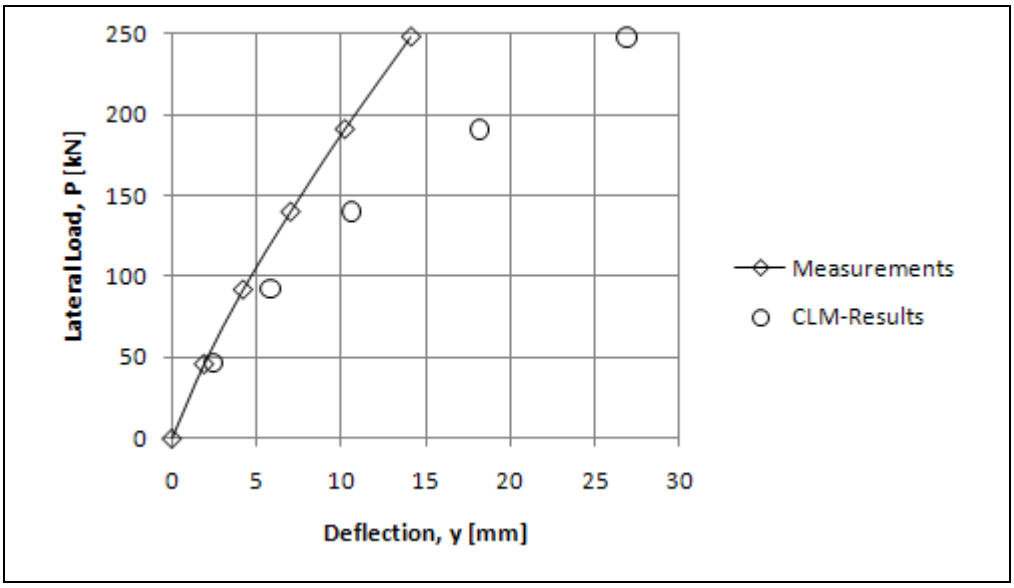

Graph 5-7 Lateral load vs. deflection, Arkansas River

5.6 CASE X-CL, FLORIDA

5.6.1 Calculation

Determine if the deflections are measured at the ground line.

Yes, the ground line deformation has been measured; therefore the calculation can legitimately be used to predict the measurements.

Determine if the pile is long enough to perform a CLM-calculation.

The pile is 7,62/1,42=5,4 diameters long. This length is insufficient to perform a CLM-calculation according to table 6-2 of Appendix A. The minimum length of the pile must be higher than 8 to 14 times the diameter of the pile, depending on the soil and pile parameters.

6 NONDIMENSIONAL METHOD

The Nondimensional Method, NDM, is developed by performing lots and lots of p-y calculations and placing the results in nondimensional graphs. With this manual method computer calculations can be checked and the user can easily choose the type of p-y curve he likes. The six field tests that have considered with the CLM method are also used here. Of these field test, three have been executed in cohesive soils, the others in cohesionless soil.

6.1 CASE I-CU, BAGNOLET

6.1.1 Determine the p-y Curves.

Because the NDM method can only deal with a homogeneous soil, the soil parameters are averaged over the first eight pile diameters. This is the same approach as for the CLM.

$$\gamma = 17{,}9\ kN/m^3$$
$$c_u = \frac{8 \times 0{,}43}{3{,}96} \times (125 - 100) + 100 = 121{,}72\ kPa$$

The P-Y curves are determined as suggested by Reese *et al.* The method is described in Appendix A, chapter 2. The P-Y curves are shown in figure 6-1.

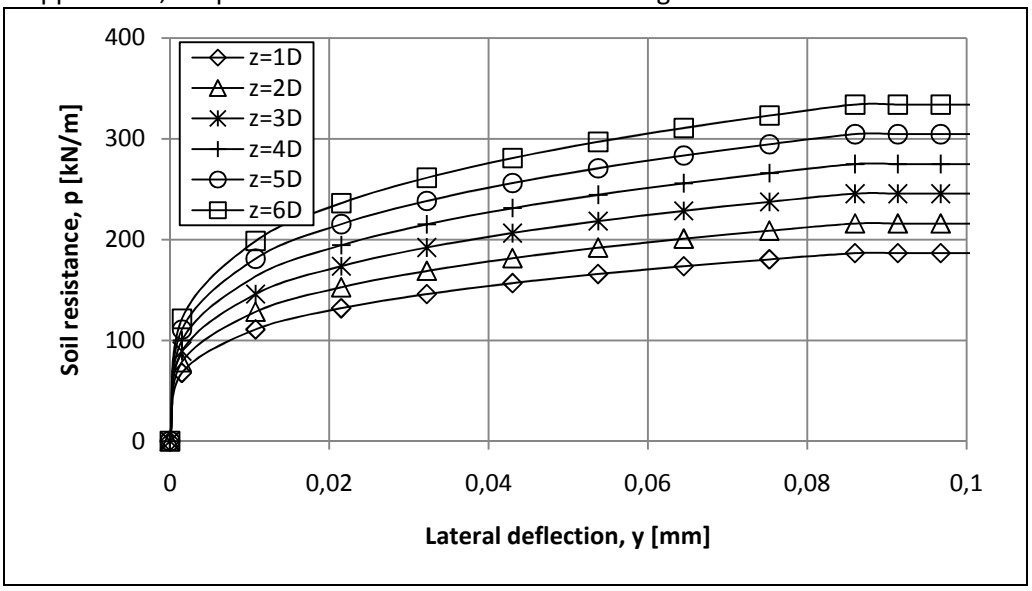

Figure 6-1 P-Y curves Bagnolet according to Reese et al.

6.1.1.1 *TEST I*

*Calculate the displacements at the ground line for a load of **29kN.***

Take $T_{tried} = 1,33m$

Then $Z_{max} = L/T_{tried} = 2,65/1,33 = 2,0$

z [m]	Z	Ay	By	Y_A [mm]	P [kN/m]	E_{py} [kPa]
0,430	0,32	3,45	2,55	12,82	115,89	9038
0,860	0,65	2,52	1,5	8,85	122,34	13817
1,290	0,97	1,45	0,75	4,94	120,14	24341
1,720	1,29	0,45	0	1,20	94,57	78549
2,150	1,62	-0,55	-0,7	-2,46	#NUM!	#NUM!
2,580	1,94	-1,4	-1,4	-5,72	#NUM!	#NUM!

If the stiffness is plotted versus the depth, K_{py} can be calculated.

$K_{py} = 1/(25,9*10^{-6}) = 38610 kN/m^3$ $T_{obtained} = (25500/38610)^{(1/5)} = 0,92m$ $T_{obtained} < T_{tried}$

Take $T_{tried} = 0,88m$ *Then* $Z_{max} = L/T_{tried} = 2,65/0,88 = 3,0$

z [m]	Z	Ay	By	Y_A [mm]	P [kN/m]	E_{py} [kPa]
0,430	0,49	1,8	1	2,01	72,93	36259
0,860	0,98	1,15	0,45	1,17	73,74	63098
1,290	1,47	0,5	0,2	0,51	68,14	133402
1,720	1,95	0,15	-0,1	0,05	43,64	799277
2,150	2,44	-0,2	-0,2	-0,28	#NUM!	#NUM!
2,580	2,93	-0,5	-0,3	-0,57	#NUM!	#NUM!

If the stiffness is plotted versus the depth, K_{py} can be calculated.

$K_{py} = 1/(10,5*10^{-6}) = 95238 kN/m^3$ $T_{obtained} = (25500/95238)^{(1/5)} = 0,77m$ $T_{obtained} > T_{tried}$

Plot the values of T_{tried} versus the values of $T_{obtained}$. This plot is shown graph 6-1. Calculate the value of T, where $T_{tried} = T_{obtained}$. Subsequently calculate y_{29kN}.

$0,3333T + 0,4767 = T$, $T = 0,4767/0,6667 = 0,72m$

$y_{29kN} = (1000)*2,75*29*0,72^3/25500+(1000)*1,75*20,3*0,72^2/25500= 1,9mm$

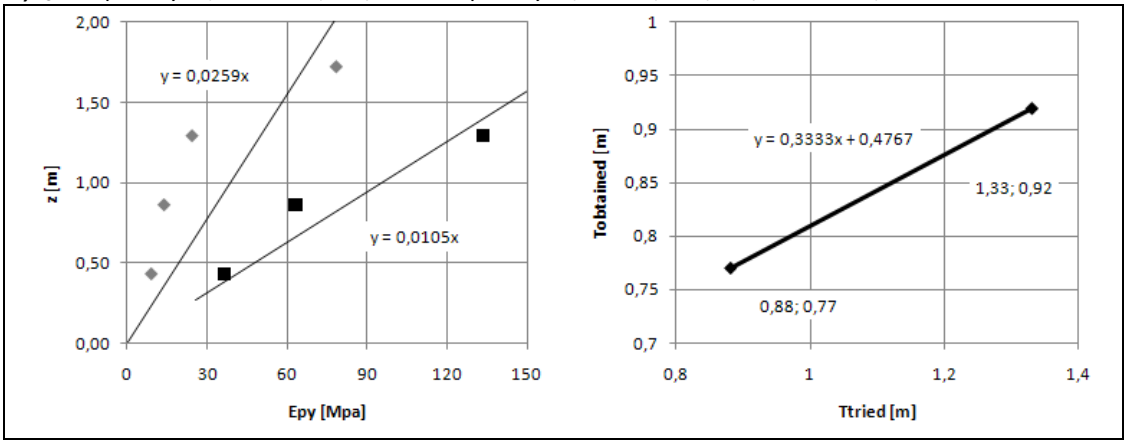

Graph 6-1 Graphs for iterative procedure of NDM, Bagnolet, Reese, 29kN

*Calculate the displacements at the ground line for a load of **49kN.***

Take $T_{tried} = 1,33m$

Then $Z_{max} = L/T_{tried} = 2,65/1,33 = 2,0$

z [m]	Z	Ay	By	Y_A [mm]	P [kN/m]	E_{py} [kPa]
0,430	0,32	3,45	2,55	21,66	132,12	6099
0,860	0,65	2,52	1,5	14,96	139,48	9323
1,290	0,97	1,45	0,75	8,34	136,97	16425
1,720	1,29	0,45	0	2,03	107,82	53002
2,150	1,62	-0,55	-0,7	-4,15	#NUM!	#NUM!
2,580	1,94	-1,4	-1,4	-9,66	#NUM!	#NUM!

If the stiffness is plotted versus the depth, K_{py} can be calculated.

$K_{py} = 1/(38,4*10^{-6}) = 26042kN/m^3$ $T_{obtained} = (25500/26042)^{(1/5)} = 1,00m$ $T_{obtained} < T_{tried}$

Take $T_{tried} = 0,88m$ *Then* $Z_{max} = L/T_{tried} = 2,65/0,88 = 3,0$

z [m]	Z	Ay	By	Y_A [mm]	P [kN/m]	E_{py} [kPa]
0,430	0,49	1,8	1	3,40	83,15	24466
0,860	0,98	1,15	0,45	1,97	84,07	42576
1,290	1,47	0,5	0,2	0,86	77,69	90015
1,720	1,95	0,15	-0,1	0,09	49,76	539323
2,150	2,44	-0,2	-0,2	-0,47	#NUM!	#NUM!
2,580	2,93	-0,5	-0,3	-0,97	#NUM!	#NUM!

If the stiffness is plotted versus the depth, K_{py} can be calculated.

$K_{py} = 1/(15,5*10^{-6}) = 64516kN/m^3$ $T_{obtained} = (25500/64516)^{(1/5)} = 0,83m$ $T_{obtained} > T_{tried}$

Plot the values of T_{tried} versus the values of $T_{obtained}$. This plot is shown graph 6-2. Calculate the value of T, where $T_{tried} = T_{obtained}$. Subsequently calculate y_{49kN}.

$0,3778T + 0,4976 = T$, $T = 0,4976/0,6222 = 0,80m$

$y_{49kN} = (1000)*2,75*49*0,80^3/25500+(1000)*1,75*34,3*0,80^2/25500= 4,22mm$

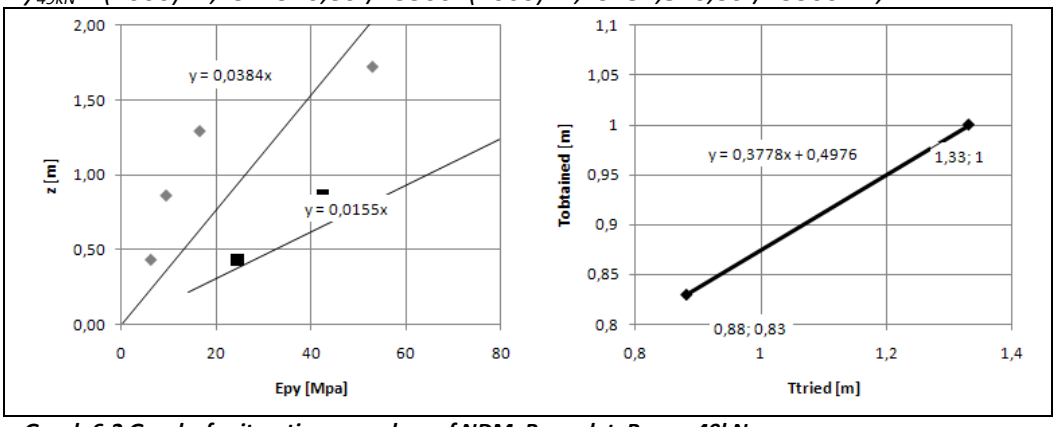

Graph 6-2 Graphs for iterative procedure of NDM, Bagnolet, Reese, 49kN

*Calculate the displacements at the ground line for a load of **59kN.***

Take $T_{tried} = 1,33m$

Then $Z_{max} = L/T_{tried} = 2,65/1,33 = 2,0$

z [m]	Z	Ay	By	Y_A [mm]	P [kN/m]	E_{py} [kPa]
0,430	0,32	3,45	2,55	26,09	138,40	5306
0,860	0,65	2,52	1,5	18,01	146,11	8111
1,290	0,97	1,45	0,75	10,04	143,48	14289
1,720	1,29	0,45	0	2,45	112,95	46110
2,150	1,62	-0,55	-0,7	-5,00	#NUM!	#NUM!
2,580	1,94	-1,4	-1,4	-11,63	#NUM!	#NUM!

If the stiffness is plotted versus the depth, K_{py} can be calculated.

$K_{py} = 1/(44,1*10^{-6}) = 22676kN/m^3$ $T_{obtained} = (25500/22676)^{(1/5)} = 1,02m$ $T_{obtained} < T_{tried}$

Take $T_{tried} = 0,88m$ *Then* $Z_{max} = L/T_{tried} = 2,65/0,88 = 3,0$

z [m]	Z	Ay	By	Y_A [mm]	P [kN/m]	E_{py} [kPa]
0,430	0,49	1,8	1	4,09	87,11	21285
0,860	0,98	1,15	0,45	2,38	88,07	37040
1,290	1,47	0,5	0,2	1,04	81,38	78311
1,720	1,95	0,15	-0,1	0,11	52,12	469199
2,150	2,44	-0,2	-0,2	-0,57	#NUM!	#NUM!
2,580	2,93	-0,5	-0,3	-1,16	#NUM!	#NUM!

If the stiffness is plotted versus the depth, K_{py} can be calculated.

$K_{py} = 1/(17,8*10^{-6}) = 56180kN/m^3$ $T_{obtained} = (25500/56180)^{(1/5)} = 0,85m$ $T_{obtained} > T_{tried}$

Plot the values of T_{tried} versus the values of $T_{obtained}$. This plot is shown graph 6-3. Calculate the value of T, where $T_{tried} = T_{obtained}$. Subsequently calculate y_{59kN}.

$0,3778T + 0,5176 = T,\ T = 0,5176/0,6222 = 0,83m$

$y_{59kN} = (1000)*2,75*59*0,83^3/25500+(1000)*1,75*41,3*0,83^2/25500= 5,59\ mm$

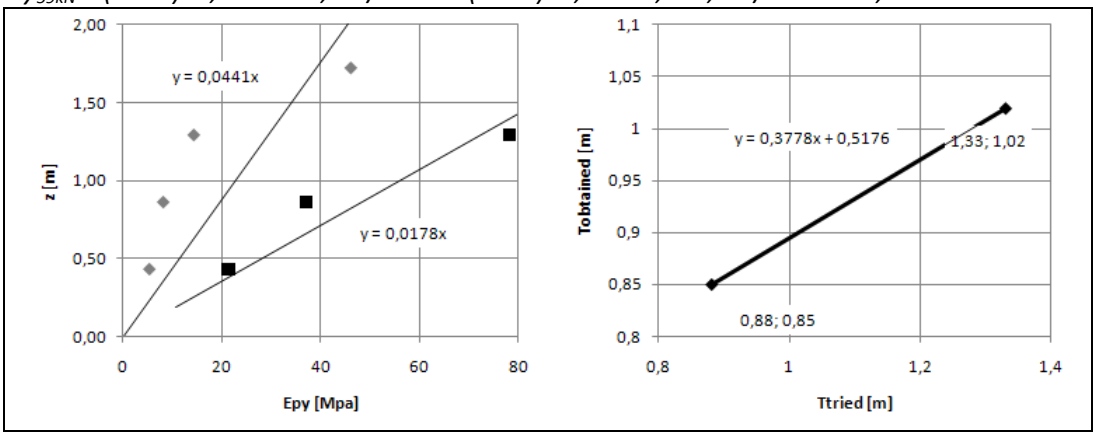

Graph 6-3 Graphs for iterative procedure of NDM, Bagnolet, Reese, 59kN

*Calculate the displacements at the ground line for a load of **79kN.***

Take $T_{tried} = 1,33m$

Then $Z_{max} = L/T_{tried} = 2,65/1,33 = 2,0$

z [m]	Z	Ay	By	Y_A [mm]	P [kN/m]	E_{py} [kPa]
0,430	0,32	3,45	2,55	34,93	148,88	4263
0,860	0,65	2,52	1,5	24,12	157,18	6516
1,290	0,97	1,45	0,75	13,45	154,35	11479
1,720	1,29	0,45	0	3,28	121,50	37044
2,150	1,62	-0,55	-0,7	-6,69	#NUM!	#NUM!
2,580	1,94	-1,4	-1,4	-15,57	#NUM!	#NUM!

If the stiffness is plotted versus the depth, K_{py} can be calculated.

$K_{py} = 1/(54,9*10^{-6}) = 18215kN/m^3$ $T_{obtained} = (25500/18215)^{(1/5)} = 1,07m$ $T_{obtained} < T_{tried}$

Take $T_{tried} = 0,88m$ *Then* $Z_{max} = L/T_{tried} = 2,65/0,88 = 3,0$

z [m]	Z	Ay	By	Y_A [mm]	P [kN/m]	E_{py} [kPa]
0,430	0,49	1,8	1	5,48	93,70	17100
0,860	0,98	1,15	0,45	3,18	94,74	29757
1,290	1,47	0,5	0,2	1,39	87,54	62913
1,720	1,95	0,15	-0,1	0,15	56,07	376943
2,150	2,44	-0,2	-0,2	-0,76	#NUM!	#NUM!
2,580	2,93	-0,5	-0,3	-1,56	#NUM!	#NUM!

If the stiffness is plotted versus the depth, K_{py} can be calculated.

$K_{py} = 1/(22,2*10^{-6}) = 45045kN/m^3$ $T_{obtained} = (25500/45045)^{(1/5)} = 0,89m$ $T_{obtained} > T_{tried}$

Plot the values of T_{tried} versus the values of $T_{obtained}$. This plot is shown graph 6-4. Calculate the value of T, where $T_{tried} = T_{obtained}$. Subsequently calculate y_{79kN}.

0,4T + 0,538 = T, T = 0,538/0,6 = 0,90m

$y_{79kN} = (1000)*2,75*79*0,9^3/25500+(1000)*1,75*55,3*0,9^2/25500= 8,2mm$

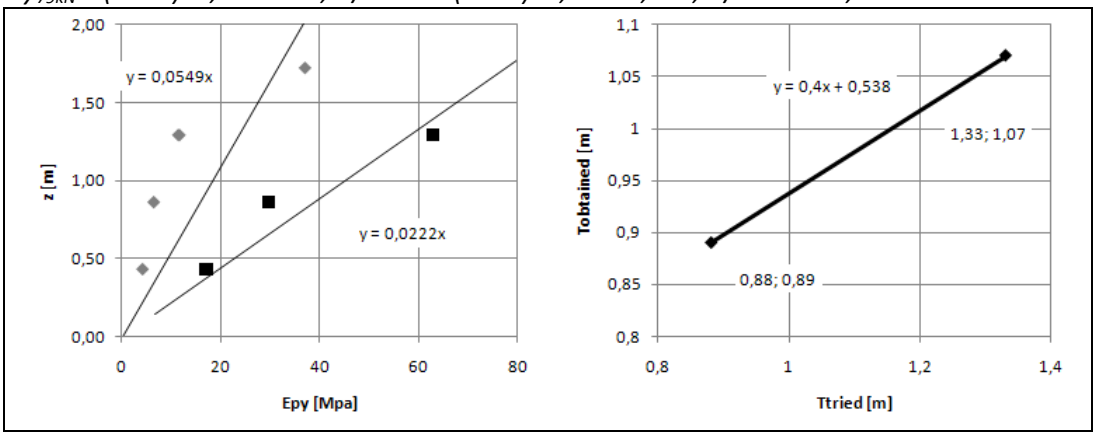

Graph 6-4 Graphs for iterative procedure of NDM, Bagnolet, Reese, 79kN

6.1.1.2 *TEST II*

*Calculate the displacements at the ground line for a load of **15kN.***

Take $T_{tried} = 1,04m$

Then $Z_{max} = L/T_{tried} = 4,15/1,04 = 4,0$

z [m]	Z	Ay	By	Y_A [mm]	P [kN/m]	E_{py} [kPa]
0,430	0,41	1,88	0,99	1,81	71,03	39249
0,860	0,83	1,21	0,50	1,08	72,34	66845
1,290	1,24	0,71	0,23	0,60	71,00	117940
1,720	1,65	0,36	0,00	0,24	62,95	266372
2,150	2,07	0,13	-0,07	0,05	47,23	948076

If the stiffness is plotted versus the depth, K_{py} can be calculated.

$K_{py} = 1/(7,5*10^{-6}) = 133333 kN/m^3$ $T_{obtained} = (25500/133333)^{(1/5)} = 0,72m$ $T_{obtained} < T_{tried}$

Take $T_{tried} = 0,5m$ *Then* $Z_{max} = L/T_{tried} = 4,15/0,5 = 8,3$

z [m]	Z	Ay	By	Y_A [mm]	P [kN/m]	E_{py} [kPa]
0,430	0,86	1,79	0,99	0,26	43,85	166824
0,860	1,72	1,16	0,50	0,15	44,22	292606
1,290	2,58	0,67	0,23	0,08	42,75	540213
1,720	3,44	0,36	0,00	0,03	36,34	1383984
2,150	4,30	0,13	-0,07	0,00	17,21	19598706
2,580	5,16	0,00	-0,09	-0,01	#NUM!	#NUM!

If the stiffness is plotted versus the depth, K_{py} can be calculated.

$K_{py} = 1/(1,5*10^{-6}) = 666667 kN/m^3$ $T_{obtained} = (25500/666667)^{(1/5)} = 0,52m$ $T_{obtained} > T_{tried}$

Plot the values of T_{tried} versus the values of $T_{obtained}$. This plot is shown graph 6-5. Calculate the value of T, where $T_{tried} = T_{obtained}$. Subsequently calculate y_{15kN}.

$0,3704T + 0,3348 = T$, $T = 0,3348/0,6296 = 0,53m$

$y_{15kN} = (1000)*2,4*15*0,53^3/25500+(1000)*1,70*13,5*0,53^2/25500 = 0,46mm$

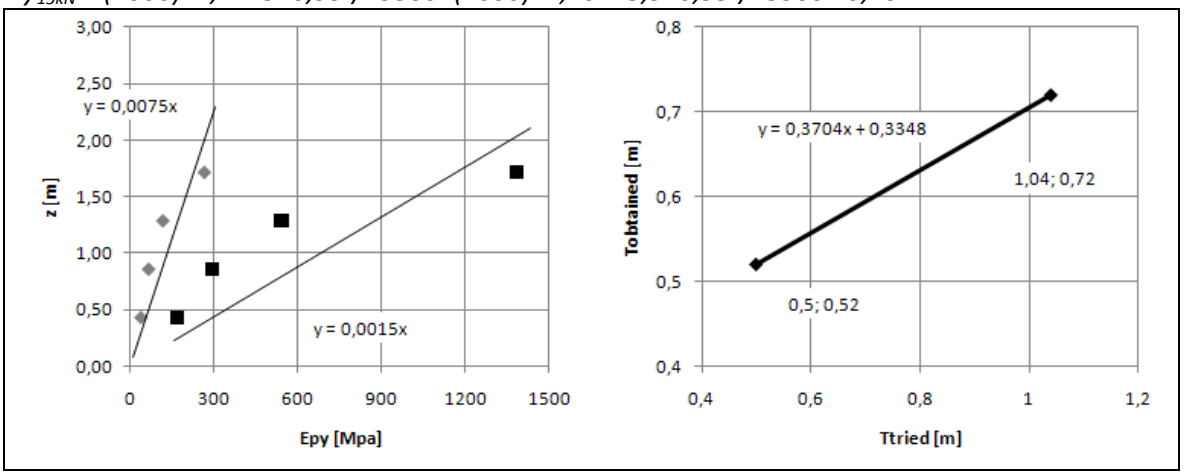

Graph 6-5 Graphs for iterative procedure of NDM, Bagnolet, Reese, 15kN

*Calculate the displacements at the ground line for a load of **39kN.***

Take $T_{tried} = 1,33m$

Then $Z_{max} = L/T_{tried} = 4,15/1,04 = 4,0$

z [m]	Z	Ay	By	Y_A [mm]	P [kN/m]	E_{py} [kPa]
0,430	0,41	1,88	0,99	4,71	90,21	19161
0,860	0,83	1,21	0,5	2,83	91,96	32539
1,290	1,24	0,71	0,23	1,56	90,14	57636
1,720	1,65	0,36	0	0,62	80,09	129319
2,150	2,07	0,13	-0,07	0,12	58,77	492036
2,580	2,48	0,00	-0,09	-0,13	#NUM!	#NUM!

If the stiffness is plotted versus the depth, K_{py} can be calculated.

$K_{py} = 1/(15,5*10^{-6}) = 64516kN/m^3$ $T_{obtained} = (25500/64516)^{(1/5)} = 0,83m$ $T_{obtained} < T_{tried}$

Take $T_{tried} = 0,5m$ *Then* $Z_{max} = L/T_{tried} = 4,15/0,5 = 8,3$

z [m]	Z	Ay	By	Y_A [mm]	P [kN/m]	E_{py} [kPa]
0,430	0,86	1,79	0,99	0,68	55,67	81525
0,860	1,72	1,16	0,5	0,39	56,18	142662
1,290	2,58	0,67	0,23	0,21	54,38	262424
1,720	3,44	0,36	0	0,07	46,24	671902
2,150	4,30	0,13	-0,07	0,00	16,62	21738148
2,580	5,16	0	-0,09	-0,03	#NUM!	#NUM!

If the stiffness is plotted versus the depth, K_{py} can be calculated.

$K_{py} = 1/(3,0*10^{-6}) = 333333kN/m^3$ $T_{obtained} = (25500/333333)^{(1/5)} = 0,60m$ $T_{obtained} > T_{tried}$

Plot the values of T_{tried} versus the values of $T_{obtained}$. This plot is shown graph 6-6. Calculate the value of T, where $T_{tried} = T_{obtained}$. Subsequently calculate y_{39kN}.

$0,4259T + 0,3870 = T$, $T = 0,3870/0,5741 = 0,67m$

$y_{39kN} = (1000)*2,4*39*0,67^3/25500+(1000)*1,7*35,1*0,67^2/25500= 2,2mm$

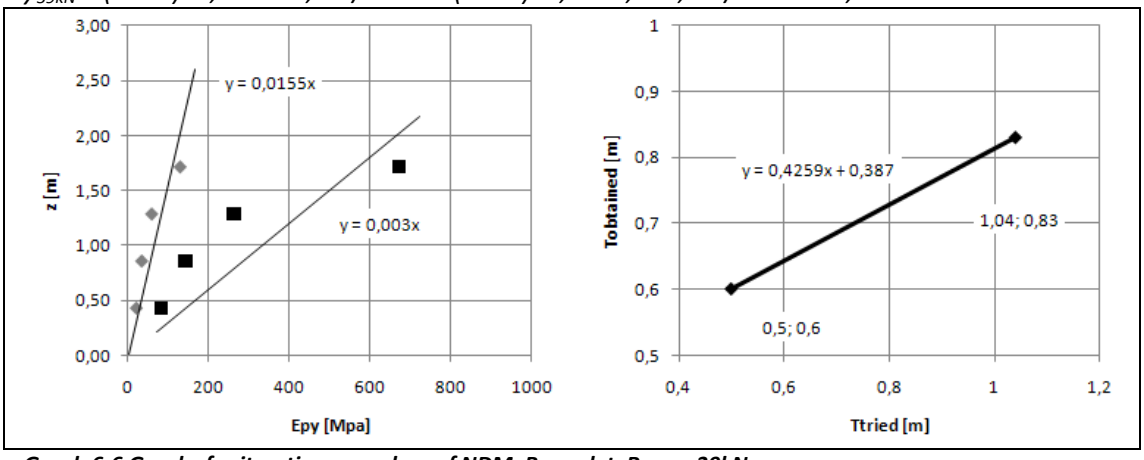

Graph 6-6 Graphs for iterative procedure of NDM, Bagnolet, Reese, 39kN

*Calculate the displacements at the ground line for a load of **59kN.***

Take $T_{tried} = 1,04m$

Then $Z_{max} = L/T_{tried} = 4,15/1,04 = 4,0$

z [m]	Z	Ay	By	Y_A [mm]	P [kN/m]	E_{py} [kPa]
0,430	0,41	1,88	0,99	7,12	100,05	14046
0,860	0,83	1,21	0,5	4,28	101,98	23854
1,290	1,24	0,71	0,23	2,37	99,97	42253
1,720	1,65	0,36	0	0,94	88,83	94803
2,150	2,07	0,13	-0,07	0,18	65,17	360709
2,580	2,48	0	-0,09	-0,20	#NUM!	#NUM!

If the stiffness is plotted versus the depth, K_{py} can be calculated.

$K_{py} = 1/(21,2*10^{-6}) = 47170kN/m^3$ $T_{obtained} = (25500/47170)^{(1/5)} = 0,88m$ $T_{obtained} < T_{tried}$

Take $T_{tried} = 0,5m$ *Then* $Z_{max} = L/T_{tried} = 4,15/0,5 = 8,3$

z [m]	Z	Ay	By	Y_A [mm]	P [kN/m]	E_{py} [kPa]
0,430	0,86	1,79	0,99	1,03	61,74	59765
0,860	1,72	1,16	0,5	0,60	62,31	104585
1,290	2,58	0,67	0,23	0,31	60,31	192381
1,720	3,44	0,36	0	0,10	51,28	492567
2,150	4,30	0,13	-0,07	0,00	18,44	15936098
2,580	5,16	0	-0,09	-0,05	#NUM!	#NUM!

If the stiffness is plotted versus the depth, K_{py} can be calculated.

$K_{py} = 1/(4,1*10^{-6}) = 243902kN/m^3$ $T_{obtained} = (25500/243902)^{(1/5)} = 0,64m$ $T_{obtained} > T_{tried}$

Plot the values of T_{tried} versus the values of $T_{obtained}$. This plot is shown graph 6-7. Calculate the value of T, where $T_{tried} = T_{obtained}$. Subsequently calculate y_{59kN}.

$0,4444T + 0,4178 = T,\ T = 0,4178/0,5556 = 0,75m$

$y_{59kN} = (1000)*2,4*59*0,75^3/25500+(1000)*1,70*41,3*0,75^2/25500= 3,91\ mm$

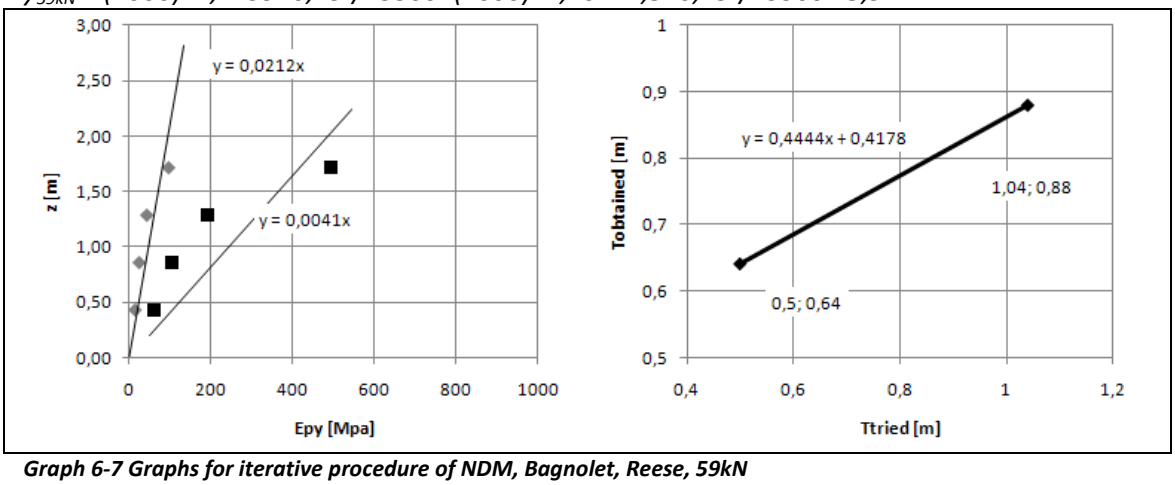

Graph 6-7 Graphs for iterative procedure of NDM, Bagnolet, Reese, 59kN

*Calculate the displacements at the ground line for a load of **83kN.***

Take $T_{tried} = 1,04m$

Then $Z_{max} = L/T_{tried} = 4,15/1,04 = 4,0$

z [m]	Z	Ay	By	Y_A [mm]	P [kN/m]	E_{py} [kPa]
0,430	0,41	1,88	0,99	10,02	108,96	10874
0,860	0,83	1,21	0,5	6,01	111,07	18467
1,290	1,24	0,71	0,23	3,33	108,87	32710
1,720	1,65	0,36	0	1,32	96,74	73393
2,150	2,07	0,13	-0,07	0,25	70,98	279246
2,580	2,48	0	-0,09	-0,29	#NUM!	#NUM!

If the stiffness is plotted versus the depth, K_{py} can be calculated.

$K_{py} = 1/(27,3*10^{-6}) = 36630kN/m^3$ $T_{obtained} = (25500/36630)^{(1/5)} = 0,93m$ $T_{obtained} < T_{tried}$

Take $T_{tried} = 0,5m$ *Then* $Z_{max} = L/T_{tried} = 4,15/0,5 = 8,3$

z [m]	Z	Ay	By	Y_A [mm]	P [kN/m]	E_{py} [kPa]
0,430	0,86	1,79	0,99	1,45	67,24	46268
0,860	1,72	1,16	0,5	0,84	67,86	80965
1,290	2,58	0,67	0,23	0,44	65,69	148934
1,720	3,44	0,36	0	0,15	55,85	381325
2,150	4,30	0,13	-0,07	0,00	20,08	12337081
2,580	5,16	0	-0,09	-0,07	#NUM!	#NUM!

If the stiffness is plotted versus the depth, K_{py} can be calculated.

$K_{py} = 1/(5,3*10^{-6}) = 188679N/m^3$ $T_{obtained} = (25500/188679)^{(1/5)} = 0,67m$ $T_{obtained} > T_{tried}$

Plot the values of T_{tried} versus the values of $T_{obtained}$. This plot is shown graph 6-8. Calculate the value of T, where $T_{tried} = T_{obtained}$. Subsequently calculate y_{83kN}.

$0,4815T + 0,4293 = T$, $T = 0,4293/0,5185 = 0,83m$

$y_{83kN} = (1000)*2,4*83*0,83^3/25500+(1000)*1,70*74,7*0,83^2/25500= 7,90mm$

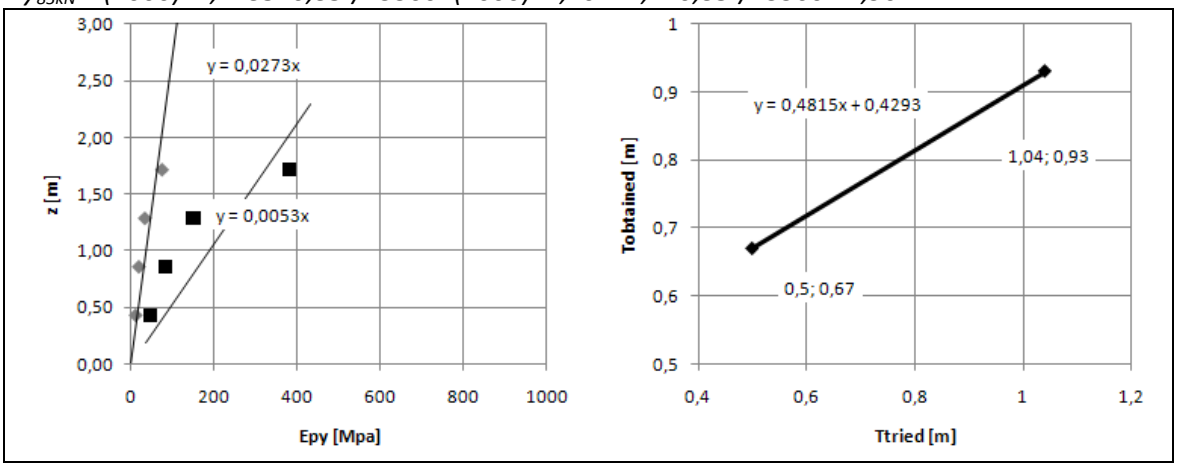

Graph 6-8 Graphs for iterative procedure of NDM, Bagnolet, Reese, 83kN

6.1.1.3 *TEST III*

*Calculate the displacements at the ground line for a load of **34kN.***

Take $T_{tried} = 1,02m$

Then $Z_{max} = L/T_{tried} = 5,1/1,02= 5,0$

z [m]	Z	Ay	By	Y_A [mm]	P [kN/m]	E_{py} [kPa]
0,430	0,42	1,79	0,99	3,91	86,10	22042
0,860	0,84	1,16	0,5	2,33	87,67	37547
1,290	1,26	0,67	0,23	1,27	85,52	67492
1,720	1,69	0,36	0	0,51	76,27	149736
2,150	2,11	0,13	-0,07	0,09	54,27	624897
2,580	2,53	0	-0,09	-0,12	#NUM!	#NUM!

If the stiffness is plotted versus the depth, K_{py} can be calculated.

$K_{py} = 1/(13,4*10^{-6}) = 74627kN/m^3$ $T_{obtained} = (25500/74627)^{(1/5)} = 0,81m$ $T_{obtained} < T_{tried}$

Take $T_{tried} = 0,5m$ *Then* $Z_{max} = L/T_{tried} = 5,1/0,5 = 10,2$

z [m]	Z	Ay	By	Y_A [mm]	P [kN/m]	E_{py} [kPa]
0,430	0,86	1,79	0,99	0,63	54,53	86778
0,860	1,72	1,16	0,5	0,36	54,94	152601
1,290	2,58	0,67	0,23	0,19	53,10	281940
1,720	3,44	0,36	0	0,06	44,68	744723
2,150	4,30	0,13	-0,07	0,00	#NUM!	#NUM!
2,580	5,16	0	-0,09	-0,03	#NUM!	#NUM!

If the stiffness is plotted versus the depth, K_{py} can be calculated.

$K_{py} = 1/(2,7*10^{-6}) = 370370\ kN/m^3$ $T_{obtained} = (25500/370370)^{(1/5)} = 0,59m$ $T_{obtained} > T_{tried}$

Plot the values of T_{tried} versus the values of $T_{obtained}$. This plot is shown graph 6-9. Calculate the value of T, where $T_{tried} = T_{obtained}$. Subsequently calculate y_{34kN}.

$0,4231T + 0,3785= T, T = 0,3785/0,5769= 0,66m$

$y_{34kN} = (1000)*2,4*34*0,66^3/25500+(1000)*1,70*34*0,66^2/25500= 1,91mm$

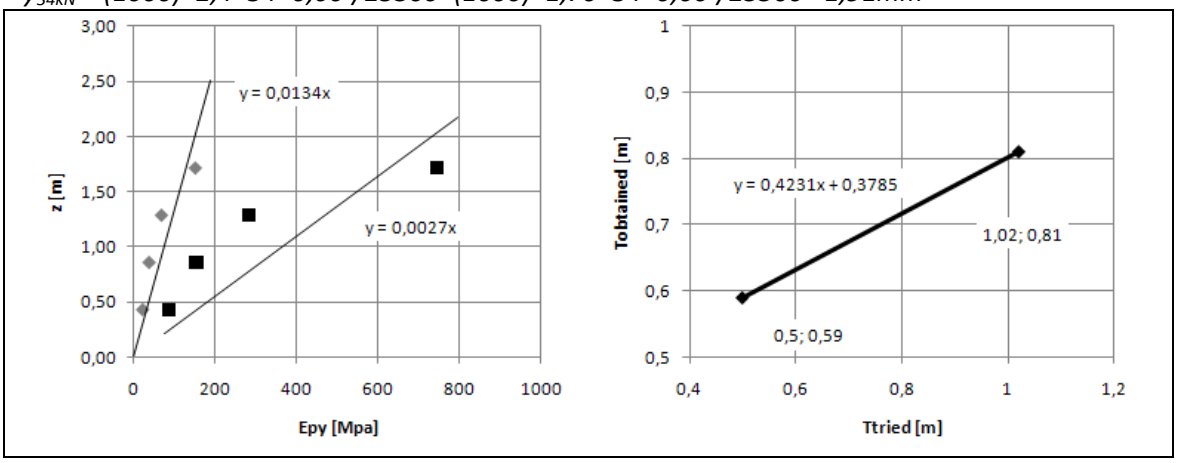

Graph 6-9 Graphs for iterative procedure of NDM, Bagnolet, Reese, 34kN

*Calculate the displacements at the ground line for a load of **46kN.***

Take $T_{tried} = 1,02m$

Then $Z_{max} = L/T_{tried} = 5,1/1,02 = 5,0$

z [m]	Z	Ay	By	Y_A [mm]	P [kN/m]	E_{py} [kPa]
0,430	0,42	1,79	0,99	5,28	92,85	17571
0,860	0,84	1,16	0,5	3,16	94,55	29931
1,290	1,26	0,67	0,23	1,71	92,23	53801
1,720	1,69	0,36	0	0,69	82,26	119362
2,150	2,11	0,13	-0,07	0,12	58,53	498137
2,580	2,53	0	-0,09	-0,17	#NUM!	#NUM!

If the stiffness is plotted versus the depth, K_{py} can be calculated.

$K_{py} = 1/(16,8*10^{-6}) = 59524N/m^3$ $T_{obtained} = (25500/59524)^{(1/5)} = 0,84m$ $T_{obtained} < T_{tried}$

Take $T_{tried} = 0,5m$ *Then* $Z_{max} = L/T_{tried} = 5,1/0,5 = 10,2$

z [m]	Z	Ay	By	Y_A [mm]	P [kN/m]	E_{py} [kPa]
0,430	0,86	1,79	0,99	0,85	58,81	69175
0,860	1,72	1,16	0,5	0,49	59,25	121646
1,290	2,58	0,67	0,23	0,25	57,27	224749
1,720	3,44	0,36	0	0,08	48,19	593657
2,150	4,30	0,13	-0,07	0,00	#NUM!	#NUM!
2,580	5,16	0	-0,09	-0,04	#NUM!	#NUM!

If the stiffness is plotted versus the depth, K_{py} can be calculated.

$K_{py} = 1/(3,4*10^{-6}) = 294118kN/m^3$ $T_{obtained} = (25500/294118)^{(1/5)} = 0,61m$ $T_{obtained} > T_{tried}$

Plot the values of T_{tried} versus the values of $T_{obtained}$. This plot is shown graph 6-10. Calculate the value of T, where $T_{tried} = T_{obtained}$. Subsequently calculate y_{46kN}.

$0,4423T + 0,3888 = T,\ T = 0,3888/0,5577 = 0,70m$

$y_{46kN} = (1000)*2,4*46*0,70^3/25500+(1000)*1,7*46*0,70^2/25500= 2,98mm$

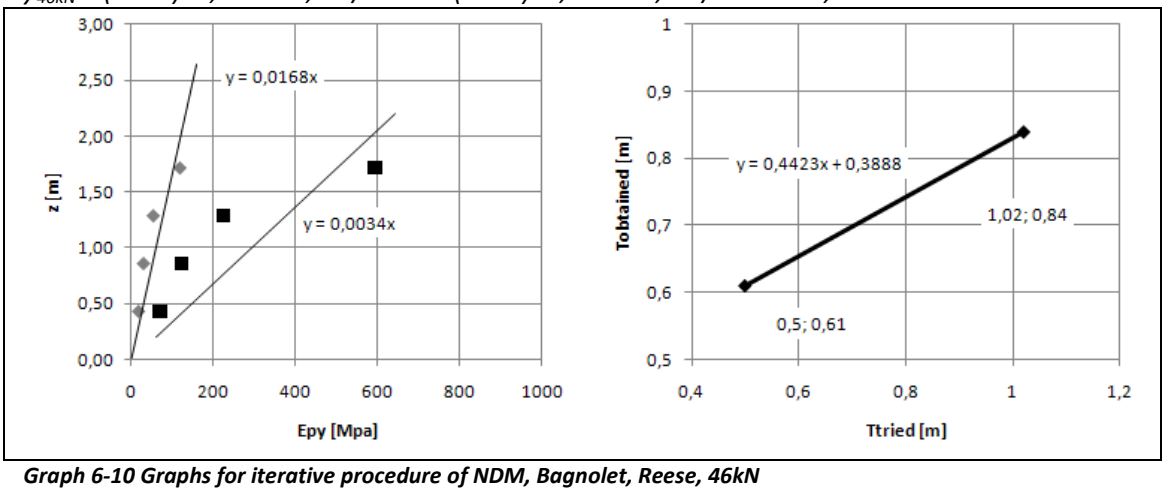

Graph 6-10 Graphs for iterative procedure of NDM, Bagnolet, Reese, 46kN

*Calculate the displacements at the ground line for a load of **59kN.***

Take $T_{tried} = 1,02m$

Then $Z_{max} = L/T_{tried} = 5,1/1,02 = 5,0$

z [m]	Z	Ay	By	Y_A [mm]	P [kN/m]	E_{py} [kPa]
0,430	0,42	1,79	0,99	6,78	98,82	14579
0,860	0,84	1,16	0,5	4,05	100,62	24834
1,290	1,26	0,67	0,23	2,20	98,15	44640
1,720	1,69	0,36	0	0,88	87,54	99037
2,150	2,11	0,13	-0,07	0,15	62,28	413312
2,580	2,53	0	-0,09	-0,22	#NUM!	#NUM!

If the stiffness is plotted versus the depth, K_{py} can be calculated.

$K_{py} = 1/(20,2*10^{-6}) = 49505kN/m^3$ $T_{obtained} = (25500/49505)^{(1/5)} = 0,88m$ $T_{obtained} < T_{tried}$

Take $T_{tried} = 0,5m$ *Then* $Z_{max} = L/T_{tried} = 5,1/0,5 = 10,2$

z [m]	Z	Ay	By	Y_A [mm]	P [kN/m]	E_{py} [kPa]
0,430	0,86	1,79	0,99	1,09	62,58	57396
0,860	1,72	1,16	0,5	0,62	63,05	100932
1,290	2,58	0,67	0,23	0,33	60,94	186477
1,720	3,44	0,36	0	0,10	51,28	492567
2,150	4,30	0,13	-0,07	0,00	#NUM!	#NUM!
2,580	5,16	0	-0,09	-0,05	#NUM!	#NUM!

If the stiffness is plotted versus the depth, K_{py} can be calculated.

$K_{py} = 1/(4,1*10^{-6}) = 243902kN/m^3$ $T_{obtained} = (25500/243902)^{(1/5)} = 0,64m$ $T_{obtained} > T_{tried}$

Plot the values of T_{tried} versus the values of $T_{obtained}$. This plot is shown graph 6-11. Calculate the value of T, where $T_{tried} = T_{obtained}$. Subsequently calculate y_{59kN}.

$0,4615T + 0,4092 = T,\ T = 0,4092/0,5385 = 0,76m$

$y_{59kN} = (1000)*2,4*59*0,76^3/25500+(1000)*1,70*59*0,76^2/25500= 4,71mm$

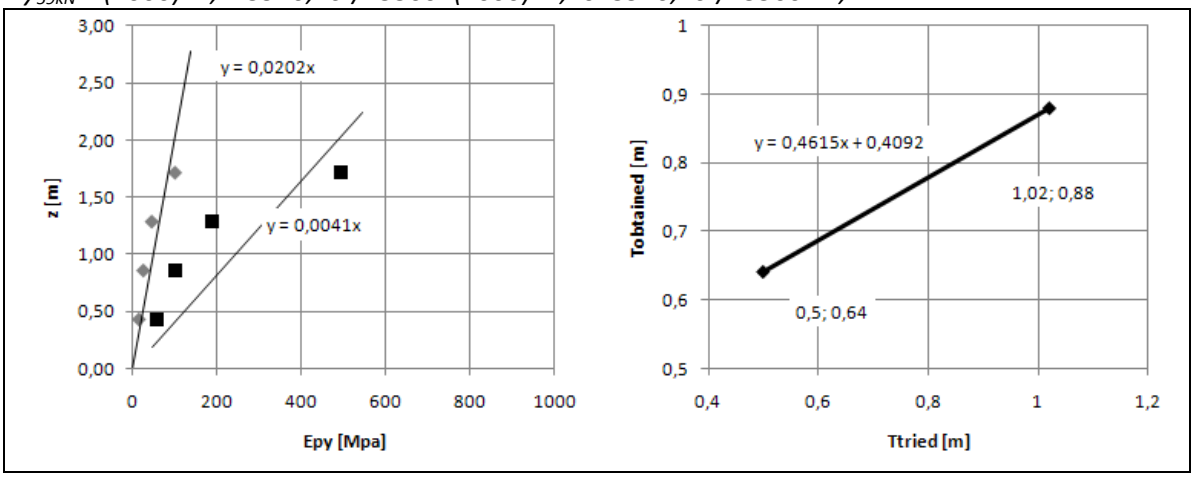

Graph 6-11 Graphs for iterative procedure of NDM, Bagnolet, Reese, 59kN

*Calculate the displacements at the ground line for a load of **79kN.***

Take $T_{tried} = 1,02m$

Then $Z_{max} = L/T_{tried} = 5,1/1,02 = 5,0$

z [m]	Z	Ay	By	Y_A [mm]	P [kN/m]	E_{py} [kPa]
0,430	0,42	1,79	0,99	9,08	106,30	11712
0,860	0,84	1,16	0,5	5,43	108,24	19951
1,290	1,26	0,67	0,23	2,94	105,58	35862
1,720	1,69	0,36	0	1,18	94,17	79564
2,150	2,11	0,13	-0,07	0,20	67,00	332045
2,580	2,53	0	-0,09	-0,29	#NUM!	#NUM!

If the stiffness is plotted versus the depth, K_{py} can be calculated.

$K_{py} = 1/(25,2*10^{-6}) = 39683kN/m^3$ $T_{obtained} = (25500/39683)^{(1/5)} = 0,92m$ $T_{obtained} < T_{tried}$

Take $T_{tried} = 0,5m$ *Then* $Z_{max} = L/T_{tried} = 5,1/0,5 = 10,2$

z [m]	Z	Ay	By	Y_A [mm]	P [kN/m]	E_{py} [kPa]
0,430	0,86	1,79	0,99	1,46	67,32	46110
0,860	1,72	1,16	0,5	0,84	67,83	81086
1,290	2,58	0,67	0,23	0,44	65,56	149811
1,720	3,44	0,36	0	0,14	55,17	395716
2,150	4,30	0,13	-0,07	0,00	#NUM!	#NUM!
2,580	5,16	0	-0,09	-0,07	#NUM!	#NUM!

If the stiffness is plotted versus the depth, K_{py} can be calculated.

$K_{py} = 1/(5,1*10^{-6}) = 196078N/m^3$ $T_{obtained} = (25500/196078)^{(1/5)} = 0,67m$ $T_{obtained} > T_{tried}$

Plot the values of T_{tried} versus the values of $T_{obtained}$. This plot is shown graph 6-12. Calculate the value of T, where $T_{tried} = T_{obtained}$. Subsequently calculate y_{79kN}.

$0,4808T + 0,4296 = T, T = 0,4296/0,5192 = 0,83m$

$y_{79kN} = (1000)*2,4*79*0,83^3/25500+(1000)*1,70*79*0,83^2/25500= 7,88mm$

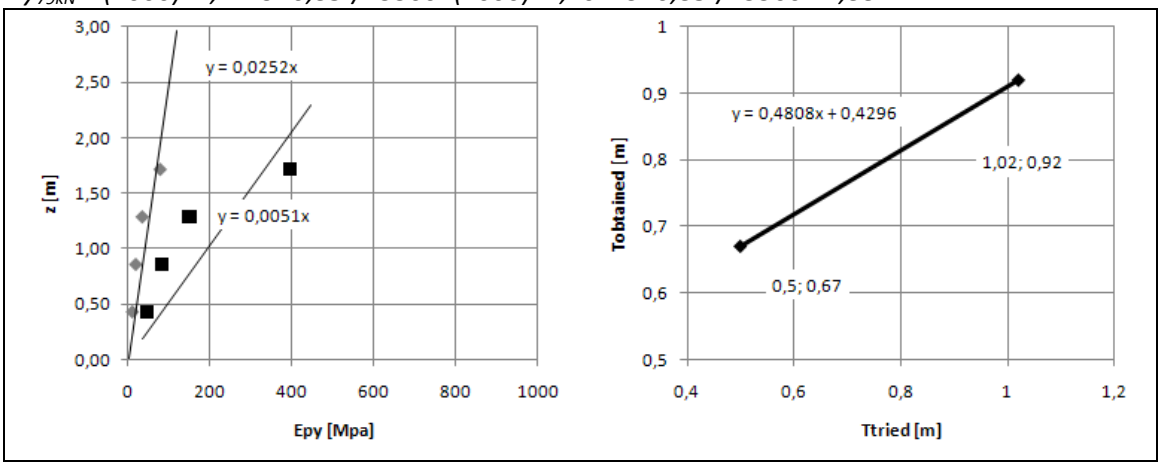

Graph 6-12 Graphs for iterative procedure of NDM, Bagnolet, Reese, 79kN

6.1.2 Calculation of Maximum moments

6.1.2.1 TEST I

Calculate the maximum moment for Load = 29kN

First the Nondimensional graphs have to be chosen to find the values of A_m and B_m. This can be found by calculating Z_{max}.

$$Z_{max} = \frac{L}{T} = \frac{2{,}95}{0{,}72} = 4{,}10$$

Choose the graph where Z_{max} = 4. Since the maximum value of A_m can be found at a depth of 1,33T, the maximum moment must be located between 0,0T and 1,33T. Now the moments between these points are determined.

$$M = A_m P_t T + B_m M_t$$

Take T = 0,72m, P_t = 29kN and M_t = 20,3kNm

Depth Coefficient, z	Am	Bm	M [kNm]
0	0	1	20,3
0,3	0,36	0,98	27,4
0,6	0,55	0,95	30,8
0,9	0,71	0,87	32,5
1,1	0,75	0,83	32,5
1,33	0,78	0,74	31,3

$$M_{max,29kN} = 33kNm$$

Calculate the maximum moment for Load = 49kN

First the Nondimensional graphs have to be chosen to find the values of A_m and B_m. This can be found by calculating Z_{max}.

$$Z_{max} = \frac{L}{T} = \frac{2{,}95}{0{,}80} = 3{,}68$$

Choose the graph where Z_{max} = 4. Since the maximum value of A_m can be found at a depth of 1,33T, the maximum moment must be located between 0,0T and 1,33T. Now the moments between these points are determined.

$$M = A_m P_t T + B_m M_t$$

Take T = 0,80m, P_t = 49kN and M_t = 34,3kNm

Depth Coefficient, z	Am	Bm	M [kNm]
0	0	1	34,3
0,3	0,36	0,98	47,7
0,6	0,55	0,95	54,1
0,9	0,71	0,87	57,7
1,1	0,75	0,83	57,9
1,33	0,78	0,74	56,0

$$M_{max,49kN} = 58kNm$$

Calculate the maximum moment for Load = 59kN

First the Nondimensional graphs have to be chosen to find the values of A_m and B_m. This can be found by calculating Z_{max}.

$$Z_{max} = \frac{L}{T} = \frac{2{,}95}{0{,}83} = 3{,}55$$

Choose the graph where Z_{max} = 4. Since the maximum value of A_m can be found at a depth of 1,33T, the maximum moment must be located between 0,0T and 1,33T. Now the moments between these points are determined.

$$M = A_m P_t T + B_m M_t$$

Take T = 0,83m, P_t = 59kN and M_t = 41,3kNm

Depth Coefficient, z	**Am**	**Bm**	**M [kNm]**
0	0	1	41,3
0,3	0,36	0,98	57,5
0,6	0,55	0,95	65,2
0,9	0,71	0,87	69,4
1,1	0,75	0,83	69,7
1,33	0,78	0,74	67,4

$$M_{max,59kN} = 70kNm$$

Calculate the maximum moment for Load = 79kN

First the Nondimensional graphs have to be chosen to find the values of A_m and B_m. This can be found by calculating Z_{max}.

$$Z_{max} = \frac{L}{T} = \frac{2{,}95}{0{,}90} = 3{,}28$$

Choose the graph where Z_{max} = 3. Since the maximum value of A_m can be found at a depth of 1,33T, the maximum moment must be located between 0,0T and 1,33T. Now the moments between these points are determined.

$$M = A_m P_t T + B_m M_t$$

Take T = 0,90m, P_t = 79kN and M_t = 55,3kNm

Depth Coefficient, z	**Am**	**Bm**	**M [kNm]**
0	0	1	55,3
0,3	0,36	0,97	79,2
0,6	0,55	0,94	91,1
0,9	0,67	0,85	94,6
1,1	0,7	0,8	94,0
1,33	0,69	0,7	87,8

$$M_{max,79kN} = 95kNm$$

6.1.2.2 TEST II

Calculate the maximum moment for Load = 15kN

First the Nondimensional graphs have to be chosen to find the values of A_m and B_m. This can be found by calculating Z_{max}.

$$Z_{max} = \frac{L}{T} = \frac{4{,}15}{0{,}53} = 7{,}83$$

Choose the graph where Z_{max} = 5. Since the maximum value of A_m can be found at a depth of 1,33T, the maximum moment must be located between 0,0T and 1,33T. Now the moments between these points are determined.

$$M = A_m P_t T + B_m M_t$$

Take T = 0,53m, P_t = 15kN and M_t = 13,5kNm

Depth Coefficient, z	Am	Bm	M [kNm]
0	0	1	13,5
0,3	0,36	0,98	16,1
0,6	0,55	0,93	16,9
0,9	0,71	0,85	17,1
1,1	0,74	0,8	16,7
1,33	0,77	0,71	15,7

$$M_{max,15kN} = 17kNm$$

Calculate the maximum moment for Load = 39kN

First the Nondimensional graphs have to be chosen to find the values of A_m and B_m. This can be found by calculating Z_{max}.

$$Z_{max} = \frac{L}{T} = \frac{2{,}95}{0{,}67} = 6{,}19$$

Choose the graph where Z_{max} = 5. Since the maximum value of A_m can be found at a depth of 1,33T, the maximum moment must be located between 0,0T and 1,33T. Now the moments between these points are determined.

$$M = A_m P_t T + B_m M_t$$

Take T = 0,67m, P_t = 39kN and M_t = 34,3kNm

Depth Coefficient, z	Am	Bm	M [kNm]
0	0	1	35,1
0,3	0,36	0,98	43,8
0,6	0,55	0,93	47,0
0,9	0,71	0,85	48,4
1,1	0,74	0,8	47,4
1,33	0,77	0,71	45,0

$$M_{max,39kN} = 48kNm$$

Calculate the maximum moment for Load = 59kN

First the Nondimensional graphs have to be chosen to find the values of A_m and B_m. This can be found by calculating Z_{max}.

$$Z_{max} = \frac{L}{T} = \frac{4{,}15}{0{,}75} = 5{,}53$$

Choose the graph where Z_{max} = 5. Since the maximum value of A_m can be found at a depth of 1,33T, the maximum moment must be located between 0,0T and 1,33T. Now the moments between these points are determined.

$$M = A_m P_t T + B_m M_t$$

Take T = 0,75m, P_t = 59kN and M_t = 53,1kNm

Depth Coefficient, z	**Am**	**Bm**	**M [kNm]**
0	0	1	53,1
0,3	0,36	0,98	68,0
0,6	0,55	0,93	73,7
0,9	0,71	0,85	76,6
1,1	0,74	0,8	75,2
1,33	0,77	0,71	71,8

$$M_{max,59kN} = 77kNm$$

Calculate the maximum moment for Load = 83kN

First the Nondimensional graphs have to be chosen to find the values of A_m and B_m. This can be found by calculating Z_{max}.

$$Z_{max} = \frac{L}{T} = \frac{4{,}15}{0{,}83} = 5{,}00$$

Choose the graph where Z_{max} = 5. Since the maximum value of A_m can be found at a depth of 1,33T, the maximum moment must be located between 0,0T and 1,33T. Now the moments between these points are determined.

$$M = A_m P_t T + B_m M_t$$

Take T = 0,83m, P_t = 83kN and M_t = 74,7kNm

Depth Coefficient, z	**Am**	**Bm**	**M [kNm]**
0	0	1	74,7
0,3	0,36	0,98	98,0
0,6	0,55	0,93	107,4
0,9	0,71	0,85	112,4
1,1	0,74	0,8	110,7
1,33	0,77	0,71	106,1

$$M_{max,83kN} = 112kNm$$

6.1.2.3 TEST III

Calculate the maximum moment for Load = 34kN

First the Nondimensional graphs have to be chosen to find the values of A_m and B_m. This can be found by calculating Z_{max}.

$$Z_{max} = \frac{L}{T} = \frac{5{,}1}{0{,}66} = 7{,}73$$

Choose the graph where Z_{max} = 5. Since the maximum value of A_m can be found at a depth of 1,33T, the maximum moment must be located between 0,0T and 1,33T. Now the moments between these points are determined.

$$M = A_m P_t T + B_m M_t$$

Take T = 0,66m, P_t = 34kN and M_t = 34kNm

Depth Coefficient, z	**Am**	**Bm**	**M [kNm]**
0	0	1	34,0
0,3	0,36	0,98	41,4
0,6	0,55	0,93	44,0
0,9	0,71	0,85	44,8
1,1	0,74	0,8	43,8
1,33	0,77	0,71	41,4

$$M_{max,34kN} = 45kNm$$

Calculate the maximum moment for Load = 46kN

First the Nondimensional graphs have to be chosen to find the values of A_m and B_m. This can be found by calculating Z_{max}.

$$Z_{max} = \frac{L}{T} = \frac{5{,}1}{0{,}70} = 7{,}29$$

Choose the graph where Z_{max} = 5. Since the maximum value of A_m can be found at a depth of 1,33T, the maximum moment must be located between 0,0T and 1,33T. Now the moments between these points are determined.

$$M = A_m P_t T + B_m M_t$$

Take T = 0,70m, P_t = 46kN and M_t = 46kNm

Depth Coefficient, z	**Am**	**Bm**	**M [kNm]**
0	0	1	49,0
0,3	0,36	0,98	60,4
0,6	0,55	0,93	64,4
0,9	0,71	0,85	66,0
1,1	0,74	0,8	64,6
1,33	0,77	0,71	61,2

$$M_{max,46kN} = 66kNm$$

Calculate the maximum moment for Load = 59kN

First the Nondimensional graphs have to be chosen to find the values of A_m and B_m. This can be found by calculating Z_{max}.

$$Z_{max} = \frac{L}{T} = \frac{5{,}1}{0{,}76} = 6{,}71$$

Choose the graph where Z_{max} = 5. Since the maximum value of A_m can be found at a depth of 1,33T, the maximum moment must be located between 0,0T and 1,33T. Now the moments between these points are determined.

$$M = A_m P_t T + B_m M_t$$

Take T = 0,76m, P_t = 59kN and M_t = 59kNm

Depth Coefficient, z	**Am**	**Bm**	**M [kNm]**
0	0	1	59,0
0,3	0,36	0,98	74,0
0,6	0,55	0,93	79,5
0,9	0,71	0,85	82,0
1,1	0,74	0,8	80,4
1,33	0,77	0,71	76,4

$$M_{max,59kN} = 82kNm$$

Calculate the maximum moment for Load = 79kN

First the Nondimensional graphs have to be chosen to find the values of A_m and B_m. This can be found by calculating Z_{max}.

$$Z_{max} = \frac{L}{T} = \frac{5{,}1}{0{,}83} = 6{,}14$$

Choose the graph where Z_{max} = 5. Since the maximum value of A_m can be found at a depth of 1,33T, the maximum moment must be located between 0,0T and 1,33T. Now the moments between these points are determined.

$$M = A_m P_t T + B_m M_t$$

Take T = 0,83m, P_t = 79kN and M_t = 79kNm

Depth Coefficient, z	**Am**	**Bm**	**M [kNm]**
0	0	1	79,0
0,3	0,36	0,98	101,0
0,6	0,55	0,93	109,5
0,9	0,71	0,85	113,7
1,1	0,74	0,8	111,7
1,33	0,77	0,71	106,6

$$M_{max,79kN} = 114kNm$$

6.1.3 Results

The result of this NDM calculation results in the same set of graphs for the CLM-method. From the graphs below it can be seen that the NDM method overestimates the deflections of the pile in all three of the cases. The maximum moments however have been predicted reasonably accurate.

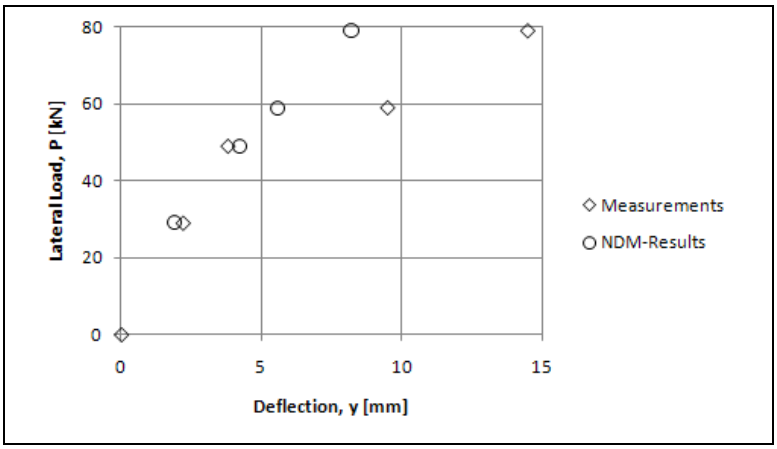

Graph 6-13 Lateral load vs. displacement Test I

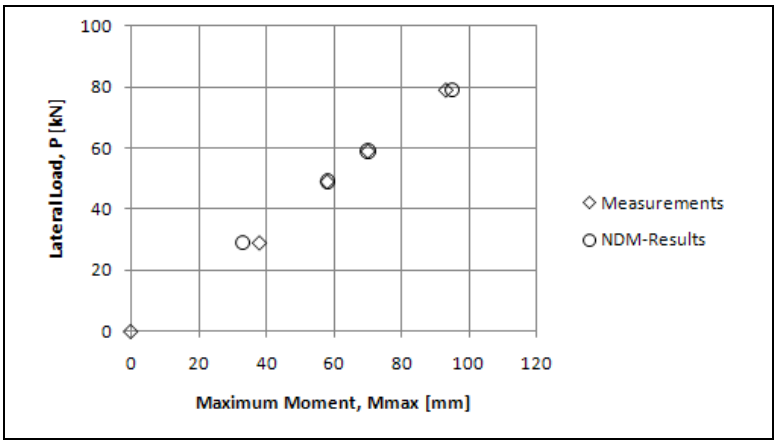

Graph 6-14 Lateral load vs. maximum moment Test I

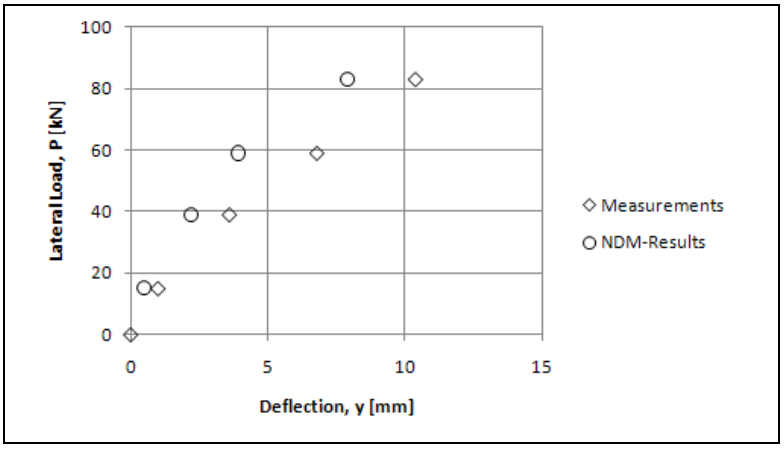

Graph 6-15 Lateral load vs. displacement Test II

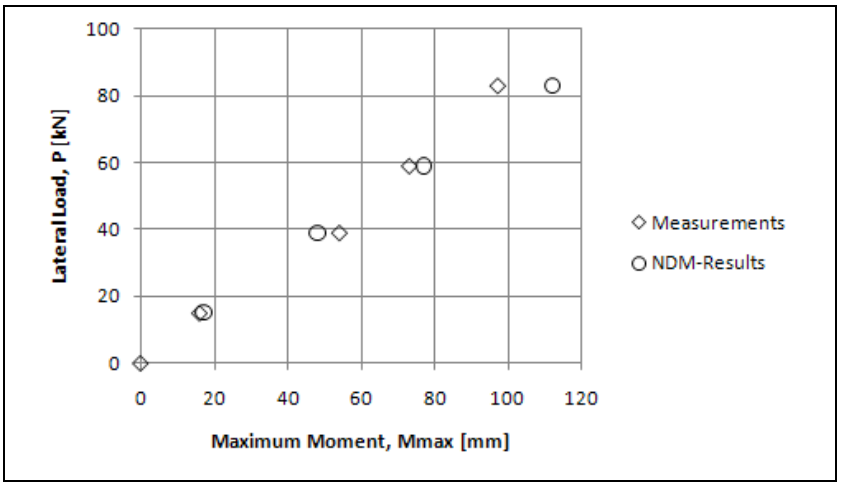

Graph 6-16 Lateral load vs. maximum moment Test II

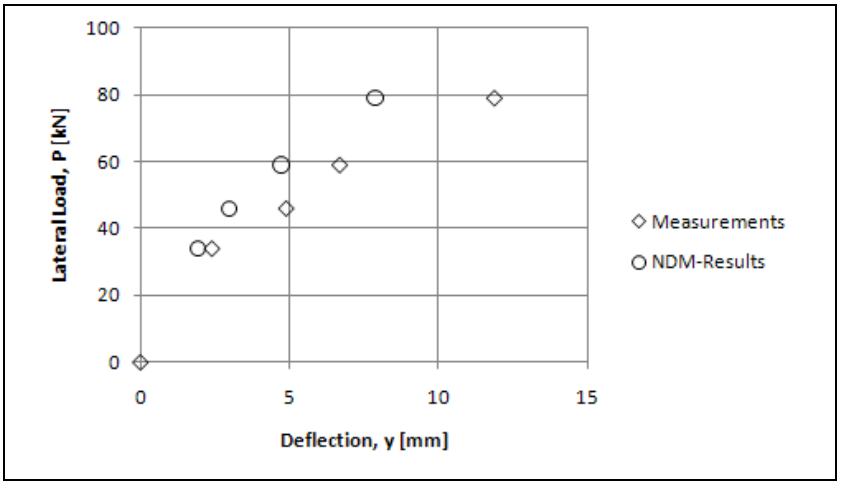

Graph 6-17 Lateral load vs. displacement Test III

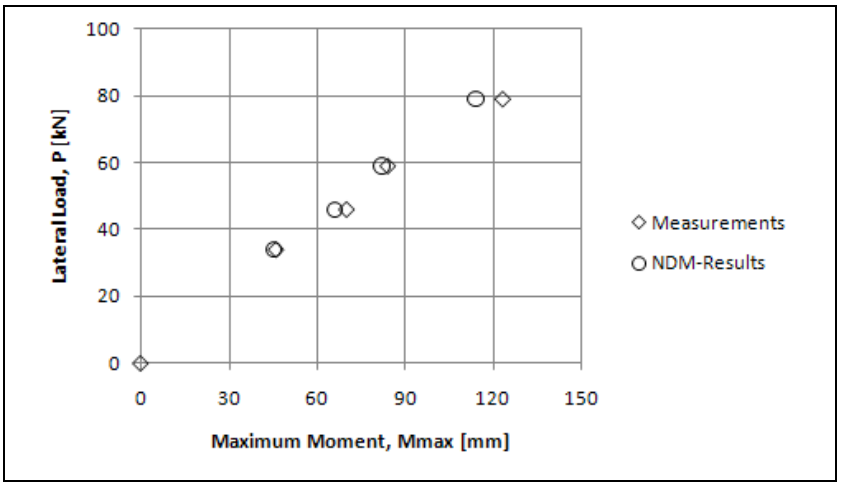

Graph 6-18 Lateral load vs. maximum moment Test III

6.2 CASE III-CU, BRENT CROSS

In the case of Brent Cross the P-Y method has been applied with both the recommendations made by the API and by Reese *et al.*

6.2.1 P-Y API

Determine the p-y Curves.

Because the NDM method can only deal with a homogeneous soil, the soil parameters are averaged over the first eight pile diameters. This is the same approach as for the CLM.

γ' = 17 kN/m^3

c_u = (((8 x 0,406) / 4,6) x (85,2-44,1)) / 2 + 44,1 = 58,6 kPa

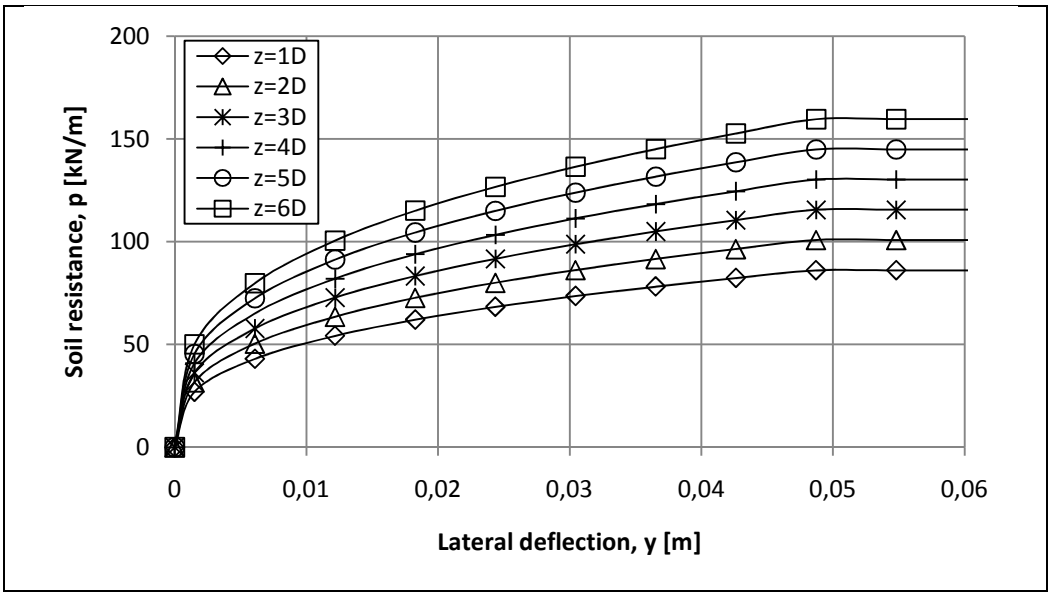

Table 6-1 P-Y curves Brent Cross according to API.

Calculate the displacements at the ground line for a load of 20kN.

Take $T_{tried} = 1{,}0m$

Then $Z_{max} = L/T_{tried} = 16{,}5/1{,}0 = 16{,}5$

z [m]	Z	Ay	By	Y_A [mm]	P [kN/m]	E_{py} [kPa]
0,406	0,41	1,79	0,94	1,06	24,03	22674
0,812	0,81	0,98	0,49	0,57	22,92	39983
1,218	1,22	0,74	0,18	0,36	22,41	62928
1,624	1,62	0,38	-0,02	0,14	18,46	132839
2,030	2,03	0,13	-0,07	0,03	11,76	451288
2,436	2,44	0,00	-0,09	-0,03	-14,26	410327

If the stiffness is plotted versus the depth, K_{py} can be calculated.

$K_{py} = 1/(14{,}1*10^{-6}) = 70922\ kN/m^3$ $T_{obtained} = (51400/70922)^{(1/5)} = 0{,}94\ m$ $T_{obtained} < T_{tried}$

Take $T_{tried} = 1{,}5\ m$ *Then* $Z_{max} = L/T_{tried} = 16{,}5/1{,}5 = 11\ m$

z [m]	Z	Ay	By	Y_A [mm]	P [kN/m]	E_{py} [kPa]
0,406	0,27	2,05	1,16	3,71	36,49	9828
0,812	0,54	1,56	0,80	2,76	38,68	14038
1,218	0,81	1,23	0,49	2,04	40,11	19641
1,624	1,08	0,92	0,29	1,46	40,39	27745
2,030	1,35	0,65	0,13	0,97	39,23	40552
2,436	1,62	0,38	0,01	0,51	34,86	68612

If the stiffness is plotted versus the depth, K_{py} can be calculated.

$K_{py} = 1/(42{,}8*10^{-6}) = 23364\ kN/m^3$ $T_{obtained} = (51400/23364)^{(1/5)} = 1{,}17\ m$ $T_{obtained} < T_{tried}$

Plot the values of T_{tried} versus the values of $T_{obtained}$. This plot is shown graph 6-13. Calculate the value of T, where $T_{tried} = T_{obtained}$. Subsequently calculate y_{20kN}.

$0{,}46T + 0{,}48 = T,\ T = 0{,}48/0{,}54 = 0{,}89\ m$

$y_{20kN} = (1000)*(2{,}4*20*0{,}89^3/51400 + 1{,}7*20*0{,}89^2/51400) = 1{,}18\ mm$

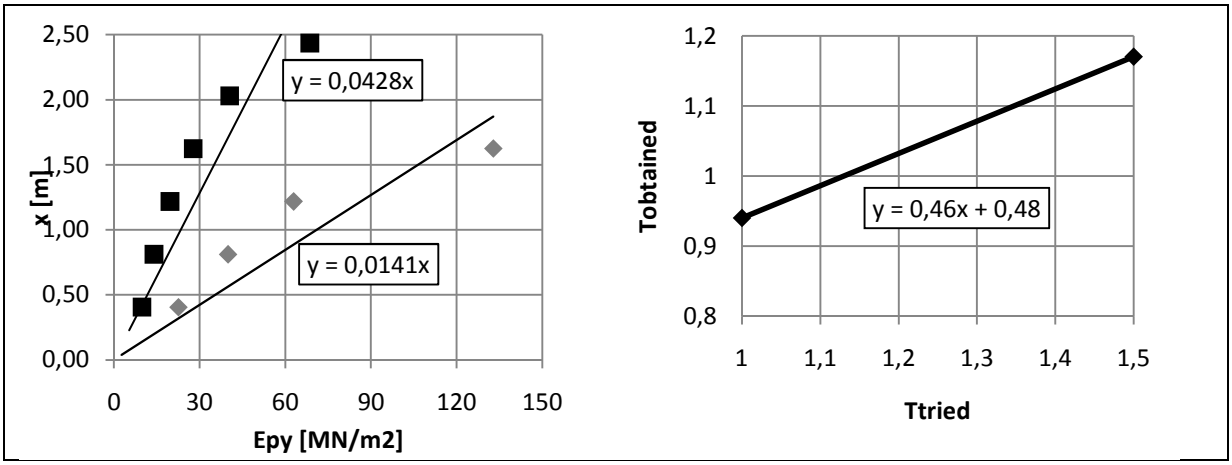

Graph 6-19 Graphs for iterative procedure of NDM, Case III-cu, Brent Cross, 20kN, p-y according to API

Calculate the displacements at the ground line for a load of 40kN.

Take $T_{tried} = 1{,}0m$

Then $Z_{max} = L/T_{tried} = 16{,}5/1{,}0 = 16{,}5$

z [m]	Z	Ay	By	Y_A [mm]	P [kN/m]	E_{py} [kPa]
0,406	0,41	1,79	0,94	2,12	30,30	14260
0,812	0,81	0,98	0,49	1,14	28,86	25225
1,218	1,22	0,74	0,18	0,72	28,28	39504
1,624	1,62	0,38	-0,02	0,28	23,32	83240
2,030	2,03	0,13	-0,07	0,05	14,28	305888
2,436	2,44	0	-0,09	-0,07	-18,01	257120

If the stiffness is plotted versus the depth, K_{py} can be calculated.

$K_{py} = 1/(22{,}5*10^{-6}) = 44444\ kN/m^3$ $T_{obtained} = (51400/44444)^{(1/5)} = 1{,}03\ m$ $T_{obtained} < T_{tried}$

Take $T_{tried} = 1{,}5\ m$ *Then* $Z_{max} = L/T_{tried} = 16{,}5/1{,}5 = 11\ m$

z [m]	Z	Ay	By	Y_A [mm]	P [kN/m]	E_{py} [kPa]
0,406	0,27	2,05	1,16	2,50	31,98	12801
0,812	0,54	1,56	0,8	1,84	33,79	18398
1,218	0,81	1,23	0,49	1,34	34,84	26030
1,624	1,08	0,92	0,29	0,94	34,93	37097
2,030	1,35	0,65	0,13	0,61	33,58	55326
2,436	1,62	0,38	0,01	0,30	29,36	96736

If the stiffness is plotted versus the depth, K_{py} can be calculated.

$K_{py} = 1/(67{,}9*10^{-6}) = 14728kN/m^3$ $T_{obtained} = (51400/14728)^{(1/5)} = 1{,}28\ m$ $T_{obtained} < T_{tried}$

Plot the values of T_{tried} versus the values of $T_{obtained}$. This plot is shown graph 6-14. Calculate the value of T, where $T_{tried} = T_{obtained}$. Subsequently calculate y_{40kN}.

$0{,}5T + 0{,}53 = T,\ T = 0{,}53/0{,}5 = 1{,}06\ m$

$y_{40kN} = (1000)*(2{,}4*40*1{,}06^3/51400 + 1{,}7*40*1{,}06^3/51400) = 3{,}71\ mm$

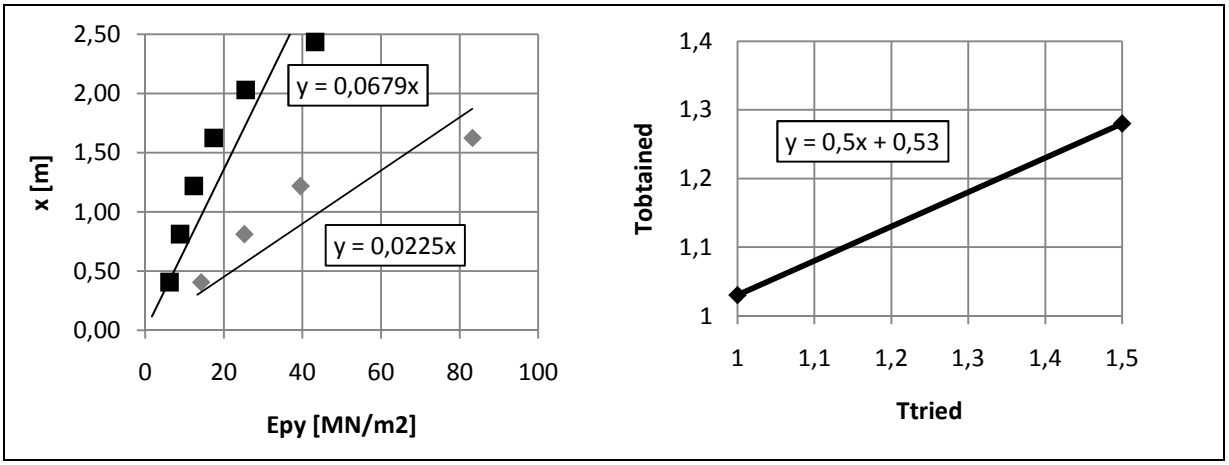

Graph 6-20 Graphs for iterative procedure of NDM, Case III-cu, Brent Cross, 40kN, p-y according to API

Calculate the displacements at the ground line for a load of 60kN.

Take $T_{tried} = 1,0m$

Then $Z_{max} = L/T_{tried} = 16,5/1,0 = 16,5$

z [m]	Z	Ay	By	Y_A [mm]	P [kN/m]	E_{py} [kPa]
0,406	0,41	1,79	0,94	3,19	34,68	10883
0,812	0,81	0,98	0,49	1,72	33,03	19250
1,218	1,22	0,74	0,18	1,07	32,38	30147
1,624	1,62	0,38	-0,02	0,42	26,69	63524
2,030	2,03	0,13	-0,07	0,07	16,35	233436
2,436	2,44	0	-0,09	-0,11	-20,61	196220

If the stiffness is plotted versus the depth, K_{py} can be calculated.

$K_{py} = 1/(29,4*10^{-6}) = 34014\ kN/m^3$ $T_{obtained} = (51400/34014)^{(1/5)} = 1,09\ m$ $T_{obtained} > T_{tried}$

Take $T_{tried} = 1,5\ m$ *Then* $Z_{max} = L/T_{tried} = 16,5/1,5 = 11\ m$

z [m]	Z	Ay	By	Y_A [mm]	P [kN/m]	E_{py} [kPa]
0,406	0,27	2,05	1,16	11,12	52,61	4729
0,812	0,54	1,56	0,8	8,25	55,74	6759
1,218	0,81	1,23	0,49	6,13	57,87	9436
1,624	1,08	0,92	0,29	4,39	58,34	13301
2,030	1,35	0,65	0,13	2,90	56,58	19494
2,436	1,62	0,38	0,01	1,52	50,27	32999

If the stiffness is plotted versus the depth, K_{py} can be calculated.

$K_{py} = 1/(89*10^{-6}) = 11236\ kN/m^3$ $T_{obtained} = (51400/11236)^{(1/5)} = 1,36\ m$ $T_{obtained} > T_{tried}$

Plot the values of T_{tried} versus the values of $T_{obtained}$. This plot is shown graph 6-15. Calculate the value of T, where $T_{tried} = T_{obtained}$. Subsequently calculate y_{60kN}.

$0,54T + 0,55 = T,\ T = 0,55/0,46 = 1,20\ m$

$y_{60kN} = (1000)*(2,4*60*1,20^3/51400 + 1,7*60*1,20^3/51400) = 7,70\ mm$

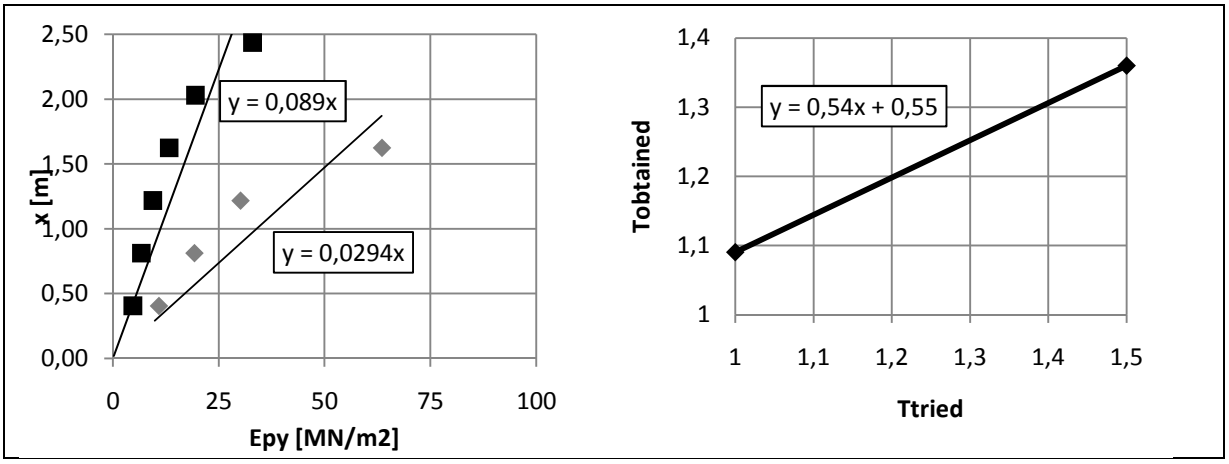

Graph 6-21 Graphs for iterative procedure of NDM, Case III-cu, Brent Cross, 60kN, p-y according to API

Calculate the displacements at the ground line for a load of 100kN.

Take $T_{tried} = 1{,}0m$

Then $Z_{max} = L/T_{tried} = 16{,}5/1{,}0 = 16{,}5$

z [m]	Z	Ay	By	Y_A [mm]	P [kN/m]	E_{py} [kPa]
0,406	0,41	1,79	0,94	5,31	41,12	7742
0,812	0,81	0,98	0,49	2,86	39,16	13694
1,218	1,22	0,74	0,18	1,79	38,39	21446
1,624	1,62	0,38	-0,02	0,70	31,65	45190
2,030	2,03	0,13	-0,07	0,12	19,38	166061
2,436	2,44	0	-0,09	-0,18	-24,44	139586

If the stiffness is plotted versus the depth, K_{py} can be calculated.

$K_{py} = 1/(41{,}4*10^{-6}) = 24155\ kN/m^3$ $T_{obtained} = (51400/24155)^{(1/5)} = 1{,}16\ m$ $T_{obtained} > T_{tried}$

Take $T_{tried} = 1{,}5\ m$ *Then* $Z_{max} = L/T_{tried} = 16{,}5/1{,}5 = 11\ m$

z [m]	Z	Ay	By	Y_A [mm]	P [kN/m]	E_{py} [kPa]
0,406	0,27	2,05	1,16	18,54	62,37	3364
0,812	0,54	1,56	0,8	13,75	66,09	4808
1,218	0,81	1,23	0,49	10,22	68,61	6713
1,624	1,08	0,92	0,29	7,31	69,17	9462
2,030	1,35	0,65	0,13	4,84	67,08	13868
2,436	1,62	0,38	0,01	2,54	59,60	23475

If the stiffness is plotted versus the depth, K_{py} can be calculated.

$K_{py} = 1/(125*10^{-6}) = 8000\ kN/m^3$ $T_{obtained} = (51400/8000)^{(1/5)} = 1{,}45\ m$ $T_{obtained} < T_{tried}$

Plot the values of T_{tried} versus the values of $T_{obtained}$. This plot is shown graph 6-16. Calculate the value of T, where $T_{tried} = T_{obtained}$. Subsequently calculate y_{100kN}.

$0{,}58T + 0{,}58 = T,\ T = 0{,}58/0{,}42 = 1{,}38\ m$

$y_{100kN} = (1000)*(2{,}4*100*1{,}38^3/51400 + 1{,}7*100*1{,}38^3/51400) = 18{,}57\ mm$

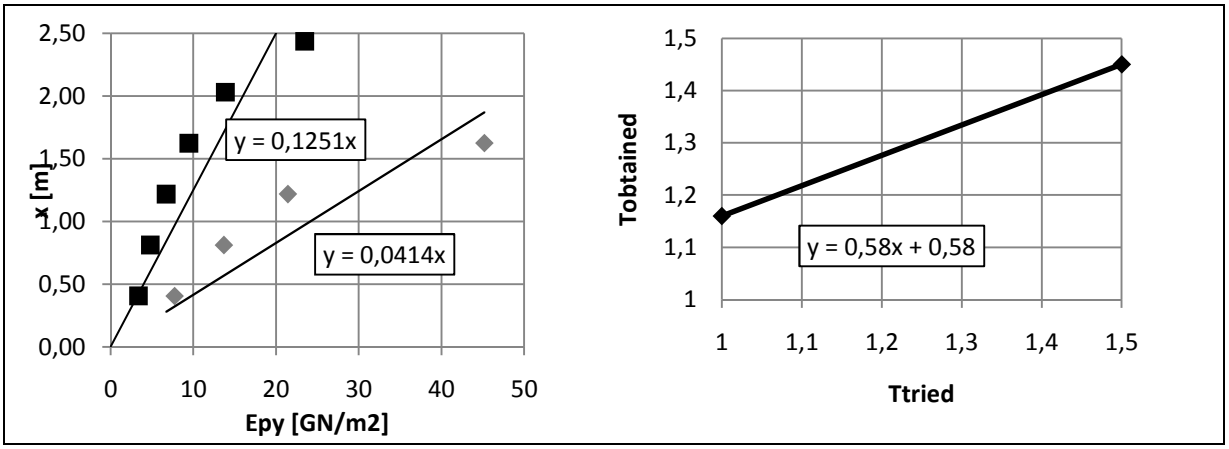

Graph 6-22 Graphs for iterative procedure of NDM, Case III-cu, Brent Cross, 60kN, p-y according to API

6.2.2 P-Y Reese et al.

The ultimate stresses on the pile according to Reese are exactly the same as the ultimate stresses by the API. The difference lies therein that the parabolic part of the two p-y curves is different. The recommendations by Reese propose a different curve for saturated clay and unsaturated clay whereas the recommendations of the API do not. The construction of the p-y curves according to Reese can be found in chapter 2 in appendix A.
The p-y curves are given in graph 6-17.

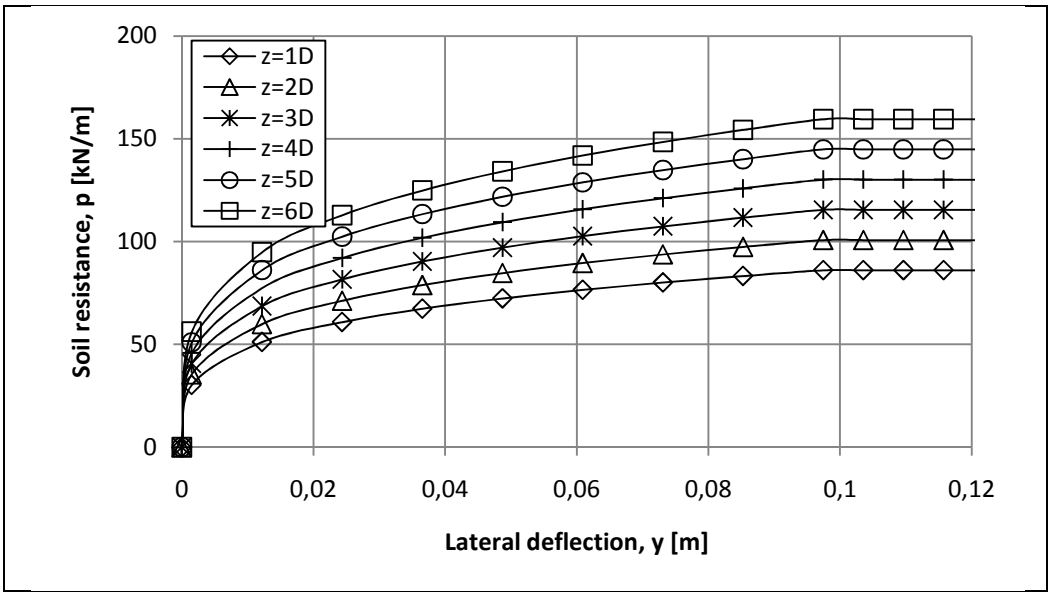

Graph 6-23 p-y Curves according to Reese, Case III-cu, Brent Cross

Calculate the displacements at the ground line for a load of 20kN.

Take $T_{tried} = 1{,}0m$

Then $Z_{max} = L/T_{tried} = 16{,}5/1{,}0 = 16{,}5$

z [m]	Z	Ay	By	Y_A [mm]	P [kN/m]	E_{py} [kPa]
0,406	0,41	1,79	0,94	1,06	27,81	26182
0,812	0,81	0,98	0,49	0,57	27,89	48765
1,218	1,22	0,74	0,18	0,36	28,43	79413
1,624	1,62	0,38	-0,02	0,14	25,35	180942
2,030	2,03	0,13	-0,07	0,02	18,02	771996
2,436	2,44	0	-0,09	-0,04	-14,29	408153

If the stiffness is plotted versus the depth, K_{py} can be calculated.

$K_{py} = 1/(10{,}5*10^{-6}) = 95238\ kN/m^3$ $T_{obtained} = (51400/95238)^{(1/5)} = 0{,}88\ m$ $T_{obtained} < T_{tried}$

Take $T_{tried} = 1{,}5\ m$ *Then* $Z_{max} = L/T_{tried} = 16{,}5/1{,}5 = 11\ m$

z [m]	Z	Ay	By	Y_A [mm]	P [kN/m]	E_{py} [kPa]
0,406	0,27	2,05	1,16	3,71	38,02	10253
0,812	0,54	1,56	0,8	2,75	41,30	15023
1,218	0,81	1,23	0,49	2,04	43,95	21497
1,624	1,08	0,92	0,29	1,46	45,56	31160
2,030	1,35	0,65	0,13	0,97	45,73	47268
2,436	1,62	0,38	0,01	0,51	34,85	68640

If the stiffness is plotted versus the depth, K_{py} can be calculated.

$K_{py} = 1/(40{,}9*10^{-6}) = 24450\ kN/m^3$ $T_{obtained} = (51400/24450)^{(1/5)} = 1{,}16\ m$ $T_{obtained} < T_{tried}$

Plot the values of T_{tried} versus the values of $T_{obtained}$. This plot is shown graph 6-18. Calculate the value of T, where $T_{tried} = T_{obtained}$. Subsequently calculate y_{20kN}.

$0{,}56T + 0{,}32 = T,\ T = 0{,}32/0{,}44 = 0{,}73\ m$

$y_{20kN} = (1000)*(2{,}4*20*0{,}73^3/51400 + 1{,}7*20*0{,}73^2/51400) = 0{,}71\ mm$

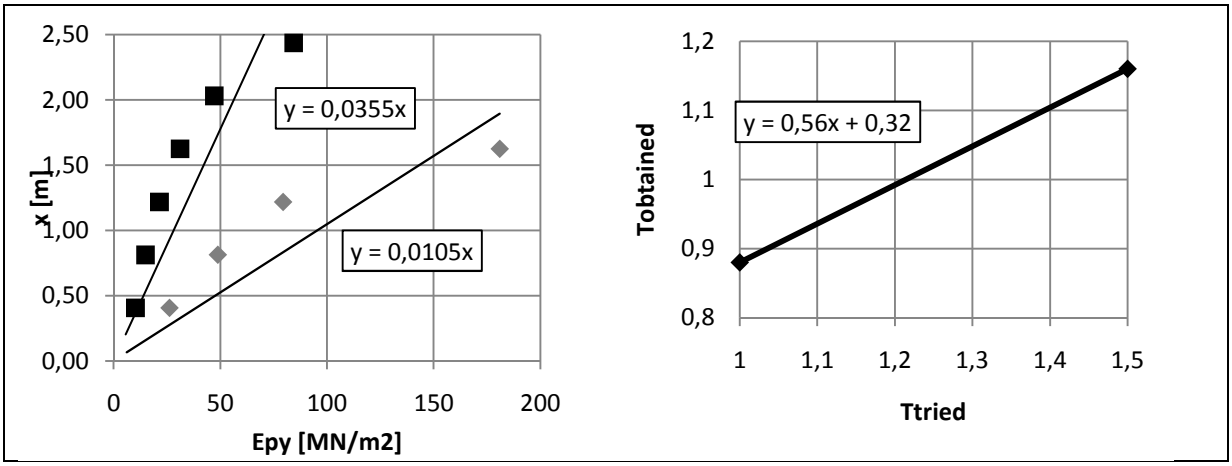

Graph 6-24 Graphs for iterative procedure of NDM, Case III-cu, Brent Cross, 20kN, p-y according to API

Calculate the displacements at the ground line for a load of 40kN.

Take $T_{tried} = 1,0m$

Then $Z_{max} = L/T_{tried} = 16,5/1,0 = 16,5$

z [m]	Z	Ay	By	Y_A [mm]	P [kN/m]	E_{py} [kPa]
0,406	0,41	1,79	0,94	2,12	33,07	15568
0,812	0,81	0,98	0,49	1,14	33,17	28996
1,218	1,22	0,74	0,18	0,72	33,81	47219
1,624	1,62	0,38	-0,02	0,28	30,14	107589
2,030	2,03	0,13	-0,07	0,05	21,43	459032
2,436	2,44	0	-0,09	-0,07	-18,01	257120

If the stiffness is plotted versus the depth, K_{py} can be calculated.

$K_{py} = 1/(17,6*10^{-6}) = 56818\ kN/m^3$ $T_{obtained} = (51400/56818)^{(1/5)} = 0,98\ m$ $T_{obtained} < T_{tried}$

Take $T_{tried} = 1,5\ m$ *Then* $Z_{max} = L/T_{tried} = 16,5/1,5 = 11\ m$

z [m]	Z	Ay	By	Y_A [mm]	P [kN/m]	E_{py} [kPa]
0,406	0,27	2,05	1,16	7,42	45,21	6097
0,812	0,54	1,56	0,8	5,50	49,11	8933
1,218	0,81	1,23	0,49	4,09	52,26	12782
1,624	1,08	0,92	0,29	2,92	54,18	18528
2,030	1,35	0,65	0,13	1,93	54,38	28106
2,436	1,62	0,38	0,01	1,02	43,91	43241

If the stiffness is plotted versus the depth, K_{py} can be calculated.

$K_{py} = 1/(59,7*10^{-6}) = 16750 kN/m^3$ $T_{obtained} = (51400/16750)^{(1/5)} = 1,25\ m$ $T_{obtained} < T_{tried}$

Plot the values of T_{tried} versus the values of $T_{obtained}$. This plot is shown graph 6-19. Calculate the value of T, where $T_{tried} = T_{obtained}$. Subsequently calculate y_{40kN}.

$0,54T + 0,44 = T,\ T = 0,44/0,46 = 0,96\ m$

$y_{40kN} = (1000)*(2,4*40*0,96^3/51400 + 1,7*40*0,96^2/51400) = 2,87\ mm$

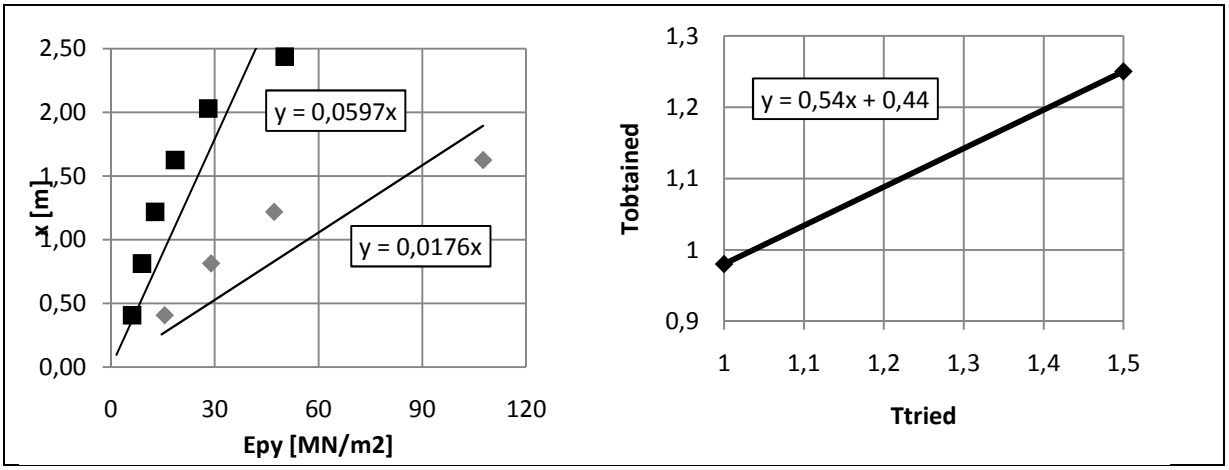

Graph 6-25 Graphs for iterative procedure of NDM, Case III-cu, Brent Cross, 40kN, p-y according to API

Calculate the displacements at the ground line for a load of 60kN.

Take $T_{tried} = 1{,}0m$

Then $Z_{max} = L/T_{tried} = 16{,}5/1{,}0 = 16{,}5$

z [m]	Z	Ay	By	Y_A [mm]	P [kN/m]	E_{py} [kPa]
0,406	0,41	1,79	0,94	3,19	36,60	11486
0,812	0,81	0,98	0,49	1,72	36,71	21393
1,218	1,22	0,74	0,18	1,07	37,41	34838
1,624	1,62	0,38	-0,02	0,42	33,36	79378
2,030	2,03	0,13	-0,07	0,07	23,72	338668
2,436	2,44	0	-0,09	-0,11	#NUM!	#NUM!

If the stiffness is plotted versus the depth, K_{py} can be calculated.

$K_{py} = 1/(23{,}9*10^{-6}) = 41841\ kN/m^3$ $T_{obtained} = (51400/41841)^{(1/5)} = 1{,}04\ m$ $T_{obtained} > T_{tried}$

Take $T_{tried} = 1{,}5\ m$ *Then* $Z_{max} = L/T_{tried} = 16{,}5/1{,}5 = 11\ m$

z [m]	Z	Ay	By	Y_A [mm]	P [kN/m]	E_{py} [kPa]
0,406	0,27	2,05	1,16	11,12	50,03	4498
0,812	0,54	1,56	0,8	8,25	54,35	6591
1,218	0,81	1,23	0,49	6,13	57,84	9431
1,624	1,08	0,92	0,29	4,39	59,96	13669
2,030	1,35	0,65	0,13	2,90	60,18	20736
2,436	1,62	0,38	0,01	1,52	56,42	37038

If the stiffness is plotted versus the depth, K_{py} can be calculated.

$K_{py} = 1/(80{,}9*10^{-6}) = 12361\ kN/m^3$ $T_{obtained} = (51400/12361)^{(1/5)} = 1{,}33\ m$ $T_{obtained} > T_{tried}$

Plot the values of T_{tried} versus the values of $T_{obtained}$. This plot is shown graph 6-20. Calculate the value of T, where $T_{tried} = T_{obtained}$. Subsequently calculate y_{60kN}.

$0{,}58T + 0{,}46 = T,\ T = 0{,}46/0{,}42 = 1{,}10\ m$

$y_{60kN} = (1000)*(2{,}4*60*1{,}10^3/51400 + 1{,}7*60*1{,}10^2/51400) = 6{,}13\ mm$

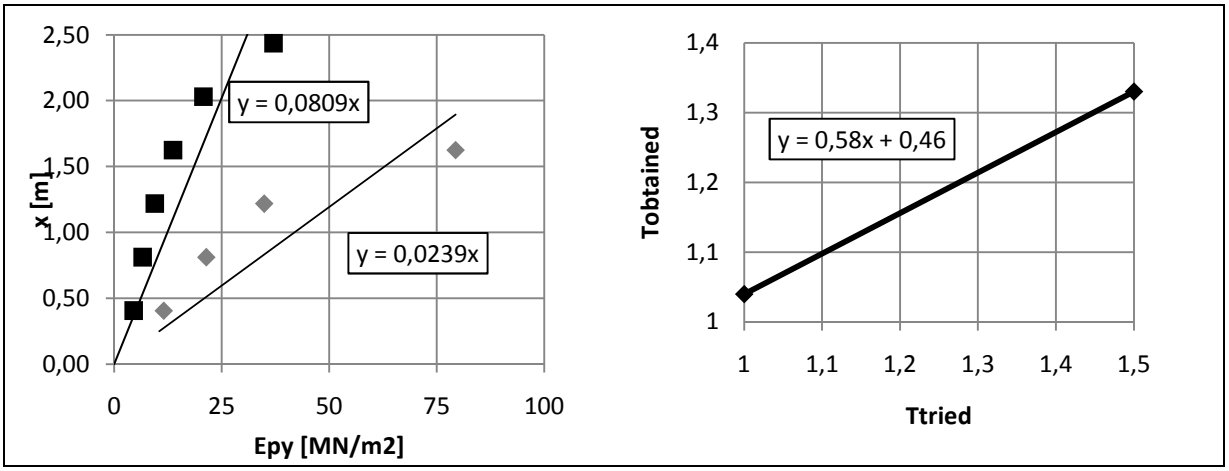

Graph 6-26 Graphs for iterative procedure of NDM, Case III-cu, Brent Cross, 60kN, p-y according to API

Calculate the displacements at the ground line for a load of 100kN.

Take $T_{tried} = 1{,}0m$

Then $Z_{max} = L/T_{tried} = 16{,}5/1{,}0 = 16{,}5$

z [m]	Z	Ay	By	Y_A [mm]	P [kN/m]	E_{py} [kPa]
0,406	0,41	1,79	0,94	5,31	41,59	7830
0,812	0,81	0,98	0,49	2,86	41,71	14584
1,218	1,22	0,74	0,18	1,79	42,51	23750
1,624	1,62	0,38	-0,02	0,70	37,90	54114
2,030	2,03	0,13	-0,07	0,12	26,95	230881
2,436	2,44	0	-0,09	-0,18	#NUM!	#NUM!

If the stiffness is plotted versus the depth, K_{py} can be calculated.

$K_{py} = 1/(35*10^{-6}) = 28571\ kN/m^3$ $T_{obtained} = (51400/28571)^{(1/5)} = 1{,}12\ m$ $T_{obtained} > T_{tried}$

Take $T_{tried} = 1{,}5\ m$ *Then* $Z_{max} = L/T_{tried} = 16{,}5/1{,}5 = 11\ m$

z [m]	Z	Ay	By	Y_A [mm]	P [kN/m]	E_{py} [kPa]
0,406	0,27	2,05	1,16	18,54	56,85	3066
0,812	0,54	1,56	0,8	13,75	61,76	4493
1,218	0,81	1,23	0,49	10,22	65,71	6429
1,624	1,08	0,92	0,29	7,31	68,12	9319
2,030	1,35	0,65	0,13	4,84	68,38	14137
2,436	1,62	0,38	0,01	2,54	64,11	25250

If the stiffness is plotted versus the depth, K_{py} can be calculated.

$K_{py} = 1/(119*10^{-6}) = 8432 kN/m^3$ $T_{obtained} = (51400/8432)^{(1/5)} = 1{,}44\ m$ $T_{obtained} < T_{tried}$

Plot the values of T_{tried} versus the values of $T_{obtained}$. This plot is shown graph 6-21. Calculate the value of T, where $T_{tried} = T_{obtained}$. Subsequently calculate y_{100kN}.

$0{,}64T + 0{,}48 = T,\ T = 0{,}48/0{,}36 = 1{,}33\ m$

$y_{100kN} = (1000)*(2{,}4*100*1{,}33^3/51400 + 1{,}7*100*1{,}33^2/51400) = 16{,}84\ mm$

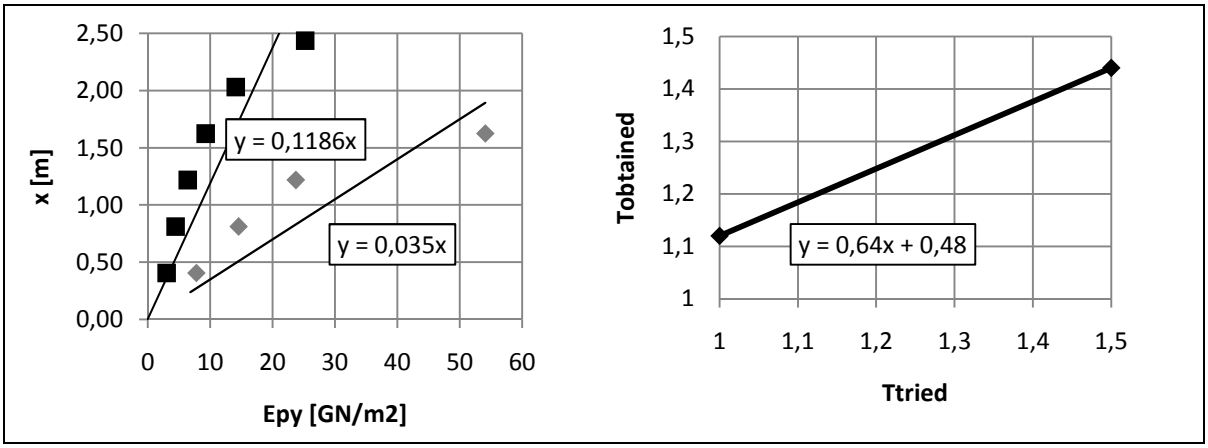

Graph 6-27 Graphs for iterative procedure of NDM, Case III-cu, Brent Cross, 100kN, p-y according to Reese et al.

6.2.3 From ground line deflection to pile head deflection

The result of the nondimensional calculation was the deflection of the pile at the ground-line under a certain load. The next step is to calculate the deflection at the pile head (One meter above the ground line), which was measured during the field test. This is done by taking the sum of the deformation at the ground line, y_{gl}, the deformation caused by the rotation of the pile at the ground line, y_s, and the deformation caused by the bending of that part of the pile that is situated above the ground line, y_{agl}.

Deformations cause by rotation of the pile at the ground line, y_S.

The rotation of the pile at the ground line can be calculated with the nondimensional method. The formula is given below:

$$S = A_s \frac{P_t T^2}{E_p I_p} + B_s \frac{M_t T}{E_p I_p}$$

Where:

S = Slope [*degree*]
T = Relative stiffness factor [*m*]
P_t = Applied lateral load at pile head [*kN*]
M_t = Applied moment at pile head [*kNm*]
A_s, B_s = nondimensional parameters for respectively: slope by lateral load and slope by moment. These parameters have to be deduced from the nondimensional charts.

API							
Pt [kN]	**Mt [kNm]**	**T [m]**	**Z_{max} [-]**	**As [-]**	**Bs [-]**	**S [degree]**	**y_S [mm]**
20	20	0,89	18,5	1,62	1,72	0,00109	1,09
40	40	1,06	15,6	1,62	1,72	0,00284	2,84
60	60	1,20	13,8	1,62	1,72	0,00513	5,13
100	100	1,38	12,0	1,62	1,72	0,01062	10,62

Reese							
Pt [kN]	**Mt [kNm]**	**T [m]**	**Z_{max} [-]**	**As [-]**	**Bs [-]**	**S [degree]**	**y_S [mm]**
20	20	0,73	22,6	1,62	1,72	0,00082	0,82
40	40	0,96	17,2	1,62	1,72	0,00245	2,45
60	60	1,1	15,0	1,62	1,72	0,00450	4,50
100	100	1,33	12,4	1,62	1,72	0,01003	10,03

Deformations of the pile by bending of the pile above the ground line.

To calculate this part the pile is fixed at the ground line. Now, y_{agl} can be calculated with the following formula:

$$y_{agl} = \frac{P_t l^2}{3E_p I_p}$$

This part of the deformation is independent on whether the recommendations by the API or by Reese were used for constructing the p-y curves.

API & Reese	
Pt [kN]	**y_{agl} [mm]**
20	0,13
40	0,26
60	0,39
100	0,65

Total deformation

The total, pile head deformation is finally found by adding the deformation of the pile above the soil surface to the deformation of the pile at the ground line.

API			
y_S [mm]	**+y_{agl} [mm]**	**+y_{gl} [mm]**	**=y_h [mm]**
1,09	0,13	1,18	2,40
2,84	0,26	3,71	6,81
5,13	0,39	7,70	13,22
10,62	0,65	18,57	29,84

Reese			
y_S [mm]	**+y_{agl} [mm]**	**+y_{gl} [mm]**	**=y_h [mm]**
0,82	0,13	0,71	1,66
2,45	0,26	2,87	5,58
4,50	0,39	6,13	11,02
10,03	0,65	16,84	27,52

6.2.4 Results

The graphs below show that, indifferent of whether the p-y curves have been established according to API or according to Reese *et al.*, the NDM predicts the deflections very accurate. At higher loads however, the deflection is underestimated and this underestimation is probably going to increase for higher loads.

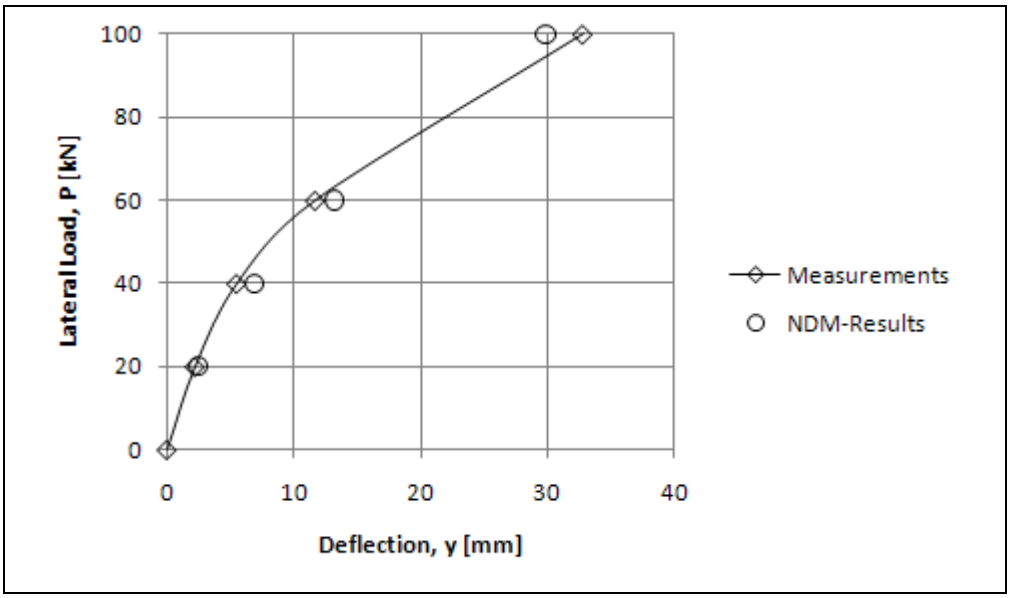

Graph 6-28 NDM Results, Pile head deflection vs. lateral load with P-Y according to API

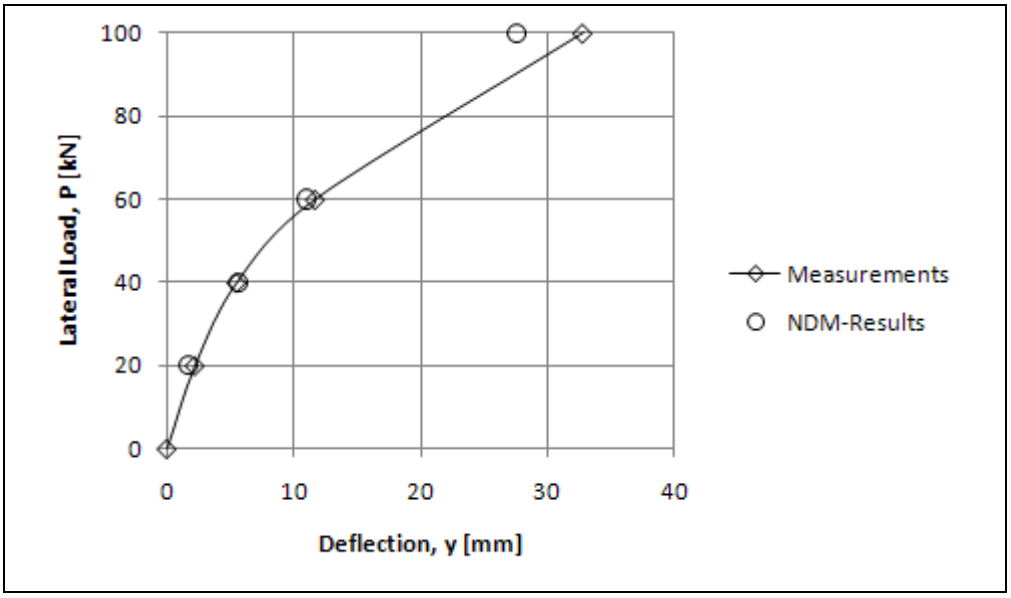

***Graph 6-29 NDM Results, Pile head deflection vs. lateral load with P-Y according to Reese* et al.**

6.3 CASE VI-CS, SABINE

6.3.1 Calculation

Determine the p-y Curves.

Because the NDM method can only deal with a homogeneous soil, the soil parameters are averaged over the first eight pile diameters. This is the same approach as for the CLM.

$\gamma' = 5{,}5\ kN/m^3$
$c_u = 14{,}4 kN/m^2$

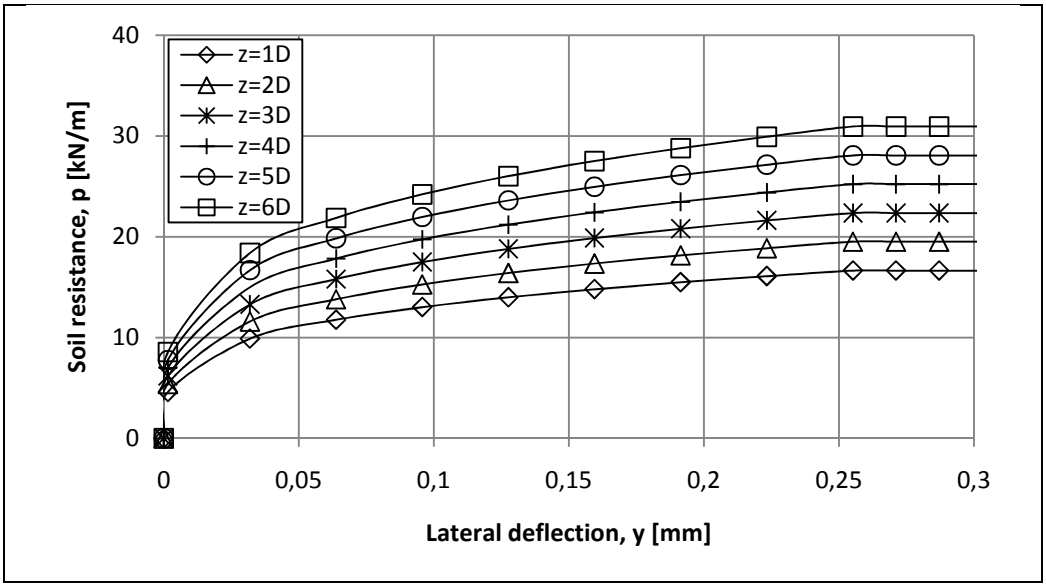

Table 6-2 P-Y curves Sabine according to Reese et al.

*Calculate the displacements at the ground line for a load of **18kN.***

Take $T_{tried} = 1{,}50m$

Then $Z_{max} = L/T_{tried} = 12{,}8/1{,}5 = 8{,}53\ m$

z [m]	Z	Ay	By	Y_A [mm]	P [kN/m]	E_{py} [kPa]
0,319	0,21	2,01	1,31	4,42	6,04	1366
0,638	0,43	1,70	0,95	3,67	6,75	1840
0,957	0,64	1,43	0,70	3,05	7,39	2422
1,276	0,85	1,12	0,47	2,35	7,81	3318
1,595	1,06	0,85	0,32	1,77	8,10	4571
1,914	1,28	0,65	0,16	1,32	8,29	6283

If the stiffness is plotted versus the depth, K_{py} can be calculated.

$K_{py} = 1/(333{,}1*10^{-6}) = 3002 kN/m^3$ $T_{obtained} = (31280/3002)^{(1/5)} = 1{,}60m$ $T_{obtained} > T_{tried}$

Take $T_{tried} = 2{,}0m$ *Then* $Z_{max} = L/T_{tried} = 12{,}8/2{,}0 = 6{,}4m$

z [m]	Z	Ay	By	Y_A [mm]	P [kN/m]	E_{py} [kPa]
0,319	0,16	2,01	1,31	10,17	7,43	731
0,638	0,32	1,70	0,95	8,48	8,32	982
0,957	0,48	1,43	0,70	7,07	9,12	1290
1,276	0,64	1,12	0,47	5,47	9,65	1763
1,595	0,80	0,85	0,32	4,13	10,01	2425
1,914	0,96	0,65	0,16	3,09	10,26	3318

If the stiffness is plotted versus the depth, K_{py} can be calculated.

$K_{py} = 1/(628{,}8*10^{-6}) = 1590\ kN/m^3$ $T_{obtained} = (31280/1590)^{(1/5)} = 1{,}81m$ $T_{obtained} < T_{tried}$

Plot the values of T_{tried} versus the values of $T_{obtained}$. This plot is shown graph 6-22. Calculate the value of T, where $T_{tried} = T_{obtained}$. Subsequently calculate y_{50kN}.

$0{,}42T + 0{,}97 = T,\ T = 0{,}97/0{,}58 = 1{,}67\ m$

$y_{18kN} = (1000)*2{,}4*18*1{,}67^3/31280+(1000)*1{,}70*5{,}49*1{,}67^2/31280 = 7{,}26mm$

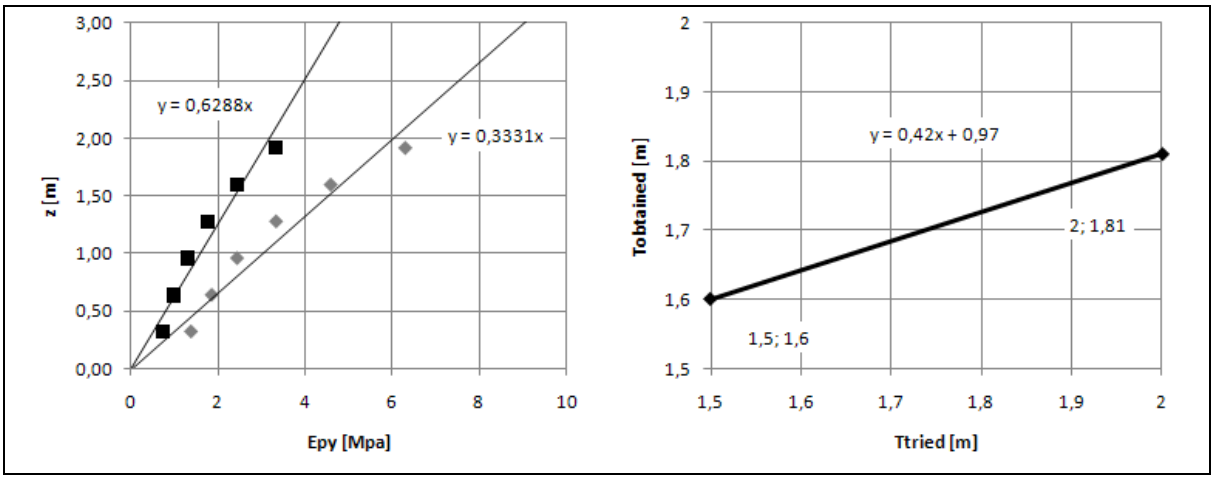

Graph 6-30 Graphs for iterative procedure of NDM, Sabine, Reese, 18kN

To go from groundline deflection to Pile head deflection, two additional displacements have to be added to the groundline deflection.

Calculate the pile-head deflection due to rotation at the groundline.

The rotation S is:

$S_{607kN} = (1000)*1{,}7*18*1{,}67^2/31280+(1000)*1{,}75*5{,}49*1{,}67/31280 = 3{,}24mm/m$

$y_{S,607kN} = 3{,}24*0{,}305 = 0{,}99mm$

Calculate the pile head deflection due to bending of the pile above the ground line.

$y_{B,607kN} = 18*0{,}305^3/(3*31280) = 5{,}44*10^{-3}\ mm.$

Calculate the pile head deflection at load 18kN

$\boldsymbol{y_h} = 7{,}26+0{,}99+0{,}0054=\mathbf{8{,}3mm}$

*Calculate the displacements at the ground line for a load of **35kN.***

Take $T_{tried} = 1,50m$

Then $Z_{max} = L/T_{tried} = 12,8/1,5 = 8,53\ m$

z [m]	Z	Ay	By	Y_A [mm]	P [kN/m]	E_{py} [kPa]
0,319	0,21	2,01	1,31	8,60	7,13	829
0,638	0,43	1,7	0,95	7,15	7,98	1116
0,957	0,64	1,43	0,7	5,94	8,73	1470
1,276	0,85	1,12	0,47	4,59	9,23	2011
1,595	1,06	0,85	0,32	3,46	9,57	2770
1,914	1,28	0,65	0,16	2,58	9,80	3803

If the stiffness is plotted versus the depth, K_{py} can be calculated.

$K_{py} = 1/(549,9*10^{-6}) = 1819kN/m^3$ $T_{obtained} = (31280/1819)^{(1/5)} = 1,77m$ $T_{obtained} > T_{tried}$

Take $T_{tried} = 2,0m$ *Then* $Z_{max} = L/T_{tried} = 12,8/2,0= 6,4m$

z [m]	Z	Ay	By	Y_A [mm]	P [kN/m]	E_{py} [kPa]
0,319	0,16	2,01	1,31	19,78	8,78	444
0,638	0,32	1,7	0,95	16,51	9,83	595
0,957	0,48	1,43	0,7	13,76	10,77	783
1,276	0,64	1,12	0,47	10,67	11,40	1068
1,595	0,80	0,85	0,32	8,05	11,83	1470
1,914	0,96	0,65	0,16	6,04	12,13	2009

If the stiffness is plotted versus the depth, K_{py} can be calculated.

$K_{py} = 1/(1,038*10^{-3}) = 964\ kN/m^3$ $T_{obtained} = (31280/964)^{(1/5)} = 2,01m$ $T_{obtained} > T_{tried}$

Take T = 2,0m

$y_{35kN} = (1000)*2,4*35*2,0^3/31280+(1000)*1,70*10,68*2,0^2/31280 = 23,80mm$

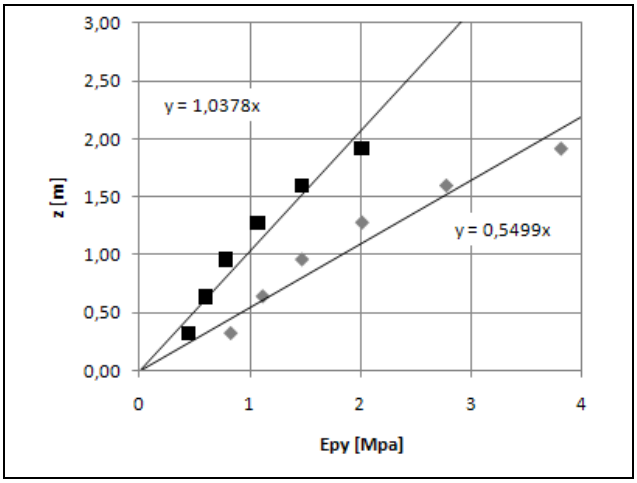

Graph 6-31 Graphs for iterative procedure of NDM, Sabine, Reese, 35kN

To go from groundline deflection to Pile head deflection, two additional displacements have to be added to the groundline deflection.

Calculate the pile-head deflection due to rotation at the groundline.

The rotation S is:

$S_{607kN} = (1000)*1,7*35*2,0^2/31280+(1000)*1,75*10,68*2,0/31280 = 8,81mm/m$

$y_{S,607kN} = 8,81*0,305 = 2,69mm$

Calculate the pile head deflection due to bending of the pile above the ground line.

$y_{B,607kN} = 35*0,305^3/(3*31280) = 10,6*10^{-3}$ mm.

Calculate the pile head deflection at load 35kN

$\boldsymbol{y_h = 23,80+2,69+0,0106=26,5mm}$

*Calculate the displacements at the ground line for a load of **53kN.***

Take $T_{tried} = 2m$

Then $Z_{max} = L/T_{tried} = 12,8/2 = 6,4m$

z [m]	Z	Ay	By	Y_A [mm]	P [kN/m]	E_{py} [kPa]
0,319	0,16	2,01	1,31	29,95	9,74	325
0,638	0,32	1,7	0,95	25,01	10,91	436
0,957	0,48	1,43	0,7	20,83	11,95	574
1,276	0,64	1,12	0,47	16,15	12,64	783
1,595	0,80	0,85	0,32	12,18	13,12	1077
1,914	0,96	0,65	0,16	9,14	13,45	1471

If the stiffness is plotted versus the depth, K_{py} can be calculated.

$K_{py} = 1/(1,4168*10^{-3}) = 706kN/m^3$ $T_{obtained} = (31280/706)^{(1/5)} = 2,13m$ $T_{obtained} > T_{tried}$

Take $T_{tried} = 2,56m$ *Then* $Z_{max} = L/T_{tried} = 12,8/2,56= 5,0m$

z [m]	Z	Ay	By	Y_A [mm]	P [kN/m]	E_{py} [kPa]
0,319	0,12	2,01	1,31	61,57	11,66	189
0,638	0,25	1,7	0,95	51,54	13,07	254
0,957	0,37	1,43	0,7	43,02	14,32	333
1,276	0,50	1,12	0,47	33,43	15,16	454
1,595	0,62	0,85	0,32	25,25	15,74	623
1,914	0,75	0,65	0,16	19,02	16,16	849

If the stiffness is plotted versus the depth, K_{py} can be calculated.

$K_{py} = 1/(2,4499*10^{-3}) = 408\ kN/m^3$ $T_{obtained} = (31280/408)^{(1/5)} = 2,38m$ $T_{obtained} < T_{tried}$

Plot the values of T_{tried} versus the values of $T_{obtained}$. This plot is shown graph 6-24. Calculate the value of T, where $T_{tried} = T_{obtained}$. Subsequently calculate y_{50kN}.

$0,4464T +1,2371 = T,\ T = 1,2371/0,5536 = 2,23\ m$

$y_{18kN} = (1000)*2,4*53*2,23^3/31280+(1000)*1,70*16,17*2,23^2/31280 =49,47mm$

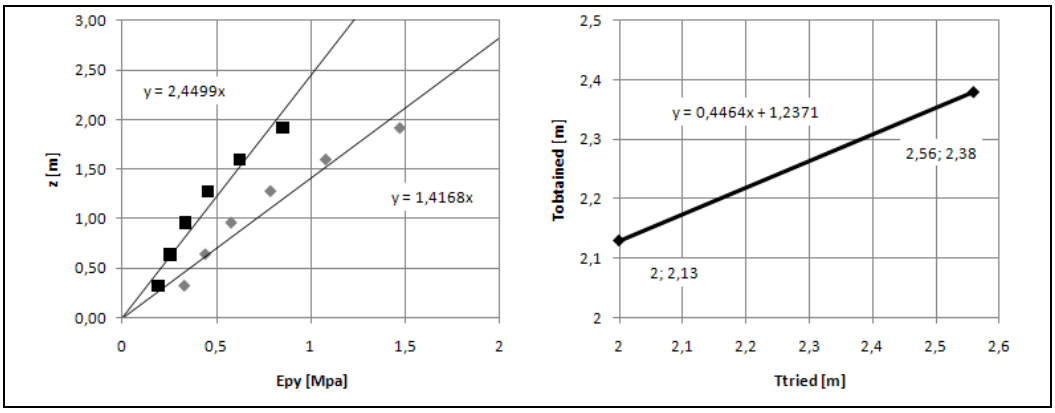

Graph 6-32 Graphs for iterative procedure of NDM, Sabine, Reese, 53kN

To go from groundline deflection to Pile head deflection, two additional displacements have to be added to the groundline deflection.

Calculate the pile-head deflection due to rotation at the groundline.

The rotation S is:

S_{607kN} *= (1000)*1,7*53*2,23²/31280+(1000)*1,75*16,17*2,23/31280 = 16,34mm/m*

$y_{S,607kN}$ *= 16,34*0,305 = 4,98mm*

Calculate the pile head deflection due to bending of the pile above the ground line.

$y_{B,607kN}$ *= 53*0,305³/(3*31280) = 16,0*10⁻³ mm.*

Calculate the pile head deflection at load 53kN

y_h = 49,47+4,98+0,0160=54,47mm

*Calculate the displacements at the ground line for a load of **80kN.***

Take T_{tried} *= 2,56m*

Then $Z_{max} = L/T_{tried} = 12,8/2,56 = 5,0$

z [m]	Z	Ay	By	Y_A [mm]	P [kN/m]	E_{py} [kPa]
0,319	0,12	2,01	1,31	92,94	12,92	139
0,638	0,25	1,7	0,95	77,80	14,49	186
0,957	0,37	1,43	0,7	64,94	15,87	244
1,276	0,50	1,12	0,47	50,46	16,81	333
1,595	0,62	0,85	0,32	38,11	17,45	458
1,914	0,75	0,65	0,16	28,71	17,91	624

If the stiffness is plotted versus the depth, K_{py} can be calculated.

$K_{py} = 1/(3,3354*10^{-3}) = 300kN/m^3$ $T_{obtained} = (31280/300)^{(1/5)} = 2,53m$ $T_{obtained} < T_{tried}$

Take $T_{tried} = 2,4m$ *Then* $Z_{max} = L/T_{tried} = 12,8/2,4= 5,3m$

z [m]	Z	Ay	By	Y_A [mm]	P [kN/m]	E_{py} [kPa]
0,319	0,13	2,01	1,31	76,95	12,33	160
0,638	0,27	1,7	0,95	64,37	13,82	215
0,957	0,40	1,43	0,7	53,70	15,14	282
1,276	0,53	1,12	0,47	41,71	16,03	384
1,595	0,66	0,85	0,32	31,49	16,63	528
1,914	0,80	0,65	0,16	23,70	17,07	720

If the stiffness is plotted versus the depth, K_{py} can be calculated.

$K_{py} = 1/(2,8908*10^{-3}) = 346\ kN/m^3$ $T_{obtained} = (31280/346)^{(1/5)} = 2,46m$ $T_{obtained} > T_{tried}$

Plot the values of T_{tried} versus the values of $T_{obtained}$. This plot is shown graph 6-25. Calculate the value of T, where $T_{tried} = T_{obtained}$. Subsequently calculate y_{80kN}.

$0,4375T + 1,41 = T,\ T = 1,41/0,5625 = 2,51\ m$

$y_{18kN} = (1000)*2,4*80*2,51^3/31280+(1000)*1,70*24,4*2,51^2/31280 = 105,41mm$

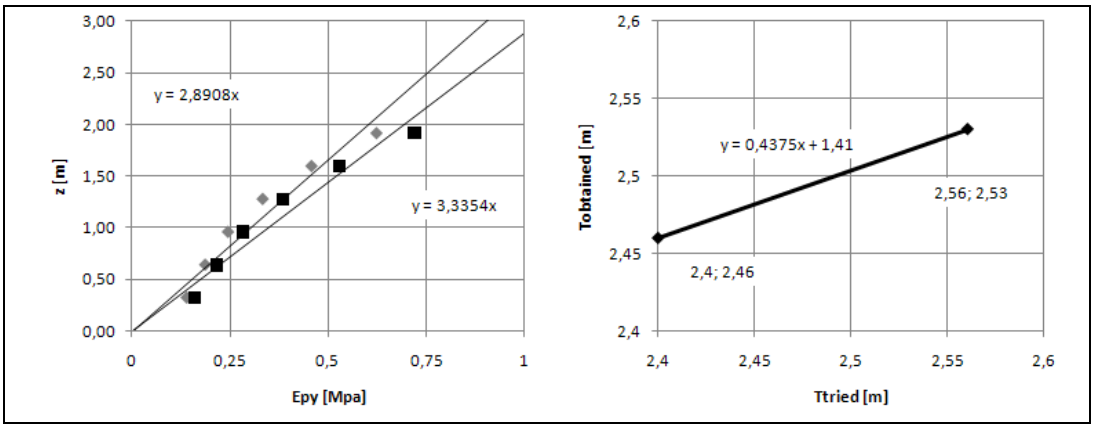

Graph 6-33 Graphs for iterative procedure of NDM, Sabine, Reese, 80kN

To go from groundline deflection to Pile head deflection, two additional displacements have to be added to the groundline deflection.

Calculate the pile-head deflection due to rotation at the groundline.

The rotation S is:

$S_{607kN} = (1000)*1,7*80*2,51^2/31280+(1000)*1,75*24,4*2,51/31280 = 30,82mm/m$

$y_{S,607kN} = 30,82*0,305 = 9,40mm$

Calculate the pile head deflection due to bending of the pile above the ground line.

$y_{B,607kN} = 80*0,305^3/(3*31280) = 24,2*10^{-3}\ mm.$

Calculate the pile head deflection at load 80kN

$\boldsymbol{y_h =}$ *105,41+9,40+0,0242=****114,83mm***

6.3.2 Calculation of Maximum moments

Calculate the maximum moment for Load = 18kN

First the Nondimensional graphs have to be chosen to find the values of A_m and B_m. This can be found by calculating Z_{max}.

$$Z_{max} = \frac{L}{T} = \frac{12{,}8}{1{,}67} = 7{,}7$$

Choose the graph where Z_{max} = 5. Since the maximum value of A_m can be found at a depth of 1,33T, the maximum moment must be located between 0,0T and 1,33T. Now the moments between these points are determined.

$$M = A_m P_t T + B_m M_t$$

Take T = 1,67m, P_t = 18kN and M_t = 5,49kNm

Depth Coefficient, z	Am	Bm	M [kNm]
0	0	1	5,5
0,3	0,36	0,98	16,2
0,6	0,55	0,93	21,6
0,9	0,71	0,85	26,0
1,1	0,74	0,8	26,6
1,33	0,77	0,71	27,0

$$M_{max,18kN} = 27kNm$$

Calculate the maximum moment for Load = 35kN

First the Nondimensional graphs have to be chosen to find the values of A_m and B_m. This can be found by calculating Z_{max}.

$$Z_{max} = \frac{L}{T} = \frac{12{,}8}{2{,}0} = 6{,}4$$

Choose the graph where Z_{max} = 5. Since the maximum value of A_m can be found at a depth of 1,33T, the maximum moment must be located between 0,0T and 1,33T. Now the moments between these points are determined.

$$M = A_m P_t T + B_m M_t$$

Take T = 2,0m, P_t = 35kN and M_t = 10,68kNm

Depth Coefficient, z	Am	Bm	M [kNm]
0	0	1	10,7
0,3	0,36	0,98	35,7
0,6	0,55	0,93	48,4
0,9	0,71	0,85	58,8
1,1	0,74	0,8	60,3
1,33	0,77	0,71	61,5

$$M_{max,35kN} = 62kNm$$

Calculate the maximum moment for Load = 53kN

First the Nondimensional graphs have to be chosen to find the values of A_m and B_m. This can be found by calculating Z_{max}.

$$Z_{max} = \frac{L}{T} = \frac{12{,}8}{2{,}23} = 5{,}7$$

Choose the graph where Z_{max} = 5. Since the maximum value of A_m can be found at a depth of 1,33T, the maximum moment must be located between 0,0T and 1,33T. Now the moments between these points are determined.

$$M = A_m P_t T + B_m M_t$$

Take T = 2,23m, P_t = 53kN and M_t = 16,17kNm

Depth Coefficient, z	**Am**	**Bm**	**M [kNm]**
0	0	1	16,2
0,3	0,36	0,98	58,4
0,6	0,55	0,93	80,0
0,9	0,71	0,85	97,7
1,1	0,74	0,8	100,4
1,33	0,77	0,71	102,5

$$M_{max,607kN} = 103kNm$$

Calculate the maximum moment for Load = 80kN

First the Nondimensional graphs have to be chosen to find the values of A_m and B_m. This can be found by calculating Z_{max}.

$$Z_{max} = \frac{L}{T} = \frac{12{,}8}{2{,}51} = 5{,}1$$

Choose the graph where Z_{max} = 5. Since the maximum value of A_m can be found at a depth of 1,33T, the maximum moment must be located between 0,0T and 1,33T. Now the moments between these points are determined.

$$M = A_m P_t T + B_m M_t$$

Take T = 2,51m, P_t = 80kN and M_t = 24,4kNm

Depth Coefficient, z	**Am**	**Bm**	**M [kNm]**
0	0	1	24,4
0,3	0,36	0,98	96,2
0,6	0,55	0,93	133,1
0,9	0,71	0,85	163,3
1,1	0,74	0,8	168,1
1,33	0,77	0,71	171,9

$$M_{max,80kN} = 172kNm$$

6.3.3 Results

The results show that the deflections are overestimated by almost a factor of two. The maximum moments on the other hand are approximated quite closely. This can be seen in the two graphs below.

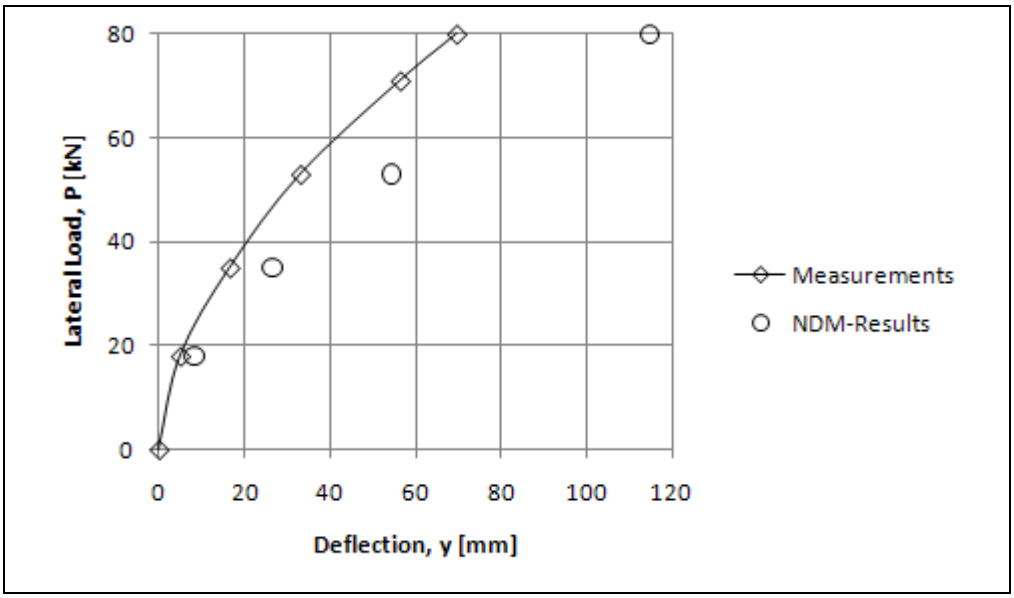

Graph 6-34 Lateral Load vs. displacement, Sabine

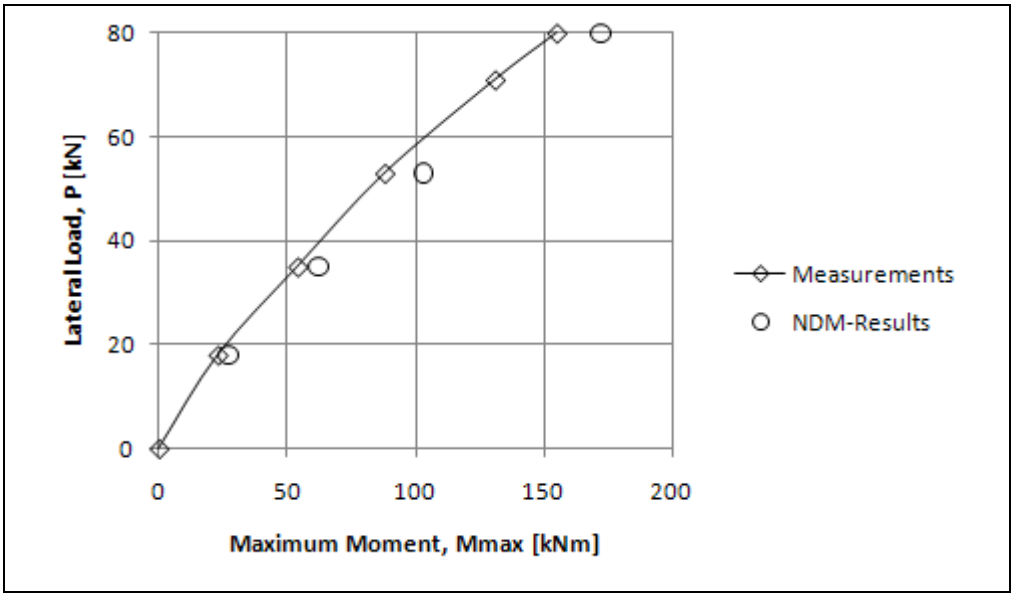

Graph 6-35 Lateral Load vs. Maximum Moment, Sabine

6.4 CASE IX-CL,GARSTON

6.4.1 Calculation

Since one NDM-calculation requires a lot of time, only three of the twelve measurements have been recalculated. This is done, because with three points and the origin in a graph the non-linear character of a load displacement curve can be seen.

Determine the p-y Curves.

Because the NDM method can only deal with a homogeneous soil, the soil parameters are averaged over the first eight pile diameters. This is the same approach as for the CLM.

$$\gamma = \frac{3{,}5 \times 21{,}5 + 3{,}0 \times 9{,}7 + 5{,}5 \times 11{,}7}{12} = 14{,}06\ kN/m^3$$

$$\varphi = \frac{3{,}5 \times 43 + 3{,}0 \times 37 + 5{,}5 \times 43}{12} = 41{,}5°$$

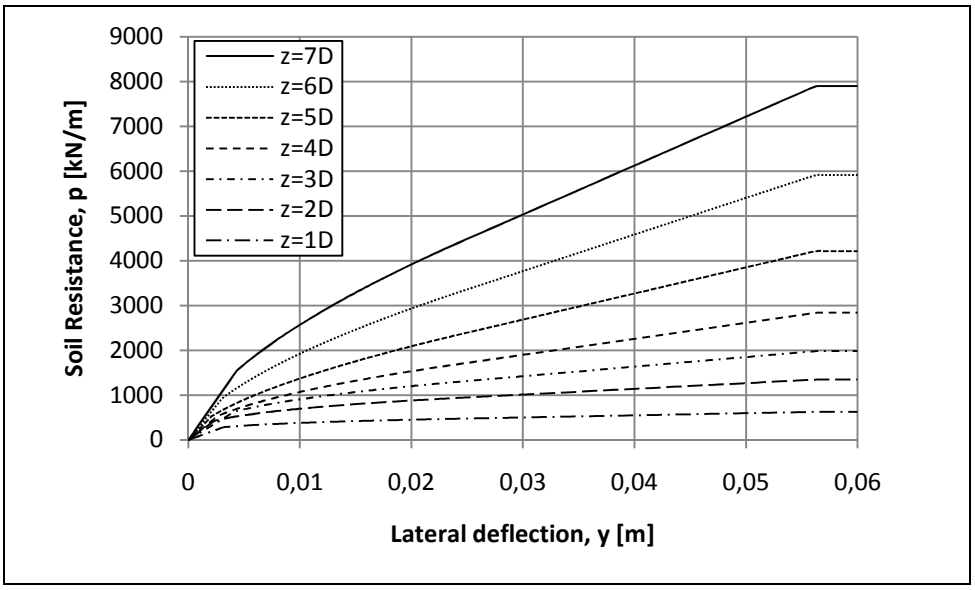

Table 6-3 P-Y curves Garston according to Reese et al.

*Calculate the displacements at the ground line for a load of **607kN.***

Take $T_{tried} = 4{,}17m$

Then $Z_{max} = L/T_{tried} = 12{,}5/4{,}17 = 3{,}0\ m$

z [m]	Z	Ay	By	Y_A [mm]	P [kN/m]	E_{py} [kPa]
1,50	0,36	2,16	1,16	9,06	372,08	41058
3,00	0,72	1,56	0,71	6,44	599,57	93103
4,50	1,08	1,07	0,40	4,34	645,72	148622
6,00	1,44	0,65	0,13	2,54	517,51	204000
7,50	1,80	0,31	-0,02	1,15	294,33	255000
9,00	2,16	0,04	-0,11	0,08	23,60	306000
10,50	2,52	-0,20	-0,20	-0,92	#NUM!	#NUM!

If the stiffness is plotted versus the depth, K_{py} can be calculated.

$K_{py} = 1/(29{,}8*10^{-6}) = 33557kN/m^3$ $\quad T_{obtained} = (11698000/33557)^{(1/5)} = 3{,}22m$ $T_{obtained} < T_{tried}$

Take $T_{tried} = 2,5\ m$ *Then* $Z_{max} = L/T_{tried} = 12,5/2,5 = 5m$

z [m]	Z	Ay	By	Y_A [mm]	P [kN/m]	E_{py} [kPa]
1,50	0,60	1,51	0,71	1,43	131,29	91500
3,00	1,20	0,56	0,20	0,51	93,25	183000
4,50	1,80	0,29	-0,04	0,22	33,90	153000
6,00	2,40	0,04	-0,09	0,01	2,06	204000
7,50	3,00	-0,04	-0,09	-0,06	#NUM!	#NUM!
9,00	3,60	-0,07	-0,04	-0,07	#NUM!	#NUM!
10,50	4,20	-0,04	0,00	-0,04	#NUM!	#NUM!

If the stiffness is plotted versus the depth, K_{py} can be calculated.

$K_{py} = 1/(16,4*10^{-6}) = 60976\ kN/m^3$ $T_{obtained} = (11698000/60976)^{(1/5)} = 2,86m$ $T_{obtained} > T_{tried}$

Plot the values of T_{tried} versus the values of $T_{obtained}$. This plot is shown graph 6-26. Calculate the value of T, where $T_{tried} = T_{obtained}$. Subsequently calculate y_{50kN}.

$0,2156T + 2,3211 = T,\ T = 2,3211/0,7844,92 = 2,96\ m$

$y_{607kN} = (1000)*2,5*607*2,96^3/11698000+(1000)*1,65*546,3*2,96^2/11698000 = 4,04\ mm$

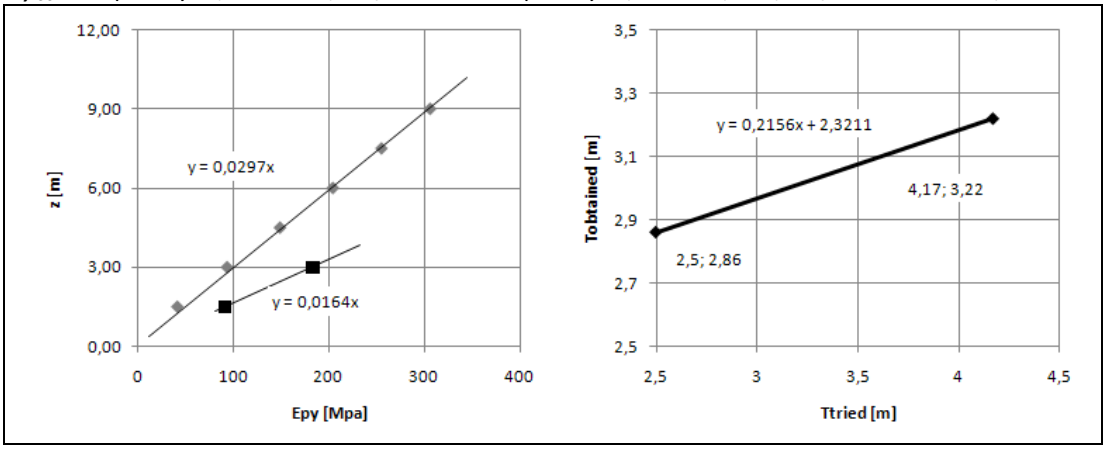

Graph 6-36 Graphs for iterative procedure of NDM, Arkansas, Reese, 607kN

To go from groundline deflection to Pile head deflection, two additional displacements have to be added to the groundline deflection.

Calculate the pile-head deflection due to rotation at the groundline.

The rotation S is:

$S_{607kN} = (1000)*1,7*607*2,96^2/11698000+(1000)*1,75*546,3*2,96/11698000 = 1,01mm/m$

$y_{S,607kN} = 1,0*0,9 = 0,9mm$

Calculate the pile head deflection due to bending of the pile above the ground line.

$y_{B,607kN} = 607*0,9^3/(3*11698000) = 12*10^{-6}\ m.$

Calculate the pile head deflection at load 607kN

$\boldsymbol{y_h = 4,04+1,01+0,01=5,1mm}$

Calculate the displacements at the ground line for a load of ***1402kN.***

Take $T_{tried} = 4,17m$

Then $Z_{max} = L/T_{tried} = 12,5/4,17 = 3,0\ m$ Also use the reduced bending stiffness of the pile.

z [m]	Z	Ay	By	Y_A [mm]	P [kN/m]	E_{py} [kPa]
1,50	0,36	2,16	1,16	51,68	606,71	11740
3,00	0,72	1,56	0,71	36,73	1094,84	29807
4,50	1,08	1,07	0,4	24,79	1309,08	52803
6,00	1,44	0,65	0,13	14,54	1298,42	89316
7,50	1,80	0,31	-0,02	6,55	1061,11	161907
9,00	2,16	0,04	-0,11	0,35	106,67	306000
10,50	2,52	-0,2	-0,2	-5,21	#NUM!	#NUM!

If the stiffness is plotted versus the depth, K_{py} can be calculated.

$K_{py} = 1/(36{,}8*10^{-6}) = 27174 kN/m^3$ $T_{obtained} = (4741700/30030)^{(1/5)} = 2{,}81m$ $T_{obtained} < T_{tried}$

Take $T_{tried} = 2{,}5$ m Then $Z_{max} = L/T_{tried} = 12{,}5/2{,}5 = 5m$

z [m]	Z	Ay	By	Y_A [mm]	P [kN/m]	E_{py} [kPa]
1,50	0,36	1,51	0,71	35,66	530,15	14867
3,00	0,72	0,56	0,2	12,93	757,84	58603
4,50	1,08	0,29	-0,04	6,03	737,71	122289
6,00	1,44	0,04	-0,09	0,44	89,99	204000
7,50	1,80	-0,04	-0,09	-1,27	#NUM!	#NUM!
9,00	2,16	-0,07	-0,04	-1,69	#NUM!	#NUM!
10,50	2,52	-0,04	0	-0,86	#NUM!	#NUM!

If the stiffness is plotted versus the depth, K_{py} can be calculated.

$K_{py} = 1/(32{,}8*10^{-6}) = 30489 kN/m^3$ $T_{obtained} = (4741700/30489)^{(1/5)} = 2{,}74m$ $T_{obtained} > T_{tried}$

Plot the values of T_{tried} versus the values of $T_{obtained}$. This plot is shown graph 6-27. Calculate the value of T, where $T_{tried} = T_{obtained}$. Subsequently calculate y_{50kN}.

0,0419T +2,6352 = T, T = 2,6352/0,9581 = 2,75m

$y_{1402kN} = (1000)*2{,}5*1402*2{,}75^3/4741700+(1000)*1{,}65*1261{,}8*2{,}75^2/4741700 = 18{,}69mm$

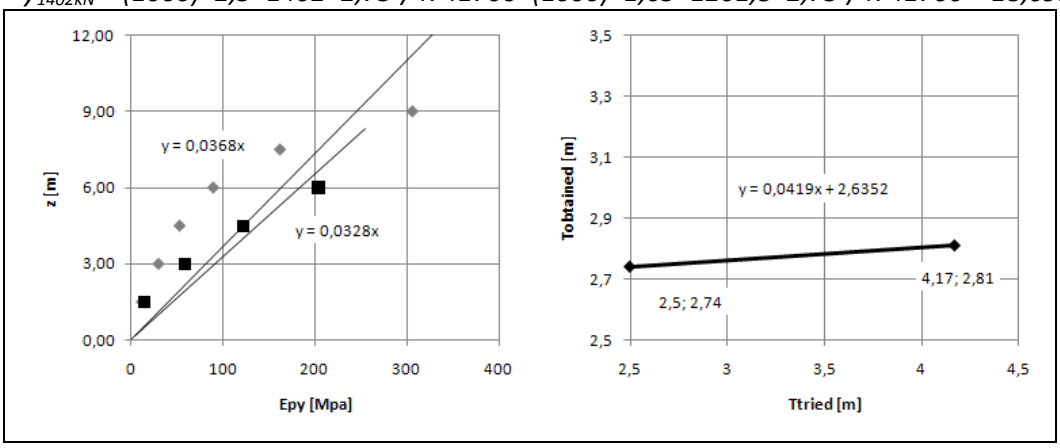

Graph 6-37 Graphs for iterative procedure of NDM, Arkansas, Reese, 1402kN

Calculate the pile-head deflection due to rotation at the groundline.

The rotation S is:

$S_{607kN} = (1000)*1{,}7*1402*2{,}75^2/4741700+(1000)*1{,}75*1261{,}8*2{,}75/4741700 = 5{,}08$ mm/m

$y_{S,1402kN} = 4{,}08*0{,}9 = 4{,}57mm$

Calculate the pile head deflection due to bending of the pile above the ground line.

$y_{B,1402kN} = 1402*0{,}9^3/(3*11698000) = 29*10^{-6}$ m.

Calculate the pile head deflection at load 1402kN

y_h = 18,69+4,57+0,03=23,3mm

Note: in this NDM-calculation reduced pile stiffness was used. This is used because in a concrete pile the concrete strength reduces as moments in the pile increase. However, the moments in the part of the pile above the groundline where sufficiently low that it was allowed to use the full bending stiffness of the pile in the calculation of the bending of the pile above the groundline. The same reduced bending stiffness is also used in the following NDM-calculation.

*Calculate the displacements at the ground line for a load of **2383kN.***

Take T_{tried} = 4,17m
Then $Z_{max} = L/T_{tried}$ = 12,5/4,17 = 3,0 m

z [m]	Z	Ay	By	Y_A [mm]	P [kN/m]	E_{py} [kPa]
1,50	0,36	2,16	1,16	87,84	628,57	7156
3,00	0,72	1,56	0,71	62,43	1342,93	21510
4,50	1,08	1,07	0,4	42,14	1678,95	39843
6,00	1,44	0,65	0,13	24,71	1709,51	69184
7,50	1,80	0,31	-0,02	11,14	1464,97	131510
9,00	2,16	0,04	-0,11	0,59	181,31	306000
10,50	2,52	-0,2	-0,2	-8,86	#NUM!	#NUM!

If the stiffness is plotted versus the depth, K_{py} can be calculated.
$K_{py} = 1/(37,4*10^{-6}) = 26738 kN/m^3$ $T_{obtained} = (4741700/26738)^{(1/5)} = 2,82m$ $T_{obtained} < T_{tried}$
Take T_{tried} = 2,5 m Then $Z_{max} = L/T_{tried}$ = 12,5/2,5 = 5m

z [m]	Z	Ay	By	Y_A [mm]	P [kN/m]	E_{py} [kPa]
1,50	0,60	1,51	0,71	13,86	413,69	29838
3,00	1,20	0,56	0,2	4,96	549,32	110687
4,50	1,80	0,29	-0,04	2,16	331,12	153000
6,00	2,40	0,04	-0,09	0,06	12,17	204000
7,50	3,00	-0,04	-0,09	-0,57	#NUM!	#NUM!
9,00	3,60	-0,07	-0,04	-0,66	#NUM!	#NUM!
10,50	4,20	-0,04	0	-0,31	#NUM!	#NUM!

If the stiffness is plotted versus the depth, K_{py} can be calculated.
$K_{py} = 1/(29,3*10^{-6}) = 34130 kN/m^3$ $T_{obtained} = (4741700/34130)^{(1/5)} = 2,68m$ $T_{obtained} > T_{tried}$

Plot the values of T_{tried} versus the values of $T_{obtained}$. This plot is shown graph 6-28. Calculate the value of T, where $T_{tried} = T_{obtained}$. Subsequently calculate y_{50kN}.
0,0838T +2,4704 = T, T = 2,4704/0,9162 = 2,70m
$y_{2383kN} = (1000)*2,5*2383*2,70^3/4741700+(1000)*1,65*2144,7*2,70^2/4741700 = 30,17$ mm

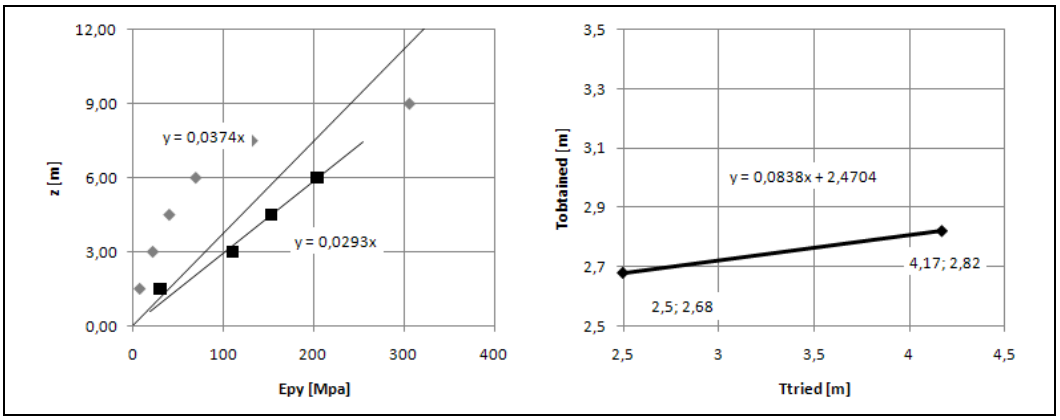

Graph 6-38 Graphs for iterative procedure of NDM, Arkansas, Reese, 2383kN

Calculate the pile-head deflection due to rotation at the groundline.

The rotation S is:

S_{607kN} *= (1000)*1,7*2383*2,70²/4741700+(1000)*1,75*2144,7*2,70/4741700= 8,37mm/m*

$y_{S,607kN}$ *= 8,37*0,9 = 7,53mm*

Calculate the pile head deflection due to bending of the pile above the ground line.

$y_{B,607kN}$ *= 2383*0,9³/(3*4741700) = 0,18mm.*

Calculate the pile head deflection at load 2383kN

y_h = 30,17+7,53+0,18=37,9mm

6.4.2 Calculation of Maximum moments

Calculate the maximum moment for Load = 607kN

First the Nondimensional graphs have to be chosen to find the values of A_m and B_m. This can be found by calculating Z_{max}.

$$Z_{max} = \frac{L}{T} = \frac{12{,}5}{2{,}96} = 4{,}22$$

Choose the graph where Z_{max} = 4. Since the maximum value of A_m can be found at a depth of 1,33T, the maximum moment must be located between 0,0T and 1,33T. Now the moments between these points are determined.

$$M = A_m P_t T + B_m M_t$$

Take T = 2,96m, P_t = 607kN and M_t = 546kNm

Depth Coefficient, z	Am	Bm	M [kNm]
0,0	0	1	546
0,3	0,36	0,98	1182
0,6	0,55	0,95	1507
0,9	0,71	0,87	1750
1,1	0,75	0,83	1800
1,33	0,78	0,74	1805

$$M_{max,607kN} = 1805kNm$$

Calculate the maximum moment for Load = 2383kN

First the Nondimensional graphs have to be chosen to find the values of A_m and B_m. This can be found by calculating Z_{max}.

$$Z_{max} = \frac{L}{T} = \frac{12{,}5}{2{,}70} = 4{,}63$$

Choose the graph where Z_{max} = 5. Since the maximum value of A_m can be found at a depth of 1,33T, the maximum moment must be located between 0,0T and 1,33T. Now the moments between these points are determined.

$$M = A_m P_t T + B_m M_t$$

Take T = 2,70m, P_t = 2383kN and M_t = 2145 kNm

Depth Coefficient, z	Am	Bm	M [kNm]
0	0	1	2145
0,3	0,36	0,98	4418
0,6	0,55	0,93	5533
0,9	0,71	0,85	6391
1,1	0,74	0,8	6477
1,33	0,77	0,71	6477

$M_{max,2383kN} = 6477kNm$

6.4.3 Results

The lateral deflection and maximum moment are calculated reasonably well for the lower loads of 607 and 1402kN. For the maximum applied load of 2483kN the lateral deflection and maximum moment are underestimated. It must be noted that the bending stiffness of the pile in this case is more uncertain than in the other cases since a reinforced concrete pile has been used. With such a pile the bending stiffness reduces as the moments in the pile become larger.

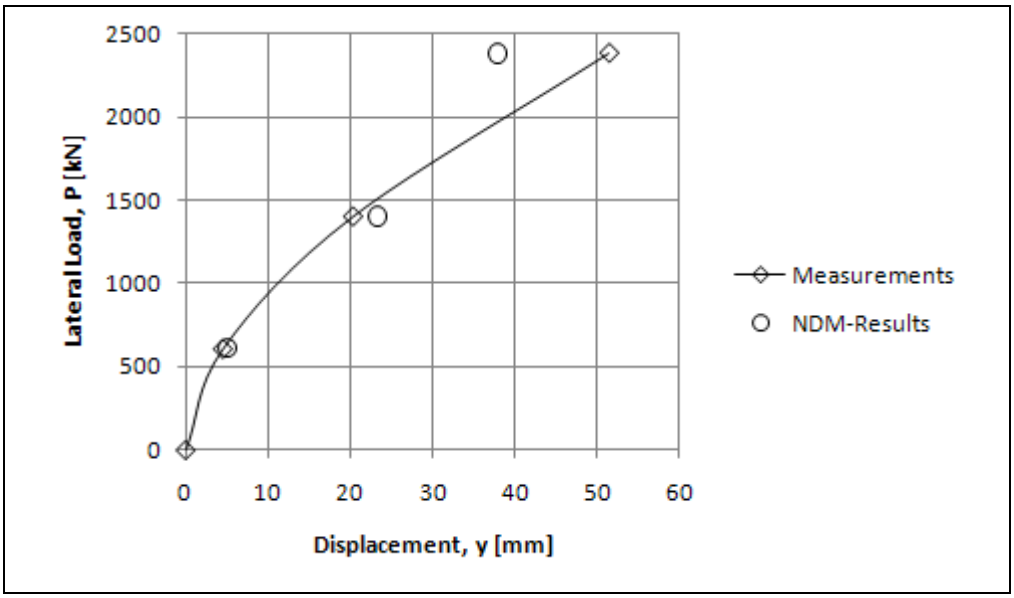

Graph 6-39 Load vs. displacement, Garston

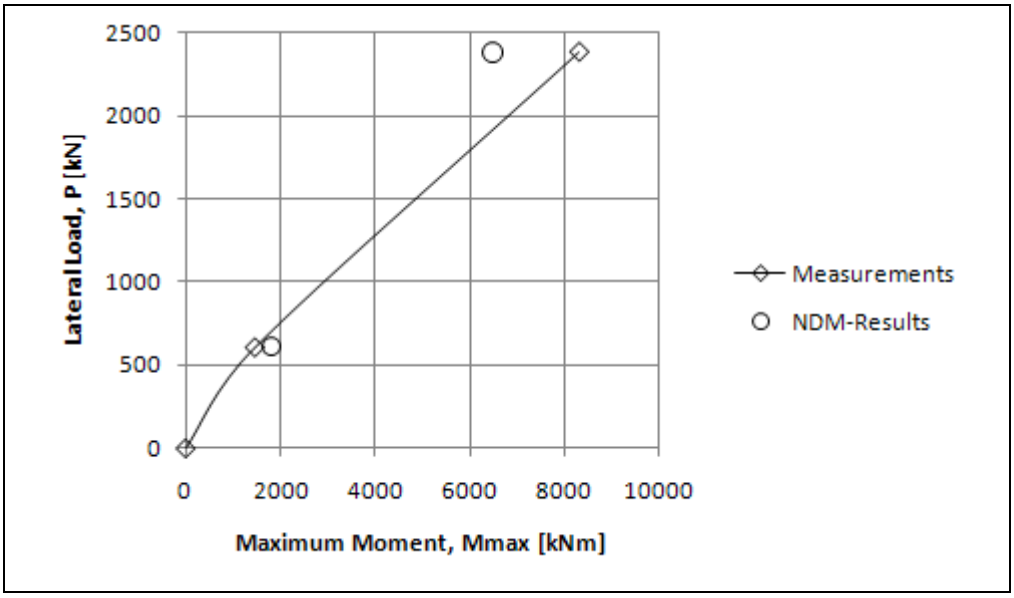

Graph 6-40 Load vs. Maximum Moment, Garston

6.5 CASE X-CL, ARKANSAS RIVER

In the case of Arkansas River the P-Y method has been applied with both the recommendations made by the API and by Reese *et al.*

6.5.1 Calculations, P-Y API

Determine the p-y Curves.

Because the NDM method can only deal with a homogeneous soil, the soil parameters are averaged over the first eight pile diameters. This is the same approach as for the CLM.

γ' = (1,5*20 + (8*0,48-1,5)*10,2)/(8*0,48) = 14,03 kN/m^3
φ' = (1,0*45 + (8*0,48-1,0)*42)/(8*0,48) = 42,8 *degree*

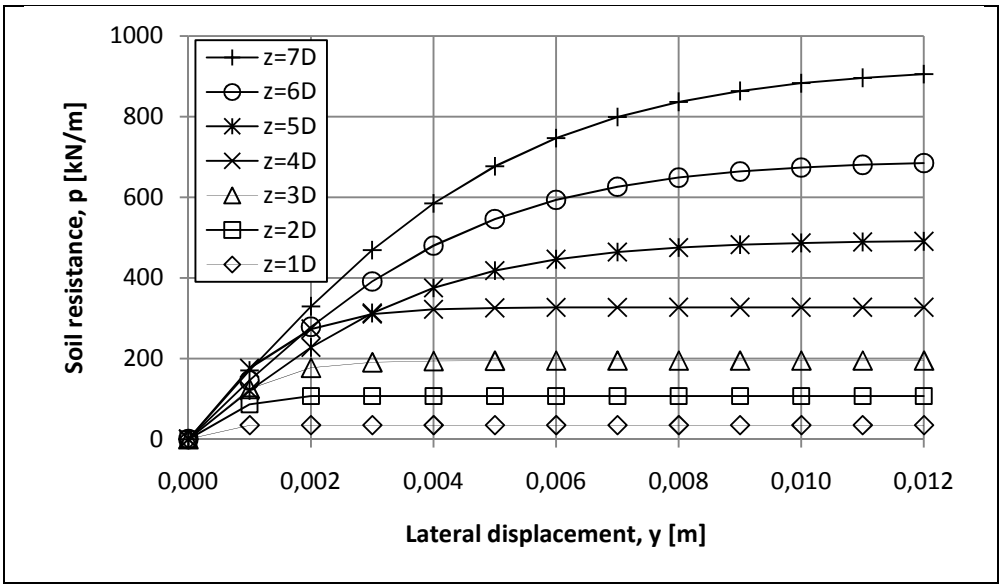

Table 6-4 P-Y curves Arkansas River according to API.

Calculate the displacements at the ground line for a load of 46kN.

Take $T_{tried} = 1,0m$

Then $Z_{max} = L/T_{tried} = 15/1,0 = 15\ m$

z [m]	Z	Ay	Y_A [mm]	P [kN/m]	E_{py} [kPa]
0,48	0,48	1,65	1,18	34,59	29305
0,96	0,96	1	0,72	65,59	91700
1,44	1,44	0,5	0,36	51,53	144071
1,92	1,92	0,25	0,18	35,05	196025
2,40	2,40	0,05	0,04	4,40	122985
2,88	2,88	-0,1	-0,07	-10,56	147574
3,36	3,36	-0,2	-0,14	-24,63	172143

If the stiffness is plotted versus the depth, K_{py} can be calculated. The points where z => 2,4 m are not taken into account, since the calculated stiffness reduces from that point.

$K_{py} = 1/(9,79*10^{-6}) = 102096\ kN/m^3$ $T_{obtained} = (69900/102096)^{(1/5)} = 0,93$ $T_{obtained} < T_{tried}$

Take $T_{tried} = 0,75m$ *Then* $Z_{max} = L/T_{tried} = 15/0,75 = 20\ m$

z [m]	Z	Ay	Y_A [mm]	P [kN/m]	E_{py} [kPa]
0,48	0,64	1,45	0,44	20,97	47924
0,96	1,28	0,6	0,18	17,73	97926
1,44	1,92	0,25	0,08	11,12	147425
1,92	2,56	0	0,00	0,00	-
2,40	3,20	-0,1	-0,03	-3,71	122986
2,88	3,84	-0,1	-0,03	-4,45	147584
3,36	4,48	0	0,00	0,00	-

If the stiffness is plotted versus the depth, K_{py} can be calculated. The points where z => 1,92 m are not taken into account, since the calculated stiffness reduces from that point.

$K_{py} = 1/(9,77*10^{-6}) = 102378\ kN/m^3$

$T_{obtained} = (69900/102378)^{(1/5)} = 0,93$ $T_{obtained} > T_{tried}$

Plot the values of T_{tried} versus the values of $T_{obtained}$. This plot is shown in graph 6-29. Calculate the value of T, where $T_{tried} = T_{obtained}$. In this case it can directly been seen that T = 0,93m. The deflection of the pile at the ground line, at a load of 46kN is: $y_{46kN} = (1000)*2,4*46*0,93^3/69900 = 1,3mm$

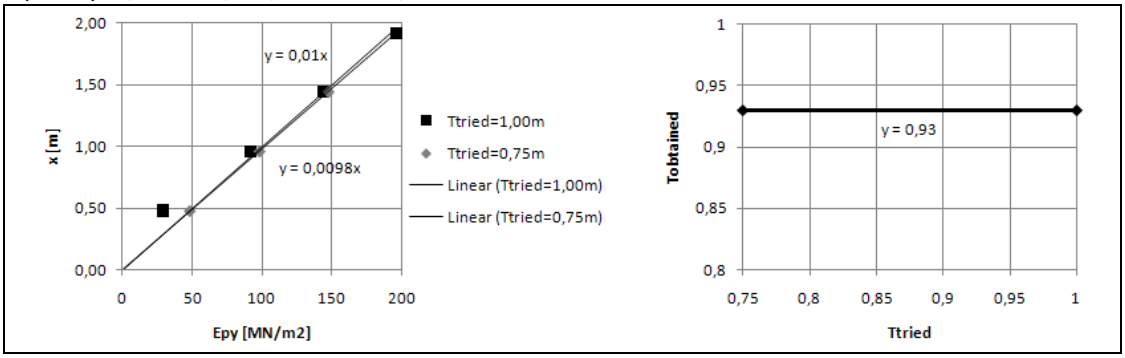

Graph 6-41Graphs for iterative procedure of NDM. The first depicts the stiffness versus depth. The second depicts the graph with which the final value of T can be calculated, Arkansas, API, 46kN.

Calculate the displacements at the ground line for a load of 92kN.

Take $T_{tried} = 1{,}0m$

Then $Z_{max} = L/T_{tried} = 15/1{,}0 = 15\ m$

z [m]	Z	Ay	Y_A [mm]	P [kN/m]	E_{py} [kPa]
0,48	0,48	1,65	2,36	34,59	14653
0,96	0,96	1	1,43	106,67	74564
1,44	1,44	0,5	0,72	96,30	134634
1,92	1,92	0,25	0,36	69,31	193798
2,40	2,40	0,05	0,07	8,80	122975
2,88	2,88	-0,1	-0,14	-21,11	147540
3,36	3,36	-0,2	-0,29	-49,22	172021

If the stiffness is plotted versus the depth, K_{py} can be calculated. The points where z => 2,4 m are not taken into account, since the calculated stiffness reduces from that point.

$K_{py} = 1/(11{,}4*10^{-6}) = 87719\ kN/m^3$ $T_{obtained} = (69900/87719)^{(1/5)} = 0{,}96$ $T_{obtained} < T_{tried}$

Take $T_{tried} = 0{,}75m$ *Then* $Z_{max} = L/T_{tried} = 15/0{,}75 = 20\ m$

z [m]	Z	Ay	Y_A [mm]	P [kN/m]	E_{py} [kPa]
0,48	0,64	1,45	0,44	20,97	47924
0,96	1,28	0,6	0,18	17,73	97926
1,44	1,92	0,25	0,08	11,12	147425
1,92	2,56	0	0,00	0,00	-
2,40	3,20	-0,1	-0,03	-3,71	122986
2,88	3,84	-0,1	-0,03	-4,45	147584
3,36	4,48	0	0,00	0,00	-

If the stiffness is plotted versus the depth, K_{py} can be calculated. The points where z => 1,92 m are not taken into account, since the calculated stiffness reduces from that point.

$K_{py} = 1/(10{,}2*10^{-6}) = 98039\ kN/m^3$

$T_{obtained} = (69900/98039)^{(1/5)} = 0{,}93$ $T_{obtained} > T_{tried}$

Plot the values of T_{tried} versus the values of $T_{obtained}$. This plot is shown in graph 6-30. Calculate the value of T, where $T_{tried} = T_{obtained}$.

$0{,}12T + 0{,}84 = T,\ T = 0{,}84/0{,}88 = 0{,}95m$

The deflection of the pile at the ground line, at a load of 92kN is:

$y_{92kN} = (1000)*2{,}4*92*0{,}95^3/69900 = 2{,}7\ mm$

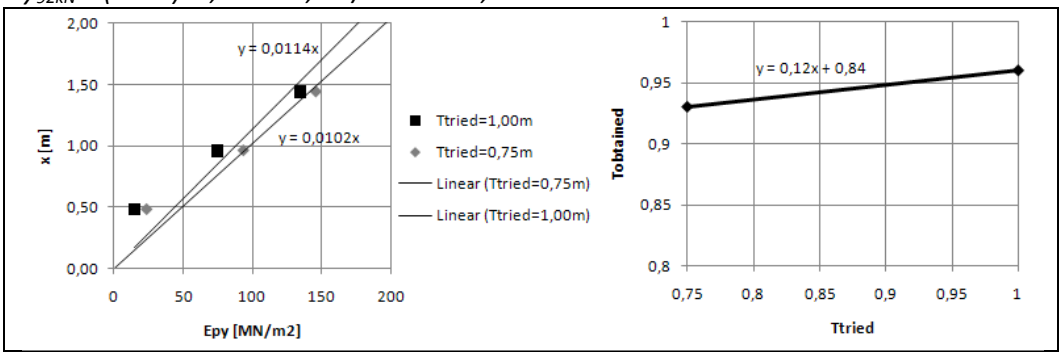

Graph 6-42 Graphs for iterative procedure of NDM, Arkansas, API, 92kN.

Calculate the displacements at the ground line for a load of 140kN.

Take $T_{tried} = 1,0m$

Then $Z_{max} = L/T_{tried} = 15/1,0 = 15\ m$

z [m]	Z	Ay	Y_A [mm]	P [kN/m]	E_{py} [kPa]
0,48	0,48	1,65	3,54	34,59	9768
0,96	0,96	1	2,15	106,67	49710
1,44	1,44	0,5	1,07	130,71	121821
1,92	1,92	0,25	0,54	102,05	190218
2,40	2,40	0,05	0,11	13,19	122959
2,88	2,88	-0,1	-0,21	-31,65	147483
3,36	3,36	-0,2	-0,43	-73,74	171819

If the stiffness is plotted versus the depth, K_{py} can be calculated. The points where z => 2,4 m are not taken into account, since the calculated stiffness reduces from that point.

$K_{py} = 1/(13,1*10^{-6}) = 76336\ kN/m^3$ $T_{obtained} = (69900/76336)^{(1/5)} = 0,98$ $T_{obtained} < T_{tried}$

Take $T_{tried} = 0,75m$ *Then* $Z_{max} = L/T_{tried} = 15/0,75 = 20\ m$

z [m]	Z	Ay	Y_A [mm]	P [kN/m]	E_{py} [kPa]
0,48	0,64	1,45	0,44	20,97	47924
0,96	1,28	0,6	0,18	17,73	97926
1,44	1,92	0,25	0,08	11,12	147425
1,92	2,56	0	0,00	0,00	-
2,40	3,20	-0,1	-0,03	-3,71	122986
2,88	3,84	-0,1	-0,03	-4,45	147584
3,36	4,48	0	0,00	0,00	-

If the stiffness is plotted versus the depth, K_{py} can be calculated. The points where z => 1,92 m are not taken into account, since the calculated stiffness reduces from that point.

$K_{py} = 1/(10,1*10^{-6}) = 99010\ kN/m^3$

$T_{obtained} = (69900/99010)^{(1/5)} = 0,93$ $T_{obtained} < T_{tried}$

Plot the values of T_{tried} versus the values of $T_{obtained}$. This plot is shown in the right graph in graph 6-31. Calculate the value of T, where $T_{tried} = T_{obtained}$.

$0,2T + 0,78 = T,\ T = 0,78/0,80 = 0,98m$

The deflection of the pile at the ground line, at a load of 140kN is:

$y_{140kN} = (1000)*2,4*140*0,98^3/69900 = 4,6\ mm$

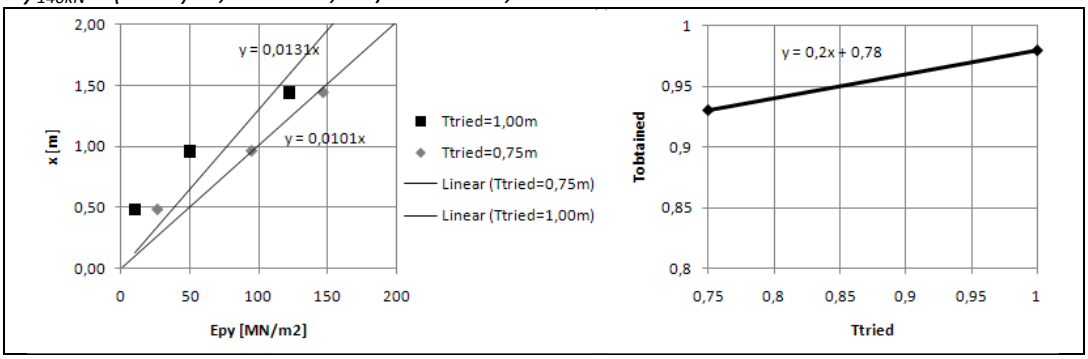

Graph 6-43 Graphs for iterative procedure of NDM, Arkansas, API, 140kN.

Calculate the displacements at the ground line for a load of 248kN.

Take $T_{tried} = 1,0m$

Then $Z_{max} = L/T_{tried} = 15/1,0 = 15\ m$

z [m]	Z	Ay	Y_A [mm]	P [kN/m]	E_{py} [kPa]
0,48	0,48	1,65	3,54	34,59	9768
0,96	0,96	1	2,15	106,67	49710
1,44	1,44	0,5	1,07	130,71	121821
1,92	1,92	0,25	0,54	102,05	190218
2,40	2,40	0,05	0,11	13,19	122959
2,88	2,88	-0,1	-0,21	-31,65	147483
3,36	3,36	-0,2	-0,43	-73,74	171819

If the stiffness is plotted versus the depth, K_{py} can be calculated.

$K_{py} = 1/(14,5*10^{-6}) = 58966kN/m^3$ $T_{obtained} = (69900/69866)^{(1/5)} = 1,00$ $T_{obtained} = T_{tried}$

No iteration is needed here, since T was guessed correctly immediately. The deflection of the pile at the ground line, at a load of 248kN is:

$y_{248kN} = (1000)*2,4*248*1,0^3/69900 = 8,6\ mm$

6.5.2 Calculation, P-Y Reese et al.

Determination of the p-y curves with the method presented by L.C. Reese *et al.* is more time consuming than with the method recommended by the API. The difference is that the Reese p-y curves consist of four parts versus two parts of an API p-y curve.
A detailed derivation for the p-y curves for sands is given in appendix A, chapter 2. The results are given in figure 6-2. The input to obtain the graphs was the same as the input for obtaining API p-y curves.

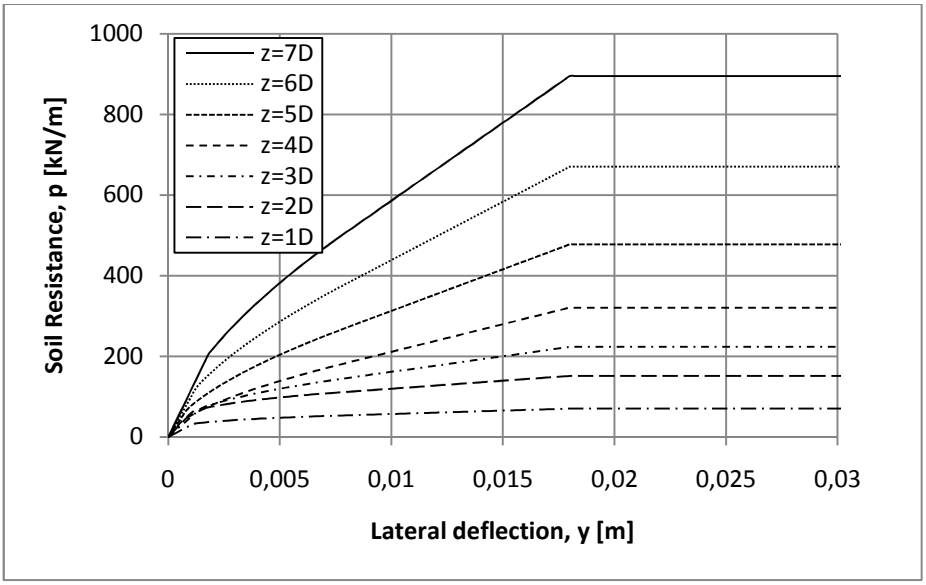

Figure 6-2 p-y curves Arkansas River according to L.C. Reese

Calculate the displacements at the ground line for a load of 46kN.

Take $T_{tried} = 1,0m$

Then $Z_{max} = L/T_{tried} = 15/1,0 = 15$ *m*

z [m]	Z	Ay	Y_A [mm]	P [kN/m]	E_{py} [kPa]
0,48	0,48	1,65	1,18	33,21	28140
0,96	0,96	1	0,72	41,89	58560
1,44	1,44	0,5	0,36	17,51	48960
1,92	1,92	0,25	0,18	11,67	65280
2,40	2,40	0,05	0,04	2,92	81600
2,88	2,88	-0,1	-0,07	-	-
3,36	3,36	-0,2	-0,14	-	-

If the stiffness is plotted versus the depth, K_{py} can be calculated.

$K_{py} = 1/(26,3*10^{-6}) = 38023\ kN/m^3$ $T_{obtained} = (69900/38023)^{(1/5)} = 1,13\ m$ $T_{obtained} > T_{tried}$

Take $T_{tried} = 1,5\ m$ *Then* $Z_{max} = L/T_{tried} = 15/1,5 = 10\ m$

z [m]	Z	Ay	Y_A [mm]	P [kN/m]	E_{py} [kPa]
0,48	0,32	1,95	4,71	46,89	9961
0,96	0,64	1,50	3,62	89,33	24669
1,44	0,96	1,05	2,53	89,81	35428
1,92	1,28	0,70	1,69	72,73	43035
2,40	1,60	0,40	0,97	75,00	77667
2,88	1,92	0,15	0,36	35,46	97920
3,36	2,24	0,05	0,12	13,79	114240

If the stiffness is plotted versus the depth, K_{py} can be calculated.

$K_{py} = 1/(31,2*10^{-6}) = 32051\ kN/m^3$

$T_{obtained} = (69900/32051)^{(1/5)} = 1,17\ m$ $T_{obtained} < T_{tried}$

Plot the values of T_{tried} versus the values of $T_{obtained}$. This plot is shown graph 6-32. Calculate the value of T, where $T_{tried} = T_{obtained}$. Subsequently calculate y_{50kN}.

$0,08T + 1,05 = T,\ T = 1,05/0,92 = 1,14\ m$

$y_{46kN} = (1000)*2,4*46*1,14^3/69900 = 2,34\ mm$

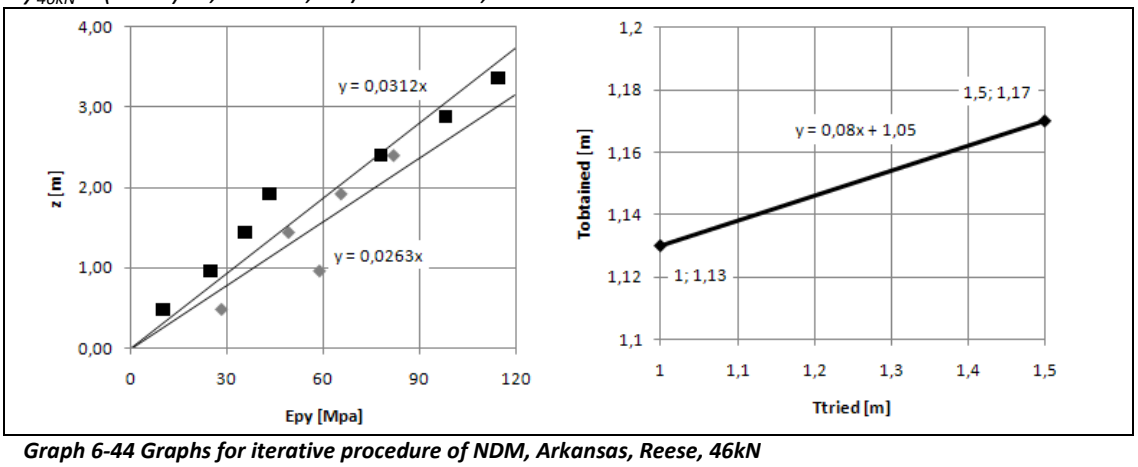

Graph 6-44 Graphs for iterative procedure of NDM, Arkansas, Reese, 46kN

Calculate the displacements at the ground line for a load of 92kN.

Take $T_{tried} = 1{,}0m$

Then $Z_{max} = L/T_{tried} = 15/1{,}0 = 15\ m$

z [m]	Z	Ay	Y_A [mm]	P [kN/m]	E_{py} [kPa]
0,48	0,32	1,65	7,97	56,40	7080
0,96	0,64	1,00	4,83	102,20	21166
1,44	0,96	0,50	2,41	92,80	38439
1,92	1,28	0,25	1,21	62,78	52006
2,40	1,60	0,05	0,24	19,70	81600
2,88	1,92	-0,10	-0,48	-	-
3,36	2,24	-0,20	-0,97	-	-

If the stiffness is plotted versus the depth, K_{py} can be calculated.

$K_{py} = 1/(33{,}1*10^{-6}) = 30211\ kN/m^3$ $T_{obtained} = (69900/30211)^{(1/5)} = 1{,}18\ m$ $T_{obtained} > T_{tried}$

Take $T_{tried} = 1{,}5\ m$ *Then* $Z_{max} = L/T_{tried} = 15/1{,}5 = 10\ m$

z [m]	Z	Ay	Y_A [mm]	P [kN/m]	E_{py} [kPa]
0,48	0,32	1,95	4,71	49,47	10508
0,96	0,64	1,50	3,62	94,24	26023
1,44	0,96	1,05	2,53	94,74	37373
1,92	1,28	0,70	1,69	76,72	45397
2,40	1,60	0,40	0,97	78,80	81600
2,88	1,92	0,15	0,36	35,46	97920
3,36	2,24	0,05	0,12	13,79	114240

If the stiffness is plotted versus the depth, K_{py} can be calculated.

$K_{py} = 1/(30{,}8*10^{-6}) = 32468\ kN/m^3$ $T_{obtained} = (69900/32468)^{(1/5)} = 1{,}17\ m$ $T_{obtained} < T_{tried}$

Plot the values of T_{tried} versus the values of $T_{obtained}$. This plot is shown graph 6-33. Calculate the value of T, where $T_{tried} = T_{obtained}$. Subsequently calculate y_{100kN}.

-0,02T + 1,2 = T, T = 1,2/1,02 = 1,18 m

$y_{100kN} = (1000)*2{,}4*92*1{,}18^3/69900 = 5{,}18\ mm$

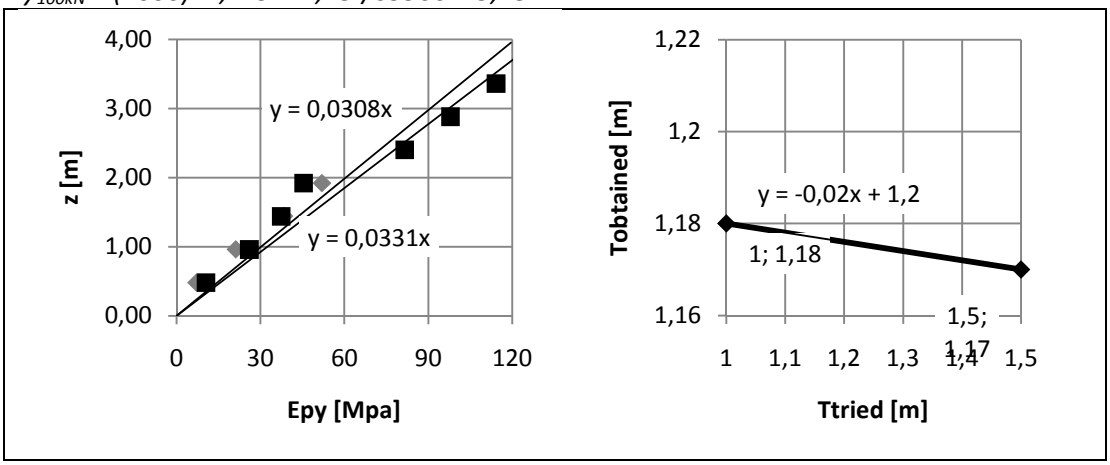

Graph 6-45 Graphs for iterative procedure of NDM, Arkansas, Reese, 92kN

Calculate the displacements at the ground line for a load of 140kN.

Take $T_{tried} = 1,0m$

Then $Z_{max} = L/T_{tried} = 15/1,0 = 15$ *m*

z [m]	Z	Ay	Y_A [mm]	P [kN/m]	E_{py} [kPa]
0,48	0,48	1,65	3,54	46,08	13013
0,96	0,96	1,00	2,15	81,31	37892
1,44	1,44	0,50	1,07	52,53	48960
1,92	1,92	0,25	0,54	35,02	65280
2,40	2,40	0,05	0,11	8,76	81600
2,88	2,88	-0,10	-0,21	-	-
3,36	3,36	-0,20	-0,43	-	-

If the stiffness is plotted versus the depth, K_{py} can be calculated.

$K_{py} = 1/(29,1*10^{-6}) = 34364\ kN/m^3$ $T_{obtained} = (69900/34364)^{(1/5)} = 1,15\ m$ $T_{obtained} > T_{tried}$

Take $T_{tried} = 1,5\ m$ *Then* $Z_{max} = L/T_{tried} = 15/1,5 = 10\ m$

z [m]	Z	Ay	Y_A [mm]	P [kN/m]	E_{py} [kPa]
0,48	0,32	1,95	14,12	67,23	4761
0,96	0,64	1,5	10,86	129,72	11941
1,44	0,96	1,05	7,60	150,86	19839
1,92	1,28	0,7	5,07	147,67	29128
2,40	1,60	0,4	2,90	154,30	53261
2,88	1,92	0,15	1,09	106,38	97920
3,36	2,24	0,05	0,36	41,37	114240

If the stiffness is plotted versus the depth, K_{py} can be calculated.

$K_{py} = 1/(33,2*10^{-6}) = 30120\ kN/m^3$ $T_{obtained} = (69900/30120)^{(1/5)} = 1,18\ m$ $T_{obtained} < T_{tried}$

Plot the values of T_{tried} versus the values of $T_{obtained}$. This plot is shown in graph 6-34. Calculate the value of T, where $T_{tried} = T_{obtained}$. Subsequently calculate y_{150kN}.

0,06T + 1,09 = T, T = 1,09/0,94 = 1,16 m

$y_{140kN} = (1000)*2,4*140*1,16^3/69900 = 7,50\ mm$

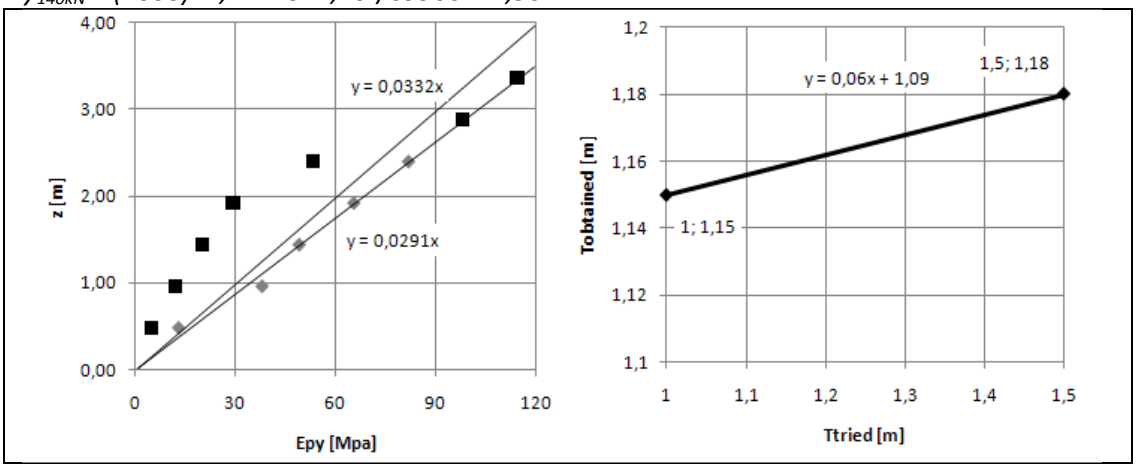

Graph 6-46Graphs for iterative procedure of NDM, Arkansas, Reese, 140kN

Calculate the displacements at the ground line for a load of 248kN.

Take $T_{tried} = 1{,}0m$

Then $Z_{max} = L/T_{tried} = 15/1{,}0 = 15\ m$

z [m]	Z	Ay	Y_A [mm]	P [kN/m]	E_{py} [kPa]
0,48	0,48	1,65	5,90	49,61	8407
0,96	0,96	1	3,58	89,02	24890
1,44	1,44	0,5	1,79	77,47	43321
1,92	1,92	0,25	0,89	49,76	55654
2,40	2,40	0,05	0,18	14,59	81600
2,88	2,88	-0,1	-0,36	-	-
3,36	3,36	-0,2	-0,72	-	-

If the stiffness is plotted versus the depth, K_{py} can be calculated.

$K_{py} = 1/(31{,}9*10^{-6}) = 31348\ kN/m^3$ $T_{obtained} = (69900/31348)^{(1/5)} = 1{,}17\ m$ $T_{obtained} > T_{tried}$

Take $T_{tried} = 1{,}5\ m$ *Then* $Z_{max} = L/T_{tried} = 15/1{,}5 = 10\ m$

z [m]	Z	Ay	Y_A [mm]	P [kN/m]	E_{py} [kPa]
0,48	0,32	1,95	23,54	70,20	2983
0,96	0,64	1,50	18,11	151,06	8343
1,44	0,96	1,05	12,67	182,28	14382
1,92	1,28	0,70	8,45	189,88	22472
2,40	1,60	0,40	4,83	199,54	41327
2,88	1,92	0,15	1,81	154,31	85223
3,36	2,24	0,05	0,60	68,95	114240

If the stiffness is plotted versus the depth, K_{py} can be calculated.

$K_{py} = 1/(35{,}1*10^{-6}) = 28490\ kN/m^3$ $T_{obtained} = (69900/28490)^{(1/5)} = 1{,}20\ m$ $T_{obtained} < T_{tried}$

Plot the values of T_{tried} versus the values of $T_{obtained}$. This plot is shown in graph 6-35. Calculate the value of T, where $T_{tried} = T_{obtained}$. Subsequently calculate y_{50kN}.

$0{,}06T + 1{,}11 = T,\ T = 1{,}11/0{,}94 = 1{,}18\ m$

$y_{248kN} = (1000)*2{,}4*248*1{,}18^3/69900 = 14{,}0\ mm$

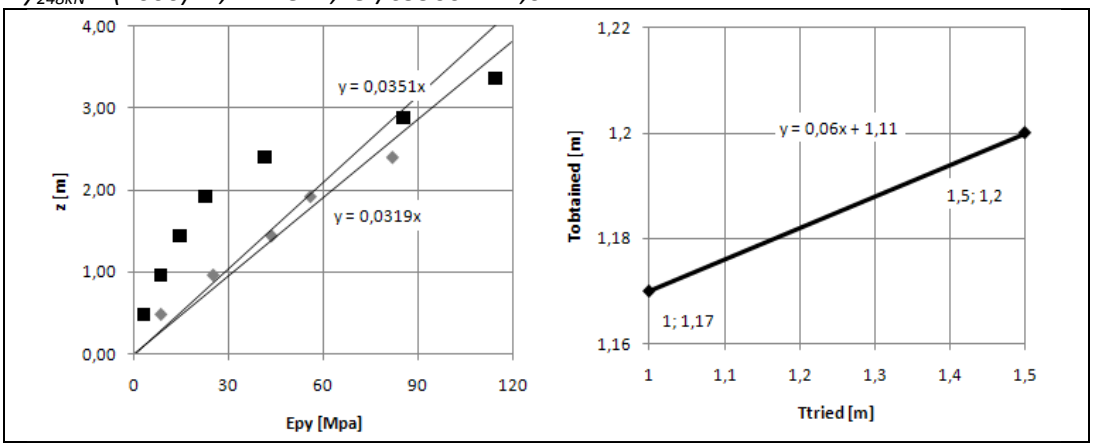

Graph 6-47 Graphs for iterative procedure of NDM, Arkansas, Reese, 248kN

6.5.3 Results

The results of the NDM calculation show a very good fit with the measurements if the p-y curves are generated according to Reese *et al.* The deflections are underestimated if the p-y curves are used that are established according to the API.

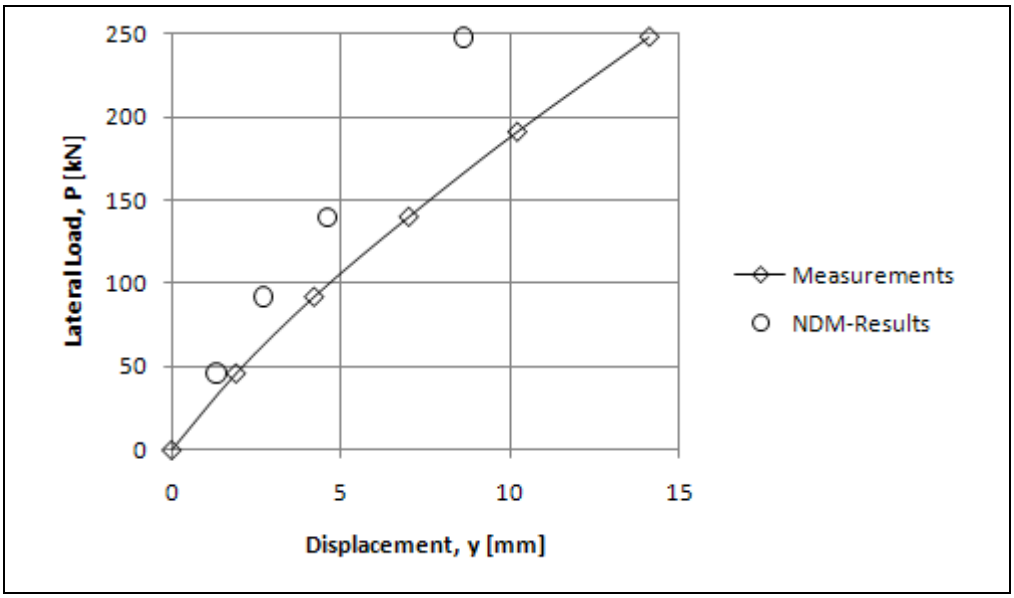

Graph 6-48 Load Displacement API

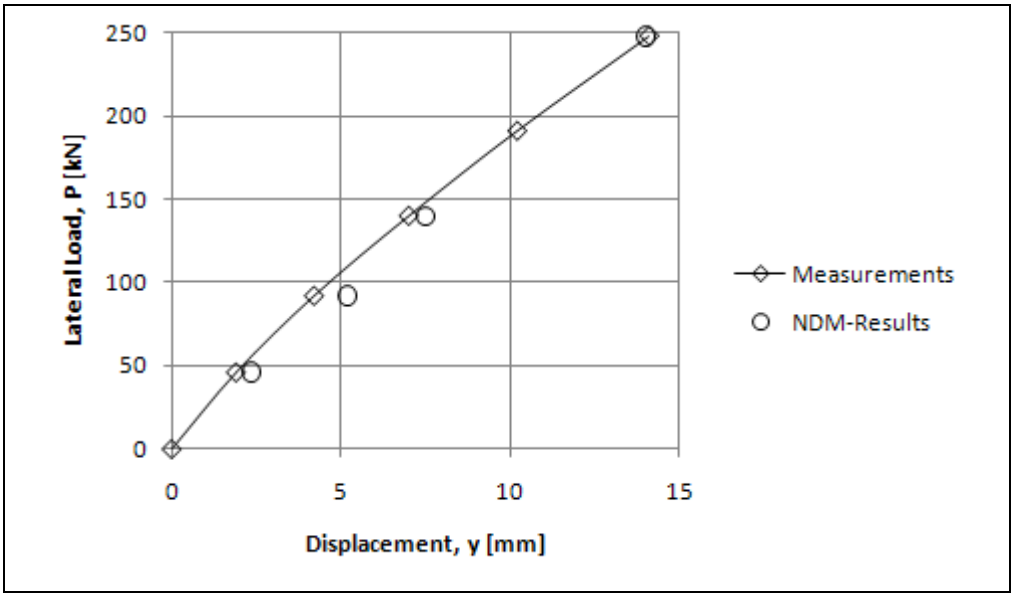

Graph 6-49 Load Displacement, Reese

6.6 CASE XIII-L, FLORIDA

It is not possible to perform a NDM-calculation in this case for two reasons. The soil consists of a clay and a sand layer and the NDM requires a homogeneous soil. (This limitation can be overcome by averaging the soil parameters over a depth of eight pile diameters, but is not preferable in this situation, since the two layers consist of a totally different material.) The second reason is that the pile consists of two sections with both a different stiffness. In the NDM the pile is assumed to have the same stiffness over the entire length of the pile. For this reasons the NDM-calculation cannot be performed.

7 MSHEET – SINGLE PILE MODULE

The single pile module of MSheet is a software program that simulates the soil as a series of bilinear springs along the pile. This calculation cannot be reported in this thesis, since it was automatically executed by a computer. The input and output of the program are given in this chapter for the six cases. First the three field tests that have been executed with clayey soil are given, followed by the three cases in sandy soil.
The software produces a detailed report after the calculation has been finished. In this report comprises both input and output of the calculation. Parts of these reports are left out of this appendix to prevent that information is given more than one time.

7.1 CASE I-CU, BAGNOLET

7.1.1 Input

For all three tests executed at Bagnolet the soil profile is the same. The profile and accompanying data is given below. The soil profile shown is given for Test I. The pile properties and the results are different for each test. They are given separately.

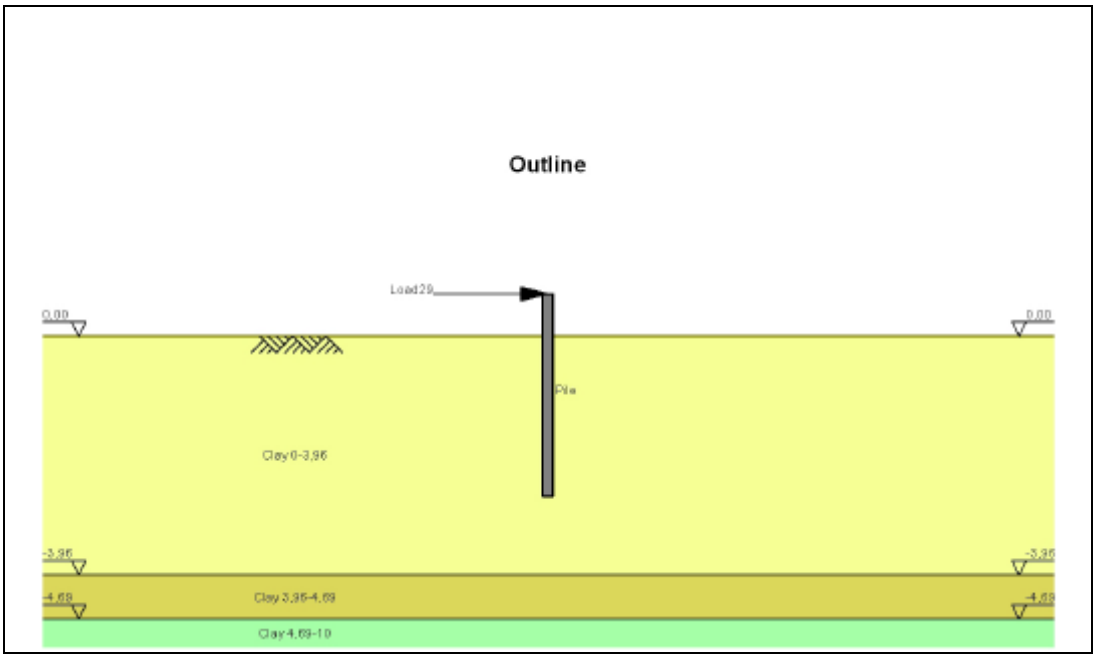

Figure 7-1 Soil Profile, Bagnolet

3.5 Water Level

Water level: -5,00 [m]

3.6 Surface

Surface level: 0,00 [m]

3.7 Soil Material Properties

Layer name	Level [m]	Unit weight		Cohesion [kN/m²]	Friction angle phi [deg]	Brinch Hansen used
		Unsat [kN/m³]	Sat [kN/m³]			
Clay 0-3,96	0,00	17,90	17,90	100,00	0,00	Yes
Clay 3,96-4,69	-3,96	17,90	17,90	125,00	0,00	Yes
Clay 4,69-10	-4,69	17,90	17,90	135,00	0,00	Yes

Layer name	Level [m]	Earth pressure coefficients			Additional pore pressure	
		Active [-]	Neutral [-]	Passive [-]	Top [kN/m²]	Bottom [kN/m²]
Clay 0-3,96	0,00	0,00	0,00	0,01	0,00	0,00
Clay 3,96-4,69	-3,96	0,00	0,00	0,01	0,00	0,00
Clay 4,69-10	-4,69	0,00	0,00	0,01	0,00	0,00

3.8 Soil Material Properties calculated using Brinch Hansen

Layer name	Level [m]	Fictive cohesion [kN/m²]
Clay 0-3,96	0,00	4695,98
Clay 3,96-4,69	-3,96	6414,12
Clay 4,69-10	-4,69	8590,14

3.9 Modulus of Subgrade Reaction

Layer name	Level [m]	Menard used	E-Mod Menard [kN/m²]	Soil type Menard	Branch 1	
					Top [kN/m³]	Bottom [kN/m³]
Clay 0-3,96	0,00	Yes	6000,00	Clay	26000,52	26000,52
Clay 3,96-4,69	-3,96	Yes	7000,00	Clay	30333,94	30333,94
Clay 4,69-10	-4,69	Yes	8000,00	Clay	34667,36	34667,36

Figure 7-2 Soil Parameters Bagnolet

7.1.2 Test I

Here the pile properties and test results for all loads that were applied in test I. Note: During the field test the deformations were measured at the ground line.

3.2 Pile Properties

Length 3,35 m
Level top side 0,70 m
Number of sections 1

Section name	From [m]	To [m]	Stiffness EI [kNm²]	Diameter [m]	Maximum moment [kNm]
Pile	-2,65	0,70	2,5500E+04	0,43	1000,00

Section name	From [m]	To [m]	Red. factor EI [-]	Red. factor max. moment [-]	Note to reduction factor
Pile	-2,65	0,70	1,00	1,00	

Section name	From [m]	To [m]	Corrected stiffness EI [kNm²]	Corrected max. moment [kNm]
Pile	-2,65	0,70	2,5500E+04	1000,00

Figure 7-3 Pile Properties Bagnolet Test I

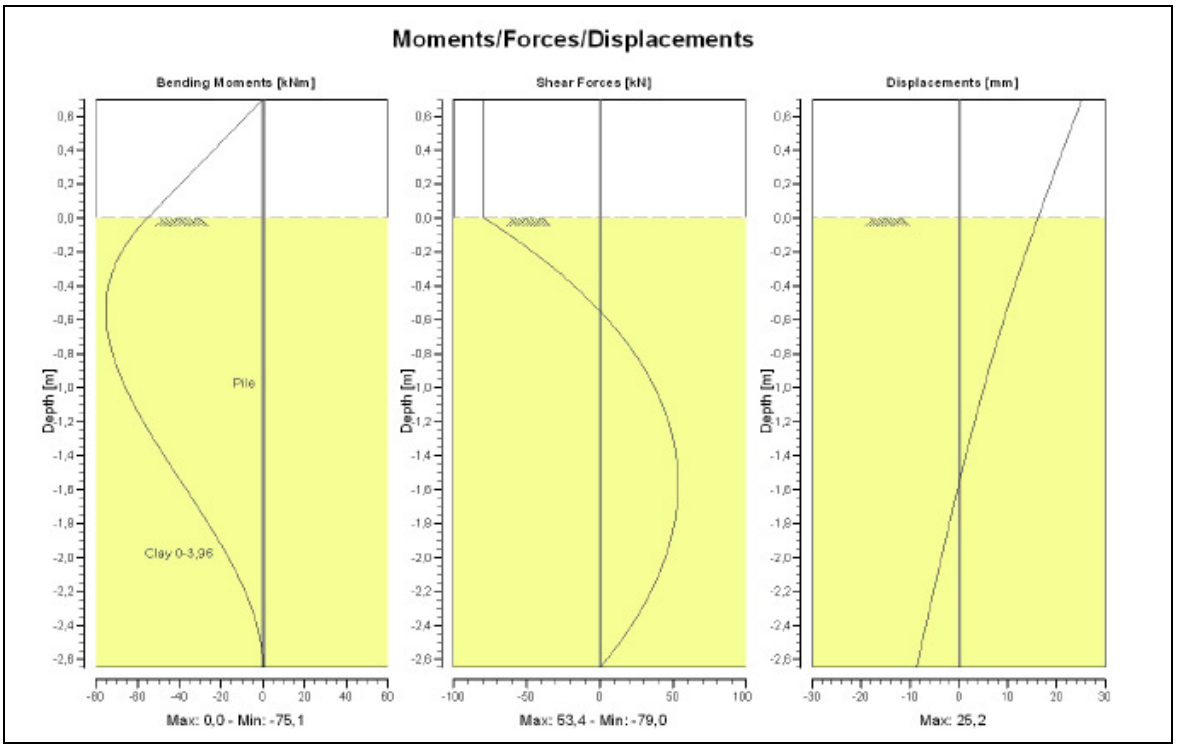

Figure 7-4 Output Bagnolet Test I, Load = 79kN

7.1.3 Test II

3.2 Pile Properties

Length 5,05 m
Level top side 0,90 m
Number of sections 1

Section name	From [m]	To [m]	Stiffness EI [kNm²]	Diameter [m]	Maximum moment [kNm]
Pile	-4,15	0,90	2,5500E+04	0,43	1000,00

Section name	From [m]	To [m]	Red. factor EI [-]	Red. factor max. moment [-]	Note to reduction factor
Pile	-4,15	0,90	1,00	1,00	

Section name	From [m]	To [m]	Corrected stiffness EI [kNm²]	Corrected max. moment [kNm]
Pile	-4,15	0,90	2,5500E+04	1000,00

Figure 7-5 Pile Properties Bagnolet Test II

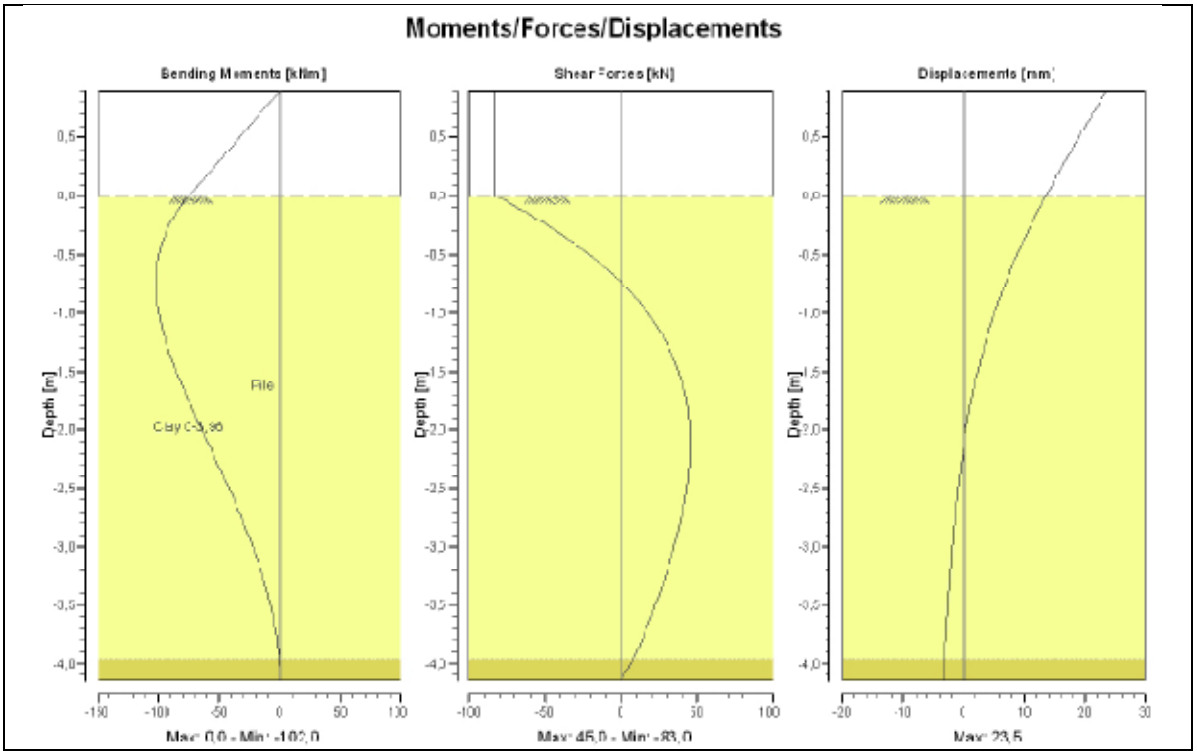

Figure 7-6 Output Bagnolet Test II, Load = 83kN

7.1.4 Test III

3.2 Pile Properties

Length	6,10 m
Level top side	1,00 m
Number of sections	1

Section name	From [m]	To [m]	Stiffness EI [kNm²]	Diameter [m]	Maximum moment [kNm]
Pile	-5,10	1,00	2,5500E+04	0,43	1000,00

Section name	From [m]	To [m]	Red. factor EI [-]	Red. factor max. moment [-]	Note to reduction factor
Pile	-5,10	1,00	1,00	1,00	

Section name	From [m]	To [m]	Corrected stiffness EI [kNm²]	Corrected max. moment [kNm]
Pile	-5,10	1,00	2,5500E+04	1000,00

Figure 7-7 Pile Properties Bagnolet Test III

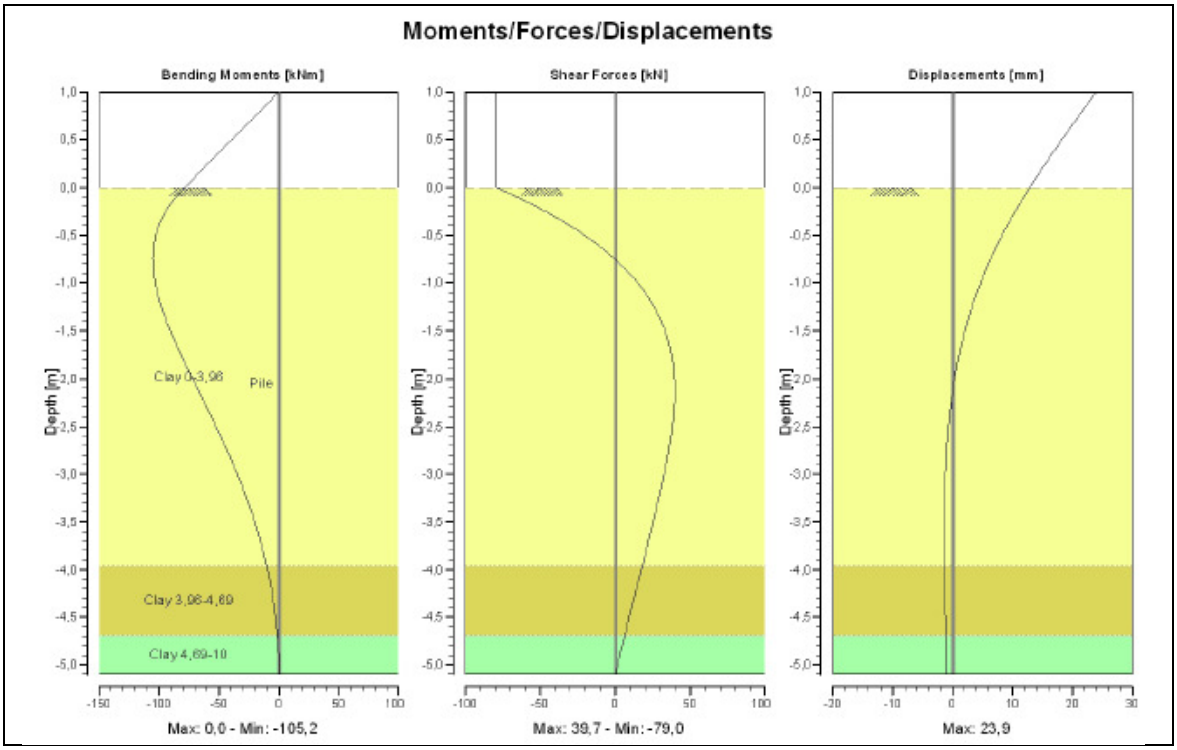

Figure 7-8 Output Bagnolet Test III, Load = 79kN

7.1.5 Results

When the calculated and measured deflections and maximum moments are plotted versus the lateral load, it can be seen that the deflections are overestimated for all three tests. The calculated maximum moments are approximated quite accurately.

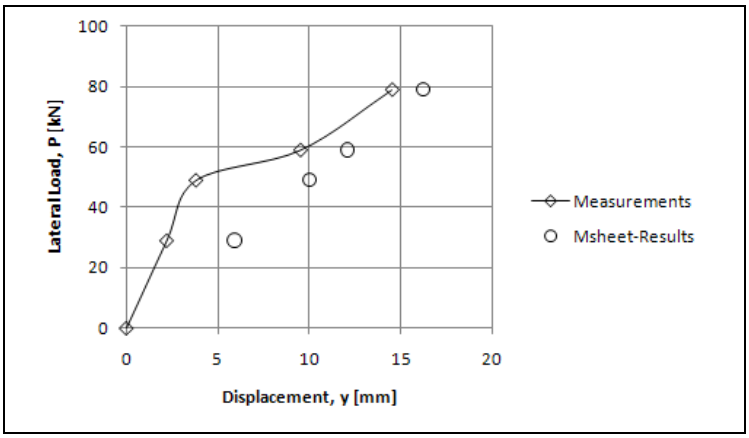

Graph 7-1 Lateral load vs. displacement Test I

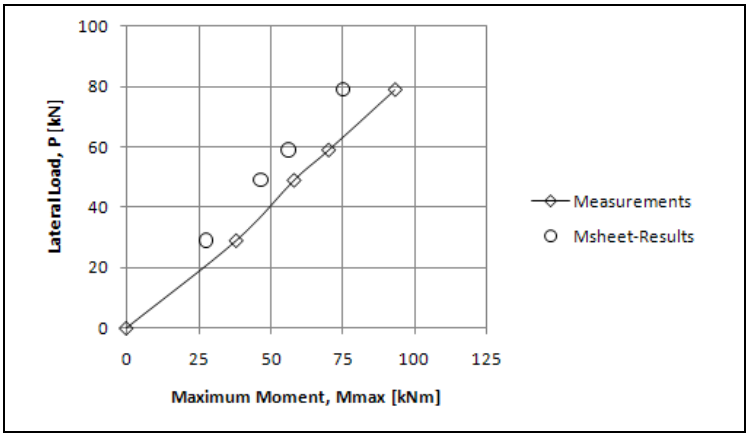

Graph 7-2 Lateral load vs. maximum moment Test I

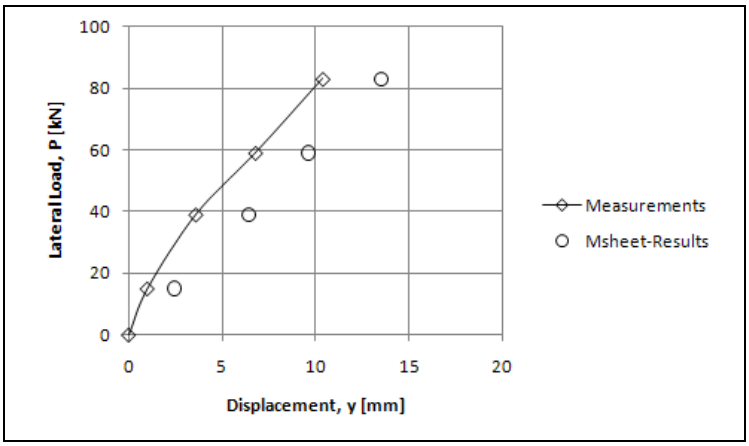

Graph 7-3 Lateral load vs. displacement Test II

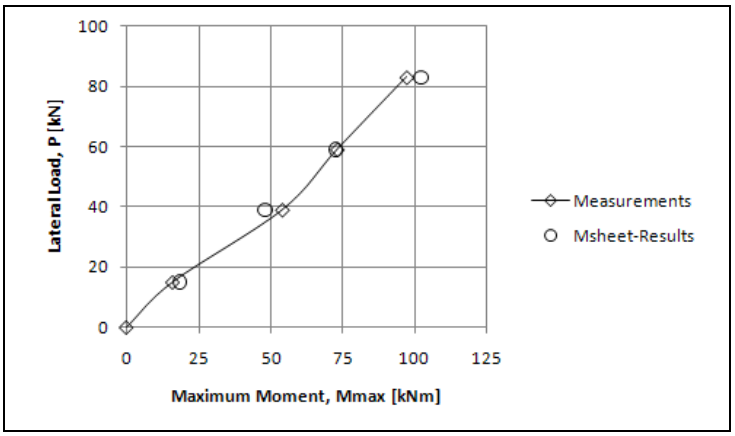

Graph 7-4 Lateral load vs. maximum moment Test II

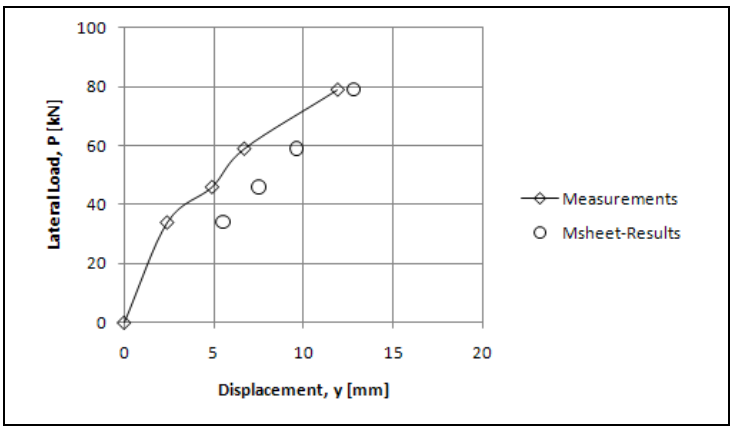

Graph 7-5 Lateral load vs. displacement Test III

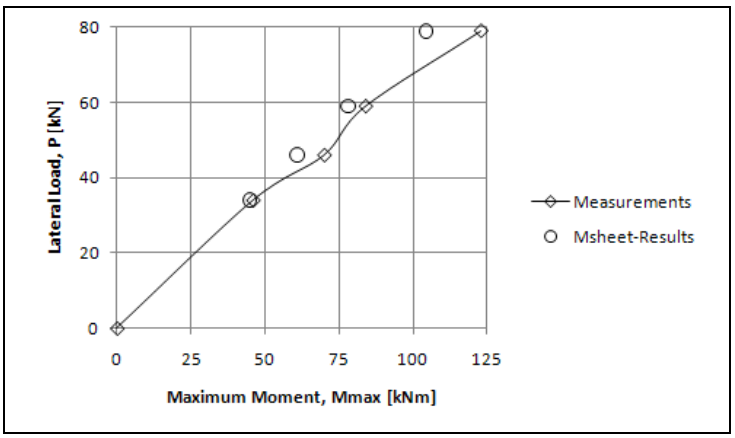

Graph 7-6 Lateral load vs. maximum moment Test III

7.2 CASE III-CU, BRENT CROSS

7.2.1 Input

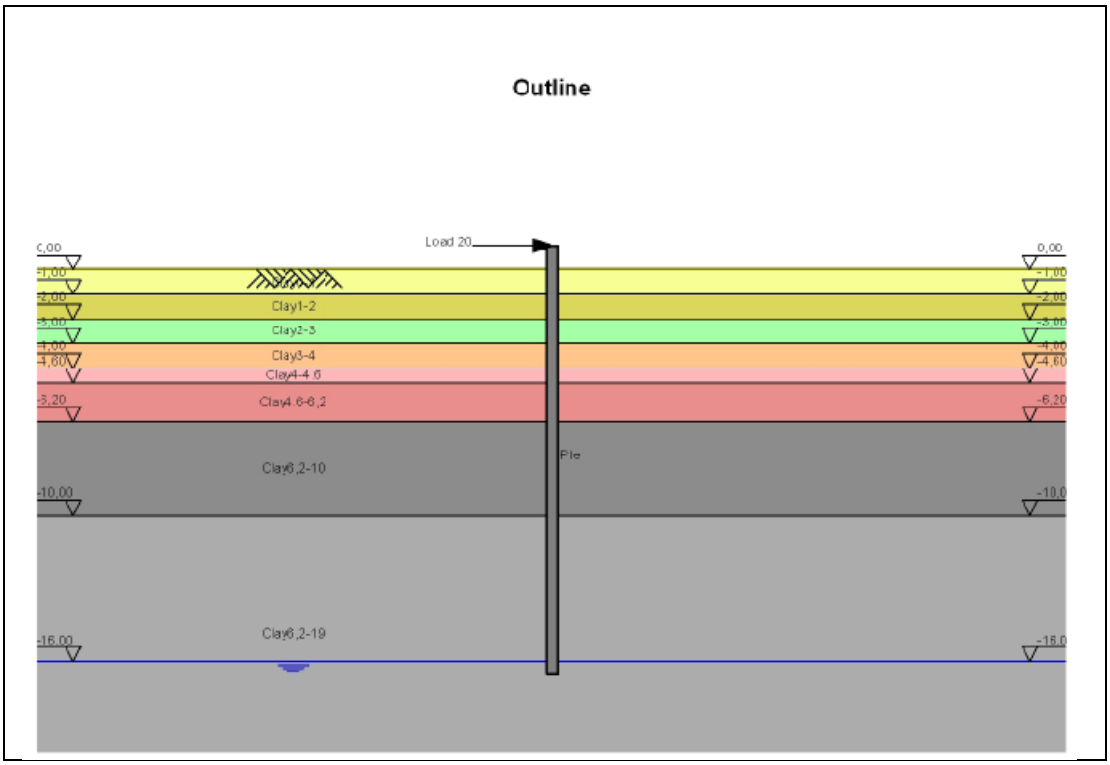

Figure 7-9 Soil Profile Brent Cross

3.5 Water Level

Water level: -16,00 [m]

3.6 Surface

Surface level: 0,00 [m]

3.7 Soil Material Properties

Layer name	Level [m]	Unit weight		Cohesion [kN/m²]	Friction angle phi [deg]	Brinch Hansen used
		Unsat [kN/m³]	Sat [kN/m³]			
Clay0-1	0,00	17,00	19,00	48,60	0,00	Yes
Clay1-2	-1,00	17,00	19,00	57,50	0,00	Yes
Clay2-3	-2,00	17,00	19,00	66,50	0,00	Yes
Clay3-4	-3,00	17,00	19,00	75,40	0,00	Yes
Clay4-4.6	-4,00	17,00	19,00	82,50	0,00	Yes
Clay4.6-6,2	-4,60	17,00	19,00	82,90	0,00	Yes
Clay6,2-10	-6,20	17,00	19,00	88,40	0,00	Yes
Clay6,2-19	-10,00	17,00	19,00	114,80	0,00	Yes

Layer name	Level [m]	Earth pressure coefficients			Additional pore pressure	
		Active [-]	Neutral [-]	Passive [-]	Top [kN/m²]	Bottom [kN/m²]
Clay0-1	0,00	0,00	0,00	0,01	0,00	0,00
Clay1-2	-1,00	0,00	0,00	0,01	0,00	0,00
Clay2-3	-2,00	0,00	0,00	0,01	0,00	0,00
Clay3-4	-3,00	0,00	0,00	0,01	0,00	0,00
Clay4-4.6	-4,00	0,00	0,00	0,01	0,00	0,00
Clay4.6-6,2	-4,60	0,00	0,00	0,01	0,00	0,00
Clay6,2-10	-6,20	0,00	0,00	0,01	0,00	0,00
Clay6,2-19	-10,00	0,00	0,00	0,01	0,00	0,00

3.8 Soil Material Properties calculated using Brinch Hansen

Layer name	Level [m]	Fictive cohesion [kN/m²]
Clay0-1	0,00	1708,57
Clay1-2	-1,00	2600,67
Clay2-3	-2,00	3245,15
Clay3-4	-3,00	3814,85
Clay4-4.6	-4,00	4247,12
Clay4.6-6,2	-4,60	4334,31
Clay6,2-10	-6,20	4711,53
Clay6,2-19	-10,00	6188,78

3.9 Modulus of Subgrade Reaction

Layer name	Level [m]	Menard used	E-Mod Menard [kN/m²]	Soil type Menard	Branch 1	
					Top [kN/m³]	Bottom [kN/m³]
Clay0-1	0,00	Yes	2916,00	Clay	13252,66	13252,66
Clay1-2	-1,00	Yes	3450,00	Clay	15679,58	15679,58
Clay2-3	-2,00	Yes	3990,00	Clay	18133,78	18133,78
Clay3-4	-3,00	Yes	4524,00	Clay	20560,70	20560,70
Clay4-4.6	-4,00	Yes	4950,00	Clay	22496,79	22496,79
Clay4.6-6,2	-4,60	Yes	4974,00	Clay	22605,87	22605,87
Clay6,2-10	-6,20	Yes	5304,00	Clay	24105,65	24105,65
Clay6,2-19	-10,00	Yes	6864,00	Clay	31195,55	31195,55

Figure 7-10 Soil Parameters Brent Cross

3.2 Pile Properties

Length	3,35 m
Level top side	0,70 m
Number of sections	1

Section name	From [m]	To [m]	Stiffness EI [kNm²]	Diameter [m]	Maximum moment [kNm]
Pile	-2,65	0,70	2,5500E+04	0,43	1000,00

Section name	From [m]	To [m]	Red. factor EI [-]	Red. factor max. moment [-]	Note to reduction factor
Pile	-2,65	0,70	1,00	1,00	

Section name	From [m]	To [m]	Corrected stiffness EI [kNm²]	Corrected max. moment [kNm]
Pile	-2,65	0,70	2,5500E+04	1000,00

Figure 7-11 Pile Properties Brent Cross

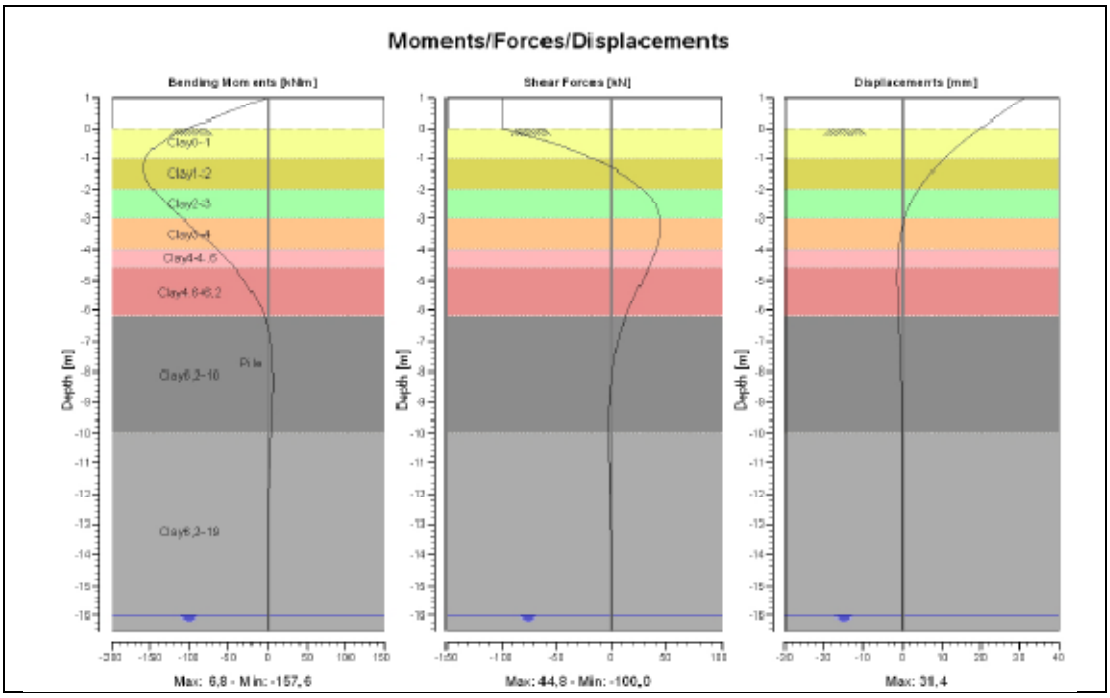

Figure 7-12 Output Brent Cross , Load = 100kN

7.2.2 Results

When the calculated and measured deflections are plotted versus the lateral load, it can be seen that the deflections are overestimated for the three lower loads. The deflection at the load of 100kN was calculated quite accurately. Looking at the shape of the graphs, it is to be expected that for higher loads the displacements will be underestimated.

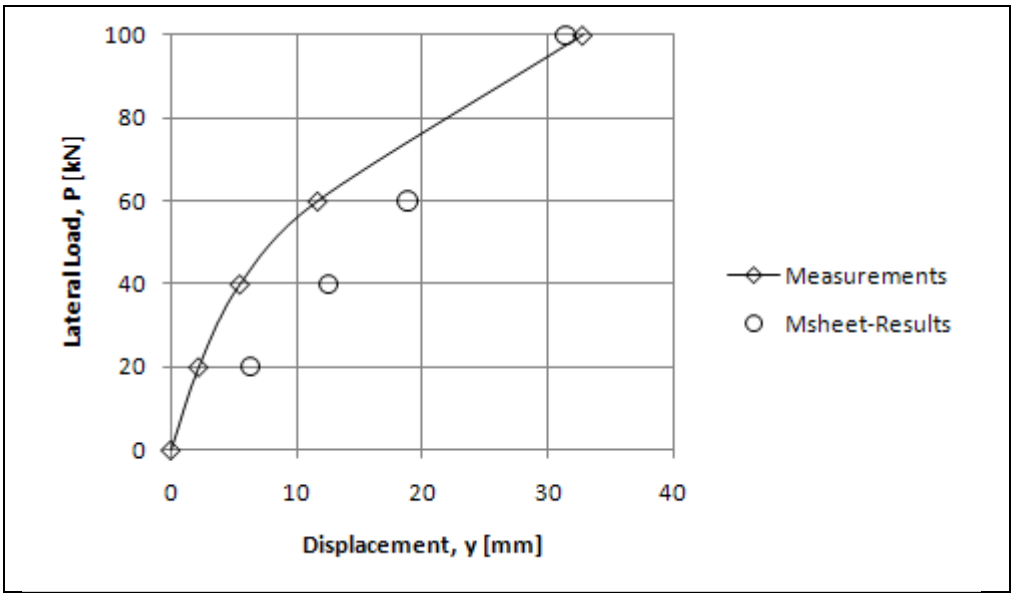

Graph 7-7 Lateral load vs. displacement, Brent Cross

7.3 CASE VI-CS, SABINE

7.3.1 Input

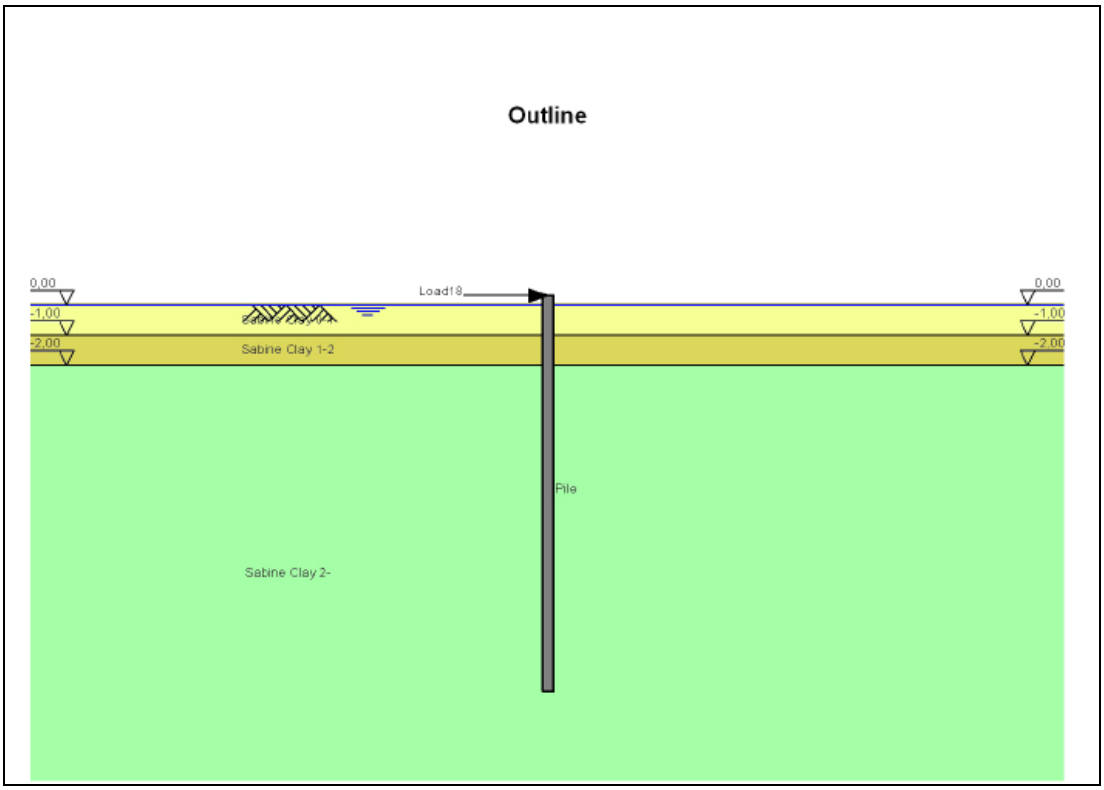

Figure 7-13 Soil Profile Sabine

3.5 Water Level

Water level: 0,00 [m]

3.6 Surface

Surface level: 0,00 [m]

3.7 Soil Material Properties

Layer name	Level [m]	Unit weight		Cohesion [kN/m²]	Friction angle phi [deg]	Brinch Hansen used
		Unsat [kN/m³]	Sat [kN/m³]			
Sabine Clay 0-1	0,00	15,50	15,50	14,40	0,00	Yes
Sabine Clay 1-2	-1,00	15,50	15,50	14,40	0,00	Yes
Sabine Clay 2-	-2,00	15,50	15,50	14,40	0,00	Yes

Layer name	Level [m]	Earth pressure coefficients			Additional pore pressure	
		Active [-]	Neutral [-]	Passive [-]	Top [kN/m²]	Bottom [kN/m²]
Sabine Clay 0-1	0,00	0,00	0,00	0,01	0,00	0,00
Sabine Clay 1-2	-1,00	0,00	0,00	0,01	0,00	0,00
Sabine Clay 2-	-2,00	0,00	0,00	0,01	0,00	0,00

3.8 Soil Material Properties calculated using Brinch Hansen

Layer name	Level [m]	Fictive cohesion [kN/m²]
Sabine Clay 0-1	0,00	540,60
Sabine Clay 1-2	-1,00	678,04
Sabine Clay 2-	-2,00	771,29

3.9 Modulus of Subgrade Reaction

Layer name	Level [m]	Menard used	E-Mod Menard [kN/m²]	Soil type Menard	Branch 1	
					Top [kN/m³]	Bottom [kN/m³]
Sabine Clay 0-1	0,00	Yes	3000,00	Clay	17469,10	17469,10
Sabine Clay 1-2	-1,00	Yes	6000,00	Clay	34938,20	34938,20
Sabine Clay 2-	-2,00	Yes	8000,00	Clay	46584,26	46584,26

Figure 7-14 Soil Parameters Sabine

3.2 Pile Properties

Length	13,11 m
Level top side	0,31 m
Number of sections	1

Section name	From [m]	To [m]	Stiffness EI [kNm²]	Diameter [m]	Maximum moment [kNm]
Pile	-12,80	0,31	3,1280E+04	0,32	1000,00

Section name	From [m]	To [m]	Red. factor EI [-]	Red. factor max. moment [-]	Note to reduction factor
Pile	-12,80	0,31	1,00	1,00	

Section name	From [m]	To [m]	Corrected stiffness EI [kNm²]	Corrected max. moment [kNm]
Pile	-12,80	0,31	3,1280E+04	1000,00

Figure 7-15 Pile Properties Sabine

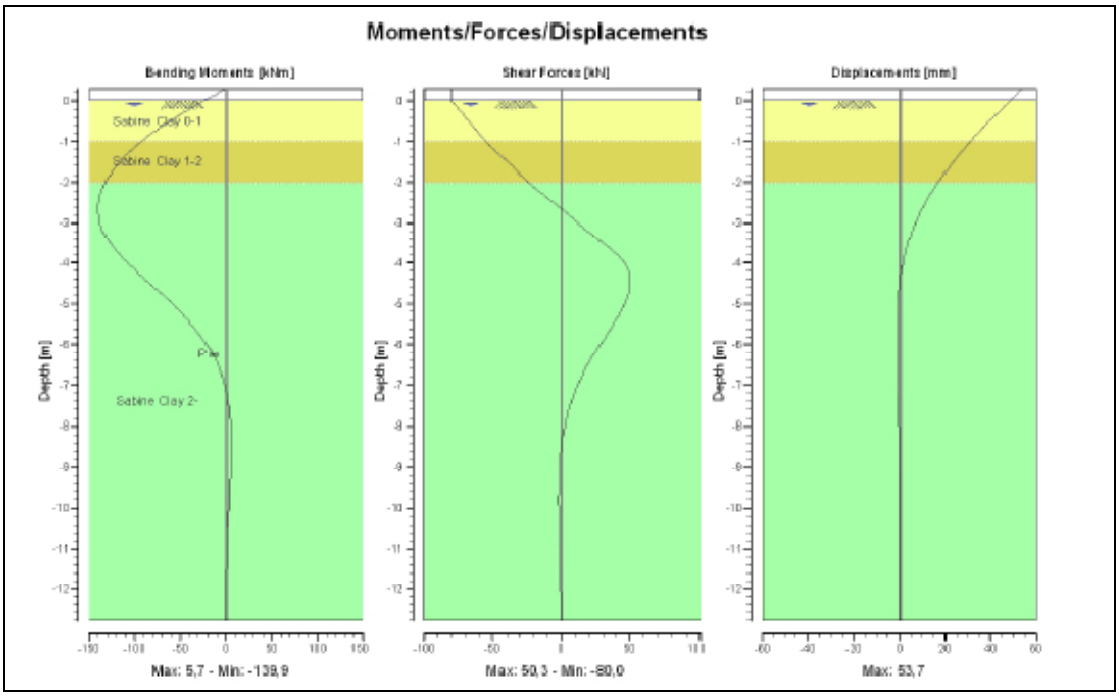

Figure 7-16 Output Sabine, Load = 80kN

7.3.2 Results

When the calculated and measured deflections are plotted versus the lateral load, it can be seen that the MSheet calculation underestimates the displacements. the shapes of the two curves however are similar. The calculated moments approach the measurements quite well.

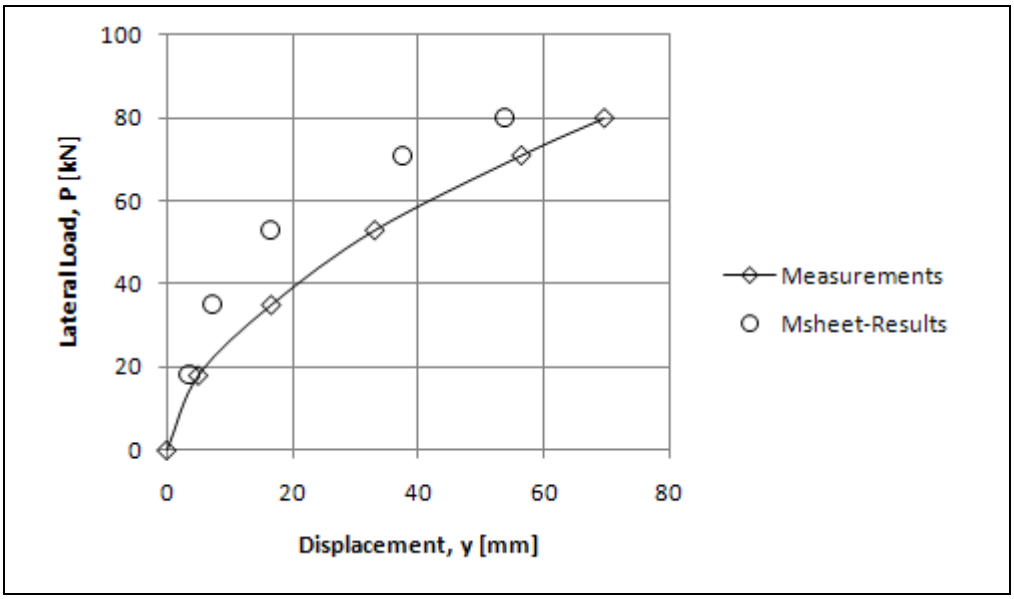

Graph 7-8 Lateral load vs. Displacement Sabine

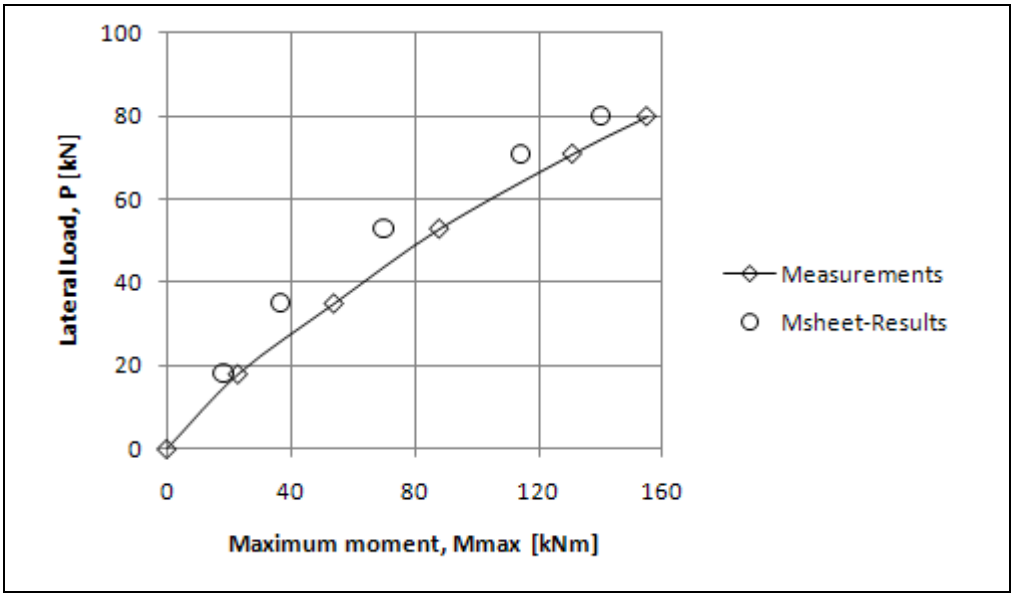

Graph 7-9 Lateral load vs. Maximum moment Sabine

7.4 CASE IX-CL, GARSTON

7.4.1 Input

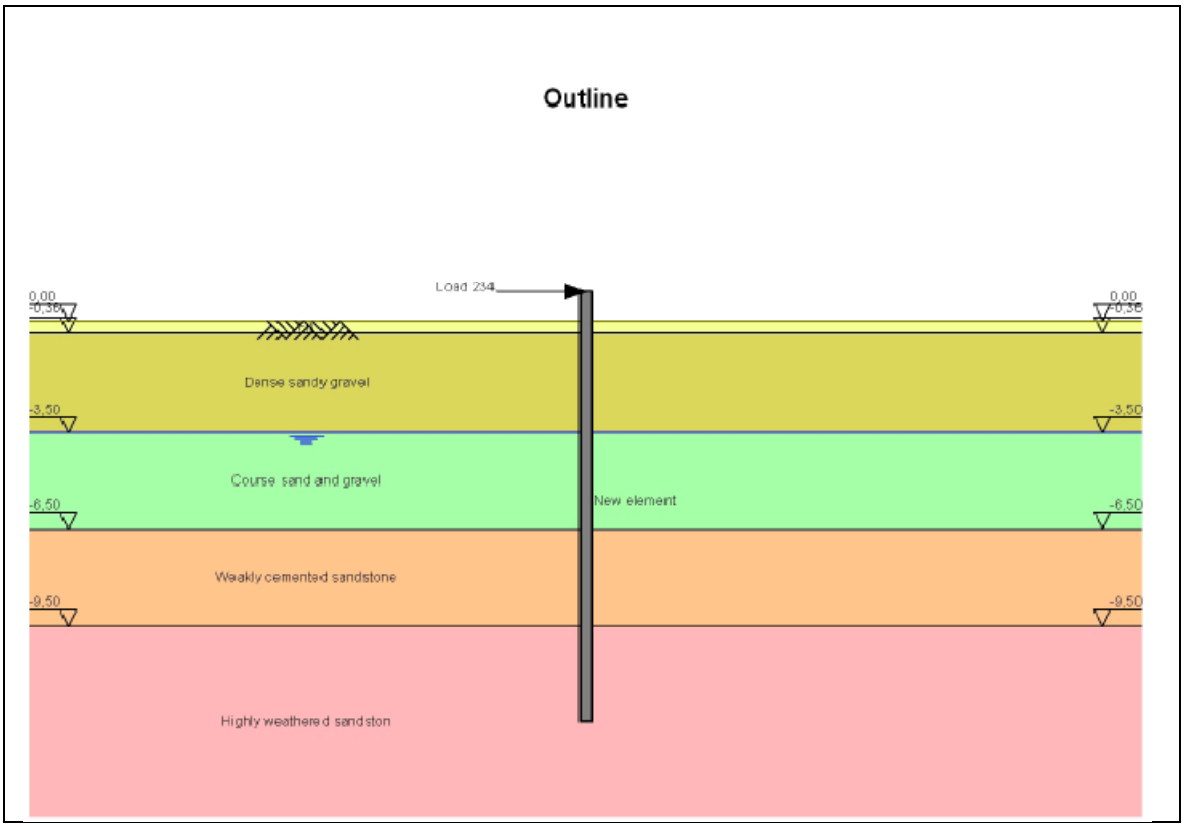

Figure 7-17 Soil Profile Garston

3.5 Water Level

Water level: -3,50 [m]

3.6 Surface

Surface level: 0,00 [m]

3.7 Soil Material Properties

Layer name	Level [m]	Unit weight Unsat [kN/m³]	Unit weight Sat [kN/m³]	Cohesion [kN/m²]	Friction angle phi [deg]	Brinch Hansen used
Fill	0,00	17,00	17,00	0,00	0,00	Yes
Dense sandy gr...	-0,36	21,50	21,50	0,00	43,00	Yes
Course sand a...	-3,50	19,70	19,70	0,00	37,00	Yes
Weakly cement...	-6,50	21,70	21,70	0,00	43,00	Yes
Highly weather...	-9,50	20,00	20,00	0,00	40,00	Yes

Layer name	Level [m]	Earth pressure coefficients Active [-]	Earth pressure coefficients Neutral [-]	Earth pressure coefficients Passive [-]	Additional pore pressure Top [kN/m²]	Additional pore pressure Bottom [kN/m²]
Fill	0,00	0,00	0,00	0,01	0,00	0,00
Dense sandy gr...	-0,36	0,00	0,00	18,77	0,00	0,00
Course sand a...	-3,50	0,00	0,00	14,57	0,00	0,00
Weakly cement...	-6,50	0,00	0,00	30,56	0,00	0,00
Highly weather...	-9,50	0,00	0,00	26,54	0,00	0,00

3.8 Soil Material Properties calculated using Brinch Hansen

Layer name	Level [m]	Fictive cohesion [kN/m²]
Fill	0,00	0,00
Dense sandy gr...	-0,36	0,00
Course sand a...	-3,50	0,00
Weakly cement...	-6,50	0,00
Highly weather...	-9,50	0,00

3.9 Modulus of Subgrade Reaction

Layer name	Level [m]	Menard used	E-Mod Menard [kN/m²]	Soil type Menard	Branch 1 Top [kN/m³]	Branch 1 Bottom [kN/m³]
Fill	0,00	Yes	10000,00	Gravel	36891,63	36891,63
Dense sandy gr...	-0,36	Yes	10000,00	Gravel	36891,63	36891,63
Course sand a...	-3,50	Yes	15000,00	Sand	45802,66	45802,66
Weakly cement...	-6,50	Yes	15000,00	Sand	45802,66	45802,66
Highly weather...	-9,50	Yes	25000,00	Sand	76337,76	76337,76

Figure 7-18 Soil Parameters Garston

3.2 Pile Properties

Length	13,40 m
Level top side	0,90 m
Number of sections	3

Section name	From [m]	To [m]	Stiffness EI [kNm²]	Diameter [m]	Maximum moment [kNm]
New element	0,00	0,90	1,1698E+07	1,50	15900,00
New element (1)	-8,79	0,00	4,7417E+06	1,50	15900,00
New element (2)	-12,50	-8,79	1,1698E+07	1,50	15900,00

Section name	From [m]	To [m]	Red. factor EI [-]	Red. factor max. moment [-]	Note to reduction factor
New element	0,00	0,90	1,00	1,00	
New element (1)	-8,79	0,00	1,00	1,00	
New element (2)	-12,50	-8,79	1,00	1,00	

Section name	From [m]	To [m]	Corrected stiffness EI [kNm²]	Corrected max. moment [kNm]
New element	0,00	0,90	1,1690E+07	15900,00
New element (1)	-8,79	0,00	4,7420E+06	15900,00
New element (2)	-12,50	-8,79	1,1690E+07	15900,00

Figure 7-19 Pile Properties Garston, Load=2383kN

Note: The concrete of the pile at Garston cracks at a moment of 2060kNm. Therefore a reduced bending stiffness has to be used at the parts of the pile where this is the case. The pile has been separated in three parts. The bending moment in the middle part is higher than 2060kNm. The depths at which the bending moment is higher than 2060kNm are determined by applying the actual load on the pile that has been used for the previous calculation with the lower load. Then the calculation is repeated, but with a reduced bending stiffness between the two points where the moment was equal to the 2060kNm. The pile section heights are given in the table below:

Load	Top Section One [m +gl]	Top Section Two [m –gl]	Top Section Three [m –gl]
234	0,90	12,50	12,50
374	0,90	12,50	12,50
607	0,90	12,50	12,50
794	0,90	12,50	12,50
981	0,90	1,62	5,66
1215	0,90	1,24	6,25
1402	0,90	0,80	6,86
1589	0,90	0,54	7,39
1776	0,90	0,40	7,71
2009	0,90	0,29	8,19
2150	0,90	0,17	8,32
2383	0,90	0,00	8,79

Table 7-1 Pile sections pile Garston under different loads

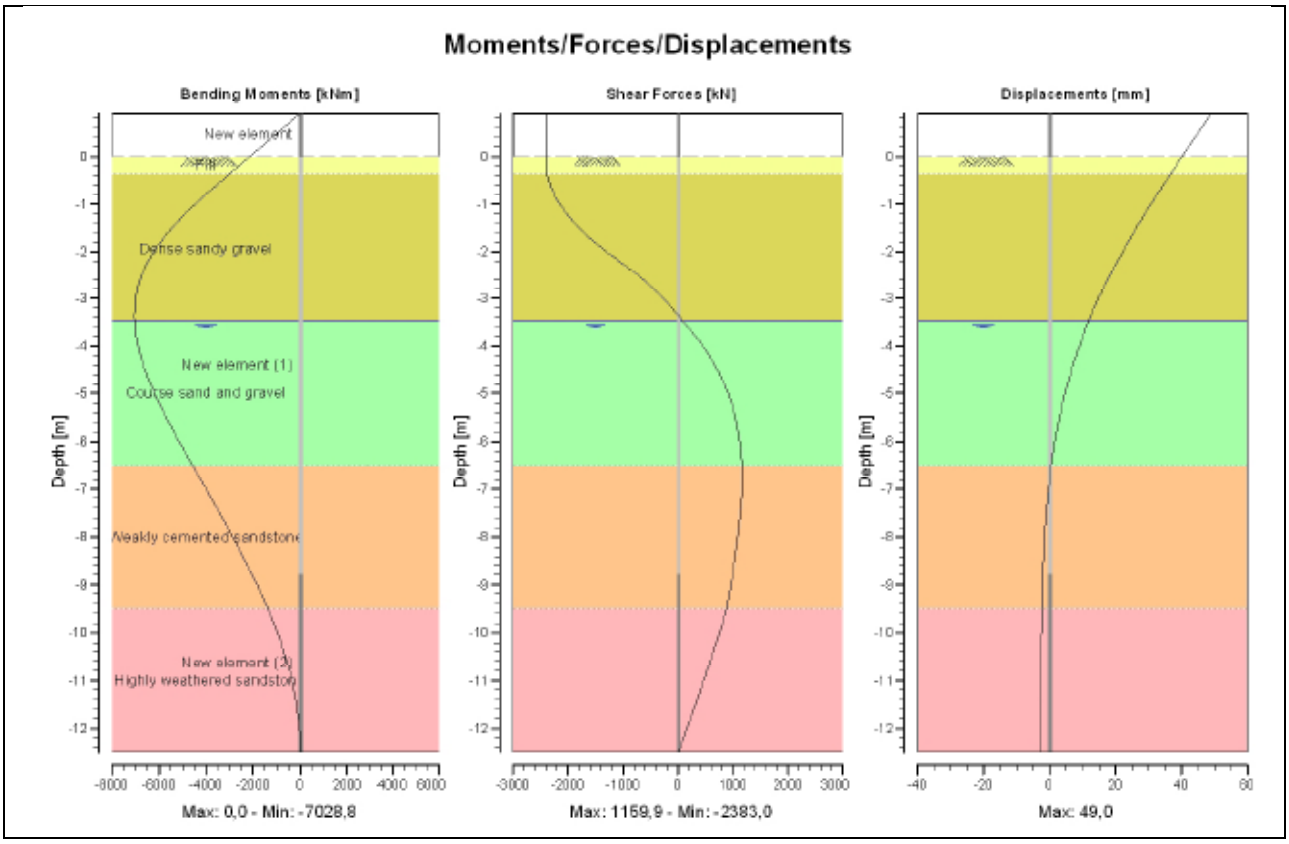

Figure 7-20 Output Garston, Load = 2383kN

7.4.2 Results

When the calculated and measured deflections are plotted versus the lateral load, it can be seen that the calculated displacement predicted the measurements almost exactly. This is also the case for the calculation of the maximum moment.

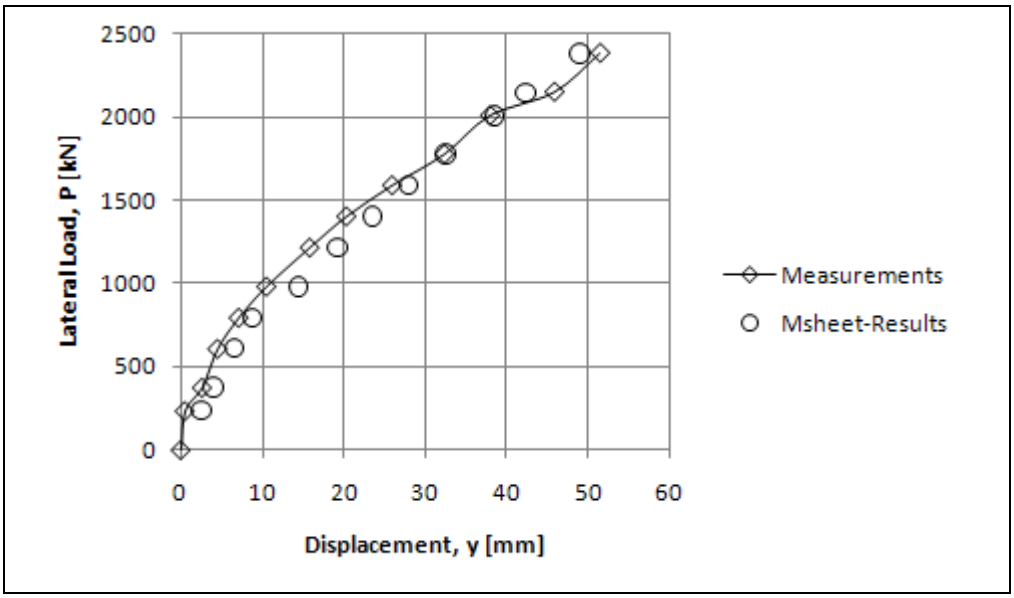

Graph 7-10 Lateral load vs. Displacement Garston

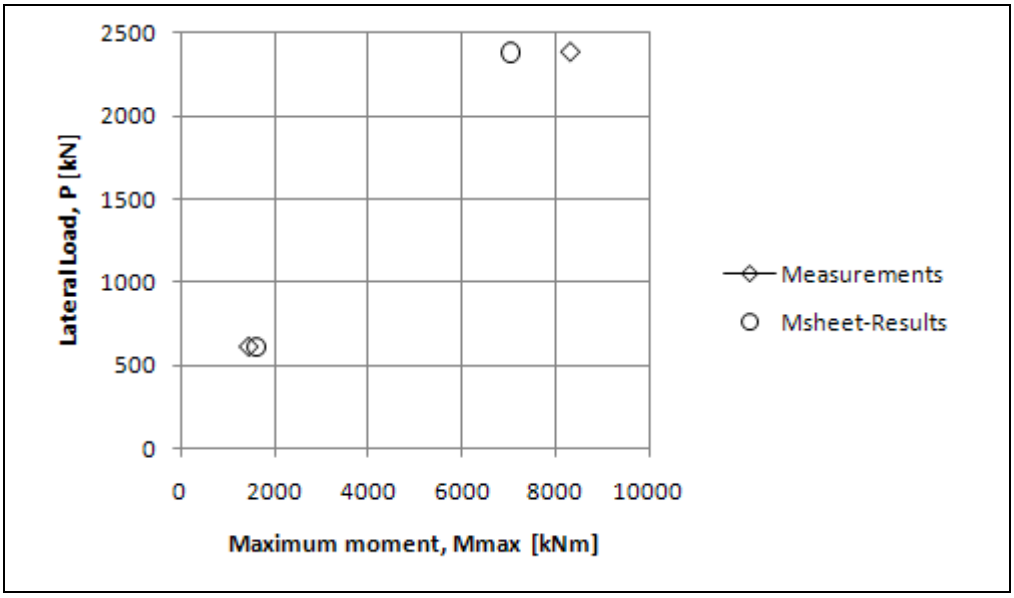

Graph 7-11 Lateral load vs. Maximum Moment Garston

7.5 CASE X-CL, ARKANSAS RIVER

7.5.1 Input

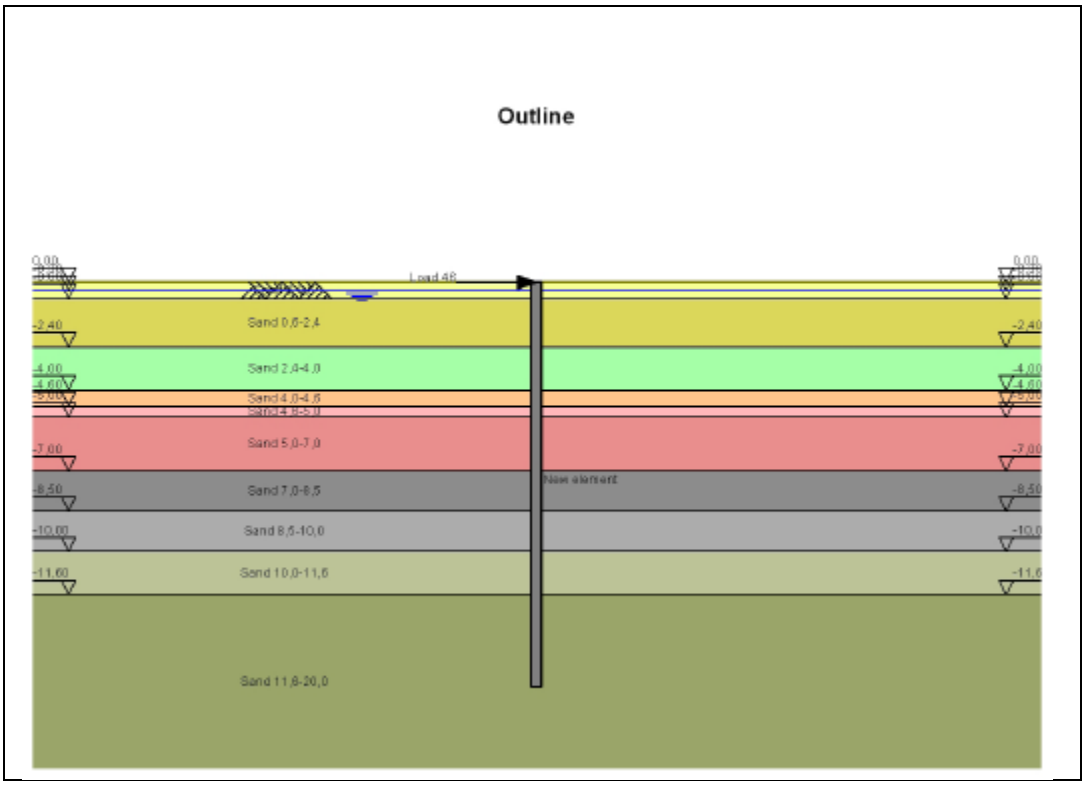

Figure 7-21 Soil Profile Arkansas River

3.5 Water Level

Water level: -0,30 [m]

3.6 Surface

Surface level: 0,00 [m]

3.7 Soil Material Properties

Layer name	Level [m]	Unit weight Unsat [kN/m³]	Unit weight Sat [kN/m³]	Cohesion [kN/m²]	Friction angle phi [deg]	Brinch Hansen used
Sand 0-0,6	0,00	20,00	20,20	0,00	45,00	Yes
Sand 0,6-2,4	-0,60	20,00	20,20	0,00	42,00	Yes
Sand 2,4-4,0	-2,40	20,00	20,20	0,00	42,00	Yes
Sand 4,0-4,6	-4,00	20,00	20,20	0,00	41,00	Yes
Sand 4,6-5,0	-4,60	20,00	20,20	0,00	42,00	Yes
Sand 5,0-7,0	-5,00	20,00	20,20	0,00	42,00	Yes
Sand 7,0-8,5	-7,00	20,00	20,20	0,00	40,00	Yes
Sand 8,5-10,0	-8,50	20,00	20,20	0,00	41,00	Yes
Sand 10,0-11,6	-10,00	20,00	20,20	0,00	40,00	Yes
Sand 11,6-20,0	-11,60	20,00	20,20	0,00	36,00	Yes

Layer name	Level [m]	Earth pressure coefficients			Additional pore pressure	
		Active [-]	Neutral [-]	Passive [-]	Top [kN/m²]	Bottom [kN/m²]
Sand 0-0,6	0,00	0,00	0,00	20,35	0,00	0,00
Sand 0,6-2,4	-0,60	0,00	0,00	22,22	0,00	0,00
Sand 2,4-4,0	-2,40	0,00	0,00	30,81	0,00	0,00
Sand 4,0-4,6	-4,00	0,00	0,00	32,18	0,00	0,00
Sand 4,6-5,0	-4,60	0,00	0,00	37,61	0,00	0,00
Sand 5,0-7,0	-5,00	0,00	0,00	42,05	0,00	0,00
Sand 7,0-8,5	-7,00	0,00	0,00	38,11	0,00	0,00
Sand 8,5-10,0	-8,50	0,00	0,00	46,23	0,00	0,00
Sand 10,0-11,6	-10,00	0,00	0,00	43,83	0,00	0,00
Sand 11,6-20,0	-11,60	0,00	0,00	28,84	0,00	0,00

3.8 Soil Material Properties calculated using Brinch Hansen

Layer name	Level [m]	Fictive cohesion [kN/m²]
Sand 0-0,6	0,00	0,00
Sand 0,6-2,4	-0,60	0,00
Sand 2,4-4,0	-2,40	0,00
Sand 4,0-4,6	-4,00	0,00
Sand 4,6-5,0	-4,60	0,00
Sand 5,0-7,0	-5,00	0,00
Sand 7,0-8,5	-7,00	0,00
Sand 8,5-10,0	-8,50	0,00
Sand 10,0-11,6	-10,00	0,00
Sand 11,6-20,0	-11,60	0,00

3.9 Modulus of Subgrade Reaction

Layer name	Level [m]	Menard used	E-Mod Menard [kN/m²]	Soil type Menard	Branch 1	
					Top [kN/m³]	Bottom [kN/m³]
Sand 0-0,6	0,00	Yes	5000,00	Sand	28690,30	28690,30
Sand 0,6-2,4	-0,60	Yes	5500,00	Sand	31559,33	31559,33
Sand 2,4-4,0	-2,40	Yes	10000,00	Sand	57380,60	57380,60
Sand 4,0-4,6	-4,00	Yes	8000,00	Sand	45904,48	45904,48
Sand 4,6-5,0	-4,60	Yes	13000,00	Sand	74594,78	74594,78
Sand 5,0-7,0	-5,00	Yes	14000,00	Sand	80332,84	80332,84
Sand 7,0-8,5	-7,00	Yes	12000,00	Sand	68856,72	68856,72
Sand 8,5-10,0	-8,50	Yes	15000,00	Sand	86070,90	86070,90
Sand 10,0-11,6	-10,00	Yes	15000,00	Sand	86070,90	86070,90
Sand 11,6-20,0	-11,60	Yes	15000,00	Sand	86070,90	86070,90

Figure 7-22 Soil Parameters Arkansas River

3.2 Pile Properties

Length	15,00 m
Level top side	0,00 m
Number of sections	1

Section name	From [m]	To [m]	Stiffness EI [kNm²]	Diameter [m]	Maximum moment [kNm]
New element	-15,00	0,00	6,9900E+04	0,48	100000,00

Section name	From [m]	To [m]	Red. factor EI [-]	Red. factor max. moment [-]	Note to reduction factor
New element	-15,00	0,00	1,00	1,00	

Section name	From [m]	To [m]	Corrected stiffness EI [kNm²]	Corrected max. moment [kNm]
New element	-15,00	0,00	6,9900E+04	100000,00

Figure 7-23 Pile Properties Arkansas River

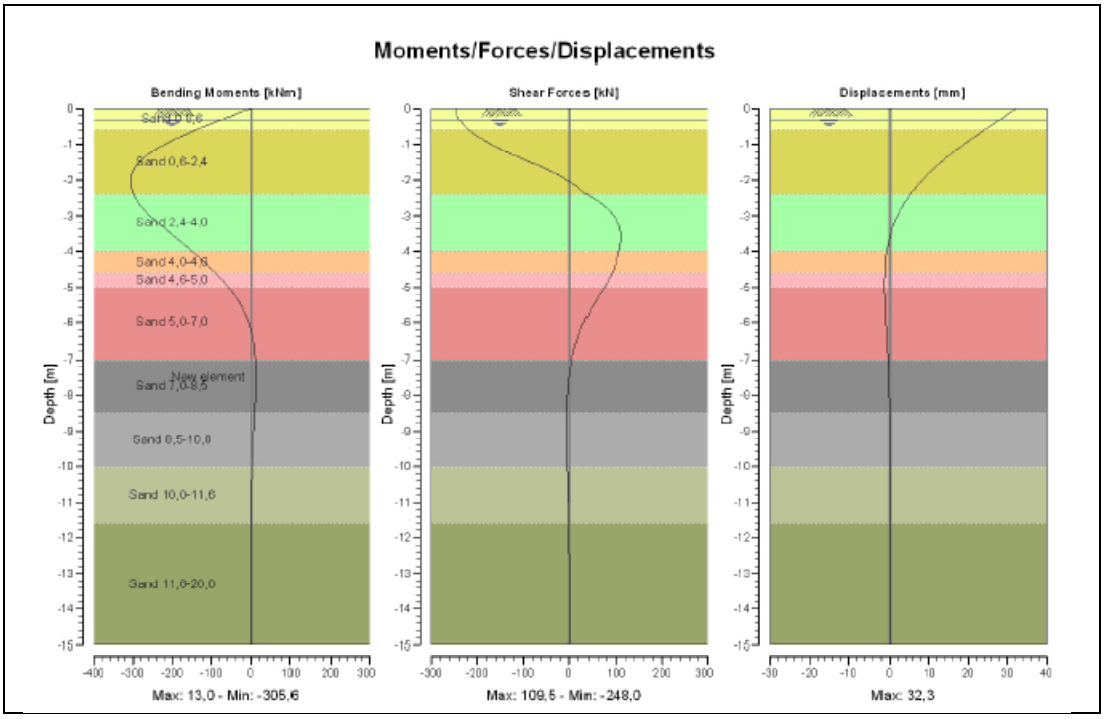

Figure 7-24 Output Arkansas River, Load = 248kN

7.5.2 Results

When the calculated and measured deflections are plotted versus the lateral load, it can be seen that the calculated displacements are overestimated by almost a factor two.

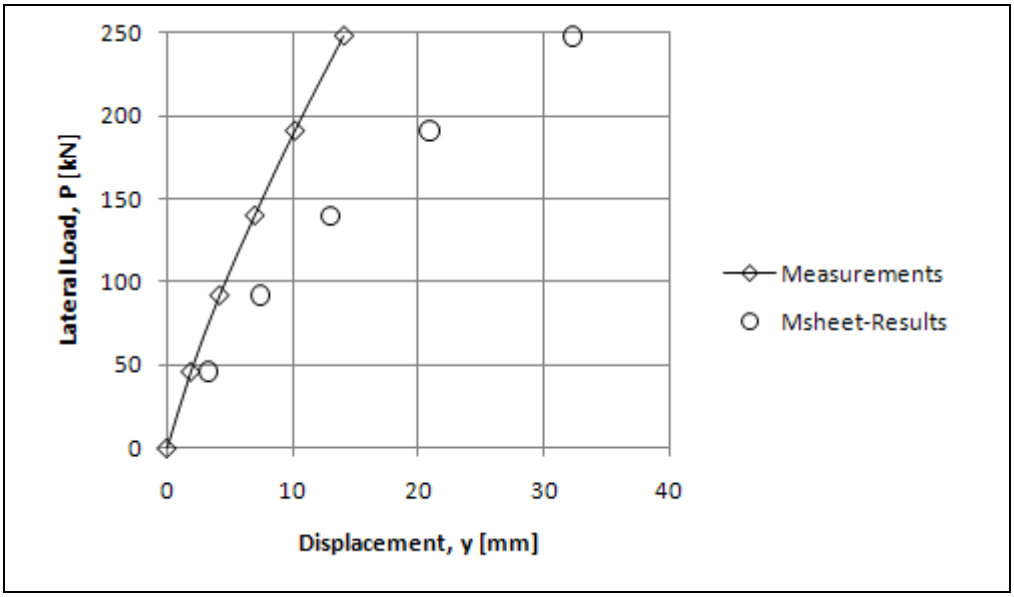

Graph 7-12 Lateral load vs. Displacement Arkansas River

7.6 CASE XIII-L, FLORIDA

7.6.1 Input

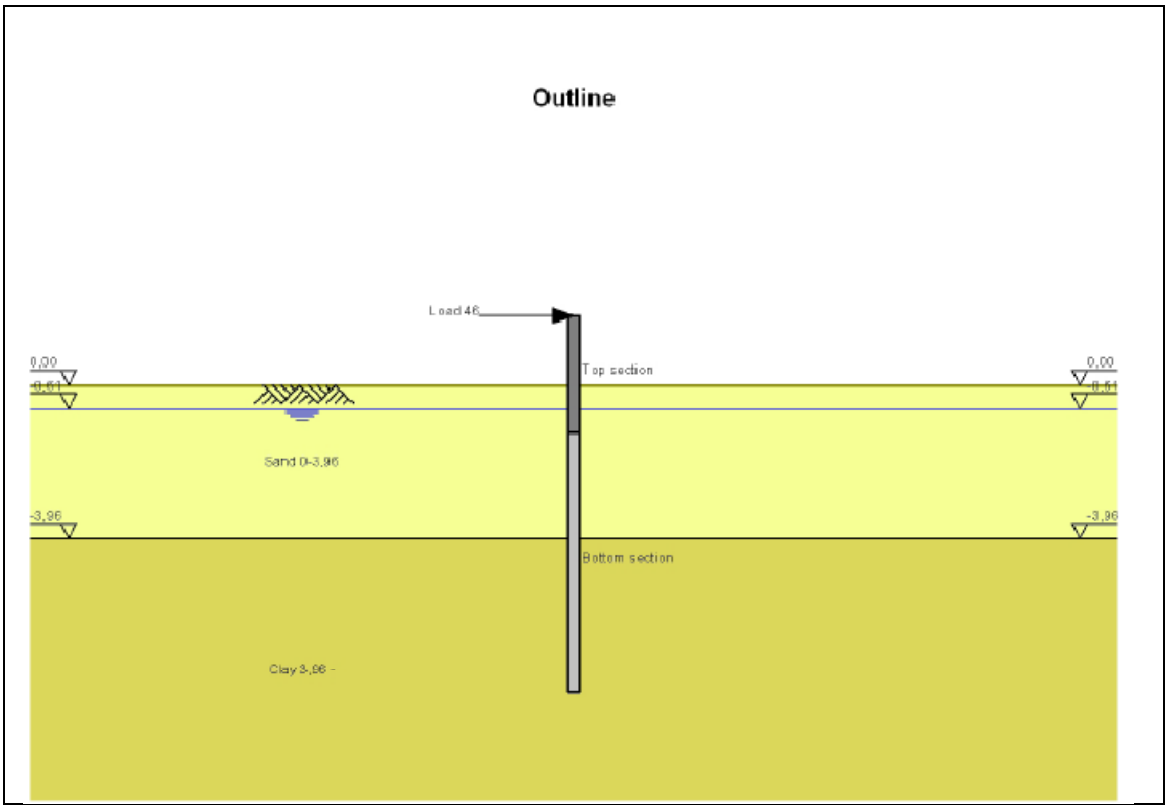

Figure 7-25 Soil Profile Florida

3.5 Water Level

Water level: -0,61 [m]

3.6 Surface

Surface level: 0,00 [m]

3.7 Soil Material Properties

Layer name	Level [m]	Unit weight Unsat [kN/m³]	Unit weight Sat [kN/m³]	Cohesion [kN/m²]	Friction angle phi [deg]	Brinch Hansen used
Sand 0-3,96	0,00	17,00	19,20	0,00	38,00	Yes
Clay 3,96 -	-3,96	19,40	19,40	120,00	0,00	Yes

Layer name	Level [m]	Earth pressure coefficients Active [-]	Neutral [-]	Passive [-]	Additional pore pressure Top [kN/m²]	Bottom [kN/m²]
Sand 0-3,96	0,00	0,00	0,00	12,18	0,00	0,00
Clay 3,96 -	-3,96	0,00	0,00	0,01	0,00	0,00

3.8 Soil Material Properties calculated using Brinch Hansen

Layer name	Level [m]	Fictive cohesion [kN/m²]
Sand 0-3,96	0,00	0,00
Clay 3,96 -	-3,96	5551,31

3.9 Modulus of Subgrade Reaction

Layer name	Level [m]	Menard used	E-Mod Menard [kN/m²]	Soil type Menard	Branch 1 Top [kN/m³]	Branch 1 Bottom [kN/m³]
Sand 0-3,96	0,00	Yes	7000,00	Sand	21969,24	21969,24
Clay 3,96 -	-3,96	Yes	6000,00	Clay	10001,84	10001,84

Figure 7-26 Soil Parameters Florida

3.2 Pile Properties

Length	9,71 m
Level top side	1,79 m
Number of sections	2

Section name	From [m]	To [m]	Stiffness EI [kNm²]	Diameter [m]	Maximum moment [kNm]
Top section	-1,22	1,79	5,0790E+06	1,42	6280,00
Bottom section	-7,92	-1,22	2,5250E+06	1,42	4410,00

Section name	From [m]	To [m]	Red. factor EI [-]	Red. factor max. moment [-]	Note to reduction factor
Top section	-1,22	1,79	1,00	1,00	
Bottom section	-7,92	-1,22	1,00	1,00	

Section name	From [m]	To [m]	Corrected stiffness EI [kNm²]	Corrected max. moment [kNm]
Top section	-1,22	1,79	5,0790E+06	6280,00
Bottom section	-7,92	-1,22	2,5250E+06	4410,00

Figure 7-27 Pile Properties Florida

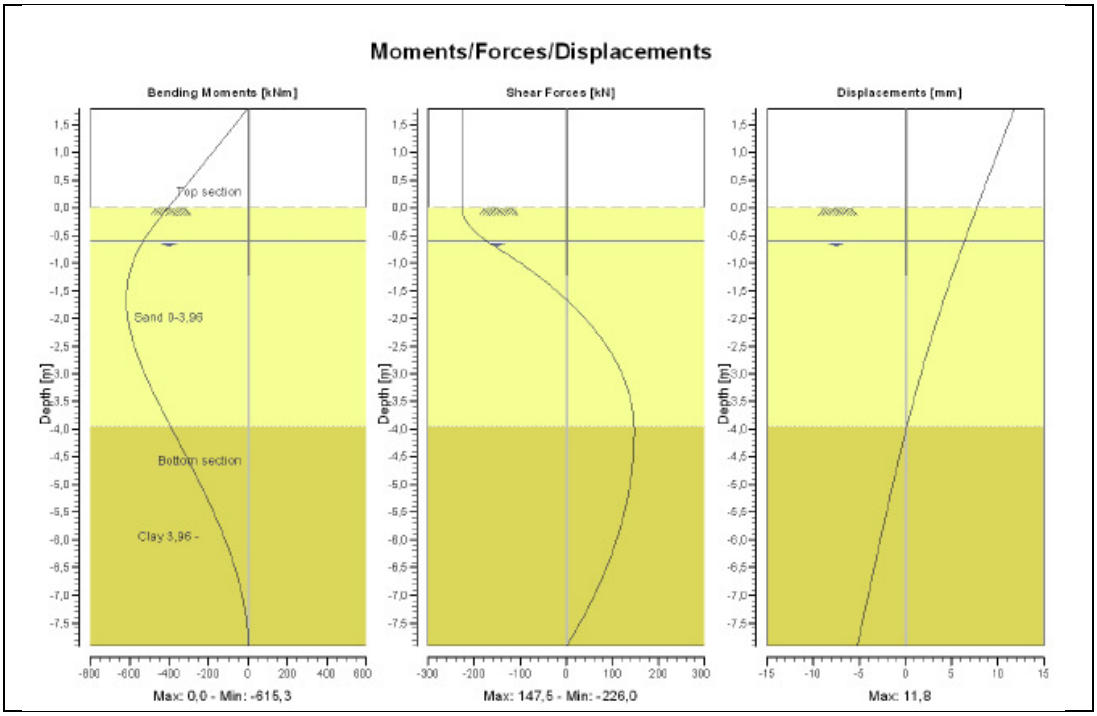

Figure 7-28 Output Florida, Load = 226kN

7.6.2 Results

When the calculated and measured deflections are plotted versus the lateral load, it can be seen that the calculated displacement at the lowest load predicted the displacement almost exactly. However, if the load increased the deflections where underestimated increasingly up to almost three times the measured displacement.

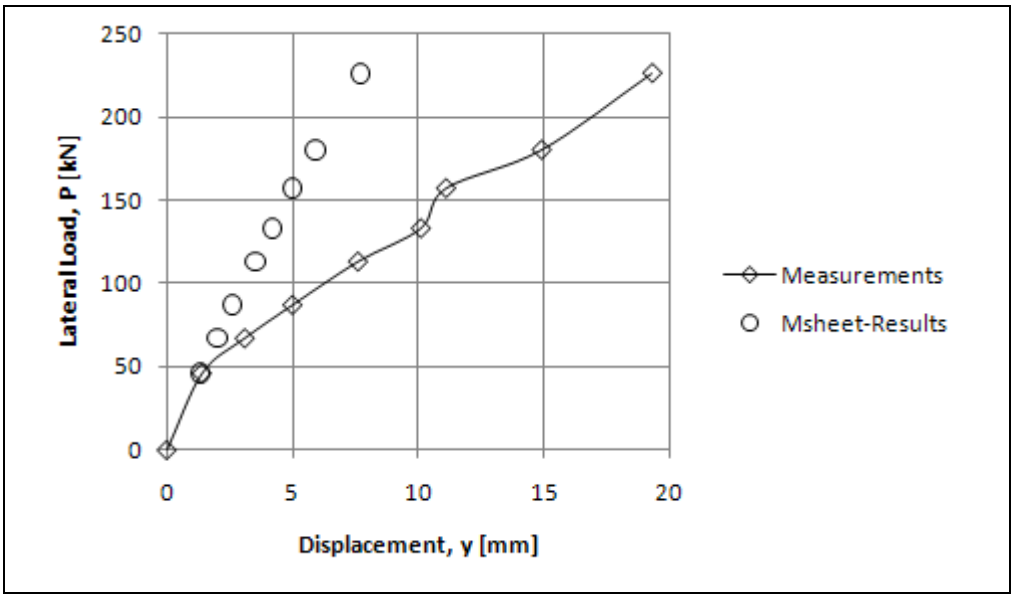

Graph 7-13 Lateral load vs. Displacement Florida

8 MPILE

MPile is a software program that simulates the soil as a series of non-linear springs. These springs are called the P-Y Curves. The shapes of the curves are parabolic until the ultimate soil resistance is reached as they are determined according to the rules of the API. Thus the program works almost exactly as the MSheet Single Pile Module, but the soil springs are modeled differently.
The calculations are here presented as the input of the MPile program. The output is not presented. The results are presented in the usual way.

8.1 CASE I-CU, BAGNOLET

8.1.1 Input

For all three tests executed at Bagnolet the soil profile and pile type is the same. The profile and accompanying data is given below. The pile- and cap properties and the results are different for each test. They are given separately.

```
 Calculation method : Cap
 Cap model          : Rigid Cap


 SOIL LAYER DATA
 ================

  Soil layername: Clay Top with soil type: STIFF CLAY
  Lateral and axial rule: API and API
-------------------------------------------------------------
  Unit weight dry             [kN/m3] |      17.90 |      17.90
  Unit weight wet             [kN/m3] |      17.90 |      17.90
  Undrained Shearstength Cu   [kN/m2] |     100.00 |     125.00
  Empirical constant J            [-] |     0.5000 |
  Strain at 50% failure load      [-] |    0.00500 |
  dz                              [m] |       0.00 |

  Soil layername: Clay Middle with soil type: STIFF CLAY
  Lateral and axial rule: API and API
-------------------------------------------------------------
  Unit weight dry             [kN/m3] |      17.90 |      17.90
  Unit weight wet             [kN/m3] |      17.90 |      17.90
  Undrained Shearstength Cu   [kN/m2] |     125.00 |     130.00
  Empirical constant J            [-] |     0.5000 |
  Strain at 50% failure load      [-] |    0.00500 |
  dz                              [m] |       0.00 |

  Soil layername: Clay Bottom with soil type: STIFF CLAY
  Lateral and axial rule: API and API
-------------------------------------------------------------
  Unit weight dry             [kN/m3] |      17.90 |      17.90
  Unit weight wet             [kN/m3] |      17.90 |      17.90
  Undrained Shearstength Cu   [kN/m2] |     130.00 |     130.00
  Empirical constant J            [-] |     0.5000 |
  Strain at 50% failure load      [-] |    0.00500 |
  dz                              [m] |       0.00 |


 SOIL PROFILE DATA
 ================


 Waterlevel:   -6.00 [m]
 Location:  x =    0.00 [m]  z =    0.00 [m]
 ------------------------------------------------------------
   layer |    Y[m]   | Soil layer name    | Soil type
 --------|-----------|--------------------|------------------
       1 |     0.00  | Clay Top           | STIFF CLAY
       2 |    -3.96  | Clay Middle        | STIFF CLAY
       3 |    -4.69  | Clay Bottom        | STIFF CLAY
```

Figure 8-1 Soil Profile MPile, Bagnolet

PILE TIP CURVES

Rt[%]	Zt[m]
0.000	0.000
100.000	0.002

PILE TYPE DATA

Pile Type nr	Pile Type Name	Pile properties Length [m]	Mass [kg]	Diam. [m]	Thickn. [m]	EI [kN/m2]	EA [kN]	Young modulus [kN/m2]
1	Pile Test 1	3.35	0.0	0.43	0.01	2.550E+04	1.129E+06	1.692E+08
2	Pile Test 2	5.05	0.0	0.43	0.01	2.550E+04	1.129E+06	1.692E+08
3	Pile Test 3	6.10	0.0	0.43	0.01	2.550E+04	1.129E+06	1.692E+08

Figure 8-2 Pile tip curve and Pile Type

8.1.2 Test I

Here the pile properties and test results for all loads that were applied in test I. Note: During the field test the deformations were measured at the ground line.

PILE DATA

Pile nr	Pile Type name	Pile coordinates [m] X	Y	Z	Angle [deg]	Skew-ness	End Bearing [kN]	Top cond.
1	Pile Test 1	0.00	0.70	0.00	0.00	0.00	1000.00	free

nr	Soil profile	Pile type name	Pile tip curve
1	1	Pile Test 1	1

CAP DATA

	X-direction	Y-direction	Z-direction
Centre of gravity [m]	0.00	0.70	0.00

LOAD DATA

Index	Loadstep number	Force [kN] X - direction	- Y - direction	- Z - direction
1	1	29.000	-	-
2	2	49.000	-	-
3	3	59.000	-	-
4	4	79.000	-	-

Figure 8-3 Pile Properties, Cap data and Load Data Bagnolet Test I

8.1.3 Test II

PILE DATA

Pile nr	Pile Type name	Pile coordinates [m] X	Y	Z	Angle [deg]	Skew-ness	End Bearing [kN]	Top cond.
1	Pile Test 2	0.00	0.90	0.00	0.00	0.00	1000.00	free

nr	Soil profile	Pile type name	Pile tip curve
1	1	Pile Test 2	1

CAP DATA

	X-direction	Y-direction	Z-direction
Centre of gravity [m]	0.00	0.90	0.00

LOAD DATA

Index	Loadstep number	Force [kN] X - direction	- Y - direction	- Z - direction
1	1	15.000	-	-
2	2	39.000	-	-
3	3	59.000	-	-
4	4	83.000	-	-

Figure 8-4 Pile Properties, Cap data and Load Data Bagnolet Test II

8.1.4 Test III

PILE DATA

Pile nr	Pile Type name	Pile coordinates [m] X	Y	Z	Angle [deg]	Skew-ness	End Bearing [kN]	Top cond.
1	Pile Test 3	0.00	1.00	0.00	0.00	0.00	1000.00	free

nr	Soil profile	Pile type name	Pile tip curve
1	1	Pile Test 3	1

CAP DATA

	X-direction	Y-direction	Z-direction
Centre of gravity [m]	0.00	1.00	0.00

LOAD DATA

Index	Loadstep number	Force [kN] X - direction	- Y - direction	- Z - direction
1	1	34.000	-	-
2	2	46.000	-	-
3	3	59.000	-	-
4	4	79.000	-	-

Figure 8-5 Pile Properties Bagnolet Test III

8.1.5 Results

When the calculated and measured deflections and maximum moments are plotted versus the lateral load, it can be seen that for all three tests the MPile calculation was very accurate. The curves in all graphs match each other almost perfectly.

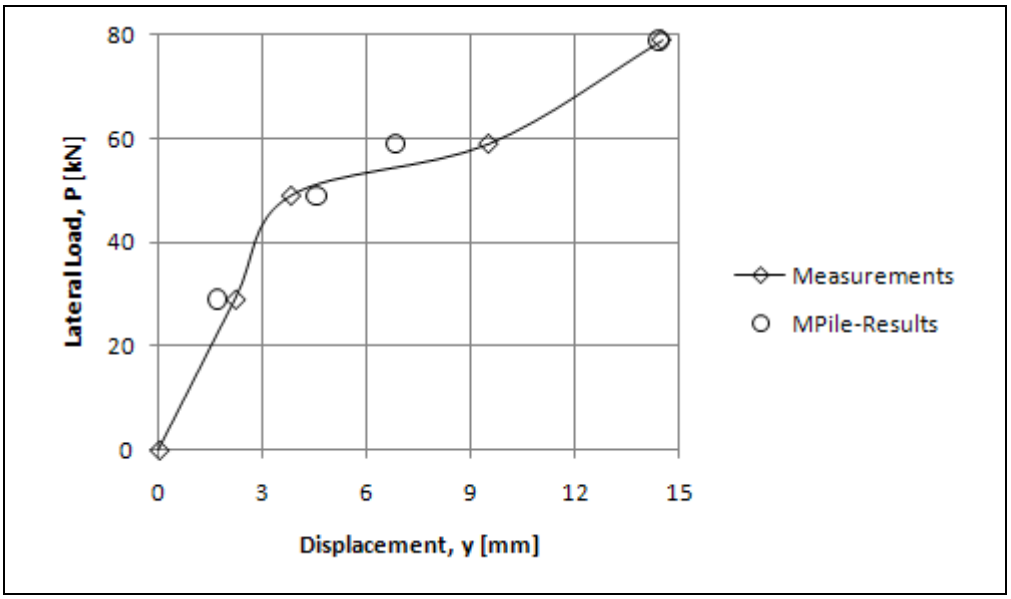

Graph 8-1 Lateral load vs. displacement Test I

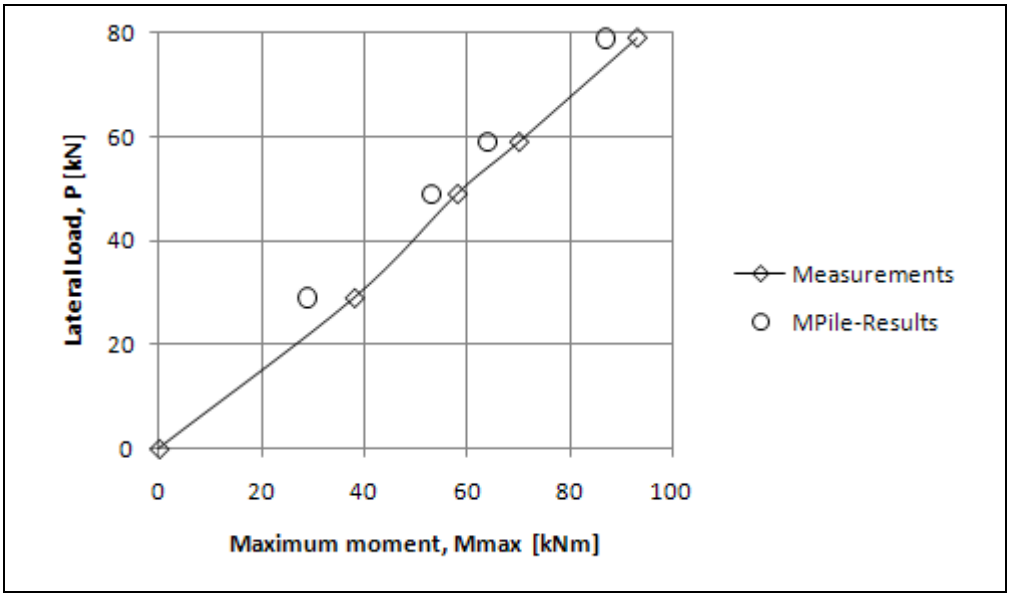

Graph 8-2 Lateral load vs. maximum moment Test I

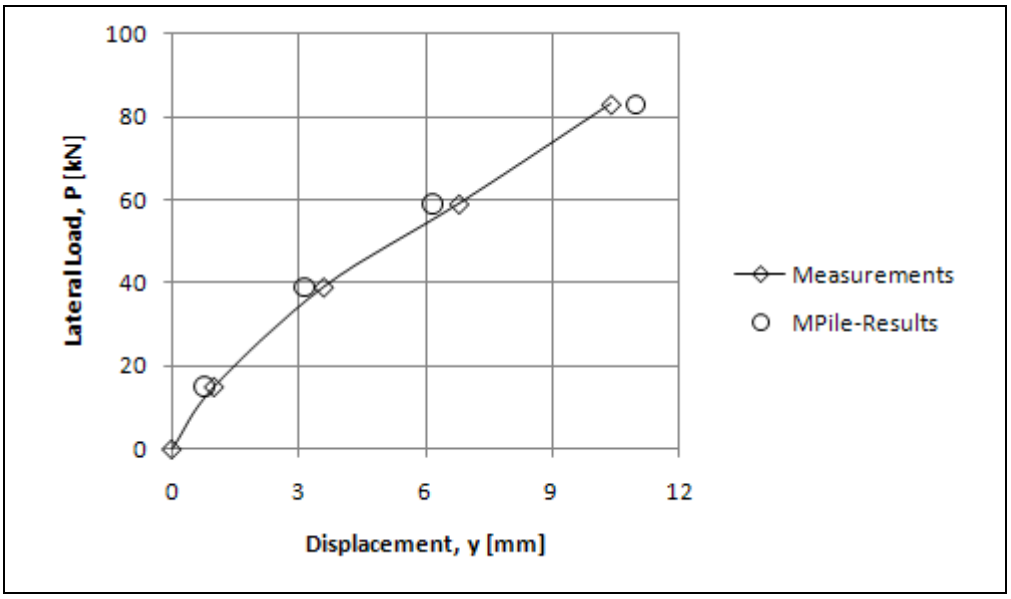

Graph 8-3 Lateral load vs. displacement Test II

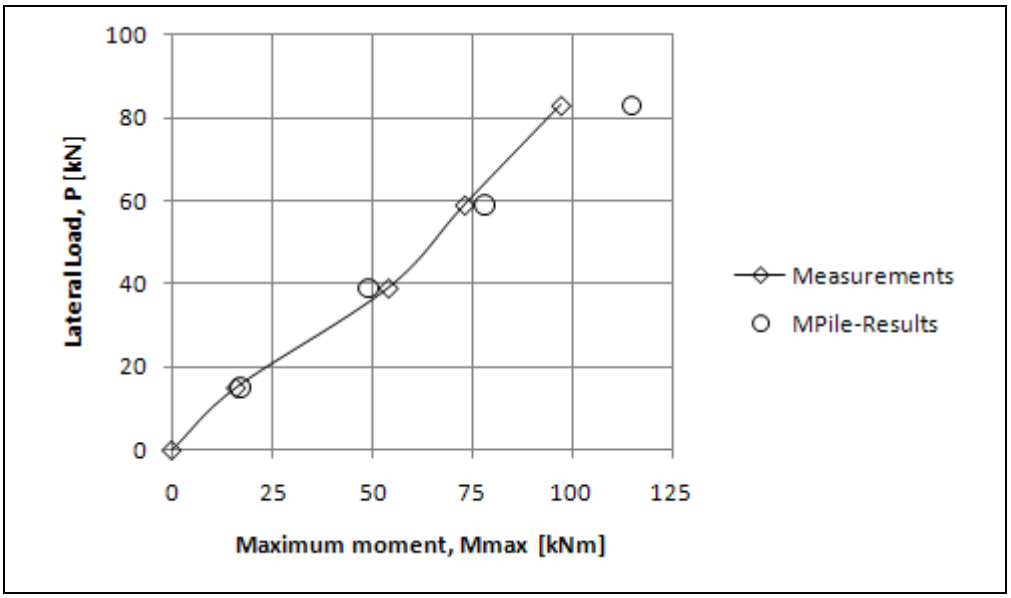

Graph 8-4 Lateral load vs. maximum moment Test II

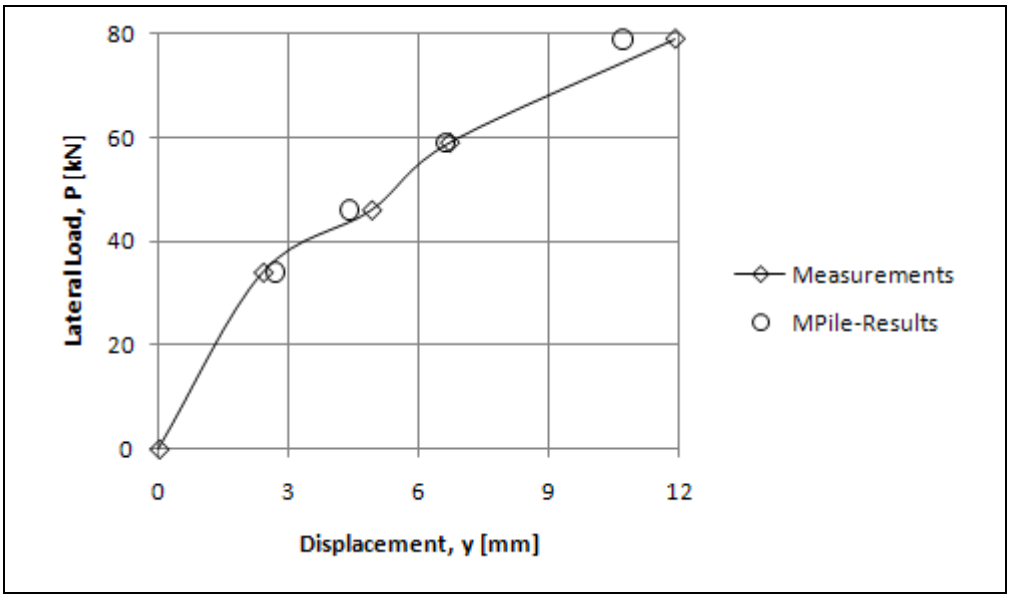

Graph 8-5 Lateral load vs. displacement Test III

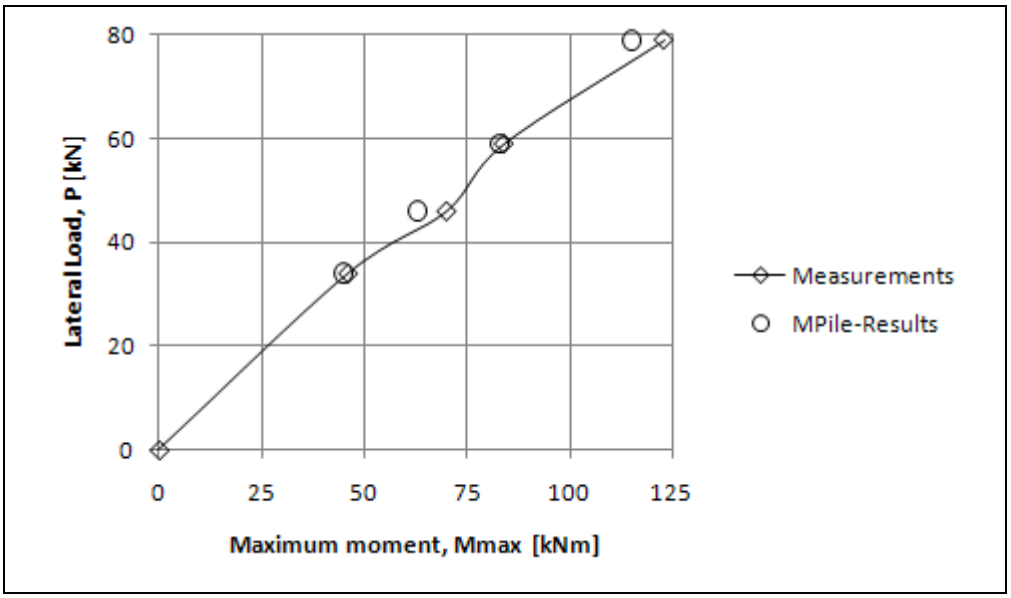

Graph 8-6 Lateral load vs. maximum moment Test III

8.2 CASE III-CU, BRENT CROSS

8.2.1 Input

```
 Calculation method : Cap
 Cap model          : Rigid Cap


 SOIL LAYER DATA
 ================

  Soil layername: Layer 1 0-4,6 with soil type: STIFF CLAY
  Lateral and axial rule: API and API
-------------------------------------------------------
  Unit weight dry             [kN/m3] |      17.00 |      17.00
  Unit weight wet             [kN/m3] |      17.00 |      17.00
  Undrained Shearstength Cu   [kN/m2] |      44.10 |      85.20
  Empirical constant J            [-] |     0.5000 |
  Strain at 50% failure load      [-] |    0.00700 |
  dz                              [m] |       0.00 |

  Soil layername: Layer 3 4,6-6,2m with soil type: STIFF CLAY
  Lateral and axial rule: API and API
-------------------------------------------------------
  Unit weight dry             [kN/m3] |      17.00 |      17.00
  Unit weight wet             [kN/m3] |      17.00 |      17.00
  Undrained Shearstength Cu   [kN/m2] |      85.20 |      80.60
  Empirical constant J            [-] |     0.5000 |
  Strain at 50% failure load      [-] |    0.00700 |
  dz                              [m] |       0.00 |

  Soil layername: Layer 4 6,2-19 with soil type: STIFF CLAY
  Lateral and axial rule: API and API
-------------------------------------------------------
  Unit weight dry             [kN/m3] |      17.00 |      17.00
  Unit weight wet             [kN/m3] |      17.00 |      17.00
  Undrained Shearstength Cu   [kN/m2] |      80.60 |     133.30
  Empirical constant J            [-] |     0.5000 |
  Strain at 50% failure load      [-] |    0.00500 |
  dz                              [m] |       0.00 |


 SOIL PROFILE DATA
 =================


 Waterlevel:  -19.00 [m]
 Location:  x =    0.00 [m]  z =    0.00 [m]
 ---------------------------------------------------------
   layer |   Y[m]  | Soil layer name    | Soil type
 --------|---------|--------------------|-----------------
       1 |    1.00 | No soil            | NO SOIL
       2 |    0.00 | Layer 1 0-4,6      | STIFF CLAY
       3 |   -4.60 | Layer 3 4,6-6,2m   | STIFF CLAY
       4 |   -6.20 | Layer 4 6,2-19     | STIFF CLAY
```

Figure 8-6 Soil Profile Brent Cross

PILE TIP CURVES

Rt[%]	Zt[m]
0.000	0.000
100.000	0.010

PILE TYPE DATA

Pile Type nr	Pile Type Name	Pile properties Length [m]	Mass [kg]	Diam. [m]	Thickn. [m]	EI [kN/m2]	EA [kN]	Young modulus [kN/m2]
1	Pile	17.50	0.0	0.41	0.01	5.140E+04	2.621E+06	2.106E+08

Figure 8-7 Pile tip curve and Pile Type Brent Cross

PILE DATA

Pile nr	Pile Type name	Pile coordinates [m] X	Y	Z	Angle [deg]	Skew-ness	End Bearing [kN]	Top cond.
1	Pile	0.00	1.00	0.00	0.00	0.00	301.00	free

nr	Soil profile	Pile type name	Pile tip curve
1	1	Pile	1

CAP DATA

	X-direction	Y-direction	Z-direction
Centre of gravity [m]	0.00	1.00	0.00

LOAD DATA

Index	Loadstep number	Force [kN] X - direction	- Y - direction	- Z - direction
1	10	100.000	-	-

Figure 8-8 Pile Properties, Cap data and Load Data Brent Cross

8.2.2 Results

When the calculated and measured displacements are plotted in the same graph it can be seen that MPile calculates the displacement fairly accurate. However, as the load increases MPile underestimates the deflections more and more.

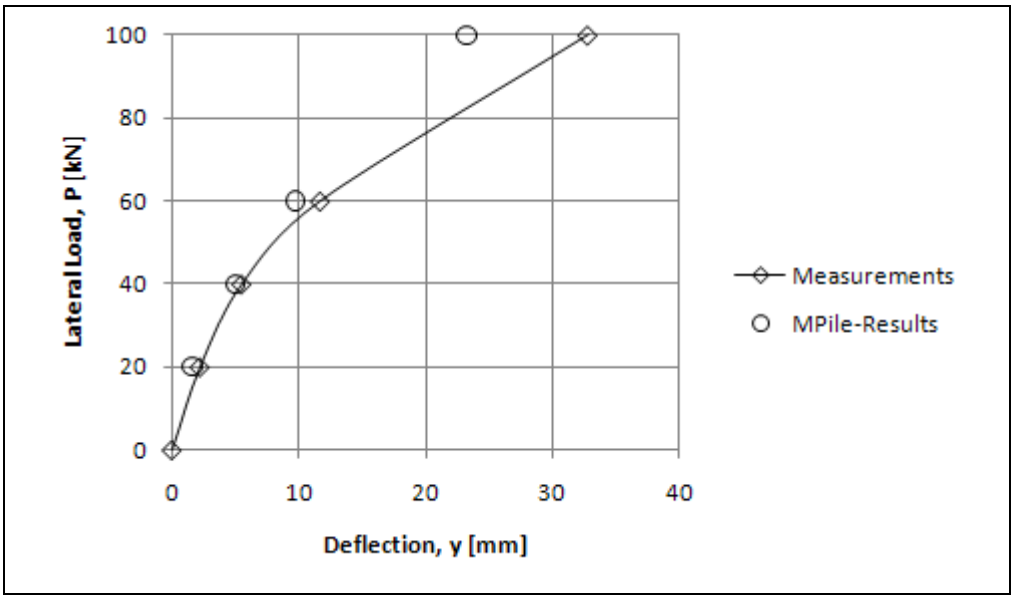

Graph 8-7 Lateral load vs. displacement Brent Cross

8.3 CASE VI-CS, SABINE

8.3.1 Input

SOIL LAYER DATA

Soil layername: Clay with soil type: SOFT CLAY
Lateral and axial rule: API and API

Unit weight dry	[kN/m3]	15.50	15.50
Unit weight wet	[kN/m3]	15.50	15.50
Undrained Shearstength Cu	[kN/m2]	14.40	14.40
Empirical constant J	[-]	0.5000	
Strain at 50% failure load	[-]	0.02000	
dz	[m]	0.00	

SOIL PROFILE DATA

Waterlevel: 0.00 [m]
Location: x = 0.00 [m] z = 0.00 [m]

layer	Y[m]	Soil layer name	Soil type
1	0.00	Clay	SOFT CLAY

Figure 8-9 Soil Profile Sabine

LOAD DATA

Index	Loadstep number	Force [kN] X - direction	- Y - direction	- Z - direction
1	1	18.000	-	-
2	2	35.000	-	-
3	3	53.000	-	-
4	4	71.000	-	-
5	5	80.000	-	-

Figure 8-10 Load Data, Sabine

PILE TIP CURVES

Rt[%]	Zt[m]
0.000	0.000
100.000	0.002

PILE TYPE DATA

Pile Type nr	Pile Type Name	Pile properties Length [m]	Mass [kg]	Diam. [m]	Thickn. [m]	EI [kN/m2]	EA [kN]	Young modulus [kN/m2]
1	Pile	12.80	0.0	0.32	0.01	3.128E+04	2.663E+06	2.179E+08

PILE DATA

Pile nr	Pile Type name	Pile coordinates [m] X	Y	Z	Angle [deg]	Skew-ness	End Bearing [kN]	Top cond.
1	Pile	0.00	0.31	0.00	0.00	0.00	1000.00	free

nr	Soil profile	Pile type name	Pile tip curve
1	1	Pile	1

CAP DATA

	X-direction	Y-direction	Z-direction
Centre of gravity [m]	0.00	0.31	0.00

Figure 8-11 Pile Properties Sabine

8.3.2 Results

When the calculated and measured deflections are plotted versus the lateral load, it can be seen that the MPile calculation overestimates the deflection by almost a factor two. The maximum moments are calculated quite accurately.

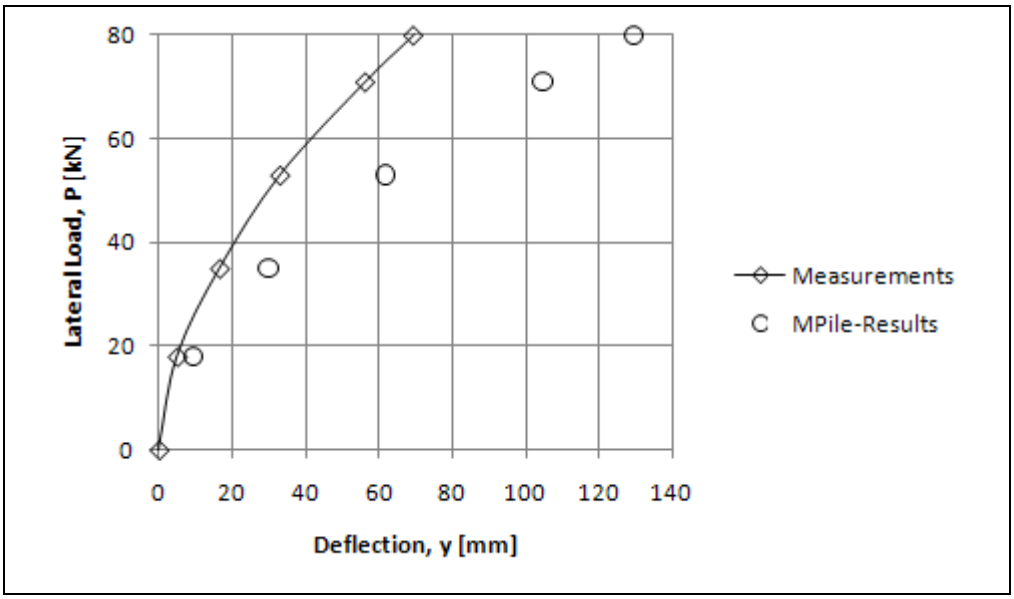

Graph 8-8 Lateral load vs. Displacement Sabine

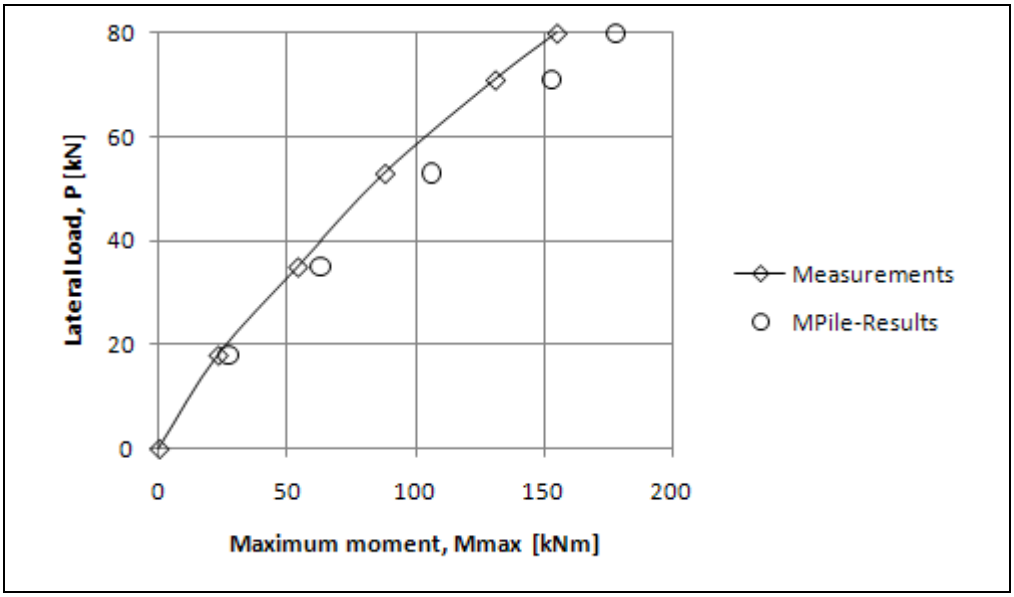

Graph 8-9 Lateral load vs. Maximum moment Sabine

8.4 CASE IX-CL, GARSTON

8.4.1 Input

```
 Calculation method : Cap
 Cap model          : Rigid Cap


 SOIL LAYER DATA
 ================

  Soil layername: Fill with soil type: SAND
  Lateral and axial rule: API and API
-------------------------------------------------------
  Unit weight dry             [kN/m3] |       21.50 |       21.50
  Unit weight wet             [kN/m3] |       21.50 |       21.50
  Angle of internal friction    [deg] |       43.00 |       43.00
  Cone resistance qc          [kN/m2] |    10000.00 |    10000.00
  Ko                              [-] |        0.32 |
  dz  at 100 %                    [m] |       0.002 |
  Friction between pile/soil    [deg] |       20.00 |       20.00

  Soil layername: Dense sandy gravel with soil type: SAND
  Lateral and axial rule: API and API
-------------------------------------------------------
  Unit weight dry             [kN/m3] |       21.50 |       21.50
  Unit weight wet             [kN/m3] |       21.50 |       21.50
  Angle of internal friction    [deg] |       43.00 |       43.00
  Cone resistance qc          [kN/m2] |    10000.00 |    10000.00
  Ko                              [-] |        0.32 |
  dz  at 100 %                    [m] |       0.002 |
  Friction between pile/soil    [deg] |       20.00 |       20.00

  Soil layername: Course sand and gravel with soil type: SAND
  Lateral and axial rule: API and API
-------------------------------------------------------
  Unit weight dry             [kN/m3] |        9.70 |        9.70
  Unit weight wet             [kN/m3] |        9.70 |        9.70
  Angle of internal friction    [deg] |       37.00 |       37.00
  Cone resistance qc          [kN/m2] |    15000.00 |    15000.00
  Ko                              [-] |        0.40 |
  dz  at 100 %                    [m] |       0.002 |
  Friction between pile/soil    [deg] |       20.00 |       20.00

  Soil layername: Weakly cemented sandstone with soil type: SAND
  Lateral and axial rule: API and API
-------------------------------------------------------
  Unit weight dry             [kN/m3] |       11.70 |       11.70
  Unit weight wet             [kN/m3] |       11.70 |       11.70
  Angle of internal friction    [deg] |       43.00 |       43.00
  Cone resistance qc          [kN/m2] |    25000.00 |    25000.00
  Ko                              [-] |        0.32 |
  dz  at 100 %                    [m] |       0.002 |
  Friction between pile/soil    [deg] |       20.00 |       20.00

  Soil layername: Highly weathered sandston with soil type: SAND
  Lateral and axial rule: API and API
-------------------------------------------------------
  Unit weight dry             [kN/m3] |       11.70 |       11.70
  Unit weight wet             [kN/m3] |       11.70 |       11.70
  Angle of internal friction    [deg] |       43.00 |       43.00
  Cone resistance qc          [kN/m2] |    25000.00 |    25000.00
  Ko                              [-] |        0.32 |
  dz  at 100 %                    [m] |       0.002 |
  Friction between pile/soil    [deg] |       20.00 |       20.00
```

Figure 8-12 Soil Layer data Garston

SOIL PROFILE DATA
==========

Waterlevel: -3.50 [m]
Location: x = 0.00 [m] z = 0.00 [m]

layer	Y[m]	Soil layer name	Soil type
1	0.00	Fill	SAND
2	-0.36	Dense sandy gravel	SAND
3	-3.50	Course sand and..	SAND
4	-6.50	Weakly cemented..	SAND
5	-9.50	Highly weathered..	SAND

Figure 8-13 Soil Profile Garston

PILE TIP CURVES

Rt[%]	Zt[m]
0.000	0.000
100.000	0.002

PILE TYPE DATA

Pile Type nr	Pile Type Name	Pile properties Length [m]	Mass [kg]	Diam. [m]	Thickn. [m]	EI [kN/m2]	EA [kN]	Young modulus [kN/m2]
1*	Pile Load 2..	13.40	0.0	1.50	0.00	1.170E+07	2.100E+08	0.000E+00
2*	Pile Load 3..	13.40	0.0	1.50	0.00	1.170E+07	2.100E+08	0.000E+00
3	Pile Load 6..	13.40	0.0	1.50	0.00	1.170E+07	2.100E+08	0.000E+00
4*	Pile Load 7..	13.40	0.0	1.50	0.00	1.170E+07	2.100E+08	0.000E+00
5*	Pile Load 9..	2.52	0.0	1.50	0.00	1.170E+07	2.100E+08	0.000E+00
		4.04	0.0	1.50	0.00	4.742E+06	2.100E+08	0.000E+00
		6.84	0.0	1.50	0.00	1.170E+07	2.100E+08	0.000E+00
6*	Pile Load 1..	2.14	0.0	1.50	0.00	1.170E+07	2.100E+08	0.000E+00
		5.01	0.0	1.50	0.00	4.742E+06	2.100E+08	0.000E+00
		6.25	0.0	1.50	0.00	1.170E+07	2.100E+08	0.000E+00
7*	Pile Load 1..	1.70	0.0	1.50	0.00	1.170E+07	2.100E+08	0.000E+00
		6.06	0.0	1.50	0.00	4.742E+06	2.100E+08	0.000E+00
		5.64	0.0	1.50	0.00	1.170E+07	2.100E+08	0.000E+00
8*	Pile Load 1..	1.44	0.0	1.50	0.00	1.170E+07	2.100E+08	0.000E+00
		6.85	0.0	1.50	0.00	4.742E+06	2.100E+08	0.000E+00
		5.11	0.0	1.50	0.00	1.170E+07	2.100E+08	0.000E+00
9*	Pile Load 1..	1.30	0.0	1.50	0.00	1.170E+07	2.100E+08	0.000E+00
		7.31	0.0	1.50	0.00	4.742E+06	2.100E+08	0.000E+00
		4.79	0.0	1.50	0.00	1.170E+07	2.100E+08	0.000E+00
10*	Pile Load 2..	1.19	0.0	1.50	0.00	1.170E+07	2.100E+08	0.000E+00
		7.90	0.0	1.50	0.00	4.742E+06	2.100E+08	0.000E+00
		4.31	0.0	1.50	0.00	1.170E+07	2.100E+08	0.000E+00
11*	Pile Load 2..	1.07	0.0	1.50	0.00	1.170E+07	2.100E+08	0.000E+00
		8.15	0.0	1.50	0.00	4.742E+06	2.100E+08	0.000E+00
		4.18	0.0	1.50	0.00	1.170E+07	2.100E+08	0.000E+00
12*	Pile Load 2..	0.90	0.0	1.50	0.00	1.170E+07	2.100E+08	0.000E+00
		8.79	0.0	1.50	0.00	4.742E+06	2.100E+08	0.000E+00
		3.71	0.0	1.50	0.00	1.170E+07	2.100E+08	0.000E+00

Marked piletypes (*) are not used

PILE DATA

Pile nr	Pile Type name	Pile coordinates [m] X	Y	Z	Angle [deg]	Skew-ness	End Bearing [kN]	Top cond.
1	Pile Load 6..	0.00	0.90	0.00	0.00	0.00	10000.00	free

nr	Soil profile	Pile type name	Pile tip curve
1	1	Pile Load 607kN..	1

Figure 8-14

Pile Properties Garston, Load=2383kN

CAP DATA

	X-direction	Y-direction	Z-direction
Centre of gravity [m]	0.00	0.90	0.00

LOAD DATA

Index	Loadstep number	Force [kN] X - direction	- Y - direction	- Z - direction
1	1	607.000	-	-

Figure 8-15 Output Garston, Load = 2383kN

8.4.2 Results

When the calculated and measured deflections are plotted versus the lateral load, it can be seen that the calculated displacement predicted the measurements almost exactly for the smaller loads. For higher loads the calculated displacements increasingly underestimate the measured values. This is also the case for the calculation of the maximum moment.

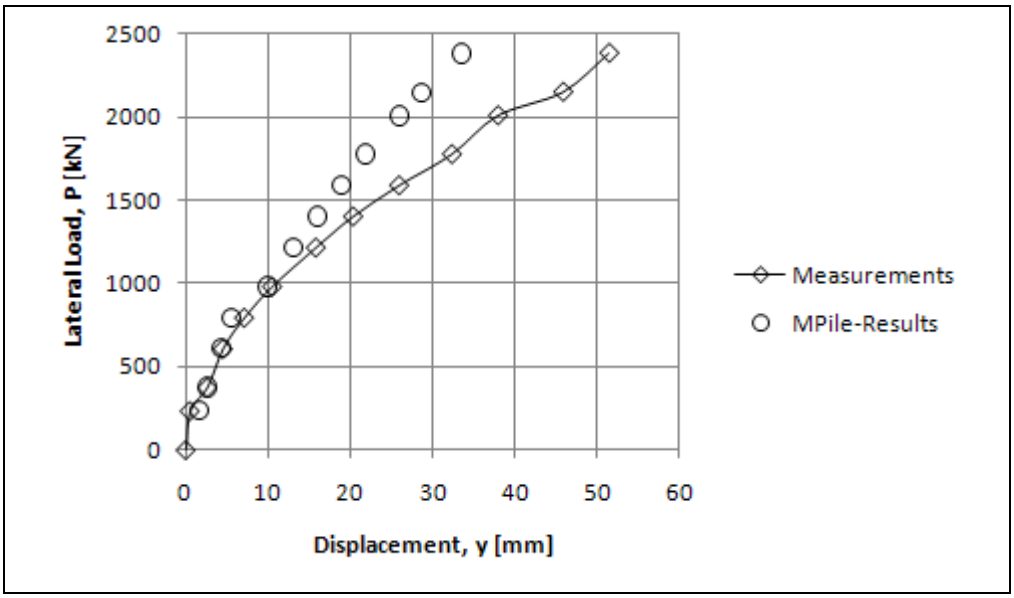

Graph 8-10 Lateral load vs. Displacement Garston

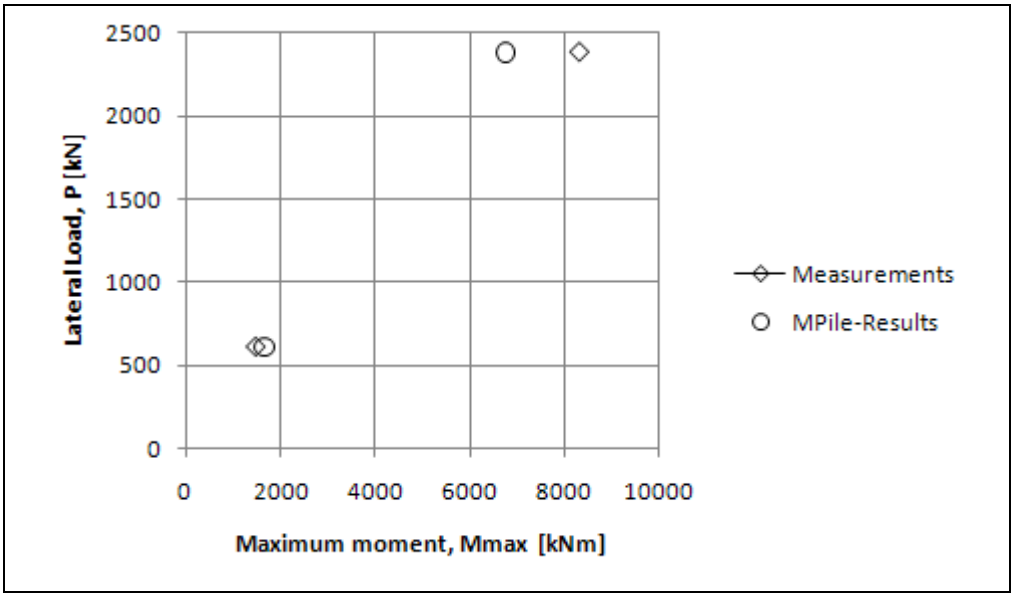

Graph 8-11 Lateral load vs. Maximum Moment Garston

8.5 CASE X-CL, ARKANSAS RIVER

8.5.1 Input

```
 Calculation method : Cap
 Cap model          : Rigid Cap


 SOIL LAYER DATA
 ================

  Soil layername: 0-0.61 with soil type: SAND
  Lateral and axial rule: API and API
-------------------------------------------------------
  Unit weight dry              [kN/m3] |      20.00 |      20.00
  Unit weight wet              [kN/m3] |      20.00 |      20.00
  Angle of internal friction     [deg] |      45.00 |      45.00
  Cone resistance qc           [kN/m2] |    5000.00 |    5000.00
  Ko                               [-] |       0.30 |
  dz  at 100 %                     [m] |      0.020 |
  Friction between pile/soil     [deg] |       1.00 |       1.00

  Soil layername: 0.61-2.4 with soil type: SAND
  Lateral and axial rule: API and API
-------------------------------------------------------
  Unit weight dry              [kN/m3] |      20.00 |      20.00
  Unit weight wet              [kN/m3] |      20.00 |      20.00
  Angle of internal friction     [deg] |      45.00 |      42.00
  Cone resistance qc           [kN/m2] |    5000.00 |    5500.00
  Ko                               [-] |       0.33 |
  dz  at 100 %                     [m] |      0.020 |
  Friction between pile/soil     [deg] |       1.00 |       1.00

  Soil layername: 2.4-4 with soil type: SAND
  Lateral and axial rule: API and API
-------------------------------------------------------
  Unit weight dry              [kN/m3] |      20.00 |      20.00
  Unit weight wet              [kN/m3] |      20.00 |      20.00
  Angle of internal friction     [deg] |      42.00 |      42.00
  Cone resistance qc           [kN/m2] |    5500.00 |   10000.00
  Ko                               [-] |       0.33 |
  dz  at 100 %                     [m] |      0.020 |
  Friction between pile/soil     [deg] |       1.00 |       1.00

  Soil layername: 4-4.6 with soil type: SAND
  Lateral and axial rule: API and API
-------------------------------------------------------
  Unit weight dry              [kN/m3] |      20.00 |      20.00
  Unit weight wet              [kN/m3] |      20.00 |      20.00
  Angle of internal friction     [deg] |      42.00 |      41.00
  Cone resistance qc           [kN/m2] |   10000.00 |    8000.00
  Ko                               [-] |       0.33 |
  dz  at 100 %                     [m] |      0.020 |
  Friction between pile/soil     [deg] |       1.00 |       1.00

  Soil layername: 4.6-5 with soil type: SAND
  Lateral and axial rule: API and API
-------------------------------------------------------
  Unit weight dry              [kN/m3] |      20.00 |      20.00
  Unit weight wet              [kN/m3] |      20.00 |      20.00
  Angle of internal friction     [deg] |      41.00 |      42.00
  Cone resistance qc           [kN/m2] |    8000.00 |   13000.00
  Ko                               [-] |       0.33 |
  dz  at 100 %                     [m] |      0.020 |
  Friction between pile/soil     [deg] |       1.00 |       1.00
```

Soil layername: 5-7 with soil type: SAND			
Lateral and axial rule: API and API			
Unit weight dry	[kN/m3]	20.00	20.00
Unit weight wet	[kN/m3]	20.00	20.00
Angle of internal friction	[deg]	42.00	42.00
Cone resistance qc	[kN/m2]	13000.00	14000.00
Ko	[-]	0.33	
dz at 100 %	[m]	0.020	
Friction between pile/soil	[deg]	1.00	1.00
Soil layername: 7-8.5 with soil type: SAND			
Lateral and axial rule: API and API			
Unit weight dry	[kN/m3]	20.00	20.00
Unit weight wet	[kN/m3]	20.00	20.00
Angle of internal friction	[deg]	42.00	40.00
Cone resistance qc	[kN/m2]	14000.00	12000.00
Ko	[-]	0.35	
dz at 100 %	[m]	0.020	
Friction between pile/soil	[deg]	1.00	1.00
Soil layername: 8.5-10 with soil type: SAND			
Lateral and axial rule: API and API			
Unit weight dry	[kN/m3]	20.00	20.00
Unit weight wet	[kN/m3]	20.00	20.00
Angle of internal friction	[deg]	40.00	41.00
Cone resistance qc	[kN/m2]	12000.00	15000.00
Ko	[-]	0.35	
dz at 100 %	[m]	0.020	
Friction between pile/soil	[deg]	1.00	1.00
Soil layername: 10-11.6 with soil type: SAND			
Lateral and axial rule: API and API			
Unit weight dry	[kN/m3]	20.00	20.00
Unit weight wet	[kN/m3]	20.00	20.00
Angle of internal friction	[deg]	41.00	40.00
Cone resistance qc	[kN/m2]	15000.00	15000.00
Ko	[-]	0.35	
dz at 100 %	[m]	0.020	
Friction between pile/soil	[deg]	1.00	1.00
Soil layername: 11.6-20 with soil type: SAND			
Lateral and axial rule: API and API			
Unit weight dry	[kN/m3]	20.00	20.00
Unit weight wet	[kN/m3]	20.00	20.00
Angle of internal friction	[deg]	40.00	36.00
Cone resistance qc	[kN/m2]	15000.00	15000.00
Ko	[-]	0.35	
dz at 100 %	[m]	0.020	
Friction between pile/soil	[deg]	1.00	1.00

Figure 8-16 Soil Layer data Arkansas River

SOIL PROFILE DATA

Waterlevel: -1.50 [m]
Location: x = 0.00 [m] z = 0.00 [m]

layer	Y[m]	Soil layer name	Soil type
1	0.00	0-0.61	SAND
2	-0.61	0.61-2.4	SAND
3	-2.40	2.4-4	SAND
4	-4.00	4-4.6	SAND
5	-4.60	4.6-5	SAND
6	-5.00	5-7	SAND
7	-7.00	7-8.5	SAND
8	-8.50	8.5-10	SAND
9	-10.00	10-11.6	SAND
10	-11.60	11.6-20	SAND

Figure 8-17 Soil Profile Arkansas River

PILE TIP CURVES

Rt[%]	Zt[m]
0.000	0.000
100.000	0.010

PILE TYPE DATA

Pile Type nr	Pile Type Name	Pile properties Length [m]	Mass [kg]	Diam. [m]	Thickn. [m]	EI [kN/m2]	EA [kN]	Young modulus [kN/m2]
1	Pile	15.00	0.0	0.48	0.01	6.991E+04	2.510E+06	2.116E+08

PILE DATA

Pile nr	Pile Type name	Pile coordinates [m] X	Y	Z	Angle [deg]	Skew-ness	End Bearing [kN]	Top cond.
1	Pile	0.00	0.00	0.00	0.00	0.00	500.00	free

nr	Soil profile	Pile type name	Pile tip curve
1	1	Pile	1

Figure 8-18 Pile Properties Arkansas River

CAP DATA

	X-direction	Y-direction	Z-direction
Centre of gravity [m]	0.00	0.00	0.00

LOAD DATA

Index	Loadstep number	Force [kN] X - direction	- Y - direction	- Z - direction
1	1	46.000	-	-
2	2	92.000	-	-
3	3	140.000	-	-
4	4	191.000	-	-
5	5	248.000	-	-

Figure 8-19 Cap- and load data Arkansas River, Load = 248kN

8.5.2 Results

When the calculated and measured deflections are plotted versus the lateral load, it can be seen that the calculated displacements almost exactly match the measured values. However, if the shapes of the curves are extrapolated, it is likely that MPile will increasingly overestimate the lateral deflections.

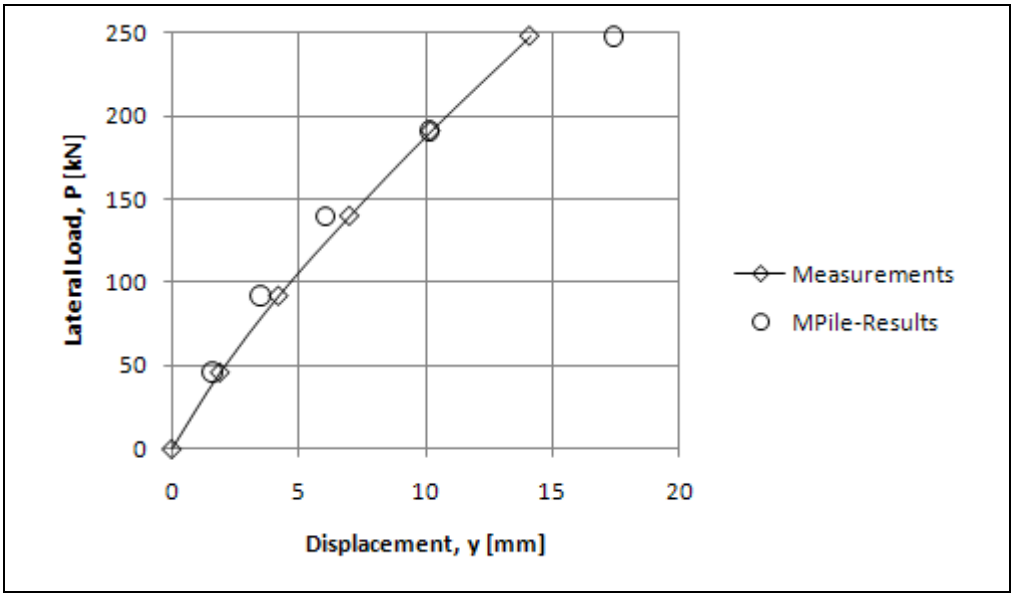

Graph 8-12 Lateral load vs. Displacement Arkansas River

8.6 CASE XIII-L, FLORIDA

8.6.1 Input

Calculation method : Cap
Cap model : Rigid Cap

SOIL LAYER DATA

Soil layername: Sand with soil type: SAND
Lateral and axial rule: API and API

Unit weight dry	[kN/m3]	19.20	19.20
Unit weight wet	[kN/m3]	19.20	19.20
Angle of internal friction	[deg]	38.00	38.00
Cone resistance qc	[kN/m2]	10000.00	15000.00
Ko	[-]	0.38	
dz at 100 %	[m]	0.002	
Friction between pile/soil	[deg]	15.00	15.00

Soil layername: Clay with soil type: STIFF CLAY
Lateral and axial rule: API and API

Unit weight dry	[kN/m3]	19.40	19.40
Unit weight wet	[kN/m3]	19.40	19.40
Undrained Shearstength Cu	[kN/m2]	120.00	120.00
Empirical constant J	[-]	0.5000	
Strain at 50% failure load	[-]	0.00500	
dz	[m]	0.00	

Figure 8-20 Soil layer data Florida

SOIL PROFILE DATA

Waterlevel: -0.61 [m]
Location: x = 0.00 [m] z = 0.00 [m]

layer	Y[m]	Soil layer name	Soil type
1	0.00	Sand	SAND
2	-3.96	Clay	STIFF CLAY

Figure 8-21 Soil Profile Florida

PILE TIP CURVES

Rt[%]	Zt[m]
0.000	0.000
100.000	0.002

PILE TYPE DATA

Pile Type nr	Pile Type Name	Pile properties Length [m]	Mass [kg]	Diam. [m]	Thickn. [m]	EI [kN/m2]	EA [kN]	Young modulus [kN/m2]
1	Pile	3.01	0.0	1.42	0.00	5.079E+06	2.000E+08	0.000E+00
		6.70	0.0	1.42	0.00	2.525E+06	1.000E+08	0.000E+00

PILE DATA

Pile nr	Pile Type name	Pile coordinates [m] X	Y	Z	Angle [deg]	Skew-ness	End Bearing [kN]	Top cond.
1	Pile	0.00	1.79	0.00	0.00	0.00	1000.00	free

nr	Soil profile	Pile type name	Pile tip curve
1	1	Pile	1

Figure 8-22 Pile Properties Florida

CAP DATA

	X-direction	Y-direction	Z-direction
Centre of gravity [m]	0.00	1.79	0.00

LOAD DATA

Index	Loadstep number	Force [kN] X - direction	- Y - direction	- Z - direction
1	1	46.000	-	-
2	2	67.000	-	-
3	3	87.000	-	-
4	4	113.000	-	-
5	5	133.000	-	-
6	6	157.000	-	-
7	7	180.000	-	-
8	8	226.000	-	-

Figure 8-23 Cap- and load data Florida, Load = 226kN

8.6.2 Results

When the calculated and measured deflections are plotted versus the lateral load, it can be seen that the calculated displacement at the lowest load predicted the displacement almost exactly. However, if the load increased the deflections where underestimated increasingly up to almost three times the measured displacement.

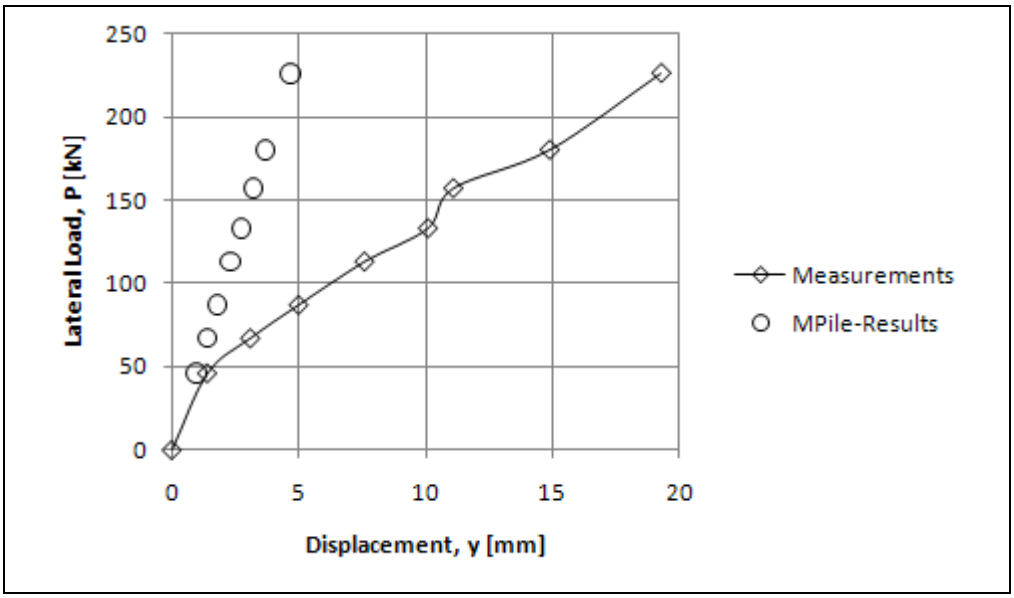

Graph 8-13 Lateral load vs. Displacement Florida

9 PLAXIS

Plaxis is a finite element program. For the single pile calculation, the 3D Foundation version is used.

9.1 GENERAL RULES FOR PLAXIS INPUT

To make sure that all Plaxis calculations are executed in a similar manner. A few simple rules have been applied to each of the cases. These rules apply to the geometry of the input, the mesh generation and the application of the load on the pile.

9.1.1 General Rules for Geometry, Mesh and Pile Input

The 3D geometry of the model is a square box. The width, in x-direction, and length, in z-direction, are 30 diameters or 2 pile lengths long, depending on which of the two values is largest. The height, in y-direction, of the model is always at least 1,5 times the length of the pile.

Because the width and length of the pile and the dimensions of the geometry are different for each of the cases, it is impossible to generate the same mesh for each of the cases. Therefore the mesh is generated as follows. First, a cluster is defined closely around the pile. The dimensions cluster are either 6x6 diameters or 0,2x0,2 pile lengths, depending of which of the two values is largest. Within this cluster a more refined mesh is chosen, since most of the deformations will occur within the cluster. After the cluster is defined, the overall mesh is globally refined. (Use once: refine global.) Then, the cluster is refined twice. (Select the cluster and use twice: refine cluster.) Finally, the vertical element distribution should be set on “fine”. This should generate a mesh which has an aspect ratio of the elements in the clusters of approximately one.

In many of the cases it is rarely known how the load was applied on the pile. Therefore it is desirable to distribute the load at the top of the pile to prevent high peaks of stresses in the pile. To do this, a floor element is placed at the top of the pile. The floor is very stiff and weightless. The thickness of the floor is modeled to be 10cm and the modulus of elasticity similar to that of steel, $2{,}1 \times 10^8$ kN/m^2. Be aware that, despite a floor-thickness of 10cm is entered, the floor will still be 0,0cm thick in the model. Therefore, the floor has no influence on the rotation of the cap, but will only distribute the load around the pile.

Finally, all the piles are modeled as circular tube piles with interfaces on the in- and outside of the pile. The “shell” option in the piles-menu is checked. The thickness of the pile is zero. This means that the pile has no volume in the model. In the material set of the pile, the thickness has been taken into account, as is the stiffness. The material is set to be isotropic and linearly elastic. This is the case for all field tests, including those with concrete piles. By adapting the elasticity and thickness the right bending stiffness of the pile is accomplished.

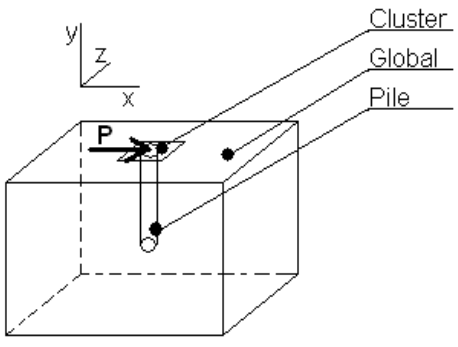

9.1.2 General Rules for Soil Parameter Selection.

In the cases where the soil consisted mainly out of clayey soil, the Mohr-Coulomb model is used. During the process it became clear that the HS and the HSS model in Plaxis did not perform that well if a friction angle of zero was used together with undrained shear strength. This decision was made together with Plaxis bv.

The required parameters for the Mohr Coulomb model have been acquired either from the available soil data or by available correlations. Below follows a summary of al used parameters.

- *Model Type - Drained:* However, the clay will react undrained. The loads are applied in short time intervals of several minutes. The stiffness parameters will be multiplied with a factor 2, to obtain the undrained values. The reason for this decision was caused by the iteration problems encountered when the undrained model type was used.
- *Unit weight - From soil data:* In all of the cases the dry and saturated unit weights are known.
- *Stiffness E_{ref} - From table 1:* The stiffnesses of the clays are not known. Therefore, these values are obtained from table one. Since the stiffness, E_{100}, is not stress dependent for clays, the values do not have to be adjusted for this reason. However, the stiffness do has to be adjusted to model the undrained behavior. The value of E_{100} is multiplied by a factor 2 to model this behavior. The value of E_{100} is obtained from table 1, NEN 6740:2006. The table is entered through the undrained shear strength and then the values of E_{100} are found by means of linear interpolation or extrapolation.
- *Poisson's Ratio:* The Poisson's ratio is assumed 0,3 for unsaturated clays and 0,4 for saturated clays.
- *Cohesion – Undrained shear strength from soil data:* In all of the field tests undrained shear strengths are given.
- *Friction angle – Zero:* The friction angle has to be zero, since the shear strength is undrained.
- *At rest lateral earth pressure – 0,5:* This value is unknown in all cases. 0,5 Is a characteristic value.

In the case where the soil consisted out of sand, the Hardening Soil model with Small strain stiffness (HSSmall) is used. This decision was made, since the model behaved logically and the strain- and stress dependency of this model are desirable. This decision is also made together with Plaxis bv.

Also for sand the material parameters are found by means of correlations and the available soil data. For some parameters just generally accepted values for sand are used.

- *Model type – Drained:* It is assumed that sand will behave drained since the application of the load lasts for several minutes.
- *Unit weight – From soil data:* In all of the cases the dry and saturated unit weights are known.
- *Stiffnesses E_{50}, E_{oed} and E_{ur} – From correlation:* In agreement with Plaxis bv. a correlation table for sandy soils is used based on the grain size distribution of the sand. The relation between the three parameters is as follows: $3E_{50} = 3E_{oed} = E_{ur}$. As is the standard setting in Plaxis.
- *Stress dependency, m –value = 0,5:* Because the material purely consists of sand.
- *Cohesion – value = 1kPa:* Because of the formulas used in the HSSmall model, the cohesion may not be equal to zero. Therefore a small value must be entered here.

- *Angle of internal friction – From soil data:* In all of the cases the angle of internal friction is known.
- *Dilatancy angle – value = 5°:* This value has been used in all cases. The dilatancy angle does not have a large influence on the results. Therefore a value of 5° is chosen in each of the cases.
- $y_{0,7} = 1{,}0x10^{-4}$*:* This value is a characteristic value for sand.
- $G_{0,ref} = E_{ur}$*:* This is an approximation of $G_{0,ref}$.
- *Reference stress level = 100kPa:* For the reference stress level the standard value of 100kPa is used since this is also the value on which the correlation table is based. This correlation table was used to find the stiffness of the soil.

9.2 CASE I-CU, BAGNOLET

9.2.1 Input

In the case of Bagnolet the following input is used for all three of the tests. The differences between the tests are the penetration depth, the point of application of the load and the magnitude of the loads. These values can be found in Appendix B, paragraph 1.1.

The case in Bagnolet is the first considered test in clayey soil. The soil can generally be described as unsaturated clay.

As can be seen from the soil input, the parameters are chosen in such a way that the stiffness and undrained shear strength of the soil increases continuously. This is shown graphically in graph 9-1 on the following page.

Parameter	Symbol	Top layer	Middle layer	Bottom Layer	Unit
Model		Mohr-Coulomb	Mohr-Coulomb	Mohr-Coulomb	-
Type		Drained	Drained	Drained	-
Volumetric weight	γ_{unsat}	17,9	17,9	17,9	kN/m^3
Saturated volumetric weight	γ_{sat}	17,9	17,9	17,9	kN/m^3
Elasticity soil	E_{ref}	8000	11000	11600	kN/m^2
Elasticity increment	E_{incr}	821,2	890,5	812,5	kN/m^2
Reference depth for increments	y_{ref}	0	-3,96	-4,69	m
Poisson's ratio	ν	0,3	0,3	0,3	-
Undrained shear strength	c_{ref}	100	125	130	kN/m^2
Undrained shear strength increment	c_{incr}	6,31	6,85	5	kN/m^2
Angle of internal friction	φ	0	0	0	°
Dilatancy angle	ψ	0	0	0	°

Table 9-1 Model parameters Plaxis, Bagnolet

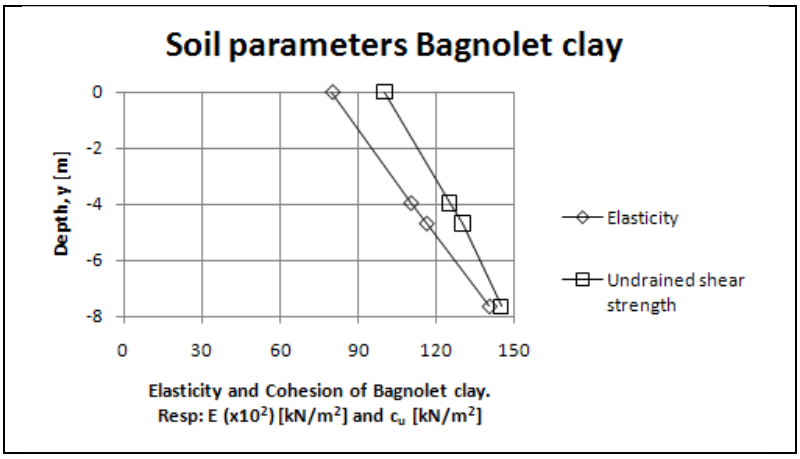

Graph 9-1 Soil parameters Bagnolet clay

9.2.2 Results

When the Plaxis results are considered for all three tests, it can be seen that the deflections are overestimated. This can be due to several reasons.

The first reason is the chosen model. Small strains occur a lot around the pile. If it was possible to use the hardening soil model with small strain stiffnesses, the deformations would be reduced.

Another cause might be found in the pile description. It might be argued that the 0,43m is less than the total width of the pile. This argument is invalidated in the following case. Here, the soil is similar and the overestimation approximately the same. Because here the pile dimensions were known exactly, 0,43m is an adequate value for the pile width.

Thus the results might improve, if another soil model is used or/and the soil stiffnesses were determined accurately by means of borings and laboratory tests.

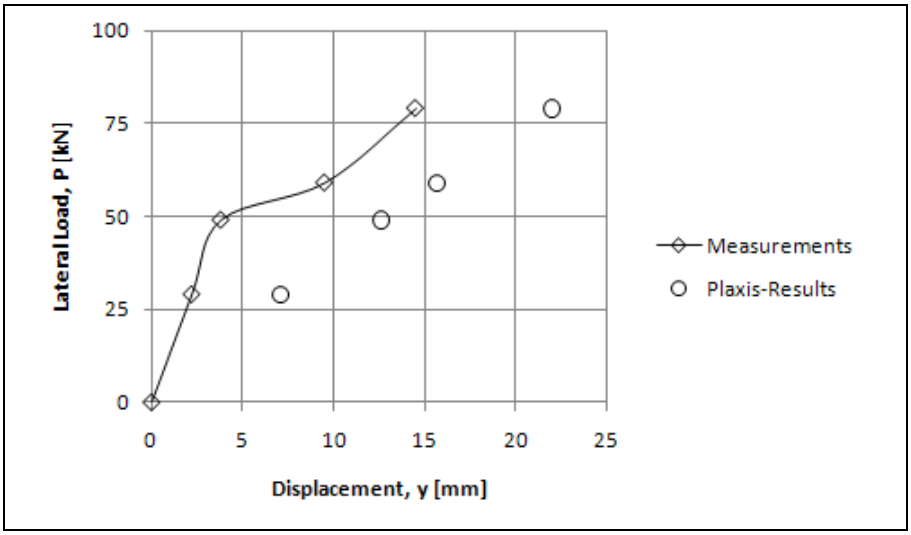

Graph 9-2 Lateral Load vs. displacements, Bagnolet Test I

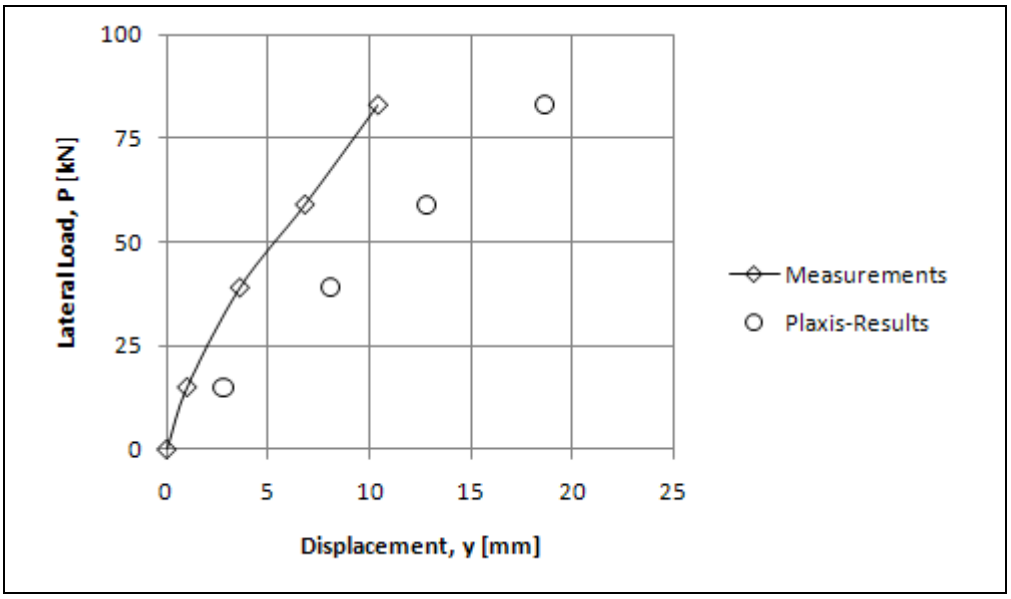

Graph 9-3 Lateral load vs. displacement, Bagnolet Test II

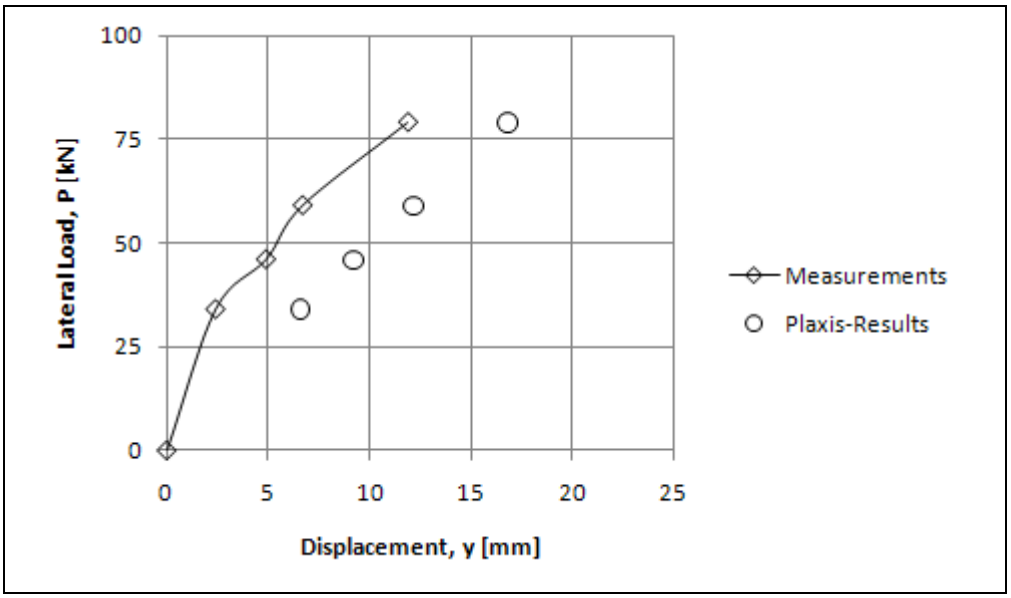

Graph 9-4 Lateral load vs. displacement, Bagnolet Test III

9.3 CASE III-CU, BRENT CROSS

9.3.1 Input

The input of the soil parameters is chosen such that the stiffnesses and undrained shear strengths are continuously increasing (or in one layer: decreasing) over the profile. The parameters of the bottom layer are chosen such that the stiffness and undrained shear strength of the soil are equal to the parameters given for a depth of 19 m –groundline.
All other input is according to the general rules and de test data from Appendix B, chapter 1.3. The soil is here mainly unsaturated clay as was the case in the previous case in Bagnolet.

Parameter	Symbol	Top layer	Middle layer	Bottom layer	Unit
Model		Mohr-Coulomb	Mohr-Coulomb	Mohr-Coulomb	-
Type		Drained	Drained	Drained	-
Volumetric weight	γ_{unsat}	17,0	17,0	17,0	kN/m^3
Saturated volumetric weight	γ_{sat}	17,0	17,0	17,0	kN/m^3
Stiffness soil	E_{ref}	3528	6816	6448	kN/m^2
Stiffness increment	E_{incr}	688,5	-221,5	417	kN/m^2
Reference depth for increments	y_{ref}	0	-4,6	-6,2	m
Poisson's ratio	v	0,3	0,3	0,3	-
Undrained shear strength	c_{ref}	44,1	85,2	80,6	kN/m^2
Undrained shear strength increment	c_{incr}	8,93	-2,875	4,11	kN/m^2
Angle of internal friction	φ	0	0	0	^{o}
Dilatancy angle	ψ	0	0	0	^{o}

Table 9-2 Model parameters Plaxis, Brent Cross

9.3.2 Results

Considering the results of Brent Cross, it can be seen that the deflections are overestimated. This is the same result as was obtained from the previous case in Bagnolet. The reasons for this can be also the same. The MC-model reacts less stiff than the HSS-model and the soil stiffnesses were not determined by means of laboratory tests, but by means of correlations with the strength parameters.

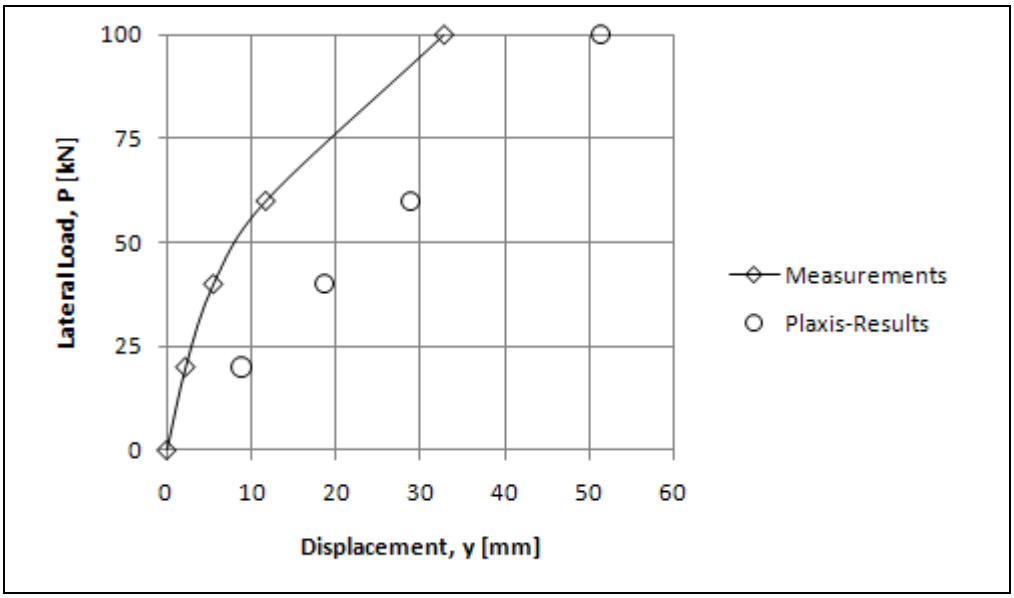

Graph 9-5 Lateral load vs. displacement, Brent Cross

9.4 CASE VI-CS, SABINE

9.4.1 Input

This is the final case in a clayey soil. The difference is the level of the ground water table. In this case the soil was completely saturated in contradiction to the previous two cases. Another difference was that the soil data was much more limited. No layers could be separated. The soil data was assumed to be valid for the first meter. Stiffness and strength increments were assumed to be present and small compared to the two unsaturated cases. An overview of the data is given below in the table.

Parameter	Symbol		Unit
Model		Mohr-Coulomb	-
Type		Drained	-
Volumetric weight	γ_{unsat}	5,5	kN/m^3
Saturated volumetric weight	γ_{sat}	15,3	kN/m^3
Stiffness soil	E_{ref}	1152	kN/m^2
Stiffness increment	E_{incr}	258,5	kN/m^2
Reference depth for increments	y_{ref}	0	m
Poisson's ratio	ν	0,4	-
Undrained shear strength	c_{ref}	14,4	kN/m^2
Undrained shear strength increment	c_{incr}	3	kN/m^2
Angle of internal friction	φ	0	^{o}
Dilatancy angle	ψ	0	^{o}

Table 9-3 Model parameters Plaxis, Sabine

9.4.2 Results

The results are remarkably accurate compared to the results in the two field tests in unsaturated clay. These results are presented in graph 9-6. The reason for this accuracy is hard to determine since the soil data was very limited in this case and a lot of assumptions had to be made. The results might still improve if the HSS model was used.

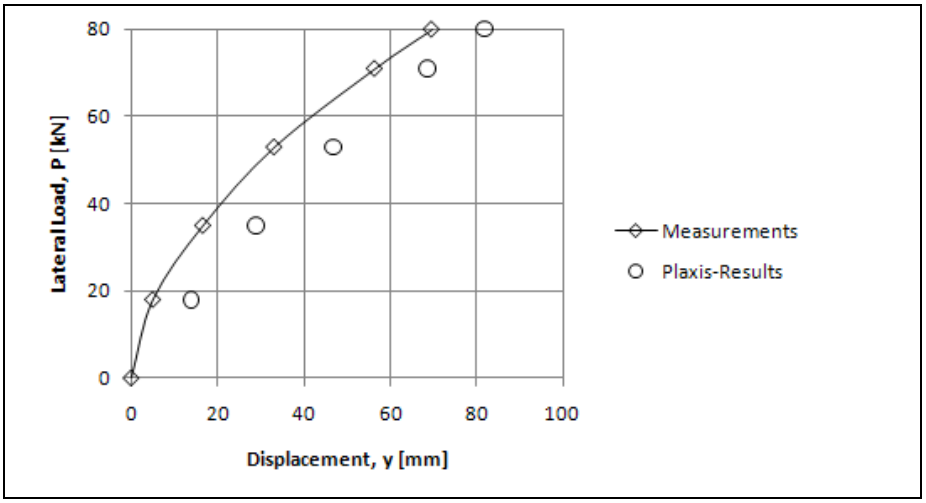

Graph 9-6 Lateral load vs. Displacement, Sabine

9.5 CASE IX-CL, GARSTON

9.5.1 Input

This is the first case in sandy soil. The pile was a bored pile, reinforced with steel bars. This resulted in the possibility to apply very high loads. The parameters were determined as stated in the general rules at the beginning of this chapter. An overview of the soil parameters is given below in the table.

Parameter	Symbol	Fill, dense sandy gravel	Sand and gravel	Sandstone	Weathered Sandstone	Unit
Model		HSSmall	HSSmall	HSSmall	HSSmall	-
Type		Drained	Drained	Drained	Drained	-
Volumetric weight	γ_{unsat}	21,5	19,7	21,7	21,7	kN/m^3
Saturated volumetric weight	γ_{sat}	21,5	19,7	21,7	21,7	kN/m^3
Stiffness soil	E_{ref}	60000	60000	60000	60000	kN/m^2
Oedometer stiffness	E_{oed}	59650	60000	59650	59650	kN/m^2
Unloading/reloading stiffness	E_{ur}	180000	180000	180000	180000	kN/m^2
Power (stress dependency)	m	0,5	0,5	0,5	0,5	-
Poisson's ratio	ν_{ur}	0,2	0,2	0,2	0,2	-
Undrained shear strength	c_{ref}	1	1	1	1	kN/m^2
Angle of internal friction	φ	43	37	43	43	^{o}
Lateral earth pressure	K_0	0,322	0,398	0,322	0,322	-
Dilatancy angle	ψ	5	5	5	5	^{o}
Small strain	$\gamma_{0,7}$	1,0x10^{-4}	1,0x10^{-4}	1,0x10^{-4}	1,0x10^{-4}	-
Small strain	G_0^{ref}	1,8 x10^5	1,8 x10^5	1,8 x10^5	1,8 x10^5	kN/m^2

Table 9-4 Model parameters Plaxis, Garston

9.5.2 Results

The obtained results in this case are reasonably good. This is despite the fact that some crude assumptions had to be made.

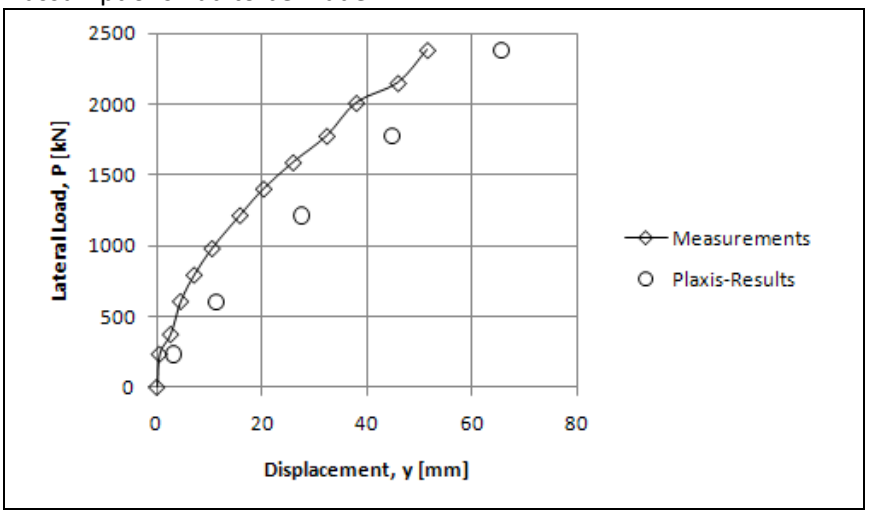

Graph 9-7 Lateral load vs. Displacement, Garston

9.6 CASE X-CL, ARKANSAS RIVER

9.6.1 Input

The input in this case is very special. In Plaxis it is possible to include a pre- overburden pressure. This is the case in Arkansas. An overburden of 6 meter of sand used to be present. If the sand is assumed to be loosely packed, the volumetric weight can be assumed to be 16kN/m^2. This leads to a overburden pressure of 96kN/m^2. This effect is examined with both the HS-model and the HSS model. It is not possible with the HSS-model to include a POP. The effect was examined by performing the calculation with and without a POP in the HS model and by performing the calculation with and without a fill over the entire surface of the soil model in the initial phase in the HSS model. If the effect of the POP in HS-model turns out to be large compared to the effect of the fill in the HSS model, the POP is preferred to be used, because this method was developed for this purpose. However it is also thought that the fill is also a good approach. The advantage of the fill is that the HSS-model can now be used.

The soil parameters are in all calculations basically the same. The difference lies therein, that the HS model does not include the small strain parameters and one of the HS calculations does and the other does not include the POP.

Together with Plaxis bv. it was determined to simulate the soil as a single layer.

Parameter	Symbol	Sand	Unit
Model		HSSmall	-
Type		Drained	-
Volumetric weight	γ_{unsat}	20,0	kN/m^3
Saturated volumetric weight	γ_{sat}	20,0	kN/m^3
Stiffness soil	E_{ref}	60000	kN/m^2
Oedometer stiffness	E_{oed}	60000	kN/m^2
Unloading/reloading stiffness	E_{ur}	180000	kN/m^2
Power (stress dependency)	m	0,5	-
Poisson's ratio	v_{ur}	0,2	-
Undrained shear strength	c_{ref}	1	kN/m^2
Angle of internal friction	φ	42	^{o}
Lateral earth pressure	K_0	0,35	-
Dilatancy angle	ψ	5	^{o}
Small strain (Not in HS-model)	$\gamma_{0,7}$	1,0x10^{-4}	-
Small strain (Not in HS model)	G_0^{ref}	1,8 x10^5	kN/m^2
Pre Overburden Pressure	POP	96,0	kN/m^2

Table 9-5 Model parameters Plaxis, Arkansas River

The fill in the HSS model is modeled as a stiff layer (high stiffness, and strength) with a volumetric weight of 16kN/m^3 and a thickness of 6 meters. These last two parameters are the most important one, since the fill is removed prior to the pile installation.

9.6.2 Results

When the deflections are plotted versus the lateral load for all four calculations, it can be seen that there is a large influence of the fill. The deformations of the top of the pile are reduced with approximately 1/3. The effect is a little larger for the HSS-model than for the HS model. Considering the results of these calculations, the HSS-model with a fill is the best approach. This because the fill effect is similar to the effect of the POP and the HSS-model is also strain dependent.

If the results of the HSS calculation with the fill are plotted besides the measurements, it can be seen that they are approximately the same.

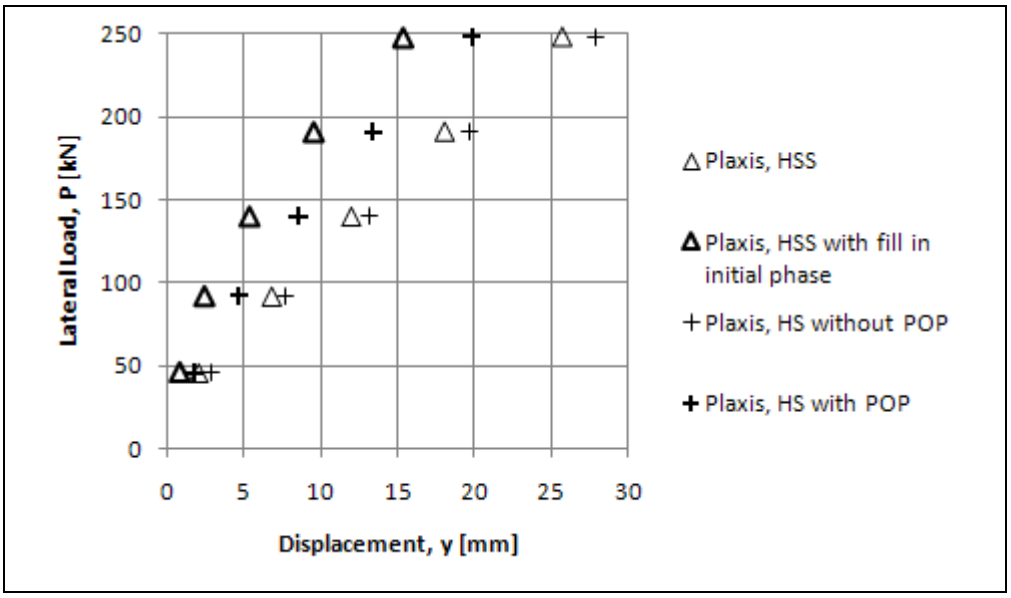

Graph 9-8 Calculated displacements Arkansas River with different soil models in Plaxis.

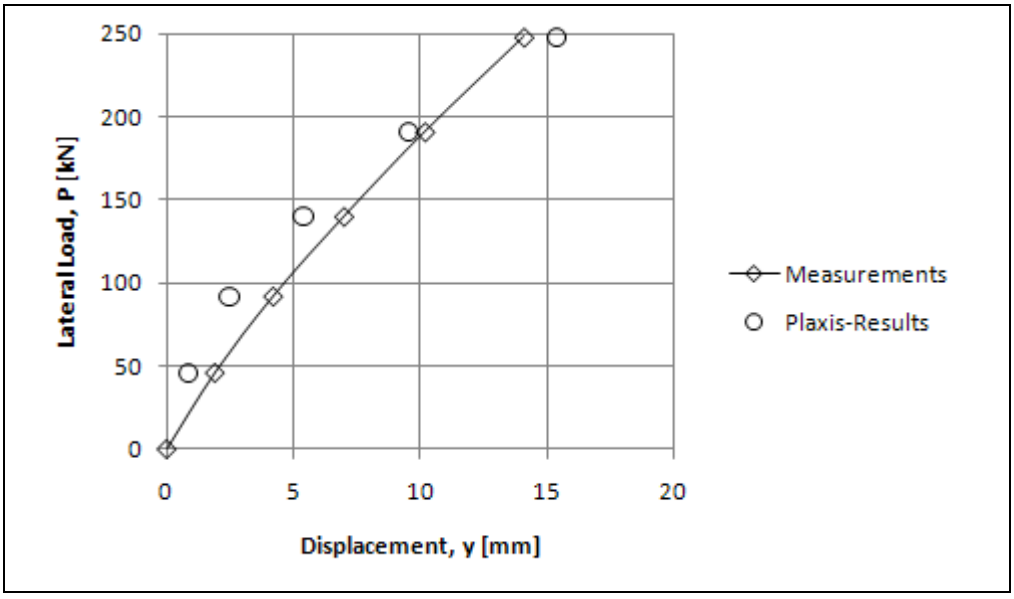

Graph 9-9 Lateral load vs. Displacements, Arkansas River

9.7 CASE XIII-L, FLORIDA

9.7.1 Input

This case is special for two reasons. The soil consists of two layers with a different material and the pile's bending stiffness is not constant over the height of the pile. The parameters of the clay layer and the sand layer are given below.

Parameter	Symbol	Sand	Clay	Unit
Model	-	HSSmall	Mohr-Coulomb	-
Type	-	Drained	Drained	-
Volumetric weight	γ_{unsat}	20,0	19,2	kN/m^3
Saturated volumetric weight	γ_{sat}	20,0	19,2	kN/m^3
Stiffness soil	E_{ref}	60000	10400	kN/m^2
Oedometer stiffness	E_{oed}	60000	-	kN/m^2
Unloading/reloading stiffness	E_{ur}	180000	-	kN/m^2
Power (stress dependency)	m	0,5	-	-
Poisson's ratio	v_{ur}	0,2	0,4	-
Undrained shear strength	c_{ref}	1	120	kN/m^2
Angle of internal friction	φ	42	0	^{o}
Lateral earth pressure	K_0	0,35	0,5	-
Dilatancy angle	ψ	5	0	^{o}
Small strain (Not in HS-model)	$\gamma_{0,7}$	$1,0x10^{-4}$	-	-
Small strain (Not in HS model)	G_0^{ref}	$1,8 x10^5$	-	kN/m^2
Cohesion increment	$c_{increment}$	-	3	$kN/m^{-2}/m$
Reference level of $c_{increment}$	y_{ref}	-	-5,94	m

Table 9-6 Model parameters Plaxis, Florida

9.7.2 Results

When the calculated and measured deflections are plotted versus the lateral load, it is clear that the deflections are severely underestimated.

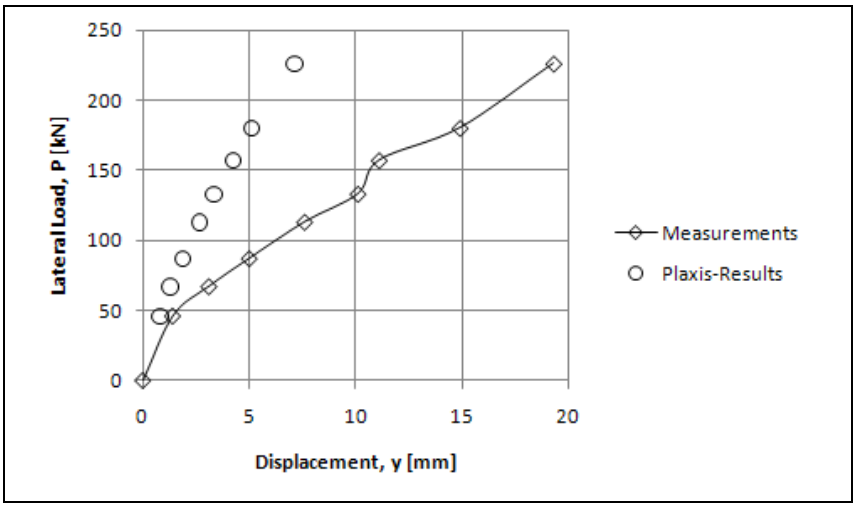

Graph 9-10 Lateral Load vs. deflection, Florida

BIBLIOGRAPHY

Bekken, L. (2009). *Lateral bahavior of large diameter offshore monopiles for wind turbines.* Nieuwegein.

Bijnagte, J. (2005). PAO cursus - Paalfunderingen. *PF13*.

Bijnagte, J., & Luger, H. (Red.). (2006). *MPile Version 4.1, 3D Analysis of single piles and pile groups.* Delft: GeoDelft.

Bijnagte, J., Van den Berg, P., Zorn, N., & Dieterman, H. (1991). Laterally loaded single pile in soft soil. *Heron , 36* (1), 1-78.

Blum, H. (1932). Wirtschaftliche dalbenformen und deren berechnung. *Bautechnik* , Heft 5.

Brinch Hansen, J. (1961). The Ultimate resistance of rigid piles against transversal forces. *The Danish geotechnical institute, Bulletin , 12*.

Broms, B. (1965). Design of laterally loaded piles. *Journal of the soil mechanics and foundation division , 91* (3), 77-99.

Broms, B. (1964). Lateral resistance of piles in cohesionless soils. *Journal of the soil mechanics and foundation division , 90* (3), 123-156.

Broms, B. (1964). Lateral resistance of piles in cohesive soils. *Journal of the soil mechanic and foundation division , 90* (2), 27-63.

Christensen, N. H. (1961). Model tests with transversally loaded rigid piles in sand. *Geoteknisk Institut, Bulletin No. 12* .

Department_for_communities_and_local_government. (2009). *Multi-criteria analysis: a manual.* London: Crown.

Duncan, J., Evans, L., & Ooi, P. (1994). Lateral load analysis of single piles and drilled shafts. *Journal of geotechnical engineering devision , 120* (5), 1018-1033.

GeoDelft. (2004). *MSheet user manual - Release 6.1.* Delft.

LPILE Plus 5.0 for windows. (sd). Opgeroepen op May 31, 2010, van Ensoft, inc: http://www.ensoftinc.com

Lupnitz, H. (1977). *Spundwand-Handbuch Berechnung.* Dortmund: Hoesch - Spundwand und Profil.

Lupnitz, H., & al., E. (2007). *Spundwand-Handbuch Berechnung (Revised version).* Gelsenkirchen: Makossa Druck und Medien GmbH.

Matlock, H., & Reese, L. (1962). Generalized solutions for laterally loaded piles. *ASCE , 127* (1), 1220-1251.

MPile, version 4.1, 3D modelling of single piles and pile groups. (sd). Opgeroepen op May 31, 2010, van Geodelftsystems: http://www.delftgeosystems.nl//EN/page64.asp

PLAXIS 3D Foundation, Material models manual, Version 2. (sd). Opgeroepen op July 27, 2010, van plaxis.com: http://www.plaxis.nl/files/files/3DF2_3_Material_Models.pdf

Plaxis 3D Foundation, Validation manual, version 2. (sd). Opgeroepen op July 27, 2010, van Plaxis.nl: http://www.plaxis.nl/files/files/3DF2_5_Validation.pdf

Reese, L., & Matlock, H. (1956). Nondimensional solutions for laterally loaded piles with soil modulus assumed proportional with depth. *Proceedings, VIII Texas conference on soil mechanics and foundation engineering* , 672-690.

Reese, L., & Van Impe, W. (2001). *Single piles and pile groups under lateral loading.* Rotterdam: A.A. Balkema.

Reese, L., Isenhower, W., & Wang, S.-T. (2006). *Analysis and design of shallow and deep foundations.* Hoboken: John Wiley & Sons, Inc.

Roctest. (sd). *Pressuremeter and dilatometer tests, interpretation and results.* Opgeroepen op June 4, 2010, van Roctest.com: http://www.roctest.com/modules/AxialRealisation/img_repository/files/documents/-PRESSUREMETER%20AND%20DILATOMETER%20TESTS-V10.pdf

Schanz, T., Vermeer, P., & Bonnier, P. (1999). The hardening soil model: Formulation and verification. *Beyond 2000 in computational geotechnics - 10 Years of PLAXIS* .

Verruijt, A. (1983). *Grondmechanica.* Delft: VSSD.